Synthesis of γ-cyclobutane amino acids via visible light

Dissertation
zur Erlangung des Doktorgrades der Naturwissenschaften
Dr. rer. nat.
der Fakultät für Chemie und Pharmazie
der Universität Regensburg

vorgelegt von
Sabine Martha Kerres
aus Burglengenfeld

Regensburg 2018

Die Arbeit wurde angeleitet von:	Prof. Dr. O. Reiser
Promotionsgesuch eingereicht am:	09.07.2018
Promotionskolloquium am:	21.09.2018
Prüfungsausschuss:	Vorsitz: Prof. Dr. R. Müller
	1. Gutachter: Prof. Dr. O. Reiser
	2. Gutachter: Prof. Dr. D. J. Aitken
	3. Gutachter: Prof. J. Wegener

Der experimentelle Teil der vorliegenden Arbeit wurde im Zeitraum von November 2014 bis Dezember 2017 am Lehrstuhl von Prof. Dr. Oliver Reiser, Institut für Organische Chemie, Universität Regensburg, angefertigt.

Herrn Prof. Dr. Oliver Reiser möchte ich herzlich für die Überlassung des interessanten Themas, die anregenden Diskussionen und seine stete Unterstützung während der Durchführung dieser Arbeit danken.

Für Florian und meine Familie

Freiheit bedeutet, dass man nicht

unbedingt alles so machen muss,

wie andere Menschen.

(Astrid Lindgren)

Abbreviations

Å	angstrom	DEE	diethyl ether
Ac	acetyl	DEPT	distortionless enhancement by polarization transfer
ACHC	amino cylcohexane carboxylic acid	dF(CF_3)ppy	(2-(2,4-difluorophenyl)-5(trifluoromethyl)pyridine
AcOH	acetic acid	DIPEA	*N,N*-diisopropylethylamine
ACC	amino cyclopropane carboxylic acid	DMA	*N,N*-dimethylaminiline
ACBC	amino cyclobutane carboxylic acid	DMAP	*N,N*-dimethyl-4-aminopyridine
ACPC	amino cyclopentane carboxylic acid	DMF	dimethylformamide
APC	amino pyrrolidine carboxylic acid	DMSO	dimethylsulfoxide
aq.	aqueous	*dr*	diastereomeric ratio
Boc	*tert*-butyloxycarbonyl	dtp-bpy	4,4'-di-*tert*-butyl-2,2'-dipyridyl
bp	boiling point	E_T	triplet energy
bpy	bipyridine	$E_{1/2}$	standard reaction potential
bpz	2,2'-bipyrazine	EDC	1-ethyl-3-(3-dimethylaminopropyl)carbodiimide
brine	saturated NaCl solution	*ee*	enantiomeric excess
Bu	butyl	equiv.	equivalent(s)
°C	degrees Celcius	ESI	electrospray ionization
calc.	calculated	*et al.*	and others
CBz	carboxybenzyl	Et	ethyl
CFL	compact fluorescent light bulb	ET	energy transfer
cm^{-1}	wavenumbers	EtOAc	ethyl acetate
conv.	conversion	*fac*	facial
CV	cyclic voltammetry	Fmoc	fluorenylmethyloxycarbonyl
d	day(s)	GABA	γ-amino butyric acid
D	electron donor	h	hour(s)
dap	2,9-bis(para-anisyl)-1,10-phenanthroline	hν	light
DCC	*N,N'*-dicyclohexylcarbodiimide	HMDS	hexamethyldisilazane
DCM	dichloromethane	HP	high pressure
decomp.	decomposition	HPLC	high performance liquid chromatography
		HRMS	high resolution mass spectrometry
		IBX	2-iodoxybenzoic acid
		i-Pr	*iso*-propyl

IR	infrared
ISC	intersystem crossing
K	reaction constant
L*	chiral ligand
LED	light-emitting diode
li.	liquid
LMCT	ligand to metal charge transfer
M	molar
Me	methyl
MeCN	acetonitrile
MHz	megahertz
min	minute(s)
MLCT	metal to ligand charge transfer
mp.	melting point
MS	mass spectrometry
MV	methyl viologen
NAC	near attack conformation
NBS	*N*-bromosuccinimide
*n*BuLi	*n*-butylithium
nm	nanometer(s)
NMR	nuclear magnetic resonance
PC	photocatalyst
PET	photoinduced electron transfer
Pg	protecting group
Ph	phenyl
ppm	part(s) per million
ppy	2-phenylpyridine
R	arbitrary rest
R_f	retention factor
rac	racemic
RP	reversed phase
R_f	retention factor
rt	room temperature
SCE	saturated calomel electrode
Su	succinimide
T	temperature
TBAF	tetrabutylammonium fluoride
TBDMS	*tert*-butyldimethylsilyl
tert-Bu	*tert*-butyl
TS	transition state
TFA	trifluoroacetic acid
TFMSA	trifluoromethanesulfonic acid
THF	tetrahydrofuran
TLC	thin-layer chromatography
UV	ultraviolet
V	Volt
W	Watt
vs	versus
X	arbitrary moiety

Table of contents

A Introduction

1 [2+2] Cycloaddition

The cyclobutane motif is ubiquitous in a wide range of natural products. Molecules containing these small ring systems are versatile molecular building blocks in organic synthesis since their inherent ring strain enables a selective cleavage of a cyclobutane bond.[1] Thus they can serve as key intermediates to build up complex molecule structures by ring contraction, ring expansion or ring opening.[2] Furthermore, cyclobutane derivatives find great application in catalytical processes.[3] During the last decades, several research groups have been working on the development to get access to such molecules. Besides C-H activation[4], direct ring closure[5] and radical cyclization to form cyclobutanes, they are also accessible by cyclopropanes[6] or sugar derivatives[7]. However, the most frequently used method to synthesize cyclobutanes is the [2+2] cycloaddition.[8]

"A cycloaddition reaction is a ring forming addition of "m" number of atoms of one group to "n" number of atoms of another group; if both groups are part of the same molecule the cycloaddition is intramolecular and if both groups are part of different molecules the cycloaddition is intermolecular [...] Most cycloadditions are characterized by the formation of two new sigma bonds as the ring is being formed."[9]

The unambiguous advantage of this reaction type is the generation of multiple bonds and stereocenters in a single step what makes this reaction a powerful and meaningful method to build up natural products, biologically active molecules and other complex structures. This type of reaction can either take place thermally or photochemically. According to the Woodward-Hoffmann rules[10], a thermal [2+2] cycloaddition is symmetrically allowed *antara-supra-facial* what is unfavorable for substituted alkenes due to steric reasons. Some exceptions herein represent cycloadditions of molecules which possess two double bonds to the same carbon and therefore two π-bonds at right angles as for example ketenes[11], isocyanates[12] or allenes[13]. The thermal [2+2] cycloaddition of ketenes with alkenes forms cyclobutanones whereas the reactions of ketene with imines or chlorosulfonyl isocyanates with alkenes construct β-lactams. Furthermore, the thermal [2+2] cycloaddition of allenes allows the introduction of exomethylene moieties at the four-membered ring.[14]

More attention has been paid to the extensively studied photochemical [2+2] cycloaddition since it is symmetrically allowed in a *suprafacial-suprafacial* manner. In 1908, Cíamician and

coworkers described the earliest example of a [2+2] photocycloaddition: the transformation of carvone **1** to carvone camphor **2** by exposure to sunlight for one year (Scheme 1).[15]

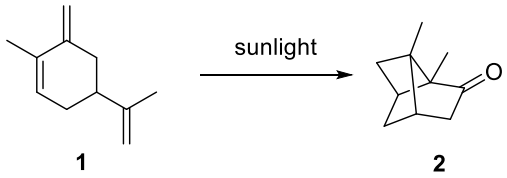

Scheme 1. Conversion of carvone to carvone camphor, reported by Cíamician *et al.*[15]

The first synthetic applications were developed by Corey[16] and Eaton[17] with the syntheses of caryophyllene **3**, a sesquiterpene, which is an ingredient of several essential oils, and cubane **4** as strained energy-rich molecule. Numerous natural and unnatural compounds have been prepared having a [2+2] photocycloaddition as crucial step in their syntheses.[18] Depending on the involved substrate different classes of this reaction can be described: [2+2] photocycloaddition of alkenes, enone-photocycloaddition, metal-catalyzed [2+2] photocycloaddition, de Mayo reaction or the Paternò-Büchi reaction. A selection of some representative examples is illustrated in figure 1.[19,20]

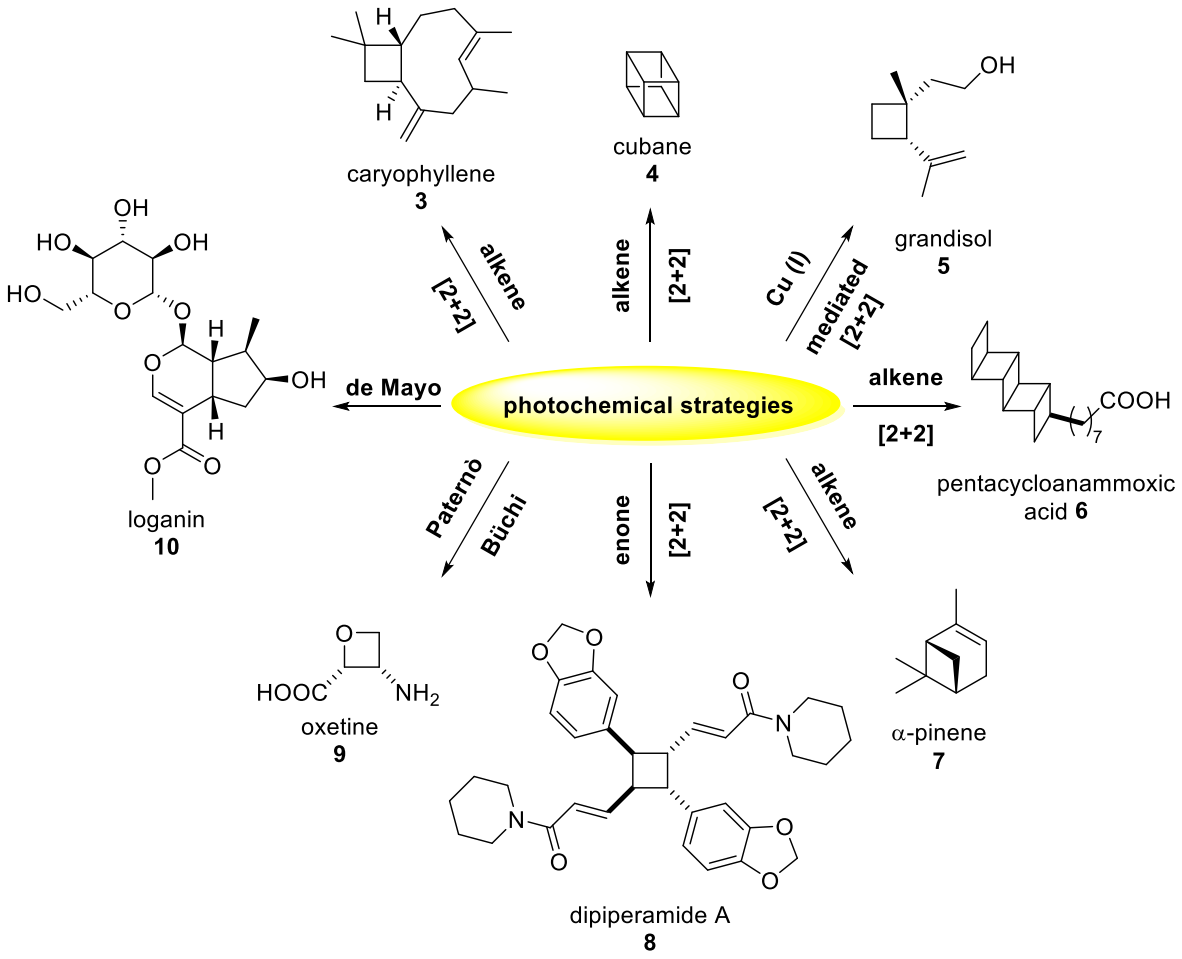

Figure 1. Representative examples of photochemical [2+2] photocycloaddition.

Depending on the used substrates, reagents and excitation mode the [2+2] photocycloaddition occurs *via* different mechanistic pathways.[21] On the one hand, direct excitation of a reacting partner can generate its excited singlet state S_1 and by a subsequent intersystem crossing (ISC) also its excited triplet state T_1 both of which can react with another alkene in its ground state giving rise to cyclobutane derivatives. On the other hand, the presence of an additive absorbing the light the [2+2] photocycloaddition can be performed either by an energy transfer or by a photoinduced electron transfer (PET) from this photoexcited species to the reactant. In the following chapter, the different reaction modes will be discussed in more detail and be exemplified by synthetic examples.

2 [2+2] Photocycloaddition *via* first excited singlet state S_1

The direct excitation of an alkene from its ground state S_0 **11** leads to its first excited state S_1 **12**. A subsequent addition to another ground state alkene **13** is called photocycloaddition, giving rise to the cyclobutane compound **15**. The reaction either occurs in a concerted manner or *via* a generation of an exciplex **14** (Scheme 2).[22]

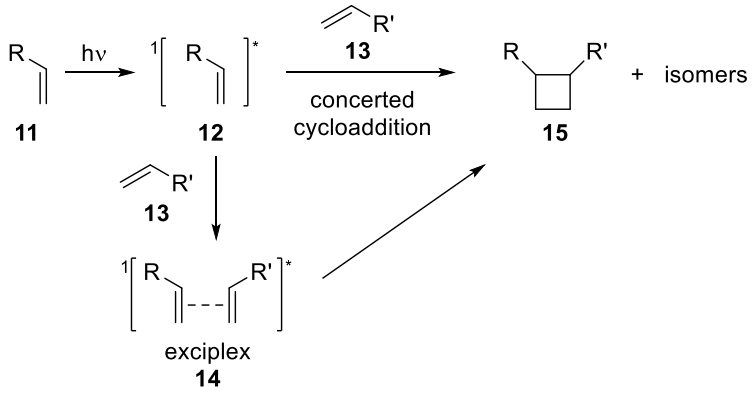

Scheme 2. Reaction mechanism of [2+2] photocycloaddition *via* S_1.[22]

Since the excited state S_1 is mostly dominated by $\pi\pi^*$ character, the *cis-trans* isomerization usually displays the competitive reaction, what serves as very fast radiationless energy decay.[22] This issue can be circumvented by using constrained molecules, as cycloalkenes with a ring size from three to five or performing the reaction in a rigid environment.[23] Therefore, there is only a limited number of singlet excited [2+2] photocycloadditions of acyclic alkenes in solution. For example, in the case of liquid *trans*-2-butene (**16**) and *cis*-2-butene (**17**) their inefficient dimerizations compete with efficient *cis-trans* isomerization. Irradiation of *trans*-2-butene (**16**) led stereospecifically to tetramethyl cyclobutanes **18** and **19** and *cis*-2-butene (**17**) reacted to dimers **19** and **20** at low conversion, respectively. At high reagent concentration, the

cycloaddition competes effectively with the *cis-trans* isomerization resulting in reduced product selectivity (Scheme 3).[9,24,25]

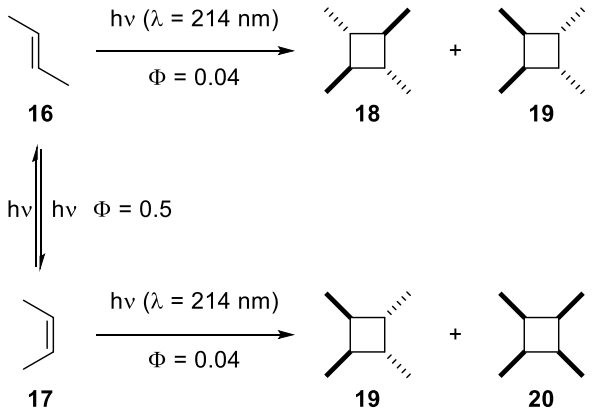

Scheme 3. Photocycloaddition of acyclic olefin.

Furthermore S_1 ($\pi\pi^*$) has a very short lifetime and the intersystem crossing (ISC) towards the more long-lived first triplet state T_1 ($\pi\pi^*$) is generally too slow to be efficient due to a very large singlet-triplet energy gap (typically > 40 kcal/mol).[9] Additionally, direct irradiation of simple alkenes is quite a challenge since they exhibit an absorption maximum λ_{max} less than or equal to 200 nm. Conventional light sources are mercury vapor lamps which are commercially available in three different types: low-, medium- and high-pressure. They differ in their spectral characteristic. The low-pressure mercury lamp emits light mainly at 253.7 nm, the weak band of 184.9 nm can be cut off by a suitable filter. Whereas the medium-pressure mercury lamp exhibits spectral lines at 265.4, 313 and 365 nm which are broadened in the case of the high-pressure mercury lamp leading roughly to a continuum.[26]

Aryl substituted alkenes absorb light at longer wavelengths and represent more suitable substrates for the [2+2] photocycloaddition *via* excited singlet state S_1. Exemplary, the state energy diagrams of *cis*-cyclooctene (**21**), 1,3-butadiene (**22**), *trans*-β-methylstyrene (**23**) and *trans*-stilbene (**24**) are illustrated in figure 2.[9]

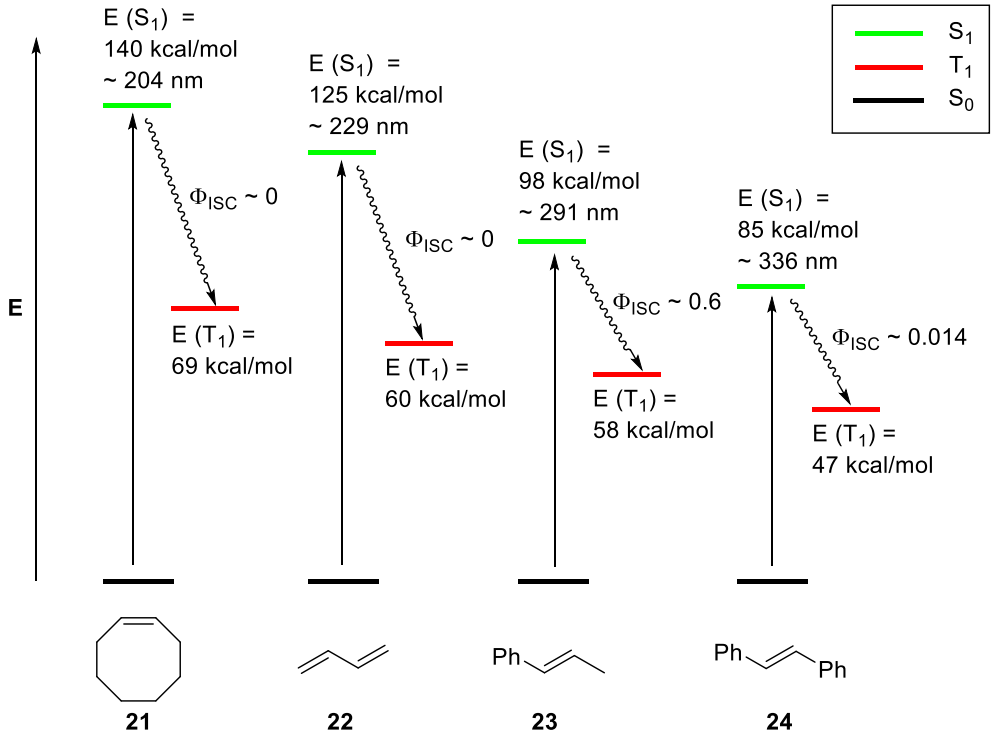

Figure 2. Representative state energy diagrams of alkenes.

Another advantage of aryl alkenes is that some of them possess a small energy barrier for the rotation around their C=C bond what makes the energy dissipation by *cis-trans* isomerization more difficult.[9,27,28]

In 2007, Abramić *et al.*[29] build up amidino-benzimidazole derivative **26** in a yield of 80% using an intermolecular [2+2] photocycloaddition of 1,2-diarylalkenes as key step in their synthesis. Herein the corresponding monomer **25** was directly irradiated in water by a 400 W high-pressure mercury lamp applying a Pyrex filter (Scheme 4). By introduction of the cyclobutane moiety as rigid conformation element, the inhibitory potential against dipeptidyl peptidase III which is involved in the mammalian pain modulatory system could be significantly improved.

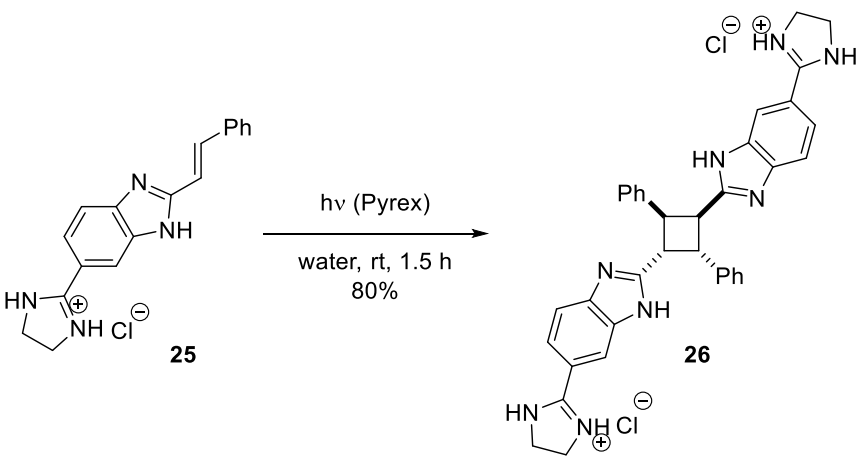

Scheme 4. Synthesis of amidino-benzimidazole **26** as an inhibitor of dipeptidyl peptidase III.

The group of Nishimura extensively applied an intramolecular variant of the [2+2] photocycloaddition occurring *via* the first excited singlet state S_1 to synthesize cyclophanes[30] as shown in compound **27** or crownethers[31] **28** (Figure 3).

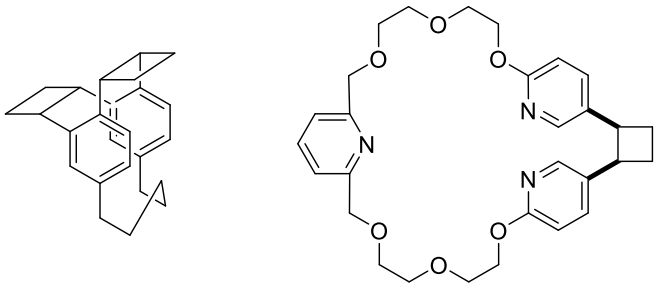

27 **28**

Figure 3. Exemplary structures of a cyclophane **27** and crownether **28**.

Fleming and coworkers performed their [2+2] photocycloaddition with silyl-tethered aryl alkenes that bears the advantage of pre-organization of the reactant alkenes.[32] Hence a better control of the regio- and stereochemistry of this reaction could be achieved. Since the likelihood of a collision of both affected double bonds could be increased by this manner, the competitive *cis-trans* isomerization could be minimized. The [2+2] photocycloaddition of the cinnamoyloxy silane **29** gave only one diastereomer **30** which was subsequently treated with ammonium fluoride to achieve the removal of the covalent bridge. Cyclobutane **31** could be obtained in an excellent yield of 94% (Scheme 5).[33]

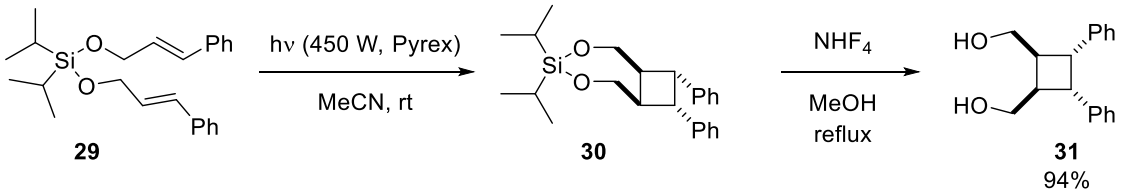

29 **30** **31**
94%

Scheme 5. Singlet [2+2] photocycloaddition of silyl-tethered derivatives, described by Fleming *et al*.[33]

3 Copper(I)-catalyzed [2+2] photocycloaddition[27,34]

In the presence of transition metal salts, a direct excitation of non-conjugated alkenes becomes feasible due to the bathochromic shift of their absorption maxima from around 200 nm to 240 nm. The most frequently used metal species were Cu(I) salts, especially the commercially available Cu(OTf) in benzene or toluene. At first, the reacting alkene moieties coordinate to a single copper(I) cation to form a ground state complex **32**. By photoexcitation of this bis-alkene-Cu(I) complex **32** the cyclobutane formation and regeneration of the Cu(I) catalyst are accomplished either *via* a metal-ligand or ligand-metal charge transfer (MLCT **33** or

LMCT **34**). The mechanism as concerted [2+2] photocycloaddition was also proposed (Scheme 6).

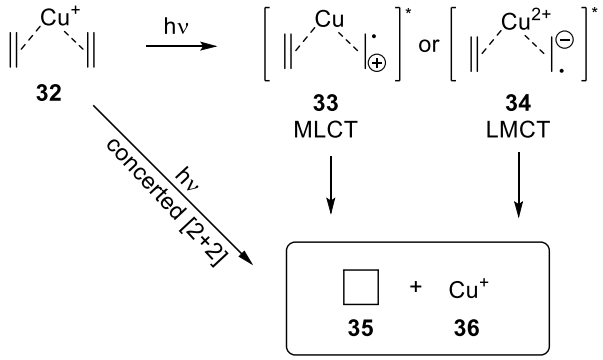

Scheme 6. Mechanism of Cu(I)-catalyzed [2+2] photocycloaddition.[22]

This methodology was especially applied for [2+2] photodimerization of the *endo*-dicyclopentadiene **37** giving rise to 88% of the dimer **38**. Interestingly, in the presence of a triplet sensitizer as acetone compound **37** reacted *via* an intramolecular [2+2] photocycloaddition to the cage hydrocarbon compound **39**. Probably due to steric reasons, the complexation of the double bonds of two substrate molecules **37** is preferred over the one of both alkene moieties of one substrate molecule **37** (Scheme 7).[35]

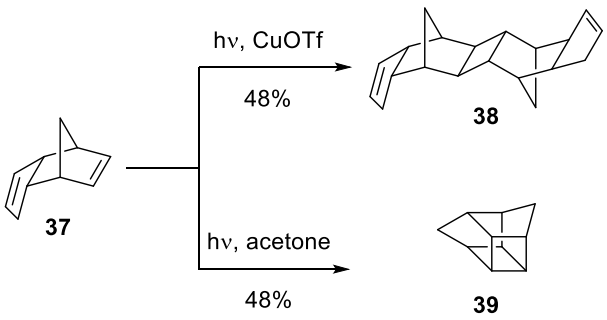

Scheme 7. Intermolecular and intramolecular [2+2] photocycloaddition of *endo*-dicyclopentadiene.

The generality as well as the scope of the intramolecular variant of this reaction type has been extensively studied by the groups of Salomon[36] and Ghosh[37]. Suitable substrate classes represent 1,6-heptadienes, diallyl ethers, homoallyl vinyl ethers and *N*,*N*-diallyl carbamates. In this manner, a huge variety of natural products and biologically active compound could be generated. Cyclobut-A **42**, a nucleoside analogue of the naturally occurring antibiotic oxetanocin, which exhibit remarkable antiviral activity, was synthesized by Ghosh *et al.*[38] using a stereoselective intramolecular Cu(I)-catalyzed [2+2] photocycloaddition as essential reaction step (Scheme 8). In the presence of Cu(OTf) the solution of triene **40** in diethyl ether was irradiated by a medium-pressure mercury lamp (450 W) through a double-walled water-cooled quartz immersion well (λ_{irr} > 250 nm) yielding 70% of an inseparable mixture of four

diastereomers **41**. The reason for obtaining diastereomers **41** is the exocyclic double bond. However, the mixture could be taken for the further synthesis towards cyclobut-A **42**, since this double bond was oxidatively cleaved off and the stereocenter at the cyclobutane ring was epimerized during the reaction sequence.

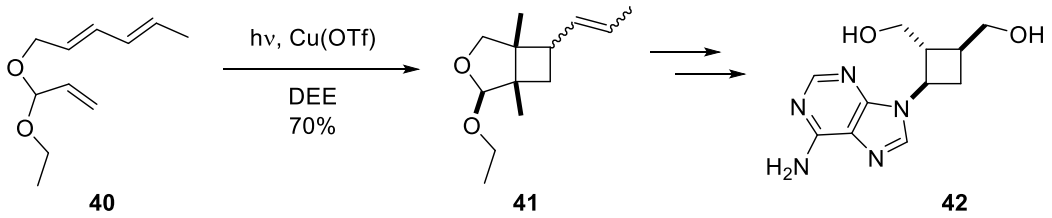

Scheme 8. The key step of the synthesis towards cyclobut-A **42**, reported by Ghosh *et al.*[38]

4 [2+2] Photocycloaddition *via* first excited triplet state T_1[22,27,39,40]

Alkenes whose double bond is in conjugation with a carbonyl group can react in the [2+2] photocycloaddition *via* their first excited triplet state T_1. Typical excitation wavelengths of α,β-unsaturated carbonyl, carboxyl and related heterocyclic compounds are over 250 nm.[41] Therefore, they are accessible by commercially available light sources and also suitable cut off filter can be used in order to avoid side reactions by irradiation with short wavelengths light. Since their excited singlet state S_1 is of nπ* character, the intersystem crossing takes place very fast and the cyclobutanation occurs from the lowest lying triplet state T_1 possessing mainly ππ* character.[42] Especially, cyclic 5- or 6-membered alkenones are widely employed substrate classes for this reaction type. Herein no energy dissipation by isomerization over the C=C double bond can take place.[43] By direct excitation of cyclopentenone **43** the first excited singlet state S_1 can be reached. By rapid intersystem crossing the long-lived triplet state **45** can be generated followed by the formation of an exciplex **47** with a ground state alkene **46**.[44] This complex **47** can either decay to the triplet 1,4-biradicals **48** and **49** or competitively to the ground state reactants **43** and **46**.[45] Weedon and coworkers confirmed the formation of the 1,4-biradical intermediates during the [2+2] photocycloaddition by trapping them with hydrogen selenide.[46] By a further intersystem crossing the singlet 1,4-biradicals **50** and **51** were obtained which either cyclize to the desired cyclobutane derivative **52** or revert to the starting material.[39,47]

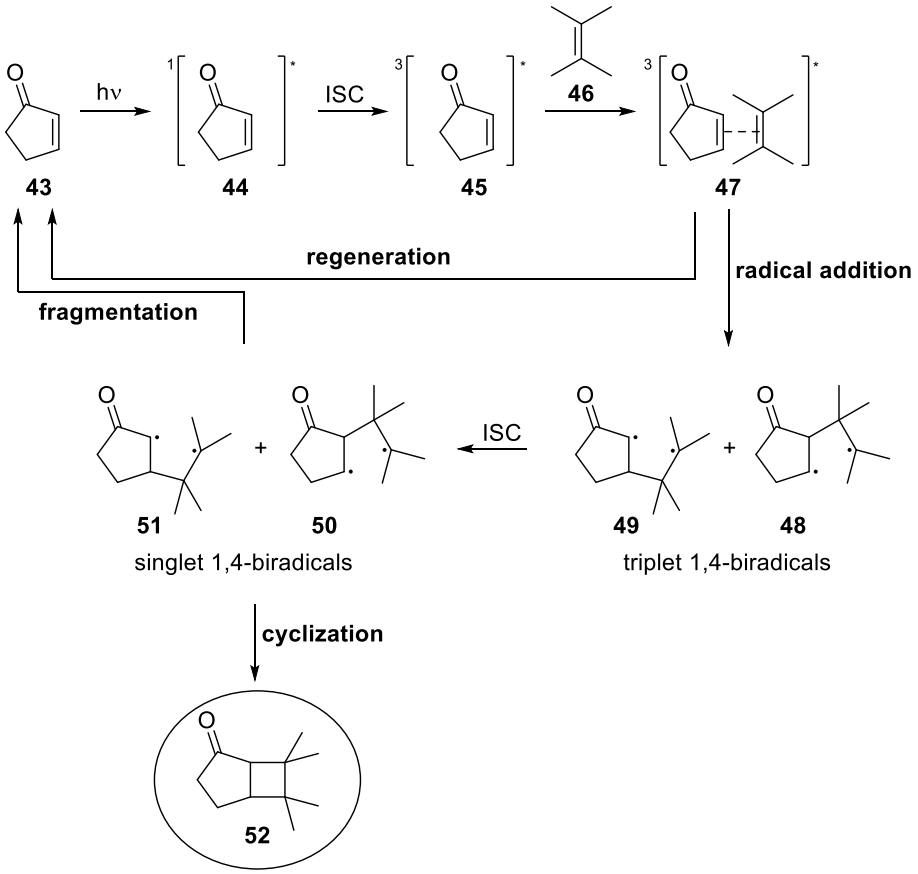

Scheme 9. Reaction mechanism of [2+2] photocycloaddition of cyclopentenone **43**.

Advantageously, the T_1 state represents a more long-lived species so that a cycloaddition of an excited enone with a ground state alkene, which is normally used in excess, becomes more likely. However, in contrast to the singlet [2+2] photocycloaddition where the stereochemistry of the starting material is preserved the stereocontrol during the triplet reaction is lost due to the formation of 1,4-biradical intermediates. On the one hand, the regioselectivity is controlled by the stability of the 1,4-biradical and on the other hand, it is influenced by the ratio between the cleavage of the singlet 1,4-biradicals to the ground state starting material and the cyclization to the product.[48]

In intermolecular [2+2] photocycloadditions of enones with alkenes, the regioselectivity depends to a certain extent on the substitution pattern of the alkene. The excited state of an enone displays an inverted polarity in contrast to its ground state (Umpolung).[49] Therefore, electron-rich alkenes prefer a head-to-tail conformation whereas electron poor ones a head-to-head conformation. In the reaction of lactam **53** with acrylonitrile **54** compound **56a** with the 1,2-relationship to the carbonyl represents the major product and with ethyl vinyl ether **55** isomer **57b** with the 1,3-relationship, respectively.[50]

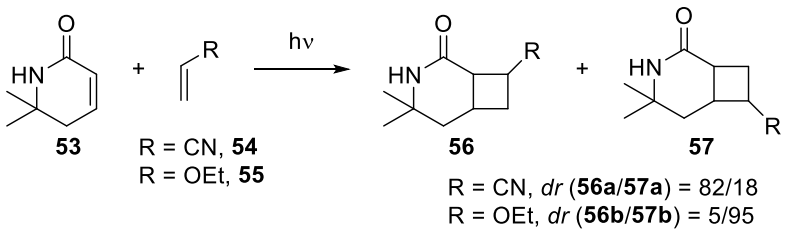

Scheme 10. [2+2] photocycloaddition of lactam **53** with an acceptor olefin **54** *vs* with a donor olefin **55**.

Applying cyclopentenone as substrate leads always to a *cis*-fusion at the cyclobutane ring whereas also a *trans*-fusion can be obtained in the case of cyclohexanone because of the twisted conformation of its excited state.[16,44]

Good diastereoselectivity can be easily achieved by the introduction of chirality to the enone derivative as for example a substituent in γ-position to the carbonyl moiety or by using a bicyclic enone since the alkene will preferably attack from the less shielded side. Piers *et al.*[51] profit from this behavior in their synthesis of (±)-kelsoene **61** obtaining only one diastereomer **60** in the [2+2] photocycloaddition (Scheme 11).

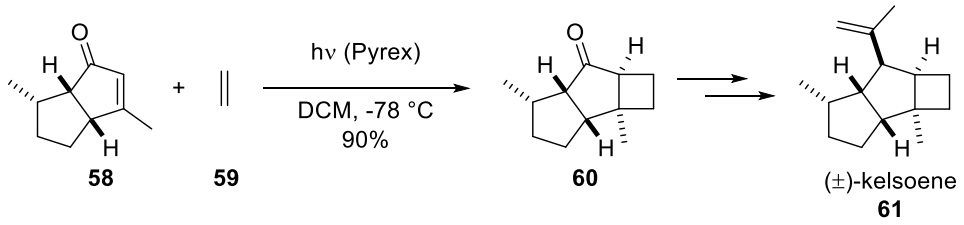

Scheme 11. Intermolecular [2+2] approach towards (±)-kelsoene **61** by Piers and coworkers.[51]

Moreover, diastereoselectivity in the intermolecular [2+2] photocycloaddition of enones can be induced using already chiral alkene reacting partner.[52]

The intramolecular variant is usually highly regio- and stereoselective, especially due to the "rule of five", which implies that 1,4-biradicals in which a cyclopentane ring has been formed are preferentially generated.[49,53]

A synthetically useful variant displays the de Mayo reaction. In the 1960s, de Mayo and coworkers described the photocycloaddition of β-diketones with alkenes giving rise to 1,5-diketones (Scheme 12). The tautomerization of the 1,3-diketone **62** yields the corresponding keto enol **63** which undergoes the [2+2] photocycloaddition. The resulting β-acyclcyclobutanol **64** reacts in a retro-aldolisation to the 1,5 diketone **65**.[54]

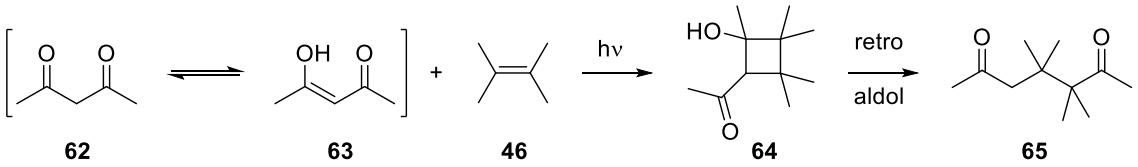

Scheme 12. De Mayo reaction.

A huge variety of natural products could be build up having de Mayo reaction as key step in the synthetical sequence as for example hirsutene[55], loganin[20], reserpine[56] or longifolene[57]. In analogy, nitrogen-containing ring systems can be generated by subjecting vinylogous amides to the [2+2] photocycloaddition followed by a retro-Mannich fragmentation.[58] For instance koumine[59], manzamine-A[60] or hetisine[61] could be synthesized.

Another important example is the [2+2] photocycloaddition of an excited carbonyl and an alkene, the so-called Paternò-Büchi reaction which is a powerful method to form oxetanes (Scheme 13). By light absorption, the carbonyl moiety is excited to its first singlet excited state S_1 **67** with nπ* character that readily undergoes intersystem crossing to the corresponding T_1 **68**. The cyclobutane formation can be furnished from both the singlet and the triplet state in which the majority of the Paternò-Büchi reactions occur.[62]

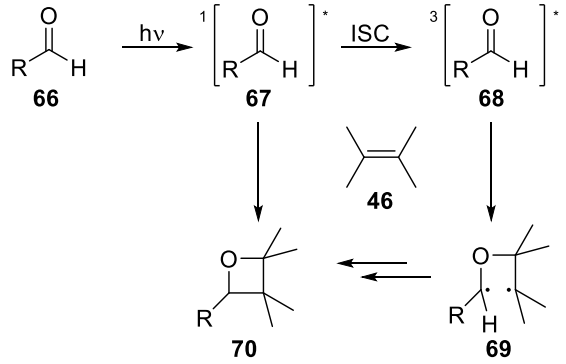

Scheme 13. Paternò-Büchi reaction, in general.[63]

One limitation of this reaction arises if the applied carbonyl derivative has a higher triplet energy than the alkene. Then the energy transfer would present the major reaction pathway and the oxetane formation will occur slowly or not at all. The irradiation of norbornene (E_T = 314 kJ/mol) in the presence of benzophenone (E_T = 288 kJ/mol) led to oxetane formation between both substrates, whereas in the presence of acetophenone (E_T = 310 kcal/mol) whose triplet energy is close to the one of norbornene the sensitized photodimerization of the alkene was obtained.[64]

5 [2+2] Photocycloaddition *via* energy transfer

As already mentioned, numerous compounds proceed an inefficient intersystem crossing (ISC) due to the big energy gap between their singlet and triplet excited state. Therefore, another possibility to generate the first triplet state T_1 of an olefin displays the energy transfer from another photoexcited molecule (Figure 4).[9]

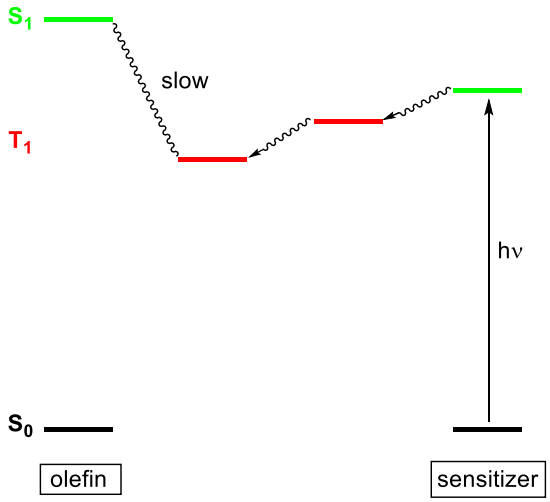

Figure 4. Energy diagram of sensitization process.

A molecule possessing following characteristics represents a good triplet photosensitizer:

- fast ISC-rate relative to another deactivation mode of S_1 (low-lying S_1 and high-lying T_1)
- high triplet energy E_T (T_1 (sensitizer) higher than T_1 (acceptor olefin))
  → energy transfer has to be exothermic
- long triplet lifetime τ_T
- different absorption spectrum relative to the one of the acceptor olefin
- low chemical reactivity

In general, a sensitization process can be achieved by performing the reaction in acetone (E_T = 326 kJ/mol) or in a transparent solvent in the presence of an aromatic ketone as benzophenone (E_T = 288 kJ/mol) or acetophenone (E_T = 310 kJ/mol).
For instance, Aitken and coworkers used this reaction type to build up several unnatural amino acids containing a cyclobutane core. In their synthetic sequence towards (±)-*cis*-2-amino-1-cyclobutanecarboxylic acid **74** the crucial step is an acetone-sensitized [2+2] photocycloaddition of uracil **71** and ethylene **59**.[65,66] The controlled degradation of the

heterocyclic ring in compound **72** led to the corresponding *N*-carbamoyl-β-amino acid **73** which was further hydrolyzed to the desired *cis*-cyclobutane amino acid **74** in an overall yield of 52% over three steps (Scheme 14).

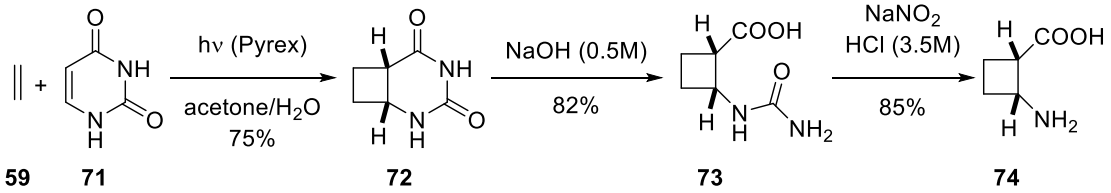

Scheme 14. Synthesis of (±)-*cis*-2-amino-1-cyclobutanecarboxylic acid **73** according to Aitken *et al.*[65]

Moreover, Aitken *et al.*[67] applied acetophenone as triplet sensitizer in the synthesis of four stereoisomers of cyclobutane analogues of glutamic acid. Herein the [2+2] photocycloaddition took place between maleic anhydride and again ethylene. By further transformations and through enzymatic transamination all four isomers of *L*-2-(2-carboxycyclobutyl)-glycine (**77**-**80**) could be obtained (Scheme 15).

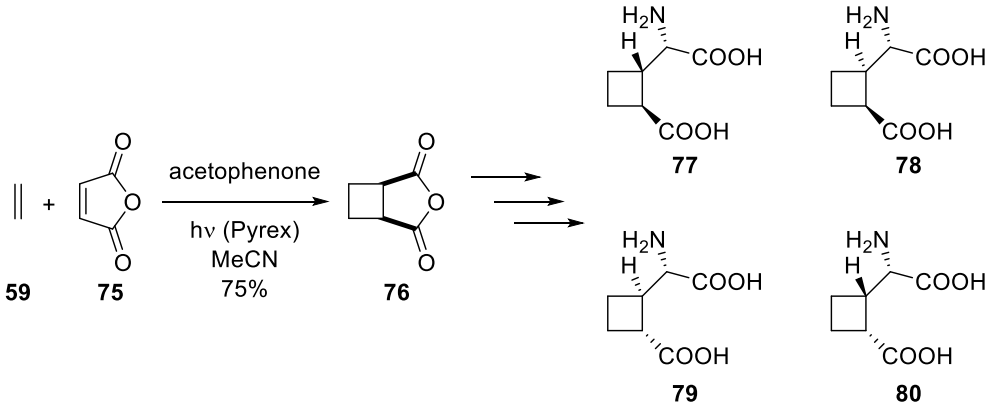

Scheme 15. The key step of the synthesis of all four isomers of *L*-2-(2-carboxycyclobutyl)-glycine (**77**-**80**).

Besides the well-studied UV-mediated triplet sensitization, the field of energy transfer by irradiation with visible light remains to be further developed. Organic dyes as flavin[68] or Eosin Y[69] are known to promote [2+2] photocycloaddition having their absorption maxima in the range of visible light. Furthermore, Yoon and coworkers described the sensitized [2+2] cycloaddition of tethered bisstyrenes whose oxidation potential has precluded the participation in a photoredox catalytic pathway, using the visible light active organometallic compound, $Ir[(dtb\text{-}bpy)(dF(CF_3)ppy)_2]PF_6$.[70]

By an energy transfer of the excited $Ru(bpy)_3Cl_2$ to 2-ylideneoxindoles Xiao *et al.*[71] succeed in their [2+2] homodimerization.

Especially, the enantioselective approach towards a sensitized [2+2] cycloaddition is still challenging.[72] For example, the group of Thorsten Bach could introduce chirality in the intramolecular [2+2] photocycloaddition of quinolone-derived substrates[73] or in the intermolecular reaction of 2-pyridones with acetylene dicarboxylates[74] by applying a chiral photosensitizer. This catalyst possesses a chromophoric unit to absorb the light and to be capable of energy transfer, as well as a lactam moiety to interact with the substrate and to pre-organize it. The incorporation of a thioxanthone unit to the catalyst **82** allowed excitation in the visible light range (Scheme 16).[75]

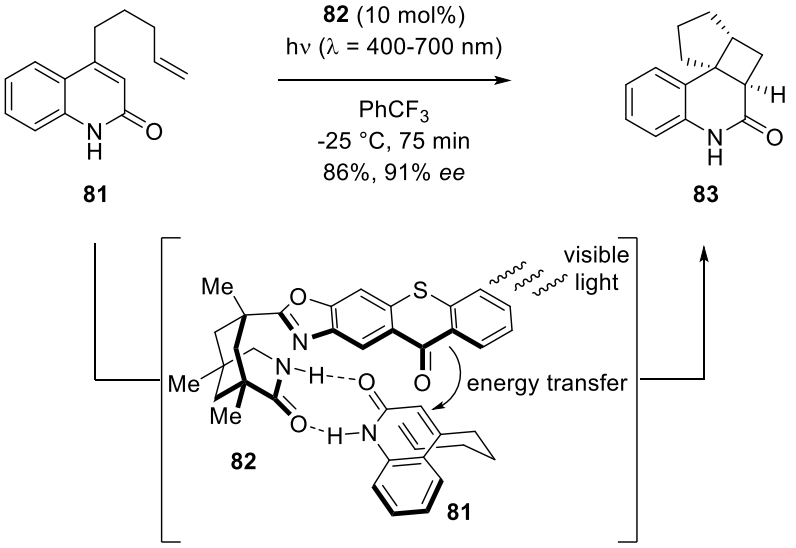

Scheme 16. Exemplary intramolecular [2+2] photocycloaddition reported by Bach *et al.*[75]

In 2017, Yoon and coworkers took a different approach to develop an enantioselective method for a sensitized [2+2] photocycloaddition *via* visible light.[76] By coordination of 2'-hydroxychalcones with a chiral Lewis acid, the singlet-triplet energy gap of these substrates can be diminished what enables $Ru(bpy)_3Cl_2$ to serve as triplet sensitizer in this reaction. The chirality of the applied Lewis acid provides the opportunity for a highly enantioselective synthesis of 1,2-diarylcyclobutane derivatives which are key structures in a variety of natural products as for example in norlignan **88**[77] (Scheme 17).

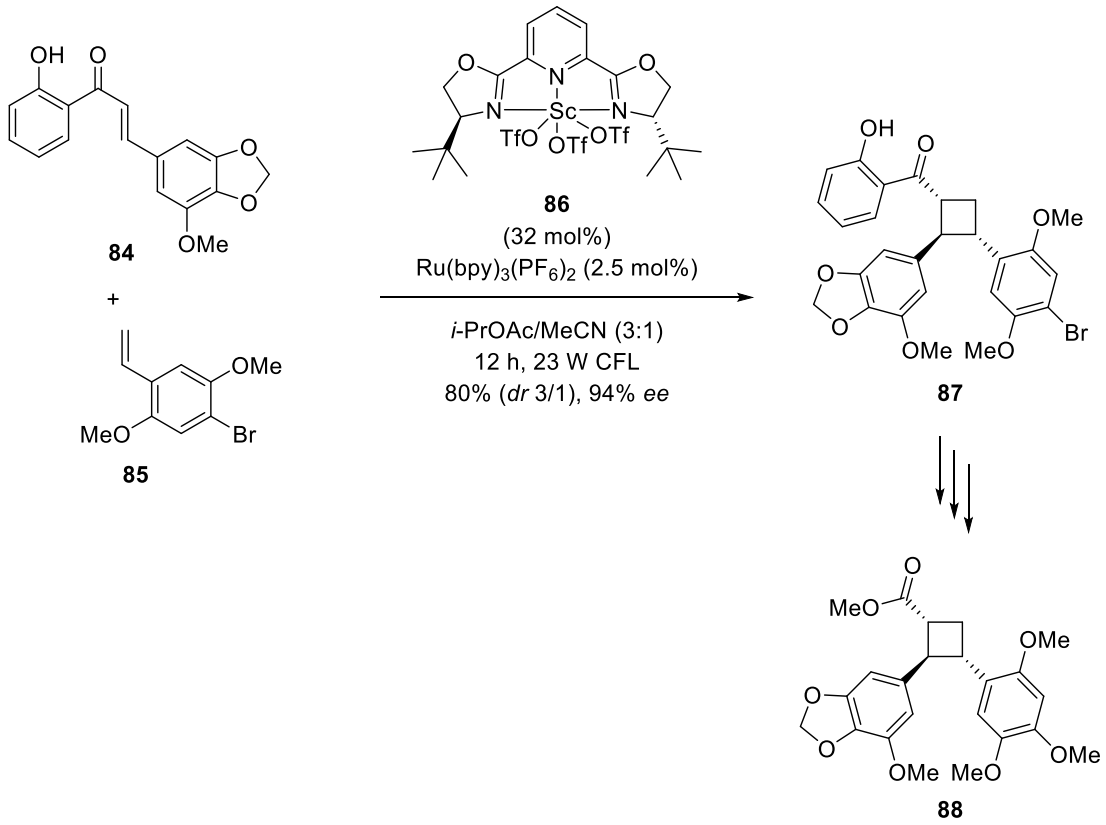

Scheme 17. The key step in the synthesis of norlignane **88** by Yoon *et al.*[76]

6 [2+2] Photocycloaddition *via* photoinduced electron transfer

In the presence of a photocatalyst such as ketones, pyrylium salts, organic dyes or metal-polypyridyl complexes the [2+2] cycloaddition can also be achieved *via* an electron transfer. Either the olefin is reduced generating a radical anion intermediate (reductive PET) or the alkene delivers an electron to the catalyst having a radical cation intermediate (oxidative PET).[9,25,78]

For instance, by an oxidative PET an ethene radical cation **89** is generated which reacts with another olefin **11** to a 1,4-radical cation dimeric species **90**. The back-electron transfer can lead to the cyclobutane formation as well as the oxidation of a further alkene **11** during the radical chain propagation (Scheme 18).[79]

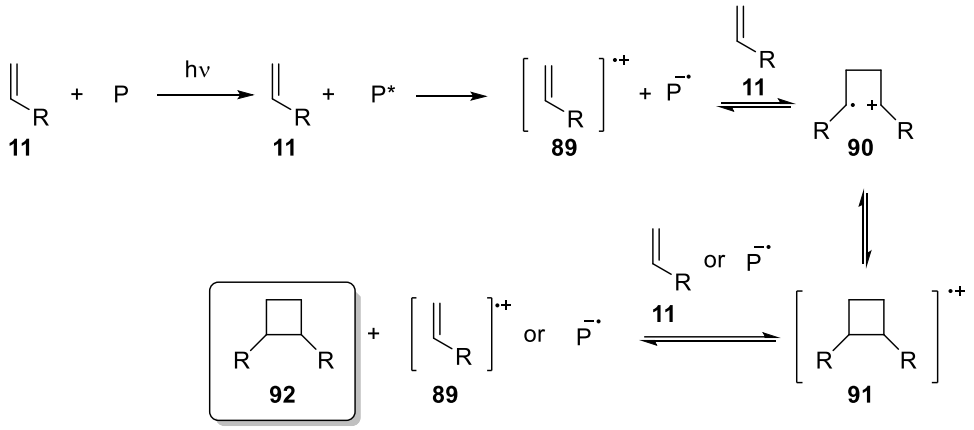

Scheme 18. Reaction mechanism of an oxidative PET.

The formation of a triplet state alkene or of a triplex as intermediates which participate rather in the cycloaddition than the free radical species are described in the literature as well.[79,80] Especially, electron-rich alkenes display a suitable substrate class for this reaction type. In analogy to T_1 sensitized [2+2] cycloaddition the regiochemistry is dominated by the formation of the most stabilized dimeric 1,4-radical cation leading mainly to head-to-head conformations. Moreover, heterodimer 1,4-radical cation formation can take place though the oxidation potentials of both substrates have to be close to each other.[81]

In recent years the photoredox catalysis *via* visible light has become very popular in this research field.[18,82] Exposuring the photoreaction to light in the range of 400-700 nm bears the advantage of an increased functional group tolerance, no need of specialized equipment, no high input of energy and the usage of environmentally friendly LEDs or fluorescent light bulbs as light sources.

In 2013, Nicewicz *et al.*[83] demonstrated the visible light induced [2+2] photocycloaddition of aryl alkenes towards cyclobutane lignans by applying triaryloxopyrylium salt **94** as photooxidation catalyst in conjunction with anthracene and naphthalene as electron relay compound (Scheme 19).

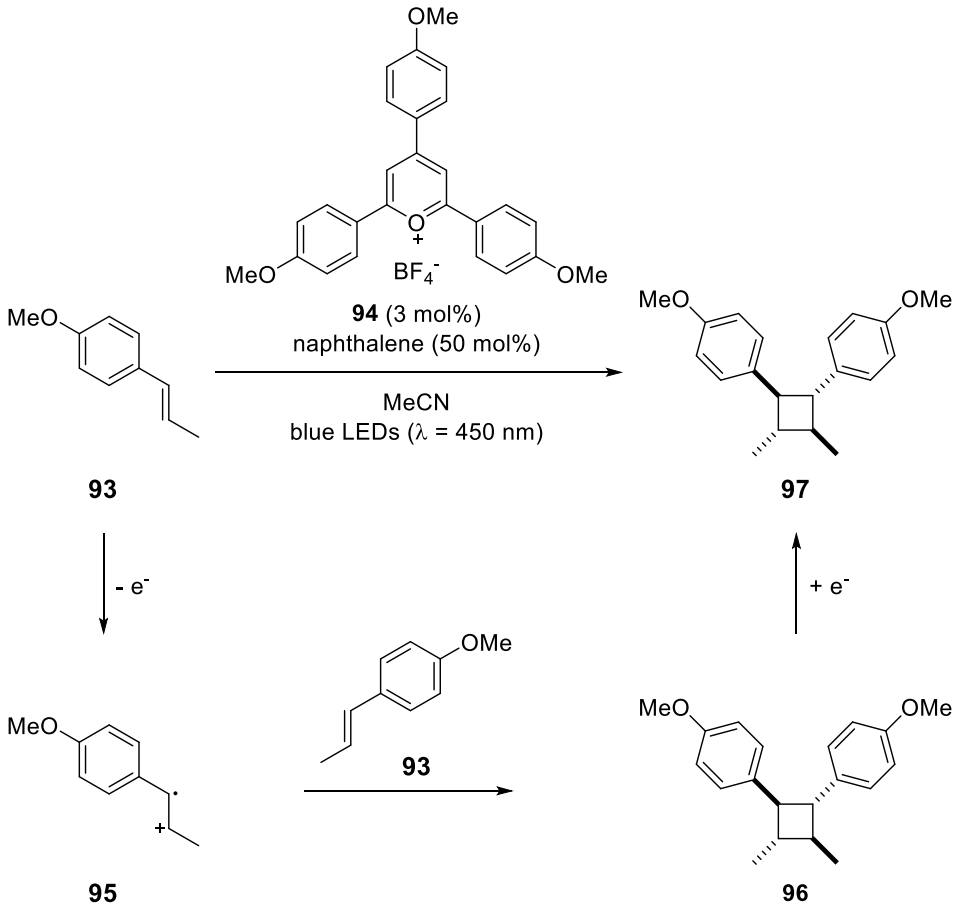

Scheme 19. Visible light induced [2+2] cycloaddition of styrenes by Nicewicz *et al.*[83]

Above all the work of Yoon and coworkers has significantly contributed to the development of visible light induced [2+2] cycloadditions of a broad range of substrates.[82] They demonstrate that Lewis acid activated enone substrates are capable of participating in [2+2] cycloaddition *via* visible light photocatalysis in an intra-[84] as well as intermolecular[85] manner. In contrast to the previously described reactions, key intermediate herein represents a photogenerated radical anion. In 2014, this work group also succeeded in establishing an enantioselective version of [2+2] photocycloaddition of α,β-unsaturated ketones by applying a dual catalyst system consisting of a visible light absorbing photocatalyst and a stereocontrolling Lewis acid cocatalyst (Scheme 20).[86]

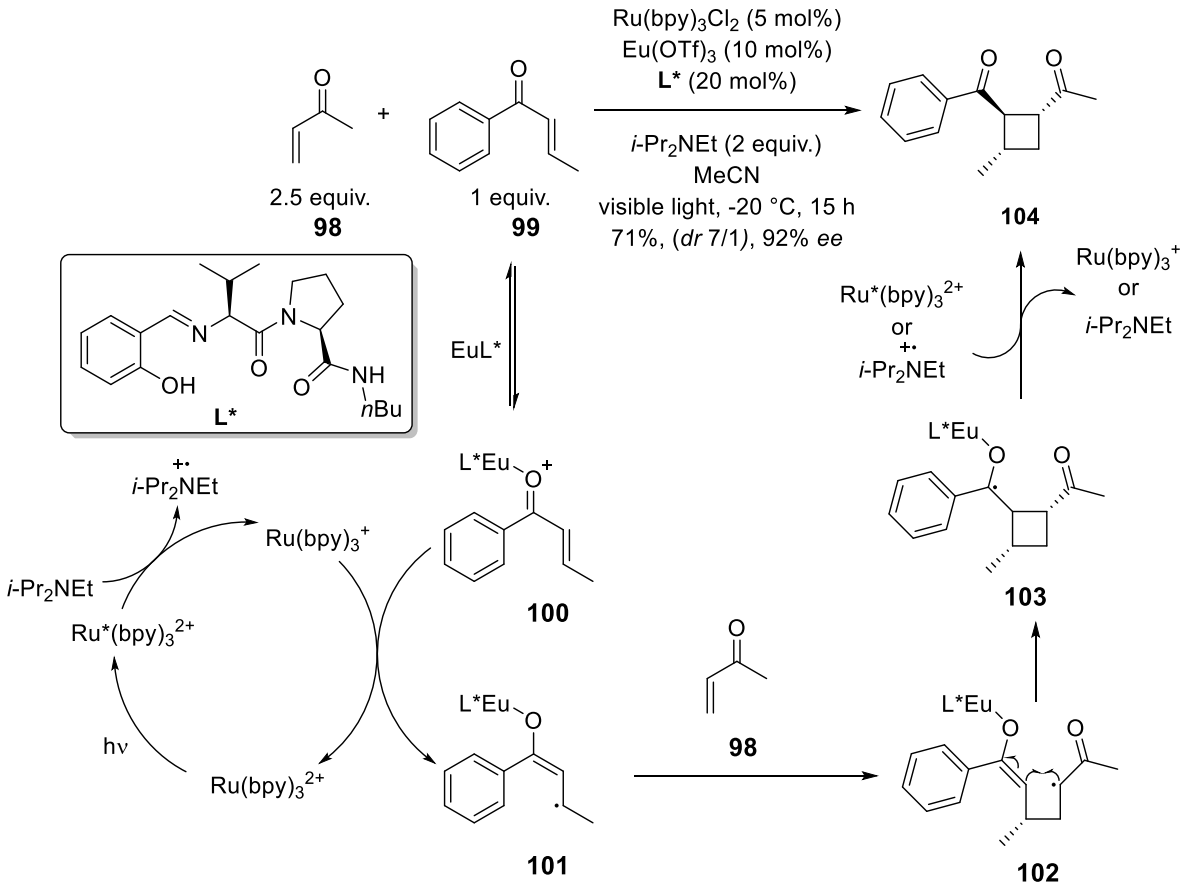

Scheme 20. Enantioselective [2+2] photocycloaddition by Yoon *et al.*[86]

The absorption of visible light induces a metal to ligand charge transfer between the Ru-species and the pyridyl ligands generating the photoexcited state $Ru^*(bpy)_3^{2+}$. The reductive quenching with DIPEA as sacrificial electron donor led to the reduced $Ru(bpy)_3^{+}$ species which transfers one electron to the Lewis acid activated enone **100** by regenerating the starting catalyst, $Ru(bpy)_3^{2+}$. A 1,4-addition of radical **101** to another α,β-unsaturated carbonyl compound **98** and a subsequent radical cyclization provides the cyclobutane radical **103** which can be oxidized either by excited $Ru^*(bpy)_3^{2+}$ or by the amine radical cation to give cyclobutane derivative **104** with an enantiomeric excess of 92% of the major diastereomer. The high enantioselectivity could be achieved by using a complex of the lanthanide salt $Eu(OTf)_3$ and the chiral Schiff base ligand **L*** as Lewis acid.

In summary, the [2+2] photocycloaddition is a powerful method to build up highly functionalized cyclobutane derivatives. Due to the different reaction pathways on which this cycloaddition can proceed, a wide range of substrates can be covered. Recently, the development of asymmetric [2+2] photocycloaddition has attracted much attention and will remain an interesting as well as challenging research topic in the future.

7 References

[1] J. C. Namyslo, D. E. Kaufmann, *Chem. Rev.* **2003**, *103*, 1485–1537.

[2] E. Lee-Ruff, G. Mladenova, *Chem. Rev.* **2003**, *103*, 1449–1483.

[3] T. Seiser, T. Saget, D. N. Tran, N. Cramer, *Angew. Chem., Int. Ed.* **2011**, *50*, 7740–7752.

[4] a) C. D. Bray, G. Pattenden, *Tetrahedron Lett.* **2006**, *47*, 3937–3939; b) M. Chaumontet, R. Piccardi, N. Audic, J. Hitce, J.-L. Peglion, E. Clot, O. Baudoin, *J. Am. Chem. Soc.* **2008**, *130*, 15157–15166.

[5] a) H. Ito, T. Toyoda, M. Sawamura, *J. Am. Chem. Soc.* **2010**, *132*, 5990–5992; b) Y. T. Han, N.-J. Kim, J.-W. Jung, H. Yun, S. Lee, Y.-G. Suh, *Arch. Pharm. Res.* **2011**, *34 (9)*, 1437–1442.

[6] a) J. Barluenga, L. Riesgo, L. A. López, E. Rubio, M. Tomás, *Angew. Chem., Int. Ed.* **2009**, *48*, 7569–7572; b) C. Guérot, B. H. Tchitchanov, H. Knust, E. M. Carreira, *Org. Lett.* **2011**, *13*, 780–783; c) S. Ye, Z.-X. Yu, *Chem. Commun.* **2011**, *47*, 794–796; d) A. F. Stepan, C. Subramanyam, I. V. Efremov, J. K. Dutra, T. J. O'Sullivan, K. J. DiRico, W. S. McDonald, A. Won, P. H. Dorff, C. E. Nolan *et al*., *J. Med. Chem.* **2012**, *55*, 3414–3424.

[7] S. Dong, G. D. Parker, T. Tei, L. A. Paquette, *Org. Lett.* **2006**, *8*, 2429–2431.

[8] a) S. L. Schreiber, *Science* **1985**, *227*, 857–863; b) J. Iriondo-Alberdi, M. F. Greaney, *Eur. J. Org. Chem.* **2007**, 4801–4815; c) N. Hoffmann, *Chem. Rev.* **2008**, *108*, 1052–1103; d) T. Bach, J. P. Hehn, *Angew. Chem., Int. Ed.* **2011**, *50*, 1000–1045.

[9] N. J. Turro, V. Ramamurthy, J. C. Scaiano, *Modern Molecular Photochemistry of Organic Molecules, Chapter 10*, University Science Books, Sausalito, **2010**.

[10] a) R. B. Woodward, R. Hoffmann, *J. Am. Chem. Soc.* **1965**, *87 (2)*, 395–397; b) R. B. Woodward, R. Hoffmann, *Angew. Chem., Int. Ed.* **1969**, *8 (11)*, 781–932.

[11] P. Rullière, J. Grisel, C. Poittevin, P. Cividino, S. Carret, J.-F. Poisson, *Org. Lett.* **2016**, *18*, 2824–2827.

[12] S. Perreault, T. Rovis, *Chem. Soc. Rev.* **2009**, *38*, 3149–3159.

[13] B. Alcaide, P. Almendros, C. Aragoncillo, *Chem. Soc. Rev.* **2010**, *39*, 783–816.

[14] J. Clayden, N. Greeves, S. Warren, *Organic Chemistry, Second Edition, Oxford University Press* **2012**, 877–908.

[15] G. Cíamician, P. Silber, *Chem. Ber.* **1908**, *41*, 1928–1935.

[16] E. J. Corey, Rajat B. Mitra., Uda Hisashi, *J. Am. Chem. Soc.* **1964**, *86*, 485–492.

[17] P. E. Eaton, T. W. Cole, *J. Am. Chem. Soc.* **1964**, *86*, 3157-3158.

[18] Markus D. Kärkäs, John A. Porco, Corey R. J. Stephenson, *Chem. Rev.* **2016**, *116*, 9683–9747.

[19] a) R. Zurflüh, L. L. Dunham, V. L. Spain, J. B. Siddall, *J. Am. Chem. Soc.* **1970**, *92 (2)*, 425–427; b) R. L. Cargill, B. W. Wright, *J. Org. Chem.* **1975**, *40 (1)*, 120-122; c) A. Meibom, N. H. Sleep, C. P. Chamberlain, R. G. Coleman, R. Frei, M. T. Hren, J. L. Wooden, *Nature*

2002, *419*, 705–708; d) S. D. Larsen, S. A. Monti, *J. Am. Chem. Soc.* **1977**, *99 (24)*, 8015–8020; e) M. Takahashi, M. Ichikawa, S. Aoyagi, C. Kibayashi, *Tetrahedron Lett.* **2005**, *46*, 57–59; f) T. Bach, J. Schröder, *Liebigs Ann.* **1997**, *11*, 2265–2267.

[20] G. Büchi, J. A. Carlson, J. E. Powell Jr., L.-F. Tietze, *J. Am. Chem. Soc.* **1970**, *92 (7)*, 2165–2167.

[21] J. Kopecky, *Organic Photochemistry: A visual Approach, Chapter 5*, VCH, New York, **1992**.

[22] P. Klán, J. Wirz, *Photochemistry of Organic Compounds: From Concepts to Practice, Chapter 6*, Wiley, Chichester, U.K, **2009**.

[23] V. Ramamurthy, J. Sivaguru, *Chem. Rev.* **2016**, *116*, 9914–9993.

[24] a) N. Sakurai, M. Murakami, M. Kumada, *J. Am. Chem. Soc.* **1969**, 520–522; b) H. Yamazaki, R. J. Cvetanovic, *J. Am. Chem. Soc.* **1969**, *91 (2)*, 520–522; c) H. Yamazaki, R. J. Cvetanovic, R. S. Irwin, *J. Am. Chem. Soc.* **1976**, *98 (8)*, 2198–2205.

[25] A. Gilbert, J. Baggot, *Essentials of Molecular Photochemistry, Chapter 6*, Blackwell Scientific Publications, Oxford, **1991**.

[26] W. Horspool, F. Lenci, *CRC Handbook of Organic Photochemistry and Photobiology, Chapter 22*, CRC Press LCC, **2004**.

[27] G. Kaupp, W. M. Horspool, P.-S. Song, *CRC Handbook of Organic Photochemistry and Photobiology, First Edition, Chapter 6*, CRC Press Inc., **1995**.

[28] F. D. Lewis, D. H. Volman, G. S. Hammond, Gollnick K., *Advances in Photochemistry (Vol 13)*, John Wiley & Sons, Inc, New York, **1986**.

[29] D. Agić, M. Hranjec, N. Jajcanin, K. Starcević, G. Karminski-Zamola, M. Abramić, *Bioorg. Chem.* **2007**, *35*, 153–169.

[30] a) J. Nishimura, H. Doi, E. Ueda, A. Ohbayashi, A. Oku, *J. Am. Chem. Soc.* **1987**, *109*, 5293–5295; b) J. Nishimura, A. Ohbayashi, E. Ueda, A. Oku, *Chem. Ber.* **1988**, *121*, 2025–2028.

[31] S. Inokuma, T. Yatsuzuka, S. Ohtsuki, S. Hino, J. Nishimura, *Tetrahedron* **2007**, *63*, 5088–5094.

[32] a) C. L. Bradford, S. A. Fleming, S. C. Ward, *Tetrahedron Lett.* **1995**, *36 (24)*, 4189–4192; b) S. A. Fleming, A. A. Parent, E. E. Parent, J. A. Pincock, L. Renault, *J. Org. Chem.* **2007**, *72*, 9464–9470.

[33] S. C. Ward, S. A. Fleming, *J. Org. Chem.* **1994**, *59*, 6476–6479.

[34] a) W. Horspool, F. Lenci, *CRC Handbook of Organic Photochemistry and Photobiology, Second Edition, Chapter 18*, CRC Press LCC, **2004**; b) A. Albini, M. Fagnoni, *Handbook of Synthetic Photochemistry, Chapter 5*, Wiley-VCH, Weinheim, **2010**.

[35] R. G. Salomon, J. K. Kochi, *J. Am. Chem. Soc.* **1974**, *96 (4)*, 1137-1144.

[36] a) R. G. Salomon, *Tetrahedron* **1983**, *39*, 485–575; b) R. G. Salomon, S. Ghosh, S. R. Raychaudhuri, T. S. Miranti, *Tetrahedron Lett.* **1984**, *25*, 3167–3170; c) S. Ghosh, S. R. Raychaudhuri, R. G. Salomon, *J. Org. Chem.* **1987**, *52*, 83–90.

[37] a) J. Panda, S. Ghosh, S. Ghosh, *ARKIVOC* **2005**, *2001*, 146–153; b) C. Malik, M. Vaultier, S. Ghosh, *Synthesis* **2007**, *2007*, 1247–1250.

[38] J. Panda, S. Ghosh, S. Ghosh, *J. Chem. Soc., Perkin Trans. 1* **2001**, 3013–3016.

[39] W. Horspool, F. Lenci, *CRC Handbook of Organic Photochemistry and Photobiology, Second Edition, Chapter 71*, CRC Press LCC, **2004**.

[40] W. Horspool, F. Lenci, *CRC Handbook of Organic Photochemistry and Photobiology, Second Edition, Chapter 72*, CRC Press LCC, **2004**.

[41] M. T. Crimmins, T. L. Reinhold, *Org. React. (Hoboken, NJ, U. S.)* **1993**, *44*, 297–339.

[42] a) G. Marsh, D. R. Kearns, K. Schaffner, *Helv. Chim. Acta* **1968**, *51 (8)*, 1890–1899; b) D. R. Kearns, G. Marsh, K. Schaffner, *J. Chem. Phys.* **1968**, *49*, 3316–3317; c) D. R. Kearns, G. Marsh, K. Schaffner, *J. Am. Chem. Soc.* **1971**, *93 (13)*, 3129.

[43] A. Albini, M. Fagnoni, *Handbook of Synthetic Photochemistry, Chapter 6*, Wiley-VCH, Weinheim, **2010**.

[44] E. J. Corey, J. D. Bass, R. LeMahieu, R. B. Mitra, *J. Am. Chem. Soc.* **1964**, *86*, 5570–5583.

[45] a) P. de Mayo, J.-P. Pete, M. F. Tchir, *J. Am. Chem. Soc.* **1967**, *89 (22)*, 5712–5713; b) P. de Mayo, J.-P. Pete, M. Thir, *Can. J. Chem.* **1968**, *46*, 2535–2547.

[46] David J. Hastings, A. C. Weedon, *J. Am. Chem. Soc.* **1991**, *113*, 8525–8527.

[47] a) D. I. Schuster, G. Lem, N. A. Kaprinidis, *Chem. Rev.* **1993**, *93*, 3–22; b) M. T. Crimmins, *Chem. Rev.* **1988**, *88*, 1453–1473.

[48] D. O. Cowan, R. L. E. Drisko, *J. Am. Chem. Soc.* **1970**, *92 (12)*, 6286–6291.

[49] J. L. Broeker, J. E. Eksterowicz, A. J. Belk, K. N. Houk, *J. Am. Chem. Soc.* **1995**, *117*, 1847–1848.

[50] T. Suishu, T. Shimo, K. Somekawa, *Tetrahedron* **1997**, *53 (10)*, 3545–3556.

[51] E. Piers, A. Orellana, *Synthesis* **2001**, *14*, 2138–2142.

[52] T. Bach, *Synthesis* **1998**, *1998*, 683–703.

[53] R. Srinivasan, K. H. Carlough, *J. Am. Chem. Soc.* **1967**, *89*, 4932–4936.

[54] P. de Mayo, *Acc. Chem. Res.* **1971**, *4 (2)*, 41–47.

[55] B. W. Disanayaka, A. C. Weedon, *J. Org. Chem.* **1987**, *52*, 2905–2910.

[56] B. A. Pearlman, *J. Am. Chem. Soc.* **1979**, *101 (21)*, 6404–6408.

[57] W. Oppolzer, T. Godel, *J. Am. Chem. Soc.* **1978**, *100 (8)*, 2853–2854.

[58] Y. Tamura, H. Ishibashi, M. Hirai, Y. Kita, M. Ikeda, *J. Org. Chem.* **1975**, *40 (19)*, 2702–2710.

[59] J. D. White, D. C. Ihle, *Org. Lett.* **2006**, *8*, 1081–1084.

[60] J. D. Winkler, J. E. Stelmach, M. G. Siegel, N. Haddad, J. Axten, W. P. Dailey, *Isr. J. Chem.* **1997**, *37*, 47–67.

[61] Y.-S. Kwak, J. D. Winkler, *J. Am. Chem. Soc.* **2001**, *123*, 7429–7430.

[62] a) W. Horspool, F. Lenci, *CRC Handbook of Organic Photochemistry and Photobiology, Second Edition, Chapter 60*, CRC Press LCC, **2004**; b) G. Büchi, C. G. Inmna, E. S. Lipinsky, *J. Am. Chem. Soc.* **1954**, *76*, 4327.

[63] M. D'Auria, R. Racioppi, *Curr. Org. Chem.* **2009**, *13*, 939–954.

[64] a) D. R. Arnold, R. L. Hinman, A. H. Glick, *Tetrahedron Lett.* **1964**, *22*, 1425–1430; b) D. R. Arnold, D. J. Trecker, E. B. Whipple, *J. Am. Chem. Soc.* **1965**, *87*, 2596–2602.

[65] D. J. Aitken, C. Gauzy, E. Pereira, *Tetrahedron Lett.* **2002**, *43*, 6177–6179.

[66] C. Gauzy, B. Saby, E. Pereira, S. Faure, D. J. Aitken, *Synlett* **2006**, *9*, 1394–1398.

[67] a) S. Faure, A. A. Jensen, V. Maurat, X. Gu, E. Sagot, D. J. Aitken, J. Bolte, T. Gefflaut, L. Bunch, *J. Med. Chem.* **2006**, *49*, 6532–6538; b) X. Gu, M. Xian, S. Roy-Faure, J. Bolte, D. J. Aitken, T. Gefflaut, *Tetrahedron Lett.* **2006**, *47*, 193–196.

[68] V. Mojr, E. Svobodová, K. Straková, T. Neveselý, J. Chudoba, H. Dvořáková, R. Cibulka, *Chem. Commun.* **2015**, *51*, 12036–12039.

[69] M. Neumann, K. Zeitler, *Eur. J. Org. Chem.* **2013**, *19*, 6950–6955.

[70] Z. Lu, T. P. Yoon, *Angew. Chem., Int. Ed.* **2012**, *51*, 10329–10332.

[71] Y.-Q. Zou, S.-W. Duan, X.-G. Meng, X.-Q. Hu, S. Gao, J.-R. Chen, W.-J. Xiao, *Tetrahedron* **2012**, *68*, 6914–6919.

[72] Y. Xu, M. L. Conner, M. K. Brown, *Angew. Chem., Int. Ed.* **2015**, *54*, 11918–11928.

[73] C. Müller, A. Bauer, T. Bach, *Angew. Chem., Int. Ed.* **2009**, *48*, 6640–6642.

[74] M. M. Maturi, T. Bach, *Angew. Chem., Int. Ed.* **2014**, *53*, 7661–7664.

[75] R. Alonso, T. Bach, *Angew. Chem., Int. Ed.* **2014**, *53*, 4368–4371.

[76] Z. D. Miller, B. J. Lee, T. P. Yoon, *Angew. Chem., Int. Ed.* **2017**, *56*, 11891–11895.

[77] Y.-Z. Li, A.-P. Tong, J. Huang, *Chem. Biodivers.* **2012**, *9*, 769–776.

[78] M. A. Ischay, T. P. Yoon, *Eur. J. Org. Chem.* **2012**, *2012*, 3359–3372.

[79] A. Albini, M. Fagnoni, *Photochemically-generated Intermediates in Synthesis*, John Wiley & Sons, Inc., Pavia (Italy), **2013**.

[80] K. Mizuno, Y. Otsuji, *Top. Curr. Chem.* **1994**, *169*, 301–346.

[81] G. Pandey, *Top. Curr. Chem* **1993**, *168*, 175–222.

[82] Corey R. J. Stephenson, T. P. Yoon, David W. C. MacMillan, *Visible Light Photocatalysis in Organic Chemistry, First Edition, Wiley-VCH* **2018**, 129–158.

[83] M. Riener, D. A. Nicewicz, *Chem. Sci.* **2013**, *4*, 2625–2629.

[84] M. A. Ischay, M. E. Anzovino, J. Du, T. P. Yoon, *J. Am. Chem. Soc.* **2008**, *130*, 12886–12887.

[85] J. Du, T. P. Yoon, *J. Am. Chem. Soc.* **2009**, *131*, 14604–14605.

[86] J. Du, K. L. Skubi, D. M. Schultz, T. P. Yoon, *Science* **2014**, *344*, 392–396.

B Main Part

1 Preliminary studies towards the synthesis of the bicyclic key intermediates

1.1 Introduction

The central part of the present thesis constitutes the development of a synthetic strategy towards enantiomerically pure γ-cyclobutane amino acids using a visible light mediated [2+2] cycloaddition as crucial step to install the cyclobutane core. The focus of this work lied on the investigation of an intramolecular version of visible light induced [2+2] photocycloaddition in order to synthesize 3-oxabicyclo-[3.2.0]-heptan-2-one **105** as well as 3-azabicyclo-[3.2.0]-heptan-2-one core **106** (Scheme 21).

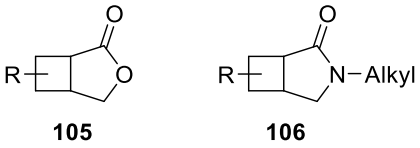

105 **106**

R = any amino side chains

Scheme 21. General motif of the desired target molecules.

These intermediates provide the required functional groups (amino and carboxylic acid functionality) of the target γ-cyclobutane amino acids in a masked form and can be liberated through further transformations.

Aitken *et al.*[1] developed a strategy for the synthesis of all four isomers of γ-cyclobutane amino acid **112** (Scheme 22). A key step in this sequence is a [2+2] photocycloaddition of enantiomerically pure unsaturated γ-lactam **107** and ethylene (**59**) by irradiation with a 400 W mercury vapor lamp with Pyrex filter. Both azabicycloheptanones **108** were separable *via* convenient column chromatography. By treatment with dissolved sodium in liquid ammonia and following protection step, the chiral appendage was exchanged by a Boc group. The resulting *N*-Boc derivatives **109** were smoothly hydrolyzed using LiOH yielding the *N*-Boc-protected γ-amino acids **111**. Simple deprotection under acidic conditions and subsequent elution through an ion exchange resin (H^+-form) gave the free *cis*-γ-amino acids **112**. For the *cis-trans* epimerization, the Boc-protected lactams **109** were treated with trimethylaluminum/ammonia in DCM to achieve the conversion into the corresponding *cis*-carboxamides **110**. By a one-pot tandem epimerization/hydrolysis process, refluxing in MeOH

in the presence of NaOH (6M), the *N*-Boc derivatives of *trans*-γ-cyclobutane amino acids **112** were obtained.

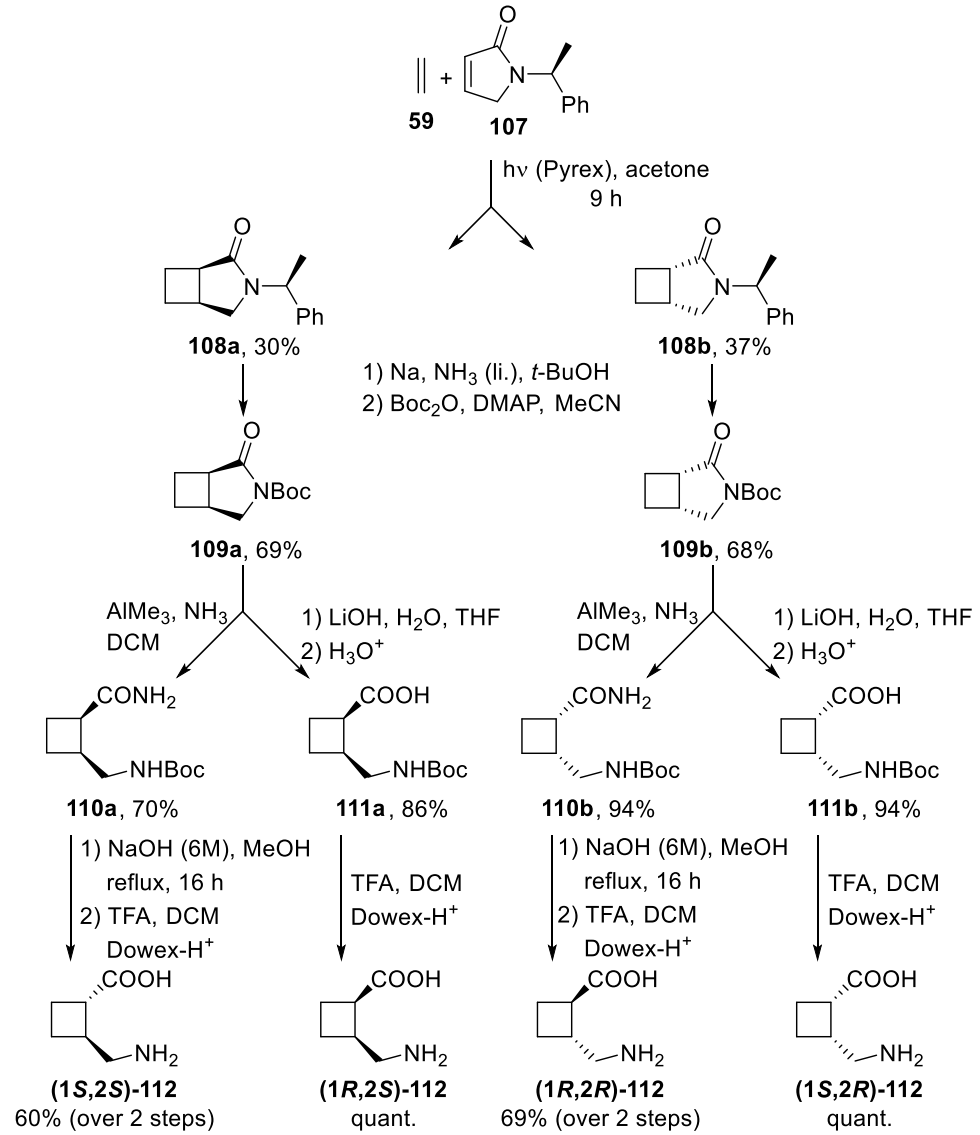

Scheme 22. Synthesis of all four γ-cyclobutane amino acid isomers by Aitken *et al*.[1]

In 2014, Aitken and coworkers also reported a synthetic sequence towards 1,2,3-trisubstituted cyclobutanes **118** using a UV-mediated [2+2] photocycloaddition of maleic anhydride **75** either with allyl alcohol or propargyl alcohol **113** (Scheme 23).[2]

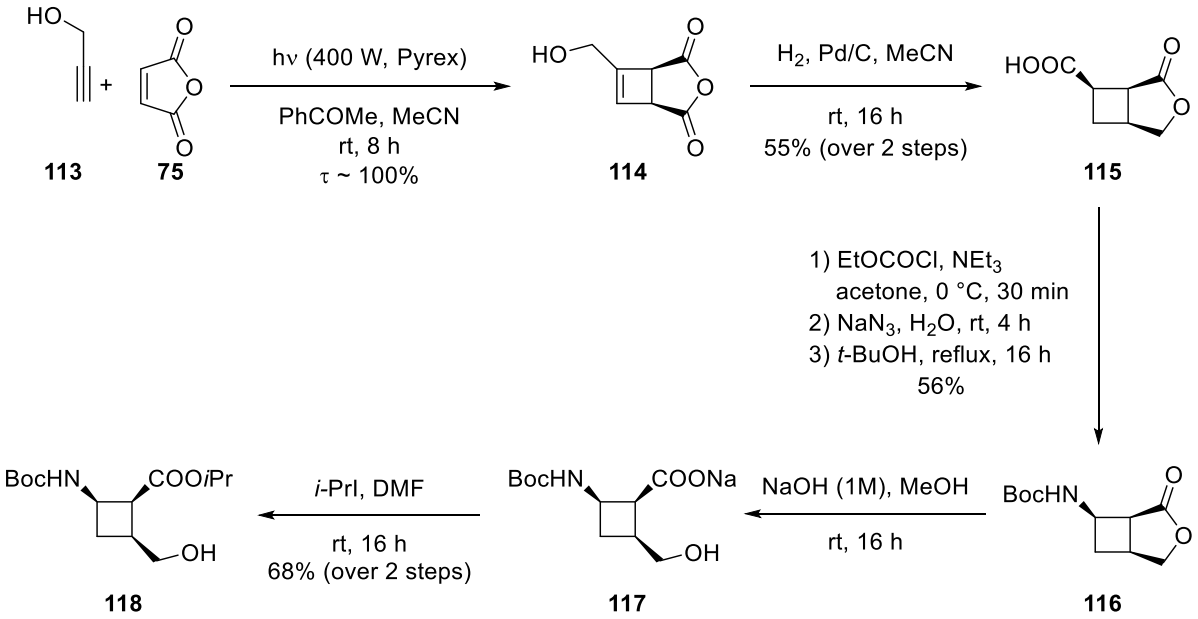

Scheme 23. The synthetic sequence towards 1,2,3-trisubstituted cyclobutanes by Aitken *et al*.[2]

By irradiation of a solution of maleic anhydride **75** with propargylic alcohol **113** *cis*-3-hydroxymethylcyclobut-3-ene-1,2-dicarboxylic anhydride (**114**) was generated as the only product. Hydrogenation of this crude compound with 10% Pd on charcoal furnished the desired lactone acid **115** stereoselective in an overall yield of 55% over 2 steps. Compound **115** was transformed into the Boc-protected amino lactone *via* acyl azide activation and subsequent Curtius rearrangement. By treatment with NaOH the corresponding sodium carboxylate **117** was obtained which was then reacted with *i*-PrI to get the amino ester **118** in moderate yield. Herein, this oxabicycloheptanone motif **105** was used to synthesize substituted cyclobutane amino acid derivatives.

In the shown procedures the cyclobutane-containing compounds were synthesized using a UV-mediated [2+2] photocycloaddition as key step in the synthesis sequence. Regarding the concept of "Green Chemistry", it is desirable to replace the UV-light source by an environmentally friendly LED or fluorescent light bulb since the use of UV-light in chemical reactions requires a high input of energy and specialized equipment for its safe generation. As extensively discussed in the introduction visible light mediated [2+2] photocycloaddition can be performed by several pathways as *via* radical anion and cation formation or *via* energy transfer. In the following chapters, the relevant literature will be presented in the context of the synthesis of appropriate substrates and their photochemical investigations. The aim constitutes the development of a reaction sequence *via* visible light induced [2+2] photocycloaddition towards the desired bicyclic key intermediates **105** and **106**.

1.2 Studies towards [2+2] photocycloaddition *via* radical anion mechanism

Bauld and Krische investigated the intramolecular cyclobutanation of several bisenones *via* an anion radical chain mechanism.[3] They demonstrated the formal [2+2] cycloaddition of tethered enones through cobalt[4] as well as copper[5] mediated single electron transfer. Furthermore, the chrysene radical anion is also capable of serving as an electron donor in this reaction type.[6] This inspired Yoon and coworkers to establish a diastereoselective [2+2] cycloaddition of bisenones *via* ruthenium-based visible light photocatalysis (Scheme 24).[7]

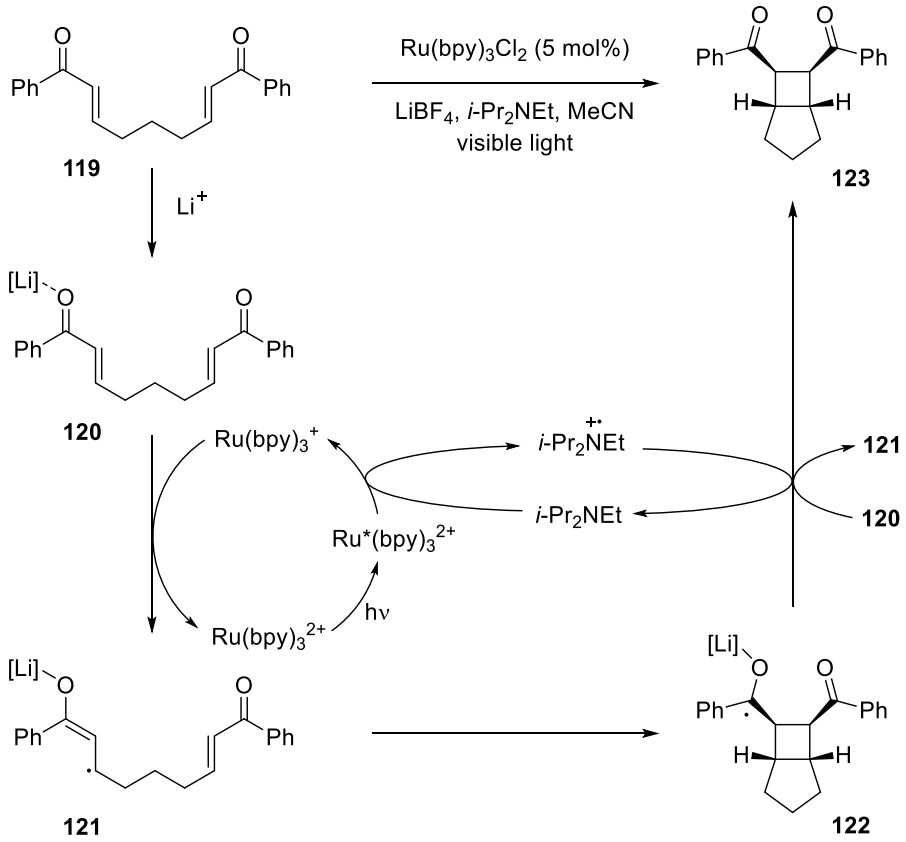

Scheme 24. Proposed mechanism for Yoon's formal [2+2] cycloaddition of enones.[7]

By absorption of visible light, the photoexcited state $Ru^*(bpy)_3^{2+}$ will be generated, which undergoes a reductive quenching pathway with DIPEA as sacrificial electron donor. The resulting $Ru(bpy)_3^{+}$ species transfers one electron to the lithium activated enone **120** leading to the regeneration of the starting catalyst, $Ru(bpy)_3^{2+}$. The cycloaddition affords a cyclobutyl ketyl radical **122**. Afterwards, the final electron transfer produces the neutral product **123**. This product-forming step takes place either as chain-terminating reduction of the photogenerated amine radical cation or as chain-propagation reduction of another equivalent of lithium activated enone **120**. Since the quantum yield is calculated with $\Phi = 77$ in this case, the product formation is dominated by a chain process.[8] Beside this intramolecular addition reaction

Yoon *et al.*[9] also developed an intermolecular version. In 2013, Zeitler *et al.*[10] demonstrated that Eosin Y as organic dye is also capable of accessing ketyl radical anions by visible light photocatalysis.

The task now was to establish a protocol for a [2+2] cycloaddition of either ester-linked or amide-linked bisenones **124** adopting the photoinduced radical anion reaction pathway in order to synthesize the target molecules, 3-oxabicyclo- as well as 3-azabicyclo-[3.2.0]-heptan-2-one derivatives **125** (Scheme 25).

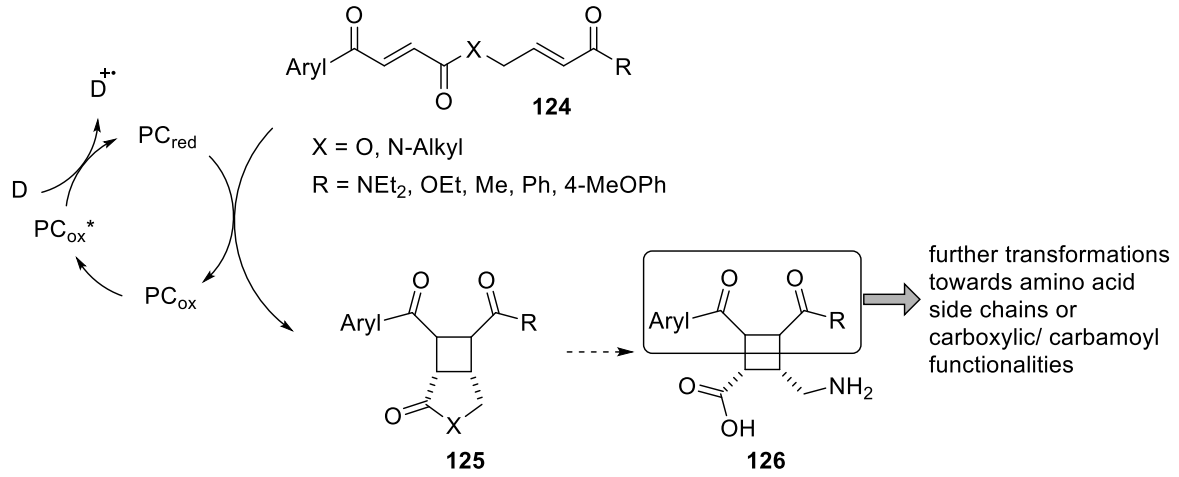

Scheme 25. Envisioned reaction sequence towards γ-cyclobutane amino acids *via* visible light.

The first goal was to synthesize the ester-linked bisenone derivative **134** according to an optimized reaction pathway of Xu *et al.*[11] (Scheme 26).

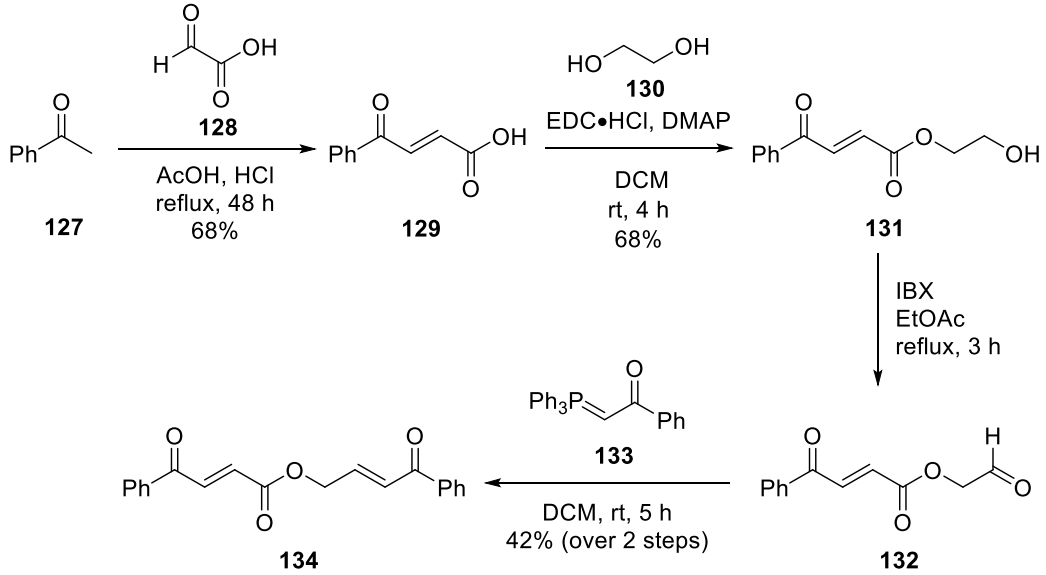

Scheme 26. Synthesis of compound **134**.

The aldol condensation between glyoxylic acid **128** and acetophenone **127** led to α,β-unsaturated acid **129** in 68% yield. However, subsequent esterification with ethylene glycol **130** using DCC and DMAP, as coupling reagent, failed as product **131** could not be isolated from the byproduct of the Steglich esterification, the dicyclohexylurea. Therefore, DCC was exchanged by EDC•HCl, since herein the corresponding coupling byproduct is water soluble and was easily removed by aqueous extraction. Ester **131** was obtained in a yield of 68%. In the following step, the hydroxyl group was oxidized with the help of iodoxybenzoic acid (IBX) to give aldehyde **132**, which finally reacted with ylide **133** in a Wittig reaction to compound **134**.

The photochemical investigation of substrate **134** mainly based on the conditions of a reductive reaction pathway (Table 1). Cyclic voltammetry (CV) measurement revealed that compound **134** possesses a potential of -1.09 V *vs* SCE[1]. Therefore, all tested metal based photocatalysts, as well as Eosin Y, should be feasible to reduce ester-linked bisenone **134**.

[1] Redoxpotential was measured against ferrocene and was converted *vs* SCE (see Experimental Part).

Table 1. Photochemical investigation of ester-linked bisenone **134**.[a)]

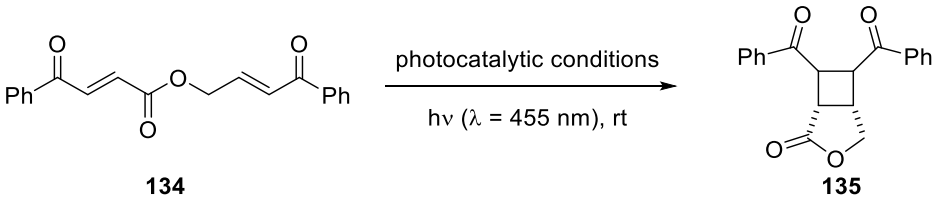

134 **135**

entry	photocatalytic conditions	solvent	time [h]	yield [%]
1	Na_2EosinY (0.5 mol%) LiBr (2 equiv.), DIPEA (2 equiv.)	MeCN	1.5	decomp.
2	Na_2EosinY (0.5 mol%) DIPEA (2 equiv.)	MeCN	1	decomp.
3	$Ru(bpy)_3Cl_2$ (5 mol%) $LiBF_4$ (2 equiv.), DIPEA (2 equiv.)	MeCN	0.75	decomp.
4	$Ru(bpy)_3Cl_2$ (5 mol%) DIPEA (2 equiv.)	MeCN	0.5	decomp.
5	$Ru(bpy)_3Cl_2$ (5 mol%) DIPEA (2 equiv.)	DCM	24	decomp.
6	$[Ir(dtb\text{-}bpy)ppy_2]PF_6$ (1 mol%) DIPEA (2 equiv.)	MeCN	1	decomp.
7	$Cu(dap)_2Cl$ (1 mol%) DIPEA (2 equiv.)	MeCN	24	decomp.
8	– DIPEA (2 equiv.)	MeCN	24	decomp.
9	$Ru(bpy)_3Cl_2$ (5 mol%) NPh_3 (2 equiv.)	DCM	48	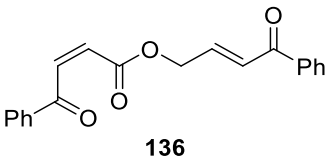 **136** 79

[a)] 0.3 mmol substrate (0.1M in corresponding solvent).

In entry 1 and 2, Eosin Y ($E_{1/2}^{PC/PC^{\bullet-}}$ = -1.14 V *vs* SCE) as organic dye served as photocatalyst.[12] However, the starting material only decomposed also in absence of the Lewis

acid LiBr (entry 2). In the following, $Ru(bpy)_3Cl_2$ ($E_{1/2}^{I/II}$ = -1.33 V *vs* SCE) was investigated to be a suitable photocatalyst for this type of reaction.[13,14] In the presence as well as the absence of $LiBF_4$ no product formation was observed (entry 3, 4). Also, the exchange of the solvent by using DCM instead of MeCN did not lead to a successful [2+2] photocycloaddition (entry 5). Using $[Ir(dtb\text{-}bpy)ppy_2]PF_6$ ($E_{1/2}^{II/III}$ = -1.51 V *vs* SCE) or $Cu(dap)_2Cl$ ($E_{1/2}^{I*/II}$ = -1.43 V *vs* SCE) in the reductive quenching cycle the starting material only decomposed (entry 6, 7). It seemed that already the used base reacted with compound **134**. No more ester-linked bisenone **134** could be recovered by stirring it in MeCN only in the presence of DIPEA (entry 8). This control experiment showed that DIPEA already led to the decomposition of the starting material **134**. Hence, NPh_3 without α-C-H bond was applied as alternative reductive quencher. Herein a *cis-trans* isomerization of the double bond in the oxo-phenylbutenoic acid part of molecule **134** took place (entry 9). The corresponding *Z*-isomer **136** was obtained in a yield of 79%.[15] The decomposition of the starting material could now be circumvented but a [2+2] photocycloaddition was not yet achieved. This could probably be explained by the preferred *S-cis* conformation of the ester moiety, instead of the less stable *S-trans* conformation required for the cycloaddition.[16] In literature, there are few examples, which confirm this observation, that ester tethered substrates similar to the tested material are not able to cyclize to bicyclic compounds under photochemical conditions.[17]

To summarize, the ester-linked bisenone **134** turned out to be a non-suitable starting material for the proposed reaction mainly due to its favored *S-cis* conformation of the ester moiety. Since this problem can be avoided in an amide-linked bisenone by choosing a suitable substituent on the amide bond in order to receive the affected double bonds in the necessary spatial proximity, the investigation was continued and focused now on the synthesis of such substrates.[18]

In accordance with the described reaction sequence above (see Scheme 26), the key steps in the synthesis of amide-linked bisenones **137** should be an amide bond formation between an aminoethanol derivative **139** and the previously synthesized acid **129**, as well as a Wittig reaction (Scheme 27). A methyl or rather a phenyl group should be bulky enough to occupy the appropriate space to bring both double bonds for the cycloaddition into the necessary spatial proximity.

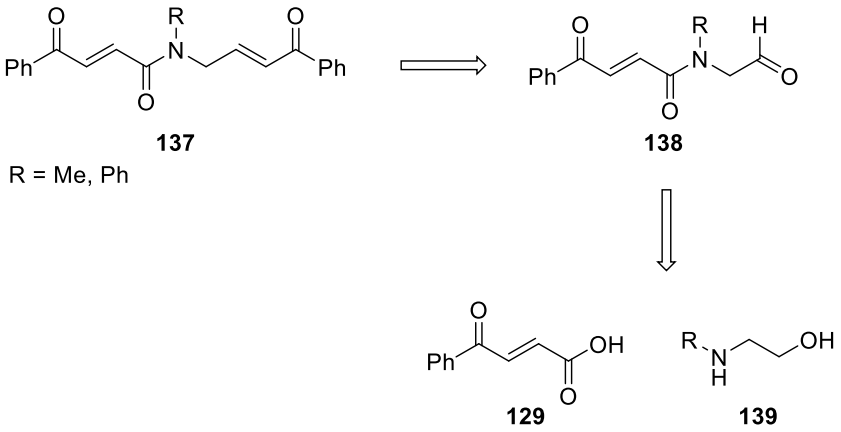

Scheme 27. The retrosynthetic approach towards amide-linked bisenone **137**.

At first, the silyl protection of 2-methylaminoethanol (**139a**) was performed (Table 2). TBDMS-protecting group seemed to be a suitable choice due to its high stability and easily selective Flouride-ion mediated cleavage.[19]

Table 2. Synthesis of the silyl-protected compound **140**.

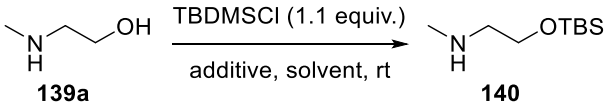

entry	additive	solvent	time [h]	yield [%]
1	imidazole (2 equiv.)	DMF	24	complex mixture
2	1-methylimidazole (3 equiv.), I_2 (2 equiv.)	DCM	1	decomp.
3	NEt_3 (1.2 equiv.), DMAP (0.01 equiv.)	DCM	18	50

Applying the protocol of Corey *et al*.,[20] dimethyl-*tert*-butylsilyl chloride and imidazole in DMF led to a complex mixture and the desired product **140** could not be isolated (entry 1). With the highly efficient reagent system, silyl-chloride-*N*-methylimidazole-iodine, only decomposition of the starting material **139a** was detectable (entry 2).[21] However, the protection using triethylamine and 4-dimethylaminopyridine gave rise to 50% of the protected amino alcohol **140** (entry 3).[19]

In the following step, the silyl-protected amino alcohol **140** was coupled with acid **129** in the presence of EDC•HCl as coupling reagent yielding 50% of compound **141** (Scheme 28).

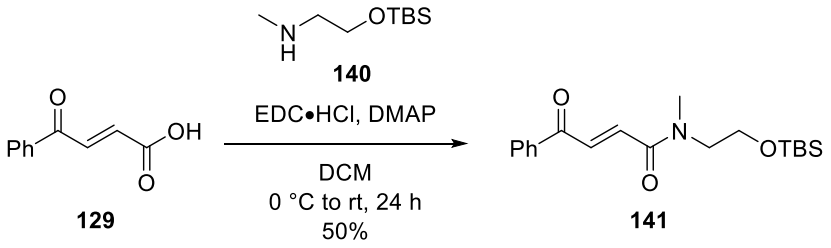

Scheme 28. Amide coupling reaction.

During the deprotection, treatment of compound **141** with TBAF, a cyclization immediately occurred and led to compound **143** instead of the desired amide **142** (Scheme 29).

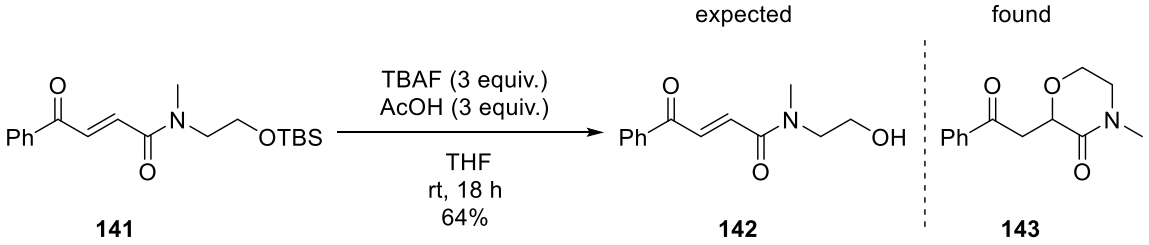

Scheme 29. Deprotection step of compound **141**.

On this account, the unprotected amino alcohol **139a** was also tried to couple with acid **129** (Scheme 30).

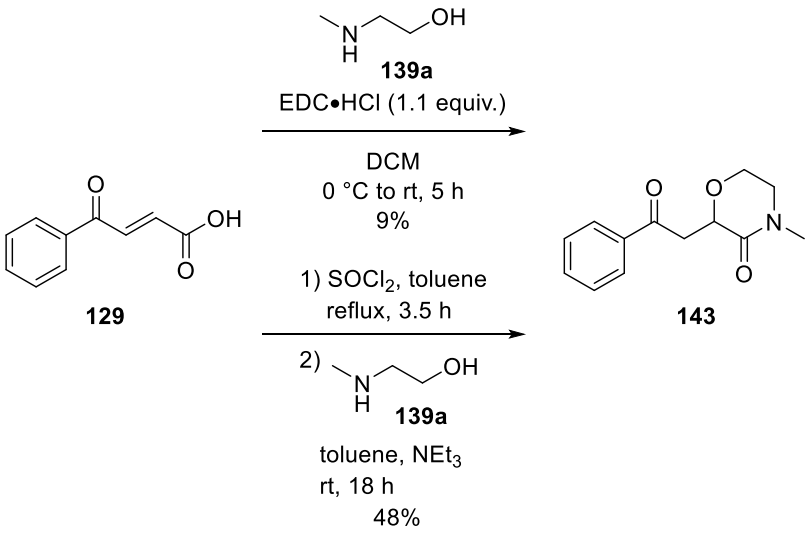

Scheme 30. Coupling attempts with the unprotected amino alcohol **139a**.

In analogy to compound **134**, EDC•HCl served as coupling reagent. In this case, only the cyclic product **143** was isolated in a yield of 9%. The transformation of acid **129** into the corresponding acid chloride as activated carbonyl compound was achieved by refluxing it with thionyl chloride. The lactam derivative **143** was obtained in a yield of 48%. In both cases, no desired product **142** was formed.

Due to this unexpected cyclization, the retrosynthetic approach was modified as followed (Scheme 31).[2]

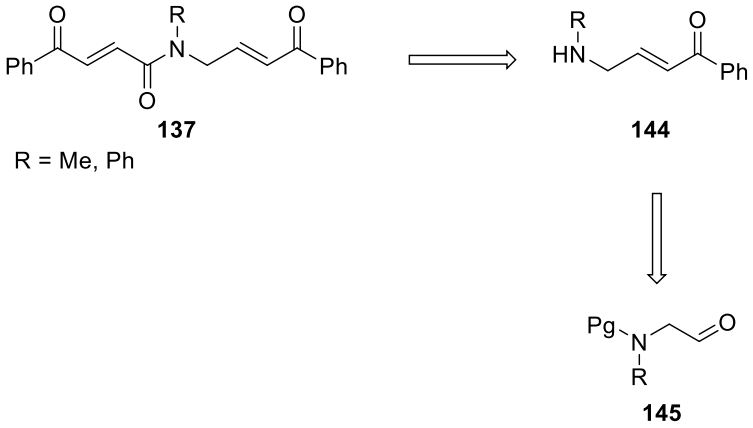

Scheme 31. The new envisioned retrosynthesis of the amide-linked bisenone **137**.

The new reaction pathway considers starting with an oxidation of a protected amino ethanol derivative to the corresponding protected α-amino aldehyde **145** which then could undergo a Wittig reaction or an aldol condensation to generate compound **144**. In contrast to the previous idea, the amide coupling should be the last reaction step. In this process, the amino functionality should be either protected by a Boc or a Fmoc group. The Boc-protection of the methyl and phenyl substrate **139** worked straightforwardly (Scheme 32). Using Boc-anhydride together with catalytic amounts of DMAP gave the desired protected derivatives **146** in excellent yield of 93% and 90%, respectively.[19]

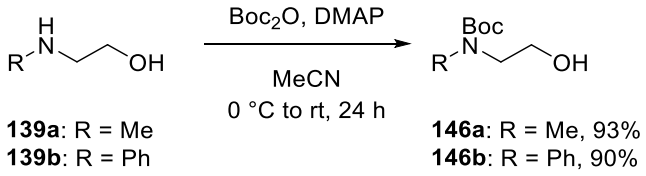

Scheme 32. Synthesis of the Boc-protected derivatives **146a** and **146b**.

Furthermore, a protocol of Chen and coworkers was applied for the Fmoc-protection (Scheme 33).[22]

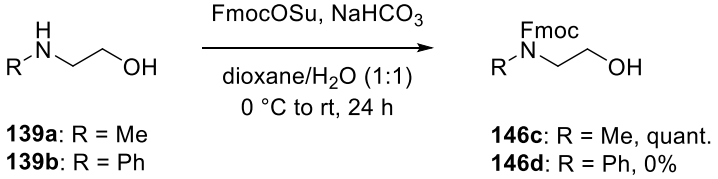

Scheme 33. Fmoc-protection of the corresponding amino alcohols **139**.

[2] Several results are adapted from the Bachelor Thesis of Lukas Wein (supervised by S. Kerres).

The amino alcohol **139** was dissolved in a dioxane/water mixture and reacted with Fmoc-succinimide in the presence of $NaHCO_3$ as an additional base. In the case of the methyl derivative **139a**, the target molecule could be synthesized quantitatively, whereas the analog phenyl substrate **139b** could not be isolated.

According to a modified procedure of Finney *et al.*[23] the obtained protected amino alcohols **146** were oxidized using IBX as oxidizing agent (Table 3).

Table 3. Oxidation step of the amino alcohols **146**.

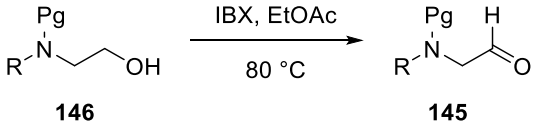

146 **145**

entry	R	Pg	146	IBX	145	yield [%]
1	Me	Boc	**a**	1.2 equiv.	**a**	90
2	Ph	Boc	**b**	1.2 equiv.	**b**	decomp.
3	Ph	Boc	**b**	2.6 equiv.	**b**	decomp.
4	Me	Fmoc	**c**	1.2 equiv.	**c**	n. r.
5	Me	Fmoc	**c**	2 equiv.	**c**	45

1.2 equivalents of the oxidizing reagent were enough in order to oxidize the Boc-derivative **146a** to the corresponding aldehyde derivative **145a** yielding 90% (entry 1). Unfortunately, during this procedure of the phenyl substituted derivative **146b** only decomposition of the starting material was observed (entry 2, 3). In the case of the Fmoc-protected derivative **146c,** an amount of 2 equivalents of IBX was necessary to afford 45% of aldehyde **145c** (entry 4, 5). With the aldehyde compounds **145** in hand the Wittig reaction with ylide **133** could be performed giving rise to both α,β-unsaturated carbonyl compounds **147** in moderate yields (Scheme 34).

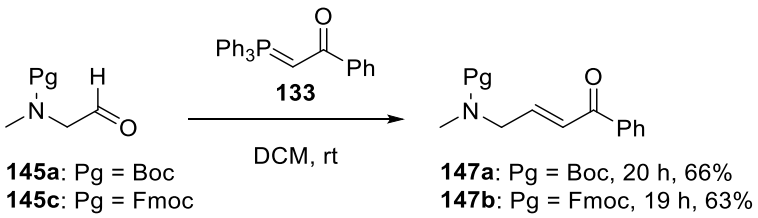

145a: Pg = Boc
145c: Pg = Fmoc

147a: Pg = Boc, 20 h, 66%
147b: Pg = Fmoc, 19 h, 63%

Scheme 34. Wittig coupling of the protected amino aldehyde **145**.

The following sequence was the deprotection of compounds **147** and the subsequent coupling with acid **129** (Table 4).

Table 4. Final reaction sequence towards amide-linked bisenone **137a**.

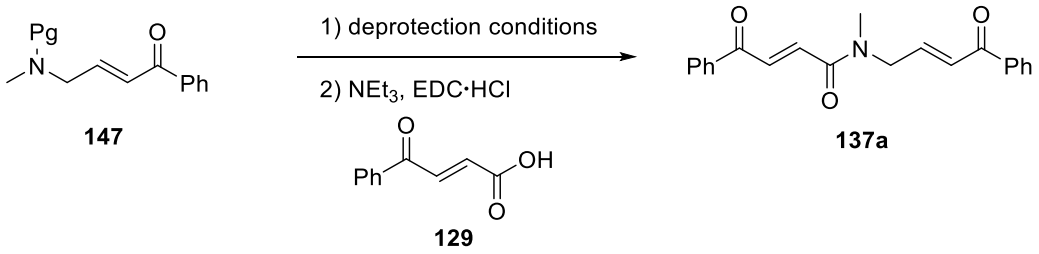

entry	Pg	147	deprotection conditions	yield [%]
1	Boc	**a**	TFA, DCM, rt, 24 h	no product formation
2	Boc	**a**	HCl in EtOAc (4.2M), 0 °C to rt, 3 h	no product formation
3	Fmoc	**b**	piperidine (20 Vol% in DMF), rt, 1 h	no product formation

At first the Boc-derivative **147a** was treated with TFA and the crude mixture was then added to a solution of the active ester of acid **129** prepared by applying EDC•HCl. However, only a complex mixture was obtained, and no product formation was detectable. Therefore, milder condition for the deprotection step reported by Reiser *et al*.[24] was tested: dissolved HCl gas in ethyl acetate as acid source. Indeed, no improvement could be achieved. Since the Fmoc group is cleaved off under basic conditions instead of acidic conditions, this could probably solve this problem. However, already the deprotection step failed and the unprotected derivative could not be synthesized at all and submitted to the last coupling reaction.

In summary, the ester-linked bisenone **134** was not a suitable substrate for the [2+2] photocycloaddition probably due to its favorable *S-cis* conformation so that the double bonds are not in spatial proximity for a successful cycloaddition. Besides the syntheses of the amide-linked bisenones **137** were lined with several problems as unexpected cyclization or decomposition in several reaction steps. As a result, this project was closed and to studies towards the preparation and photochemical behavior of amide-linked bisstyrenes were moved on.

1.3 Studies towards [2+2] photocycloaddition *via* radical cation mechanism

The cyclodimerization of *N*-vinylcarbazole catalyzed by ferric, ceric or cupric salts is the first unambiguous example of a cycloaddition mediated by a radical cation chain mechanism.[25]

Later, Ledwith *et al*.[26] also described a photoinduced electron transfer initiated version of this reaction. During the 1980s, Bauld and coworkers studied radical cation [2+2] cycloadditions of a variety of electron-rich olefins mediated by stable aminium radical salts.[27] In general, [2+2] cycloadditions are net redox-neutral transformations since they involve no overall change in the oxidation states of the substrates. An advantage of this is that no stoichiometric amount of a terminal oxidant is required what is characteristic for a chain propagation mechanism.[28,29]

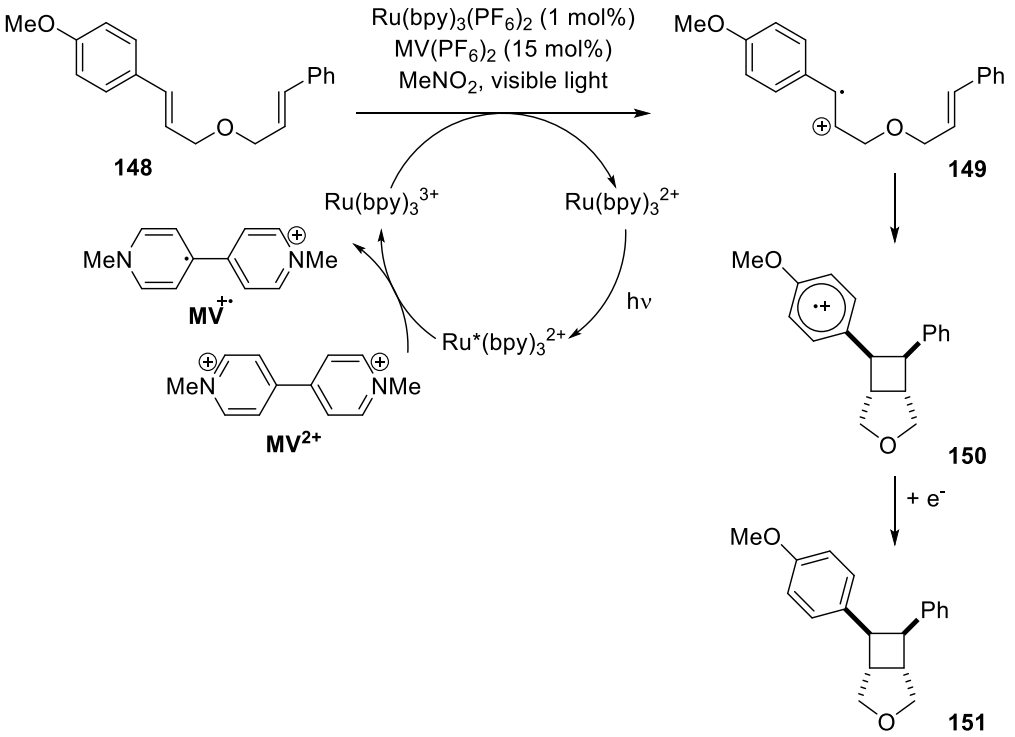

Scheme 35. [2+2] cycloaddition of electron-rich bisstyrenes.[30]

In 2010, Yoon and coworkers used the advantage of the ability of $Ru(bpy)_3^{2+}$ to generate olefin radical cations by photooxidation to establish a photooxidative [2+2] cycloaddition of electron-rich bisstyrenes (Scheme 35).[30] In the presence of methyl viologen (**MV^{2+}**), a pyridinium salt, the photoactivated $Ru^*(bpy)_3^{2+}$ is oxidatively quenched to $Ru(bpy)_3^{3+}$ which is capable of oxidizing the electron-rich bisstyrene **148**. The so obtained radical cation **149** can undergo the [2+2] cycloaddition followed by single electron reduction yielding cyclobutane-containing compound **151**. Besides, Yoon and coworkers published a variant of this reaction, achieving an intermolecular [2+2] photocycloaddition between electron-rich styrenes and a variety of acceptor olefins.[31]

Inspired by this, the focus was put on the construction of amide-linked bisstyrenes **153** and on the investigation of their behavior in a photochemical radical cation mediated [2+2] cycloaddition.

At first, four derivatives **153** were synthesized by an easy coupling reaction between cinnamic acid **152** and the corresponding amine (Table 5).

Table 5. Coupling reaction of several amines with the cinnamic acid **152**.

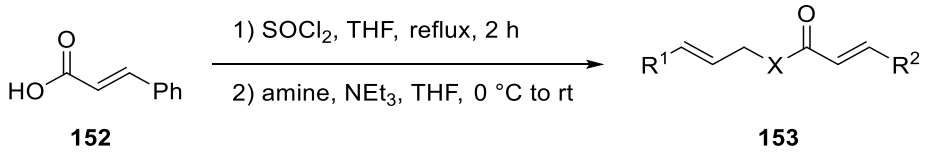

152 **153**

entry	amine	time [h]	yield [%]	153	$E_{1/2}$[3] *vs* SCE [V]
1	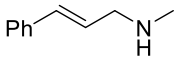 **154**[4]	19	77	**a**	1.37
2	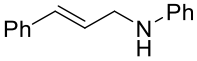 **155**[5]	19	81	**b**	1.32
3	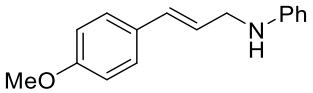 **156**[6]	19	66	**c**	1.06
4	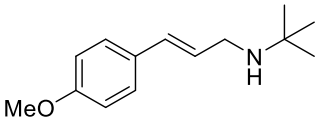 **157**[7]	21	56	**d**	1.12

By refluxing with $SOCl_2$ cinnamoyl chloride was generated *in situ* and subsequently reacted with the corresponding amine derivative. All four substrates **153** were obtained in moderate to good yields. The 4-methoxyphenyl derivatives **153c** and **153d** were synthesized, since they were estimated to have a lower potential due to the electron donating substituent and were so easy to oxidize. Substrate **153b** has a potential $E_{1/2}$ = +1.32 V *vs* SCE, whereas **153c** has a potential $E_{1/2}$ = +1.06 V *vs* SCE. In addition, compound **153d** with the *tert*-butyl group as the bulkiest group in this raw of materials is an interesting test molecule because it should have the necessary conformation for the [2+2] cycloaddition anyways.

[3] Redox potentials were measured against ferrocene and were converted *vs* SCE (see Experimental Part).

[4] Compound **154** was prepared from cinnamyl bromide and methylamine according to a procedure of Wolfe *et al.*[32]

[5] Compound **155** was synthesized by reductive amination of cinnamylaldehyde with aniline using $NaBH_4$ and amberlyst 15.[33]

[6] A stannous catalyzed reductive amination of Kumar *et al.*[34] furnished compound **156**.

[7] For the reaction condition of the preparation of compound **157** see chapter 2.1.

In the following, the synthesized compounds **153** were subjected to different photocatalytic conditions benefiting from the oxidative photocatalytic pathway (Table 6).

Table 6. Photochemical investigations of amide-linked bisstyrenes **153**.

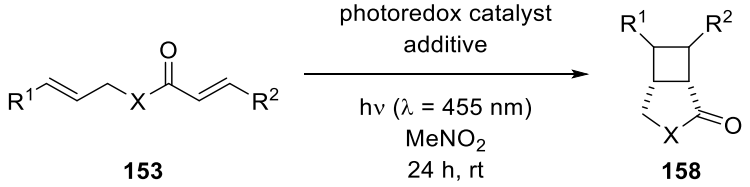

entry	R^1	X	R^2	catalyst	additive	yield
1	H	*N*-Me	Ph	$Ru(bpy)_3Cl_2$ (2.5 mol%)	$MVCl_2$ (15 mol%), $MgSO_4$ (2 wt equiv.)	n. r.
2				$Ru(bpz)_3Cl_2$ (2.5 mol%)	$MVCl_2$ (15 mol%), $MgSO_4$ (2 wt equiv.)	n. r.
3				$Ru(bpz)_3(PF_6)_2$ (2.5 mol%)	O_2	n. r.
4	H	*N*-Ph	Ph	$Ru(bpy)_3Cl_2$ (2.5 mol%)	$MVCl_2$ (15 mol%), $MgSO_4$ (2 wt equiv.)	n. r.
5				$Ru(bpz)_3Cl_2$ (2.5 mol%)	$MVCl_2$ (15 mol%), $MgSO_4$ (2 wt equiv.)	n. r.
6				$Ru(bpz)_3(PF_6)_2$ (2.5 mol%)	O_2	n. r.
7	4-MeOPh	*N*-Ph	Ph	$Ru(bpy)_3Cl_2$ (2.5 mol%)	$MVCl_2$ (15 mol%), $MgSO_4$ (2 wt equiv.)	n. r.
8				$Ru(bpz)_3Cl_2$ (2.5 mol%)	$MVCl_2$ (15 mol%), $MgSO_4$ (2 wt equiv.)	n. r.
9	4-MeOPh	*N-tert*-butyl	Ph	$Ru(bpy)_3Cl_2$ (2.5 mol%)	$MVCl_2$ (15 mol%), $MgSO_4$ (2 wt equiv.)	n. r.
10				$Ru(bpz)_3Cl_2$ (2.5 mol%)	$MVCl_2$ (15 mol%), $MgSO_4$ (2 wt equiv.)	n. r.

Applying the same reaction conditions as the ones from Yoon and coworkers[30], the participating species $Ru(bpy)_3^{3+}$ in this oxidative photocatalytic pathway with a potential $E_{1/2}^{III/II}$ = +1.29 V *vs* SCE[13,14] should be sufficient to oxidize the methoxy-substituted

derivatives **153c** and **153d**, whereas in the case of the other two substrates **153a** and **153b** it would be difficult due to their slightly higher redox potential. However, all four derivatives appeared to be unreactive as the corresponding starting material was recovered (entry 1, 4, 7, 9). Then the reaction conditions were changed to replace $Ru(bpy)_3Cl_2$ with $Ru(bpz)_3Cl_2$ (entry 2, 5, 8, 10). This catalyst has a higher redox potential $E_{1/2}^{III/II}$ = +1.86 V *vs* SCE[35] and thus a higher oxidative power. Nevertheless, the derivatives did not participate in the [2+2] cycloaddition. In contrast to $Ru(bpy)_3^{2+}$ which must be oxidized to its $Ru(bpy)_3^{3+}$ oxidation state before it can serve as electron acceptor for the electron-rich styrenes the more oxidizing analog $Ru(bpz)_3^{2+}$ is capable of performing this oxidation directly from its photoexcited state $Ru^*(bpz)_3^{2+}$ ($E_{1/2}^{*II/I}$ = +1.45 V). In this case molecular oxygen served as sacrificial electron acceptor to close the catalytic cycle again.[36] Under these conditions, derivative **153a** and **153b** could not cyclize either (entry 3, 6).

1.4 Studies towards [2+2] photocycloaddition *via* energy transfer

Finally, the third possibility was tested: a visible light mediated [2+2] cycloaddition *via* an energy transfer. Transition metal complexes can also be involved in energy transfer processes that generate highly reactive organic molecules. In these cases, successful activation depends on the relative triplet-state energies of the catalyst and substrate and not on the redox potentials. Reactions involving thermodynamically unfavorable electron transfer processes can be performed in this manner. Due to the different activation mode the substrate scope is considerably broader.[28,37]

In 2012, Yoon and coworkers demonstrated a triplet sensitized [2+2] photocycloaddition of especially electron-neutral bisstyrene derivative **159**, whose oxidation potential has precluded a participation in the radical cation cycloaddition (Scheme 36).[38] The iridium-based catalyst, $[Ir(dtb\text{-}bpy)(dF(CF_3)ppy)_2]PF_6$, was the suitable triplet sensitizer for this [2+2] photocycloaddition *via* visible light. This method could also be applied to 1,3-dienes.[39] The intramolecular variant afforded mostly carbocycles or oxygen-containing heterocycles.

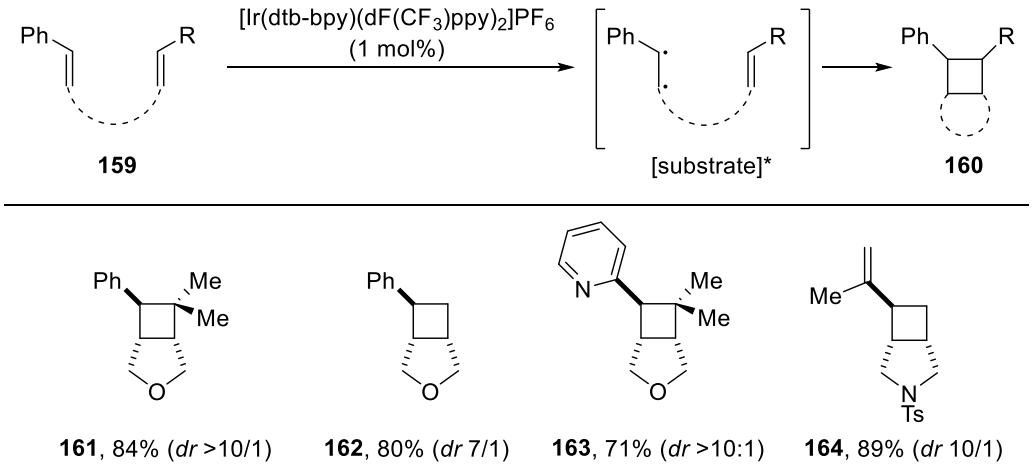

Scheme 36. [2+2] photocycloaddition enabled *via* energy transfer by Yoon *et al.*[38,39]

In contrast to this metal-based photocatalyst, also flavin derivatives **166** can serve as triplet sensitizer for this reaction type.[40] In this case, nitrogen- and sulfur-containing aryl dienes **165** were cyclized to the corresponding aryl-bicyclo-[3.2.0]-heptanes **167**. The nitrogen has been protected either by quaternisation or by acylation and the sulfur had to be in the oxidation state of a sulfone (Scheme 37).[41]

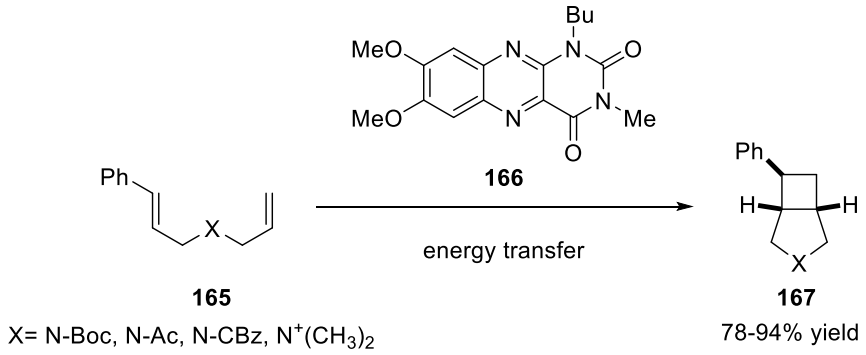

Scheme 37. Flavin-mediated [2+2] photocycloaddition by Cibulka *et al*.[41]

The previous synthesized amide-linked bisstyrenes **153** served as substrates and were subjected to [Ir(dtb-bpy)(dF(CF$_3$)ppy)$_2$]PF$_6$ in DMSO (0.04M substrate concentration) at room temperature under irradiation with blue light (Table 7).

Table 7. [2+2] photocycloaddition of amide-linked bisstyrenes **153** *via* energy transfer mechanism.[a)]

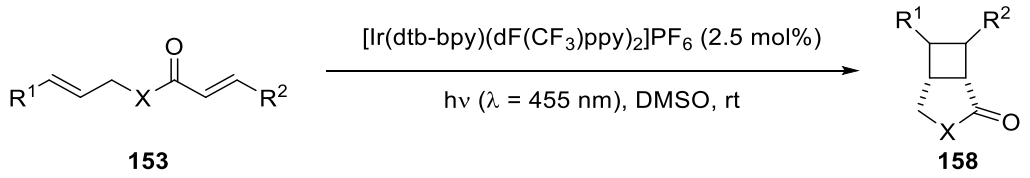

153 **158**

entry	R^1	X	R^2	153	time [h]	158	yield [%]
1	H	*N*-Me	Ph	**a**	48	**a**	isomerization
2	H	*N*-Ph	Ph	**b**	48	**b**	isomerization
3	4-MeOPh	*N*-Ph	Ph	**c**	48	**c**	isomerization
4	OMe	*N*-*tert*-butyl	Ph	**d**	24	**d**	60 (*dr* 76/24)[b)]

[a)] 0.3 mmol substrate (0.04M in DMSO), 2.5 mol% $[Ir(dtb\text{-}bpy)(dF(CF_3)ppy)_2]PF_6$. [b)] Diastereomeric ratio was estimated by crude H^1-NMR.

Having a methyl or a phenyl substituent on the amide bond led to an inseparable mixture of different *E*/*Z*-isomers of the corresponding starting materials in each case (entry 1-3).[42] This indicates that the used photocatalyst has the suitable triplet energy in order to activate the tested substrate. In general, the *cis-trans* inversion about the reactive double bond is faster than the cyclization. By irradiation, a quasistationary state is generated between both geometric isomers and from the excited intermediate, the cyclization takes place.[43] However, one prerequisite for cyclization is the spatial proximity of the two double bonds to one another. Finally, the *tert*-butyl compound **153d** took part in this visible light mediated [2+2] photocycloaddition giving rise to 60% of cyclobutane-containing derivative **158d** with a diastereomeric ratio of 76 to 24. The bulkier *tert*-butyl group forces the amide-linked diene in the necessary conformation for the cycloaddition.

In 1976, Weber *et al.*[44] already observed the corresponding [2+2] cycloadduct as byproduct in the thermolysis of benzyl substituted cinnamyl cinnamide. Its structure was later also confirmed by a UV-mediated [2+2] cycloaddition yielding 50%. More recently, Mykhailiuk and coworkers irradiated benzyl substituted amide-linked dienes at 366 nm and in the presence of acetophenone as photosensitizer. The achieved [2+2] photocycloaddition served as key step in the synthesis towards 3-azabicylo-[3.2.0]-heptanes which are attractive building blocks for drug discovery.[45]

In conclusion, the energy transfer mechanism is the suitable pathway to generate the desired bicyclic target molecules **158**. Furthermore, the [2+2] photocycloaddition occurs only when the substituent is large enough to bring the two affected double bonds close to each other (Scheme 38).

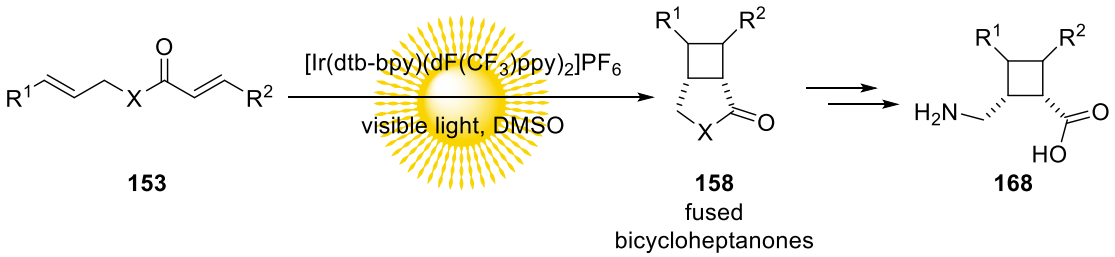

Scheme 38. The envisioned strategy towards the synthesis of γ-cyclobutane amino acids.

In the following chapters, the focus lied on the photochemical investigation of *N*-*tert*-butyl-, *N*-Boc- and *N*-benzyl-protected dienes **153** and their transformation towards γ-cyclobutane amino acids **168**.

2 Synthesis of precursors for [2+2] photocycloaddition

2.1 Synthesis of amines

In general, amine derivatives **170** were prepared *via* a S_{N2} reaction of allyl bromide **169** with the corresponding primary amine (Table 8). The used bromides were either commercially available or synthesized according to literature known procedures. For the coupling step an optimized procedure of Buchholz *et al.*[46] was applied. On this occasion, the bromide derivative **169** was treated with 3 equivalents of K_2CO_3 and the same amount of primary amine. Except for compound **170a**, which was prepared according to a procedure of Ballmann *et al.*[47] In this case no additional base was necessary.

Table 8. Synthesis of allylamines.

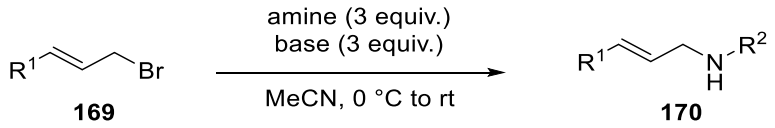

entry	R^1	169	amine	base	time [h]	R^2	product	yield [%]
1[a)]	H	**a**	*tert*-butyl amine	-	17	*tert*-butyl	**170a**	90
2	Ph	**b**	*tert*-butyl amine	K_2CO_3	27	*tert*-butyl	**170b**	95
3	4-MeOPh	**c**	*tert*-butyl amine	K_2CO_3	16	*tert*-butyl	**157**	40
4	CO_2Me	**d**	*tert*-butyl amine	K_2CO_3	21	*tert*-butyl	**170c**	91
5	H	**a**	benzylamine	K_2CO_3	21	benzyl	**170d**	54
6	Ph	**b**	benzylamine	K_2CO_3	19	benzyl	**170e**	92

[a)] 10 equivalents of amine.

In addition, the Boc-protected amine derivatives were prepared. In the presence of $LiAlH_4$ and $AlCl_3$ nitril **171** was reduced to amine **172** which was subsequently Boc-protected using a general procedure with a catalytic amount of DMAP (Scheme 39).[19,48]

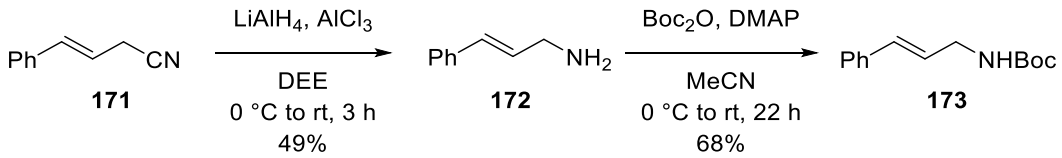

Scheme 39. Synthesis of the phenyl substituted and Boc-protected amine derivative **173**.

Allylamine **174** was protected by using Boc-anhydride and triethylamine as base to give compound **175** in a yield of 90% (Scheme 40).[49]

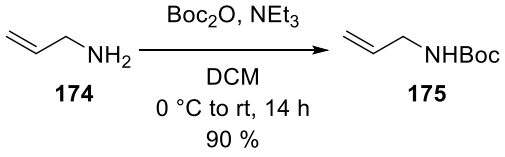

Scheme 40. Protection reaction of allylamine **174**.

2.2 Synthesis of acids

In accordance with a procedure of Worral *et al.*,[50] monomethyl fumarate **177** was synthesized by the reaction of maleic anhydride **75** with methanol followed by the isomerization of the *Z*-intermediate **176** with the help of acetyl chloride (Scheme 41).

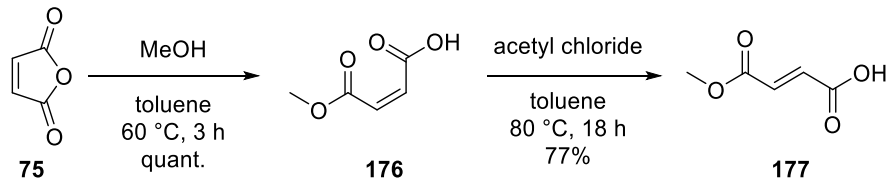

Scheme 41. Synthesis of monomethyl fumarate **177**.

Another goal was the preparation of *trans*-heterocyclic-propenoic acids **180** (Scheme 42). The heterocyclic aldehydes **178** underwent a Knoevenagel condensation to give the α,β-unsaturated acid **180** in the case of furane and thiophene in good yields.[51] However, using pyrrole-carbaldehyde **178c** led only to a total polymerization of the reaction mixture.

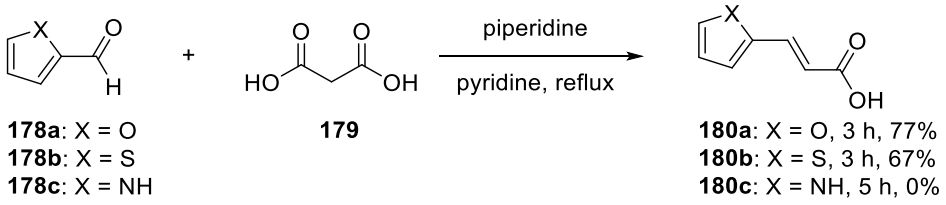

Scheme 42. Synthesis of 3-substituted acrylic acids **180**.

Therefore, the pyrrole-2-carbaldehyde **178c** was transformed into the corresponding ethyl ester derivative **181a** by a Horner-Wadsworth-Emmons reaction. Subsequent saponification with LiOH led to the desired pyrrole acrylic acid **180c** (Scheme 43).[52]

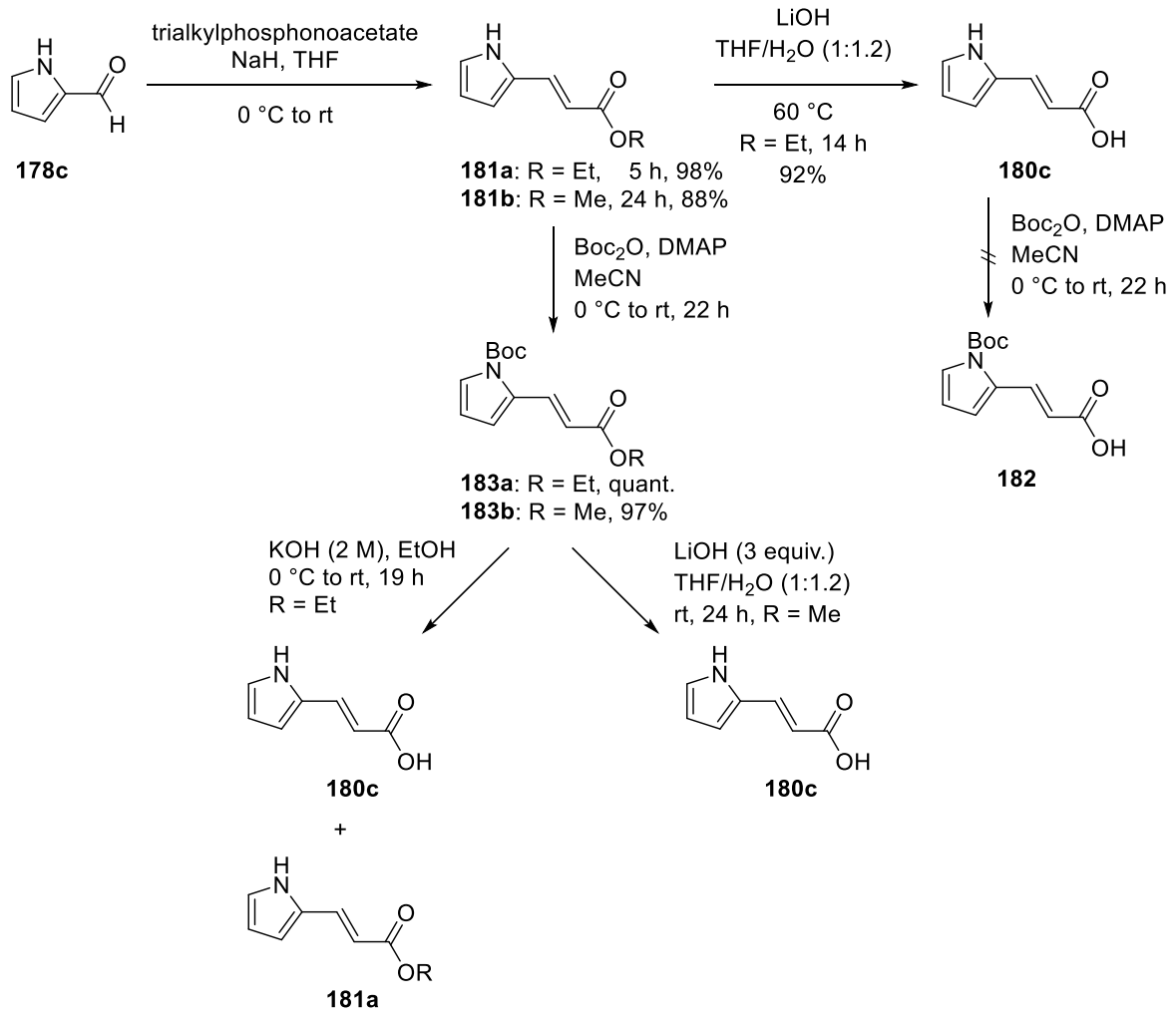

Scheme 43. Studies towards the synthesis of a suitable pyrrole-containing acid derivative.

Since a direct coupling between acid **180c** and amine **170a** to the corresponding amide-linked diene failed, investigations were ongoing to prepare a *N*-protected compound **182**.

The subsequent Boc-protection of compound **180c** led only to a polymerization of the starting material. Because of this, the desired compound **182** should be synthesized by protecting the ester intermediates **181a** and **181b** followed by an ester hydrolysis. Compound **183a** and **183b** were generated quantitatively and in 97% yield, respectively. Unfortunately, under basic conditions also a cleavage of the protecting group was observed. Avoiding this side reaction an acetyl group was chosen as next potential protecting group (Scheme 44).

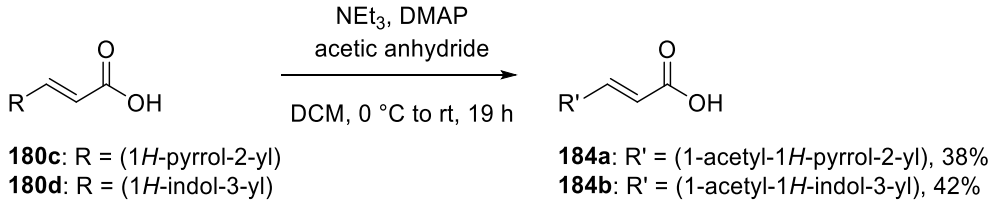

Scheme 44. Acetylation of *trans*-propenoic acid derivatives **180c** and **180d**.

The acetyl group was introduced by reacting acid derivative **180c** and **180d** with acetic anhydride in the presence of NEt_3 and DMAP.[53] Herein the desired *N*-heterocycle-containing acid derivatives **184a** and **184b** could be synthesized in moderate yield.

2.3 Synthesis of amide-linked dienes

With required acid and amine compounds in hand, a variety of amide-linked dienes **153** could be prepared (Table 9). Either the *in situ* generated or the commercially available acid chlorides **186** were reacted with the amine derivatives **187** which were previously deprotonated by NEt_3.

Table 9. Synthesis of the amide-linked dienes **153**.

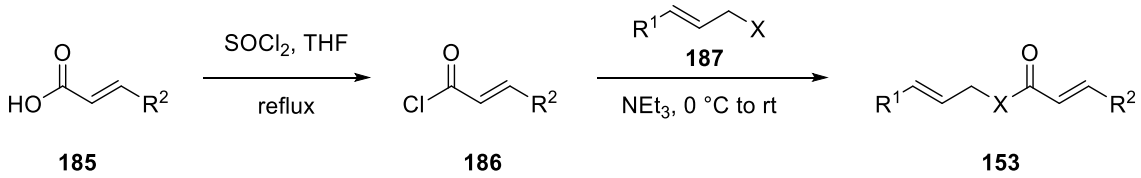

entry	R^1	X	R^2	153	time [h]	yield [%]
1	Ph	*N*-H	Ph	**e**	26	72
2	Ph	*N*-H	H	**f**	24	99
3	Ph	*N*-*tert*-butyl	Ph	**g**	16	71
4[a)]	4-MeOPh	*N*-*tert*-butyl	Ph	**d**	21	56
5	H	*N*-*tert*-butyl	Ph	**h**	19	38
6	Ph	*N*-*tert*-butyl	H	**i**	24	85
7	H	*N*-*tert*-butyl	H	**j**	24	74
8	H	*N*-*tert*-butyl	2-furanyl	**k**	20	61
9	H	*N*-*tert*-butyl	2-thiophenyl	**l**	19	66
10	H	*N*-*tert*-butyl	*N*-acetyl-3-indolyl	**m**	26	6
11	H	*N*-*tert*-butyl	*N*-acetyl-2-pyrrolyl	**n**	24	0
12	CO_2Me	*N*-*tert*-butyl	Ph	**o**	19	44
13	Ph	*N*-*tert*-butyl	CO_2Me	**p**	19	0
14	Ph	*N*-benzyl	Ph	**q**	24	59
15	H	*N*-benzyl	Ph	**r**	24	71
16	Ph	*N*-benzyl	H	**s**	19	61
17[b)]	Ph	*N*-Boc	Ph	**t**	20	38
18[b)]	Ph	*N*-Boc	H	**u**	21	traces
19[b)]	H	*N*-Boc	Ph	**v**	19	52
20	Ph	O	Ph	**w**	24	79

[a)] Results are listed again for completeness. [b)] KHMDS was used as base instead of NEt_3.

Using the pyrrole-containing acid **184a** the reaction mixture turned black and all the starting material decomposed (entry 11). In entry 13, the monomethyl fumaric acid **177** reacted with the allylamine derivative **170b** in a [4+2] manner followed by a [1,3]-*H*-shift to achieve rearomatization (Scheme 45). The structure of the tricycle **189** was verified *via* X-ray analysis.

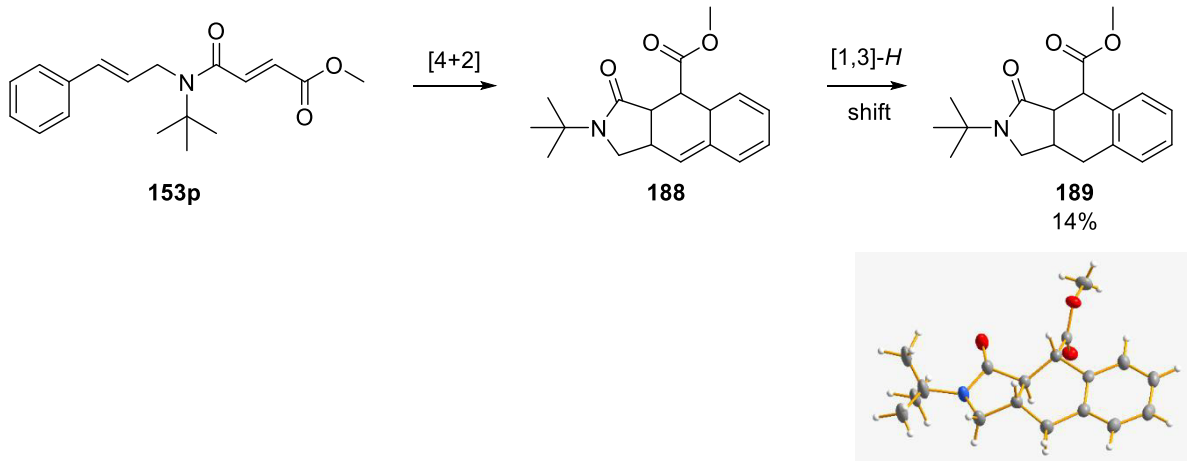

Scheme 45. [4+2] cycloaddition of compound **153p**, followed by [1,3]-*H*-shift.

In the case of Boc-protected amines (entry 17-19), KHMDS was used as base for the deprotonation since it is more basic than NEt_3.[54] In order to improve the yield of compound **153t** and **153u**, the unsubstituted derivatives **153e** and **153f** were Boc-protected giving rise to 85% of compound **153t** and 84% of compound **153u**.[55] All in all, the amide-linked dienes **153e-v** as well as the only ester-linked compound **153w** could be generated in moderate to good yields.

3 Theoretical studies towards the reaction mechanism of [2+2] photocycloaddition of amide-linked dienes

The photochemical investigation of the different substituted amide-linked dienes **153** revealed that an appropriate substituent that occupies a certain space is necessary to direct both double bonds in spatial proximity for a successful cyclization (Table 10).

Table 10. Screening of the substituents on the amide bond.[a)]

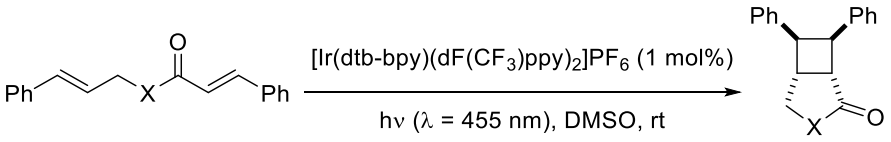

153 **158**

entry	X	153	time [h]	158	yield [%]
1	*N*-H	**e**	48	**e**	-
2	*N*-Me	**a**	48	**a**	-
3	*N*-Ph	**b**	48	**b**	-
4	*N*-*tert*-butyl	**g**	3	**g**	79 (*dr*[a)] 81/19)

[a)] 1 mmol substrate (0.04M in DMSO), 1 mol% [Ir(dtb-bpy)(dF(CF$_3$)ppy)$_2$]PF$_6$. [b)] Diastereomeric ratio was estimated by crude ^{1}H-NMR.

Applying an unsubstituted derivative **153e**, a methyl **153a** or a phenyl substituent **153b** led to an *E-Z* isomerization of the double bond moieties in the used dienes. However, testing the *tert*-butyl-protected derivative **153g** gave the desired cyclobutane compound **158g** in a yield of 79% within 3 h irradiation time. It seemed that the bulkier *tert*-butyl group forces the amide-linked diene in the necessary conformation for a successful cycloaddition.

In order to get a deeper look in the reaction mechanism a cooperation with the group of Prof. J. Rehbein whose research is mainly focused on reaction dynamics was started. The theoretical calculations were carried out by Simon Malcherek (PhD student of AK Rehbein). Since the experimental data suggested a preference for large substituents, the calculations were performed for the limiting cases. The *tert*-butyl derivative **153g** served as model substrate possessing a large substituent whereas the unprotected derivative **153e** as one having a small substituent.

Table 11. Analysis of the stationary points.

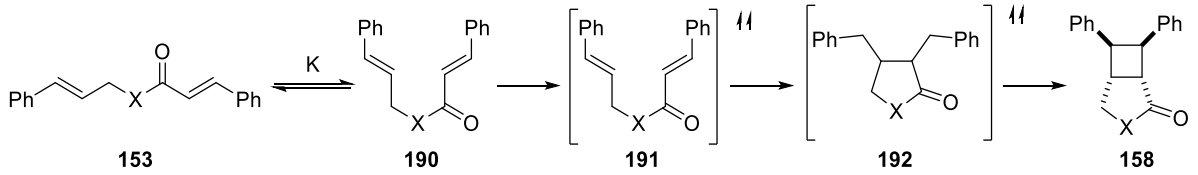

entry	LOT	X	K	$\Delta G^{\neq}$ [kcal/mol]	$\Delta_R G$ [kcal/mol] ^{3}NAC 191 - ^{3}intermediate (*cis*) 192	$\Delta_R G$ [kcal/mol] ^{1}NAC 190 – ^{1}product (*cis*) 158
1	B3LYP/ 6-311+G**	*N*-H **153e**	$2.2 \cdot 10^{-4}$	11.5	-15.0	5.6
2		*N-tert*-butyl **153g**	67.7	7.7	-22.9	-1.2
3	B3LYP-D3/ 6-311+G**	*N*-H **153e**	$5.4 \cdot 10^{-3}$	7.9	-17.4	+0.8
4		*N-tert*-butyl **153g**	133.0	5.2	-25.0	-6.1

The reaction constant (K) showed, that in the case of the *tert*-butyl derivative **153g** the near attack conformation (NAC) **190** of the diene is preferred whereas having a proton as substituent the linear conformation **153e** predominates. In the following, the reaction can be described as a two-step process. First, the substrate is activated by the triplet sensitizer whose triplet energy suits the calculated energy gap between singlet and triplet state of the substrate. After excitation to the triplet excited state **191**, the first elementary step is the formation of intermediate **192** followed by the generation of the bicyclic compound **158**. Activation barrier of the elemental step $\Delta G^{\neq}$ from ^{3}NAC **191** to ^{3}intermediate **192** is 2.7 kcal/mol higher for X = *N*-H than for X = *N-tert*-butyl. Therefore, a higher reaction rate for compound **153g** would be obtained. The overall reaction from ^{1}NAC **190** to ^{1}product **158** is exothermic for compound **153g** (-6.1 kcal/mol), whereas for compound **153e** close to neutral (+ 0.8 kcal/mol).

The level of theory (LOT) expended with Grimmes Dispersion Correction (D3) considered also the interactions in the molecule. Since there are differences in the relative energy values

between both methods (Table 11) and therefore a clear effect of dispersion exists, the dispersion correction was maintained in the following.

For a deeper insight, the correlation between the activation barrier $\Delta G^{\neq}$ and thermodynamic properties $\Delta_R G$ was investigated and the intrinsic barrier $\Delta G_0^{\neq}$ was calculated. Therefore, the Marcus-analysis[56] was applied for the first reaction step, the formation of intermediate **192** (Table 12).

Table 12. Marcus-analysis of the first reaction step.

$$\Delta G^{\ddagger} = \Delta G_o^{\ddagger} + 0.5\,\Delta_R G + \frac{\Delta_R G^2}{16\Delta G_0^{\ddagger}}$$

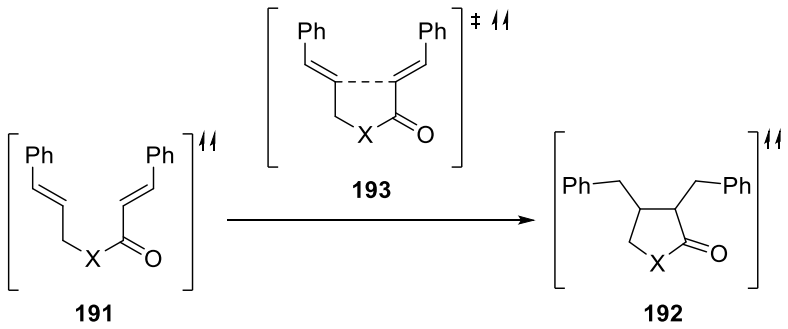

entry	X	conformation intermediate	$\Delta G^{\neq}$ [kcal/mol]	$\Delta G_0^{\neq}$ [kcal/mol]	$\Delta_R G$ [kcal/mol]
1	*N*-H **191a**	*cis*	+7.9	+15.6	-17.4
2	*N*-*tert*-butyl **191b**	*cis*	+5.2	+15.1	-25.0

The intrinsic contribution to the activation barrier, $\Delta G_0^{\neq}$, is quite the same in both cases (Δ = 0.5 kcal/mol). The most significant difference between both substrates seems to be the thermodynamic one, $\Delta_R G$. The reaction step is in the case of the *tert*-butyl derivative **191b** 7.6 kcal/mol more exothermic than having a proton as substituent.

For further investigation of the transition state, the bonding situation in accordance with Pauling[57] was examined using a factor of 0.6 (suggested for transition states) (Table 13).

Table 13. Pauling-analysis of the first elemental step, c = 0.6.

$$n_x = n_0 e^{\frac{r_0 - r_x}{c}}$$

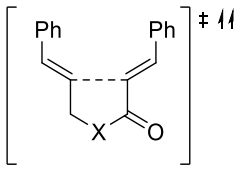

193

entry	X	distance in TS [Å]	reference [Å]	bond order
1	*N*-H **193a**	2.56	1.58	0.20
2	*N*-*tert*-butyl **193b**	2.69	1.57	0.15

The bonding situation according to Pauling resembled the starting material more than the products. The *tert*-butyl substituted transition state **193b** has a bond order of 15% whereas the unsubstituted one **193a** a slightly higher bond order of 20%. Therefore, the *H*-substituted transition state **193a** has a slightly more established bond (Δ = 5 %) compared to *tert*-butyl one **193b**.

Moreover, the Bell-Evans-Polanyi principle[58] shows that the difference in activation energy of two reactions of the same family is proportional to the difference in their reaction enthalpy: $E_\propto = E_0 + \propto \Delta H$. A significant parameter is herein α which characterize the transition state along the reaction coordinate. For large substituents an earlier, lower transition state (TS) is achieved, whereas for small substituents a later, higher TS. In context of the Bell-Evans-Polanyi principle, the results from the Marcus-analysis and Pauling-analysis suggest a preference of the *tert*-butyl derivative **153g** in this reaction type over the unsubstituted derivative **153e**.

In conclusion, all investigated features (stationary points, energy barriers, nature of transition state) prefer the [2+2] cycloaddition of derivatives with large substituents (see Figure 19 and Figure 20 in E Experimental Part, chapter 3). The main differences have been observed for the overall thermodynamic driving force of the overall reaction being exothermic for X = *N*-*tert*-butyl and endothermic for X = *N*-H. Additionally, the steric arrangement of the starting material: a large substituent force the diene into its near attack conformation (NAC) while having a less spatial demanding substituent the linear conformation is preferred. The combination of Marcus-, Pauling-analysis as well as the Bell-Evans-Polanyi principle described

well the essential steps of the reaction and explained the better driving force for the *tert*-butyl substituted dienes. Overall the computational data were in good agreement with the experimental observations.

4 Optimization of reaction conditions of [2+2] photocycloaddition

For the optimization of the reaction conditions of [2+2] photocycloaddition different photocatalysts, light sources and reaction temperature were tested (Table 14).

Table 14. Screening of different reaction conditions for the [2+2] photocycloaddition.[a)]

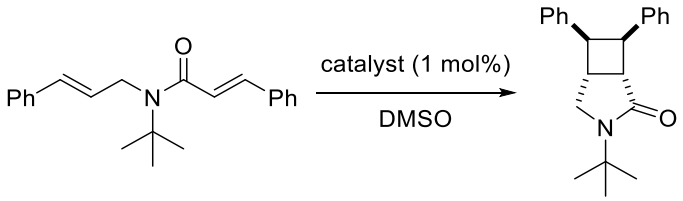

153g **158g**

entry	catalyst	time [h]	T	light source	conv. [%]	yield [%] (*dr* a/b)[c)]
1	[Ir(dtb-bpy)(dF(CF$_3$)ppy)$_2$]PF$_6$	48	rt	CFL	100	64 (*dr* 81/19)
2	*fac*-Ir(ppy)$_3$	48	rt	CFL	100	57 (*dr* 82/18)
3	Ir[(dtb-bpy)ppy$_2$]PF$_6$	48	rt	CFL	0	0
4	[Ir(dtb-bpy)(dF(CF$_3$)ppy)$_2$]PF$_6$	6.5	rt	blue LED	100	75 (*dr* 81/19)
5	*fac*-Ir(ppy)$_3$	20.5	rt	blue LED	100	88 (*dr* 83/17)
6	Ir[(dtb-bpy)ppy$_2$]PF$_6$	48	rt	blue LED	86	67 (*dr* 83/17)
7	[Ir(dtb-bpy)(dF(CF$_3$)ppy)$_2$]PF$_6$	3	rt	blue LED-stick	100	79 (*dr* 82/18)
8	[Ir(dtb-bpy)(dF(CF$_3$)ppy)$_2$]PF$_6$	3	40 °C	blue LED-stick	100	84 (*dr* 81/19)

entry	catalyst	time [h]	T	light source	conv. [%]	yield [%]
9	*fac*-Ir(ppy)$_3$	3	rt	blue LED-stick	100	75 (*dr* 82/18)
10	*fac*-Ir(ppy)$_3$	3	40 °C	blue LED-stick	100	80 (*dr* 83/17)
11[b)]	-	90	rt	HP Hg-lamp	100	74 (*dr* 80/20)
12	-	24	40 °C	-	0	0
13		24	40 °C	blue LED-stick	0	0

[a)] 1 mmol substrate (0.04M in DMSO), 1 mol% catalyst, 40 °C. [b)] 1 mmol substrate (0.1M in acetone). [c)] Diastereomeric ratio was estimated by crude ^{1}H-NMR.

The photocatalyst possess decreasing emissive energy in the following series: [Ir(dtb-bpy)(dF(CF$_3$)ppy)$_2$]PF$_6$ (E_T = 61 kcal/mol)[59], *fac*-Ir(ppy)$_3$ (E_T = 55 kcal/mol)[60] and [Ir(dtb-bpy)ppy$_2$]PF$_6$ (49 kcal/mol)[61]. [Ir(dtb-bpy)(dF(CF$_3$)ppy)$_2$]PF$_6$ with the highest energy value was the most efficient sensitizer in this experimental raw. Furthermore, the reaction time was highly affected by the used light source. Three different irradiation setups were tested as shown in figure 5.

Setup with CFL (**A**)

Setup with six blue LEDs on a plate (**B**)

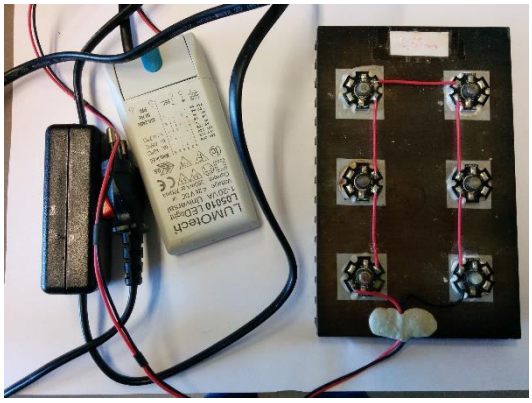

Setup with blue LED-Stick (**C**)

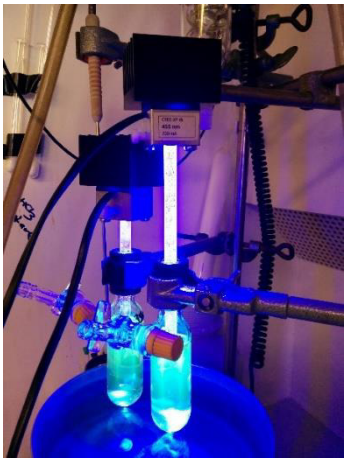

Figure 5. Different light sources.

The irradiation *via* fluorescent household bulb was structured as followed: the light source was put approximately 15 cm away from the reaction flask (Figure 5 **A**). The compact fluorescent light bulb has several emission maxima (Figure 6), whereas the plate with six high power LEDs as well as LED-stick has an emission maximum at a wavelength of 455 nm.

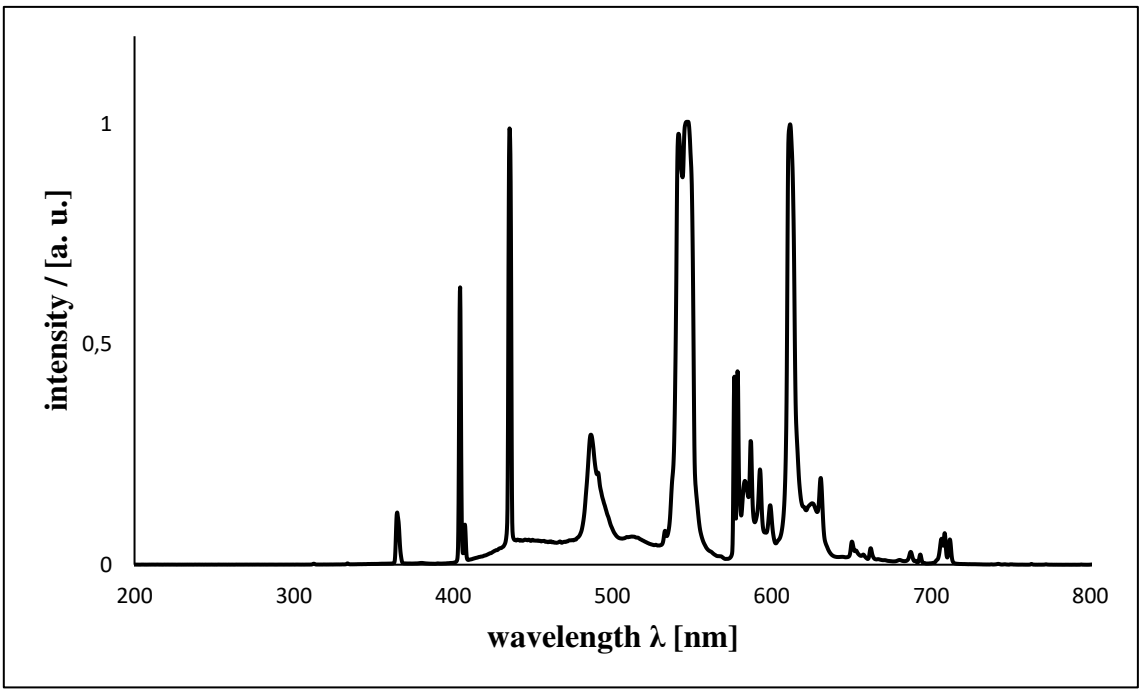

Figure 6. The emission spectrum of CFL.[8]

The advantages of using LED-containing lighting devices are the narrow emission peak at a specific wavelength, in this case $\lambda = 455$ nm, higher light intensities and a more efficient energy transfer. A common irradiation setup is built up by a suitable vessel equipped with the reaction mixture and an external lighting device, as the LED-plate which were put below the round bottom flask (Figure 5 **B**). Dr. Peter Kreitmeier, member of the group of Prof. O. Reiser, improved the irradiation in this respect that the light generated by a LED is channelled through a glass rod directly in the reaction mixture (Figure 5 **C**). In this manner, the light scattering on the glass wall of the reaction vessel can be circumvented and therefore more emitted photons can excite the used photocatalyst. This issue was verified by the done optimization reactions (Table 14). The direct irradiation *via* an optical fibre allowed the best results in comparison with the external lighting devices (entry 1 *vs* 4 *vs* 7). Direct excitation with the used light sources is not possible since the absorption maximum of substrate **153g** has a value of $\lambda = 256$ nm (Figure 7).

[8] Emission spectrum was measured by Simon Düsel (PhD student of Prof. B. König) using a Radiometer/Photometer (ILT 1400 by NIST Traceable Light Measurement Systems & Sources).

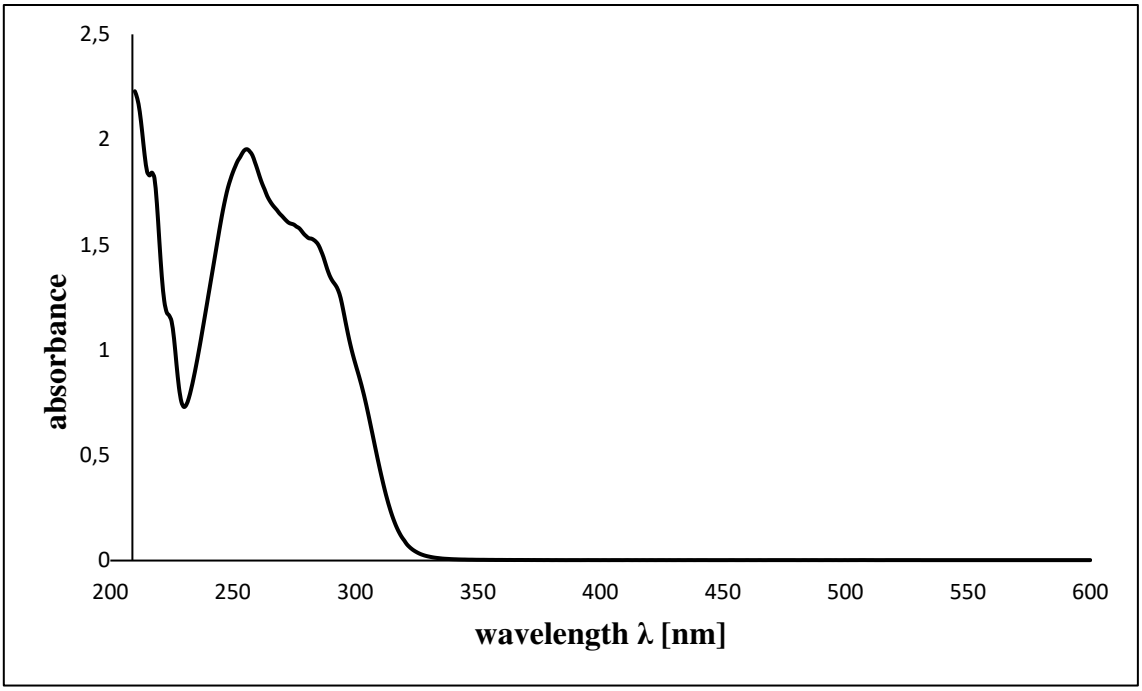

Figure 7. The absorption spectrum of substrate **153g**.[9]

By UV irradiation by a 125 W Phillips high-pressure mercury lamp full conversion was achieved by increased reaction time of 90 h and only 74% of the desired product **158g** was achieved compared to using visible light (entry 7). The control experiments (entry 12, 13) showed, that the [2+2] photocycloaddition occurred only in the presence of light and photocatalyst. By increasing the reaction temperature to 40 °C the yield could be improved to 84% (entry 8).

To sum up, all further reactions for the investigation of the substrate scope were performed using 1 mmol substrate and 1 mol% $[Ir(dtb\text{-}bpy)(dF(CF_3)ppy)_2]PF_6$ in DMSO (0.04M substrate concentration) at 40 °C using the blue LED-stick-setup.

[9] Absorption spectrum was measured on a UV/Vis spectrometer (Specord(R) 200 Plus from Analytik Jena).

5 Substrate scope of the [2+2] photocycloaddition

The previously synthesized *N*-*tert*-butyl, *N*-benzyl and *N*-Boc-protected amide derivatives **153** cyclize to the cyclobutane-containing compounds **158** in moderate to good yields with an excellent diastereoselectivity by applying the optimized reaction conditions (table 15).

Table 15. Substrate scope of the [2+2] photocatalyzed cycloaddition.[a)]

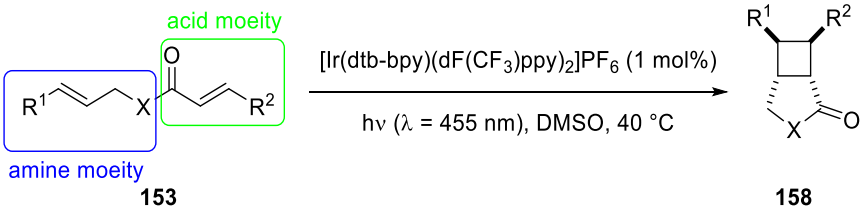

153 **158**

entry	R^1	X	R^2	158	time	yield [%] (dr a/b)[b)]
1	Ph	*N*-*tert*-butyl	Ph	**g**	3 h	85 (*dr* 81/19)
2	4-MeOPh	*N*-*tert*-butyl	Ph	**d**	7 h	63 (*dr* 72/28)
3	Ph	*N*-benzyl	Ph	**f**	4 h	75 (*dr* 77/23)
4	Ph	*N*-Boc	Ph	**h**	24 h	61 (*dr* 78/22)
5	Ph	*N*-*tert*-butyl	H	**i**	3 h	78 (*dr* 83/17)
6	Ph	*N*-benzyl	H	**j**	4 h	72 (*dr* 85/15)
7	Ph	*N*-Boc	H	**k**	48 h	73 (*dr* 81/19)
8	CO_2Me	*N*-*tert*-butyl	Ph	**l**	48 h	67 (*dr* 76/24)
9	H	*N*-*tert*-butyl	Ph	**m**	23 h	60
10	H	*N*-benzyl	Ph	**n**	19 h	83 (*dr* 93/7)
11	H	*N*-Boc	Ph	**o**	14 d	47
12	H	*N*-*tert*-butyl	2-furanyl	**p**	3 h	73
13	H	*N*-*tert*-butyl	2-thiophenyl	**q**	3 h	78
14	H	*N*-*tert*-butyl	*N*-acetyl-3-indolyl	**r**	48 h	35
15	H	*N*-*tert*-butyl	H	**s**	48 h	0
16[c)]	Ph	O	Ph	**t**	48 h	29 (*dr* 72/28)

[a)] 1 mmol substrate (0.04M in DMSO), 1 mol% $[Ir(dtb\text{-}bpy)(dF(CF_3)ppy)_2]PF_6$, 40 °C. [b)] Diastereomeric ratio was estimated by crude ^{1}H-NMR. [c)] 80 °C reaction temperature.

Depending on the location of the phenyl group on the involved double bonds, the reaction times varied dramatically. If the aromatic substituent is placed on the amine moiety (R^1) the [2+2] photocycloaddition is done within 3 h (entry 5) and 4 h (entry 6), respectively. Whereas in the case of the contrary starting material the [2+2] photocycloaddition takes longer 23 h (entry 9) and 19 h (entry 10). Using the Boc group as substituent also longer reaction times for the cyclization steps are necessary which is obviously caused by additional electronic effects of this protecting group. This is most clearly reflected in entry 11 where full conversion has been only reached after 14 d. After 48 h, only *E*-*Z* photoisomerization of compound **153v** was observed yielding to a diastereomeric ratio of 35 to 65 wherein the less stable *Z*-isomer predominates. In contrast to ground-state reactivity where rotation about the $C(sp^2)=C(sp^2)$ bond is hindered by high rotational barriers, it is known that the photochemical mode can circumvent this constraint either by direct excitation or by involving a photosensitizer. The photoisomerization is an ever-present competitive reaction when the olefinic bonds are of cinnamoylic character.[15,62] Increasing the catalyst amount to 2.5 mol% or applying UV-light irradiation in combination with acetone as sensitizer did not expedite the [2+2] photocycloaddition of compound **153v**. The electron rich heterocycles furan and thiophene on the carbonyl side accelerated the photochemical reaction in contrast to the phenyl substituent (entry 12, 13). Additionally, if the aromatic substituent is located on the carbonyl side (R^2) a better diastereoselectivity was achieved. Either only one diastereomer (entry 9, 11, 12-14) was obtained or in the case of the benzylated compound (entry 10) an excellent diastereoselectivity of 93 to 7 was determined.

The [2+2] photocycloaddition of tethered dienes **153** possessing two aromatic substituents (entry 1-4, 16) resulted in an inseparable diastereomeric mixture whereas having only one aromatic substituent has the advantage that both generated diastereomers could be isolated from each other (entry 5-7). In the structure of the diaryl-substituted main diastereomers, both phenyl groups are in *cis*-conformation what was clearly proven by X-ray crystallography of substrate **158ha** (Figure 8).

Figure 8. X-ray structure of compound **158ha**.

Major diastereomers of the monosubstituted compounds are the *trans*-derivatives whereas the minor diastereomers are the *cis*-isomers. For instance, the *trans*-configuration was manifested by X-ray structure of major compound **158ka** and the minor diastereomer was confirmed to be the *cis*-derivative by X-ray analysis of compound **158ib** (Figure 9).

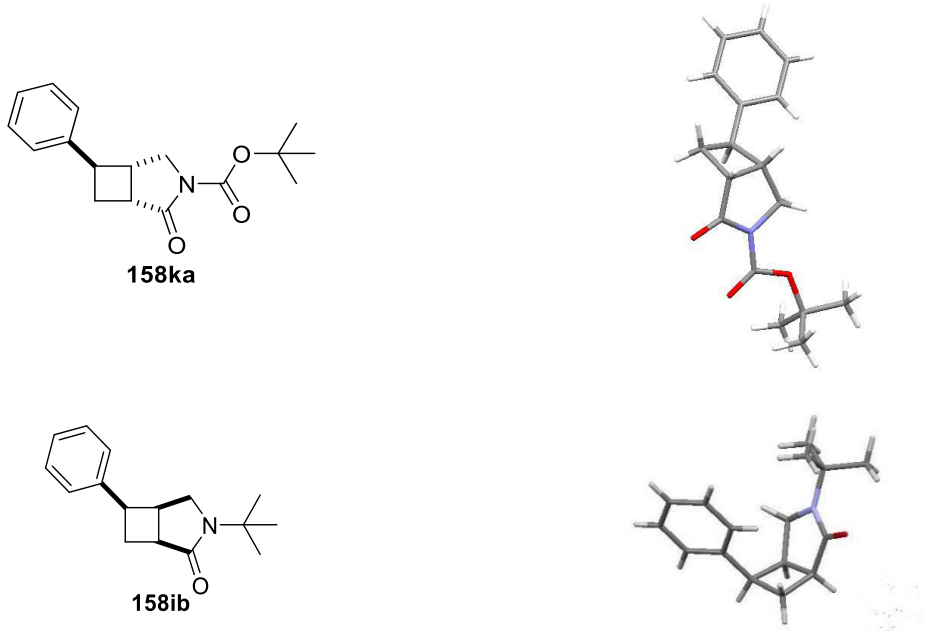

Figure 9. Exemplarily X-ray structures of major diastereomer **158ka** and minor diastereomer **158ib**.

In the case of the ester-linked derivative **153w,** the cyclobutane **158t** was only synthesized in a yield of 29% by increasing the reaction temperature to 80 °C. The low yield, as well as the need for higher temperatures, can be explained by the favorable *S-cis* conformation of the ester moiety as previously discussed in chapter 1.2.[63]

The azabicycloheptanones **158** were synthesized in moderate to good yields with good diastereoselectivity. In general, a suitable substituent of the amide bond is necessary for a successful [2+2] cycloaddition as well as at least one aromatic substituent on one of the double bonds (entry 15) what is consistent with previous observations.

6 Upscaling of the [2+2] photocycloaddition

Since the resulting bicycles **158** should be converted into the corresponding γ-cyclobutane amino acids in the further course, the azabicycloheptanones **158** should be able to be prepared in sufficient quantity. The starting material **153i** was prepared on a multigram scale within two steps without purification in-between in a good overall yield of 91%, about 27 g. Subsequently, investigations were started towards the appropriate amount of catalyst and substrate concentration for a sufficient [2+2] cycloaddition in order to upscale this photochemical reaction (Table 16).

Table 16. Catalyst loading of the [2+2] photocycloaddition of compound **153i**.[a)]

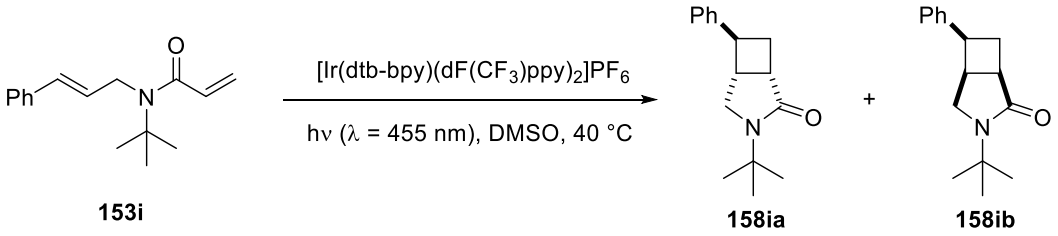

153i 158ia 158ib

entry	catalyst amount [mol%]	concentration of 153i [M]	time [h]	yield [%] (*dr* a/b)[b)]
1	1	0.04	3	78 (*dr* 83/17)
2	0.5	0.04	3	73 (*dr* 82/18)
3	0.5	0.08	3	75 (*dr* 83/17)
4	0.1	0.04	5	80 (*dr* 83/17)
5	0.1	0.16	5	79 (*dr* 84/16)
6	0.01	0.16	48	41 (*dr* 83/17)
7	0.05	0.16	43	56 (*dr* 84/16)

[a)] Irradiation with 1 W LED (λ = 455 nm). [b)] Diastereomeric ratio was estimated by crude ^{1}H-NMR.

The screening revealed that the most suitable result was obtained by applying 0.1 mol% of catalyst with a substrate concentration of 0.16M giving rise to 79% of the cyclobutane-containing product **158i**. A further decrease of catalyst amount led to a prolonged reaction time and concurrently the yield dropped to 41% and 56%, respectively (entry 6/7).

For the reactions on large scale, a reactor was developed adopting the principle of an immersion shaft exposure unit which is generally used for UV irradiation (Figure 10).

Figure 10. Setup of an immersion shaft exposure unit.

The apparatus was equipped with 30 blue LED units (λ_{max} = 455 nm) and an additional water cooling since LED lights despite their low energy consumption generate significant heat. Depending on the used reaction vessel the [2+2] photocycloaddition could be performed either with 200 mL or 600 mL volume capacity. The reaction was up-graded stepwise (Table 17).

Table 17. Upscaling of the [2+2] photocycloaddition.

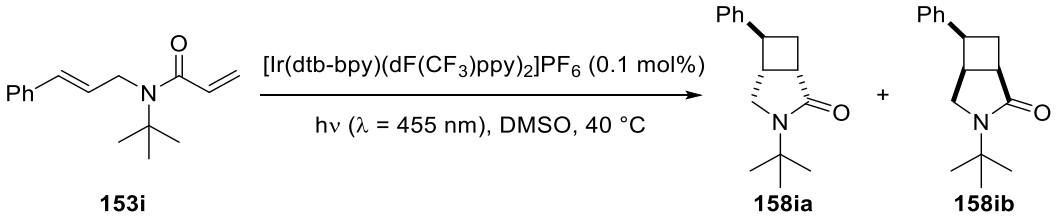

153i 158ia 158ib

entry	amount of 153i [mmol]	concentration of 153i [M]	time	conv. [%]	yield [%] (*dr* a/b)[a]
1[b]	1	0.040	5 h	100	80 (*dr* 83/17)
2[c]	10	0.040	18 h	100	58 (*dr* 83/17)
3[c]	30	0.046	24 h	100	67 (*dr* 83/17)
4[c]	110	0.169	7 d	95	70 (*dr* 81/19)

[a] Diastereomeric ratio was estimated by crude ^{1}H-NMR. [b] Irradiation with one LED (1 W, λ = 455 nm). [c] Irradiation with 30 LEDs (each 1 W, λ = 455 nm).

Converting 10 mmol or 30 mmol starting material **153i** 58% or 67% of the cyclobutane-containing compound **158i** was achieved, respectively. After 7 d a conversion of 95% of the used 110 mmol substrate **153i** was achieved and the [2+2] photocycloaddition gave 70% of the desired product **158i**. Due to the limitation of the applied photoapparatus especially the light power, the long reaction time and the incomplete conversion can be explained. However, the cyclobutane derivatives could be synthesized now on a multi-gram scale in order to have enough material for further studies towards the transformations into the corresponding amino acid derivatives.

7 Transformations of the bicyclic key intermediates into racemic γ-cyclobutane amino acids

7.1 Removal of the *tert*-butyl group

The cleavage of the *N*-*tert*-butyl protecting group is generally performed in acidic media. H_2SO_4[64], TFA[65] and TFMSA[66] were successfully applied to transform *N*-*tert*-butyl substituted amides or carbamates into the corresponding deprotected derivatives. Aqueous HCl was mainly used in the deprotection step of secondary[67] or tertiary[68] *N*-*tert*-butyl amine derivatives.

Chen *et al.*[69,70] reported in their synthesis of gabapentin **197** that the treatment of γ-lactam **195** with aqueous HCl led to an effective removal of the *tert*-butyl group and a simultaneous hydrolysis of the lactam ring (Scheme 46).

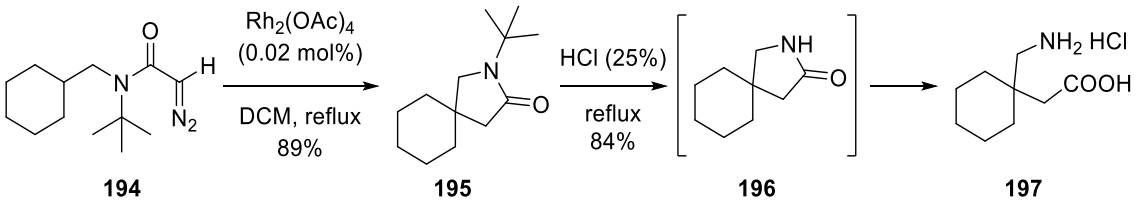

Scheme 46. A concise synthesis of gabapentin **197** *via* intramolecular C-H insertion reaction.[69]

To investigate different acidic conditions for the efficient removal of the *tert*-butyl group, the biphenyl derivative **158g** was chosen as model substrate (Table 18).

Table 18. Removal of the *tert*-butyl substituent.

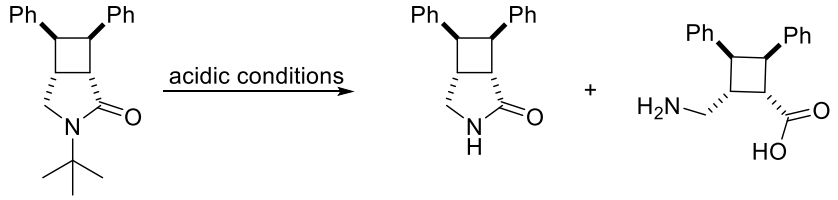

158g **158e** **198**

entry	conditions	T [°C]	time	yield
1	TFA	80	72 h	0% conv.
2	TFMSA	160	1 h	decomp.
3	96% H_2SO_4 (aq.)	55	24 h	0% conv.
4	25% HCl (aq.)	90	3 d	no full conv. **198** 34%
5	25% HCl (aq.)	90	5 d	100% conv. **198** 43%
6	25% HCl (aq.)/dioxane	90	24 h	traces of **198**
7	25% HCl (aq.)/AcOH	90	72 h	traces of **198**
8	HCl in EtOAc (4.2M)	0	5 d	0% conv.

Similar to the results observed by Chen and coworkers, applying trifluoroacetic acid, trifluoromethanesulfonic acid or sulfuric acid did not furnish the desired product **198** (entry 1-3). However, compound **198** was obtained in 34% yield by refluxing model substrate **158g** in 25% aqueous HCl (entry 4). To achieve full conversion of the starting material **158g** the reaction time was prolonged from 3 d to 5 d resulting in an improved yield of 43% (entry 5). During these investigations, it was observed that the bicyclic compound **158g** is slightly soluble in aqueous HCl. Therefore, the involvement of a cosolvent was examined. In the case of dioxane, a complex mixture was generated and only traces of **198** were formed (entry 6). The same result was achieved by using acetic acid as additional solvent (entry 7). For a better solubility, a solution of dissolved HCl gas in ethyl acetate (4.2M) was tested (entry 8). The starting material **158g** was completely dissolved but even after 5 d no conversion was detectable. Obviously, this reaction condition seemed to be too mild.

The substrate scope of this reaction was investigated for amides of type **158** by applying a 25% aqueous HCl under reflux for 5 to 6 days (Scheme 47).

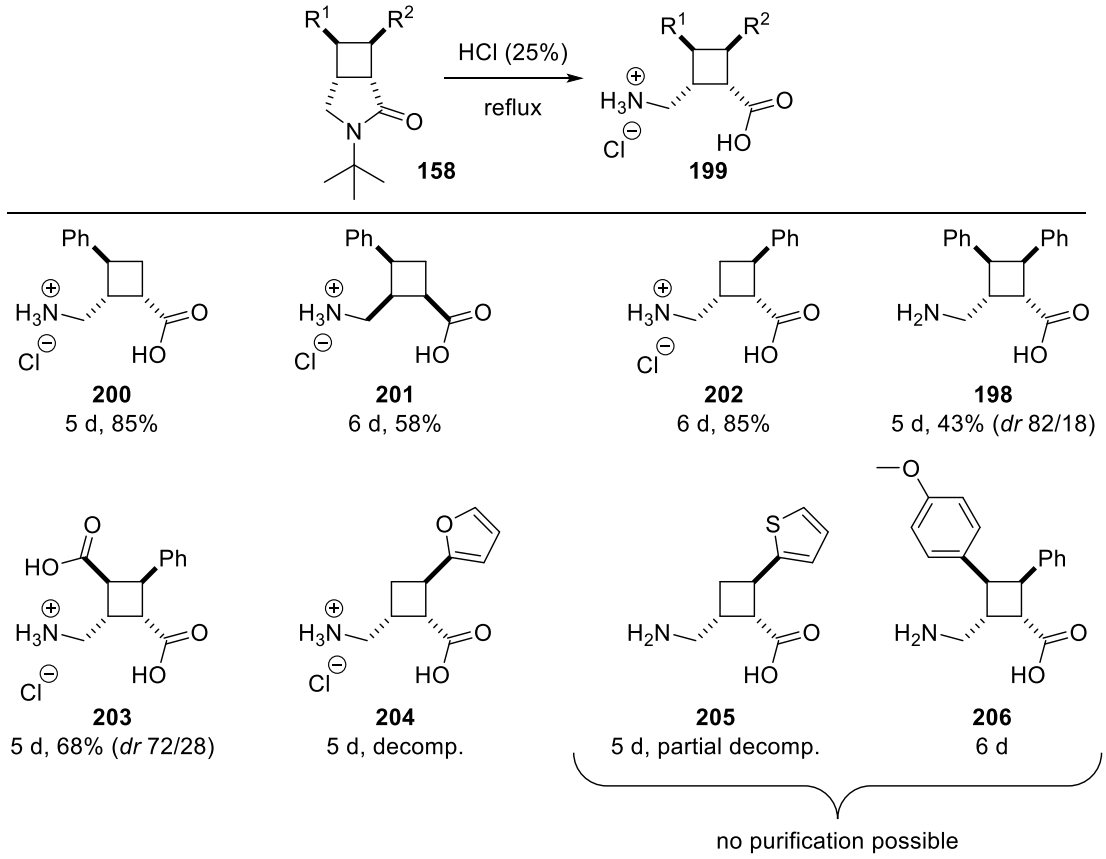

Scheme 47. Substrate scope of the *tert*-butyl removal.

Both single and double aryl-substituted derivatives **199** were synthesized in moderate to good yields. Moreover, an additional carboxylic acid group was also tolerated. It is notable, that either the chloride salt of the free amino acid or the free amino acid itself were obtained since some products required purification by an elution through an ion exchange resin (H^+-form). Treatment of ester derivative **158l** with 25% aqueous HCl led to a simultaneous cleavage of the *N*-*tert*-butyl group as well as the ester moiety. Exposure of compound **158p** and **158q** to this acidic condition led to a decomposition of the heterocyclic compounds. In the case of the thiophene derivative **158q**, a slight formation of compound **205** was observed but purification was not possible. In addition, compound **206** could not be isolated either.

The proposed mechanism for this reaction is shown in scheme 48. The first protonation causes an activation of the carbonyl group, followed by the release of *tert*-butyl cation and the formation of lactim derivative **209**. By a proton exchange, the unprotected lactam derivative **210** is obtained as well as *iso*-butene. A further acidic activation of the carbonyl moiety enables

the nucleophilic attack of water resulting in hydrate **213**. Finally, ring opening gives rise to free γ-cyclobutane amino acid **214.**

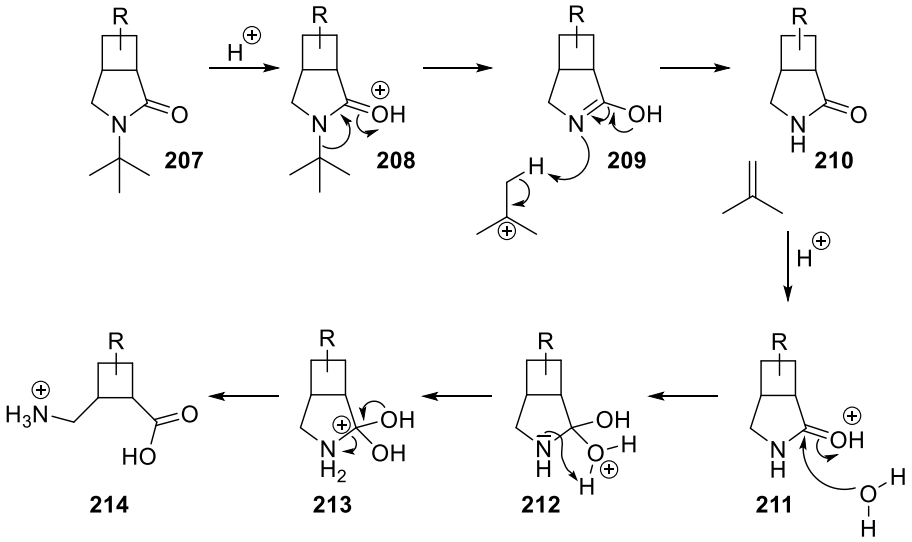

Scheme 48. The proposed reaction mechanism for the formation of the ring opening product **214**.

7.2 Studies towards debenzylation

The benzyl group is a frequently used protective group in organic synthesis and its removal is a well-researched area. The common deprotection method represents the palladium-catalyzed hydrogenation.[19] In the following, different reaction conditions were investigated to remove the benzyl group from compound **158f** (Table 19).

Table 19. Debenzylation of compound **158f**.

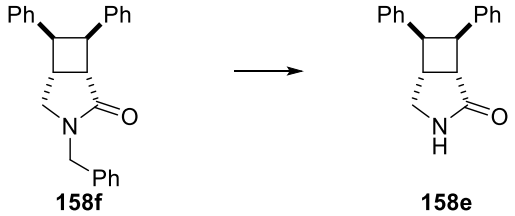

entry	conditions	T [°C]	time	yield
1	5 bar, AcOH, $Pd(OH)_2/C$	25	20 h	0% conv.
2	5 bar, AcOH, $Pd(OH)_2/C$	60	20 h	0% conv.
3	20 bar, AcOH, $Pd(OH)_2/C$	60	20 h	0% conv.
4[a)]	80 bar, H-cube, MeOH/AcOH (5:1) 10% Pd/C	80	0.5 mL/min	0% conv.
5	$AlCl_3$, benzene	0 to 25	20 h	0% conv.
6	MeLi, THF	-40	1 h	complex mixture
7	TFA, MW	210	20 min	decomp.
8	NMA, NBS, $CHCl_3$	rt	20 h	complex mixture
9[b)]	Na (10 equiv.), NH_3 (li.), *t*-BuOH	-33	1 h	complex mixture
10[b)]	Na (3.5 equiv.), NH_3 (li.), *t*-BuOH	-33	0.5 h	complex mixture

[a)] The total reaction volume was 5 mL. [b)] Complete debenzylation was detectable.

The first test reactions needing molecular hydrogen pressure from 5 to 20 bar were performed in an autoclave. Applying the Pearlman catalyst[71], $Pd(OH)_2$, and acetic acid as solvent under 5 bar hydrogen pressure at 25 °C did not result in debenzylation of starting material **158f** (entry 1). An increase in the reaction temperature to 60 °C (entry 2) and simultaneously the hydrogen pressure to 20 bar (entry 3) did not lead to any improvement. Thus, the hydrogenation was then performed in a heterogeneous catalytic flow hydrogenation system:

ThalesNano H-Cube Pro™[72] (entry 4). The advantages of this device are on the one hand the *in situ* generation of hydrogen *via* electrolysis of deionized water and on the other hand the high active area ratio of catalyst to hydrogen and substrate resulting in increased reaction rates. For this purpose, compound **158f** was dissolved in a 5:1 mixture of methanol and acetic acid and passed through this reactor containing a cartridge with an immobilized Pd catalyst (10% Pd/C) at a flow rate of 0.5 mL/min. However, no conversion was detectable. Since the reductive method of debenzylation failed, condition applying a Lewis acid was examined. In entry 5, the benzylated compound was treated with $AlCl_3$ as Lewis acid in benzene which served as solvent and trapping agent of benzyl cations generated during the reaction.[73] Also, herein no conversion was observed. In 1995, Murakami *et al.*[74] have published a lithium base mediated debenzylation. This procedure was applied to the starting material by treating it with MeLi in THF leading to a complex mixture and attempts to isolate the desired compound (entry 6) were unsuccessful. In the following, the condition of a microwave-assisted *N*-debenzylation with trifluoroacetic acid was tested without success (entry 7).[75] The combination of NMA and NBS involving probably an amide *NH*-initiated free radical process did not form the product either (entry 8).[76] Finally, debenzylation was achieved under dissolving metal conditions with sodium in ammonia (entry 9, 10).[77] In this manner, an excellent reducing medium, a blue solution of 'solvated electrons' is generated (Figure 11).

Figure 11. Experimental setup of the Birch reduction.

A complete removal of the benzyl group was observed, but also further reduction – potentially of the two additional phenyl groups – occurred thereby and isolation of the target molecule was not possible. Furthermore, no improvement was associated with using less amount of sodium and shortened reaction time (entry 10). Therefore, the testing substrate **158f** was changed to the monosubstituted derivatives **158ja** and **158na** to facilitate the purification step.

Interestingly, depending on the location of the phenyl group on the cyclobutane core the resulting products of the Birch reduction varied in the cases of the monosubstituted compounds (Scheme 49).

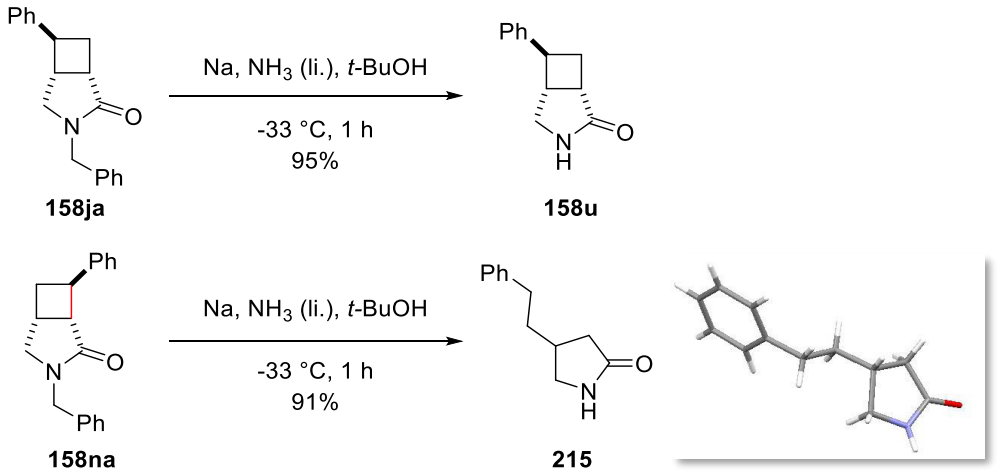

Scheme 49. Birch reduction of compound **158ja** and **158n**. In addition, X-ray analysis of compound **215**.

In the case of 6-substituted derivative **158ja** a simple deprotection took place, whereas an analog transformation of 7-substituted derivative **158na** provided product **215** resulting from deprotection and a simultaneous ring opening of the cyclobutane moiety. The structure of the ring opening product **215** was verified by X-ray analysis.

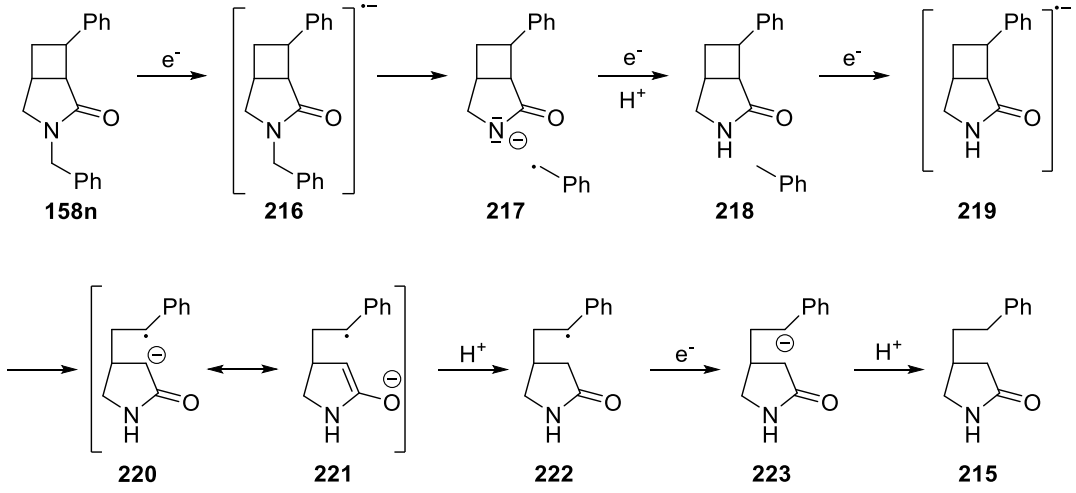

Scheme 50. Proposed reaction mechanism of the debenzylation/ring opening process.

These results are in accordance with the literature.[78] The deprotected bicyclic compound **218** can accept another electron giving rise to a cyclobutane radical anion intermediate **219** that leads to a stabilized tetramethylene radical anion **220/221**. The intermediate can subsequently

react with *t*-BuOH, as proton donor. Another electron transfer and subsequent protonation form the phenylethylpyrrolidinone **215** as saturated derivative (Scheme 50).

In 2009, SiGNa Chemistry established a safer and more convenient method for the Birch reduction by encapsulating alkali metals into nano-structure porous oxides, as silica gel or alumina, with retained reducing power of the metal.[79] This method utilizes sodium in silica gel (Na-SG I[10]), a black powder with a loading of 35 wt% which can be easily handled under air. Unfortunately, after two days no conversion of **158ja** was detectable (Scheme 51).

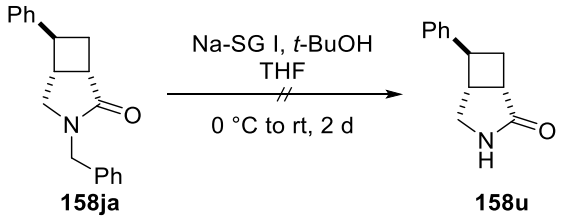

Scheme 51. Birch reduction of compound **158ja** using Na-SG.

7.3 Hydrolysis of the *N*-Boc derivatives

In 1983, Grieco *et al.*[55] developed a mild method for the hydrolysis of *N*-Boc derivatives of lactams into their acyclic amino acid derivatives. Their amino functionality remained in the protected form by employing lithium hydroxide. An analog treatment of *N*-Boc-protected derivatives **158** with an excess of LiOH gave rise to the Boc-protected γ-cyclobutane amino acids **225**, **226** and **227** in good yields (Scheme 52).

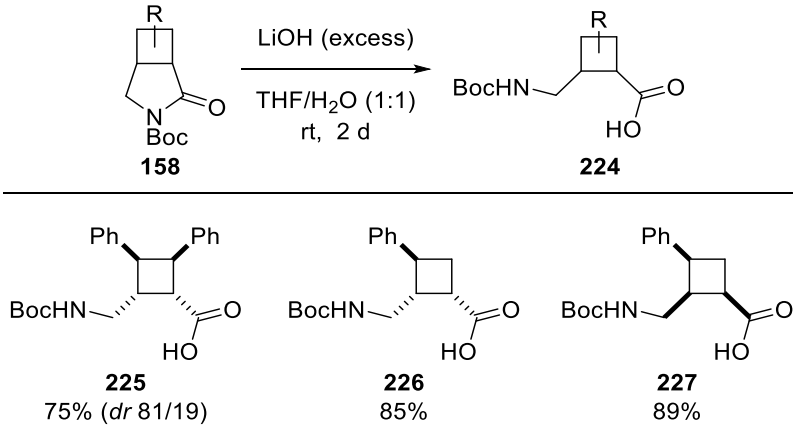

Scheme 52. Hydrolysis of the *N*-Boc-protected bicyclic compounds **158**.

[10] *SiGNa Chemistry Inc. (http://signachem.com/) has developed three categories of alkali metals in silica gel (M-SG): Stage 0 materials are strongly reducing pyrophoric powders; stage I materials are synthetically useful reducing agents; stage II materials have the least reducing capability but react with water to form H_2. All three stages are commercially available.*[79]

The structure of Boc-protected amino acid **227** was ascertained by X-ray crystallography (Figure 12).

Figure 12. X-ray analysis of compound **227**.

7.4 Conclusion

In summary, three different *N*-protected products of the photocatalytic [2+2] cycloaddition were successfully converted into the racemic *N*-Boc-protected γ-cyclobutane amino acid **(±)-226**, which served as starting material for the chiral resolution (Scheme 53).

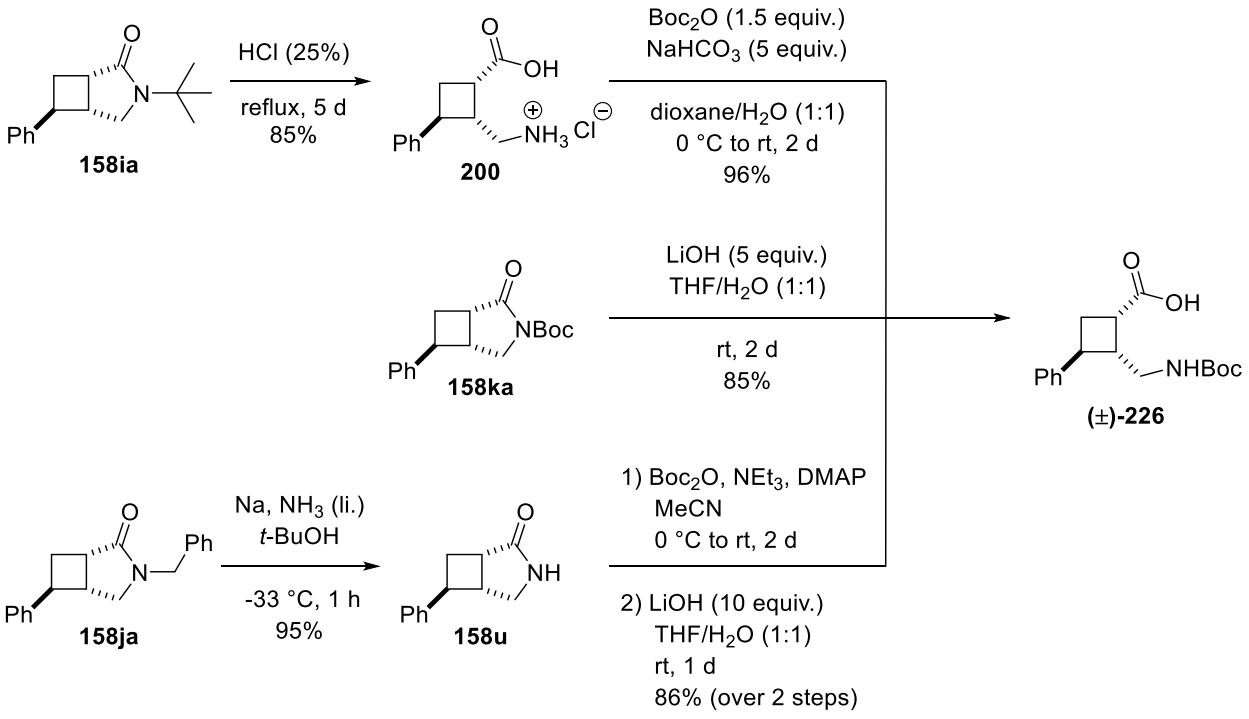

Scheme 53. Three different synthetic routes towards racemic *N*-Boc-*cis*-γ-cyclobutane amino acid **(±)-226**.

The *tert*-butyl derivative **158ia** was firstly transformed into the chloride salt of the free amino acid **200** by refluxing in 25% aqueous solution of HCl. The subsequent Boc-protection gave rise to *N*-Boc-*cis*-γ-cyclobutane amino acid **(±)-226** in a yield of 96%. Starting from the already

Boc-protected bicyclic compound **158ka**, target molecule (±)-**226** was easily accessible in a single step and 85% yield by treatment with lithium hydroxide in a THF/H_2O mixture at ambient temperature. Applying Birch conditions enabled the removal of the benzyl group in compound **158ja** and the synthesis of the unprotected amide derivative **158u** in an excellent yield of 95%. In two subsequent steps, Boc-protection and basic hydrolysis, derivative **158u** was converted to racemic γ-cyclobutane amino acid **(±)-226** in 86% yield.

8 Chiral resolution

"The chiral auxiliary is actually an enantiopure chiral molecule which temporarily attaches to the substrate to induce chirality to the resulting compound. […] Probably, the most suitable and common chiral auxiliaries, which meet nearly all these required criteria, are oxazolidin-2-ones, the so-called Evans' 2-oxazolidinones. Initially, it was discovered and presented by Evans and coworkers in 1981 and since then, a large number of structural modifications of these auxiliaries have been accomplished and reported."[80]

Oxazolidinone can also be used for chiral resolution processes. Covalent derivatization of a racemate with this type of chiral reagents affords a pair of diastereomers which can be separated by common separation techniques since they differ in physical as well as chemical properties. Afterwards, the oxazolidinone moiety needs to be cleaved from the isolated derivatives giving rise to the desired pure enantiomers and the oxazolidinone shall be preferably recyclable.

Aitken and coworkers used this strategy in several synthesis of cyclobutane amino acid derivatives and succeeded in generating a number of enantiomerically pure cyclobutane-containing amino acids for example β-amino cyclobutane amino acid **228**[81], *N*-aminoazetidinecarboxylic acid **230**[82], *cis*-(2-aminocyclobutyl)acetic acid **232**[83] or hydroxyl-β-amino cyclobutane carboxylic acid **234**[84] (Scheme 54).

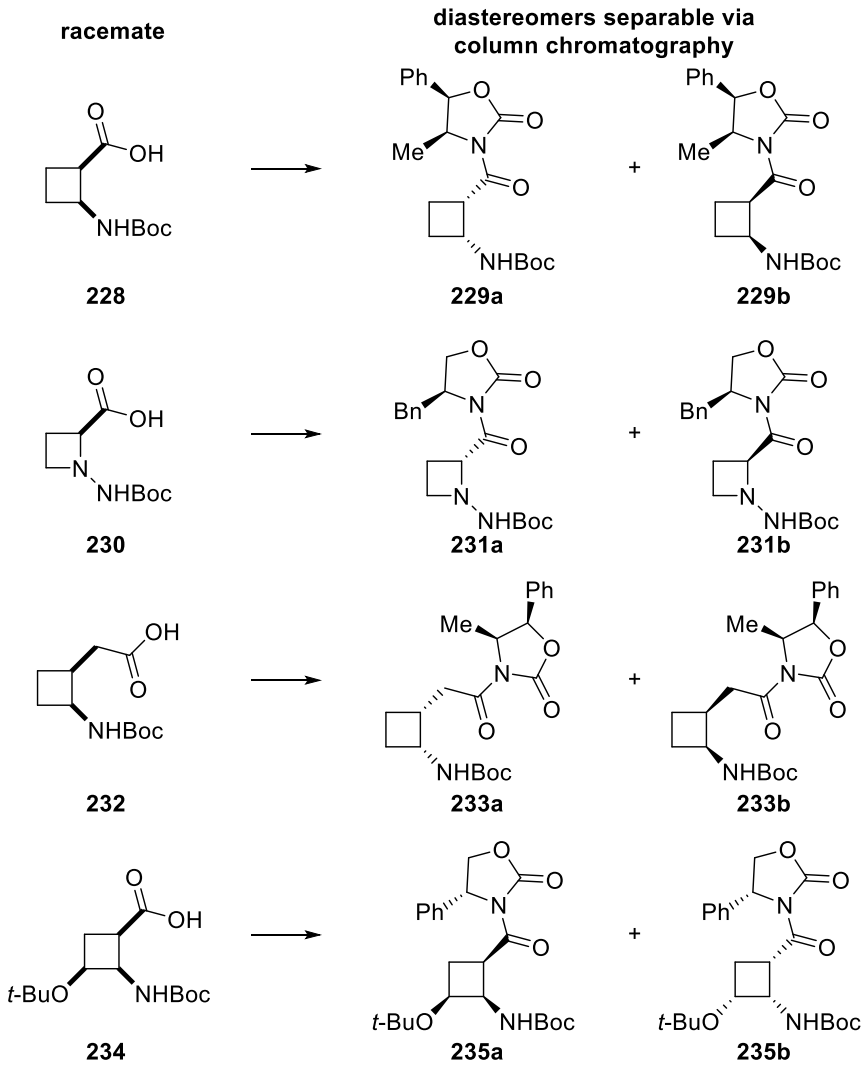

Scheme 54. Selected examples for the chiral resolution of the work group of Prof. D. J. Aitken.[81–84]

Adopting the procedure for chiral resolution developed by Aitken *et al.*[81] racemic *N*-Boc-protected γ-cyclobutane amino acid **(±)-226** was coupled with (4*S*,5*R*)-4-methyl-5-phenyloxazolidin-2-one[11] (**236**). For this purpose, the acid moiety was firstly activated with pivaloyl chloride and the oxazolidinone was introduced as its lithium salt.[85] The resulting pair of diastereomers **237** was separable *via* silica gel column chromatography. Thus diastereomer **237a** could be isolated in 42% and diastereomer **237b** in 39% yield. The absolute conformation of diastereomer **237a** was unambiguously assigned by X-ray crystallography. Treatment with lithium hydroperoxide in aqueous THF allowed the exocyclic cleavage[86] of the chiral auxiliary **237** and both enantiomers of *N*-Boc-*cis*-γ-cyclobutane amino acid **226** were

[11] Oxazolidinone **236** was available on gram scale at the work group of Prof. O. Reiser since it was a chemical donation of a company several years before.

accessible. It is notable that the used chiral oxazolidinone **236** was almost quantitatively recovered (Scheme 55).

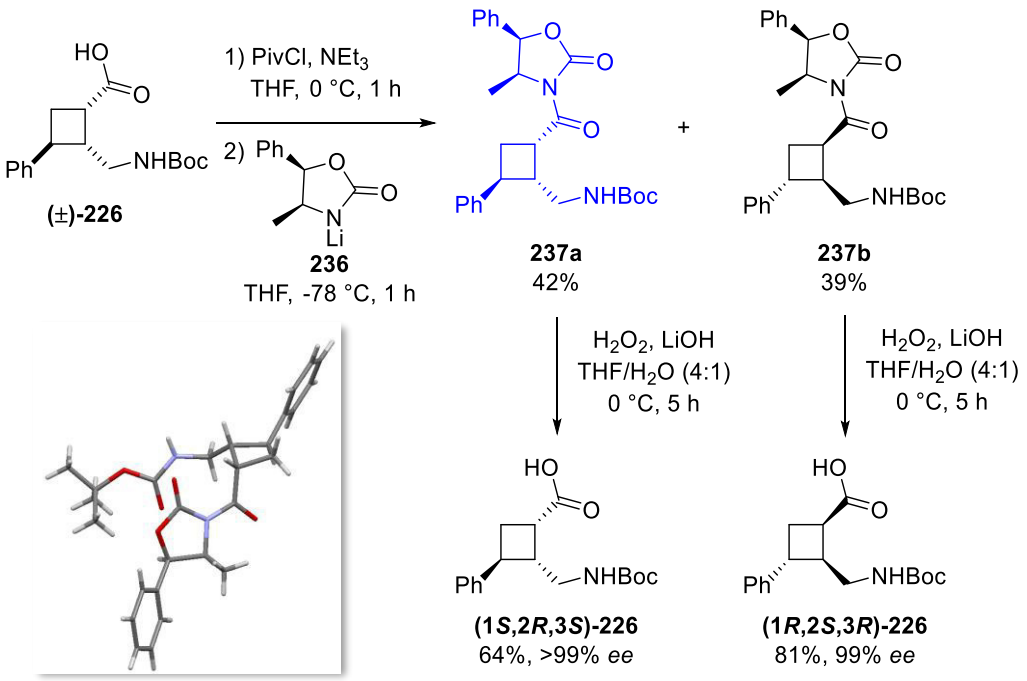

Scheme 55. Chiral resolution of compound **(±)-226**.

In conclusion, both *cis*-*N*-Boc-γ-cyclobutane amino acids **226** were accessible in good yield and excellent enantiomeric excess *via* the chiral resolution using (4*S*,5*R*)-4-methyl-5-phenyloxazolidin-2-one (**236**) as chiral auxiliary.

9 Second synthetic route towards enantioselective γ-cyclobutane amino acids

In 2011, Aitken *et al.*[87] took advantage of the good diastereoselectivity of the [2+2] photocycloaddition of ethylene (**59**) with an enantiomerically pure unsaturated γ-lactam **238** for the synthesis of both stereoisomers of *cis*-γ-cyclobutane amino acids (Table 20). The photochemical reaction led exclusively to the *cis*-configuration at the ring junction. The presence of a chiral and removable substituent on the nitrogen atom enabled a separation of the obtained pair of diastereomers by simple column chromatography. Only in the case of the (*S*)-methyl benzyl lactam **242** the diastereomers **246** were successfully isolated from each other followed by transformation into the desired target *cis*-γ-amino acids **112** (see chapter 1.1).

Table 20. Photochemical [2+2] cycloaddition of Aitken *et al*.[87]

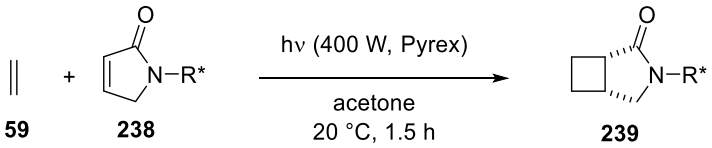

59 238 239

entry	substrate	product	yield [%]	*dr*	diastereomer separation
1	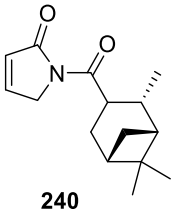 240	**243**	76	50/50	no
2	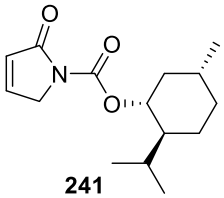 241	**244**	71	50/50	no
3	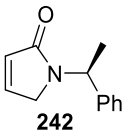 242	**246**	67	55/45	yes

These results served as inspiration for the development of another synthetic route to the previously described 2-(aminomethyl)-3-phenylcyclobutane-1-carboxylic acid (**226**) starting with an already enantiomerically pure amide-linked diene.[12] The photochemical cycloaddition of such a chiral diene *via* visible light should generate diastereomers with a good diastereoselectivity which might be separable by column chromatography.

The synthesis of the starting material worked straightforwardly as described in chapter 2.3. Cinnamyl bromide **169b** was coupled in basic medium with (*S*)-α-methyl benzylamine (**247**) giving rise to chiral amine **248** in a yield of 76% with an enantiomeric excess of 98%. The following amide formation led to 82% of compound **153x** with constant *ee*. The [2+2] photocycloaddition produced four stereoisomers **158v** with an excellent diastereomeric ratio of 43/43/7/7 and an overall yield of 83%. After column chromatography, both major diastereomers **158va** and **158vb** were isolated in 34% and 32% yield, respectively. The

[12] Several results were adapted from the Bachelor Thesis of Fabian Späth (supervised by S. Kerres).

configuration of the three stereocenters on the cyclobutane core structure in compound **158vb** could be determined by X-ray analysis having the chiral appendage as already fixed stereocenter (Scheme 56).

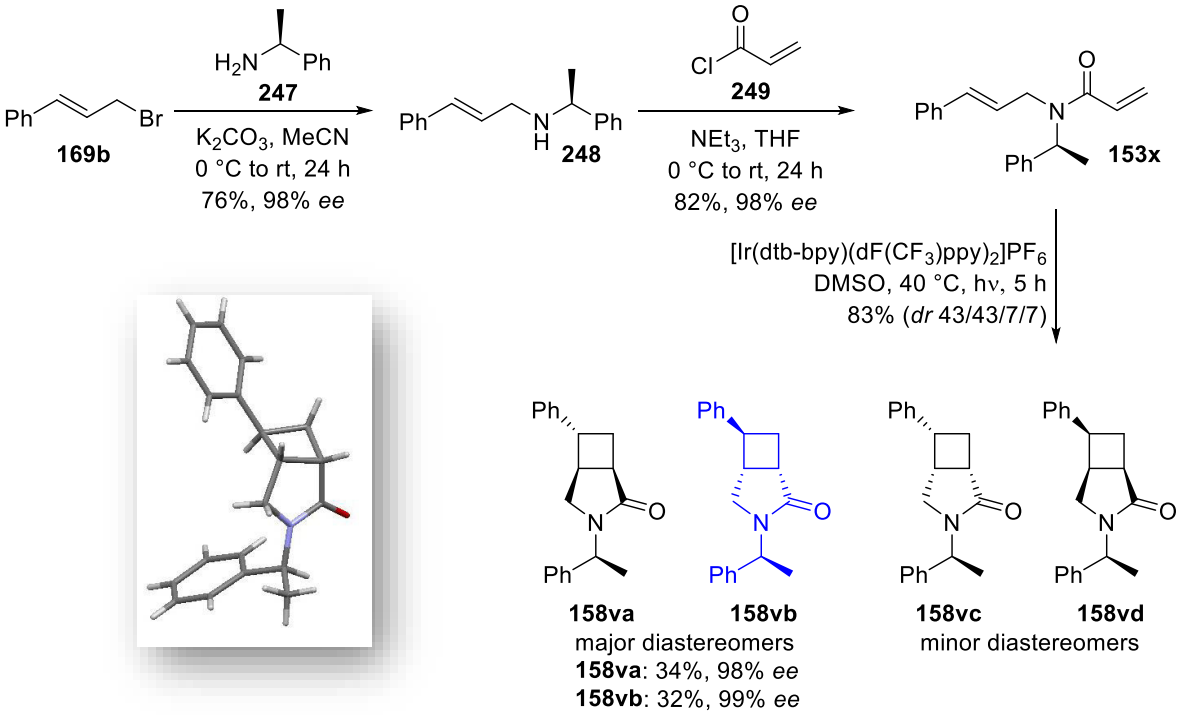

Scheme 56. Reaction sequence with a chiral amide-linked diene (pathway A).

The transformations towards the corresponding *N*-Boc-*cis*-γ-cyclobutane amino acids **226** proceeded in analogy to the reaction sequence for the racemic compound described in chapter 7.4 (Scheme 57).

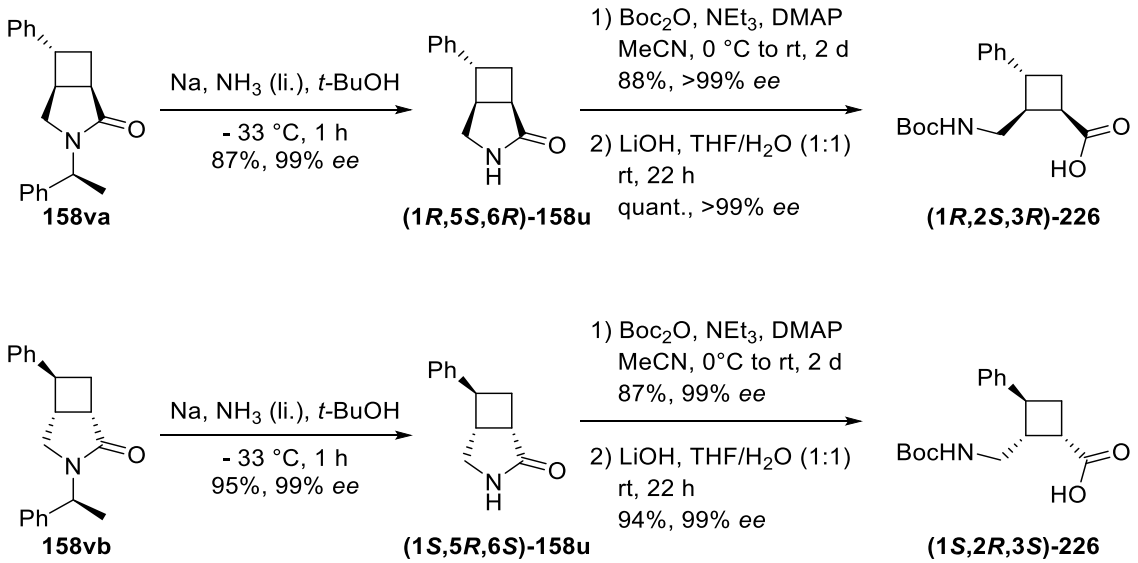

Scheme 57. Reaction sequences towards both enantiomers of compound **226**.

In summary, two different routes were developed to get both *cis*-2-(aminomethyl)-3-phenylcyclobutane-1-carboxylic acid enantiomers (**226**). On the one hand a procedure with a chiral amide-linked diene as starting material (pathway A) and on the other hand a method applying a chiral resolution step with an enantiopure oxazolidinone (pathway B). For comparison, pathway B is again summarized in the following scheme 58.

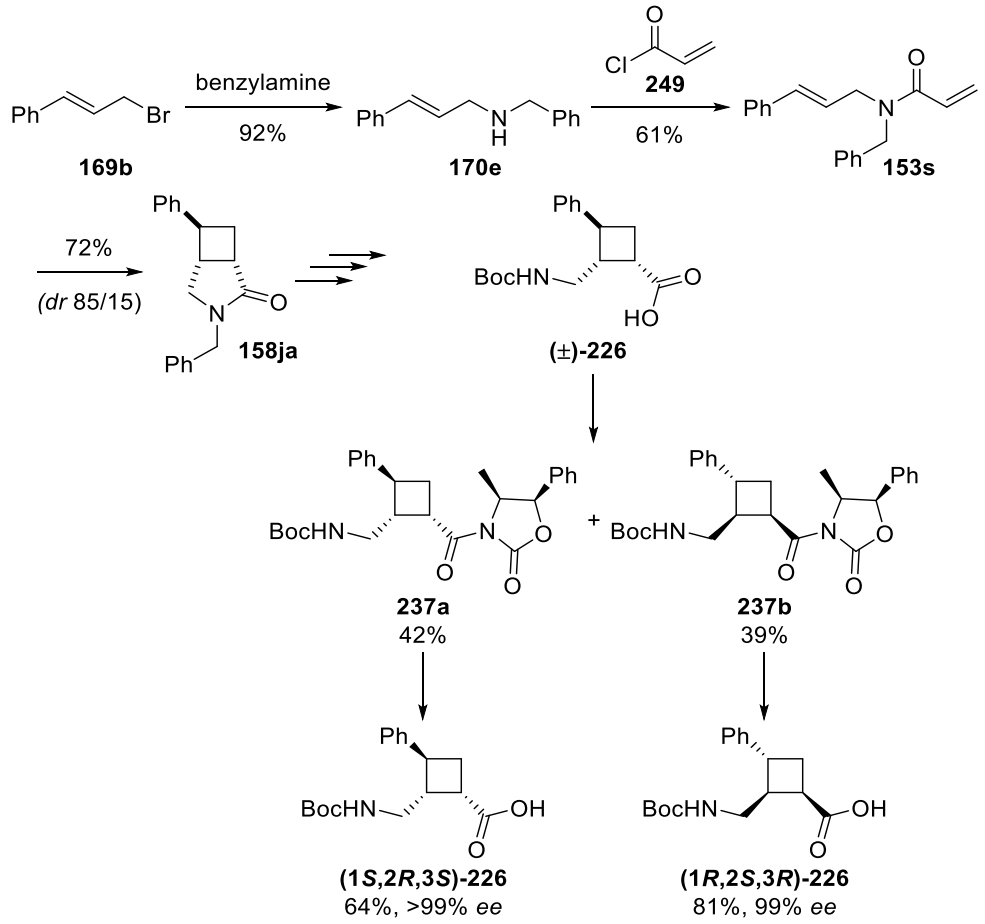

Scheme 58. Pathway B using the chiral auxiliary.

In pathway A the chiral information is introduced by starting already with an enantiomerically pure compound **153x**. In this process, both amino acids **(1*S*,2*R*,3*S*)-226** and **(1*R*,2*S*,3*R*)-226** were obtained over 6 steps in an overall yield of 15% and 16%, respectively. Pathway B includes the chiral resolution applying a chiral auxiliary. In this manner, the chiral amino acids **(1*S*,2*R*,3*S*)-226** and **(1*R*,2*S*,3*R*)-226** were synthesized over 8 steps with an overall yield of 7% and 9%, respectively. However, in both cases, the amount of performed reactions which were necessary to synthesize both enantiomers are the same: 9 experiments. The advantage of pathway B is the recyclability of the chiral auxiliary after the separation of both diastereomers **237**. In pathway A the chiral appendage was simply lost after the Birch reduction.

10 Synthesis of chiral 3-(aminomethyl)-5-phenylpentanoic acid

γ-Amino acids play an important role in the clinical treatment of diseases related to the central nervous system such as epilepsy, neuropathic pain or anxiety.[88] The most prominent representative of this family is γ-aminobutyric acid (GABA) **250** which is the major inhibitory neurotransmitter in the mammalian central nervous system. Its physiological activity is based on the interaction with three receptor subtypes. Two of them are ligand-gated ion channels and the third one is a G-protein coupled receptor, all of them affect the synaptic transmission.[89] For example, abnormally low levels of GABA in the brain are associated with serious neurological disorders as epilepsy which is characterized by recurrent seizures.[90] About 45 million people worldwide are affected by epilepsy and its prevalence is approximately 4 to 8 per 1000 in Western countries.[91,92] However, the administration of GABA orally or intravenously is not efficient because of its limited ability to cross the blood-brain barrier due to its low lipophilicity.[91] Therefore, the synthesis of more lipophilic GABA derivatives has been the aim of a great number of studies. One possibility to achieve this might be the incorporation of a phenyl ring into the GABA molecule.[93] A wide variety of GABA compounds have been synthesized and investigated over recent years. Figure 13 shows a variety of marketed GABA-analogues which have been commercialized in their racemic form.

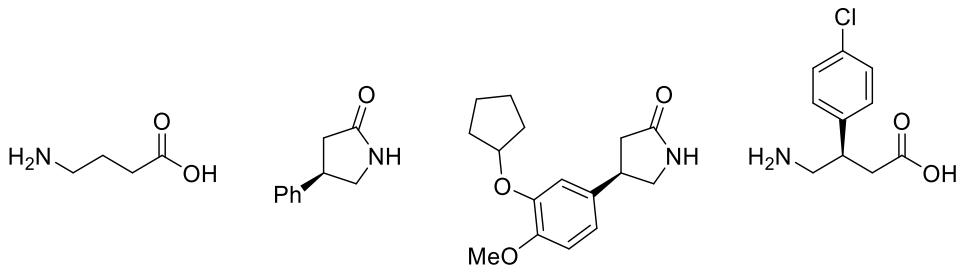

GABA **250** | *R*-Phenibut **251** | *R*-Rolipram **252** | *R*-Baclofen **253**

Figure 13. Structure of GABA **250** and its derivatives.

For instance, Phenibut **251**[93] is a neuropsychotropic drug and Rolipram **252**[94] is applied in the therapy against depression. Furthermore, Baclofen **253**[95] possesses muscle relaxing as well as antispastic activities.

As described in chapter 7.2, the unexpected cyclobutane ring opening of compound **158na** during the Birch reduction furnished 4-phenethylpyrrolidin-2-one (**215**) which is itself a GABA-analogue and is also a key intermediate in the synthesis of 3-(aminomethyl)-5-phenylpentanoic acid (**257**).[96,97] This derivative is an anticonvulsant and used in a variety of

disorders like epilepsy, depression, anxiety, pain, cranial disorders, neurodegenerative disorders or inflammatory disease. In the literature-known process[97], first a Horner-Wadsworth-Emmons reaction of hydrocinnamaldehyde **254** with the corresponding phosphonate was performed, followed by a Michael addition of nitromethane. The resulting nitro ester **256** was then reduced to phenylethylpyrrolidinone **(±)-215** with an overall yield of 45% over 3 steps. Applying the method with [2+2] photocycloaddition as key step this lactam **(±)-215** was synthesized in an overall yield of 49% over 4 steps, which is comparable to the literature reported result. Finally, the opening of the lactam ring was achieved by refluxing in aqueous solution of HCl giving rise to 89% of 3-(aminomethyl)-5-phenylpentanoic acid (**(±)-257**) (Scheme 59).

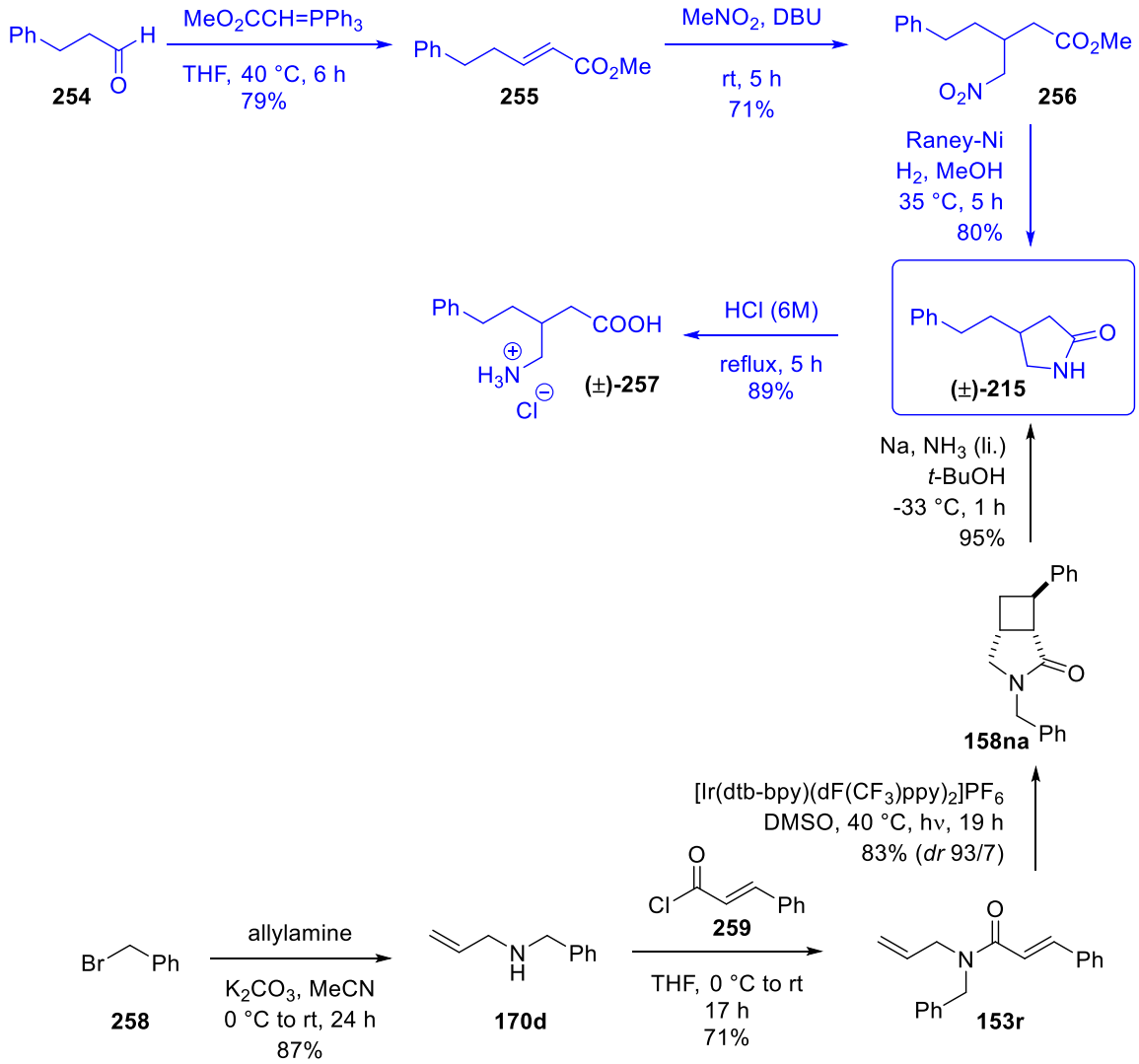

Scheme 59. Comparison of literature procedure with the herein established methodology towards 4-phenethylpyrrolidin-2-one (**(±)-215**).

Up to now, only Wu *et al.*[98] developed an asymmetric synthesis of GABA derivative **257** the *R*-enantiomer ***R*-257**, with a highly enantioselective Michael addition of an aromatic ketone to α,β,γ,δ-nitro compound as crucial step. In contrast to this approach, performing the [2+2] photocycloaddition with a chiral starting material in analogy to chapter 7.2 might give access to both enantiomers **257** (Scheme 60).

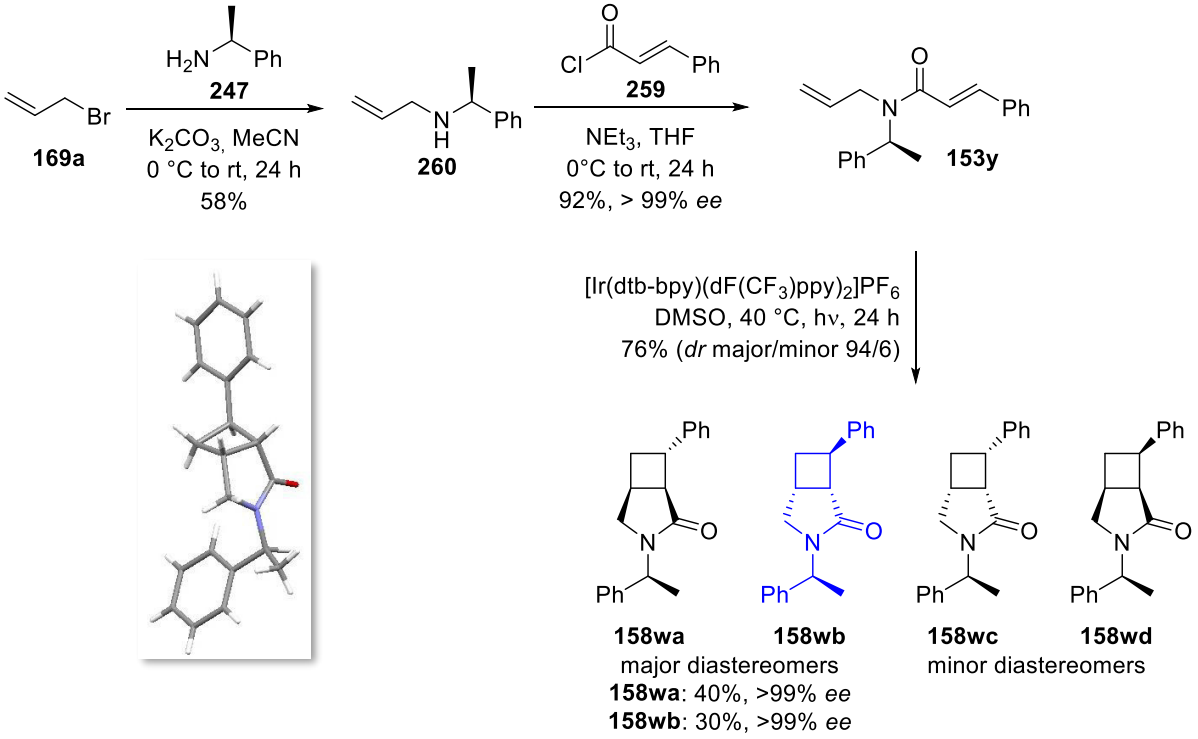

Scheme 60. [2+2] photocycloaddition of chiral amide-linked derivative **153y**.

In the case of the enantiomerically pure diene **153y** again four diastereomers **158w** were formed. The absolute configuration of product **158wb** was ascertained by X-ray analysis with the chiral appendage as already fixed stereocenter. Major diastereomer **158wa** was successfully isolated, whereas major diastereomer **158wb** could not be completely separated from the minor diastereomers **158wc** and **158wd**.

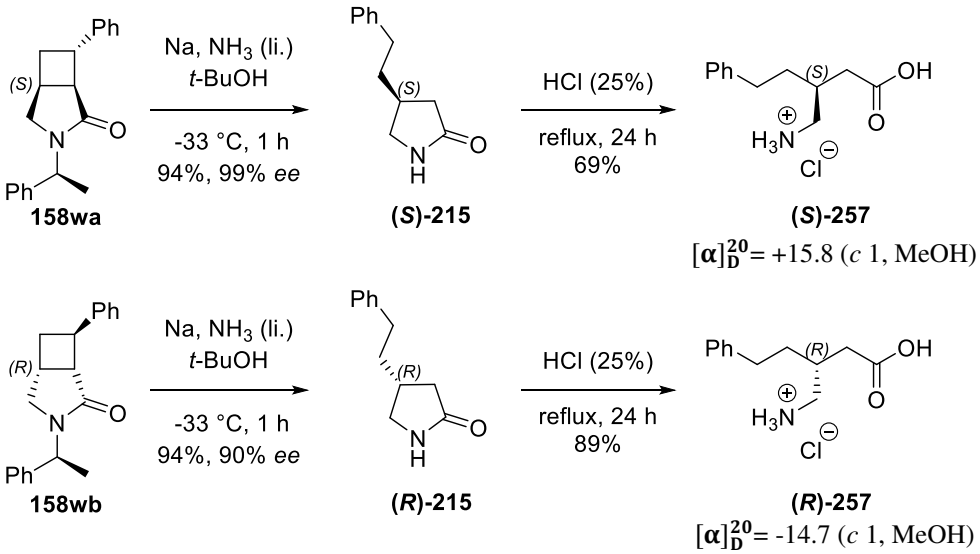

Scheme 61. Transformation into both enantiomers of compound **257**.

Therefore, the Birch reduction of compound **158wb** led only to an enantiomeric excess of 90% of the corresponding (*R*)-4-phenethylpyrrolidin-2-one **(*R*)-215** while (*S*)-4-phenethylpyrrolidin-2-one **(*S*)-215** was amenable in this process with >99% *ee*. By refluxing both pyrrolidinones **215** in a 25% aqueous solution of HCl both enantiomers of anticonvulsant 3-(aminomethyl)-5-phenylpentanoic acid (**257**) could be obtained. One discrepancy was observed: the optical rotation in the literature[98] of *R*-enantiomer **(*R*)-215** has a value of $[\alpha]_D^{25}$ = +48.2 (*c* 4.02, MeOH, 95% *ee*) whereas in this work an optical rotation of $[\alpha]_D^{20}$ = -14.7 (*c* 1, MeOH, 90% *ee*) was determined (Scheme 61). However, the performed measurements of both synthesized enantiomers **(*R*)-257** and **(*S*)-257** are consistent. Additionally, the configuration of each enantiomer could be ascertained by X-ray analysis (Figure 14) and already the X-ray crystallographic data of the bicyclic compound **158wb** confirmed the *R*-configuration of compound **(*R*)-257** (Scheme 60). Nevertheless, with the developed methodology both enantiomers of **257** are now accessible.

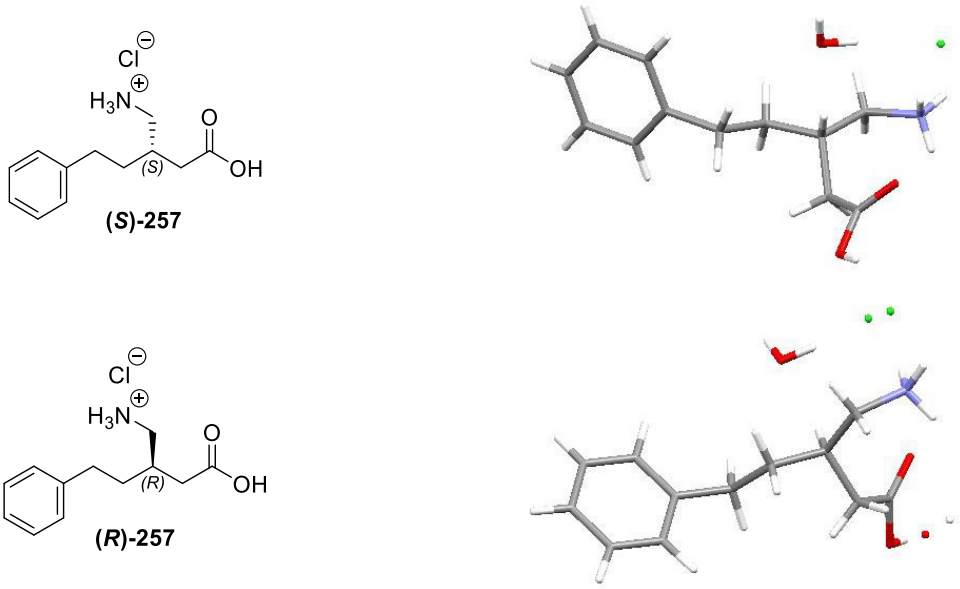

Figure 14. X-ray structures of (*S*)- and (*R*)-enantiomer **257**.

11 Neuropeptide Y analogues

11.1 Neuropeptide Y

In 1981, the 36 residue peptide amide neuropeptide Y (NPY) was isolated from porcine brain by Tatemoto and Mutt and is one of the most abundant neuropeptides in the mammalian brain.[99] Together with the pancreatic polypeptide (PP) and peptide YY (PYY), NPY has been classified into a family of homologous hormones due to their similar physiological activities.[100] The first model of its three-dimensional structure was verified by X-ray analysis from avian pancreatic polypeptide consisting of a polyproline-like helix (amino acids 1-8), followed by a turn (amino acids 9-13) which displays the connection to the α-helix (amino acids 14-31). The amidated C-terminus (amino acids 32-36) is present as flexible loop conformation (Figure 15).[101]

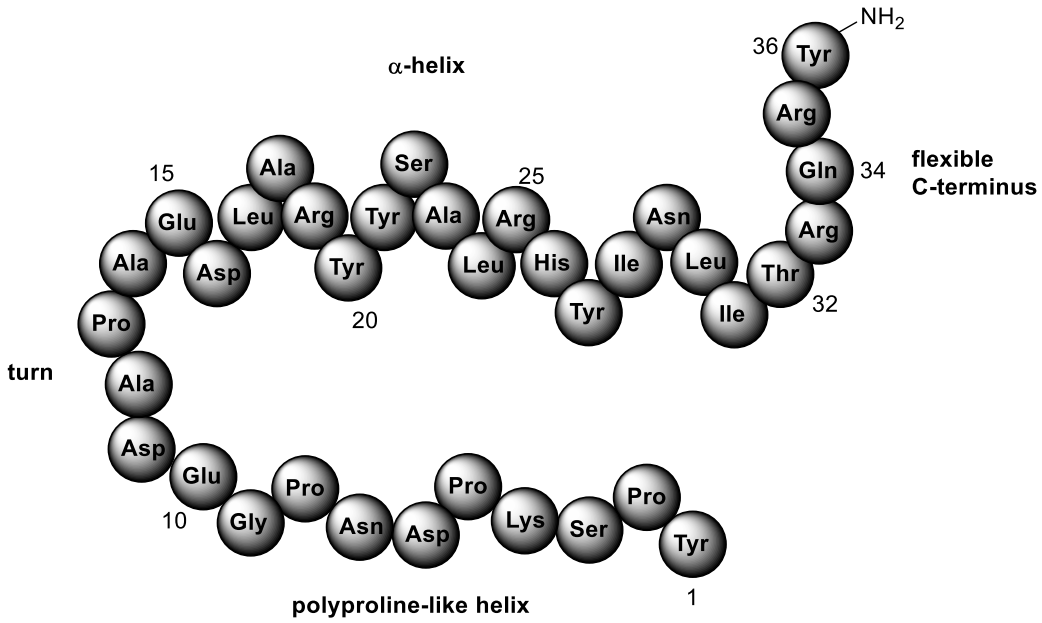

Figure 15. Structure of porcine NPY according to Allen *et al*.[102]

In humans, central and peripheral biological effects of the members of the NPY family are mediated by four G-protein coupled receptor subtypes, labelled Y_nR (n = 1, 2, 4, 5) which are involved in numerous physiological effects in the human body. Several investigations demonstrated that NPY plays a key role in the pathophysiology of a number of diseases.[103] Relevant biological functions of the different receptors are depicted in table 21.[91,104,105]

Table 21. Overview of biological effects mediated by Y_nR (n = 1,2,4,5) in humans.

receptor subtype	biological effect
Y_1	mediation of vasoconstriction and anxiolysis, regulation of food intake, control of alcohol consumption, expression in various tumor entities
Y_2	suppression of neurotransmitter release, regulation of memory retention and of circadian rhythm, implication in epilepsy
Y_4	cardiac function, gastrointestinal regulation, control of emotional and stress-related behavior
Y_5	regulation of food intake, control of seizures

In 2001, Schaer *et al.*[106] determined an overexpression of Y_1 receptor in one of the most frequent harmful cancers, breast carcinoma. Indeed, this receptor may be of functional relevance in tumor cell proliferation. Due to the high incidence of Y_1R in breast cancers NPY related drugs may represent relevant targets for anti-cancer therapy. Therefore, the development of potent and selective agonists and antagonists of the different receptors has attracted much attention.

Substitutions of single amino acids have revealed that especially the highly conserved C-terminal part of NPY, with its two positively charged arginine side chains in positions 33 and 35 and the tyrosine amide in position 36, is most important for the recognition process by the respective receptor.[104,107] Different substitution patterns close to these significant C-terminal positions allow a distinction between the various receptor subtypes. Potent and selective agonists and antagonists are already available for Y_1R, Y_2R and Y_5R, however, the amount of known selective Y_4R ligands is rather small. An attempt to generate more Y_4R selective ligands seems to be the introduction of cyclic amino acids since they rigidify the peptide backbone and induce or stabilize various secondary structure motifs.[107]

In 2013 Reiser *et al.*[108] reported a high Y_4-receptor selectivity and agonistic activity by replacing Thr^{32} and Gln^{34} in the C-terminal Neuropeptide Y fragment 25-36 by *cis*-cyclobutane **(1*R*,2*S*)-74** and *cis*-cyclopentane β-amino acids **(1*R*,2*S*)-262**. Using such unnatural building blocks for peptides is attractive since they are more stable against proteolytic degradation. More recently, Thomas Ertl demonstrated that the introduction of β-aminopyrrolidine carboxylic acid **(3*R*,4*R*)-263** to the truncated NPY (25-36) gave access to new Y_4R selective analogues as

well.[109] Whereas the incorporation of β-amino cyclopropane carboxylic acids **(1*R*,2*R*,3*R*)-261** led to a Y_1R selectivity (Figure 16.).[107]

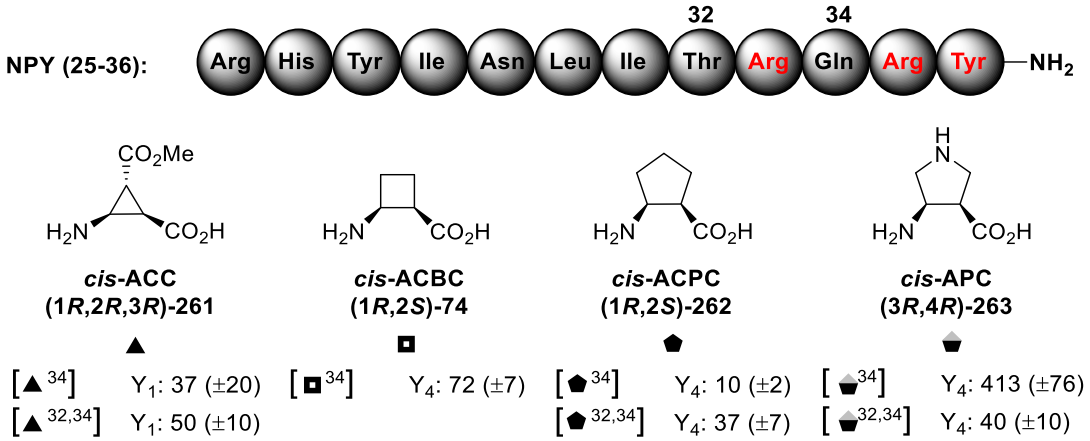

Figure 16. Overview of K_i values [nM] of NPY-analogues containing unnatural cyclic amino acids.

Due to various functionalities of the different receptor subtypes, it is of great interest to extend the development of highly selective synthetic analogues of NPY. Especially, the investigation of unnatural cyclic amino acids as potent building blocks for the NPY analogues seems to be very promising.

11.2 Incorporation of γ-cyclobutane amino acids

The incorporation of both 2-amino-3-phenylcyclobutane-1-carboxylic acid enantiomers **(1*S*,2*R*,3*S*)-227** and **(1*R*,2*S*,3*R*)-227** is worthwhile, since the influence of a γ-amino acid derivative, as well as the effect of a hydrophobic substituent, can be evaluated in this manner. In order to introduce both synthesized *N*-Boc-γ-cyclobutane amino acid enantiomers **227**, an exchange of the protecting group was performed yielding the corresponding *N*-Fmoc-protected derivatives **264**. Under acidic condition applying TFA, the Boc group was successfully cleaved off. Subsequently, the crude TFA salts of the free amino acids were subjected to basic medium each and were coupled with Fmoc-succinimide giving rise to 84% of enantiomer **(1*S*,2*R*,3*S*)-264** and 91% of enantiomer **(1*R*,2*S*,3*R*)-264** each with an unrelieved enantiomeric excess of 99% (Scheme 62).

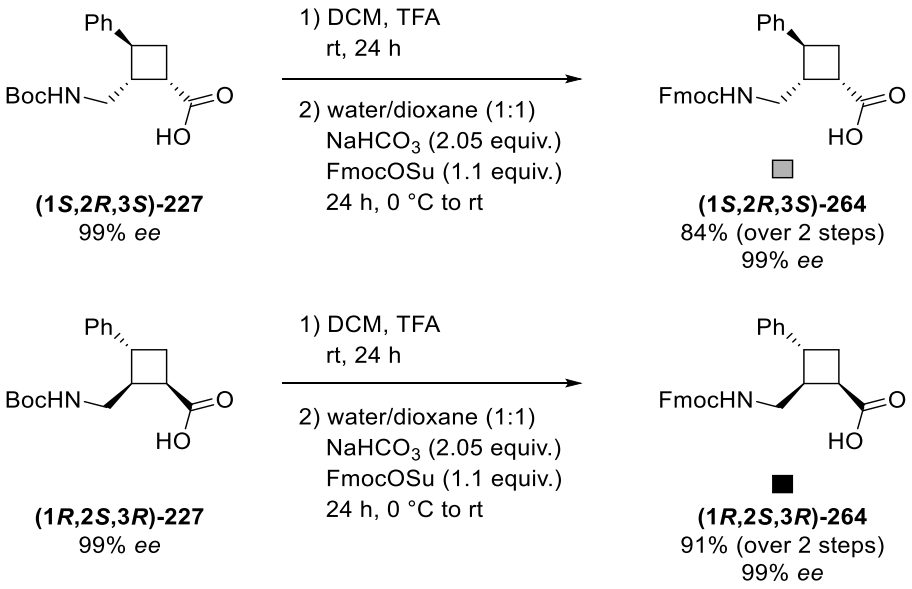

Scheme 62. Exchange of the Boc-protecting group by Fmoc group.

Reiser *et al*.[108] additionally investigated very short NPY-sequences consisting of only five residues (amino acids 32-36). This truncated C-terminal NPY-analogues **265** exhibit a Y_4R affinity with a K_i-value of 50 (± 17) nM. Furthermore, the introduction of an additional Arg-residue in position 31 even improved the selectivity towards the Y_4-receptor to the single-digit nanomolar range, K_i of 3.43 (±1.3) nM (Figure 17).[110]

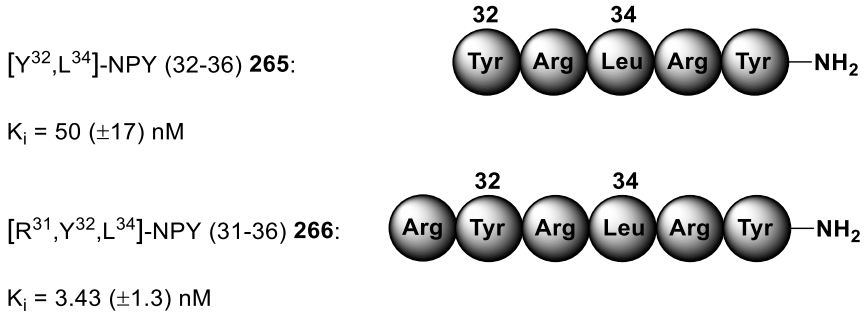

Figure 17. Amino acid sequences of the pentapeptide **265** and hexapeptide **266** NPY-analogues.

In context of these described results and in order to find new selective ligands for Y_4R, both 2-amino-3-phenylcyclobutane-1-carboxylic acid enantiomers **(1*S*,2*R*,3*S*)-264** and **(1*R*,2*S*,3*R*)-264** were each introduced in position 34 in the pentapeptide NPY (32-36) and in the case of the double substitution in position 32 and 34 the building blocks were incorporated in the sequence of the hexapeptide NPY (31-36) (Figure 18).

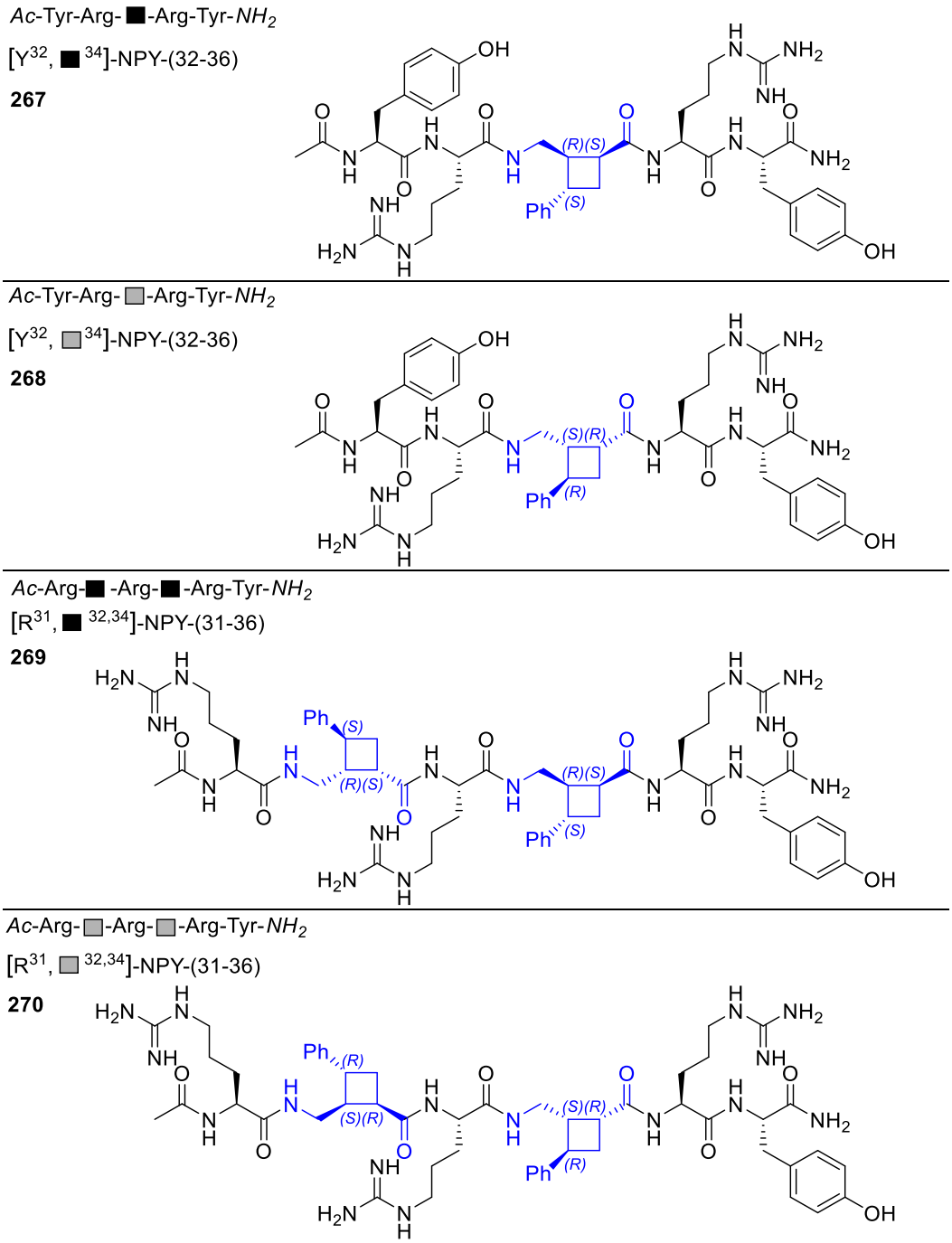

Figure 18. Amino acid sequences of the prepared NPY analogues **267-270**.

In cooperation with Prof. C. Cabrele from the University of Salzburg, the truncated NPY-analogues **267-270** were synthesized on an automated peptide synthesizer, applying Fmoc-chemistry and double-coupling procedure with HBTU/HOBt/DIPEA. The synthesis was performed on a Rink-amide MBHA resin producing C-terminally amide form peptides. Additionally, the peptides were purified by preparative RP-HPLC achieving a purity of more than 95%. The investigations of the binding profiles of all synthesized NPY analogues **267-270** are currently ongoing in cooperation with the group of Prof. A. Buschauer.

12 References

[1] V. André, M. Gras, H. Awada, R. Guillot, S. Robin, D. J. Aitken, *Tetrahedron* **2013**, *69*, 3571–3576.

[2] F. Hernvann, G. Rasore, V. Declerck, D. J. Aitken, *Org. Biomol. Chem.* **2014**, *12*, 8212–8222.

[3] Y. Roh, H.-Y. Jang, V. Lynch, N. L. Bauld, M. J. Krische, *Org. Lett.* **2002**, *4*, 611–613.

[4] a) L.-C. Wang, H.-Y. Jang, Y. Roh, V. Lynch, A. J. Schultz, X. Wang, M. J. Krische, *J. Am. Chem. Soc.* **2002**, *124*, 9448–9453; b) T.-G. Baik, A. L. Luis, L.-C. Wang, M. J. Krische, *J. Am. Chem. Soc.* **2001**, *123*, 6716–6717.

[5] J. Yang, D. F. Cauble, A. J. Berro, N. L. Bauld, M. J. Krische, *J. Org. Chem.* **2004**, *69*, 7979–7984.

[6] J. Yang, G. A. N. Felton, N. L. Bauld, M. J. Krische, *J. Am. Chem. Soc.* **2004**, *126*, 1634–1635.

[7] M. A. Ischay, M. E. Anzovino, J. Du, T. P. Yoon, *J. Am. Chem. Soc.* **2008**, *130*, 12886–12887.

[8] M. A. Cismesia, T. P. Yoon, *Chem. Sci.* **2015**, *6*, 5426–5434.

[9] J. Du, T. P. Yoon, *J. Am. Chem. Soc.* **2009**, *131*, 14604–14605.

[10] M. Neumann, K. Zeitler, *Eur. J. Org. Chem.* **2013**, *19*, 6950–6955.

[11] S. Zhao, J.-B. Lin, Y.-Y. Zhao, Y.-M. Liang, P.-F. Xu, *Org. Lett.* **2014**, *16*, 1802–1805.

[12] a) D. Ravelli, M. Fagnoni, *ChemCatChem* **2012**, *4*, 169–171; b) X.-F. Zhang, I. Zhang, L. Liu, *Photochem. Photobiol.* **2010**, *86*, 492–498.

[13] K. Kalyanasundaram, *Coord. Chem. Rev.* **1982**, *46*, 159–244.

[14] A. Juris, V. Balzani, P. Belser, A. von Zelewsky, *Helv. Chim. Acta* **1981**, *64*, 2175–2182.

[15] K. Singh, S. J. Staig, J. D. Weaver, *J. Am. Chem. Soc.* **2014**, *136*, 5275–5278.

[16] D. M. Pawar, A. A. Khalil, D. R. Hooks, K. Collins, *J. Am. Chem. Soc.* **1998**, *120*, 2108–2112.

[17] a) A. Throup, L. H. Patterson, H. M. Sheldrake, *Org. Biomol. Chem.* **2016**, *14*, 9554–9559; b) J. Panda, S. Ghosh, S. Ghosh, *ARKIVOC* **2005**, *2001*, 146–153.

[18] V. P. Manea, K. J. Wilson, J. R. Cable, *J. Am. Chem. Soc.* **1997**, *119*, 2033–2039.

[19] P. G. M. Wuts, T. W. Greene, *Greene's Protective Groups in Organic Synthesis*, John Wiley & Sons, Inc, Hoboken, NJ, USA, **2006**.

[20] Corey, E. J., A. Venkateswarlu, *J. Am. Chem. Soc.* **1972**, *94*, 6190–6191.

[21] A. Bartoszewicz, M. Kalek, J. Nilsson, R. Hiresova, J. Stawinski, *Synlett* **2008**, 37–40.

[22] M. Chen, A. Maetzke, Knak Jensen, Svend J., K. V. Gothelf, *Eur. J. Org. Chem.* **2007**, *2007*, 5826–5833.

[23] J. D. More, N. S. Finney, *Org. Lett.* **2002**, *4*, 3001–3003.

[24] F. Gnad, M. Poleschak, O. Reiser, *Tetrahedron Lett.* **2004**, *45*, 4277–4280.

[25] F. A. Bell, R. A. Crellin, H. Fujii, A. Ledwith, *Chem. Commun.* **1969**, 251–252.

[26] R. A. Crellin, M. C. Lambert, A. Ledwith, *Chem. Commun.* **1970**, 682–683.

[27] a) N. L. Bauld, *Tetrahedron* **1989**, *45*, 5307–5363; b) N. L. Bauld, D. J. Bellville, B. Harirchian, K. T. Lorenz, R. A. Pabon, D. W. Reynolds, D. D. Wirth, H. S. Chiou, B. K. Marsh, *Acc. Chem. Res.* **1987**, *20*, 371–378; c) R. A. Pabon, D. J. Bellville, N. L. Bauld, *J. Am. Chem. Soc.* **1984**, *1984*, 2730–2731; d) N. L. Bauld, R. Pabon, *J. Am. Chem. Soc.* **1983**, *105*, 633–634.

[28] C. K. Prier, D. A. Rankic, D. W. C. MacMillan, *Chem. Rev.* **2013**, *113*, 5322–5363.

[29] M. A. Ischay, T. P. Yoon, *Eur. J. Org. Chem.* **2012**, *2012*, 3359–3372.

[30] M. A. Ischay, Z. Lu, T. P. Yoon, *J. Am. Chem. Soc.* **2010**, *132*, 8572–8574.

[31] M. A. Ischay, M. S. Ament, T. P. Yoon, *Chem. Sci.* **2012**, *3*, 2807–2811.

[32] B. P. Zavesky, N. R. Babij, J. A. Fritz, J. P. Wolfe, *Org. Lett.* **2013**, *15*, 5420–5423.

[33] H. Alinezhad, M. Tajbakhsh, N. Mahdavi, *Synth. Commun.* **2010**, *40*, 951–956.

[34] O. S. Nayal, V. Bhatt, S. Sharma, N. Kumar, *J. Org. Chem.* **2015**, *80*, 5912–5918.

[35] a) M.-A. Haga, E. S. Dodsworth, G. Eryavec, P. Seymour, A. B. P. Lever, *Inorg. Chem.* **1985**, *24*, 1901–1906; b) R. J. Crutchley, A. B. P. Lever, *J. Am. Chem. Soc.* **1980**, *102*, 7128–7129.

[36] S. Lin, M. A. Ischay, C. G. Fry, T. P. Yoon, *J. Am. Chem. Soc.* **2011**, *133*, 19350–19353.

[37] D. M. Schultz, T. P. Yoon, *Science (New York, N.Y.)* **2014**, *343*, 1239176.

[38] Z. Lu, T. P. Yoon, *Angew. Chem., Int. Ed.* **2012**, *51*, 10329–10332.

[39] A. E. Hurtley, Z. Lu, T. P. Yoon, *Angew. Chem., Int. Ed.* **2014**, *53*, 8991–8994.

[40] V. Mojr, E. Svobodová, K. Straková, T. Neveselý, J. Chudoba, H. Dvořáková, R. Cibulka, *Chem. Commun.* **2015**, *51*, 12036–12039.

[41] M. Jirásek, K. Straková, T. Neveselý, E. Svobodová, Z. Rottnerová, R. Cibulka, *Eur. J. Org. Chem.* **2016**.

[42] A. Singh, C. J. Fennell, J. D. Weaver, *Chem. Sci.* **2016**, *7*, 6796–6802.

[43] P. L. Egerton, E. M. Hyde, J. Trigg, A. Payne, P. Beynon, M. V. Mijovic, A. Reiser, *J. Am. Chem. Soc.* **1981**, *103*, 3859–3863.

[44] W. Oppolzer, R. Achini, E. Pfenninger, H. P. Weber, *Helv. Chim. Acta* **1976**, *59*, 1186–1202.

[45] A. V. Denisenko, T. Druzhenko, Y. Skalenko, M. Samoilenko, O. O. Grygorenko, S. Zozulya, P. K. Mykhailiuk, *J. Org. Chem.* **2017**, *82*, 9627–9636.

[46] R. Buchholz, H. Martin R. Hoffmann, *Helv. Chim. Acta* **1991**, *1991*, 1213–1220.

[47] M. Sietzen, S. Batke, L. Merz, H. Wadepohl, J. Ballmann, *Organometallics* **2015**, *34*, 1118–1128.

[48] X. Huang, N. Jiao, *Org. Biomol. Chem.* **2014**, *12*, 4324–4328.

[49] A. Dhami, M. F. Mahon, M. D. Lloyd, M. D. Threadgill, *Tetrahedron* **2009**, *65*, 4751–4765.

[50] S. P. Raillard, R. A. Scheuerman, S. K. Manthati, T. A. Worral, Patent: PCT/US2014/041406, **2014**.

[51] P. Zhang, H.-R. Hu, Z.-H. Huang, J.-Y. Lei, Y. Chu, D.-Y. Ye, *Bioorg. Med. Chem.* **2012**, *22*, 7232–7236.

[52] P. Kancharla, J. X. Kelly, K. A. Reynolds, *J. Med. Chem.* **2015**, *58*, 7286–7309.

[53] D. R. Stuart, K. Fagnou, *Science (New York, N.Y.)* **2007**, *316*, 1172–1175.

[54] H. Zhang, K. O. Jeon, E. B. Hay, S. J. Geib, D. P. Curran, M. G. LaPorte, *Org. Lett.* **2014**, *16*, 94–97.

[55] Flynn, Daniel L., R. E. Zelle, P. A. Grieco, *J. Org. Chem.* **1983**, *48*, 2424–2426.

[56] R. A. Marcus, *J. Phys. Chem.* **1968**, *72*, 891–899.

[57] L. Pauling, *J. Am. Chem. Soc.* **1947**, *69*, 542–553.

[58] a) R. P. Bell, *Proc. Roy. Soc. London* **1936**, 414–429; b) M. G. Evans, M. Polanyi, *Trans. Faraday Soc.* **1938**, *34*, 11–24.

[59] X. Cui, C. Zhang, K. Xu, J. Zhao, *J. Mater. Chem. C* **2015**, *3*, 8735–8759.

[60] a) S. Sprouse, K. A. King, P. J. Spellane, R. J. Watts, *J. Am. Chem. Soc.* **1984**, *106*, 6647–6653; b) L. Flamigni, A. Barbieri, C. Sabatini, B. Ventura, F. Barigelletti, *Top. Curr. Chem.* **2007**, *281*, 143–203.

[61] J. D. Slinker, A. A. Gorodetsky, M. S. Lowry, J. Wang, S. Parker, R. Rohl, S. Bernhard, G. G. Malliaras, *J. Am. Chem. Soc.* **2004**, *126*, 2763–2767.

[62] a) J. B. Metternich, D. G. Artiukhin, M. C. Holland, M. von Bremen-Kühne, J. Neugebauer, R. Gilmour, *J. Org. Chem.* **2017**; b) J. Metternich, R. Gilmour, *Synlett* **2016**, *27*, 2541–2552; c) J. B. Metternich, R. Gilmour, *J. Am. Chem. Soc.* **2015**, *137*, 11254–11257; d) D. C. Fabry, M. A. Ronge, M. Rueping, *Chem. Eur. J.* **2015**, *21*, 5350–5354.

[63] G. I. L. Jones, N. L. Owen, *Journal of Molecular Structure* **1973**, *18*, 1–32.

[64] a) F. Diaba, J. A. Montiel, A. Martínez-Laporta, J. Bonjoch, *Tetrahedron Lett.* **2013**, *54*, 2619–2622; b) S. H. Rosenberg, H. Rapoport, *J. Org. Chem.* **1985**, 3979–3982.

[65] a) D. Albrecht, B. Basler, T. Bach, *J. Org. Chem.* **2008**, *73*, 2345–2356; b) M. J. Earle, R. A. Fairhurst, H. Heaney, G. Papageorgiou, *Synlett* **1990**, *10*, 621–623.

[66] G. López-Valdez, S. Olguín-Uribe, A. Millan-Ortíz, R. Gamez-Montaño, L. D. Miranda, *Tetrahedron* **2011**, *67*, 2693–2701.

[67] N. de Kimpe, P. Sulmon, P. Brunet, *J. Org. Chem.* **1990**, *55*, 5777–5784.

[68] E. Leclerc, E. Vrancken, P. Mangeney, *J. Org. Chem.* **2002**, *67*, 8928–8937.

[69] Z. Chen, Z. Chen, Y. Jiang, W. Hu, *Tetrahedron* **2005**, *61*, 1579–1586.

[70] a) Z. Du, Z. Chen, Z. Chen, X. Yu, W. Hu, *Chirality* **2004**, *16*, 516–519; b) Z. Chen, Y. Jiang, W. Hu, *Synlett* **2003**, 2444.

[71] W. M. Pearlman, *Tetrahedron Lett.* **1967**, *8*, 1663–1664.

[72] G. Dormán, L. Kocsis, R. Jones, F. Darvas, *J. Chem. Health Safety* **2013**, *20*, 3–8.

[73] Y. Murakami, T. Watanabe, A. Kobayashi, Y. Yokoyama, *Synth. Commun.* **1984**, 738–740.

[74] H. Suzuki, A. Tsukuda, M. Kondo, M. Aizawa, Y. Senoo, M. Nakajima, T. Watanabe, Y. Yokoyama, Y. Murakami, *Tetrahedron Lett.* **1995**, *36*, 1671–1672.

[75] F. Rombouts, D. Franken, C. Martínez-Lamenca, M. Braeken, C. Zavattaro, J. Chen, A. A. Trabanco, *Tetrahedron Lett.* **2010**, *51*, 4815–4818.

[76] L. Kuang, J. Zhou, S. Chen, K. Ding, *Synthesis* **2007**, *20*, 3129–3134.

[77] V. Du Vigneaud, O. K. Behrens, *J. Biomol. Chem* **1937**, *117*, 27–36.

[78] J. Nishimura, A. Ohbayashi, E. Ueda, A. Oku, *Chem. Ber.* **1988**, *121*, 2025–2028.

[79] M. J. Costanzo, M. N. Patel, K. A. Petersen, P. F. Vogt, *Tetrahedron Lett.* **2009**, *50*, 5463–5466.

[80] M. M. Heravi, V. Zadsirjan, B. Farajpour, *RSC Adv.* **2016**, *6*, 30498–30551.

[81] V. Declerck, D. J. Aitken, *Amino Acids* **2011**, *41*, 587–595.

[82] V. Declerck, D. J. Aitken, *J. Org. Chem.* **2011**, *76*, 708–711.

[83] H. Awada, S. Robin, R. Guillot, O. Yazbeck, D. Naoufal, N. Jaber, A. Hachem, D. J. Aitken, *Eur. J. Org. Chem.* **2014**, 7148–7155.

[84] Z. Chang, F. Boyaud, R. Guillot, T. Boddaert, D. J. Aitken, *J. Org. Chem.* **2018**, *83*, 527–534.

[85] D. A. Evans, J. A. Ellman, *J. Am. Chem. Soc.* **1989**, *111*, 1063–1072.

[86] D. J. Ager, I. Prakash, D. R. Schaad, *Aldrichimica Acta* **1997**, *1*, 3–11.

[87] V. André, A. Vidal, J. Ollivier, S. Robin, D. J. Aitken, *Tetrahedron Lett.* **2011**, *52*, 1253–1255.

[88] J. Aguilera, A. G. Moglioni, G. Y. Moltrasio, R. M. Ortuño, *Tetrahedron: Asymmetry* **2008**, *19*, 302–308.

[89] M. Chebib, Johnston, Graham A. R., *J. Med. Chem.* **2000**, *43*, 1427–1447.

[90] K. Gale, *Epilepsia (N. Y.)* **1989**, *30*, S1-S11.

[91] M. S. Hildebrand, H.-H. M. Dahl, J. A. Damiano, Smith, Richard J H, I. E. Scheffer, S. F. Berkovic, *J. Med. Genet.* **2013**, *50*, 271–279.

[92] a) J. F. Annegers, S. Dubinsky, S. P. Coan, M. E. Newmark, L. Roht, *Epilepsia* **1999**, *40*, 502–506; b) W. A. Hauser, J. F. Annegers, L. T. Kurland, *Epilepsia* **1993**, *34*, 453–468; c) W. A. Hauser, J. F. Annegers, L. T. Kurland, *Epilepsia* **1991**, *32*, 429–445.

[93] I. Lapin, *CNS Drug Reviews* **2001**, *7*, 471–481.

[94] H. Wachtel, *Neuropharmacology* **1983**, *22*, 267–272.

[95] a) A. Mann, T. Boulanger, B. Brandau, F. Durant, G. Evrard, M. Heaulme, E. Desaulles, C. G. Wermuth, *J. Med. Chem.* **1991**, *34*, 1307–1313; b) N. G. Bowery, D. R. Hill, A. L. Hudson, A. Doble, D. N. Middlemiss, J. Shaw, M. Turnbull, *Nature* **1980**, *283*, 92–94.

[96] A. Leyva-Pérez, P. García-García, A. Corma, *Angew. Chem., Int. Ed.* **2014**, *53*, 8687–8690.

[97] J. S. Bryans, D. C. Horwell, C. O. Kneen, D. J. Wustrow, A. J. Thorpe, WO 9817627, **1998**.

[98] X.-T. Guo, F. Sha, X.-Y. Wu, *Synthesis* **2017**, *49*, 647–656.

[99] K. Tatemoto, *Proc. Natl. Acad. Sci. U. S. A.* **1982**, *79*, 5485–5489.

[100] A. Balasubramaniam, *Peptides* **1997**, *18*, 445–457.

[101] T. L. Blundell, J. E. Pitts, J. Tickle, S. P. Wood, C.-W. Wu, *Proc. Natl. Acad. Sci. USA* **1981**, *78*, 4175–4179.

[102] J. Allen, J. Novotný, J. Martin, G. Heinrich, *Proc. Natl. Acad. Sci. USA* **1987**, *84*, 2532-2536.

[103] A. Balasubramaniam, *Am. J. Surg.* **2002**, *183*, 430–434.

[104] C. Cabrele, A. G. Beck-Sickinger, *J. Pept. Sci.* **2000**, *6*, 97–122.

[105] a) S. Lin, D. Boey, H. Herzog, *Neuropeptides* **2004**, *38*, 189–200; b) C. Walther, K. Mörl, A. G. Beck-Sickinger, *J. Pept. Sci* **2011**, *17*, 233–246.

[106] J. C. Reubi, M. Gugger, B. Waser, J.-C. Schaer, *Cancer Res.* **2001**, *61*, 4636–4641.

[107] N. Koglin, C. Zorn, R. Beumer, C. Cabrele, C. Bubert, N. Sewald, O. Reiser, A. G. Beck-Sickinger, *Angew. Chem., Int. Ed.* **2003**, *42*, 202–205.

[108] L. Berlicki, M. Kaske, R. Gutiérrez-Abad, G. Bernhardt, O. Illa, R. M. Ortuño, C. Cabrele, A. Buschauer, O. Reiser, *J. Med. Chem.* **2013**, *56*, 8422–8431.

[109] T. Ertl, *Dissertation*, Regensburg, **2017**.

[110] K. K. Kuhn, T. Littmann, S. Dukorn, M. Tanaka, M. Keller, T. Ozawa, G. Bernhardt, A. Buschauer, *ACS Omega* **2017**, *2*, 3616–3631.

C Summary

In the present thesis an intramolecular visible light mediated [2+2] photocycloaddition of amide-linked dienes **153** was developed to build up azabicycloheptanones **158** which were transformed into γ-cyclobutane amino acids. Furthermore, these cyclobutane-containing amino acids were generated enantioselective and incorporated in shortened NPY-analogues to find new selective ligands for Y_4R.

The investigations revealed that the suitable reaction mode for the [2+2] photocycloaddition of amide-linked dienes **153** is an energy transfer mechanism using the Iridium-based photocatalyst $[Ir(dtb\text{-}bpy)(dF(CF_3)ppy)_2]PF_6$ as sensitizer. The substituent on the nitrogen atom is crucial for the diene to adopt the necessary conformation for a successful cycloaddition (near attack conformation, NAC, **190**). *N*-*tert*-butyl, *N*-benzyl and *N*-Boc amide derivatives cyclized to the corresponding bicyclic compounds in moderate to good yields with an excellent diastereoselectivity (Scheme 63)

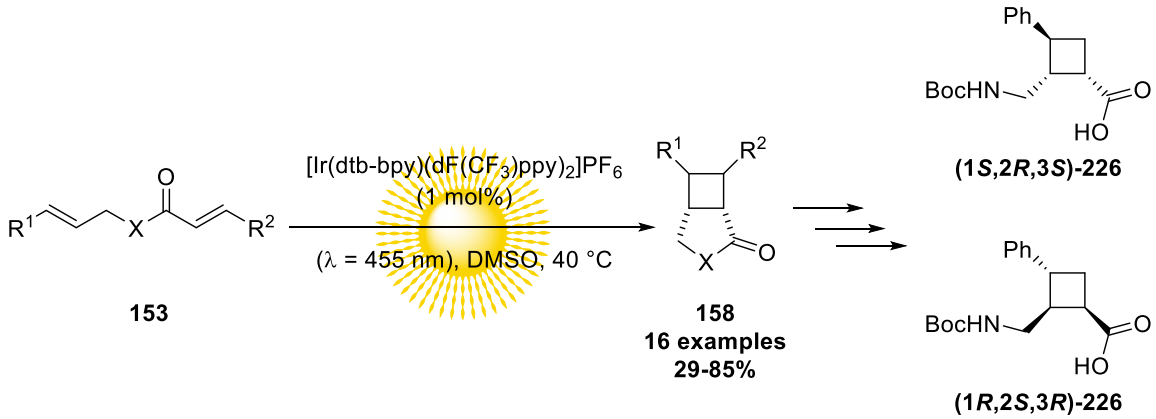

Scheme 63. Visible light mediated [2+2] photocycloaddition of amide-linked dienes.

In cooperation with the work group of Prof. J. Rehbein DFT-calculations were performed investigating the influence of the *N*-substituent of the amide-linked dienes on the [2+2] photocycloaddition (Scheme 64). All investigated features as stationary points, energy barriers and the nature of transition states prefer the [2+2] photocycloaddition of substrates with a large substituent.

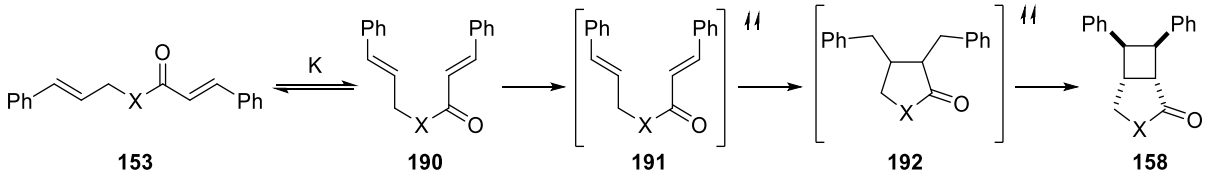

Scheme 64. Overview of the stepwise formation of the bicyclic compounds **158**.

The following part is devoted to the upscaling of the photoreaction. Therefore, a reactor with 30 LEDs (λ = 455 nm) was developed in which photoreactions with either 200 mL or 600 mL reaction volumina could be performed. Up to 110 mmol, 26 g, amide-linked diene **153i** was converted to the target bicyclic compounds **158i**, whereby the catalyst loading was reduced to 0.1 mol% (Scheme 65).

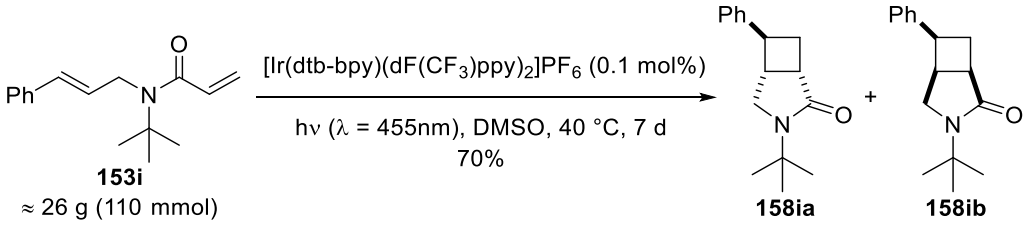

Scheme 65. Big scale [2+2] photocycloaddition of compound **153i**.

Another important issue of this thesis constitutes the transformation of the obtained bicyclic compounds **158** into the desired γ-cyclobutane amino acids (Scheme 66). The *tert*-butyl derivatives **A** were firstly transformed into the chloride salts of the free amino acids **199** by refluxing in 25% aqueous solution of HCl. The subsequent Boc-protection gave rise to *N*-Boc-*cis*-γ-cyclobutane amino acids **224**. Starting from the already Boc-protected bicyclic compounds **B**, target molecules **224** were easily accessible in a single step by treatment with lithium hydroxide in a THF/H_2O mixture at ambient temperature. Applying Birch conditions enabled the removal of the benzyl group in compounds **C** and the synthesis of the unprotected amide derivatives **271**. In two subsequent steps, Boc-protection and basic hydrolysis, derivatives **271** were converted to racemic γ-cyclobutane amino acids **224**.

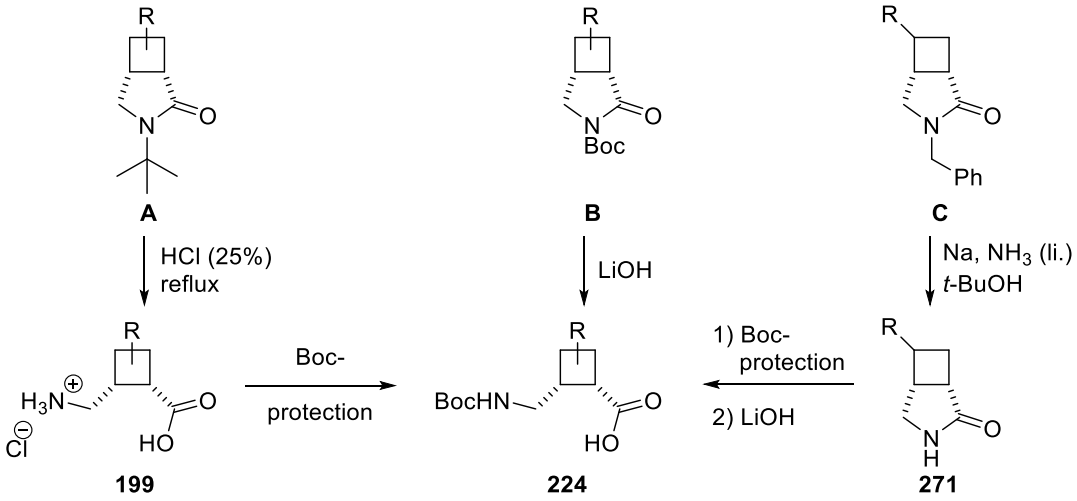

Scheme 66. Three different synthetic routes towards racemic *N*-Boc-*cis*-γ-cyclobutane amino acids **224**.

Three different *N*-protected products of the photocatalytic [2+2] cycloaddition were successfully transformed into the racemic *N*-Boc-protected γ-cyclobutane amino acid **(±)-226**, which served as starting material for the chiral resolution using (4*S*,5*R*)-4-methyl-5-

phenyloxazolidin-2-one (**236**) as chiral auxiliary giving rise to both enantiomers **(1*S*,2*R*,3*S*)-226** and **(1*R*,2*S*,3*R*)-226** (Scheme 67).

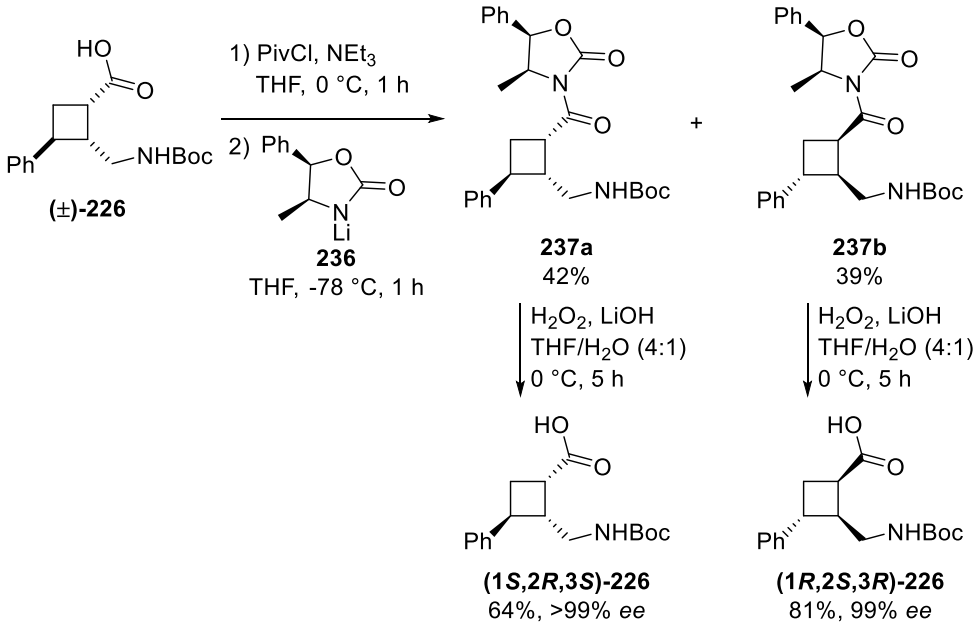

Scheme 67. Chiral resolution of compound **(±)-226**.

Another part of this thesis represents the investigation of the Birch reduction of the *N*-benzyl substituted bicyclic compounds, especially of the enantiomerically pure derivatives. In the case of 6-substituted derivatives such as **158v** a simple deprotection took place, whereas an analog transformation of 7-substituted derivatives **158w** provided product **215** which is itself a GABA-analogue and also a key intermediate in the synthesis of 3-(aminomethyl)-5-phenylpentanoic acid (**257**), an anticonvulsant. By applying this reaction mode, on the one hand a second enantioselective synthetic route towards γ-cyclobutane amino acids **(1*S*,2*R*,3*S*)-226** and **(1*R*,2*S*,3*R*)-226** and on the other hand a methodology towards both enantiomers **(*R*)-257** and **(*S*)-257** was developed (Scheme 68).

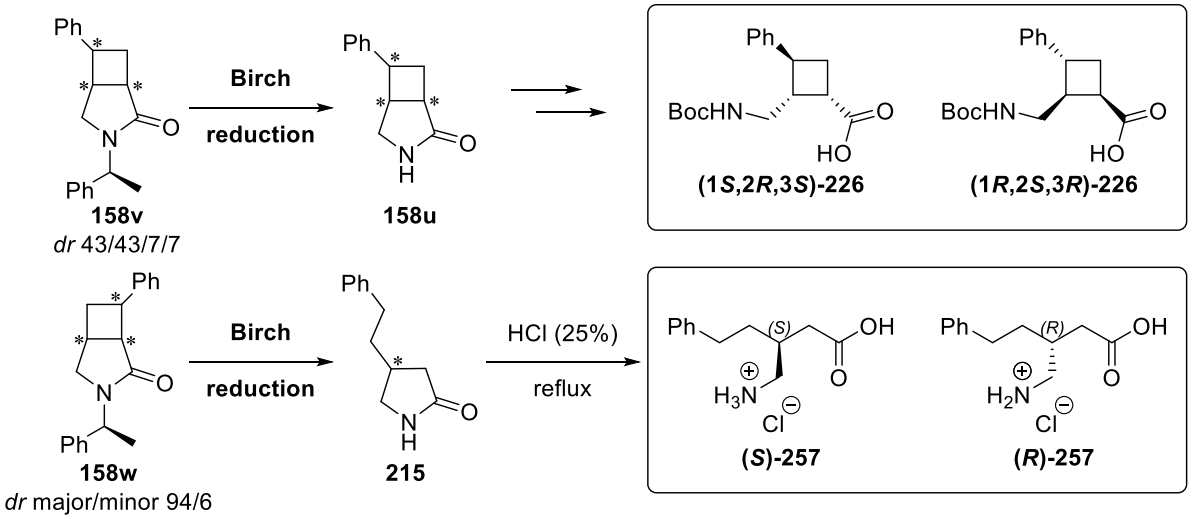

Scheme 68. Birch reduction of the enantiopure amide-linked dienes **158v** and **158w**.

The last chapter describes the incorporation of *N*-Fmoc-*cis*-γ-cyclobutane amino acids **(1*S*,2*R*,3*S*)-264** and **(1*R*,2*S*,3*R*)-264** in shortened NPY-analogues to develop new selective ligands for Y_4R in cooperation with the work group of Prof. C. Cabrele. The biological evaluation is currently ongoing in cooperation with the work group of Prof. A. Buschauer.

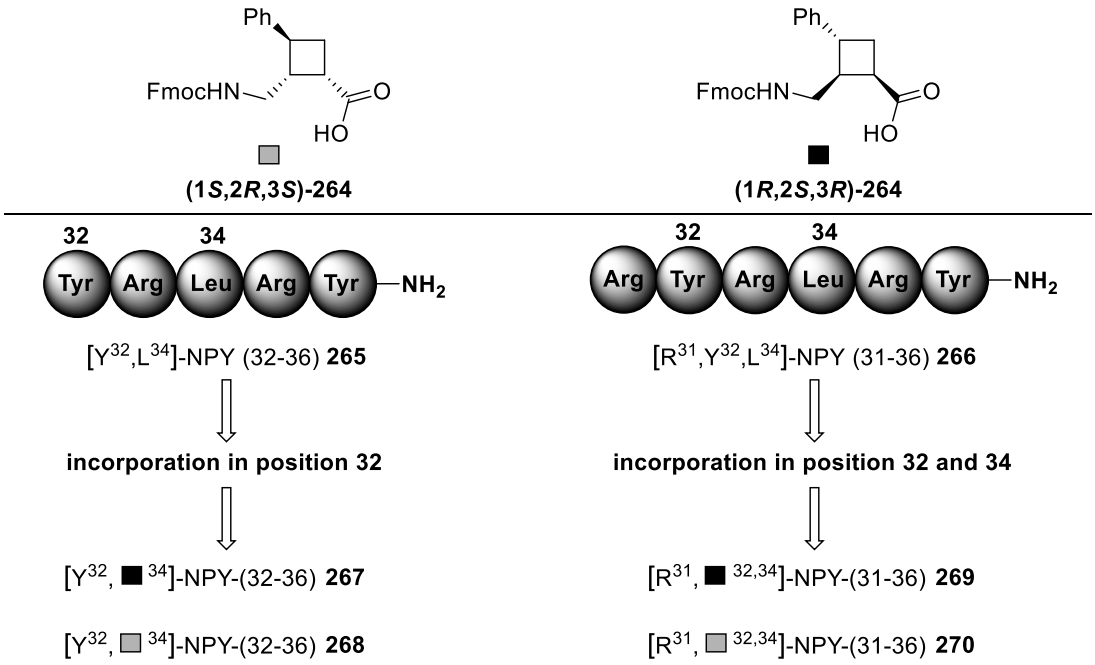

Scheme 69. Incorporation of *N*-Fmoc-*cis*-γ-cyclobutane amino acids **264** resulting in NPY-analogues (**267-270**).

D Zusammenfassung

Die vorliegende Arbeit beschreibt die Etablierung einer intramolekularen und mittels sichtbaren Licht induzierten [2+2] Photocycloaddition von amidverbrückten Dienen **153** zum Aufbau von Azabicycloheptanonen **158**, die im weiteren Verlauf zu γ-Cyclobutanaminosäuren umgewandelt wurden. Diese unnatürlichen cyclischen Aminosäuren wurden zudem für den Einbau in verkürzte NPY-Analoga enantioselektiv hergestellt, um selektive Liganden für den Y_4-Rezeptor zu gewinnen.

Die experimentellen Untersuchungen ergaben, dass der geeignete Reaktionsmodus für diese [2+2] Photocycloaddition auf einem Energieübertragungsmechanismus beruht. Der Iridium-basierte Photokatalysator $[Ir(dtb\text{-}bpy)(dF(CF_3)ppy)_2]PF_6$ diente in dieser Reaktion als Sensibilisator. Für die erfolgreiche Cycloaddition ist der Substituent am Stickstoffatom entscheidend. Hierdurch kann das Dien die notwendige Konformation **190** einnehmen. Die Umsetzung von *N*-*tert*-Butyl-, *N*-Benzyl- und *N*-Boc-amidderivate zu den entsprechenden Bicyclen gelang mit moderaten bis hin zu guten Ausbeuten mit jeweils hervorragender Diastereoselektivität (Abbildung 1).

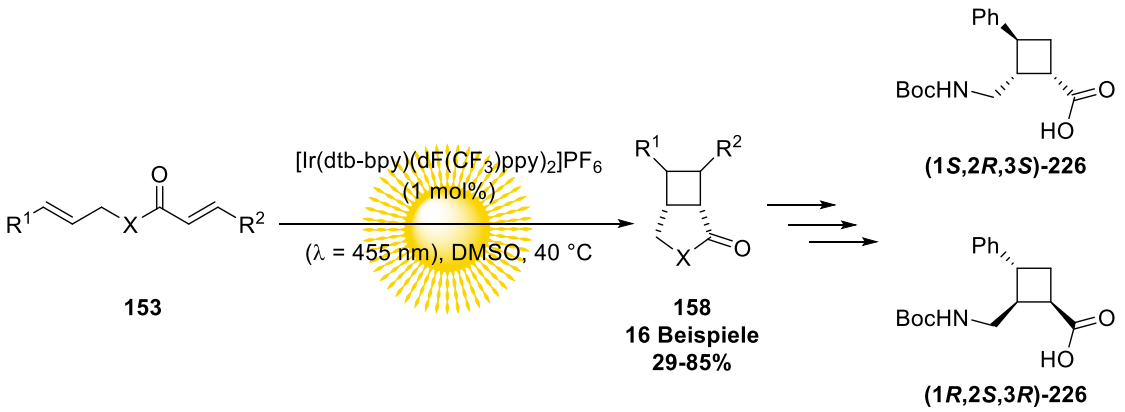

Abbildung 1: [2+2] Photocycloaddition von amidverbrückten Dienen **153** mittels sichtbarem Licht.

In Zusammenarbeit mit der Arbeitsgruppe von Frau Prof. J. Rehbein wurden DFT-Berechnungen durchgeführt, die den Einfluss des *N*-Substituenten der amidverbrückten Diene auf den Ausgang der [2+2] Photocycloaddition untersuchten (Abbildung 2). Alle berechneten Merkmale, wie die stationären Energiewerte, die Energiebarrieren und die Art der Übergangszustände wiesen darauf hin, dass für eine erfolgreiche [2+2] Cycloaddition ein ausreichend großer Substituent notwendig ist.

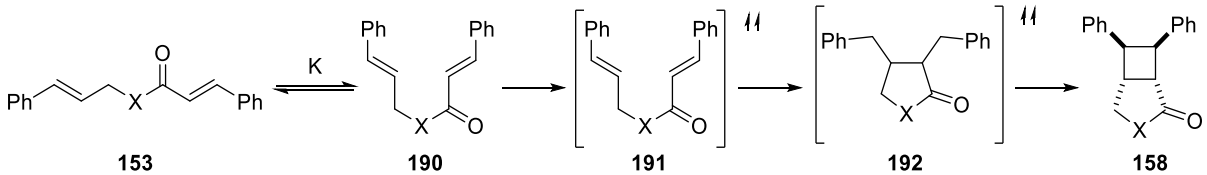

Abbildung 2: Überblick über die schrittweise Bildung der Bicyclen **158**.

Der nächste Abschnitt dieser Dissertation widmet sich dem Upscaling der Photoreaktion. Hierfür wurde ein Reaktor mit 30 LEDs (λ = 455nm) entwickelt, in dem Photoreaktionen entweder mit 200 mL oder 600 mL Reaktionsvolumen durchgeführt werden können. Mit Hilfe dieser Apparatur wurden bis zu 110 mmol (≈ 26 g) amidverbrücktes Startmaterial **153i** in das Zielmolekül Bicyclus **158i** umgesetzt (Abbildung 3). Die Katalysatormenge konnte hierbei auf 0,1 mol% herabgesetzt werden.

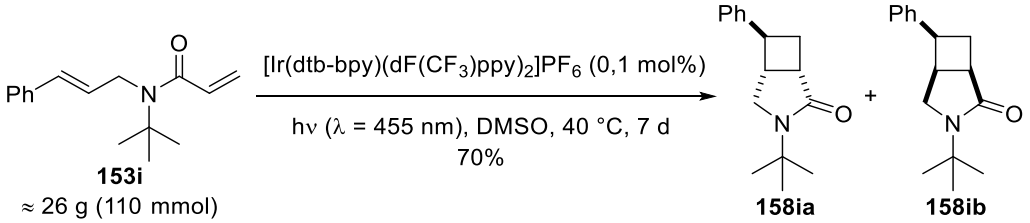

Abbildung 3: [2+2] Photoreaktion im Multigrammmaßstab.

Ein weiteres wichtiges Ziel dieser Arbeit stellte die Umwandlung der erhaltenen bicyclischen Verbindungen **158** in die gewünschten γ-Cyclobutanaminosäuren **224** dar (Abbildung 4). Durch Refluxieren der *tert*-Butylderivate **A** in 25%iger wässriger HCl-Lösung wurden diese zunächst in Chloridsalze der freien Aminosäuren **199** umgewandelt. Die anschließende Boc-Schützung führte zur Bildung der *N*-Boc-*cis*-γ-Cyclobutanaminosäuren **224**. Ausgehend von den bereits Boc-geschützten bicyclischen Verbindungen **B** waren die Zielmoleküle **224** durch den Einsatz von Lithiumhydroxid leicht zugänglich. Unter Birch-Bedingungen konnte die Benzylgruppe in Verbindungen **C** entfernt werden und derart die ungeschützten Amidderivate **271** erhalten werden. In zwei weiteren Schritten, einer Boc-Schützung und einer basischen Hydrolyse, wurden diese Derivate **271** schließlich in die racemische γ-Cyclobutanaminosäuren **224** umgewandelt.

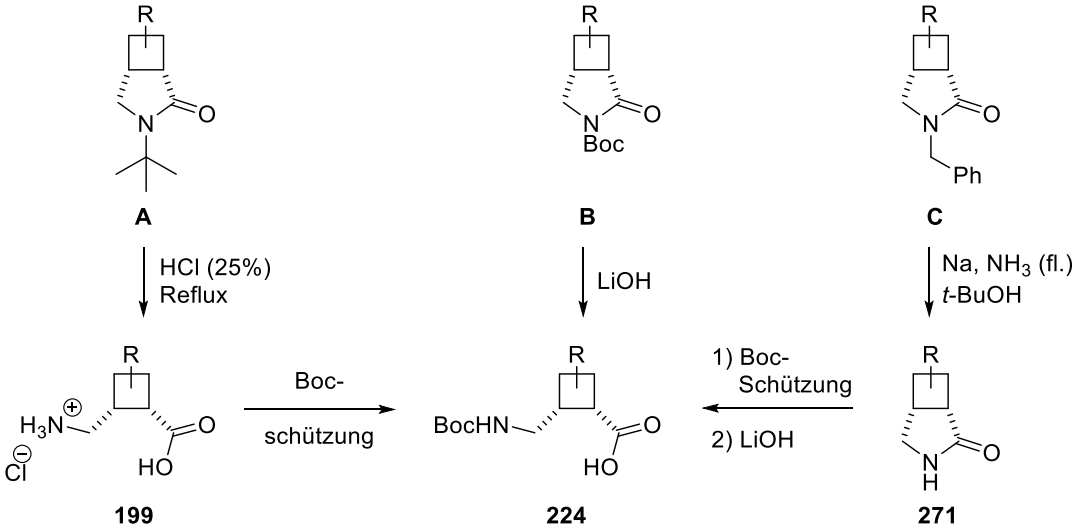

Abbildung 4: Drei verschiedene Syntheserouten zu *N*-Boc-*cis*-γ-Cylcobutanaminosäuren **224**.

Drei unterschiedlich *N*-geschützte Produkte der photokatalytischen [2+2] Cycloaddition wurden somit erfolgreich in die racemische *N*-Boc-geschützte γ-Cyclobutanaminosäure **(±)-226** umgesetzt, die als Ausgangsmaterial für die Racematspaltung mit (4*S*,5*R*)-4-Methyl-5-phenyloxazolidin-2-on (**236**) als chirales Hilfsmittel diente (Abbildung 5).

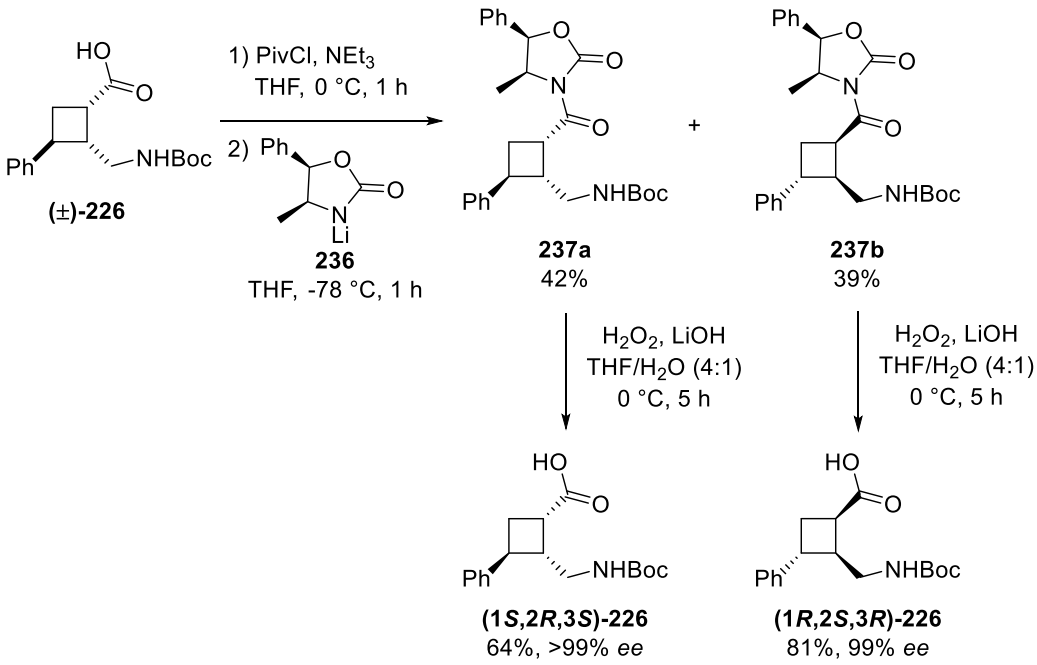

Abbildung 5: Racematspaltung des Produktes **(±)-226**.

Ein weiterer Teil dieser Arbeit befasst sich mit der Untersuchung der Birch-Reduktion der *N*-benzylsubstituierten bicyclischen Verbindungen, insbesondere der enantiomerenreinen Derivate. Im Falle von 6-substituierten Derivaten, wie **158v,** erfolgte lediglich eine Entschützung, während eine analoge Umwandlung der 7-substituierten Derivate, wie **158w**, das Produkt **215** lieferte. Bei Letzterem handelt es sich um ein GABA-Analogon sowie um ein wichtiges Zwischenprodukt in der Synthese von 3-(Aminomethyl)-5-phenylpentansäure (**257**), einer spasmolytischer Substanz. Durch diesen Reaktionstyp wurde einerseits ein zweiter enantioselektiver synthetischer Weg zu γ-Cyclobutanaminosäuren **(1*S*,2*R*,3*S*)-226** und **(1*R*,2*S*,3*R*)-226** und andererseits eine Methodik zur Darstellung beider Enantiomere **(*R*)-257** und **(*S*)-257** entwickelt (Abbildung 6).

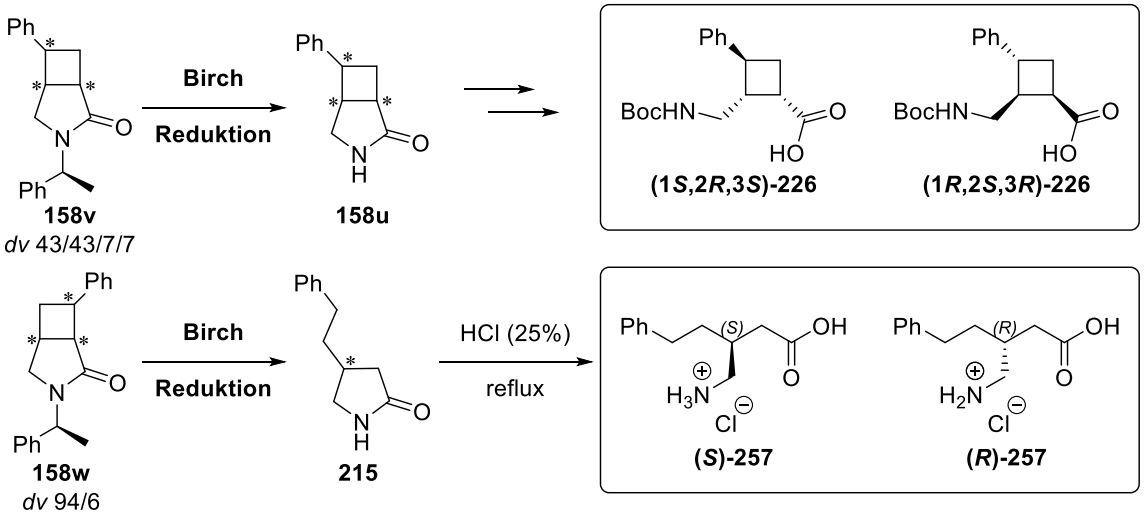

Abbildung 6: Birch-Reduktion der enantiomerenreinen Startmaterialen **158v** und **158w**.

Das letzte Kapitel beschreibt den Einbau der synthetisierten *N*-Fmoc-*cis*-γ-Cyclobutanaminosäuren **(1*S*,2*R*,3*S*)-264** und **(1*R*,2*S*,3*R*)-264** in verkürzte NPY-Analoga zur Entwicklung selektiver Liganden für den Y_4-Rezeptor in Zusammenarbeit mit der Arbeitsgruppe von Frau Prof. C. Cabrele (Abbildung 7). Die biologischen Testungen der dargestellten Substanzen erfolgen gegenwärtig in Zusammenarbeit mit der Arbeitsgruppe von Herrn Prof. A. Buschauer.

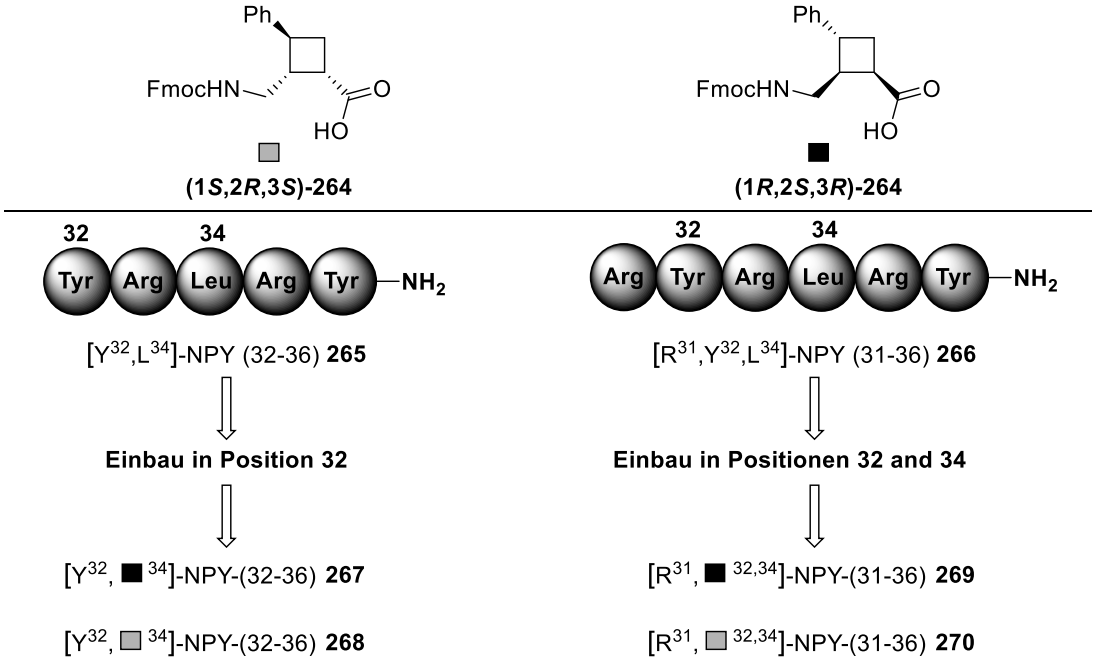

Abbildung 7: Einbau der *N*-Fmoc-*cis*-γ-Cyclobutanaminosäuren **264** zur Darstellung der NPY-Analoga (**267-270**).

E Experimental Part

1 General information

Synthesis

All chemicals were used as received or purified according to Purification of Common Laboratory Chemicals if necessary. Glassware was dried in an oven at 110 °C or flame-dried and cooled under a dry atmosphere prior to use. Solvents were applied in puriss p. a. grade and absolute solvents were prepared by established laboratory procedures. Larger quantities of dried solvents were purchased from a MB-SPS solvent purification system. Ethyl acetate, hexanes (40/60) and DCM for chromatography were distilled prior to use. Reactions with moisture and oxygen sensitive reagents were carried out in flame-dried glassware under an atmosphere of pre-dried nitrogen.

^{1}H-NMR spectra were recorded on Bruker Avance 300 (300 MHz) and Bruker Avance 400 (400 MHz). All measurements were performed at ambient temperature. Chemical shifts are reported in δ [ppm] relative to the solvent signals as internal standard, coupling constants *J* are given in [Hz]. Splitting patterns for the spin multiplicity were described in abbreviations: s = singlet, bs = broad singlet, d = doublet, t = triplet, q = quartet, p = pentet, dd = doublet of doublet, ddd = doublet of doublet of doublet, dt = doublet of triplet, dq = doublet of quartet, m = multiplet.

^{13}C-NMR spectra were recorded on Bruker Avance 300 (75 MHz) and Bruker Avance 400 (101 MHz). The chemical shifts are reported in δ [ppm] relative to the solvent signals as internal standard. In addition, DEPT 135 spectra (DEPT = distortion less enhancement by polarization transfer; primary or tertiary carbon (positive signal), secondary carbon (negative signal), quaternary carbon (no signal)) were recorded.

High-performance liquid chromatography (HPLC) was performed on a Varian 920-LC with DAD. Phenomenex Lux Cellulose-1 and 2, Chiracel OD-H and AS served as chiral stationary phase and mixtures of *n*-heptane and *i*PrOH were used for elution.

RP High-performance liquid chromatography (RP-HPLC) was performed on a Shimadzu LC-20A series. Marchery-Nagel EC 250/4 Nucleodur 100-5 C18ec and Marchery-Nagel VP

250/10 Nucleodur 100-5 C18ec served as stationary phase and mixtures of MeCN + 0.05% TFA and Millipore water + 0.05% TFA were used for elution. MeCN was removed before lyophilization. Lyophilization was carried out with a Christ Alpha 2-4 LC equipped with a vacuubrand RZ 6 rotary vane vacuum pump.

Infra-red spectroscopy (IR) was carried out on a Cary 630 FTIR Spectrometer (Agilent Technology) with ZnSe windows and Diamond Single Reflection Accessory. Solid and liquid compounds were measured neatly, and the wavenumbers are reported in cm^{-1}.

Mass spectrometry (MS) was performed on Finnigan MAT95, Agilent Q-TOF 6540 UHD, Finnigan MAT SSQ 710 A, ThermoQuest Finnigan TSQ 7000 at the Central Analytical Department of the University of Regensburg.

Melting points (mp) were measured automatically on a MPA 100 Optimelt (Automated Melting Point System, Digital Image Processing Technology).

Optical rotations were determined in a Perkin Elmer 241 polarimeter or an Anton Paar MCP 500 at 589 nm wavelength (sodium-*d*-line) in a 1.0 dm measuring cell of ca. 2 mL volume and the specified solvent.

Cyclic voltammetric measurements (CV) were carried out with an Autolab PGSTAT302N Metrohm (working electrode: glassy carbon, counter electrode: platinum wire, pseudo-reference electrode: silver wire, supporting electrolyte: tetrabutylammonium tetrafluoroborate Fluka 0.1 M). All measurements were performed by Regina Hoheisel form the work group of Prof. B. König. Prior to the measurement, the solvent was purged with argon. All experiments were performed under argon atmosphere. Ferrocene was used as an internal reference for determining the reduction and oxidation potentials. Afterwards, the so measured potentials were transferred into potential values *vs* SCE.[1]

Column chromatography was carried out on silica gel Merck Geduran 60 (0.063-0.200 mm) and flash silica gel Merck Geduran Si 60 (0.040-0.063 mm). Furthermore, the flash system Intelli Flash 310 (AnaLogix) was used with flash silica gel Merck Geduran Si 60 (0.040-0.063 mm).

Thin layer chromatography (TLC) was performed on alumina plates with silica gel (Merck silica gel 60 F 254). Visualization was accomplished using UV light (λ = 254 nm), iodine, vanillin/sulfuric acid solution (1.25 g vanillin, 8 mL conc. H_2SO_4 , 25 mL conc. acetic acid, 215 mL methanol), potassium permanganate solution (3 g $KMnO_4$, 20 g Na_2CO_3, 5 mL 5%

NaOH (aq.), 300 mL H_2O), Seebach's stain (2.5 g phosphomolybdic acid, 1 g $Ce(SO_4)_2$, 6 mL conc. H_2SO_4, 94 ml H_2O), bromocresol green (40 mg bromocresol, 100 mL ethanol, 0.1M NaOH added until solution got blue) or ninhydrin (450 mg ninhydrin, 1.5 mL conc. acetic acid, 500 mL ethanol).

Light sources

Blue light irradiation was performed using either a CREE-XP rb Lamp (700 mA, λ = 455nm) or an Oslon 80 rb Lamp (700 mA, λ = 455 nm). For the big scale reaction an immersion shaft exposure unit (30x Osram Oslon SSL 80 deep blue, 1 W/ LED @ 700 mA, λ = 455 nm, 3x Meanwell LPC-35-700, Input: 90-260 VAC, Output: 700 mA, 9-48 VDC) was used. For the UV-irradiation a Phillips HPK lamp (125 W) was used.

2 Syntheses of compounds

Following compounds were synthesized according to literature procedures and spectroscopic data matched well with those reported:

$Ru(bpz)_3Cl_2$[2], $Cu(dap)_2Cl$[3], *fac*-$Ir(ppy)_3$[4], $[Ir(dtb\text{-}bpy)ppy_2]PF_6$[5], $[Ir(dtb\text{-}bpy)(dF(CF_3)ppy)_2]PF_6$[6], 1-phenyl-2-(triphenylphosphaneylidene)ethan-1-one (**133**)[7], (*E*)-4-oxo-4-phenylbut-2-en-1-yl-(*E*)-4-oxo-4-phenylbut-2-enoate (**134**)[8], *tert*-butyl methyl(2-oxoethyl)carbamate (**145a**)[9], (9H-fluoren-9-yl)methyl methyl(2-oxoethyl)carbamate (**145c**)[10], (*E*)-*N*-methyl-3-phenylprop-2-en-1-amine (**154**)[11], *N*-cinnamylaniline (**155**)[12], (*E*)-*N*-(3-(4-methoxyphenyl)allyl)aniline (**156**)[13], (*E*)-3-(4-methoxyphenyl)prop-2-en-1-ol[14], (*E*)-1-(3-bromoprop-1-en-1-yl)-4-methoxybenzene (**169c**)[15], methyl (*E*)-4-bromobut-2-enoate (**169d**)[16], *N*-(*tert*-butyl)prop-2-en-1-amine (**170a**)[17], (*E*)-3-phenylprop-2-en-1-amine (**172**)[18], *tert*-butyl cinnamylcarbamate (**173**)[19], *tert*-butyl allylcarbamate (**175**)[20], (*E*)-4-methoxy-4-oxobut-2-enoic acid (**177**)[21], (*E*)-3-(furan-2-yl)acrylic acid (**180a**)[22], (*E*)-3-(thiophen-2-yl)acrylic acid (**180b**)[22], (*E*)-3-(1*H*-pyrrol-2-yl)acrylic acid (**180c**)[23], (*E*)-3-(1*H*-indol-3-yl)acrylic acid (**180d**)[24], methyl (*E*)-3-(1*H*-pyrrol-2-yl)acrylate (**181b**)[23].

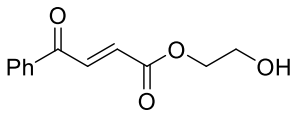

2-Hydroxyethyl (*E*)-4-oxo-4-phenylbut-2-enoate (131)[8]

In a round bottom flask, *trans*-3-benzoylacrylic acid **129** (4.40 g, 25.0 mmol, 1.0 equiv.) and ethanediol **130** (5.60 mL, 6.21 g, 100 mmol, 4.0 equiv.) were dissolved in dry DCM (100 mL). This solution was cooled down to 0 °C by an ice-bath and then EDC•HCl (5.28 g, 27.5 mmol, 1.1 equiv.), as well as DMAP (0.310 g, 2.50 mmol, 0.1 equiv.), were added, successively. The reaction mixture was stirred for 1 h at 0 °C and for further 4.5 h at ambient temperature. Afterwards, the organic phase was washed with 1M HCl (3x). The combined aqueous phases were back-extracted with DCM (30 mL). Finally, the organic phases were dried over $MgSO_4$, filtered and the solvent was removed under vacuo. By flash silica gel column chromatography (hexanes/EtOAc 2:1) compound **131** (3.22 g, 14.6 mmol, 58%) was obtained as yellow oil.

^{1}H-NMR (400 MHz, $CDCl_3$) δ = 8.03 – 7.98 (m, 2H), 7.95 (d, *J* = 15.6 Hz, 1H), 7.67 – 7.59 (m, 1H), 7.56 – 7.48 (m, 2H), 6.93 (d, *J* = 15.6 Hz, 1H), 4.43 – 4.33 (m, 2H), 3.97 – 3.87 (m, 2H), 1.78 (bs, 1H); **^{13}C-NMR** (75 MHz, $CDCl_3$) δ = 189.4, 165.8, 137.1, 136.5, 134.0, 132.0, 128.94, 128.91, 66.9, 61.0.

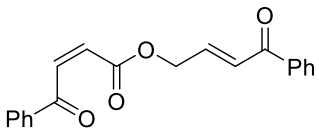

(*E*)-4-Oxo-4-phenylbut-2-en-1-yl (*Z*)-4-oxo-4-phenylbut-2-enoate (136)

A flame-dried heavy-wall Schlenk flask was equipped with compound **134** (94.7 mg, 296 µmol, 1 equiv.), NPh_3 (148 mg, 603 µmol, 2 equiv.), $Ru(bpy)_3Cl_2$ (11.2 mg, 15.0 µmol, 5 mol%) and dry DCM (3 mL). The reaction mixture was degassed via three freeze-pump-thaw cycles and was irradiated via blue LED for 48 h at rt. Afterwards, the solvent was removed, and the crude mixture was purified by silica gel column chromatography (hexanes/EtOAc 5:1) giving rise to compound **136** (75.6 mg, 236 µmol, 79%) as yellow oil.

R_f = 0.12 (hexanes/EtOAc 5:1); **^{1}H-NMR** (300 MHz, $CDCl_3$) δ = 8.01 – 7.87 (m, 4H), 7.63 – 7.41 (m, 6H), 7.05 – 6.96 (m, 2H, two signals are overlapping: 7.02 (d, *J* = 15.5 Hz, 1H) + 7.00 (dt, *J* = 15.5, 1.8 Hz, 1H)), 6.83 (dt, *J* = 15.5, 4.4 Hz, 1H), 6.38 (d, *J* = 12.2 Hz, 1H), 4.78 (dd,

J = 4.4, 1.8 Hz, 2H); **^{13}C-NMR** (101 MHz, $CDCl_3$) δ = 193.7, 189.8, 164.2, 141.7, 139.9, 137.3, 135.6, 133.9, 133.1, 128.9, 128.8, 128.72, 128.67, 128.4, 126.1, 125.5, 63.72; **IR (neat)** [cm^{-1}] = 3354, 3026, 2948, 1692, 1602, 1528, 1446, 1319, 1274, 1241, 1148, 1028, 991, 939, 894, 827, 734, 700; **HRMS**: (ESI-MS) m/z calc. for $[C_{20}H_{16}O_4Na]^+$ $[M+Na]^+$ 343.0941, found 343.0941, m/z calc. for $[C_{20}H_{17}O_4]^+$ $[M+H]^+$ 321.1121, found 321.1127, m/z calc. for $[C_{20}H_{20}NO_4]^+$ $[M+NH_4]^+$ 338.1387, found 338.1388.

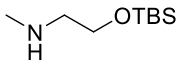

2-((*tert*-Butyldimethylsilyl)oxy)-*N*-methylethan-1-amine (140)[25]

Methylamino ethanol **139a** (1.50 g, 1.6 mL, 20 mmol, 1.0 equiv.) was dissolved in dry DCM (20 mL) and then TBS-Cl (3.32 g, 22 mmol, 1.1 equiv.) was added portionwise. Afterwards NEt_3 (2.43 g, 3.3 mL, 24 mmol, 1.2 equiv.) and DMAP (24.4 mg, 0.20 mmol, 0.01 equiv.) were added. After 20 h reaction time at ambient temperature, the reaction mixture was quenched by addition of a saturated aqueous solution of NH_4Cl (40 mL). After phase separation, the aqueous phase was extracted with DCM (3 x 20 mL). The combined organic phases were dried over $MgSO_4$, filtered and the solvent was removed under reduced pressure. Compound **140** (1.95 g, 10 mmol, 50%) was obtained as a white solid and was used in the following without further purification.

^{1}H-NMR (400 MHz, $CDCl_3$) δ = 4.01 – 3.73 (m, 2H), 3.11 – 2.83 (m, 2H), 2.79 – 2.49 (m, 3H), 0.85 (s, 9H), 0.06 (s, 6H); **^{13}C-NMR** (75 MHz, $CDCl_3$) δ = 59.0, 50.8, 33.6, 25.9, 18.2, –5.4.

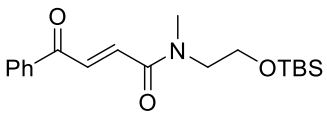

(*E*)-*N*-(2-((*tert*-Butyldimethylsilyl)oxy)ethyl)-*N*-methyl-4-oxo-4-phenylbut-2-enamide (141)

(*E*)-4-Oxo-4-phenylbut-2-enoic acid (**129**) (793 mg, 4.5 mmol, 1.0 equiv.), amine **140** (983 mg, 5.0 mmol) and DMAP (54.5 mg, 0.45 mmol, 0.1 equiv.) were dissolved in dry DCM (15 mL). After cooling to 0 °C, EDC•HCl (955 mg, 5.0 mmol, 1.1 equiv.) in dry DCM (7 mL) was added.

The reaction mixture was stirred for additional 15 min at 0 °C and then for 24 h at ambient temperature. The organic phase was washed twice with 1M HCl, dried over $MgSO_4$, filtered and the solvent was evaporated. The purification by flash column chromatography on silica gel (hexanes/EtOAc 2:1) yielded compound **141** (776 mg, 2.2 mmol, 50%) as yellow oil.

R_f = 0.39 (hexanes/EtOAc 2:1); **^{1}H-NMR** (400 MHz, $CDCl_3$) δ = 8.04 – 7.97 (m, 2H), 7.92 (dd, *J* = 15.0, 4.0 Hz, 1H), 7.61 – 7.41 (m, 4H), 3.77 (dt, *J* = 29.0, 5.3 Hz, 2H), 3.57 (dt, *J* = 7.5, 5.3 Hz, 2H), 3.23 (s, 1.25H) + 3.07 (s, 2.75H), 0.86 (s, 3.9H) + 0.81 (s, 5.1H), 0.02 (s, 2.57H) + 0.00 (s, 3.43H) (signal doubling due to rotameres); **^{13}C-NMR** (101 MHz, $CDCl_3$) δ = 189.74, 189.72, 165.8, 165.0, 137.1, 137.0, 134.0, 133.7, 133.6, 133.5, 133.4, 132.8, 128.9, 128.83, 128.81, 128.78, 61.5, 60.8, 52.2, 51.4, 38.0, 34.7, 25.9, 25.8, 18.2, –5.4, –5.5 (signal doubling due to rotameres). **HRMS**: (ESI-MS) calc. for $[C_{19}H_{30}NO_3Si]^+$ $[M+H]^+$ 348.1989, found 348.1995.

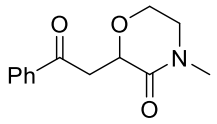

4-Methyl-2-(2-oxo-2-phenylethyl)morpholin-3-one (143)

Compound **141** (776 mg, 2.2 mmol, 1 equiv.) was dissolved in abs. THF (6 mL). Then TBAF (2.08 g, 6.6 mmol, 3 equiv.) and acetic acid (396 mg, 380 µL, 6.6 mmol, 3 equiv.) were added successively. The resulting black solution was stirred for 17.5 h at room temperature and was quenched by addition of water (3 mL) as well as brine (3 mL). After phase separation, the aqueous phase was extracted with DCM (2x). The combined organic phases were dried over $MgSO_4$, filtered and the solvent was evaporated. Purification by flash column chromatography on silica gel (hexanes/EtOAc 1:1) gave compound **143** (332 mg, 1.4 mmol, 64%) as slightly yellow oil.

R_f = 0.07 (hexanes/EtOAc 1:1); **^{1}H-NMR** (300 MHz, $CDCl_3$) δ = 7.99 – 7.93 (m, 2H), 7.59 – 7.52 (m, 1H), 7.48 – 7.41 (m, 2H), 4.69 (dd, *J* = 7.4, 3.1 Hz, 1H), 4.01 (ddd, *J* = 11.8, 4.6, 1.8 Hz, 1H), 3.93 – 3.83 (m, 1H), 3.69 (ddd, *J* = 10.6, 9.2, 3.8 Hz, 2H), 3.48 (dd, *J* = 17.4, 7.5 Hz, 1H), 3.22 – 3.14 (m, 1H), 3.03 (s, 3H); **^{13}C-NMR** (101 MHz, $CDCl_3$) δ = 196.8, 169.0, 136.8, 133.2, 128.6, 128.2, 74.0, 63.0, 48.9, 41.1, 34.5; **IR** (neat) ν [cm^{-1}] = 2926, 2866, 1684, 1640, 1502, 1449, 1345, 1259, 1215, 1118, 756, 689; **LRMS**: (APCI-MS) 234.1129 $[M+H]^+$.

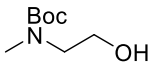

***tert*-Butyl (2-hydroxyethyl)(methyl)carbamate (146a)[26]**

Methylaminoethanol **139a** (751 mg, 0.8 mL, 10 mmol, 1 equiv.) was dissolved in MeCN (50 mL) and the solution was cooled down to 0 °C. Boc_2O (2.18 g, 10 mmol, 1 equiv.) and DMAP (12.7 mg, 0.10 mmol, 0.01 equiv.) were added and the reaction mixture was stirred for 24 h. Then the solvent was removed under reduced pressure. The residue was dissolved again in DCM and water. After phase separation, the aqueous phase was extracted twice with DCM. The combined organic phases were dried over $MgSO_4$, filtered and the solvent was removed by rotatory evaporator. Compound **146a** (1.62 g, 9.3 mmol, 93%) was obtained as clear oil and was used without further purification.

^{1}H-NMR (400 MHz, $CDCl_3$) δ = 3.75 (t, *J* = 5.3 Hz, 2H), 3.39 (t, *J* = 5.3 Hz, 2H), 2.92 (s, 3H), 1.46 (s, 9H); **^{13}C-NMR** (101 MHz, $CDCl_3$) δ = 157.3, 79.9, 61.3, 51.4, 35.5, 28.4.

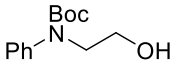

***tert*-Butyl (2-hydroxyethyl)(phenyl)carbamate (146b)[27]**

Phenylaminoethanol **139b** (1.37 g, 1.25 mL, 10 mmol, 1 equiv.) was dissolved in MeCN (50 mL) and the solution was cooled down to 0 °C. Boc_2O (2.18 g, 10 mmol, 1 equiv.) and DMAP (13.7 mg, 0.10 mmol, 0.01 equiv.) were added and the reaction mixture was stirred for 24 h. Then the solvent was removed under reduced pressure. The residue was dissolved again in DCM and water. After phase separation, the aqueous phase was extracted twice with DCM. The combined organic phases were dried over $MgSO_4$, filtered and the solvent was removed by rotatory evaporator. Compound **146b** (2.14 g, 9.0 mmol, 90%) was obtained as clear oil and was used without further purification.

^{1}H-NMR (300 MHz, $CDCl_3$) δ = 7.22 – 7.15 (m, 2H), 6.77 – 6.69 (m, 1H), 6.67 – 6.60 (m, 2H), 4.31 – 4.24 (m, 2H), 3.46 – 3.37 (m, 2H), 1.50 (s, 9H); **^{13}C-NMR** (101 MHz, $CDCl_3$) δ =153.5, 147.3, 129.3, 118.1, 113.2, 82.5, 65.4, 43.0, 27.8.

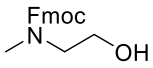

(9*H*-Fluoren-9-yl)methyl (2-hydroxyethyl)(methyl)carbamate (146c)[28]

Methylaminoethanol **139a** (751 mg, 0.8 mL, 10.0 mmol, 1.0 equiv.) was dissolved in a mixture of dioxane/water (1:1, 50 mL). After cooling down to 0 °C, FmocOSu (3.83 g, 11.3 mmol, 1.1 equiv.) and $NaHCO_3$ (1.72 g, 20.5 mmol, 2.05 equiv.) were added. The reaction mixture was stirred in the defrosting ice-bath for 24 h. Afterwards, the solvent was evaporated in vacuo and the residue was dissolved again in saturated aqueous solution of NH_4Cl and DCM. After phase separation, the aqueous phase was extracted with DCM (2x). The combined organic phases were dried over $MgSO_4$, filtered and the solvent was removed under reduced pressure. Compound **146c** (2.97 g, 10.0 mmol, quant.) was obtained as clear oil.

R_f = 0.45 (hexanes/EtOAc 1:2); **^{1}H-NMR** (300 MHz, $CDCl_3$) δ = 7.77 (d, *J* = 7.4 Hz, 2H), 7.60 (d, *J* = 6.7 Hz, 2H), 7.36 (ddd, *J* = 13.8, 10.9, 6.9 Hz, 4H), 4.63 – 4.32 (m, 2H), 4.25 (t, *J* = 6.5 Hz, 1H), 3.86 – 3.69 (m, 1H), 3.59 – 3.31 (m, 2H), 3.16 (s, 1H), 3.04 – 2.85 (m, 3H) (signal broading due to rotameres); **^{13}C-NMR** (101 MHz, $CDCl_3$) δ = 157.4, 156.4, 144.1, 141.4, 127.7, 127.1, 125.0, 124.9, 120.0, 67.6, 67.2, 60.9, 60.5, 51.8, 51.0, 47.4, 35.7, 35.3 (signal doubling due to rotameres); **LRMS**: (ESI-MS) 234.1129 $[M+H]^+$.

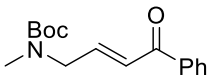

***tert*-Butyl (*E*)-methyl(4-oxo-4-phenylbut-2-en-1-yl)carbamate (147a)**

Compound **145a** (519 mg, 3.0 mmol, 1.0 equiv.) was dissolved in dry DCM (10 mL). Then ylide **133** (1.71 g, 4.5 mmol, 1.5 equiv.) was added and the reaction mixture was stirred for 20 h at ambient temperature. The solvent was removed, and the residue was purified by silica gel column chromatography (hexanes/EtOAc 7:1) yielding compound **147a** (542 mg, 2.0 mmol, 66%) as orange oil.

R_f = 0.17 (hexanes/EtOAc = 7:1); **^{1}H-NMR** (300 MHz, $CDCl_3$) δ = 7.92 (d, *J* = 7.2 Hz, 2H), 7.53 (dt, *J* = 30.2, 7.3 Hz, 3H), 7.11 – 6.74 (m, 2H), 4.09 (bs, 2H), 2.92 (bs, 3H), 1.47 (s, 9H) (signal broading due to rotameres); **^{13}C-NMR** (101 MHz, $CDCl_3$) δ = 190.4, 190.0, 155.5, 143.8, 137.6, 132.9, 128.6, 128.5, 126.3, 125.3, 50.4, 49.8, 34.5, 28.4 (signal doubling and

broading due to rotamers); **IR** (neat) ν [cm^{-1}] = 3058, 3026, 2926, 2859, 1652, 1617, 1591, 1492, 1453, 1385, 1237, 1196, 970, 764, 697; **HRMS**: (ESI-MS) calc. for $[C_{16}H_{22}NO_3]^+$ $[M+H]^+$ 276.1594, found 276.1598.

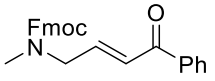

(9*H*-Fluoren-9-yl)methyl (*E*)-methyl(4-oxo-4-phenylbut-2-en-1-yl)carbamate (147b)

Compound **145c** (1.74 g, 5.9 mmol, 1.0 equiv.) was dissolved in dry DCM (20 mL). Then ylide **133** (2.32 g, 6.1 mmol, 1.03 equiv.) was added and the reaction mixture was stirred for 19 h at ambient temperature. The solvent was removed, and the residue was purified by silica gel column chromatography (hexanes/EtOAc 3:1→1:1) yielding compound **147b** (1.46 g, 3.7 mmol, 63%) as yellow oil.

R_f = 0.16 (hexanes/EtOAc 3:1); **^{1}H-NMR** (300 MHz, $CDCl_3$) δ = 7.90 (t, *J* = 7.9 Hz, 2H), 7.74 (dd, *J* = 20.1, 7.5 Hz, 2H), 7.64 – 7.28 (m, 8H), 7.25 – 7.14 (m, 1H), 7.09 – 6.59 (m, 2H), 4.49 (t, *J* = 7.7 Hz, 2H), 4.32 – 4.13 (m, 2H), 4.00 (d, *J* = 2.9 Hz, 1H), 2.97 (s, 3H); **^{13}C-NMR** (75 MHz, $CDCl_3$) δ = 190.4, 189.9, 156.3, 156.1, 144.0, 143.9, 143.0, 142.8, 141.4, 137.5, 133.1, 128.7, 127.8, 127.1, 126.6, 125.5, 125.0, 124.8, 120.0, 67.7, 67.5, 50.4, 50.1, 47.3, 35.0, 34.3; **IR** (neat) ν [cm^{-1}] = 3276, 3063, 3015, 2952, 1673, 1625, 1479, 1446, 1401, 1356, 1282, 1207, 1148, 1073, 1017, 984, 883, 738, 693; **HRMS**: (ESI-MS) calc. for $[C_{26}H_{24}NO_3]^+$ $[M+H]^+$ 398.1751, found 398.1754.

Amine and acid syntheses

General procedure for the amine synthesis A[29]

The amine (3 equiv.) and K_2CO_3 (3 equiv.) were suspended in MeCN and cooled to 0 °C with a cooling bath. To this suspension, a solution of the corresponding bromide (1 equiv.) in MeCN was added dropwise. The reaction mixture was stirred in the defrosting ice-bath for the given time. Then the inorganic salts were filtered off and the filter cake was washed with small portions of MeCN. The solvent was removed under reduced pressure. The crude product was purified by column chromatography using a hexanes/EtOAc mixture.

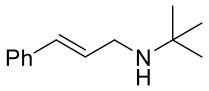

(*E*)-*N*-(*tert*-Butyl)-3-phenylprop-2-en-1-amine (170b)[30]

According to the general procedure **A** *tert*-butylamine (26.3 g, 38 mL, 360 mmol, 3 equiv.) and K_2CO_3 (49.8 g, 360 mmol, 3 equiv.) in MeCN (200 mL) were used and (*E*)-(3-bromoprop-1-en-1-yl)benzene (**169b**) (23.6 g, 120 mmol, 1 equiv.) in MeCN (100 mL) was added. The reaction mixture was stirred for 27 h. After filtration (*E*)-*N*-(*tert*-butyl)-3-phenylprop-2-en-1-amine (**170b**) (21.6 g, 114 mmol, 95%) was obtained as yellow oil which was used in following steps without further purification.

^{1}H-NMR (400 MHz, $CDCl_3$) δ = 7.40 – 7.34 (m, 2H), 7.33 – 7.24 (m, 2H), 7.24 – 7.17 (m, 1H), 6.52 (dd, *J* = 14.6, 7.6 Hz, 1H), 6.34 (dt, *J* = 15.8, 6.4 Hz, 1H), 3.38 (dd, *J* = 6.4, 1.2 Hz, 2H), 1.16 (s, 9H); **^{13}C-NMR** (101 MHz, $CDCl_3$) δ = 137.3, 130.9, 129.4, 128.5, 127.3, 126.3, 50.6, 45.2, 29.1.

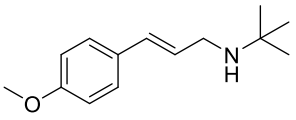

(*E*)-*N*-(*tert*-Butyl)-3-(4-methoxyphenyl)prop-2-en-1-amine (157)

According to the general procedure **A** *tert*-butylamine (2.63 g, 3.8 mL, 36 mmol, 3 equiv.) and K_2CO_3 (4.94 g, 36 mmol, 3 equiv.) in MeCN (30 mL) were used and (*E*)-1-(3-bromoprop-1-en-1-yl)-4-methoxybenzene (**169c**) (2.67 g, 12 mmol, 1 equiv.) in MeCN (30 mL) was added. The reaction mixture was stirred for 16 h. After column chromatography (hexanes/EtOAc 5:1) (*E*)-1-(3-bromoprop-1-en-1-yl)-4-methoxybenzene (**157**) was obtained as yellow oil in a yield of 40% (1.06 g, 4.8 mmol).

R_f = 0.19 (hexanes/EtOAc 3:1); **^{1}H-NMR** (300 MHz, $CDCl_3$) δ = 7.37 – 7.20 (m, 2H), 6.93 – 6.76 (m, 2H), 6.47 (d, *J* = 15.8 Hz, 1H), 6.20 (dt, *J* = 15.8, 6.5 Hz, 1H), 3.79 (s, 3H), 3.35 (dd, *J* = 6.5, 1.3 Hz, 2H), 1.16 (s, 9H); **^{13}C-NMR** (75 MHz, $CDCl_3$) δ = 159.0, 130.6, 130.0, 127.4, 126.6, 113.9, 55.3, 50.8, 45.2, 29.0; **IR** (neat) ν [cm^{-1}] = 3034, 2959, 2836, 1714, 1696, 1509, 1461, 1396, 1300, 1244, 1174, 1103, 1036, 965, 838, 805, 760, 697; **HRMS**: (EIC-MS) m/z calc. for $[C_{14}H_{21}NO]^{+\bullet}$ $[M]^{+\bullet}$ 219.16177, found 219.16189.

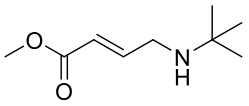

Methyl (*E*)-4-(*tert*-butylamino)but-2-enoate (170c)[31]

According to the general procedure **A** *tert*-butylamine (6.36 g, 9.1 mL, 87.0 mmol, 3 equiv.) and K_2CO_3 (12.0 g, 87.0 mmol, 3 equiv.) in MeCN (100 mL) were used and methyl (*E*)-4-bromobut-2-enoate (**169d**) (5.13 g, 3.6 ml, 29.0 mmol, 1 equiv.) in MeCN (50 mL) was added. The reaction mixture was stirred for 21 h. After filtration methyl (*E*)-4-(*tert*-butylamino)but-2-enoate (**170c**) (4.50 g, 26.3 mmol, 91%) was obtained as yellow oil which was used in following steps without further purification.

^{1}H-NMR (300 MHz, $CDCl_3$) δ = 7.04 (dt, *J* = 15.7, 5.5 Hz, 1H), 5.99 (dt, *J* = 15.7, 1.8 Hz, 1H), 3.72 (s, 3H), 3.37 (dd, *J* = 5.5, 1.8 Hz, 2H), 1.11 (s, 9H); **^{13}C-NMR** (101 MHz, $CDCl_3$) δ = 167.0, 148.2, 120.6, 51.5, 50.6, 43.7, 29.0.

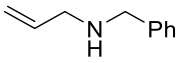

***N*-Benzylprop-2-en-1-amine (170d)[32]**

According to the general procedure **A** allylamine (5.14 g, 6.7 mL, 90.0 mmol, 3 equiv.) and K_2CO_3 (12.4 g, 90.0 mmol, 3 equiv.) in MeCN (100 mL) were used and benzylbromide (5.13 g, 3.6 mL, 30.0 mmol, 1 equiv.) in MeCN (50 mL) was added. The reaction mixture was stirred for 21 h. Distillitation under reduced pressure (1.0 mbar, 60 °C) yielded *N*-benzylprop-2-en-1-amine (**170d**) (2.40 g, 16.3 mmol, 54%) as colorless oil.

^{1}H-NMR (300 MHz, $CDCl_3$) δ = 7.39 – 7.22 (m, 5H), 5.95 (ddt, *J* = 16.2, 10.2, 6.0 Hz, 1H), 5.17 (ddq, *J* = 21.5, 10.2, 1.4 Hz, 2H), 3.81 (s, 2H), 3.29 (dt, *J* = 6.0, 1.3 Hz, 2H), 1.42 (s, 1H); **^{13}C-NMR** (75 MHz, $CDCl_3$) δ = 140.3, 136.8, 128.8, 128.4, 128.2, 127.0, 116.0, 53.3, 51.8.

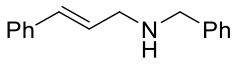

(*E*)-*N*-Benzyl-3-phenylprop-2-en-1-amine (170e)[33]

According to the general procedure **A** benzylamine (9.64 g, 9.8 mL, 90.0 mmol, 3 equiv.) and K_2CO_3 (12.4 g, 90.0 mmol, 3 equiv.) in MeCN (100 mL) were used and (*E*)-(3-bromoprop-1-en-1-yl)benzene (**169b**) (5.91 g, 4.5 mL, 30.0 mmol, 1 equiv.) in MeCN (50 mL) was added. The reaction mixture was stirred for 19 h. The excess benzylamine used was removed by distillation (4.3 mbar, 86 °C). (*E*)-*N*-benzyl-3-phenylprop-2-en-1-amine(**170e**) (6.15 g, 27.5 mmol, 92%) was obtained as yellow liquid.

^{1}H-NMR (300 MHz, $CDCl_3$) δ = 7.63 – 7.48 (m, 2H), 7.47 – 7.19 (m, 8H), 6.66 – 6.51 (m, 1H), 6.47 – 6.29 (m, 1H), 4.03 (bs, 2H), 3.55 (d, *J* = 6.6 Hz, 2H); **^{13}C-NMR** (101 MHz, $CDCl_3$) δ = 138.4, 135.4, 130.9, 130.2, 129.3, 129.2, 128.72, 128.70, 128.6, 126.9, 126.5, 118.9, 49.5, 47.8.

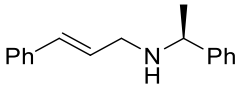

(*S,E*)-3-Phenyl-*N*-(1-phenylethyl)prop-2-en-1-amine (248)[34]

According to the general procedure **A** (*S*)-1-phenylethan-1-amine (**247**) (3.94 g, 5.2 mL, 40.0 mmol, 2 equiv.) and K_2CO_3 (5.53 g, 40.0 mmol, 2 equiv.) in MeCN (35 mL) were used and (*E*)-(3-bromoprop-1-en-1-yl)benzene (**169b**) (3.94 g, 20.0 mmol, 1 equiv.) in MeCN (35 mL) was added. The reaction mixture was stirred for 26 h. After purification by silica gel column chromatography (hexanes/EtOAc 2:1) (*S,E*)-3-phenyl-*N*-(1-phenylethyl)prop-2-en-1-amine (**248**) (3.59 g, 15.1 mmol, 76%) was obtained as yellow liquid.

^{1}H-NMR (300 MHz, $CDCl_3$) δ = 7.43 – 7.13 (m, 10H), 6.48 (d, *J* = 15.9 Hz, 1H), 6.29 (dt, *J* = 15.9, 6.2 Hz, 1H), 3.87 (q, *J* = 6.6 Hz, 1H), 3.27 (d, *J* = 6.2 Hz, 2H), 1.41 (d, *J* = 6.6 Hz, 3H); **^{13}C-NMR** (75 MHz, $CDCl_3$) δ = 145.4, 137.2, 131.2, 128.5, 127.3, 127.0, 126.7, 126.3, 57.6, 49.7, 24.3; **IR** (neat) ν [cm^{-1}] = 3060, 3026, 2967, 2926, 2886, 2825, 1599, 1494, 1449, 1367, 1304, 1118, 965, 909, 745, 693; **HRMS**: (ESI-MS) m/z calc. for $[C_{17}H_{19}N]^+$ $[M+H]^+$ 238.1590, found 238.1594; $[\boldsymbol{\alpha}]_{\boldsymbol{D}}^{\boldsymbol{20}}$ = –48.6 (*c* 0.1, CH_2Cl_2); **chiral HPLC**: >99% *ee* (Chiralpak AS-H, 4.6 x 250 mm, heptane/i-PrOH = 99:1, 0.5 mL/min, t_R (***S***), (*R*) = **10.4**, 13.7 min).

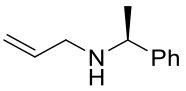

(*S*)-*N*-(1-Phenylethyl)prop-2-en-1-amine (260)[34]

According to the general procedure **A** (*S*)-1-phenylethan-1-amine (**247**) (9.69 g, 10.3 mL, 80.0 mmol, 2 equiv.) and K_2CO_3 (11.1 g, 80.0 mmol, 2 equiv.) in MeCN (100 mL) were used and 3-bromoprop-1-ene (**169a**) (4.84 g, 3.50 mL, 40.0 mmol, 1 equiv.) in MeCN (15 mL) was added. The reaction mixture was stirred for 24 h. After purification by silica column chromatography (hexanes/EtOAc 2:1) (*S*)-*N*-(1-phenylethyl)prop-2-en-1-amine (**260**) (3.74 g, 23.2 mmol, 58%) was obtained as yellow liquid.

^{1}H-NMR (300 MHz, $CDCl_3$) δ = 7.40 – 7.19 (m, 5H), 5.91 (ddt, *J* = 17.0, 10.2, 6.0 Hz, 1H), 5.22 – 5.00 (m, 2H), 3.82 (q, *J* = 6.6 Hz, 1H), 3.17 – 3.02 (m, 2H), 1.38 (d, *J* = 6.6 Hz, 3H); **^{13}C-NMR** (101 MHz, $CDCl_3$) δ = 145.5, 137.0, 128.5, 127.0, 126.7, 115.7, 57.6, 50.3, 24.3; **IR** (neat) ν [cm^{-1}] = 3063, 3026, 2967, 2926, 2870, 2810, 1643, 1602, 1490, 1449, 1371, 1207, 1118, 1077, 991, 916, 760, 700; **HRMS**: (ESI-MS) m/z calc. for $[C_{11}H_{16}N]^+$ $[M+H]^+$ 162.1277, found 162.1278.

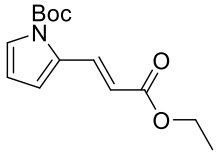

***tert*-Butyl (*E*)-2-(3-ethoxy-3-oxoprop-1-en-1-yl)-1*H*-pyrrole-1-carboxylate (183a)**[35]

Under nitrogen atmosphere ethyl (*E*)-3-(1*H*-pyrrol-2-yl)acrylate (**181a**) (2.48 g, 15.0 mmol, 1.0 equiv.) was dissolved in dry MeCN (45 mL) and the solution was cooled to 0 °C by an ice-bath. Then, Boc_2O (3.60 g, 16.5 mmol, 1.1 equiv.) and DMAP (27.5 mg, 0.230 mmol, 0.015 equiv.) were subsequently added. The reaction mixture was stirred for 22 h in defrosting ice-bath. Solvent was removed under reduced pressure and the residue was dissolved again in ethyl acetate and sat. NH_4Cl. After phase separation the aqueous phase was extracted with EtOAc (3x). The combined organic phases were dried over $MgSO_4$, filtered and evaporated. Compound **183a** (3.98 g, 15.0 mmol, quant.) was obtained quantitatively and was used in following reactions without further purification.

^{1}H-NMR (300 MHz, $CDCl_3$) δ = 8.28 (d, *J* = 15.9 Hz, 1H), 7.41 (ddd, *J* = 14.4, 3.2, 1.7 Hz, 1H), 6.69 (ddd, *J* = 3.6, 1.6, 0.7 Hz, 1H), 6.26 – 6.14 (m, 2H), 4.23 (q, *J* = 7.1 Hz, 2H), 1.63 (s, 9H), 1.31 (t, *J* = 7.1 Hz, 3H); **^{13}C-NMR** (75 MHz, $CDCl_3$) δ = 167.2, 149.0, 134.9, 131.1, 124.9, 116.6, 114.8, 111.5, 84.9, 60.3, 28.0, 14.4.

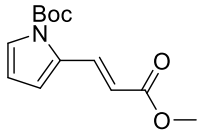

***tert*-Butyl (*E*)-2-(3-methoxy-3-oxoprop-1-en-1-yl)-1*H*-pyrrole-1-carboxylate (183b)[36]**

Under nitrogen atmosphere methyl (*E*)-3-(1*H*-pyrrol-2-yl)acrylate (**181b**) (1.99 g, 13.2 mmol, 1 equiv.) was dissolved in dry MeCN (45 mL) and the solution was cooled to 0 °C by an ice-bath. Then, Boc_2O (3.16 g, 14.5 mmol, 1.1 equiv.) and DMAP (24.1 mg, 0.200 mmol, 0.015 equiv.) were subsequently added. The reaction mixture was stirred for 24 h in defrosting ice-bath. The solvent was removed under reduced pressure and the residue was dissolved again in ethyl acetate and sat. NH_4Cl. After phase separation, the aqueous phase was extracted with ethyl acetate (3x). The combined organic phases were dried over $MgSO_4$, filtered and evaporated. Compound **183b** (3.19 g, 12.7 mmol, 93%) was obtained as brownish solid and was used in following reactions without further purification.

^{1}H-NMR (300 MHz, $CDCl_3$) δ = 8.30 (d, *J* = 16.0 Hz, 1H), 7.39 (dd, *J* = 3.2, 1.6 Hz, 1H), 6.76 – 6.60 (m, 1H), 6.27 – 6.13 (m, 2H), 3.77 (s, 3H), 1.62 (s, 9H); **^{13}C-NMR** (75 MHz, $CDCl_3$) δ = 167.6, 149.0, 135.1, 131.1, 124.9, 116.1, 114.9, 111.5, 84.9, 51.6, 28.0.

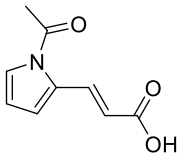

(*E*)-3-(1-Acetyl-1*H*-pyrrol-2-yl)acrylic acid (184a)

Under inert atmosphere (*E*)-3-(1*H*-pyrrol-2-yl)acrylic acid (**180c**) (1.71 g, 12.5 mmol, 1.0 equiv.) was dissolved in dry DCM (20 mL). Then DMAP (153 mg, 1.25 mmol, 0.1 equiv.) and NEt_3 (3.16 g, 4.3 mL, 31.2 mmol, 2.5 equiv.) were subsequently added. The reaction

mixture was cooled to 0 °C with an ice-bath. In the following acetic anhydride (2.55 g, 2.4 mL, 25.0 mmol, 2.0 equiv.) was added dropwise to the reaction mixture. After 18 h stirring at rt the reaction was quenched by adding sat. NH_4Cl. The phases were separated, and the aqueous phase was extracted with EtOAc (3x). The combined organic phases were dried over $MgSO_4$, filtered and the solvent was removed under reduced pressure. Recrystallization from EtOAc gave (*E*)-3-(1-acetyl-1*H*-pyrrol-2-yl)acrylic acid (**184a**) (1.54 g, 8.60 mmol, 69%) as brownish solid.

mp = 129 130 °C; **^{1}H-NMR** (300 MHz, $CDCl_3$) δ = 8.43 (dd, *J* = 26.6, 15.9 Hz, 1H), 7.22 – 7.16 (m, 1H), 6.75 (dd, *J* = 18.7, 3.2 Hz, 1H), 6.30 – 6.09 (m, 2H), 2.54 (s, 3H); **^{13}C-NMR** (75 MHz, $CDCl_3$) δ = 171.5, 169.4, 137.4, 131.9, 124.8, 124.4, 116.3, 113.0, 24.3; **IR** (neat) ν [cm^{-1}] = 3153, 2937, 2605, 1755, 1722, 1610, 1457, 1423, 1371, 1341, 1289, 1252, 1155, 1077, 1028, 976, 879, 812, 738; **HRMS**: (ESI-MS) m/z calc. for $[C_9H_9NO_3]^-$ $[M-H]^-$ 178.0510, found 178.0510.

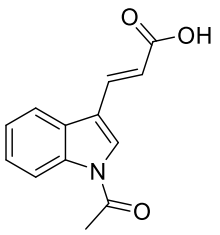

(*E*)-3-(1-Acetyl-1*H*-indol-3-yl)acrylic acid (184b)[37]

Under inert atmosphere (*E*)-3-(1*H*-indol-3-yl)acrylic acid (**180d**)(1.44 g, 7.70 mmol, 1.0 equiv.) was dissolved in dry DCM (15 mL). Then DMAP (94.1 mg, 0.770 mmol, 0.1 equiv.) and NEt_3 (1.95 g, 2.8 mL, 19.3 mmol, 2.5 equiv.) were subsequently added. The reaction mixture was cooled to 0 °C with an ice-bath. In the following acetic anhydride (1.57 g, 1.5 mL, 15.4 mmol, 2 equiv.) was added dropwise to the reaction mixture. After 18 h stirring at rt the reaction was quenched by adding sat. NH_4Cl. The phases were separated, and the aqueous phase was extracted with EtOAc (3x). The combined organic phases were dried over $MgSO_4$, filtered and the solvent was removed under reduced pressure. Recrystallization from EtOAc gave (*E*)-3-(1-acetyl-1*H*-indol-3-yl)acrylic acid (**184b**) (1.20 g, 5.20 mmol, 68%) as brownish solid.

^{1}H-NMR (300 MHz, $CDCl_3$) δ = 8.57 – 8.42 (m, 1H), 8.06 – 7.70 (m, 3H), 7.52 – 7.34 (m, 2H), 6.65 (dd, *J* = 28.1, 16.0 Hz, 1H), 2.71 (d, *J* = 4.2 Hz, 3H); **^{13}C-NMR** (101 MHz, $CDCl_3$) δ = 168.3, 162.9, 140.1, 138.2, 136.8, 129.3, 126.5, 124.8, 120.2, 118.0, 117.1, 116.6, 24.0.

Synthesis of the amide-linked dienes

General protocol for the coupling of the carboxylic acid with the amine B

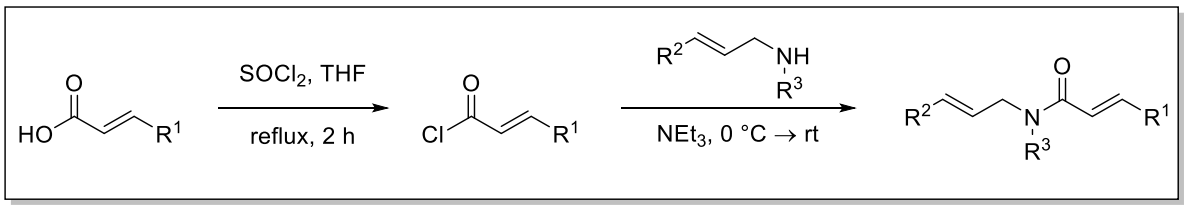

Either the acid chloride was generated *in situ* or was commercially available. For the generation *in situ* the corresponding carboxylic acid (1.0 equiv.) was dissolved in dry THF and then thionyl chloride (1.0 equiv.) was added dropwise. The reaction mixture was stirred under reflux for 2 h. The obtained acid chloride solution was then cooled down to 0 °C by an ice-bath. The solution containing the corresponding amine (1.0 equiv.) and triethylamine (1.1 equiv.) in dry THF was added via a dropping funnel and the mixture was stirred for the reported time at rt. Afterwards, the solvent was removed under reduced pressure. The residue was dissolved again in DCM and washed twice with sat. $NaHCO_3$. The organic phase was dried over $MgSO_4$, filtered and the solvent was removed under reduced pressure. The crude product was purified by column chromatography using hexanes and EtOAc as eluent to obtain the required product.

General protocol for the Boc-protection of the free amide-linked dienes C

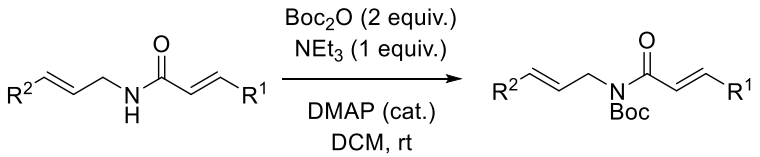

Under nitrogen atmosphere, the corresponding amide-linked diene (1.0 equiv.) was dissolved in dry DCM. Then triethylamine (1.0 equiv.), di-*tert*-butyl dicarbonate (2.0 equiv.) and DMAP (0.1 equiv.) were added successively. After the reported time the solvent was evaporated, and the crude product was purified via silica gel column chromatography using hexanes and EtOAc as eluent.

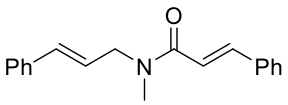

_N_-Cinnamyl-_N_-methylcinnamamide (153a)

Following the general procedure **B**, cinnamoyl chloride was generated *in situ* using cinnamic acid **152** (993 mg, 6.7 mmol, 1 equiv.) and thionyl chloride (797 mg, 486 µL, 6.7 mmol, 1 equiv.) in dry THF (20 mL). Then the reaction mixture was cooled to 0 °C and the solution of (*E*)-*N*-methyl-3-phenylprop-2-en-1-amine (**154**) (986 mg, 6.7 mmol, 1 equiv.) with triethylamine (749 mg, 1.1 mL, 7.4 mmol, 1.1 equiv.) in dry THF (12 mL) was added. The reaction mixture was stirred for 19 h at rt. After silica gel column chromatography (hexanes/EtOAc 5:1) *N*-cinnamyl-*N*-methylcinnamamide (**153a**) (1.42 g, 5.1 mmol, 77%) was obtained as white solid.

R_f = 0.12 (hexanes/EtOAc 5:1); **mp** = 97.6 °C; **^{1}H-NMR** (400 MHz, $CDCl_3$) δ = 7.75 (dd, *J* = 15.7, 5.9 Hz, 1H), 7.53 (bs, 2H), 7.44 – 7.20 (m, 8H), 6.89 (t, *J* = 15.3 Hz, 1H), 6.54 (d, *J* = 15.9 Hz, 1H), 6.21 (dt, *J* = 15.9, 5.9 Hz, 1H), 4.25 (bs, 2H), 3.13 (d, *J* = 12.4 Hz, 3H); **^{13}C-NMR** (75 MHz, $CDCl_3$) δ = 167.0, 166.4, 143.0, 142.8, 136.6, 136.2, 135.3, 133.0, 131.9, 129.68, 129.65, 128.9, 128.8, 128.7, 128.6, 128.2, 128.0, 127.9, 127.7, 126.48, 126.46, 124.5, 124.1, 117.4, 51.9, 50.1, 34.9, 34.3 (signal doubling and broadening due to rotamers); **IR** (neat) ν [cm^{-1}] = 3026, 2959, 1740, 1647, 1610, 1474, 1449, 1401, 1244, 1118, 976, 745, 693; **HRMS**: (ESI-MS) m/z calc. for $[C_{19}H_{20}NO]^+$ $[M+H]^+$: 278.1539, found 278.1546.

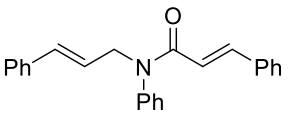

_N_-Cinnamyl-_N_-phenylcinnamamide (153b)

Following the general procedure **B**, cinnamoyl chloride was generated *in situ* using cinnamic acid **152** (340 mg, 2.3 mmol, 1.0 equiv.) and thionyl chloride (274 mg, 160 µL, 2.3 mmol, 1.0 equiv.) in dry THF (10 mL). Then the reaction mixture was cooled to 0 °C and the solution of *N*-cinnamylaniline **155** (475 mg, 2.3 mmol, 1.0 equiv.) with triethylamine (263 mg, 360 µL, 2.6 mmol, 1.1 equiv.) in dry THF (6 mL) was added. The reaction mixture was stirred at rt for 19 h. After silica gel column chromatography (hexanes/EtOAc 9:1) *N*-cinnamyl-*N*-phenylcinnamamide (**153b**) (636 mg, 1.9 mmol, 81%) was obtained as yellowish oil.

R_f = 0.24 (hexanes/EtOAc 9:1); **^{1}H-NMR** (300 MHz, $CDCl_3$) δ = 7.72 (d, *J* = 15.5 Hz, 1H), 7.45 – 7.10 (m, 15H), 6.49 – 6.22 (m, 3H), 4.58 (d, *J* = 5.9 Hz, 2H); **^{13}C-NMR** (75 MHz, $CDCl_3$) δ = 165.8, 142.14, 142.12, 136.7, 135.2, 133.2, 129.65, 129.60, 129.58, 128.7, 128.5, 128.4, 127.9, 127.7, 126.5, 124.5, 118.9, 52.1; **IR** (neat) ν [cm^{-1}] = 3058, 3026, 2926, 1651, 1613, 1490, 1449, 1328, 1237, 1196, 969, 760, 693; **HRMS**: (ESI-MS) m/z calc. for $[C_{24}H_{22}NO]^+$ $[M+H]^+$: 340.1696, found 340.1704.

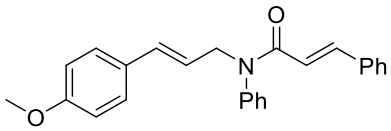

***N*-((*E*)-3-(4-Methoxyphenyl)allyl)-*N*-phenylcinnamamide (153c)**

Following the general procedure **B**, cinnamoyl chloride was generated *in situ* using cinnamic acid **152** (933 mg, 6.3 mmol, 1.0 equiv.) and thionyl chloride (750 mg, 460 µL, 6.3 mmol, 1.0 equiv.) in dry THF (20 mL). Then the reaction mixture was cooled to 0 °C and a solution of (*E*)-*N*-(3-(4-methoxyphenyl)allyl)aniline (**156**) (1.51 g, 6.3 mmol, 1.0 equiv.) with triethylamine (701 mg, 960 µL, 6.9 mmol, 1.1 equiv.) in dry THF (10 mL) was added. The reaction mixture was stirred for 19 h at rt. After silica gel column chromatography (hexanes/EtOAc 9:1 → 7:1 → 2:1) *N*-((*E*)-3-(4-methoxyphenyl)allyl)-*N*-phenylcinnamamide (**153c**) (1.53 g, 4.2 mmol, 66%) was obtained as white solid.

R_f = 0.09 (hexanes/EtOAc 9:1); **mp** = 107.4 °C; **^{1}H-NMR** (300 MHz, $CDCl_3$) δ = 7.72 (d, *J* = 15.6 Hz, 1H), 7.48 – 7.20 (m, 12H), 6.87 – 6.79 (m, 2H), 6.36 (t, *J* = 16.0 Hz, 2H), 6.21 (dt, *J* = 15.8, 6.6 Hz, 1H), 4.57 (dd, *J* = 6.6, 0.9 Hz, 2H), 3.79 (s, 3H); **^{13}C-NMR** (75 MHz, $CDCl_3$) δ = 165.8, 159.3, 142.2, 142.1, 135.2, 132.7, 129.6, 128.7, 128.4, 128.0, 127.8, 127.7, 122.2, 119.0, 113.9, 55.3, 52.2; **IR** (neat) ν [cm^{-1}] = 3060, 3034, 2959, 2933, 2836, 1651, 1591, 1490, 1449, 1386, 1330, 1300, 1241, 1174, 1032, 969, 834, 760, 700; **HRMS**: (ESI-MS) m/z calc for $[C_{25}H_{23}NO_3]^+$ $[M+H]^+$ 370.1802, found 370.1802.

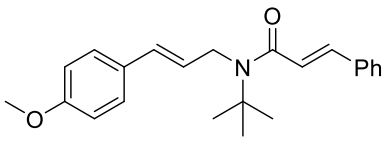

***N*-(*tert*-Butyl)-*N*-((*E*)-3-(4-methoxyphenyl)allyl)cinnamamide (153d)**

Following the general procedure **B**, cinnamoyl chloride was generated *in situ* using cinnamic acid **152** (711 mg, 4.8 mmol, 1.0 equiv.) and thionyl chloride (571 mg, 350 µL, 4.8 mmol, 1.0 equiv.) in dry THF (20 mL). Then the reaction mixture was cooled to 0 °C and the solution of (*E*)-*N*-(*tert*-butyl)-3-(4-methoxyphenyl)prop-2-en-1-amine (**157**) (1.06 g, 4.8 mmol, 1.0 equiv.) with triethylamine (537 mg, 735 µL, 5.3 mmol, 1.1 equiv.) in dry THF (10 mL) was added. The reaction mixture was stirred for 21 h at rt. After silica gel column chromatography (hexanes/EtOAc 9:1) *N*-(*tert*-butyl)-*N*-((*E*)-3-(4-methoxyphenyl)allyl)cinnamamide (**153d**) (934 mg, 2.7 mmol, 56%) was obtained as yellowish solid.

R_f = 0.16 (hexanes/EtOAc 9:1); **mp** = 113.1 °C; **^{1}H-NMR** (300 MHz, $CDCl_3$) δ = 7.64 (d, *J* = 15.4 Hz, 1H), 7.50 – 7.41 (m, 2H), 7.37 – 7.27 (m, 5H), 6.91 – 6.78 (m, 3H), 6.60 – 6.49 (m, 1H), 6.15 (dt, *J* = 16.0, 4.4 Hz, 1H), 4.22 (dd, *J* = 4.4, 1.9 Hz, 2H), 3.82 (s, 3H), 1.55 (s, 9H); **^{13}C-NMR** (75 MHz, $CDCl_3$) δ = 168.5, 159.4, 141.6, 135.6, 130.7, 129.3, 128.7, 127.7, 127.6, 125.4, 121.8, 114.1, 57.5, 55.4, 47.2, 28.7; **IR** (neat) ν [cm^{-1}] = 3060, 2955, 2840, 1743, 1654, 1606, 1509, 1449, 1382, 1271, 1244, 1196, 1036, 980, 838, 771; **HRMS**: (ESI-MS) calc. for $[C_{23}H_{28}NO_2]^+$ $[M+H]^+$ 350.2115, found 350.2113.

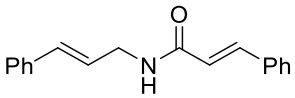

***N*-Cinnamylcinnamamide (153e)**

Following the general procedure **B**, cinnamoyl chloride was generated *in situ* using cinnamic acid **152** (1.48 g, 10 mmol, 1.0 equiv.) and thionyl chloride (1.19 g, 725 µL, 10 mmol, 1.0 equiv.) in dry THF (15 mL). Then the reaction mixture was cooled to 0 °C and the solution of (*E*)-3-phenylprop-2-en-1-amine (**172**) (1.33 g, 10 mmol, 1.0 equiv.) with triethylamine (1.11 g, 1.5 mL, 11 mmol, 1.1 equiv.) in dry THF (10 mL) was added. The reaction mixture was stirred for 26 h at rt. After purification using the flash system (hexanes/EtOAc) *N*-cinnamylcinnamamide (**153e**) (1.89 g, 7.2 mmol, 72%) was obtained as white solid.

R_f = 0.34 (hexanes/EtOAc 3:1); **mp** = 124-125 °C; **^{1}H-NMR** (300 MHz, $CDCl_3$) δ = 7.68 (d, *J* = 15.6 Hz, 1H), 7.56 – 7.43 (m, 2H), 7.40 – 7.18 (m, 8H), 6.55 (d, *J* = 15.9 Hz, 1H), 6.48 (d, *J* = 15.6 Hz, 1H), 6.24 (dt, *J* = 15.9, 6.3 Hz, 1H), 6.13 (bs, 1H), 4.17 (td, *J* = 6.1, 1.3 Hz, 2H); **^{13}C-NMR** (75 MHz, $CDCl_3$) δ = 165.9, 141.3, 136.5, 134.8, 132.3, 129.8, 128.9, 128.6, 127.9, 127.8, 126.4, 125.4, 120.6, 41.8; **IR** (neat) ν [cm^{-1}] =3280, 3082, 3030, 2907, 1654, 1617, 1550, 1494, 1448, 1423, 1338, 1222, 1036, 989, 864, 741, 685; **HRMS**: (ESI-MS) m/z calc for $[C_{18}H_{18}NO]^+$ $[M+H]^+$ 264.1383, found 264.1391; calc. for $[C_{18}H_{17}NONa]^+$ $[M+Na]^+$ 286.1202, found 286.1207.

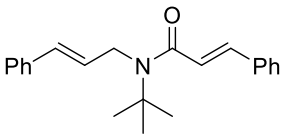

***N*-(*tert*-Butyl)-*N*-cinnamylcinnamamide (153g)**

Following the general procedure **B**, cinnamoyl chloride was generated *in situ* using cinnamic acid **152** (1.51 g, 10 mmol, 1.0 equiv.) and thionyl chloride (1.19 g, 730 µL, 10 mmol, 1.0 equiv.) in dry THF (25 mL). Then the reaction mixture was cooled to 0 °C and the solution of (*E*)-*N*-(*tert*-butyl)-3-phenylprop-2-en-1-amine (**170b**) (1.89 g, 10 mmol, 1.0 equiv.) with triethylamine (1.11 g, 1.5 mL, 11 mmol, 1.1 equiv.) in dry THF (12 mL) was added. The reaction mixture was stirred for 16 h at rt. After silica gel column chromatography (hexanes/EtOAc 9:1) *N*-(*tert*-butyl)-*N*-cinnamylcinnamamide (**153g**) (2.26 g, 7.1 mmol, 71%) was obtained as white solid.

R_f = 0.32 (hexanes/EtOAc 9:1); **mp** = 119.3 °C; **^{1}H-NMR** (300 MHz, $CDCl_3$) δ = 7.65 (d, *J* = 15.4 Hz, 1H), 7.53 – 7.22 (m, 10H), 6.82 (d, *J* = 15.4 Hz, 1H), 6.62 (dt, *J* = 16.0, 1.7 Hz, 1H), 6.31 (dt, *J* = 16.0, 4.4 Hz, 1H), 4.25 (dd, *J* = 4.4, 1.9 Hz, 2H), 1.56 (s, 9H); **^{13}C-NMR** (75 MHz, $CDCl_3$) δ = 168.5, 141.4, 136.5, 135.6, 131.3, 129.3, 128.73, 128.72, 127.8, 127.7, 126.4, 121.7, 57.5, 47.2, 28.7; **IR** (neat) ν [cm^{-1}] = 3022, 2955, 2918, 1651, 1613, 1446, 1390, 1356, 1192, 976, 764, 700; **HRMS**: (ESI-MS) m/z calc. for $[C_{22}H_{25}NO]^+$ $[M+H]^+$ 320.2009, found 320.2014.

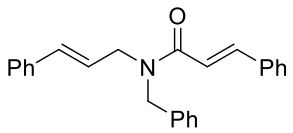

***N*-Benzyl-*N*-cinnamylcinnamamide (153q)[38,39]**

Following the general procedure **B**, cinnamoyl chloride was generated *in situ* using cinnamic acid **152** (4.1 g, 28.0 mmol, 1 equiv.) and thionyl chloride (3.3 g, 2 mL, 28.0 mmol, 1 equiv.) in dry THF (100 mL). Then the reaction mixture was cooled to 0 °C and the solution of (*E*)-*N*-benzyl-3-phenylprop-2-en-1-amine (**170e**) (6.2 g, 28.0 mmol, 1 equiv.) with triethylamine (3.4 g, 4.7 mL, 34.0 mmol, 1.1 equiv.) in dry THF (100 mL) was added. The reaction mixture was stirred at rt for 24 h. After silica gel column chromatography (hexanes/EtOAc 9:1 → 5:1 → EtOAc) *N*-benzyl-*N*-cinnamylcinnamamide (**153q**) (5.8 g, 16.4 mmol, 59%) was obtained as yellow oil.

R_f = 0.47 (hexanes/EtOAc 3:1); **^{1}H-NMR** (300 MHz, $CDCl_3$) δ = 7.83 (dd, *J* = 15.4, 4.6 Hz, 1H), 7.50 (ddd, *J* = 19.3, 6.6, 2.9 Hz, 2H), 7.43 – 7.20 (m, 13H), 6.90 (dd, *J* = 17.0, 15.6 Hz, 1H), 6.51 (dd, *J* = 15.9, 10.8 Hz, 1H), 6.33 – 6.09 (m, 1H), 4.86 – 4.66 (m, 2H), 4.37 – 4.10 (m, 2H); **^{13}C-NMR** (75 MHz, CDCl3) δ = 167.0, 167.0, 143.7, 143.6, 137.6, 137.0, 136.6, 136.2, 135.3, 135.2, 133.3, 132.1, 129.7, 129.0, 128.8, 128.72, 128.67, 128.6, 128.4, 128.0, 127.9, 127.7, 127.5, 126.6, 126.5, 124.5, 124.2, 117.4, 50.2, 49.0, 48.8, 48.1 (signal doubling due to rotamers); **IR** (neat) ν [cm^{-1}] = 3060, 3026, 2922, 1647, 1602, 1494, 1416, 1356, 1196, 1077, 1028, 969, 760, 730, 693; **HRMS**: (ESI-MS) m/z calc. for $[C_{25}H_{24}NO]^+$ $[M+H]^+$ 354.1852, found 354.1858; calc. for $[C_{25}H_{23}NONa]^+$ $[M+Na]^+$ 376.1672, found 376.1669.

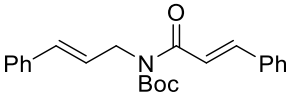

***tert*-Butyl cinnamoyl(cinnamyl)carbamate (153t)**

According to the general protocol **C** *tert*-butyl cinnamoyl(cinnamyl)carbamate (**153t**) was prepared using *N*-cinnamylcinnamamide (**153e**) (263 mg, 1.0 mmol, 1.0 equiv.), di-*tert*-butyl dicarbonate (458 mg, 2.1 mmol, 2.1 equiv.), triethylamine (102 mg, 140 µL, 1.0 mmol, 1.0 equiv.) and DMAP (12.2 mg, 0.10 mmol, 0.10 equiv.) in dry DCM (2 mL). The reaction

mixture was stirred for 21 h. After purification using flash system (hexanes/EtOAc) *tert*-butyl cinnamoyl(cinnamyl)carbamate (**153t**) (308 mg, 0.85 mmol, 85%) was obtained as white solid.

R_f = 0.2 (hexanes/EtOAc 19:1); **mp** = 108 109 °C; **^{1}H-NMR** (300 MHz, $CDCl_3$) δ = 7.73 (d, *J* = 15.6 Hz, 1H), 7.61 – 7.48 (m, 3H), 7.43 – 7.18 (m, 8H), 6.58 (d, *J* = 15.9 Hz, 1H), 6.26 (dt, *J* = 15.9, 6.3 Hz, 1H), 4.53 (dd, *J* = 6.3, 1.2 Hz, 2H), 1.56 (s, 9H); **^{13}C-NMR** (75 MHz, $CDCl_3$) δ = 168.6, 153.2, 143.4, 136.7, 135.2, 132.7, 130.0, 128.8, 128.6, 128.2, 127.7, 126.4, 124.8, 121.4, 83.3, 46.7, 28.2; **IR** (neat) ν [cm^{-1}] = 3063, 3026, 2955, 1722, 1669, 1617, 1494, 1449, 1353, 1271, 1200, 1140, 767, 969, 863, 767, 700; **HRMS**: (ESI-MS) m/z calc. for $[C_{23}H_{26}NO_3]^+$ $[M+H]^+$ 364.1907, found 364.1903.

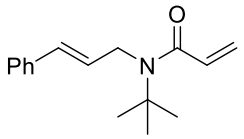

***N*-(*tert*-Butyl)-*N*-cinnamylacrylamide (153i)**

Following the general procedure **B** a solution of acryloyl chloride **249** (10.3 g, 9.30 mL, 114 mmol, 1.0 equiv.) in dry THF (120 mL) was cooled to 0 °C and (*E*)-*N*-(*tert*-butyl)-3-phenylprop-2-en-1-amine (**170b**) (21.6 g, 114 mmol, 1.0 equiv.) with triethylamine (12.7 g, 17.4 mL, 125 mmol, 1.1 equiv.) in dry THF (80 mL) was added. After stirring for 42 h at rt *N*-(*tert*-butyl)-*N*-cinnamylacrylamide (**153i**) (26.5 g, 109 mmol, 96%) was obtained as brown oil which was used in the following step without further purification.

R_f = 0.38 (hexanes/EtOAc 5:1); **^{1}H-NMR** (300 MHz, $CDCl_3$) δ = 7.42 – 7.18 (m, 5H), 6.58 – 6.45 (m, 2H), 6.33 – 6.17 (m, 2H), 5.58 (dd, *J* = 10.3, 2.1 Hz, 1H), 4.16 (dd, *J* = 4.4, 2.0 Hz, 2H), 1.51 (s, 9H); **^{13}C NMR** (101 MHz, $CDCl_3$) δ = 168.2, 136.5, 131.7, 131.2, 128.7, 128.6, 127.8, 127.5, 126.8, 126.3, 57.4, 47.0, 28.7; **IR** (neat) ν [cm^{-1}] = 3060, 3026, 2967, 2926, 1647, 1613, 1412, 1353, 1192, 965, 797, 738, 693; **HRMS**: (APCI-MS) m/z calc. for $[C_{16}H_{22}NO]^+$ $[M+H]^+$ 244.1696, found 244.1699.

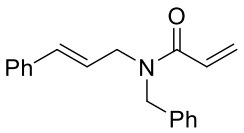

***N*-Benzyl-*N*-cinnamylacrylamide (153s)**

Following the general procedure **B** a solution of acryloyl chloride **249** (1.86 g, 1.7 mL, 20.6 mmol, 1.0 equiv.) in dry THF (50 mL) was cooled to 0 °C and (*E*)-*N*-benzyl-3-phenylprop-2-en-1-amine (**170e**) (4.60 g, 20.6 mmol, 1.0 equiv.) with triethylamine (2.32 g, 3.2 mL, 23.0 mmol, 1.1 equiv.) in dry THF (20 mL) was added. The reaction mixture was stirred for 19 h at rt. After silica gel column chromatography (hexanes/EtOAc 3:1) *N*-benzyl-*N*-cinnamylacrylamide (**153s**) (3.72 g, 13.4 mmol, 65%) was obtained as yellow sticky oil.

R_f = 0.35 (hexanes/EtOAc 3:1); **^{1}H-NMR** (400 MHz, $CDCl_3$) δ = 7.42 – 7.19 (m, 10H), 6.61 (ddd, *J* = 22.7, 16.7, 10.2 Hz, 1H), 6.53 – 6.38 (m, 2H), 6.29 – 6.04 (m, 1H), 5.74 (ddd, *J* = 14.9, 10.3, 1.9 Hz, 1H), 4.73 (s, 1H), 4.62 (s, 1H), 4.23 (d, *J* = 6.5 Hz, 1H), 4.07 (d, *J* = 4.5 Hz, 1H); **^{13}C-NMR** (101 MHz, $CDCl_3$) δ = 166.9, 166.8, 137.4, 136.8, 136.6, 136.1, 133.4, 132.1, 129.0, 128.9, 128.72, 128.67, 128.6, 128.4, 128.0, 127.8, 127.7, 127.5, 126.51, 126.46, 124.4, 124.0, 50.1, 48.8, 48.7, 47.9 (signal doubling due to rotameres); **IR** (neat) ν [cm^{-1}] = 3060, 3026, 2922, 1677, 1647, 1610, 1494, 1423, 1356, 1215, 1080, 1028, 965, 793, 730, 693; **HRMS**: (ESI-MS) m/z calc. for $[C_{19}H_{20}NO]^+$ $[M+H]^+$ 278.1539, found 278.1544.

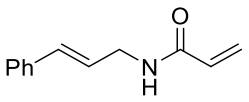

***N*-Cinnamylacrylamide (153f)**

Following the general procedure **B** a solution of acryloyl chloride **249** (4.10 g, 3.7 mL, 45.3 mmol, 1.0 equiv.) in dry THF (75 mL) was cooled to 0 °C and (*E*)-3-phenylprop-2-en-1-amine (**172**) (6.03 g, 45.3 mmol, 1.0 equiv.) with triethylamine (5.04 g, 6.9 mL, 49.8 mmol, 1.1 equiv.) in dry THF (50 mL) was added. After stirring for 24 h at rt, *N*-cinnamylacrylamide (**153f**) (8.39 g, 44.8 mmol, 99%) was obtained as a yellow solid and was used in the following step without further purification.

R_f = 0.47 (hexanes/EtOAc 1:1); **mp** = 72 73 °C; **^{1}H-NMR** (300 MHz, $CDCl_3$) δ 7.39 – 7.20 (m, 6H), 6.55 (d, *J* = 15.9 Hz, 1H), 6.33 (dd, *J* = 17.0, 1.5 Hz, 1H), 6.28 – 6.05 (m, 2H), 5.68

(dd, *J* = 10.2, 1.5 Hz, 1H), 4.13 (td, *J* = 6.1, 1.4 Hz, 2H); **^{13}C-NMR** (101 MHz, $CDCl_3$) δ = 165.4, 136.5, 132.5, 130.7, 128.6, 127.8, 126.8, 126.4, 125.3, 41.7; **IR** (neat) ν [cm^{-1}] = 3283, 3092, 3030, 2922, 1654, 1550, 1408, 1308, 1241, 1095, 1069, 991, 961, 734, 689; **HRMS**: (ESI-MS) m/z calc. for $[C_{12}H_{14}NO]^+$ $[M+H]^+$ 188.1070, found 188.1075; calc. for $[C_{12}H_{13}NONa]^+$ $[M+Na]^+$ 210.0889, found 210.0895.

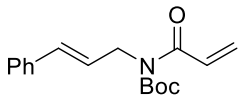

***tert*-Butyl acryloyl(cinnamyl)carbamate (153u)**

According to the general protocol **C** *tert*-butyl acryloyl(cinnamyl)carbamate (**153u**) was prepared using *N*-cinnamylacrylamide (**172**) (8.39 g, 44.8 mmol, 1.0 equiv.), di-*tert*-butyl dicarbonate (19.6 g, 89.7 mmol, 2.1 equiv.), triethylamine (4.54 g, 6.2 mL, 44.8 mmol, 1.0 equiv.) and DMAP (549 mg, 4.50 mmol, 0.10 equiv.) in dry DCM (90 mL). The reaction mixture was stirred for 21 h. The crude reaction mixture was washed once with sat. $KHSO_4$, once with sat. $NaHCO_3$ and finally with H_2O. The organic phase was dried over $MgSO_4$, filtered and the solvent was removed under reduced pressure. *Tert*-butyl acryloyl(cinnamyl)carbamate (**153u**) (10.8 g, 37.6 mmol, 84%) was obtained as yellow oil and was used in the following steps without further purification.

R_f = 0.45 (hexanes/EtOAc 9:1); **^{1}H-NMR** (400 MHz, $CDCl_3$) δ = 7.40 – 7.17 (m, 5H), 7.05 (dd, *J* = 16.9, 10.4 Hz, 1H), 6.55 (d, *J* = 15.9 Hz, 1H), 6.35 (dd, *J* = 16.9, 1.8 Hz, 1H), 6.21 (dt, *J* = 15.9, 6.4 Hz, 1H), 5.71 (dd, *J* = 10.4, 1.8 Hz, 1H), 4.46 (dd, *J* = 6.4, 1.2 Hz, 2H), 1.53 (s, 9H); **^{13}C-NMR** (101 MHz, $CDCl_3$) δ = 168.4, 153.1, 136.7, 132.9, 131.4, 128.6, 128.0, 127.7, 126.4, 124.6, 83.5, 46.5, 28.1; **IR** (neat) ν [cm^{-1}] = 3026, 2978, 1729, 1681, 1617, 1405, 1367, 1319, 1256, 1215, 1148, 1080, 985, 853, 775, 745, 693; **HRMS**: (ESI-MS) m/z calc. for $[C_{17}H_{22}NO_3]^+$ $[M+H]^+$ 288.1594, found 288.1600; m/z calc. for $[C_{17}H_{21}NO_3Na]^+$ $[M+Na]^+$ 310.1414, found 310.1424.

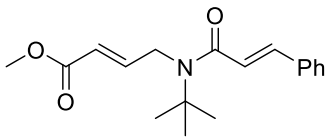

Methyl (*E*)-4-(*N*-(*tert*-butyl)cinnamamido)but-2-enoate (153o)

Following the general procedure **B** cinnamoyl chloride was generated *in situ* using cinnamic acid **152** (3.9 g, 26.3 mmol, 1.0 equiv.) and thionyl chloride (3.1 g, 1.9 mL, 26.3 mmol, 1.0 equiv.) in dry THF (50 mL). Then the reaction mixture was cooled to 0 °C and the solution of methyl (*E*)-4-(*tert*-butylamino)but-2-enoate (**170c**) (4.5 g, 26.3 mmol, 1.0 equiv.) with triethylamine (2.9 g, 4 mL, 28.9 mmol, 1.1 equiv.) in dry THF (20 mL) was added. The reaction mixture was stirred for 19 h at rt. After silica gel column chromatography (hexanes/EtOAc 9:1 → 7:1 → 5:1) methyl (*E*)-4-(*N*-(*tert*-butyl)cinnamamido)but-2-enoate (**153o**) (3.5 g, 11.6 mmol, 44%) was obtained as yellowish solid.

R_f = 0.24 (hexanes/EtOAc 5:1); **mp** = 65 66 °C; **^{1}H-NMR** (400 MHz, $CDCl_3$) δ = 7.62 (d, *J* = 15.4 Hz, 1H), 7.43 (dd, *J* = 7.5, 2.0 Hz, 2H), 7.37 – 7.29 (m, 3H), 7.09 (dt, *J* = 15.7, 3.8 Hz, 1H), 6.59 (d, *J* = 15.4 Hz, 1H), 6.08 (dt, *J* = 15.7, 2.0 Hz, 1H), 4.22 (dd, *J* = 3.8, 2.1 Hz, 2H), 3.76 (s, 3H), 1.49 (s, 9H); **^{13}C-NMR** (101 MHz, $CDCl_3$) δ = 168.3, 166.5, 146.6, 142.5, 135.3, 129.6, 128.8, 127.8, 122.4, 120.8, 57.6, 51.8, 46.4, 28.7; **IR** (neat) ν [cm^{-1}] = 3022, 2959, 1714, 1651, 1613, 1438, 1386, 1360, 1278, 1196, 1155, 1021, 976, 924, 760, 685; **HRMS**: (ESI-MS) m/z calc. for $[C_{18}H_{24}NO_3]^+$ $[M+H^+]$ 302.1751, found 302.1754; m/z calc. for $[C_{36}H_{47}N_2O_6]^+$ $[2M+H]^+$ 603.3429 found 603.3429.

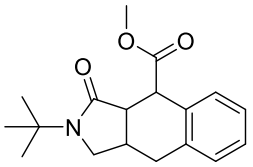

Methyl 2-(*tert*-butyl)-3-oxo-2,3,3a,4,9,9a-hexahydro-1*H*-benzo[f]isoindole-4-carboxylate (189)

Monomethyl fumarate (**177**) (1.30 g, 10 mmol, 1.0 equiv.) was dissolved in dry THF (25 mL) and thionyl chloride (1.23 g, 750 µL, 10 mmol, 1.0 equiv.) was added. After refluxing for 2 h, the reaction mixture was cooled down to 0 °C. *Via* an additional funnel, amine **170b** (1.92 g, 10 mmol, 1.0 equiv.) and NEt_3 (1.11 g, 1.5 mL, 11 mmol, 1.1 equiv.) in dry THF (10 mL) were

dropwise added. The resulting reaction mixture was stirred for 20 h in defrosting ice bath. Then the solvent was removed under reduced pressure. The residue was dissolved again in DCM and was washed twice with sat. $NaHCO_3$. The organic phase was dried over $MgSO_4$, filtered and evaporated. By purification *via* silica gel column chromatography (hexanes/EtOAc 3:1) compound **189** (414 mg, 14 mmol, 14%) was obtained as white solid.

R_f = 0.32 (hexanes/EtOAc 3:1); **mp** = 133.7 °C; **^{1}H-NMR** (300 MHz, $CDCl_3$) δ = 7.29 – 7.05 (m, 4H), 3.88 – 3.83 (m, 1H), 3.83 (s, 3H), 3.63 (dd, *J* = 9.3, 6.9 Hz, 1H), 3.16 (t, *J* = 9.7 Hz, 1H), 2.93 (dd, *J* = 15.6, 4.9 Hz, 1H), 2.88 – 2.66 (m, 2H), 2.20 – 1.98 (m, 1H), 1.38 (s, 9H); **^{13}C-NMR** (75 MHz, $CDCl_3$) δ = 174.1, 174.0, 135.6, 133.4, 130.2, 127.8, 127.3, 126.9, 54.2, 52.4, 49.7, 48.8, 46.8, 35.9, 33.5, 28.1; **IR** (neat) ν [cm^{-1}] = 2959, 2907, 2862, 1744, 1677, 1476, 1405, 1364, 1328, 1271, 1241, 1200, 1144, 1006, 980, 905, 760; **HRMS**: (APCI-MS) (m/z) calc. for $[C_{18}H_{24}NO_3]^+$ $[M+H]^+$ 302.1751, found 302.1757.

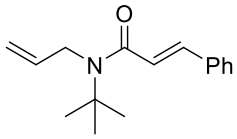

***N*-Allyl-*N*-(*tert*-butyl)cinnamamide (153h)**

Following the general procedure **B** cinnamoyl chloride was generated *in situ* using cinnamic acid **152** (1.48 g, 10 mmol, 1.0 equiv.) and thionyl chloride (1.19 g, 730 µL, 10 mmol, 1.0 equiv.) in dry THF (20 mL). Then the reaction mixture was cooled to 0 °C and the solution of *N*-(*tert*-butyl)prop-2-en-1-amine (**170a**) (1.14 g, 10 mmol, 1.0 equiv.) with triethylamine (1.11 g, 1.5 mL, 11 mmol, 1.1 equiv.) in dry THF (10 mL) was added. The reaction mixture was stirred for 19 h at rt. After silica gel column chromatography (hexanes/EtOAc 9:1) *N*-allyl-*N*-(*tert*-butyl)cinnamamide (**153h**) (927 mg, 3.8 mmol, 38%) was obtained as white solid.

R_f = 0.4 (hexanes/EtOAc 9:1); **mp** = 85.6 °C; **^{1}H-NMR** (300 MHz, $CDCl_3$) δ = 7.68 – 7.51 (m, 1H), 7.49 – 7.29 (m, 5H), 6.75 (d, *J* = 15.5 Hz, 1H), 6.05 – 5.89 (m, 1H), 5.37 – 5.31 (m, 1H), 5.29 (t, *J* = 1.9 Hz, 1H), 4.07 (dt, *J* = 4.0, 2.0 Hz, 2H), 1.51 (s, 9H); **^{13}C-NMR** (101 MHz, $CDCl_3$) δ = 168.5, 141.5, 136.3, 135.7, 129.3, 128.7, 127.7, 121.8, 116.4, 57.4, 47.5, 28.6; **IR** (neat) ν [cm^{-1}] =3060, 3026, 2967, 2926, 1766, 1699, 1651, 1602, 1449, 1386, 1192, 1073, 984, 760, 682; **HRMS**: (ESI-MS) m/z calc. for $[C_{16}H_{22}NO]^+$ $[M+H]^+$ 244.1696, found 244.1697.

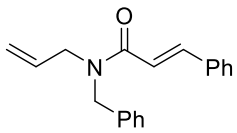

_N_-Allyl-_N_-benzylcinnamamide (153r)[40]

Following the general procedure **B** cinnamoyl chloride was generated *in situ* using cinnamic acid **152** (7.68 g, 52.0 mmol, 1.0 equiv.) and thionyl chloride (6.17 g, 3.8 mL, 52.0 mmol, 1.0 equiv.) in dry THF (60 mL). Then the reaction mixture was cooled to 0 °C and the solution of *N*-benzylprop-2-en-1-amine (**170d**) (7.63 g, 52.0 mmol, 1.0 equiv.) with triethylamine (5.80 g, 7.9 mL, 57.0 mmol, 1.1 equiv.) in dry THF (40 mL) was added. The reaction mixture was stirred for 24 h at rt. After silica gel column chromatography (hexanes/EtOAc 19:1 → 9:1 → 5:1) *N*-allyl-*N*-benzylcinnamamide (**153r**) (10.4 g, 37.5 mmol, 72%) was obtained as slightly yellow oil.

R_f = 0.26 (hexanes/EtOAc 5:1); **^{1}H-NMR** (400 MHz, $CDCl_3$) δ = 7.79 (d, *J* = 15.4 Hz, 1H), 7.48 (dd, *J* = 30.4, 4.9 Hz, 2H), 7.42 – 7.15 (m, 8H), 6.84 (d, *J* = 15.4 Hz, 1H), 5.96 – 5.71 (m, 1H), 5.36 – 5.03 (m, 2H), 4.69 (d, *J* = 19.1 Hz, 2H), 4.17 – 3.96 (m, 2H); **^{13}C-NMR** (101 MHz, $CDCl_3$) δ = 167.1, 166.9, 143.6, 143.3, 137.6, 137.0, 135.4, 135.2, 133.02, 132.98, 129.7, 129.0, 128.82, 128.80, 128.6, 128.3, 127.9, 127.7, 127.4, 126.5, 117.7, 117.5, 117.4, 117.1, 50.2, 49.3, 49.1, 48.7 (signal doubling due to rotamers); **IR** (neat) ν [cm^{-1}] = 3063, 3026, 2922, 1647, 1602, 1494, 1408, 1356, 1326, 1200, 976, 916, 760, 738, 697; **HRMS**: (APCI-MS): m/z calc. for $[C_{19}H_{20}NO]^+$ $[M+H]^+$ 278.1539, found 278.1543.

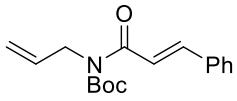

***tert*-Butyl allyl(cinnamoyl)carbamate (153v)**

At first cinnamoyl chloride was generated *in situ* using cinnamic acid **152** (741 mg, 5.0 mmol, 1.0 equiv.) and thionyl chloride (595 mg, 364 µL, 5.0 mmol, 1.0 equiv.) in dry THF (10 mL). Then the reaction mixture was cooled to 0 °C. Meanwhile, *tert*-butyl allyl carbamate (**175**) (787 mg, 5.0 mmol, 1.0 equiv.) was dissolved in dry THF (10 mL) and the solution was also cooled down to 0 °C. Then a solution of KHMDS (1M in THF, 6.0 mL, 6.0 mmol, 1.2 equiv.) was added dropwise. After stirring for 1 h at 0 °C the acid chloride solution was added dropwise

and the reaction mixture was stirred for 19 h. Afterwards, the crude mixture was diluted with H_2O and DEE. The phases were separated, and the aqueous phase was extracted twice with DEE. The combined organic layers were dried over $MgSO_4$, filtered and the solvent was removed under reduced pressure. Silica gel column chromatography (hexanes/EtOAc 19:1) gave *tert*-butyl allyl(cinnamoyl)carbamate (**153v**) (747 mg, 2.6 mmol, 52%) as a colorless oil.

R_f = 0.37 (hexanes/EtOAc 19:1); **^{1}H-NMR** (300 MHz, $CDCl_3$) δ = 7.70 (d, *J* = 15.6 Hz, 1H), 7.54 – 7.46 (m, 3H), 7.37 (dd, *J* = 5.1, 1.9 Hz, 3H), 5.88 (ddt, *J* = 17.2, 10.3, 5.6 Hz, 1H), 5.26 – 5.09 (m, 2H), 4.37 (dt, *J* = 5.6, 1.4 Hz, 2H), 1.54 (s, 9H); **^{13}C-NMR** (101 MHz, $CDCl_3$) δ = 168.5, 153.2, 143.3, 135.2, 133.5, 129.9, 128.8, 128.2, 121.4, 116.6, 83.2, 47.0, 28.1; **IR** (neat) ν [cm^{-1}] = 3086, 2981, 1722, 1673, 1617, 1449, 1341, 1244, 1207, 1136, 1099, 1025, 849, 764, 685.; **HRMS**: (ESI-MS) m/z calc. for $[C_{17}H_{21}NO_3Na]^+$ [M+Na]$^+$ 310.1414, found 310.1418.

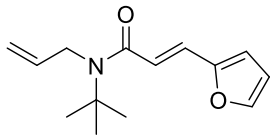

(*E*)-*N*-Allyl-*N*-(*tert*-butyl)-3-(furan-2-yl)acrylamide (153k)

Following the general procedure **B** (*E*)-3-(furan-2-yl)acryloyl chloride was generated *in situ* using (*E*)-3-(furan-2-yl)acrylic acid (**180a**) (967 mg, 7.0 mmol, 1.0 equiv.) and thionyl chloride (833 mg, 508 µL, 7.0 mmol, 1.0 equiv.) in dry THF (25 mL). Then the reaction mixture was cooled to 0 °C and the solution of *N*-(*tert*-butyl)prop-2-en-1-amine (**170a**) (792 mg, 7.0 mmol, 1.0 equiv.) with triethylamine (779 mg, 1.1 mL, 7.7 mmol, 1.1 equiv.) in dry THF (10 mL) was added. The reaction mixture was stirred for 20 h at rt. After silica gel column chromatography (hexanes/EtOAc 3:1) (*E*)-*N*-allyl-*N*-(*tert*-butyl)-3-(furan-2-yl)acrylamide (**153k**) (989 mg, 4.2 mmol, 61%) was obtained as orange oil.

R_f = 0.17 (hexanes/EtOAc 9:1); **^{1}H-NMR** (300 MHz, $CDCl_3$) δ = 7.43 – 7.32 (m, 2H), 6.63 (d, *J* = 15.2 Hz, 1H), 6.47 (d, *J* = 3.6 Hz, 1H), 6.41 (dd, *J* = 3.4, 1.9 Hz, 1H), 5.95 (ddt, *J* = 17.4, 10.3, 4.0 Hz, 1H), 5.37 – 5.19 (m, 2H), 4.05 (dt, *J* = 4.0, 2.0 Hz, 2H), 1.48 (s, 9H); **^{13}C-NMR** (75 MHz, $CDCl_3$) δ = 168.2, 152.0, 143.6, 136.2, 128.5, 119.2, 116.3, 113.1, 112.0, 57.4, 47.4, 28.6; **IR** (neat) ν [cm^{-1}] = 3090, 2963, 2929, 1654, 1610, 1483, 1386, 1256, 1196, 1013, 969, 924, 741, 667; **HRMS**: (APCI-MS): m/z calc. for $[C_{14}H_{19}NO_2]^+$ [M+H]$^+$ 234.1489, found 234.1491.

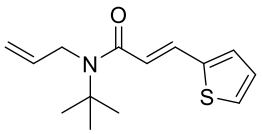

(*E*)-*N*-Allyl-*N*-(*tert*-butyl)-3-(thiophen-2-yl)acrylamide (153l)

Following the general procedure **B** (*E*)-3-(thiophen-2-yl)acryloyl chloride was generated *in situ* using (*E*)-3-(thiophenyl-2-yl)acrylic acid (**180b**) (1.04 g, 6.8 mmol, 1.0 equiv.) and thionyl chloride (804 mg, 490 µL, 6.8 mmol, 1.0 equiv.) in dry THF (25 mL). Then the reaction mixture was cooled to 0 °C and the solution of *N*-(*tert*-butyl)prop-2-en-1-amine (**170a**) (764 mg, 6.8 mmol, 1.0 equiv.) with triethylamine (751 mg, 1.0 mL, 7.4 mmol, 1.1 equiv.) in dry THF (10 mL) was added. The reaction mixture was stirred for 19 h at rt. After silica gel column chromatography (hexanes/EtOAc 3:1) (*E*)-*N*-allyl-*N*-(*tert*-butyl)-3-(thiophen-2-yl)acrylamide (**153l**) (1.11 g, 4.5 mmol, 66%) was obtained as orange oil.

R$_f$ = 0.25 (hexanes/EtOAc 9:1); **^{1}H-NMR** (300 MHz, $CDCl_3$) δ = 7.76 – 7.66 (m, 1H), 7.29 – 7.22 (m, 1H), 7.17 – 7.11 (m, 1H), 7.00 (dd, *J* = 5.1, 3.6 Hz, 1H), 6.55 (d, *J* = 15.1 Hz, 1H), 5.95 (ddt, *J* = 17.4, 10.2, 4.1 Hz, 1H), 5.35 – 5.22 (m, 2H), 4.04 (dt, *J* = 4.1, 2.0 Hz, 2H), 1.49 (s, 9H); **^{13}C-NMR** (75 MHz, $CDCl_3$) δ = 168.1, 140.9, 136.2, 134.2, 129.6, 127.9, 126.7, 120.6, 116.4, 57.4, 47.5, 28.6; **IR** (neat) ν [cm^{-1}] = 3082, 2926, 2963, 1643, 1599, 1386, 1349, 1196, 1125, 1043, 969, 916, 823, 700; **HRMS**: (APCI-MS): m/z calc. for $[C_{14}H_{19}NOS]^+$ $[M+H]^+$ 250.1260, found 250.1263.

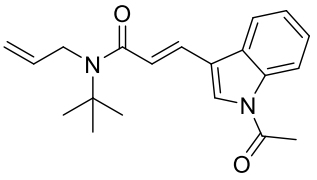

(*E*)-3-(1-Acetyl-1*H*-indol-3-yl)-*N*-allyl-*N*-(*tert*-butyl)acrylamide (153m)

Following the general procedure **B** (*E*)-3-(1-acetyl-1*H*-indol-3-yl)acryloyl chloride was generated *in situ* using (*E*)-3-(1-acetyl-1*H*-indol-3-yl)acrylic acid (**184b**) (1.15 g, 5.0 mmol, 1.0 equiv.) and thionyl chloride (595 mg, 364 µL, 5.0 mmol, 1.0 equiv.) in dry THF (16 mL). Then the reaction mixture was cooled to 0 °C and the solution of *N*-(*tert*-butyl)prop-2-en-1-amine (**170a**) (566 mg, 5.0 mmol, 1.0 equiv.) with triethylamine (557 mg, 762 µL, 5.5 mmol, 1.1 equiv.) in dry THF (10 mL) was added. The reaction mixture was stirred at rt for 26 h. After silica gel column chromatography (hexanes/EtOAc 3:1) (*E*)-3-(1-acetyl-1*H*-indol-3-yl)-*N*-

allyl-*N*-(*tert*-butyl)acrylamide (**153m**) (213 mg, 0.70 mmol, 13%) was obtained as yellowish solid.

R_f = 0.22 (hexanes/EtOAc 2:1); **mp** = 97.5 100 °C; **^{1}H-NMR** (300 MHz, $CDCl_3$) δ = 8.47 (d, *J* = 8.0 Hz, 1H), 7.78 – 7.68 (m, 2H), 7.57 (s, 1H), 7.37 (dtd, *J* = 19.7, 7.3, 1.3 Hz, 2H), 6.91 (d, *J* = 15.5 Hz, 1H), 6.04 (ddt, *J* = 17.8, 10.3, 3.9 Hz, 1H), 5.47 – 5.28 (m, 2H), 4.12 (dt, *J* = 3.9, 2.0 Hz, 2H), 2.66 (s, 3H), 1.53 (s, 9H); **^{13}C-NMR** (101 MHz, $CDCl_3$) δ = 168.6, 168.4, 136.7, 136.3, 132.7, 128.2, 126.6, 125.9, 124.3, 122.2, 120.1, 119.4, 116.9, 116.5, 57.5, 47.6, 28.6, 24.1; **IR** (neat) ν [cm^{-1}] = 2959, 1707, 1651, 1599, 1449, 1382, 1349, 1222, 1189, 1017, 987, 924, 734; **HRMS**: (ESI-MS) m/z calc. for $[C_{20}H_{25}N_2O_2]^+$ $[M+H]^+$ 325.1911, found 325.1914, calc. for $[C_{20}H_{24}N_2O_2Na]^+$ $[M+Na]^+$ 347.1730, found 347.1728.

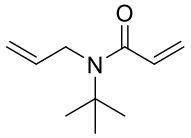

***N*-Allyl-*N*-(*tert*-butyl)acrylamide (153j)**

Following the general procedure **B** a solution of acryloyl chloride **249** (425 mg, 390 µL, 4.7 mmol, 1.0 equiv.) in dry THF (5 mL) was cooled to 0 °C and *N*-(*tert*-butyl)prop-2-en-1-amine (**170a**) (532 mg, 4.7 mmol, 1.0 equiv.) with triethylamine (523 mg, 720 µL, 5.2 mmol, 1.1 equiv.) in dry THF (5 mL) was added. After stirring for 24 h at rt, *N*-allyl-*N*-(*tert*-butyl)acrylamide (**153j**) (581 mg, 3.5 mmol, 74%) was obtained as a yellow liquid and was used in the following step without further purification.

R_f = 0.77 (hexanes/EtOAc 2:1); **^{1}H-NMR** (300 MHz, $CDCl_3$) δ = 6.43 (dd, *J* = 16.7, 10.2 Hz, 1H), 6.23 (dd, *J* = 16.7, 2.2 Hz, 1H), 5.96 – 5.79 (m, 1H), 5.54 (dd, *J* = 10.2, 2.2 Hz, 1H), 5.26 (td, *J* = 2.0, 0.7 Hz, 1H), 5.23 – 5.19 (m, 1H), 3.97 (dt, *J* = 4.1, 2.0 Hz, 2H), 1.45 (s, 9H); **^{13}C-NMR** (75 MHz, $CDCl_3$) δ = 168.2, 136.0, 131.6, 126.6, 116.2, 57.2, 47.4, 28.5; **IR** (neat) ν [cm^{-1}] = 3090, 2929, 2967, 1651, 1613, 1412, 1360, 1196, 980, 916, 797; **HRMS**: (APCI-MS) m/z calc. for $[C_{10}H_{18}NO]^+$ $[M+H]^+$ 168.1383, found 168.1387.

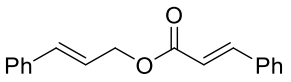

Cinnamyl cinnamate (153w)

At first cinnamoyl chloride was generated *in situ* using cinnamic acid **152** (1.48 g, 10 mmol, 1 equiv.) and thionyl chloride (1.19 g, 725 µL, 10 mmol, 1 equiv.) in dry THF (15 mL). The reaction mixture was cooled to 0 °C and a solution of (*E*)-3-phenylprop-2-en-1-ol (1.34 g, 10 mmol, 1 equiv.), triethylamine (3.00 g, 4.2 mL, 30 mmol, 3 equiv.) and DMAP (305 mg, 2.5 mmol, 0.25 equiv.) in dry THF (15 mL) was added dropwise. The reaction mixture was stirred then for 24 h. After purification using flash system (hexanes/EtOAc) cinnamyl cinnamate (**153w**) (2.09 g, 7.9 mmol, 79%) was obtained as colorless oil.

R_f = 0.3 (hexanes/EtOAc 9:1); **^{1}H-NMR** (300 MHz, $CDCl_3$) δ = 7.74 (d, *J* = 16.0 Hz, 1H), 7.60 – 7.49 (m, 2H), 7.47 – 7.20 (m, 8H), 6.72 (d, *J* = 15.9 Hz, 1H), 6.50 (d, *J* = 16.0 Hz, 1H), 6.37 (dt, *J* = 15.9, 6.4 Hz, 1H), 4.88 (dd, *J* = 6.4, 1.3 Hz, 2H); **^{13}C-NMR** (75 MHz, $CDCl_3$) δ = 166.8, 145.2, 136.3, 134.4, 134.3, 130.4, 128.9, 128.7, 128.2, 128.1, 126.7, 123.3, 117.9, 65.2; **IR** (neat) ν [cm^{-1}] = 3060, 3026, 2944, 1707, 1638, 1580, 1494, 1449, 1308, 1252, 1200, 1155, 1069, 965, 864, 745, 685; **HRMS**: (TICC/EIC-MS) m/z calc. for $[C_{18}H_{16}O_2]^{\bullet+}$ $[M]^{\bullet+}$ 264.11448, found 264.11395.

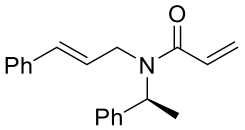

(*S*)-*N*-Cinnamyl-*N*-(1-phenylethyl)acrylamide (153x)

Following the general procedure **B,** a solution of acryloyl chloride **249** (860 mg, 775 µL, 9.50 mmol, 1.0 equiv.) in dry THF (10 mL) was cooled to 0 °C. (*S,E*)-3-phenyl-*N*-(1-phenylethyl)prop-2-en-1-amine (**248**) (2.25 g, 9.50 mmol, 1.0 equiv.) dissolved together with triethylamine (1.06 g, 1.45 mL, 10.5 mmol, 1.1 equiv.) in dry THF (10 mL) was added. The reaction mixture was stirred for 22 h at rt. After purification by silica column chromatography (hexanes/EtOAc 7:1), (*S*)-*N*-cinnamyl-*N*-(1-phenylethyl)acrylamide (**153x**) (2.26 g, 7.7 mmol, 82%) was obtained as a yellowish sticky oil.

R_f = 0.4 (hexanes/EtOAc 3:1); **^{1}H-NMR** (300 MHz, $CDCl_3$) δ = 7.40 – 7.18 (m, 10H), 6.76 – 5.85 (m, 5H), 5.71 (dd, *J* = 9.8, 2.7 Hz, 1H), 4.09 – 3.62 (m, 2H), 1.64 – 1.50 (m, 3H); **^{13}C-NMR** (75 MHz, $CDCl_3$) δ = 166.8, 140.8, 136.3, 131.4, 128.7, 128.6, 128.5, 127.8, 127.7, 127.6, 126.6, 126.3, 51.4, 45.3, 16.7; **IR (neat)** ν [cm^{-1}] = 3060, 3026, 2978, 2937, 1644, 1610, 1494, 1446, 1420, 1364, 1326, 1282, 1203, 1170, 1062, 961, 793, 730, 693. **HRMS**: (ESI-MS) m/z calc. for $[C_{20}H_{21}NOK]^+$ $[M+K]^+$ 330.1255, found 330.1256; $[\alpha]_D^{20}$ = 154.6 (*c* 0.1, CH_2Cl_2); **chiral HPLC**: 98% *ee* (Phenomenex Lux Cellulose-1, 4.6 x 250 mm, heptane/*i*-PrOH = 90:10, 0.5 mL/min, t_R (*R*), (***S***) = 20.1, **24.3** min).

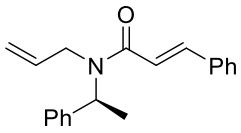

(*S*)-*N*-Allyl-*N*-(1-phenylethyl)cinnamamide (153y)

Following the general procedure **B,** a solution of cinnamoyl chloride **259** (3.86 g, 23.2 mmol, 1.0 equiv) in dry THF (25 mL) was cooled to 0 °C. (*S*)-*N*-(1-phenylethyl)prop-2-en-1-amine (**260**) (3.74 g, 23.2 mmol, 1.0 equiv.) dissolved together with triethylamine (2.58 g, 3.54 mL, 25.5 mmol, 1.1 equiv.) in dry THF (15 mL) was added. The reaction mixture was stirred for 24 h at rt. After purification by flash system (hexanes/EtOAc), (*S*)-*N*-allyl-*N*-(1-phenylethyl)cinnamamide (**153y**) (6.23 g, 21.4 mmol, 92%) was obtained as a colorless oil.

R_f = 0.13 (hexanes/EtOAc 5:1); **^{1}H-NMR** (400 MHz, $CDCl_3$) δ = 7.70 (d, *J* = 15.4 Hz, 1H), 7.40 (d, *J* = 6.1 Hz, 2H), 7.31 – 7.18 (m, 8H), 6.71 (d, *J* = 15.5 Hz, 1H), 6.15 (dd, *J* = 13.6, 6.6 Hz, 1H), 5.72 – 5.53 (m, 1H), 5.12 – 5.00 (m, 2H), 3.89 – 3.57 (m, 2H), 1.47 (d, *J* = 6.9 Hz, 3H); **^{13}C-NMR** (101 MHz, $CDCl_3$) δ = 167.1, 142.9, 140.9, 135.7, 135.5, 129.6, 128.8, 128.5, 127.8, 127.6, 127.4, 118.7, 116.5, 51.4, 45.9, 16.7. **IR** (neat) ν [cm^{-1}] = 3060, 3026, 2978, 2937, 1647, 1602, 1494, 1449, 1405, 1330, 1300, 1203, 1129, 1072, 976, 916, 857, 760, 697; **HRMS**: (ESI-MS) m/z calc. for $[C_{20}H_{21}NOK]^+$ $[M+K]^+$ 330.1255, found 330.1255; m/z calc. for $[C_{20}H_{22}NO]^+$ $[M+H]^+$ 292.1696, found 292.1702; m/z calc. for $[C_{20}H_{21}NONa]^+$ $[M+Na]^+$ 314.1515, found 314.1521; $[\alpha]_D^{20}$ = -204.1 (*c* 1, $CHCl_3$); **chiral HPLC**: 98% *ee* (Phenomenex Lux Cellulose-21, 4.6 x 250 mm, heptane/*i*-PrOH = 70:30, 0.5 mL/min, t_R (R), (**S**) = 11.7, **14.4** min).

[2+2]-Photocycloaddition

General procedure for [2+2]-Photocycloaddition D

The amide-linked diene **153** (1 mmol, 1 equiv.) was dissolved in DMSO (25 mL, 0.04M) together with Ir[(dtb-bpy)(dF(CF_3)ppy)$_2$]PF_6 (0.01 mmol, 1 mol%). The reaction mixture was stirred at 40 °C for the reported time under irradiation with the blue LED-setup. After completion, the reaction mixture was diluted with H_2O (10 mL) and DEE (30 mL). Then the phases were separated, and the aqueous phase was extracted three times with DEE (each 30 mL). The combined organic phases were washed twice with H_2O (each 10 mL) and once with brine (20 mL). Finally, the combined aqueous phases were back-extracted with DEE (30 mL). The combined organic phases were dried over $MgSO_4$, filtered and the solvent was removed under reduced pressure. The crude product was then purified by column chromatography using hexanes and EtOAc as eluent.

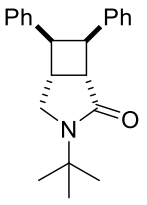

(±)-3-(*tert*-Butyl)-6,7-diphenyl-3-azabicyclo[3.2.0]heptan-2-one (158g)

Compound **158g** was prepared from **153g** (321.8 mg, 1.0 mmol, 1.0 equiv.) and Ir[(dtb-bpy)(dF(CF_3)ppy)$_2$]PF_6 (11.5 mg, 0.010 mmol) in 3 h following general protocol **D**. After silica gel column chromatography (hexanes/EtOAc 5:1) a diastereomeric mixture of compound **158g** (272.5 mg, 0.85 mmol, 85%, *dr* 81:19) was obtained as yellow oil.

In the proton NMR, the signals of both diastereomers are overlapping. Characteristic signals of the minor diastereomer are marked.

R_f = 0.23 (hexanes/EtOAc 5:1); **^{1}H-NMR** (400 MHz, $CDCl_3$) δ 7.42 – 7.27 (m, 3H), 7.26 – 7.17 (m, 1H), 7.13 – 7.05 (m, 4H), 7.05 – 6.94 (m, 4H), 6.86 (d, *J* = 7.3 Hz, 2H), 4.06 (dd, *J* = 9.4, 2.3 Hz, 1H), 4.03 – 3.96^{minor} (m, 0.36H), 3.94 (t, *J* = 8.5 Hz, 1H), 3.79 (dd, J = 10.3, 6.6 Hz, 1H), 3.48 (d, J = 10.3 Hz, 1H), 3.46 – 3.42^{minor} (m, 0.32H), 3.38 (q, *J* = 7.5 Hz, 1H), 3.27 – 3.22 (m, 1H), 3.22 – 3.11 (m, 1H), 1.51 (s, 9H), 1.35^{minor} (s, 2.42H); **^{13}C-NMR** (75.5 MHz, $CDCl_3$): major diastereomer: δ = 176.6, 140.0, 139.3, 128.1, 127.9, 127.8, 127.6,

126.0, 54.2, 51.2, 48.8, 48.6, 45.3, 34.0, 27.7; minor diastereomer: δ = 176.4, 143.5, 139.4, 128.6, 128.5, 127.7, 126.8, 126.4, 54.1, 47.3, 47.1, 47.0, 46.5, 30.3, 27.4; **IR** (neat) ν [cm^{-1}] = 3063, 3030, 2974, 1654, 1405, 1364, 1282, 1222, 909, 730, 697; **HRMS**: major diastereomer (acquisition time 3.173-3.218 min): (ESI-MS) calc. for $[C_{22}H_{26}NO]^+$ $[M+H]^+$ 320.2009, found 320.2014; minor diastereomer (acquisition time 3.323-3.373 min): (ESI-MS) calc. for $[C_{22}H_{26}NO]^+$ $[M+H]^+$ 320.2009, found 320.2017.

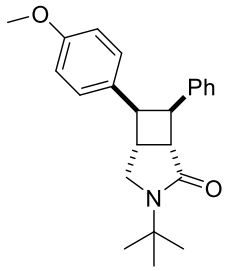

(±)-3-(*tert*-Butyl)-6-(4-methoxyphenyl)-7-phenyl-3-azabicyclo[3.2.0]heptan-2-one (158d)

Compound **158d** was prepared from **153d** (347.9 mg, 996 µmol, 1.0 equiv.) and $Ir[(dtb\text{-}bpy)(dF(CF_3)ppy)_2]PF_6$ (12.1 mg, 0.010 mmol) in 7 h following general protocol **D**. After silica gel column chromatography (hexanes/EtOAc 4:1) a diastereomeric mixture of compound **158d** (217.5 mg, 622 µmol, 63%, *dr* 72:28) was obtained as yellow oil.

In the proton and carbon NMR, the signals of both diastereomers are overlapping. Characteristic signals of the minor diastereomer are marked.

R_f = 0.25 (hexanes/EtOAc 3:1); **^{1}H-NMR** (300 MHz, $CDCl_3$) δ = 7.37 – 7.27 (m, 2H), 7.25 – 6.84 (m, 8H), 6.81 – 6.70 (m, 2H), 6.65 – 6.55 (m, 2H), 4.02 (dd, *J* = 9.3, 2.1 Hz, 1H), 3.91 – 3.83 (m, 1.5H), 3.82^{minor} (s, 1H), 3.81 – 3.71 (m, 1.75H), 3.68 (s, 3H), 3.45 (d, *J* = 10.3 Hz, 1H), 3.35 – 3.07 (m, 3H), 1.50 (s, 9H), 1.37^{minor} (s, 3.7H); **^{13}C-NMR** (75 MHz, $CDCl_3$) δ = 176.7, 176.5^{minor}, 157.8, 140.0, 131.4, 128.8^{minor}, 128.7, 128.5^{minor}, 128.1, 127.9, 126.4, 126.0, 114.0^{minor}, 113.2, 55.3^{minor}, 55.1, 54.2, 54.1^{minor}, 51.1, 48.5, 48.3, 47.4^{minor}, 47.0^{minor}, 46.8^{minor}, 46.4^{minor}, 45.0, 34.5, 30.4, 27.7, 27.6^{minor}; **IR** (neat) ν [cm^{-1}] = 3063, 2974, 2036, 1666, 1610, 1513, 1405, 1285, 1177, 1032, 831, 749, 700; **HRMS**: major diastereomer (acquisition time 3.095-3.151 min): (ESI-MS) m/z calc. for $[C_{23}H_{28}NO_2]^+$ $[M+H]^+$ 350.2115, found 350.2121; minor diastereomer (acquisition time 3.234-3.289 min): (ESI-MS) m/z calc. for $[C_{23}H_{28}NO_2]^+$ $[M+H]^+$ 350.2115, found 350.2118.

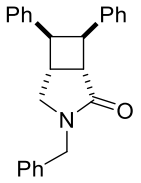

(±)-3-Benzyl-6,7-diphenyl-3-azabicyclo[3.2.0]heptan-2-one (158f)[38]

Compound **158f** was prepared from **153q** (350.2 mg, 991 µmol, 1.0 equiv.) and Ir[(dtb-bpy)(dF(CF_3)ppy)$_2$]PF_6 (11.9 mg, 0.010 mmol) in 4 h following general protocol **D**. After silica gel column chromatography (hexanes/EtOAc 2:1) a diastereomeric mixture of compound **158f** (263.1 mg, 744 µmol, 75%, *dr* 72:28) was obtained as yellow oil.

In the proton and carbon NMR, the signals of both diastereomers are overlapping. Characteristic signals of the minor diastereomer are marked.

R_f = 0.26 (hexanes/EtOAc 2:1); **^{1}H-NMR** (300 MHz, $CDCl_3$) δ = 7.56 – 7.27 (m, 10H), 7.26 – 7.19 (m, 2H), 7.17 – 6.94 (m, 9H), 6.80 (dt, *J* = 25.4, 9.5 Hz, 2H), 4.73 (d, *J* = 14.5 Hz, 1H), 4.49 (d, *J* = 14.6, 1H), 4.36^{minor} (d, *J* = 14.5 Hz, 0.35H), 4.14 (dd, *J* = 9.4, 2.5 Hz, 1H), 4.09 – 3.94^{minor} (m, 0.63H), 3.92 – 3.82 (m, 1H), 3.60 (dd, *J* = 10.2, 6.5 Hz, 1H), 3.46 (q, *J* = 10.4 Hz, 1H), 3.38 (dd, *J* = 2.04, 7.83, 1H), 3.35 – 3.26^{minor} (m, 0.67H), 3.23 (d, *J* = 10.3 Hz, 1H), 3.12 – 3.03^{minor} (m, 0.43H); **^{13}C-NMR** (75 MHz, $CDCl_3$) δ = 176.1, 175.8^{minor}, 139.7, 139.0, 136.4, 128.9, 128.7^{minor}, 128.60^{minor}, 128.58^{minor}, 128.4^{minor}, 128.3, 128.1, 128.0, 127.80, 127.79, 127.6, 127.4^{minor}, 126.4^{minor}, 126.2, 126.1, 52.0, 48.9, 48.3, 47.2^{minor}, 47.1, 45.5^{minor}, 43.9, 34.6, 31.1^{minor}; **IR** (neat) ν [cm^{-1}] = 3026, 3003, 2974, 2918, 2873, 1673, 1494, 1423, 1282, 1233, 1028, 745, 693; **HRMS**: major diastereomer (acquisition time 3.166-3.216 min): (ESI-MS) calc. for $[C_{25}H_{24}NO]^+$ $[M+H]^+$ 354.1852, found 354.1858; minor diastereomer (acquisition time 3.277-3.322 min): (ESI-MS) calc. for $[C_{25}H_{24}NO]^+$ $[M+H]^+$ 354.1852, found 354.1855.

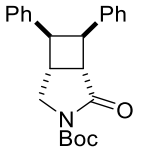

(±)-*tert*-Butyl-2-oxo-6,7-diphenyl-3-azabicyclo[3.2.0]heptane-3-carboxylate (158h)

Compound **158h** was prepared from **153t** (337.6 mg, 929 µmol, 1.0 equiv.) and Ir[(dtb-bpy)(dF(CF_3)ppy)$_2$]PF_6 (11.2 mg, 0.010 mmol) in 24 h following general protocol **D**.

After silica gel column chromatography (hexanes/EtOAc 7:1) a diastereomeric mixture of compound **158h** (206.5 mg, 568 µmol, 61%, *dr* 78:22) was obtained as yellowish solid.

In the proton and carbon NMR, the signals of both diastereomers are overlapping. Characteristic signals of the minor diastereomer are marked.

R_f = 0.18 (hexanes/EtOAc 5:1); **^{1}H-NMR** (300 MHz, $CDCl_3$) δ = 7.38 – 7.23 (m, 2H), 7.15 – 6.97 (m, 5H), 6.97 – 6.89 (m, 2H), 6.85 – 6.76 (m, 2H), 4.08 (dd, *J* = 9.4, 2.1 Hz, 1H), 4.04 – 3.90 (m, 2H), 3.80 (d, *J* = 11.4 Hz, 1H), 3.47 – 3.33 (m, 2H), 1.54 (s, 9H), 1.46^{minor} (s, 1.66H); **^{13}C-NMR** (101 MHz, $CDCl_3$) δ = 176.0, 150.7, 142.1^{minor}, 138.9, 138.5, 129.1, 128.8, 128.7, 128.1, 128.0, 127.9, 127.6, 127.2, 126.9, 126.5, 126.4, 126.3, 83.2, 83.0^{minor}, 51.6, 48.6, 48.3, 47.2^{minor}, 46.9^{minor}, 46.9^{minor}, 45.9^{minor}, 45.0, 33.4, 29.9^{minor}, 28.10, 28.05^{minor}; **IR** (neat) ν [cm^{-1}] = 3063, 3026, 2974, 2922, 1763, 1714, 1364, 1304, 1252, 1148, 1058, 752, 697; **HRMS**: major diastereomer (acquisition time 3.253-3.297 min): (ESI-MS) calc. for $[C_{23}H_{25}NO_3]^+$ $[M+H]^+$ 387.1760, found 387.1763; minor diastereomer (acquisition time 3.336-3.386 min): (ESI-MS) calc. for $[C_{23}H_{25}NO_3]^+$ $[M+H]^+$ 387.1760, found 387.1758.

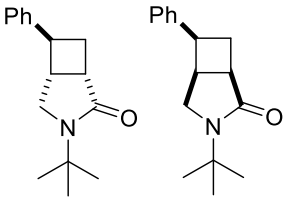

158ia **158ib**

(±)-3-(*tert*-Butyl)-6-phenyl-3-azabicyclo[3.2.0]heptan-2-one (158i)

Compound **158i** was prepared from **153i** (241.0 mg, 990 µmol, 1.0 equiv.) and $Ir[(dtb\text{-}bpy)(dF(CF_3)ppy)_2]PF_6$ (11.2 mg, 0.010 mmol) in 3 h following general protocol **D**. By silica gel column chromatography (hexanes/EtOAc 3:1) both diastereomers of compound **158i** were separated and were obtained in an overall yield of 78% (*dr* 76:24; major diastereomer **158ia**: yellow oil, 157.5 mg, 647 µmol; minor diastereomer **158ib**: yellow solid, 32.4 mg, 133 µmol)

158ia:

R_f = 0.33 (hexanes/EtOAc 2:1); **^{1}H-NMR** (400 MHz, $CDCl_3$) δ = 7.36 – 7.29 (m, 2H), 7.24 – 7.18 (m, 3H), 3.66 (dd, *J* = 10.2, 6.3 Hz, 1H), 3.48 – 3.35 (m, 2H), 3.03 – 2.86 (m, 2H), 2.66 – 2.41 (m, 2H), 1.47 (s, 9H); **^{13}C-NMR** (75 MHz, $CDCl_3$) δ = 177.4, 144.1, 128.5, 126.4, 126.3,

54.0, 51.6, 44.4, 39.5, 38.2, 31.8, 27.7; **IR** (neat) ν [cm^{-1}] = 3060, 3020, 2970, 2870, 1669, 1401, 1364, 1289, 1222, 749, 700; **HRMS**: (APCI-MS) calc. for $[C_{16}H_{22}NO]^+$ $[M+H]^+$ 244.1696, found 244.1700.

158ib:

R_f = 0.2 (hexanes/EtOAc 2:1); **mp** = 51 52 °C; **^{1}H-NMR** (400 MHz, $CDCl_3$) δ = 7.33 (t, *J* = 7.5 Hz, 2H), 7.28 – 7.14 (m, 3H), 3.91 (dd, *J* = 16.5, 9.6 Hz, 1H), 3.31 (dd, *J* = 10.5, 8.2 Hz, 1H), 3.17 – 3.00 (m, 2H), 2.92 (d, *J* = 10.9 Hz, 1H), 2.87 – 2.75 (m, 1H), 2.53 (ddd, *J* = 11.2, 6.6, 4.2 Hz, 1H), 1.22 (s, 9H); **^{13}C-NMR** (101 MHz, $CDCl_3$) δ = 177.4, 139.7, 128.3, 128.1, 126.5, 53.8, 46.8, 40.1, 39.9, 32.7, 28.3, 27.5; **HRMS**: (APCI-MS) calc. for $[C_{16}H_{22}NO]^+$ $[M+H]^+$ 244.1696, found 244.1707, calc for $[C_{32}H_{43}N_2O_2]^+$ $[2•(M+H)]^+$ 488.3352, found 488.3355.

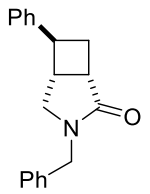

158ja

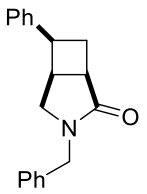

158jb

(±)-3-Benzyl-6-phenyl-3-azabicyclo[3.2.0]heptan-2-one (158j)

Compound **158j** was prepared from **153s** (280.9 mg, 1.01 mmol, 1.0 equiv.) and $Ir[(dtb\text{-}bpy)(dF(CF_3)ppy)_2]PF_6$ (11.1 mg, 0.010 mmol) in 4 h following general protocol **D**. By silica gel column chromatography (hexanes/EtOAc 2:1) both diastereomers of compound **158j** were separated and were obtained in an overall yield of 73% (*dr* 85:15, major diastereomer **158ja**: white solid, 180.4 mg, 650 µmol; minor diastereomer **158jb**: colorless oil, 22.9 mg, 83 µmmol,)

158ja:

R_f = 0.34 (hexanes/EtOAc 1:1); **mp** = 69 °C; **^{1}H-NMR** (400 MHz, $CDCl_3$): δ = 7.44 – 7.26 (m, 7H), 7.25 – 7.09 (m, 3H), 4.66 (d, *J* = 14.6 Hz, 1H), 4.47 (d, *J* = 14.6 Hz, 1H), 3.48 (dd, *J* = 10.3, 6.6 Hz, 1H), 3.36 (dd, *J* = 16.2, 8.8 Hz, 1H), 3.20 (d, *J* = 10.3 Hz, 1H), 3.10 (t, *J* = 8.0 Hz, 1H), 3.00 (dd, *J* = 14.0, 6.9 Hz, 1H), 2.72 – 2.52 (m, 2H); **^{13}C-NMR** (101 MHz, $CDCl_3$): δ = 176.9, 143.8, 136.5, 128.8, 128.6, 128.2, 127.7, 126.5, 126.3, 52.3, 47.0, 44.5, 38.8, 38.0, 31.6; **IR** (neat) ν [cm^{-1}] = 3063, 3027, 2978, 2929, 2873, 1662, 1491, 1443, 1300, 1267, 1077,

1028, 931, 905, 745, 697; **HRMS**: (ESI-MS) m/z calc. for $[C_{19}H_{19}NONa]^+$ [M+Na]$^+$ 300.1359, found 300.1357.

158jb:

R$_f$ = 0.23 (hexanes/EtOAc 1:1); **^{1}H-NMR** (400 MHz, $CDCl_3$): δ = 7.39 – 7.09 (m, 8H), 7.03 (d, *J* = 7.0 Hz, 2H), 4.48 (t, *J* = 11.6 Hz, 1H), 4.07 (d, *J* = 14.5 Hz, 1H), 3.95 (dd, *J* = 17.1, 9.5 Hz, 1H), 3.26 – 3.18 (m, 2H), 3.18 – 3.08 (m, 1H), 2.95 – 2.82 (m, 1H), 2.77 (d, *J* = 10.4 Hz, 1H), 2.54 (ddd, *J* = 13.2, 7.6, 4.0 Hz, 1H); **^{13}C-NMR** (101 MHz, $CDCl_3$): δ = 176.9, 139.5, 136.3, 128.6, 128.40, 128.39, 127.7, 127.5, 126.5, 47.6, 46.7, 39.7, 38.3, 33.7, 28.7; **IR** (neat) ν [cm^{-1}] = 3060, 3027, 2980, 2866, 1669, 1491, 1423,1300, 1256, 1077, 1028, 950, 738, 700; **HRMS**: (ESI-MS) m/z calc. for $[C_{19}H_{19}NONa]^+$ [M+Na]$^+$ 300.1359, found 300.1358.

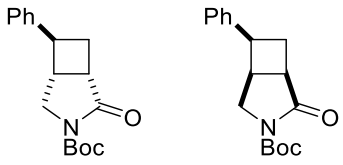

158ka **158kb**

(±)-*tert*-Butyl-2-oxo-6-phenyl-3-azabicyclo[3.2.0]heptane-3-carboxylate (158k)

Compound **158k** was prepared from **153u** (287.4 mg, 1.00 mmol, 1.0 equiv.) and Ir[(dtb-bpy)(dF(CF$_3$)ppy)$_2$]PF$_6$ (11.2 mg, 0.010 mmol) in 48 h following general protocol **D**. By silica gel column chromatography (hexanes/EtOAc 3:1) both diastereomers of compound **158k** were separated and were obtained in an overall yield of 73% (*dr* 81:19, major diastereomer **158ka**: yellowish solid, 161 mg, 560 µmol; minor diastereomer **158kb**: yellow solid, 35.5 mg, 124 µmmol,).

158ka:

R$_f$ = 0.28 (hexanes/EtOAc 3:1); **mp** = 104 105 °C; **^{1}H-NMR** (300 MHz, $CDCl_3$) δ = 7.36 – 7.28 (m, 2H), 7.27 – 7.17 (m, 3H), 3.90 – 3.73 (m, 2H), 3.58 – 3.45 (m, 1H), 3.17 – 3.07 (m, 1H), 2.99 (dd, *J* = 13.6, 6.6 Hz, 1H), 2.69 – 2.48 (m, 2H), 1.56 (s, 9H); **^{13}C-NMR** (75 MHz, $CDCl_3$) δ = 177.1, 150.6, 143.2, 128.6, 126.7, 126.3, 83.1, 52.0, 44.0, 39.4, 37.6, 31.3, 28.1; **IR** (neat) ν [cm^{-1}] = 3063, 2978, 2000, 1777, 1740, 1710, 1476, 1364, 1289, 1252, 1148, 991, 749, 700; **HRMS**: (ESI-MS) m/z calc. for $[C_{17}H_{22}NO_3]^+$ [M+H$^+$] 288.1594, found 288.1598.

158kb:

R_f = 0.13 (hexanes/EtOAc 3:1); **mp** = 84 85 °C; **^{1}H-NMR** (300 MHz, $CDCl_3$) δ = 7.40 – 7.29 (m, 2H), 7.27 – 7.20 (m, 1H), 7.17 – 7.09 (m, 2H), 4.04 – 3.88 (m, 1H), 3.68 – 3.56 (m, 1H), 3.31 (dd, *J* = 12.0, 3.1 Hz, 1H), 3.27 – 3.12 (m, 2H), 3.00 – 2.86 (m, 1H), 2.66 – 2.56 (m, 1H), 1.43 (s, 9H); **^{13}C-NMR** (101 MHz, $CDCl_3$) δ = 176.8, 150.1, 139.3, 128.7, 128.6, 127.4, 126.7, 126.3, 82.7, 47.2, 39.5, 39.4, 32.4, 28.6, 28.0; **IR** (neat) ν [cm^{-1}] = 3063, 2978, 1774, 1740, 1714, 1476, 1367, 1293, 1256, 1148, 1028, 849, 752, 700; **HRMS**: (ESI-MS) m/z calc. for $[C_{17}H_{22}NO_3]^+$ $[M+H^+]$ 288.1594, found 288.1602.

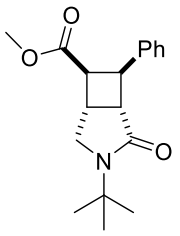

(±)-Methyl-3-(*tert*-butyl)-2-oxo-7-phenyl-3-azabicyclo[3.2.0]heptane-6-carboxylate (158l)

Compound **158l** was prepared from **153o** (305.8 mg, 1.02 mmol, 1.0 equiv.) and $Ir[(dtb\text{-}bpy)(dF(CF_3)ppy)_2]PF_6$ (11.3 mg, 0.010 mmol) in 7 h following general protocol **D**. After silica gel column chromatography (hexanes/EtOAc 2:1) a diastereomeric mixture of compound **158l** (206.2 mg, 684 µmol, 67%, *dr* 76:24) was obtained as yellow oil.

In the proton and carbon NMR, the signals of both diastereomers are overlapping. Characteristic signals of the minor diastereomer are marked.

R_f = 0.46 (hexanes/EtOAc 2:1); **^{1}H-NMR** (400 MHz, $CDCl_3$): δ = 7.37 – 7.27 (m, 2H), 7.24 – 7.15 (m, 3H), 4.00^{minor} (dd, *J* = 7.9, 5.1 Hz, 0.31H), 3.93 (dd, *J* = 8.8, 2.7 Hz, 1H), 3.76 (s, *J* = 3.0 Hz, 1H), 3.70 (dd, *J* = 11.1, 4.7 Hz, 1H), $3.65\text{-}3.58^{minor}$ (m, 0.64 H), 3.48 (p, *J* = 7.1 Hz, 2H), 3.39 (d, *J* = 10.5 Hz, 1H), 3.21 (s, 3H), 3.17 – 3.07 (m, 1H), 1.46 (s, 9H), 1.43^{minor} (s, 2.57 H); **^{13}C-NMR** (101 MHz, $CDCl_3$): major diastereomer: δ = 175.6, 171.8, 139.7, 128.3, 127.5, 127.0, 77.5, 77.3, 77.1, 76.6, 54.2, 51.3, 51.0, 48.4, 46.6, 45.7, 30.5, 27.7; minor diastereomer: δ = 175.4, 172.4, 142.2, 128.6, 126.8, 126.3, 77.5, 77.3, 77.1, 76.6, 54.1, 53.1, 51.9, 47.4, 46.8, 45.9, 45.0, 28.7, 27.6; **IR** (neat) ν[cm^{-1}] = 3064, 3030, 2974, 1729, 1669, 1405, 1364, 1222, 1196, 1166, 745, 700; **HRMS**: major diastereomer (acquisition time 2.501-2.551 min): (ESI-MS) calc. for $[C_{18}H_{24}NO_3]^+$ $[M+H]^+$ 302.1751, found 302.1760; minor diastereomer

(acquisition time 2.573-2.623 min): (ESI-MS) calc. for $[C_{18}H_{24}NO_3]^+$ $[M+H]^+$ 302.1751, found 302.1756.

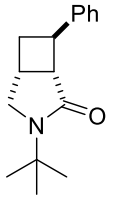

(±)-3-(*tert*-Butyl)-7-phenyl-3-azabicyclo[3.2.0]heptan-2-one (158m)

Compound **158m** was prepared from **153h** (243.1 mg, 998 µmol, 1.0 equiv.) and Ir[(dtb-bpy)(dF(CF_3)ppy)$_2$]PF_6 (11.4 mg, 0.010 mmol) in 23 h following general protocol **D**. After silica gel column chromatography (hexanes/EtOAc 3:1) compound **158m** (146.5 mg, 602 µmol, 60%) was obtained as yellowish solid.

R_f = 0.47 (hexanes/EtOAc 3:1); **mp** = 47 – 47.5 °C; **^{1}H-NMR** (300 MHz, $CDCl_3$) δ = 7.36 – 7.29 (m, 4H), 7.25 – 7.16 (m, 1H), 3.71 (dd, *J* = 10.1, 7.6 Hz, 1H), 3.67 – 3.58 (m, 1H), 3.43 (dd, *J* = 10.2, 1.2 Hz, 1H), 3.14 – 2.96 (m, 1H), 3.00 – 2.82 (m, 1H), 2.59 – 2.29 (m, 2H), 1.47 (s, 9H); **^{13}C-NMR** (75 MHz, $CDCl_3$) δ = 176.7, 144.8, 128.5, 126.4, 126.2, 54.0, 52.5, 50.0, 42.8, 33.6, 27.6, 26.8; **IR** (neat) ν [cm^{-1}] = 3026, 2967, 2922, 1654, 1408, 1364, 1297, 1230, 749, 697; **HRMS**: (APCI-MS) calc for $[C_{16}H_{21}NO]^+$ $[M+H]^+$ 244.1696, found 244.1702.

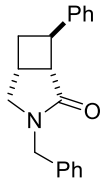

158na

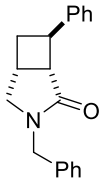

158nb

(±)-3-Benzyl-7-phenyl-3-azabicyclo[3.2.0]heptan-2-one (158n)

Compound **158na** was prepared from **153r** (299.3 mg, 1.08 mmol, 1.0 equiv.) and Ir[(dtb-bpy)(dF(CF_3)ppy)$_2$]PF_6 (11.9 mg, 0.010 mmol) in 19 h following general protocol **D**. After silica gel column chromatography (hexanes/EtOAc 2:1) the major diastereomer of compound **158na** (247.2 mg, 891 µmol, 83%) was obtained as yellowish solid.

R_f = 0.34 (hexanes/EtOAc 3:1); **mp** = 61.5 – 63 °C; **^{1}H-NMR** (300 MHz, $CDCl_3$) δ = 7.42 – 7.27 (m, 9H), 7.26 – 7.19 (m, 1H), 4.68 (d, *J* = 14.6 Hz, 1H), 4.43 (d, *J* = 14.6 Hz, 1H), 3.78 – 3.63 (m, 1H), 3.51 (dd, *J* = 10.3, 7.7 Hz, 1H), 3.27 – 3.14 (m, 2H), 3.08 – 2.93 (m, 1H), 2.57 – 2.44 (m, 1H), 2.40 – 2.26 (m, 1H); **^{13}C-NMR** (101 MHz, $CDCl_3$) δ = 176.1, 144.5, 136.6, 128.8, 128.6, 128.2, 127.7, 126.5, 126.4, 53.2, 48.5, 46.8, 42.8, 33.8, 27.4; **IR** (neat) ν [cm^{-1}] = 3080, 2981, 2940, 2855, 1669, 1602, 1490, 1446, 1326, 1274, 950, 752, 700; **HRMS**: major diastereomer (acquisition time 8.141-8.258 min): (APCI-MS) calc. for $[C_{19}H_{20}NO]^+$ $[M+H]^+$ 278.1539, found 278.1542; minor diastereomer (acquisition time 2.733-2.777 min): LRMS: (ESI-MS) calc. for $[C_{19}H_{20}NO]^+$ $[M+H]^+$ 278.1539, found 278.1546.

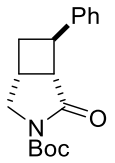

(±)-*tert*-Butyl-2-oxo-7-phenyl-3-azabicyclo[3.2.0]heptane-3-carboxylate (158o)

Compound **158o** was prepared from **153v** (293.9 mg, 1.02 mmol, 1.0 equiv.) and $Ir[(dtb\text{-}bpy)(dF(CF_3)ppy)_2]PF_6$ (11.4 mg, 0.010 mmol) in 14 d following general protocol **D**. By silica gel column chromatography (hexanes/EtOAc 5:1 → 4:1) compound **158o** was obtained as clear oil (138.1 mg, 481 µmol, 47%).

R_f = 0.43 (hexanes/EtOAc 4:1); **^{1}H-NMR** (400 MHz, $CDCl_3$) δ = 7.38 – 7.27 (m, 4H), 7.26 – 7.19 (m, 1H), 3.97 (dd, *J* = 11.5, 8.3 Hz, 1H), 3.83 – 3.70 (m, 2H), 3.25 – 3.17 (m, 1H), 3.04 – 2.92 (m, 1H), 2.63 – 2.52 (m, 1H), 2.51 – 2.39 (m, 1H), 1.57 (s, 9H). **^{13}C-NMR** (101 MHz, $CDCl_3$) δ = 175.8, 150.7, 143.6, 128.6, 126.6, 126.4, 83.0, 52.9, 49.7, 42.4, 33.2, 28.1, 25.8; IR (neat) [cm^{-1}] = 3373, 3060, 2978, 2937, 1774, 1740, 1710, 1476, 1304, 1285, 1148, 1062, 943, 849, 756, 697; **HRMS**: (ESI-MS) m/z calc. for $[C_{17}H_{25}N_2O_3]^+$ $[M+NH_4]^+$ 305.1860, found 305.1860; m/z calc. for $[C_{17}H_{21}NO_3Na]^+$ $[M+Na]^+$ 310.1414, found 310.1414; m/z calc. for $[C_{17}H_{22}NO_3]^+$ $[M+H]^+$ 288.1594, found 288.1594.

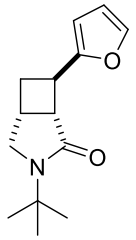

(±)-3-(*tert*-Butyl)-7-(furan-2-yl)-3-azabicyclo[3.2.0]heptan-2-one (158p)

Compound **158p** was prepared from **153k** (228.5 mg, 979 µmol, 1.0 equiv.) and Ir[(dtb-bpy)(dF(CF_3)ppy)$_2$]PF_6 (11.2 mg, 0.010 mmol) in 3 h following general protocol **D**. After silica gel column chromatography (hexanes/EtOAc 4:1) compound **158p** (167.7 mg, 719 µmol, 73%) was obtained as yellow oil.

R_f = 0.36 (hexanes/EtOAc 4:1); **^{1}H-NMR** (300 MHz, $CDCl_3$) δ = 7.34 (dd, *J* = 1.9, 0.9 Hz, 1H), 6.30 (dd, *J* = 3.2, 1.9 Hz, 1H), 6.08 (dt, *J* = 3.2, 0.8 Hz, 1H), 3.65 (dd, *J* = 10.2, 7.1 Hz, 1H), 3.62 – 3.53 (m, 1H), 3.36 (dt, *J* = 10.2, 1.0 Hz, 1H), 3.11 – 2.92 (m, 2H), 2.50 (dddd, *J* = 12.5, 8.5, 4.6, 2.7 Hz, 1H), 2.29 (ddd, *J* = 12.2, 9.0, 6.0 Hz, 1H), 1.45 (s, 9H); **^{13}C-NMR** (75 MHz, $CDCl_3$) δ = 176.0, 157.4, 141.4, 110.2, 104.7, 54.0, 52.2, 48.2, 36.2, 32.1, 27.6, 27.4; **IR** (neat) ν [cm^{-1}] = 3116, 2974, 1669, 1405, 1287, 1230, 730; **HRMS**: (APCI-MS) m/z calc. for $[C_{14}H_{20}NO_2]^+$ $[M+H]^+$ 234.1489, found 234.1496.

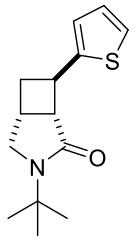

(±)-3-(*tert*-Butyl)-7-(thiophen-2-yl)-3-azabicyclo[3.2.0]heptan-2-one (158q)

Compound **158q** was prepared from **153l** (249.9 mg, 1.00 mmol, 1 equiv.) and Ir[(dtb-bpy)(dF(CF_3)ppy)$_2$]PF_6 (11.6 mg, 0.010 mmol) in 3 h following general protocol **D**. After silica gel column chromatography (hexanes/EtOAc 4:1) compound **158q** (195.5 mg, 782 µmol, 78%) was obtained as colorless oil.

R_f = 0.36 (hexanes/EtOAc 4:1); **^{1}H-NMR** (300 MHz, $CDCl_3$) δ = 7.16 (dd, *J* = 5.0, 1.3 Hz, 1H), 6.94 (dd, *J* = 5.0, 3.5 Hz, 1H), 6.92 – 6.89 (m, 1H), 3.87 – 3.77 (m, 1H), 3.66 (dd, *J* = 10.2,

7.2 Hz, 1H), 3.37 (dt, *J* = 10.2, 1.1 Hz, 1H), 3.11 – 2.96 (m, 2H), 2.51 – 2.40 (m, 2H), 1.46 (s, 9H); **^{13}C-NMR** (75 MHz, $CDCl_3$) δ = 175.8, 149.2, 126.9, 123.4, 123.3, 54.0, 52.1, 51.3, 38.5, 35.4, 27.6, 27.2; **IR** (neat) ν [cm^{-1}] = 3071, 2974, 2933, 1666, 1401, 1364, 1285, 1226, 693; **HRMS**: (APCI-MS) m/z calc. for $[C_{14}H_{20}NOS]^+$ $[M+H]^+$ 250.1260 found 250.1262.

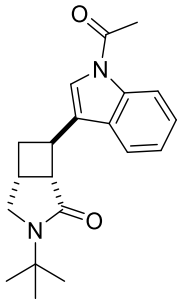

(±)-7-(1-Acetyl-1*H*-indol-3-yl)-3-(*tert*-butyl)-3-azabicyclo[3.2.0]heptan-2-one (158r)

Compound **158r** was prepared from **153m** (146.9 mg, 453 µmol, 1.0 equiv.) and $Ir[(dtb\text{-}bpy)(dF(CF_3)ppy)_2]PF_6$ (5.6 mg, 0.0045 mmol) in 48 h following general protocol **D**. After silica gel column chromatography (hexanes/EtOAc 1:1) compound **158r** (51.9 mg, 160 µmol, 35%) was obtained as yellowish solid.

R_f = 0.27 (hexanes/EtOAc 1:1); **mp** = 134 – 138 °C; **^{1}H-NMR** (300 MHz, $CDCl_3$) δ = 8.38 (bs, 1H), 7.74 – 7.68 (m, 1H), 7.39 – 7.22 (m, 3H), 3.83 – 3.64 (m, 2H), 3.45 (d, *J* = 10.2 Hz, 1H), 3.10 (d, *J* = 7.7 Hz, 1H), 3.01 – 2.84 (m, 1H), 2.62 (s, *J* = 5.7 Hz, 3H), 2.60 – 2.53 (m, 1H), 2.50 – 2.36 (m, 1H), 1.49 (s, 9H); **^{13}C-NMR** (75 MHz, $CDCl_3$) δ = 176.4, 168.4, 136.4, 129.6, 125.7, 125.5, 123.7, 120.5, 119.8, 116.5, 54.1, 52.5, 48.6, 34.6, 31.6, 27.7, 27.1, 24.1; **IR** (neat) ν [cm^{-1}] = 3112, 3049, 2959, 2937, 1699, 1666, 1453, 1379, 1300, 1252, 1215, 1017, 943, 752; **HRMS**: (ESI-MS) m/z calc. for $[C_{20}H_{25}N_2O_2]^+$ $[M+H]^+$ 325.1911, found 325.1915.

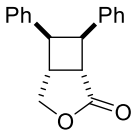

(±)-6,7-Diphenyl-3-oxabicyclo[3.2.0]heptan-2-one (158t)

Compound **158t** was prepared from **153w** (264.3 mg, 1.00 mmol, 1.0 equiv.) and Ir[(dtb-bpy)(dF(CF$_3$)ppy)$_2$]PF$_6$ (11.5 mg, 0.010 mmol) in 48 h at 80 °C following general protocol **D**. After silica gel column chromatography (hexanes/EtOAc 5:1) a diastereomeric mixture of compound **158t** (77.8 mg, 294 µmol, 29%, *dr* 72:28) was obtained as clear oil.

In the proton and carbon NMR the signals of both diastereomers are overlapping. Characteristic signals of the minor diastereomer are marked.

R$_f$ = 0.14 (hexanes/EtOAc 5:1); **^{1}H-NMR** (300 MHz, CDCl$_3$) δ = 7.43 – 7.31 (m, 2H), 7.23 – 7.02 (m, 6H), 7.01 – 6.93 (m, 2H), 6.89 – 6.81 (m, 2H), 4.57 (dd, *J* = 9.6, 6.1 Hz, 1H), 4.48 – 4.36 (m, 1H), 4.27^{minor} (dd, *J* = 10.3, 5.0 Hz, 0.39H), 4.21 – 4.05 (m, 2H), 3.77 – 3.64 (m, 1H), 3.60 – 3.48^{minor} (m, 0.46H), 3.48 – 3.40 (m, 1H), 3.36 – 3.28^{minor} (m, 0.41H); **^{13}C-NMR** (101 MHz, CDCl$_3$) δ = 179.4, 141.6, 138.4, 138.1, 128.9, 128.8, 128.2, 128.0, 127.9, 127.7, 127.19, 127.16, 127.1, 126.6, 126.5, 126.3, 72.7, 69.0, 48.1, 47.6, 46.7, 45.8, 42.5, 40.6, 38.9, 35.3; **IR** (neat) ν [cm^{-1}] = 3063, 3030, 2970, 2907, 1759, 1602, 1494, 1453, 1371, 1151, 1043, 1002, 976, 730, 697; **HRMS**: major diastereomer (acquisition time 10.1301-10.1501 min): (EIC-MS) calc. for [C$_{18}$H$_{16}$O$_2$]$^{+\bullet}$ [M]$^{+\bullet}$ 264.11448, found 264.11373; minor diastereomer (acquisition time 10.4099-10.4299 min): (ECI-MS) calc. for [C$_{18}$H$_{16}$O$_2$]$^{+\bullet}$ [M]$^{+\bullet}$ 264.11448, found 264.11304.

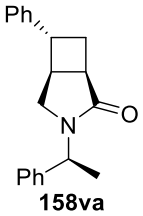

158va

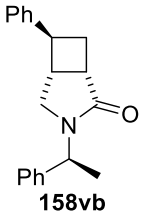

158vb

(1*R*,5*S*,6*R*)-6-Phenyl-3-((*S*)-1-phenylethyl)-3-azabicyclo[3.2.0]heptan-2-one (158va)
(1*S*,5*R*,6*S*)-6-Phenyl-3-((S)-1-phenylethyl)-3-azabicyclo[3.2.0]heptan-2-one (158vb)

Compound **158v** was prepared from **153x** (296.4 mg, 1.02 µmol, 1.0 equiv.) and Ir[(dtb-bpy)(dF(CF$_3$)ppy)$_2$]PF$_6$ (11.2 mg, 0.010 mmol) in 5 h following general protocol **D**. By silica gel column chromatography (hexanes/EtOAc 3:1) all four diastereomers of compound

158v were obtained in an overall yield of 83% (*dr* 43:43:7:7, major diastereomer **158va**: yellow oil, 98.6 mg, 338 µmol; major diastereomer **158vb**: white solid, 94.0 mg, 322 µmol).

158va:

R_f = 0.5 (hexanes/EtOAc 1:1); **^{1}H-NMR** (400 MHz, $CDCl_3$) δ = 7.39 – 7.25 (m, 7H), 7.25 – 7.19 (m, *J* = 7.9 Hz, 3H), 5.65 (q, *J* = 7.1 Hz, 1H), 3.42 (dd, *J* = 16.3, 8.6 Hz, 1H), 3.26 (d, *J* = 10.3 Hz, 1H), 3.13 (dd, *J* = 10.3, 6.5 Hz, 1H), 3.06 (t, *J* = 8.2 Hz, 1H), 2.95 (q, *J* = 6.9 Hz, 1H), 2.70 – 2.62 (m, 1H), 2.60 – 2.50 (m, 1H), 1.64 (d, *J* = 7.1 Hz, 3H); **^{13}C-NMR** (101 MHz, $CDCl_3$) δ = 176.3, 143.9, 139.8, 128.63, 128.61, 127.6, 127.4, 126.6, 126.3, 49.3, 48.2, 44.6, 38.7, 38.5, 31.6, 16.4; **IR** (neat) ν[cm^{-1}] = 3060, 3026, 2974, 2937, 2877, 1669, 1494, 1449, 1416, 1300, 1271, 1218, 1192, 1025, 902, 782, 749, 697; **HRMS**: (ESI-MS) m/z calc. for $[C_{20}H_{22}NO]^+$ $[M+H]^+$ 292.1696, found 292.1700; $[\alpha]_D^{20}$= – 167.4 (*c* 1, DCM); **chiral HPLC**: 98% *ee* (Phenomenex Lux Cellulose-2, 4.6 x 250 mm, heptane/*i*-PrOH = 80:20, 0.5 mL/min, t_R (***R*,*S*,*R*,*S***), (*S*,*R*,*S*,*R*) = **21.8**, 25.8 min).

158vb:

R_f = 0.3 (hexanes/EtOAc: 1/1); **mp** = 60.5 – 62 °C; **^{1}H-NMR** (300 MHz, $CDCl_3$): δ = 7.45 – 7.23 (m, 7H), 7.21 – 7.14 (m, 1H), 7.14 – 7.01 (m, 2H), 5.63 (q, *J* = 7.2 Hz, 1H), 3.52 (dd, *J* = 10.2, 6.4 Hz, 1H), 3.11 (dd, *J* = 15.9, 9.3 Hz, 2H), 2.97 (dd, *J* = 13.8, 7.0 Hz, 1H), 2.91 (d, *J* = 10.2 Hz, 1H), 2.68 – 2.48 (m, 2H), 1.57 (d, *J* = 7.1 Hz, 3H); **^{13}C-NMR** (101 MHz, $CDCl_3$): δ = 176.4, 143.8, 140.4, 128.7, 128.5, 127.6, 127.1, 126.5, 126.3, 49.0, 47.7, 44.0, 38.7, 38.5, 31.7, 15.7; **IR** (neat) ν[cm^{-1}] = 3082, 3022, 2967, 2933, 2881, 1666, 1494, 1446, 1304, 1215, 1118, 1066, 1025, 902, 786, 745, 697; **HRMS**: (ESI-MS) m/z calc. for $[C_{20}H_{22}NO]^+$ $[M+H]^+$ 292.1696, found 292.1698; $[\alpha]_D^{20}$ = 22.0 (*c* 1, DCM); **chiral HPLC**: 99% *ee* (Phenomenex Lux Cellulose-2, 4.6 x 250 mm, heptane/*i*-PrOH = 80:20, 0.5 mL/min, t_R (*R*,*S*,*R*,*R*), (***S*,*R*,*S*,*S***) = 19.2, **24.3** min).

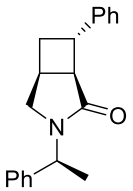

158wa

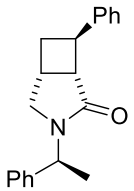

158wb

(1*R*,5*S*,7*S*)-7-Phenyl-3-((*S*)-1-phenylethyl)-3-azabicyclo[3.2.0]heptan-2-one (158wa)
(1*S*,5*R*,7*R*)-7-Phenyl-3-((*S*)-1-phenylethyl)-3-azabicyclo[3.2.0]heptan-2-one (158wb)

Compound **158w** was prepared from **153y** (290.5 mg, 997 µmol, 1 equiv.) and Ir[(dtb-bpy)(dF(CF$_3$)ppy)$_2$)]PF$_6$ (11.7 mg, 0.010 mmol) in 24 h following general protocol **D**. By purification via flash system (hexanes/EtOAc) all four diastereomers of compound **158w** were obtained in an overall yield of 76% (*dr* 94:6, major diastereomer **158wa**: white solid, 93.1 mg, 320 µmol; major diastereomer **158wb** (with minor diastereomer): white solid, 128.4 mg, 441 µmol).

158wa:

R$_f$ = 0.45 (hexanes/EtOAc 3:1); **mp** = 54 – 56 °C; **^{1}H-NMR** (400 MHz, $CDCl_3$) δ = 7.38 – 7.32 (m, 8H), 7.32 – 7.26 (m, 1H), 7.26 – 7.19 (m, 1H), 5.61 (q, *J* = 7.1 Hz, 1H), 3.68 (dt, *J* = 9.1, 4.6 Hz, 1H), 3.28 – 3.12 (m, 3H), 3.00 – 2.88 (m, 1H), 2.52 (dddd, *J* = 12.6, 8.8, 5.5, 2.1 Hz, 1H), 2.38 (ddd, *J* = 12.7, 9.1, 5.7 Hz, 1H), 1.63 (d, *J* = 7.1 Hz, 3H); **^{13}C-NMR** (101 MHz, $CDCl_3$) δ = 175.6, 144.5, 139.8, 128.56, 128.55, 127.5, 127.3, 126.4, 126.3, 49.2, 48.93, 48.87, 42.7, 33.8, 27.4, 16.3; **IR** (neat) ν[cm^{-1}] = 3190, 3060, 3030, 2978, 2937, 2877, 1669, 1490, 1449, 1416, 1349, 1285, 1215, 1185, 1025, 916, 846, 786, 752, 697; **HRMS**: (ESI-MS) m/z calc. for $[C_{20}H_{21}NO]^+$ $[M+H]^+$ 292.1696, found 292.1706; m/z calc. for $[C_{20}H_{21}NOK]^+$ $[M+K]^+$ 330.1255, found 330.1258; m/z calc. for $[C_{20}H_{21}NONa]^+$ $[M+Na]^+$ 314.1515, found 314.1520; $[\alpha]_D^{20}$ = −138.8 (*c* 1, $CHCl_3$); **chiral HPLC**: >99% *ee* (Phenomenex Lux Cellulose-2, 4.6 x 250 mm, heptane/*i*-PrOH = 90:10, 1 mL/min, t_R (***R*,*S*,*S*,*S***), (*S*,*R*,*R*,*R*) = **31.01**, 40.16 min).

158wb:

R$_f$ = 0.32 (hexanes/EtOAc 3:1); **mp** = 93 – 96.5 °C; **^{1}H-NMR** (400 MHz, $CDCl_3$) δ = 7.37 – 7.29 (m, 4H), 7.29 – 7.21 (m, 5H), 7.20 – 7.11 (m, 1H), 5.55 (q, *J* = 7.1 Hz, 1H), 3.61 – 3.53 (m, 1H), 3.48 (dd, *J* = 10.1, 7.6 Hz, 1H), 3.15 – 3.07 (m, 1H), 2.97 – 2.87 (m, 1H), 2.82 (d, *J* = 10.1 Hz, 1H), 2.37 – 2.26 (m, 1H), 2.13 – 2.01 (m, 1H), 1.51 (d, *J* = 7.1 Hz, 3H); **^{13}C-NMR** (101 MHz, $CDCl_3$) δ = 175.6, 144.6, 140.6, 128.65, 128.64, 128.57, 127.5, 127.0, 126.4, 126.3, 48.9, 48.5, 42.9, 33.4, 27.5, 15.7; **IR** (neat) ν[cm^{-1}] = 3058, 2970, 2937, 2881, 1658, 1490,

1449, 1349, 1297, 1241, 1181, 1025, 935, 782, 697; **HRMS**: (ESI-MS) m/z calc. for $[C_{20}H_{21}NO]^+$ $[M+H]^+$ 292.1696, found 292.1703; m/z calc. for $[C_{20}H_{21}NOK]^+$ $[M+K]^+$ 330.1255, found 330.1258; m/z calc. for $[C_{20}H_{21}NONa]^+$ $[M+Na]^+$ 314.1515, found 314.1521; $[\alpha]_D^{20}$= −194.6 (*c* 1, $CHCl_3$); **chiral HPLC**: >99% *ee* (Phenomenex Lux Cellulose-2, 4.6 x 250 mm, heptane/*i*-PrOH = 90:10, 1 mL/min, t_R (*R*,*S*,*S*,*R*), (***S*,*R*,*R*,*S***) = 32.15, **43.29** min).

Big Scale [2+2]-Photocycloaddition

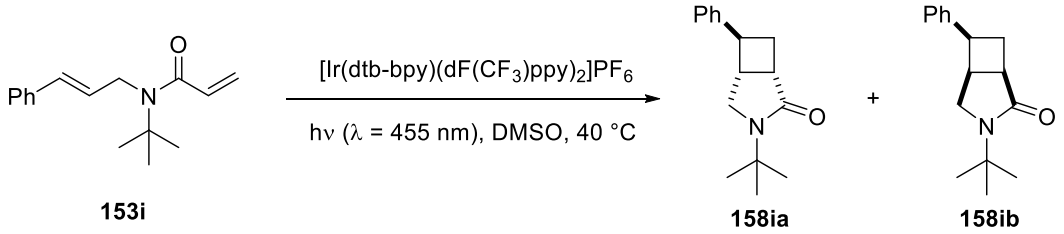

153i 158ia 158ib

Compound **153i** (26.8 g, 110 mmol, 1.0 equiv.) and $Ir[(dtb\text{-}bpy)(dF(CF_3)ppy)_2]PF_6$ (123 mg, 0.110 mmol, 0.1 mol%) were dissolved in DMSO (650 mL) in an immersion shaft exposure unit. After irradiation for 7 d, the solvent was removed under reduced pressure. The residue was dissolved in DEE (200 mL) and H_2O (100 mL). The phases were separated, and the aqueous phase was extracted with DEE (4x100 mL). Then the organic phases were washed with H_2O (100 mL) and brine (2x100 mL). After column chromatography, both diastereomers were obtained in an overall yield of 70% (major diastereomer **158ia**: 12.6 g, 52.0 mmol; minor diastereomer **158ib**: 5.45 g, 23.0 mmol).

Transformation of the azabicycloheptanones

General Procedure for the removal of the *tert*-butyl group E

The bicyclic compound was dissolved in an aqueous solution of HCl (25%) and was stirred for the reported time under reflux. Afterwards, the reaction mixture was extracted once with DEE. Then water was removed under reduced pressure to give the corresponding crude chloride salt of the free amino acid.

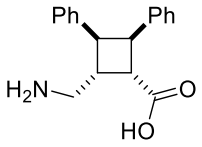

(±)-2-(Aminomethyl)-3,4-diphenylcyclobutane-1-carboxylic acid (198)

Compound **198** was prepared from **158g** (558.8 mg, 1.75 mmol, 1.0 equiv) in HCl (25%, 15 mL) after 5 d following general procedure **E**. After elution through an ion-exchange resin (protonated form, Dowex® 50WX8, 200-400 mesh) the diastereomeric mixture of compound **198** (212.5 mg, 753 µmol, 43%, *dr* 82:18) was obtained as white powder.

In the proton and carbon NMR the signals of both diastereomers are overlapping. Characteristic signals of the minor diastereomer are marked.

mp = 119 – 124 °C; **^{1}H-NMR** (300 MHz, MeOD) δ = 7.47 – 6.86 (m, 10H), 4.42 - 4.23 (m, 1H), 4.15 – 3.78 (m, 2H), 3.74 – 3.61^{minor} (m, 0.19H), 3.56 – 3.19 (m, 3H); **^{13}C-NMR** (75 MHz, MeOD) δ = 176.5, 175.2, 139.9, 139.83, 139.78, 139.6, 130.0, 129.6, 129.3, 129.2, 129.12, 129.09, 129.05, 129.0, 127.54, 127.50, 127.4, 127.3, 47.4, 47.3, 46.3 (2xCH), 43.1, 42.9, 42.2, 41.9, 38.3, 38.2; **IR** (neat) ν [cm^{-1}] = 3056, 3026, 2926, 2363, 1558, 1494, 1453, 1394, 1191, 1073, 913, 846, 745, 697; **HRMS**: major diastereomer (retention time 1.720-1.770 min): (ESI-MS) m/z calc. for $[C_{18}H_{20}NO_2]^+$ $[M+H]^+$ 282.1489 found 282.1493; minor diastereomer (retention time 1.637-1.692 min): (ESI-MS) m/z calc. for $[C_{18}H_{20}NO_2]^+$ $[M+H]^+$ 282.1489 found 282.1493.

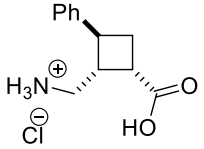

(±)-2-(Aminomethyl)-3-phenylcyclobutane-1-carboxylic acid (200)

Compound **200** was prepared from **158ia** (1.10 g, 4.52 mmol, 1.0 equiv) in HCl (25%, 50 mL) after 5 d following the general procedure **E**. After recrystallization from $CHCl_3$ compound **200** (930 mg, 3.86 mmol, 85%) was obtained as beige powder.

Mp = 204.5 – 206 °C; **^{1}H-NMR** (300 MHz, MeOD) δ = 7.37 – 7.28 (m, 4H), 7.27 – 7.18 (m, 1H), 3.51 – 3.32 (m, 2H), 3.30 – 3.22 (m, 1H), 3.10 – 2.93 (m, 2H), 2.65 (ddd, *J* = 12.2, 9.2,

3.3 Hz, 1H), 2.37 (dt, *J* = 11.6, 9.3 Hz, 1H); **^{13}C-NMR** (75 MHz, MeOD) δ = 177.1, 143.7, 129.8, 128.0, 127.8, 43.40, 43.38, 41.7, 38.5, 30.2; **IR** (neat) ν [cm^{-1}] = 3194, 3026, 2978, 2914, 2780, 2598, 2527, 2460, 1688, 1584, 1498, 1453, 1394, 1222, 1159, 872, 756, 700; **HRMS**: (ESI-MS) m/z calc. for $[C_{12}H_{15}NNaO_2]^+$ $[M+Na]^+$ 228.0995 found 228.0994.

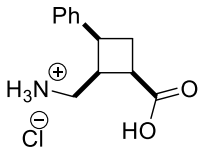

(±)-2-(Aminomethyl)-3-phenylcyclobutane-1-carboxylic acid (201)

Compound **201** was prepared from **158ib** (797.3 mg, 3.28 mmol, 1.0 equiv) in HCl (25%, 40 mL) after 6 d following the general procedure **E**. After cooling to rt, a white powder precipitated which was subsequently filtered. Compound **201** (462.2 mg, 1.91 mmol, 58%) was obtained as white powder.

mp = 209 – 210 °C; **^{1}H-NMR** (300 MHz, MeOD) δ = 7.40 – 7.30 (m, 2H), 7.29 – 7.18 (m, 3H), 3.88 (dt, *J* = 10.6, 8.3 Hz, 1H), 3.62 (ddd, *J* = 10.4, 9.1, 7.4 Hz, 1H), 3.19 – 2.97 (m, 2H), 2.83 (q, *J* = 10.9 Hz, 1H), 2.60 (dtd, *J* = 11.3, 9.0, 2.6 Hz, 1H), 2.47 (d, *J* = 10.4 Hz, 1H); **^{13}C-NMR** (75 MHz, MeOD) δ = 178.27, 139.29, 129.81, 128.80, 128.13, 41.05, 39.80, 38.85, 38.26, 28.61; **IR** (neat) ν [cm^{-1}] = 3022, 2974, 1725, 1572, 1505, 1453, 1408, 1244, 1215, 1181, 1080, 916, 875, 816, 749, 700; **HRMS**: (ESI-MS) m/z calc. for $[C_{12}H_{15}NO_2]^+$ $[M+H]^+$ 206.1176 found 206.1178.

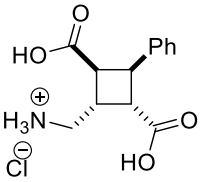

(±)-2-(Aminomethyl)-4-phenylcyclobutane-1,3-dicarboxylic acid (203)

Compound **203** was prepared from **158l** (358.5 mg, 1.19 mmol, 1.0 equiv) in HCl (25%, 15 mL) after 5 d following general procedure **E**. The diastereomeric mixture of compound **203** (240.7 mg, 844 µmol, 71%, *dr* 72:28) was obtained as beige powder and was not further purified.

In the proton and carbon NMR the signals of both diastereomers are overlapping. Characteristic signals of the minor diastereomer are marked.

mp = 196 – 199 °C; **^{1}H-NMR** (400 MHz, MeOD) δ = 7.41 – 7.32^{minor} (m, 0.4H), 7.32 – 7.18 (m, 5H), 4.30 – 4.18 (m, 1H), 4.07^{minor} (t, *J* = 10.4 Hz, 0.13H), 3.84 (t, *J* = 8.5 Hz, 1H), 3.56^{minor} (t, *J* = 9.4 Hz, 0.20H), 3.50 – 3.42 (m, 1H), 3.42 – 3.27 (m, 3H), 3.21 (dd, *J* = 11.3, 8.0 Hz, 1H); **^{13}C-NMR** (101 MHz, MeOD) δ = 174.3, 173.5, 140.6^{minor}, 138.4, 128.1^{minor}, 128.0, 127.2, 126.8, 126.5^{minor}, 45.4, 42.6, 42.3, 40.1, 34.0; **HRMS**: major diastereomer (retention time 0.855-0.910 min): (ESI-MS) m/z calc. for $[C_{13}H_{15}NO_4]^+$ $[M+H]^+$ 250.1074 found 250.1079; minor diastereomer (retention time 1.054-1.110 min): (ESI-MS) m/z calc. for $[C_{13}H_{15}NO_4]^+$ $[M+H]^+$ 250.1074 found 250.1078.

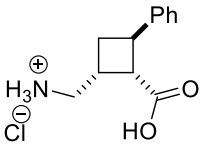

(±)-2-(Aminomethyl)-4-phenylcyclobutane-1-carboxylic acid (202)

Compound **202** was prepared from **158m** (221.9 mg, 912 µmol, 1.0 equiv.) in HCl (25%, 12 mL) after 6 d following the general procedure **E**. The crude product was dissolved in a small amount of MeOH and pure product was then precipitated in cold DEE. Compound **202** (212.2 mg, 880 µmol, 96%) was obtained as beige powder.

mp = 213 – 217 °C; **^{1}H-NMR** (400 MHz, MeOD) δ = 7.30 (dd, *J* = 10.3, 2.8 Hz, 4H), 7.25 – 7.15 (m, 1H), 3.91 (q, *J* = 9.5 Hz, 1H), 3.54 (t, *J* = 9.4 Hz, 1H), 3.41 (dd, *J* = 12.8, 7.5 Hz, 1H), 3.22 (dd, *J* = 12.8, 8.5 Hz, 1H), 2.86 (pd, *J* = 8.2, 2.7 Hz, 1H), 2.39 (dt, *J* = 11.8, 9.2 Hz, 1H), 2.21 (ddd, *J* = 12.2, 9.6, 3.0 Hz, 1H); **^{13}C-NMR** (101 MHz, MeOD) δ = 174.8, 142.7, 128.1, 126.3, 126.1, 46.2, 40.8, 40.1, 31.2, 28.2; **IR** (neat) ν [cm^{-1}] = 3131, 3037, 2948, 2586, 1703, 1553, 1494, 1408, 1237, 1181, 823, 752, 704; **HRMS**: (ESI-MS) m/z calc. for $[C_{12}H_{15}NO_2]^+$ $[M+H]^+$ 206.1176 found 206.1179.

General procedure for the Boc-protection of the unsubstituted azabicycloheptanones F

Under nitrogen atmosphere, unsubstituted azabicycloheptanone **158u** (1 equiv.) was dissolved in dry MeCN (10 mL) and the solution was cooled to 0 °C by an ice-bath. Then NEt_3 (1 equiv.), Boc_2O (2 equiv.) and DMAP (0.1 mmol, 0.1 equiv.) were subsequently added. The reaction mixture was stirred in defrosting ice-bath for 2 d. The solvent was removed under reduced pressure giving rise to compound **158ka**.

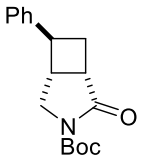

(±)-*tert*-Butyl-2-oxo-6-phenyl-3-azabicyclo[3.2.0]heptane-3-carboxylate ((±)-158ka)

Compound **(±)-158ka** was synthesized from compound **(±)-158u** (189.8 mg, 1.01 mmol, 1.0 equiv.), NEt_3 (102.6 mg, 140 µL, 1.01 mmol, 1.0 equiv.), Boc_2O (442.5 mg, 2.03 mmol, 2.0 equiv.) and DMAP (12.4 mg, 0.1 mmol, 0.10 equiv.) following the general procedure **F**. Compound **(±)-158ka**(291.3 mg, 1.01 mmol, quant.) was obtained as yellow solid.

Spectral data are in accordance with compound **(±)-158ka** (see page 138).

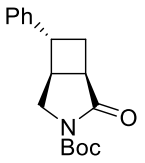

***tert*-Butyl (1*R*,5*S*,6*R*)-2-oxo-6-phenyl-3-azabicyclo[3.2.0]heptane-3-carboxylate ((1*R*,5*S*,6*R*)-158ka)**

Compound **(1*R*,5*S*,6*R*)-158ka** was synthesized from compound **(1*R*,5*S*,6*R*)-158u** (112.4 mg, 0.60 mmol, 1.0 equiv.), NEt_3 (60.7 mg, 85 µL, 0.60 mmol, 1.0 equiv.), Boc_2O (261.9 mg, 1.2 mmol, 2.0 equiv.) and DMAP (7.4 mg, 0.060 mmol, 0.10 equiv.) following the general procedure **F**. After silica gel column chromatography (hexanes/EtOAc 4:1) compound **(1*R*,5*S*,6*R*)-158ka** (151.2 mg, 0.53 mmol, 88%) was obtained.

Spectral data are in accordance with compound **(±)-158ka**.

mp = 94 95 °C; **HRMS**: (ESI-MS) m/z calc. for $[C_{17}H_{22}NO]^+$ $[M+H]^+$ 288.1594, found 288.1597; m/z calc. for $[C_{17}H_{21}NONa]^+$ $[M+Na]^+$ 310.1414, found 310.1418; m/z calc. for $[C_{17}H_{21}NONH_4]^+$ $[M+NH_4]^+$ 305.1860, found 305.1863; $[\alpha]_D^{20}$= – 138.8 (*c* 1, DCM); **chiral HPLC**: >99% *ee* (Phenomenex Lux Cellulose-2, 4.6 x 250 mm, heptane/*i*-PrOH = 70:30, 0.5 mL/min, t_R (*S,R,S*), (***R,S,R***) = 13.4, **18.3** min).

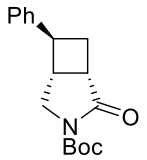

***tert*-Butyl (1*S*,5*R*,6*S*)-2-oxo-6-phenyl-3-azabicyclo[3.2.0]heptane-3-carboxylate ((1*S*,5*R*,6*S*)-158ka)**

Compound **(1*S*,5*R*,6*S*)-158ka** was synthesized from compound **(1*S*,5*R*,6*S*)-158u** (112.4 mg, 0.60 mmol, 1.0 equiv.), NEt_3 (60.7 mg, 85 µL, 0.60 mmol, 1.0 equiv.), Boc_2O (261.9 mg, 1.2 mmol, 2.0 equiv.) and DMAP (7.4 mg, 0.060 mmol, 0.10 equiv.) following the general procedure **F**. After silica gel column chromatography (hexanes/EtOAc 4:1) compound **(1*S*,5*R*,6*S*)-158ka** (148 mg, 0.52 mmol, 87%) was obtained.

Spectral data are in accordance with compound **(±)-158ka**.

mp = 99 °C; **HRMS**: (ESI-MS) m/z calc. for $[C_{17}H_{22}NO]^+$ $[M+H]^+$ 288.1594, found 288.1598; m/z calc. for $[C_{17}H_{21}NONa]^+$ $[M+Na]^+$ 310.1414, found 310.1419; m/z calc. for $[C_{17}H_{21}NONH_4]^+$ $[M+NH_4]^+$ 305.1860, found 305.1863; $[\alpha]_D^{20}$= 146.7 (*c* 1, DCM); **chiral HPLC**: 98% *ee* (Phenomenex Lux Cellulose-2, 4.6 x 250 mm, heptane/*i*-PrOH = 70:30, 0.5 mL/min, t_R (***S,R,S***), (*R,S,R*) = **11.8**, 15.5 min).

Lactam ring opening of the Boc-protected bicyclic compounds

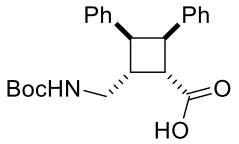

(±)-2-(((*tert*-Butoxycarbonyl)amino)methyl)-3,4-diphenylcyclobutane-1-carboxylic acid (225)

Compound **158ha** (709.7 mg, 1.95 mmol, 1.0 equiv.) was dissolved in a mixture of H_2O/THF (1:1, 0.1M, 44 mL). After addition of LiOH (473.8 mg, 19.8 mmol, 10 equiv.) the reaction mixture was stirred at rt for 2 d. The solvent was removed under reduced pressure, the residue was again dissolved in EtOAc and water was added. After phase separation, the aqueous phase was brought to a pH of 1 with aq. HCl (2 M) and extracted with EtOAc (3x). The combined organic phases were dried over $MgSO_4$, filtered and the solvent was removed under reduced pressure. After purification by silica gel column chromatography (DCM/MeOH 95:5) compound **225** (557.6 mg, 1.46 mmol, 75%, *dr* 88:12) was obtained as white solid.

In the proton and carbon NMR, the signals of both diastereomers are overlapping. Characteristic signals of the minor diastereomer are marked.

R_f = 0.36 (DCM/MeOH 95:5); **mp** = 61 63 °C; **^{1}H-NMR** (300 MHz, $CDCl_3$) δ = 7.48 – 7.27 (m, 2H), 7.16 – 6.98 (m, 5H), 6.98 – 6.88 (m, 3H), 4.95 (bs, 0.5H, NH), 4.40 – 4.23 (m, 1H), 3.92 – 3.64 (m, 2H), 3.63 – 3.26 (m, 3H), 1.43 (s, 9H), 1.35minor (s, 1.19H); **^{13}C-NMR** (75 MHz, MeOD) δ = 176.8, 158.5, 143.6, 141.6, 140.8, 129.7, 129.5, 129.3, 129.1, 129.0, 128.88, 128.85, 127.9, 127.7, 127.6, 127.0, 126.9, 80.1, 47.7, 45.2, 43.6, 43.0, 40.6, 28.8; **IR** (neat) ν [cm^{-1}] = 3313, 3083, 3026, 2974, 2933, 1699, 1493, 1449, 1416, 1307, 1248, 1109, 1080, 969, 909, 853, 749, 697; **HRMS**: major diastereomer (retention time 2.939-2.989 min): (ESI-MS) m/z calc. for $[C_{23}H_{28}NO_4]^+$ $[M+H]^+$ 382.2013 found 382.2015, m/z calc. for $[C_{23}H_{27}NO_4Na]^+$ $[M+Na]^+$ 404.1832 found 404.1836, m/z calc. for $[C_{23}H_{27}NO_4K]^+$ $[M+K]^+$ 420.1572 found 420.1558; minor diastereomer (retention time 3.072-3.121 min): (ESI-MS) m/z calc. for $[C_{23}H_{27}NO_4Na]^+$ $[M+Na]^+$ 404.1832 found 404.1834, m/z calc. for $[C_{23}H_{27}NO_4K]^+$ $[M+K]^+$ 420.1572 found 420.1569.

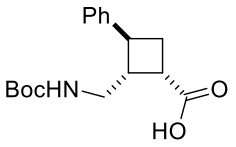

(±)-*trans*-2-(((*tert*-Butoxycarbonyl)amino)methyl)-3-phenylcyclobutane-1-carboxylic acid ((±)-226)

Method 1:

Compound **200** (240 mg, 995 µmol, 1.0 equiv.) was dissolved in a H_2O/dioxane mixture (1:1, 5 mL), $NaHCO_3$ (420 mg, 5.00 mmol, 5.0 equiv.) was added and the reaction mixture was cooled to 0 °C. Then a solution of Boc_2O (327 mg, 1.50 mmol, 1.5 equiv.) in dioxane (5 mL) was added dropwise. The reaction mixture was stirred for 2 d at rt. H_2O (10 mL) was added and the aqueous phase was extracted twice with EtOAc (each 15 mL). The combined organic phases were washed twice with $NaHCO_3$ (each 15 mL). Then the aqueous phase was brought to a pH of 1 with aq. HCl (5%) and again extracted with EtOAc (3x20 mL). The combined organic phases were dried over Na_2SO_4, filtered and the solvent was removed under reduced pressure. After silica gel column chromatography (DCM/MeOH 95:5) compound **(±)-226** (293 mg, 959 µmol, 96%) was obtained as white solid.

Method 2:

Compound **158ka** (4.31 g, 15.0 mmol, 1.0 equiv.) was dissolved in a mixture of H_2O/THF (1:1, 0.1M, 150 mL). After addition of LiOH (1.79 g, 75.0 mmol, 5.0 equiv.) the reaction mixture was stirred at rt for 2 d. The solvent was removed under reduced pressure, the residue was again dissolved in EtOAc and water was added. After phase separation, the aqueous phase was brought to a pH of 1 with aq. HCl (2 M) and extracted with EtOAc (3x). The combined organic phases were dried over $MgSO_4$, filtered and the solvent was removed under reduced pressure. After recrystallization from $CHCl_3$ compound **(±)-226** (3.88 g, 12.7 mmol, 85%) was obtained as white solid.

R_f = 0.27 (DCM/MeOH 95:5); **mp** = 112 114 °C; **^{1}H-NMR** (400 MHz, $CDCl_3$) δ = 10.89 (bs, 1H), 7.31 (t, *J* = 7.5 Hz, 2H), 7.22 (dd, *J* = 14.7, 7.2 Hz, 3H), 4.90 (bs, 1H), 3.49 (dd, *J* = 18.5, 8.9 Hz, 2H), 3.29 (t, *J* = 7.5 Hz, 2H), 2.98 (dt, *J* = 16.2, 8.3 Hz, 1H), 2.69 (ddd, *J* = 11.7, 9.2, 2.9 Hz, 1H), 2.24 (dd, *J* = 20.4, 9.4 Hz, 1H), 1.41 (s, 9H); **^{13}C-NMR** (101 MHz, $CDCl_3$) δ = 179.2, 156.1, 143.3, 128.5, 126.6, 126.5, 79.6, 45.3, 42.1, 42.0, 38.1, 28.4; **IR** (neat) ν [cm^{-1}] = 3380, 3060, 3030, 2978, 2940, 2713, 2519, 1714, 1654, 1543, 1442, 1364, 1289, 1252, 1162,

991, 816, 861, 894, 745; **HRMS**: (ESI-MS) m/z calc. for $[C_{17}H_{24}NO_4]^+$ $[M+H]^+$ 306.1700 found 306.1698.

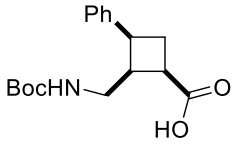

(±)-*cis*-2-(((*tert*-Butoxycarbonyl)amino)methyl)-3-phenylcyclobutane-1-carboxylic acid (227)

Compound **158kb** (862.1 mg, 3.00 mmol, 1.0 equiv.) was dissolved in a mixture of H_2O/THF (1:1, 0.1 M, 30 mL). After addition of LiOH (359.2 mg, 15.0 mmol, 5.0 equiv.) the reaction mixture was stirred at rt for 2 d. The solvent was removed under reduced pressure, the residue was again dissolved in EtOAc and water was added. After phase separation the aqueous phase was brought to a pH of 1 with aq. HCl (2 M) and extracted with EtOAc (3x). The combined organic phases were dried over $MgSO_4$, filtered and the solvent was removed under reduced pressure. After recrystallization from $CHCl_3$ compound **227** (814.5 mg, 2.67 mmol, 89%) was obtained as white solid.

R_f = 0.45 (DCM/MeOH 95:5); **mp** = 133 134 °C; **^{1}H-NMR** (300 MHz, MeOD) δ = 7.37 – 7.14 (m, 5H), 3.75 (dt, *J* = 10.9, 8.3 Hz, 1H), 3.40 – 3.31 (m, 1H, overlapping with solvent signal), 3.19 – 2.74 (m, 4H), 2.30 (dtd, *J* = 11.0, 8.0, 2.9 Hz, 1H), 1.32 (s, 9H); **^{13}C-NMR** (101 MHz, MeOD) δ = 175.3, 156.3, 139.3, 128.0, 127.5, 1262, 78.6, 42.2, 38.0, 37.7, 36.3, 27.3, 25.0; **IR** (neat) ν [cm^{-1}] = 3388, 3034, 2981, 2952, 2855, 2680, 2553, 1684, 1513, 1435, 1394, 1328, 1237, 1174, 1083, 995, 868, 745, 700; **HRMS**: (-ESI-MS) m/z calc. for $[C_{17}H_{23}NO_4]^-$ $[M-H]^-$ 304.1554 found 304.1564, m/z calc. for $[C_{17}H_{23}NO_4Cl]^-$ $[M+Cl]^-$ 304.1321 found 304.1324.

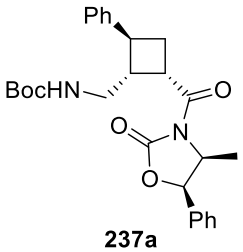

237a

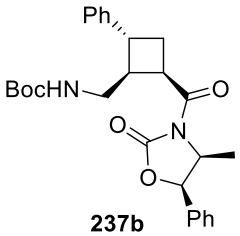

237b

***tert*-Butyl(((1*R*,2*S*,4*S*)-2-((4*S*,5*R*)-4-methyl-2-oxo-5-phenyloxazolidine-3-carbonyl)-4-phenylcyclobutyl)methyl)carbamate (237a)**
***tert*-Butyl(((1*S*,2*R*,4*R*)-2-((4*S*,5*R*)-4-methyl-2-oxo-5-phenyloxazolidine-3-carbonyl)-4-phenylcyclobutyl)methyl)carbamate (237b)**

Compound **(±)-226** (1.78 g, 5.82 mmol, 1.0 equiv.) was dissolved together with triethylamine (730 mg, 7.20 mmol, 1.2 equiv.) in dry THF (50 mL) and cooled to -78 °C. Then pivaloyl chloride (702 mg, 5.82 mmol, 1.0 equiv.) was added dropwise and the reaction mixture was stirred for 1 h at 0 °C. Meanwhile, (4*S*,5*R*)-4-methyl-5-phenyloxazolidin-2-one (1.03 g, 5.82 mmol, 1.0 equiv.) was dissolved in dry THF (35 mL), cooled to -40 °C, *n*-BuLi (2.7M in toluene, 2.16 mL, 5.82 mmol, 1.0 equiv.) was added dropwise and this reaction mixture was stirred for 5 min at -40 °C. The resulting solution was added by rapid cannulation to the cooled solution of the mixed anhydride. The reaction mixture was stirred for 1 h at -78 °C. After warming to 0 °C, the mixture was treated with saturated $NaHCO_3$ (50 mL), and the solvent was removed under reduced pressure. The aqueous phase was extracted with DCM (4x50 mL). The combined organic phases were washed once with sat. $NaHCO_3$ (20 mL) and once with brine (20 mL), dried over $MgSO_4$, filtered and the solvent was removed under reduced pressure. After purification by using the flash system (hexanes/acetone) both diastereomers **237** were obtained as white solids in an overall yield of 85% (**237a**: 1.15 g, 2.46 mmol, 42%; **237b**: 1.05 g, 2.26 mmol, 39%).

237a:

R_f = 0.36 (hexanes/acetone 4:1); **mp** = 129 – 130 °C; **^{1}H-NMR** (400 MHz, $CDCl_3$) δ = 7.45 – 7.19 (m, 10H), 5.77 (d, *J* = 7.4 Hz, 1H), 4.85 (p, *J* = 6.6 Hz, 1H), 4.63 – 4.46 (m, 2H), 3.52 – 3.24 (m, 3H), 3.09 – 2.96 (m, 1H), 2.90 – 2.77 (m, 1H), 2.25 (dt, *J* = 11.7, 8.7 Hz, 1H), 1.40 (s, 9H), 0.92 (d, *J* = 6.6 Hz, 3H); **^{13}C-NMR** (101 MHz, $CDCl_3$) δ = 173.4, 155.9, 153.2, 143.6, 133.6, 128.7, 128.6, 126.7, 126.6, 126.3, 125.7, 79.4, 79.0, 54.9, 45.5, 41.7, 41.2, 37.5, 28.4, 27.5, 14.8; **IR** (neat) ν [cm^{-1}] = 3406, 3328, 3030, 2981, 2933, 2855, 1774, 1692, 1602, 1524, 1453, 1364, 1241, 1196, 1148, 1121, 1088, 1062, 984, 946, 868, 764, 723, 700; **HRMS**: (ESI-

MS) m/z calc. for $[C_{27}H_{33}N_2O_5]^+$ $[M+H]^+$ 465.2384 found 465.2385; m/z calc. for $[C_{27}H_{32}N_2O_5Na]^+$ $[M+Na]^+$ 487.2203 found 487.2208.

237b:

R_f = 0.30 (hexanes/acetone 4:1); **mp** = 121 – 122 °C; **^{1}H-NMR** (300 MHz, $CDCl_3$) δ = 7.49 – 7.17 (m, 10H), 5.69 (d, *J* = 7.2 Hz, 1H), 4.82 (p, *J* = 6.7 Hz, 1H), 4.65 (bs, 1H), 4.34 (td, *J* = 8.6, 4.6 Hz, 1H), 3.44 (dd, *J* = 17.3, 8.9 Hz, 1H), 3.36 – 3.04 (m, 3H), 2.98 – 2.80 (m, 1H), 2.23 (dt, *J* = 11.7, 8.6 Hz, 1H), 1.39 (s, 9H), 0.97 (d, *J* = 6.6 Hz, 3H); **^{13}C-NMR** (101 MHz, $CDCl_3$) δ = 173.2, 155.7, 153.3, 143.8, 133.2, 128.9, 128.8, 128.6, 126.7, 126.5, 125.7, 79.3, 79.1, 55.2, 45.2, 42.1, 41.3, 37.6, 28.4, 27.1, 14.5; **IR** (neat) ν [cm^{-1}] = 3414, 3063, 3030, 2974, 2922, 1770, 1714, 1684, 1513, 1453, 1386, 1345, 1248, 1148, 1118, 1039, 976, 924, 887, 767, 693; **HRMS**: (ESI-MS) m/z calc. for $[C_{27}H_{32}N_2O_5K]^+$ $[M+K]^+$ 503.1943 found 503.1947; m/z calc. for $[C_{27}H_{32}N_2O_5Na]^+$ $[M+Na]^+$ 487.2203 found 487.2209.

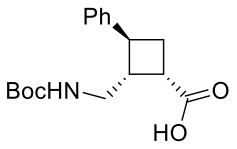

(1*S*,2*R*,3*S*)-2-(((*tert*-Butoxycarbonyl)amino)methyl)-3-phenylcyclobutane-1-carboxylic acid ((1*S*,2*R*,3*S*)-226)

Method 1:

To an ice-cooled solution of compound **237a** (911.6 mg, 1.96 mmol, 1.0 equiv.) in a mixture of H_2O/THF (4:1, 0.05 M, 40 mL) H_2O_2 (30 wt%, 1.2 mL, 6.0 equiv.) was added. The resulting mixture was stirred for 5 min and an aqueous solution of LiOH (0.3M, 13 mL, 94 mg, 3.92 mmol, 2.0 equiv.) was added. The reaction mixture was stirred for 5 h at rt. Afterwards, it was quenched with Na_2SO_3 (1 M, 15 mL) and $NaHCO_3$ (sat., 15 mL). The solvent was removed under reduced pressure. The aqueous residue was washed with DCM (4x15 mL) in order to recover the chiral auxiliary (almost quantitatively). Then the aqueous phase was acidified to a pH of 1 with aq. HCl (conc.) and extracted with DCM (4x20 mL). The combined organic phases were dried over $MgSO_4$, filtered and the solvent was removed under reduced pressure to give the compound **(1*S*,2*R*,3*S*)-226** (379.9 mg, 1.24 mmol, 63%) as white solid.

Method 2:

Compound **(1*S*,2*R*,3*S*)-158ka** (134.3 mg, 467 µmol, 1.0 equiv.) was dissolved in a mixture of H_2O/THF (1:1, 0.1M, 5 mL). After addition of LiOH (111.9 mg, 4.67 mmol, 10 equiv.) the reaction mixture was stirred at rt for 22 h. Then the solvent was removed under reduced pressure, the residue was again dissolved in EtOAc and water was added. After phase separation, the aqueous phase was brought to a pH of 1 with aq. HCl (2M) and extracted with EtOAc (3x). The combined organic phases were dried over $MgSO_4$, filtered and the solvent was removed under reduced pressure. After purification via flash system (DCM/MeOH) compound **(1*S*,2*R*,3*S*)-226** (142.7 mg, 467 µmol, quant.) was obtained as a white solid.

The spectral data are in accordance with the racemic compound **(±)-226**.

mp = 112 – 113 °C; $[\alpha]_D^{20}$ = 32.5 (*c* 1, CH_2Cl_2); **chiral HPLC**: >99% *ee* (Phenomenex Lux Cellulose-1, 4.6 x 250 mm, heptane/*i*-PrOH = 90:10, 1.0 mL/min, t_R (***S,R,S***), (*R,S,R*) = **6.43**, 8.78 min).

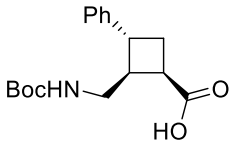

(1*R*,2*S*,3*R*)-2-(((*tert*-Butoxycarbonyl)amino)methyl)-3-phenylcyclobutane-1-carboxylic acid ((1*R*,2*S*,3*R*)-226)

Method 1:

To an ice-cooled solution of compound **237b** (715.6 mg, 1.54 mmol, 1.0 equiv.) in a mixture of H_2O/THF (4:1, 0.05M, 30 mL) H_2O_2 (30 wt%, 944 µL, 6 equiv.) was added. The resulting mixture was stirred for 5 min and then an aqueous solution of LiOH (0.3M, 10 mL, 74 mg, 3.08 mmol, 2.0 equiv.) was added. The reaction mixture was stirred for 5 h at rt. Afterwards, it was quenched with Na_2SO_3 (1M, 15 mL) and $NaHCO_3$ (sat., 15 mL). The solvent was removed under reduced pressure. The aqueous residue was washed with DCM (4x15 mL) in order to recover the chiral auxiliary (almost quantitatively). Then the aqueous phase was acidified to a pH of 1 with aq. HCl (conc.) and extracted with DCM (4x20 mL). The combined organic phases were dried over $MgSO_4$, filtered and the solvent was removed under reduced pressure to give compound **(1*R*,2*S*,3*R*)-226** (380.8 mg, 1.25 mmol, 81%) as white solid.

Method 2:

Compound **(1*R*,2*S*,3*R*)-158ka** (129 mg, 449 µmol, 1.0 equiv.) was dissolved in a mixture of H_2O/THF (1:1, 0.1M, 5 mL). After addition of LiOH (108 mg, 4.49 mmol, 10 equiv.) the reaction mixture was stirred at rt for 21 h. Then the solvent was removed under reduced pressure, the residue was again dissolved in EtOAc and water was added. After phase separation the aqueous phase was brought to a pH of 1 with aq. HCl (2 M) and extracted with EtOAc (3x). The combined organic phases were dried over $MgSO_4$, filtered and the solvent was removed under reduced pressure. After purification via flash system (DCM/MeOH) compound **(1*R*,2*S*,3*R*)-226** (129 mg, 421 µmol, 94%) was obtained as a white solid.

The spectral data are in accordance with the racemic compound **(±)-226**.

mp = 114 – 115 °C; $[\boldsymbol{\alpha}]_{\boldsymbol{D}}^{\mathbf{20}}$ = − 33.9 (*c* 1, CH_2Cl_2); **chiral HPLC**: 99% *ee* (Phenomenex Lux Cellulose-1, 4.6 x 250 mm, heptane/*i*-PrOH = 90:10, 1.0 mL/min, t_R (*S,R,S*), (***R,S,R***) = 6.43, **8.78** min).

General Procedure for the Fmoc-Protection G

The Boc-protected amino acid **226** was dissolved in dry DCM (10 mL) and TFA (5 mL) was added. After stirring the reaction mixture for 24 h at ambient temperature, the volatiles were removed *in vacuo*. The crude TFA salt of the amino acid was dissolved again in a mixture of dioxane and water (1:1) and the solution was cooled down to 0 °C. Then $NaHCO_3$ (2.05 equiv.) and FmocOSu (1.1 equiv.) were added. After 24 h reaction time, the solvent was removed under reduced pressure and sat. NH_4Cl, as well as ethyl acetate, were added. The phases were separated, and the aqueous phase was extracted with EtOAc (3 x). The combined organic phases were dried over $MgSO_4$, filtered and evaporated. By silica gel column chromatography (DCM/MeOH) followed by recrystallization from MeOH, the corresponding Fmoc-protected amino acid was purified.

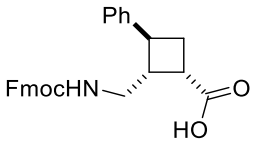

(±)-2-(((((9*H*-Fluoren-9-yl)methoxy)carbonyl)amino)methyl)-3-phenylcyclobutane-1-carboxylic acid ((±)-264)

According to the general procedure **G** compound **(±)-264** was synthesized from amino acid **(±)-226** (305.4 mg, 1.00 mmol, 1.0 equiv.), $NaHCO_3$ (172.2 mg, 2.05 mmol, 2.05 equiv.) and FmocOSu (371.1 mg, 1.10 mmol, 1.1 equiv.). By purification with the flash system (DCM/MeOH) and recrystallization from MeOH, compound **(±)-264** (370.3 mg, 866 µmol, 87%) was obtained as a white solid.

R_f = 0.38 (DCM/ MeOH 95:5); **mp** = 165 166 °C; **^{1}H-NMR** (400 MHz, MeOD) δ = 7.76 (d, *J* = 7.6 Hz, 2H), 7.57 – 7.50 (m, 2H), 7.36 (t, *J* = 7.4 Hz, 2H), 7.27 – 7.19 (m, 6H), 7.10 (t, *J* = 7.0 Hz, 1H), 4.19 (d, *J* = 7.0 Hz, 2H), 4.05 (t, *J* = 6.9 Hz, 1H), 3.48 (q, *J* = 9.1 Hz, 1H), 3.36 – 3.27 (m, 4H), 3.21 (td, *J* = 9.1, 3.1 Hz, 1H), 2.97 (p, *J* = 8.5 Hz, 1H), 2.63 – 2.53 (m, 1H), 2.18 (dt, *J* = 11.3, 9.0 Hz, 1H); **^{13}C-NMR** (101 MHz, MeOD) δ = 176.3, 157.3, 144.0, 143.91, 143.88, 141.1, 128.0, 127.3, 126.7, 126.3, 125.9, 124.8, 119.5, 66.4, 43.9, 42.5, 42.1, 37.3, 28.0. **IR** (neat) ν [cm^{-1}] = 3354, 3026, 2948, 1692, 1602, 1528, 1446, 1274, 1241, 1148, 1028, 991, 939, 894, 827, 734, 700; **HRMS**: (ESI-MS) m/z calc. for $[C_{27}H_{26}NO_4]^+$ $[M+H]^+$ 428.1856, found 428.1867.

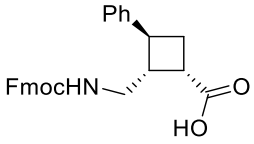

(1*S*,2*R*,3*S*)-2-(((((9*H*-Fluoren-9-yl)methoxy)carbonyl)amino)methyl)-3-phenylcyclobutane-1-carboxylic acid ((1*S*,2*R*,3*S*)-264)

According to the general procedure **G** compound **(1*S*,2*R*,3*S*)-264** was synthesized from amino acid **(1*S*,2*R*,3*S*)-226** (925 mg, 3.03 mmol, 1.0 equiv.), $NaHCO_3$ (522 mg, 6.21 mmol, 2.05 equiv.) and FmocOSu (1.12 g, 3.33 mmol, 1.1 equiv.). By purification with the flash system (DCM/MeOH) and recrystallization from MeOH, compound **(1*S*,2*R*,3*S*)-264** (1.09 g, 2.55 mol, 84%) was obtained as a white solid.

Spectral data are in accordance with those of **(±)-264**.

mp = 173.3 °C; **HRMS**: (ESI-MS) m/z calc. for $[C_{27}H_{26}NO_4]^+$ $[M+H]^+$ 428.1856, found 428.1863; m/z calc. for $[C_{27}H_{25}NO_4Na]^+$ $[M+Na]^+$ 450.1676, found 450.1677. $[\alpha]_D^{20}$ = 13.4 (*c* 1, DMSO); **chiral HPLC**: 99% *ee* (Chiralpak AS-H, 4.6 x 250 mm, heptane/*i*-PrOH = 70:30, 0.5 mL/min, t_R (***S,R,S***), (*R,S,R*) = **13.7**, 20.2 min).

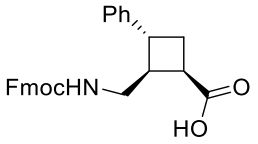

(1*R*,2*S*,3*R*)-2-(((((9*H*-Fluoren-9-yl)methoxy)carbonyl)amino)methyl)-3-phenylcyclobutane-1-carboxylic acid ((1*R*,2*S*,3*R*)-264)

According to the general procedure **G** compound **(1*R*,2*S*,3*R*)-264** was synthesized from amino acid **(1*R*,2*S*,3*R*)-226** (933 mg, 3.05 mmol, 1.0 equiv.), $NaHCO_3$ (525 mg, 6.25 mmol, 2.05 equiv.) and FmocOSu (1.13 g, 3.36 mmol, 1.1 equiv.). By purification with the flash system (DCM/MeOH) and recrystallization from MeOH, compound **(1*R*,2*S*,3*R*)-264** (1.19 g, 2.78 mol, 91%) was obtained as a white solid.

Spectral data are in accordance with those of **(±)-264**.

mp = 174 – 175 °C; **HRMS**: (ESI-MS) m/z calc. for $[C_{27}H_{26}NO_4]^+$ $[M+H]^+$ 428.1856, found 428.1860; m/z calc. for $[C_{27}H_{25}NO_4Na]^+$ $[M+Na]^+$ 450.1676, found 450.1669. $[\alpha]_D^{20}$ = −12.1 (*c* 1, DMSO); **chiral HPLC**: 99% *ee* (Chiralpak AS-H, 4.6 x 250 mm, heptane/*i*-PrOH = 70:30, 0.5 mL/min, t_R (***S,R,S***), (*R,S,R*) = **13.7**, 20.2 min).

General Protocol for Birch Reduction H

In a three-necked round bottom flask under inert gas atmosphere Na (7.0 equiv.) was dissolved in condensed ammonia (ca. 25 ml) at -78 °C. The reaction mixture became dark blue and was stirred for further 15 min until Na was completely dissolved. Then a solution of compound **158** (1.0 equiv.) and *t*-BuOH (2.2 equiv.) in abs. THF was added dropwise and the reaction mixture was stirred for 1 h at −33 °C. Afterwards, the reaction was quenched by the addition of NH_4Cl. The ammonia was allowed to evaporate at ambient temperature. Water (2 mL) and aqueous

HCl (1M, 30 mL) were added. After phase separation, the aqueous phase was extracted with DCM (6x20 mL). The combined organic phases were dried over Na_2SO_4, filtered and the solvent was removed under reduced pressure.

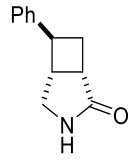

(±)-6-Phenyl-3-azabicyclo[3.2.0]heptan-2-one((±)-158u)

Following the general procedure **H** compound **(±)-158u** was prepared from **158ja** (416.1 mg, 1.50 mmol, 1.0 equiv.) using Na (241.4 mg, 10.5 mmol, 7.0 equiv.) and *t*-BuOH (244.6 mg, 310 µL, 3.30 mmol, 2.2 equiv.). Compound **(±)-7** (270.6 mg, 1.43 mmol, 95%) was obtained as a white solid and was used in the following reaction without further purification.

The spectral data are in accordance with those of enantiomer **(1*R*,5*S*,6*R*)-158u**.

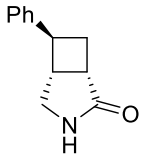

(1*S*,5*R*,6*S*)-6-Phenyl-3-azabicyclo[3.2.0]heptan-2-one ((1*S*,5*R*,6*S*)-158u)

Following the general procedure **H** compound **(1*S*,5*R*,6*S*)-158u** was prepared from **158vb** (272.4 mg, 935 µmol, 1.0 equiv.) using Na (150.4 mg, 6.50 mmol, 7.0 equiv.) and *t*-BuOH (152.4 mg, 155 µL, 2.00 mmol, 2.2 equiv.). Compound **(1*S*,5*R*,6*S*)-158u** (168.5 mg, 890 µmol, 95%) was obtained as a white solid and was used in the following reaction without further purification.

The spectral data are in accordance with those of the enantiomer **(1*R*,5*S*,6*R*)-158u**.

HRMS: (ESI-MS) m/z calc. for $[C_{12}H_{14}NO]^+$ $[M+H]^+$ 188.1070, found 188.1072; $[\alpha]_D^{20}$= 167.5 (*c* 1, DCM); **chiral HPLC**: 99% *ee* (Phenomenex Lux Cellulose-1, 4.6 x 250 mm, heptane/*i*-PrOH = 90:10, 0.5 mL/min, t_R (*R,S,R*), (***S,R,S***) = 29.5, **36.6** min).

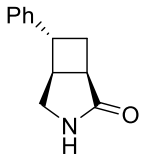

(1*R*,5*S*,6*R*)-6-Phenyl-3-azabicyclo[3.2.0]heptan-2-one ((1*R*,5*S*,6*R*)-158u)

Following the general procedure **G** compound **(1*R*,5*S*,6*R*)-158u** was prepared from **158va** (399.1 mg, 1.37 mmol, 1 equiv.) using Na (220.4 mg, 9.6 mmol, 7.0 equiv.) and *t*-BuOH (223.4 mg, 285 µL, 3.00 mmol, 2.2 equiv.). Compound **(1*R*,5*S*,6*R*)-158u** (226.2 mg, 1.21 mmol, 88%) was obtained as a white solid and was used in the following reaction without further purification.

R_f = 0.63 (DCM/MeOH 9:1); **mp** = 70 °C; **^{1}H-NMR** (300 MHz, $CDCl_3$) δ = 7.39 – 7.29 (m, 2H), 7.27 – 7.16 (m, 3H), 6.32 (d, *J* = 47.0 Hz, 1H), 3.66 – 3.50 (m, 2H), 3.38 (d, *J* = 10.1 Hz, 1H), 3.17 (q, *J* = 6.9 Hz, 1H), 3.03 – 2.91 (m, 1H), 2.69 – 2.49 (m, 2H); **^{13}C-NMR** (75 MHz, $CDCl_3$) δ = 180.9, 143.8, 128.6, 126.6, 126.3, 47.6, 44.3, 42.3, 36.6, 31.2. **IR** (neat) ν [cm^{-1}] = 3227, 3030, 2959, 2933, 2862, 1688, 1643, 1487, 1431, 1304, 1259, 1066, 1025, 797, 745, 697; **HRMS**: (ESI-MS) m/z calc. for $[C_{12}H_{14}NO]^+$ $[M+H]^+$ 188.1070, found 188.1069; $[\alpha]_D^{20}$ = – 152.0 (*c* 1, DCM); **chiral HPLC**: >99% *ee* (Phenomenex Lux Cellulose-1, 4.6 x 250 mm, heptane/*i*-PrOH = 90:10, 0.5 mL/min, t_R (***R,S,R***), (*S,R,S*) = **33.2**, 37.5 min).

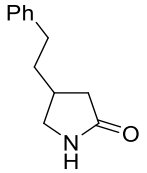

(±)-4-Phenethylpyrrolidin-2-one ((±)-215)[41]

Following the general procedure **H** compound **(±)-215** was prepared from **158na** (832.1 mg, 3.00 mmol, 1.0 equiv.) using Na (482.8 mg, 21.0 mmol, 7.0 equiv.) and *t*-BuOH (487 mg, 620 µL, 6.60 mmol, 2.2 equiv.). Compound **(±)-215** (509.7 mg, 2.72 mmol, 91%) was obtained as a white solid and was used in the following reaction without further purification.

R_f = 0.58 (DCM/MeOH 9:1); **mp** = 86 87 °C; **^{1}H-NMR** (300 MHz, $CDCl_3$) δ = 7.34 – 7.12 (m, 5H), 6.26 (s, 1H), 3.49 (dd, *J* = 9.4, 7.7 Hz, 1H), 3.05 (dd, *J* = 9.4, 6.6 Hz, 1H), 2.72 – 2.55 (m, 2H), 2.46 (ddd, *J* = 15.4, 8.7, 5.6 Hz, 2H), 2.12 – 1.98 (m, 1H), 1.80 (dd, *J* = 14.8, 7.5 Hz,

2H);**^{13}C-NMR** (101 MHz, $CDCl_3$) δ = 178.2, 141.3, 128.5, 128.3, 126.1, 48.0, 36.6, 36.3, 34.4, 33.8; **IR** (neat) ν [cm^{-1}] = 3182, 3082, 3026, 2929, 2855, 1684, 1599, 1453, 1420, 1364, 1297, 1140, 1062, 1025, 916, 887, 849, 805, 745, 700; **HRMS**: (ESI-MS) m/z calc. for $[C_{12}H_{16}NO]^+$ $[M+H]^+$ 190.1226, found 190.1234; m/z calc. for $[C_{12}H_{15}NONa]^+$ $[M+Na]^+$ 212.1046, found 212.1052.

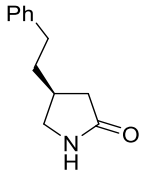

(*S*)-4-Phenethylpyrrolidin-2-one ((*S*)-215)

Following the general procedure **H** compound **(*S*)-215** was prepared from **156wa** (435.9 mg, 1.50 mmol, 1.0 equiv.) using Na (241.4 mg, 10.5 mmol, 7.0 equiv.) and *t*-BuOH (244.6 mg, 310 µL, 3.30 mmol, 2.2 equiv.). Compound **(*S*)-215** (266.4 mg, 1.41 mmol, 94%) was obtained as a white solid and was used in the following reaction without further purification.

The spectral data are in accordance with those of the compound **(±)-215**

mp = 78 – 79 °C; **HRMS**: (ESI-MS) m/z calc. for $[C_{12}H_{16}NO]^+$ $[M+H]^+$ 190.1226, found 190.1234; m/z calc. for $[C_{12}H_{15}NONa]^+$ $[M+Na]^+$ 212.1046, found 212.1052. $[\alpha]_D^{20}$ = 4.7 (*c* 1, $CHCl_3$); **chiral HPLC**: 99% *ee* (Phenomenex Lux Cellulose-2, 4.6 x 250 mm, heptane/*i*-PrOH = 70:30, 0.5 mL/min, t_R (***S***), (*R*) = **23.1**, 25.3 min).

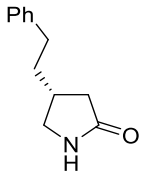

(*R*)-4-Phenethylpyrrolidin-2-one ((*R*)-215)[42]

Following the general procedure **G** compound **(*R*)-215** was prepared from **158wb** (378.8 mg, 1.30 mmol, 1.0 equiv.) using Na (209.2 mg, 9.10 mmol, 7.0 equiv.) and *t*-BuOH (212 mg, 270 µL, 2.90 mmol, 2.2 equiv.). Compound **(*R*)-215** (231 mg, 1.22 mmol, 94%) was obtained as a white solid and was used in the following reaction without further purification.

The spectral data are in accordance with those of the compound **(±)-215**.

mp = 71 – 73.5 °C; **HRMS**: (ESI-MS) m/z calc. for $[C_{12}H_{16}NO]^+$ $[M+H]^+$ 190.1226, found 190.1234; m/z calc. for $[C_{12}H_{15}NONa]^+$ $[M+Na]^+$ 212.1046, found 212.1052. $[\alpha]_D^{20} = -9.0$ (*c* 1, $CHCl_3$); **chiral HPLC**: 90% *ee* (Phenomenex Lux Cellulose-2, 4.6 x 250 mm, heptane/*i*-PrOH = 70:30, 0.5 mL/min, t_R (*S*), (***R***) = 23.5, **24.7** min).

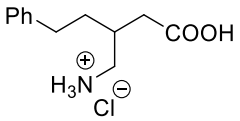

(±)-3-(Aminomethyl)-5-phenylpentanoic acid hydrochloride ((±)-257)[41]

Compound **(±)-215** (189.3 mg, 1.00 mmol, 1.0 equiv.) was dissolved in aq. HCl (25%, 10 mL) and the reaction mixture was stirred for 13 h at 90 °C. The solvent was removed under reduced pressure. The resulting residue was triturated and washed with EtOAc yielding compound **(±)-257** (220.6 mg, 0.91 mmol, 91%) as beige powder.

mp = 164 – 166.5 °C; **^{1}H-NMR** (300 MHz, MeOD) δ = 7.32 – 7.12 (m, 5H), 3.09 – 2.93 (m, 2H), 2.81 – 2.61 (m, 2H), 2.60 – 2.40 (m, 2H), 2.23 – 2.07 (m, 1H), 1.86 – 1.60 (m, 2H); **^{13}C-NMR** (101 MHz, MeOD) δ = 174.5, 141.3, 128.1, 128.0, 125.7, 42.9, 35.5, 33.23, 33.16, 32.2; **IR (neat)** ν [cm^{-1}] = 3168, 3082, 3022, 2937, 2370, 1722, 1572, 1528, 1453, 1408, 1300, 1259, 1200, 1092, 1053, 969, 946, 846, 801, 756, 730, 663 **HRMS**: (ESI-MS) m/z calc. for $[C_{12}H_{17}NO_2]^+$ $[M+H]^+$ 208.1332, found 208.1331.

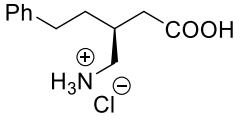

(*S*)-3-(Aminomethyl)-5-phenylpentanoic acid hydrochloride ((*S*)-257)

Compound **(*S*)-215** (184.6 mg, 0.98 mmol, 1.0 equiv.) was dissolved in aq. HCl (25%, 10 mL) and the reaction mixture was stirred for 24 h at 90 °C. The solvent was removed under reduced pressure. The resulting residue was triturated and washed with EtOAc yielding compound **(*S*)-257** (164.3 mg, 0.67 mmol, 69%) as beige powder.

The spectral data were in accordance with those of compound **(±)-257**.

mp = 145 – 148 °C; $[\alpha]_D^{20}$ = 15.8 (*c* 1, MeOH); **HRMS**: (ESI-MS) m/z calc. for $[C_{12}H_{17}NO_2]^+$ $[M+H]^+$ 208.1332, found 208.1330.

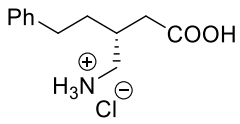

(*R*)-3-(Aminmethyl)-5-phenylpentanoic acid hydrochloride ((*R*)-257)[43]

Compound **(*R*)-215** (169.6 mg, 0.90 mmol, 1.0 equiv.) was dissolved in aq. HCl (25%, 10 mL) and the reaction mixture was stirred for 24 h at 90 °C. The solvent was removed under reduced pressure. The resulting residue was triturated and washed with EtOAc yielding compound **(*R*)-257** (197.2 mg, 0.81 mmol, 89%) as beige powder.

The spectral data were in accordance with those of compound **(±)-257**.

mp = 131 – 136; $[\alpha]_D^{20}$ = − 14.7 (*c* 1; MeOH); **HRMS**: (ESI-MS) m/z calc. for $[C_{12}H_{17}NO_2]^+$ $[M+H]^+$ 208.1332, found 208.1331.

NPY-analogues

NPY-analogues were synthesized on an automated peptide synthesizer, applying Fmoc-chemistry in cooperation with Prof. C. Cabrele from the University of Salzburg. At the University of Regensburg the obtained peptides were purified by preparative reversed phase HPLC. In the following, conditions of the purification, as well as the analytical data, were described.

Ph-ACBC ≡ Phenylamino cyclobutane amino acid

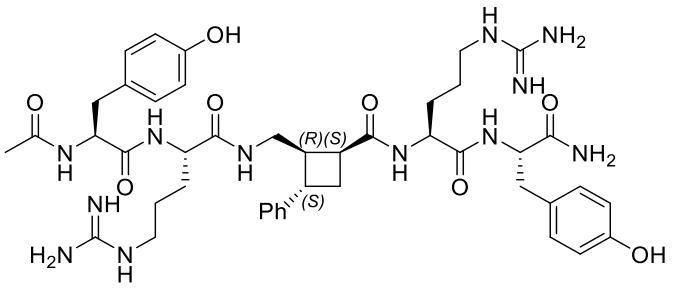

Ac-[Tyr-Arg-(1*S*,2*R*,3*S*)-Ph-ACBC-Arg-Tyr]-CONH$_2$ (267)

Purification by preparative RP-HPLC (Machery-Nagel VP 250/10 Nucleodur 100-5 C18ec, MeCN + 0.05% TFA 10-31% over 23 min, 5 mL/min, 220 nm, t_r = 16.7 min) gave **267** as white fluffy solid.

HPLC analysis (Machery-Nagel EC 250/4 Nucleodur 100-5 C18ec, MeCN + 0.05% TFA 10-60% over 40 min, 60-90% over 3 min, 90% for 10 min, 0.8 mL/min, 220 nm, t_R = 17.7 min); **HRMS**: (ESI-MS) m/z calc. for $[C_{44}H_{61}N_{12}O_8]^+$ $[M+H]^+$ 885.4730, found 885.4721; m/z calc. for $[C_{44}H_{62}N_{12}O_8]^{2+}$ $[M+2H]^{2+}$ 443.2401, found 443.2405.

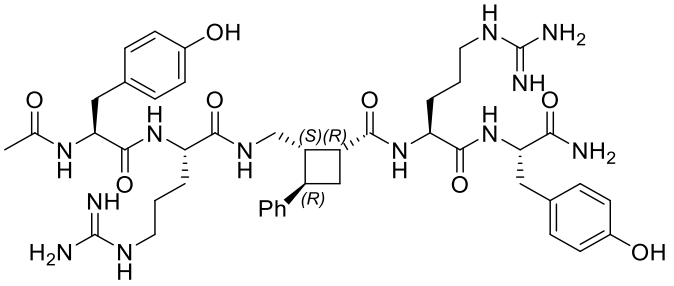

Ac-[Tyr-Arg-(1*R*,2*S*,3*R*)-Ph-ACBC-Arg-Tyr]-CONH$_2$ (268)

Purification by preparative RP-HPLC (Machery-Nagel VP 250/10 Nucleodur 100-5 C18ec, MeCN + 0.05% TFA 10-31% over 23 min, 5 mL/min, 220 nm, t_r = 16.2 min) gave **268** as white fluffy solid.

HPLC analysis (Machery-Nagel EC 250/4 Nucleodur 100-5 C18ec, MeCN + 0.05% TFA 10-60% over 40 min, 60-90% over 3 min, 90% for 10 min, 0.8 mL/min, 220 nm, t_R = 17.3 min); **HRMS**: (ESI-MS) m/z calc. for $[C_{44}H_{61}N_{12}O_8]^+$ $[M+H]^+$ 885.4730, found 885.4721, m/z calc. for $[C_{44}H_{62}N_{12}O_8]^{2+}$ $[M+2H]^{2+}$ 443.2401, found 443.2406.

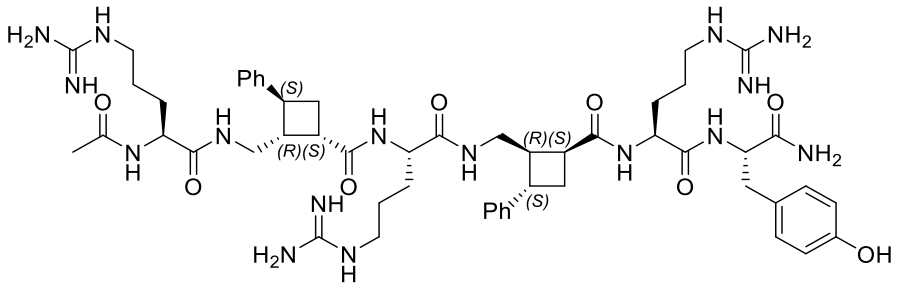

Ac-[Arg-(1*S*,2*R*,3*S*)-Ph-ACBC-Arg-(1*S*,2*R*,3*S*)-Ph-ACBC-Arg-Tyr]-CONH$_2$ (269)

Purification by preparative RP-HPLC (Machery-Nagel VP 250/10 Nucleodur 100-5 C18ec, MeCN + 0.05% TFA 10-35% over 25 min, 5 mL/min, 220 nm, t_r = 17.9 min) gave **269** as white fluffy solid.

HPLC analysis (Machery-Nagel EC 250/4 Nucleodur 100-5 C18ec, MeCN + 0.05% TFA 10-60% over 40 min, 60-90% over 3 min, 90% for 10 min, 0.8 mL/min, 220 nm, t_R = 19.5 min); **HRMS**: (ESI-MS) m/z calc. for $[C_{53}H_{77}N_{16}O_8]^+$ $[M+H]^+$ 1065.6105, found 1065.6106, m/z calc. for $[C_{53}H_{78}N_{16}O_8]^{2+}$ $[M+2H]^{2+}$ 533.3089, found 533.3095, m/z calc. for $[C_{53}H_{79}N_{16}O_8]^{2+}$ $[M+3H]^{3+}$ 355.8750, found 355.8757.

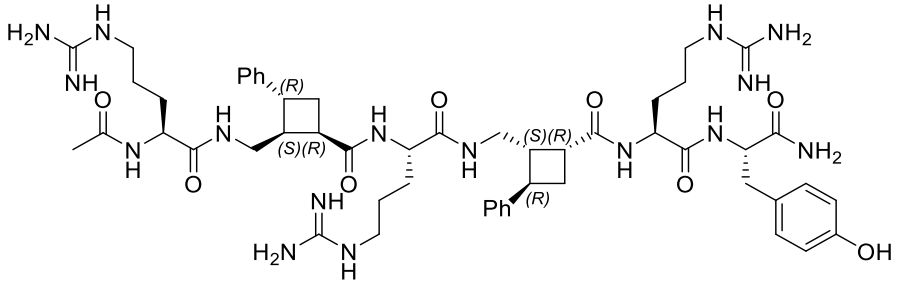

Ac-[Arg-(1R,2*S*,3*R*)-Ph-ACBC-Arg-(1*R*,2*S*,3*R*)-Ph-ACBC-Arg-Tyr]-CONH$_2$ (270)

Purification by preparative RP-HPLC (Machery-Nagel VP 250/10 Nucleodur 100-5 C18ec, MeCN + 0.05% TFA 10-35% over 25 min, 5 mL/min, 220 nm, t_r = 17.2 min) gave **270** as white fluffy solid.

HPLC analysis (Machery-Nagel EC 250/4 Nucleodur 100-5 C18ec, MeCN + 0.05% TFA 10-60% over 40 min, 60-90% over 3 min, 90% for 10 min, 0.8 mL/min, 220 nm, t_R = 18.6 min); **HRMS**: (ESI-MS) m/z calc. for $[C_{53}H_{78}N_{16}O_8]^{2+}$ $[M+2H]^{2+}$ 533.3089, found 533.3091, m/z calc. for $[C_{53}H_{79}N_{16}O_8]^{2+}$ $[M+3H]^{3+}$ 355.8750, found 355.8756.

3 DFT-calculations

All DFT calculations were run using the Gaussian09 Revision E01[44] suite of programs. The chosen level of theory is B3LYP/6-311+G**[45,46,47,48,49] with the addition of Grimmes Empirical Dispersion GD3[50]. After comparison it was found that adding dispersion correction does have a significant impact on the system, therefore dispersion corrected values were used going forward. To compute non-covalent interactions the NCI package was used.[51,52]

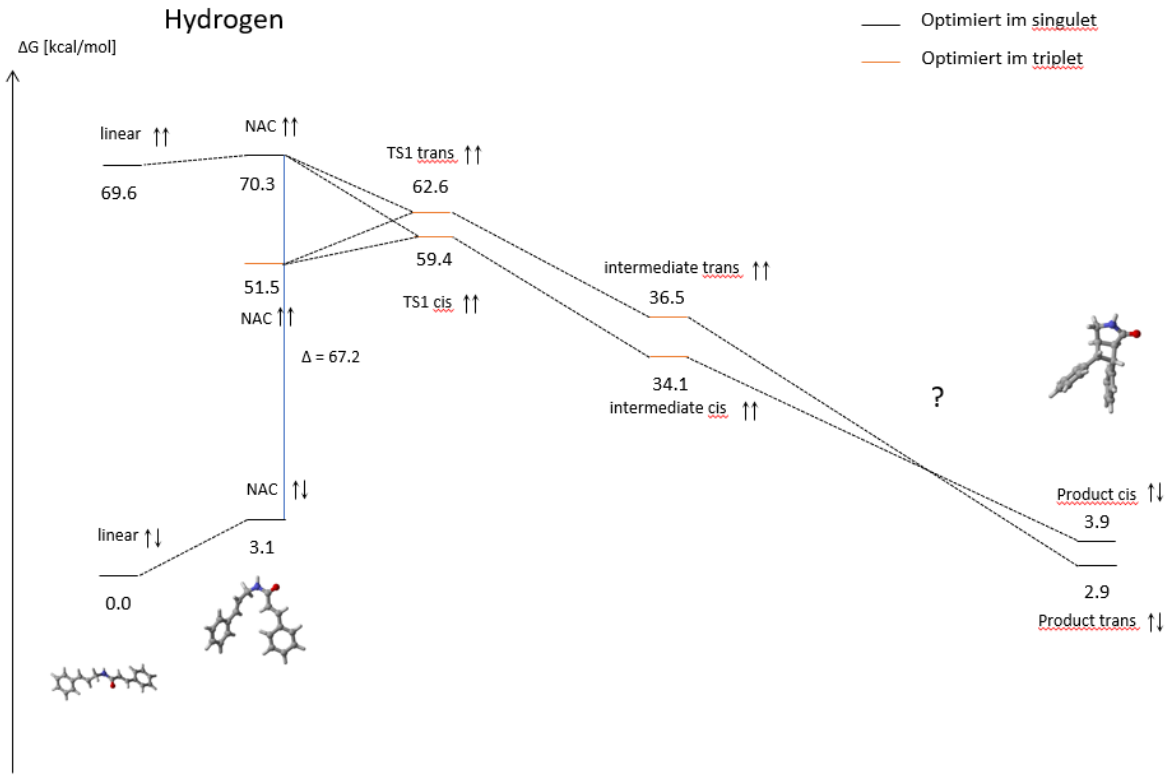

Figure 19. Reaction coordination diagram for [2+2] photocycloaddition of substrate **153e** with the level of theory B3LYP-D3/6-311+G**.

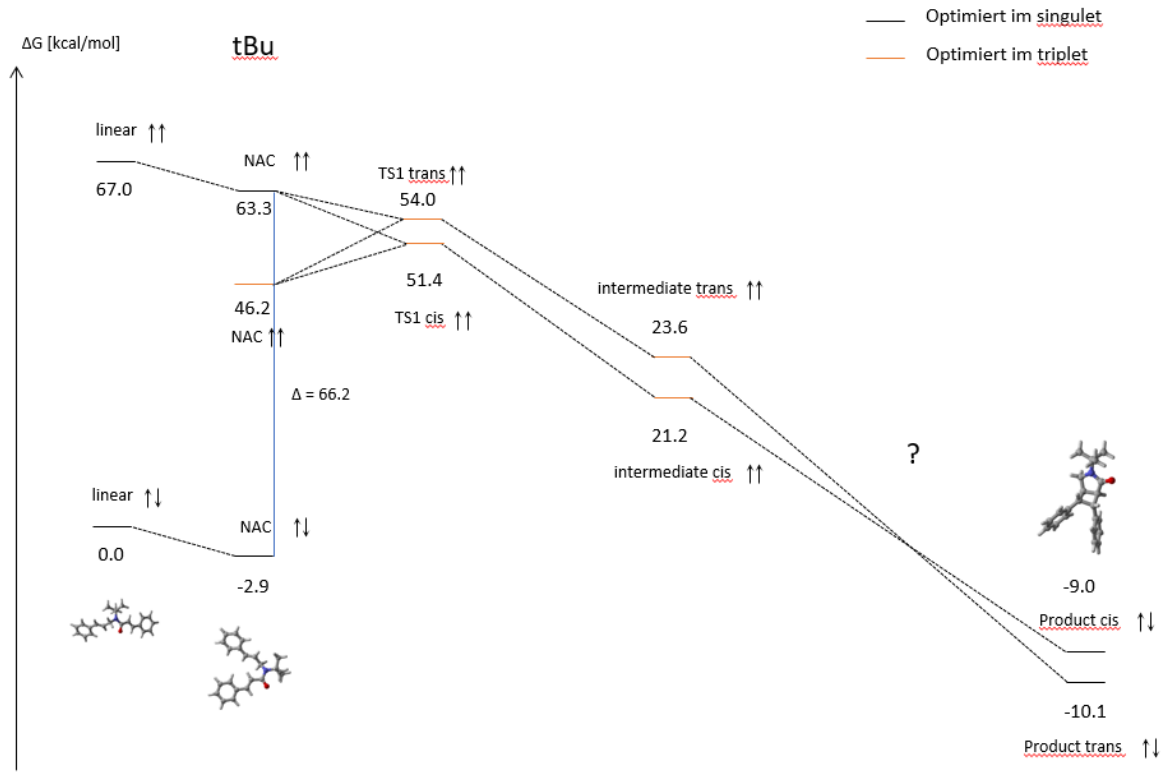

Figure 20. Reaction coordination diagram for [2+2] photocycloaddition of substrate **153g** with the level of theory B3LYP-D3/6-311+G**.

#B3LYP/6-311+G**	**Singulett-153g**

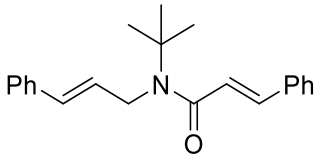

0 1

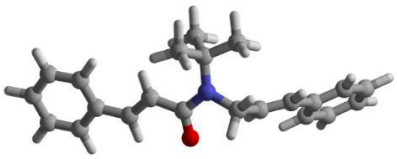

xyz-matrix

6	-3.611896000	0.390215000	0.667884000
6	-2.319144000	0.102421000	0.859879000
6	-1.326527000	1.048454000	1.480485000
7	-0.074516000	1.201265000	0.701516000
6	0.849856000	0.201744000	0.961136000
6	0.059755000	2.301859000	-0.324070000
6	2.219267000	0.248415000	0.370054000
8	0.551385000	-0.730393000	1.710166000
6	3.055888000	-0.784200000	0.562172000
6	-1.265389000	3.081075000	-0.466390000
6	1.122988000	3.332405000	0.117415000
6	0.354411000	1.710807000	-1.721011000
6	-4.651585000	-0.495137000	0.119692000
6	-5.906700000	0.045936000	-0.200610000
6	-6.920166000	-0.745057000	-0.736414000
6	-6.701646000	-2.102309000	-0.959993000
6	-5.462246000	-2.659044000	-0.637386000
6	-4.452212000	-1.868741000	-0.101896000
6	4.435087000	-0.915537000	0.086778000
6	5.125829000	-2.108073000	0.359591000
6	6.437606000	-2.295888000	-0.066856000
6	7.090330000	-1.290674000	-0.776347000
6	6.420132000	-0.096961000	-1.054598000
6	5.111278000	0.088884000	-0.629016000
1	-3.961058000	1.388006000	0.932469000
1	-1.916886000	-0.872864000	0.604634000
1	-1.775022000	2.025330000	1.644374000
1	-1.034393000	0.651281000	2.454523000
1	2.541122000	1.110121000	-0.190450000
1	2.667171000	-1.620325000	1.136442000
1	-1.145919000	3.798949000	-1.280731000
1	-2.101161000	2.427762000	-0.717251000
1	-1.515223000	3.651720000	0.430181000
1	1.157467000	4.160196000	-0.596701000
1	2.128053000	2.921176000	0.194693000
1	0.859291000	3.740786000	1.096294000
1	-0.466046000	1.056958000	-2.026677000
1	0.434786000	2.519019000	-2.453246000
1	1.273837000	1.130533000	-1.764523000
1	-6.085539000	1.102723000	-0.028735000
1	-7.879862000	-0.301126000	-0.977092000
1	-7.488100000	-2.722821000	-1.374336000
1	-5.286153000	-3.717082000	-0.797752000
1	-3.503701000	-2.324536000	0.156668000
1	4.621151000	-2.892825000	0.913040000
1	6.949079000	-3.225530000	0.155812000
1	8.112223000	-1.431921000	-1.109489000
1	6.923550000	0.690548000	-1.604332000
1	4.612373000	1.024661000	-0.852741000

Zero-point correction= 0.414712 (Hartree/Particle)
Thermal correction to Energy= 0.437996
Thermal correction to Enthalpy= 0.438940
Thermal correction to Gibbs Free Energy= 0.357909
Sum of electronic and zero-point Energies= -983.197296
Sum of electronic and thermal Energies= -983.174011
Sum of electronic and thermal Enthalpies= -983.173067
Sum of electronic and thermal Free Energies= -983.254098

	E (Thermal)	CV	S
	KCal/Mol	Cal/Mol-Kelvin	Cal/Mol-Kelvin
Total	274.847	89.685	170.544

#UB3LYP/6-311+G**	**triplet-153g**

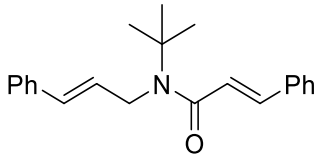

0 3

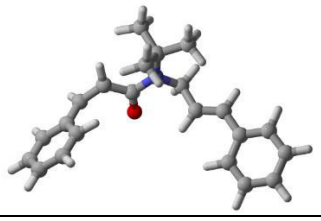

xyz-matrix

6	3.245781000	0.418777000	-0.643149000
6	1.928139000	0.413350000	-0.877402000
6	1.141443000	1.627552000	-1.294194000
7	-0.075929000	1.860356000	-0.483031000
6	-1.167609000	1.116055000	-0.918517000
6	-0.035357000	2.754204000	0.730792000
6	-2.502479000	1.280811000	-0.333621000
8	-1.037486000	0.306912000	-1.846927000
6	-3.624205000	0.489355000	-0.838077000
6	1.402753000	3.247312000	0.997330000
6	-0.896647000	4.017486000	0.506858000
6	-0.460625000	1.974993000	1.995474000
6	4.095339000	-0.728612000	-0.287293000
6	5.426479000	-0.497144000	0.093492000
6	6.269868000	-1.546481000	0.450495000
6	5.799717000	-2.857330000	0.430275000
6	4.480577000	-3.106236000	0.045521000
6	3.640377000	-2.058323000	-0.311158000
6	-4.116021000	-0.702754000	-0.259860000
6	-5.238959000	-1.366433000	-0.831395000
6	-5.742900000	-2.528707000	-0.275715000
6	-5.153687000	-3.082236000	0.867991000
6	-4.045726000	-2.451753000	1.445764000
6	-3.532107000	-1.287867000	0.898807000
1	3.775394000	1.368574000	-0.713130000
1	1.350165000	-0.503397000	-0.815101000
1	1.767842000	2.516214000	-1.276943000
1	0.802112000	1.482216000	-2.321830000
1	-2.709898000	2.045194000	0.403626000
1	-4.118780000	0.854795000	-1.736971000
1	1.396217000	3.814450000	1.930536000
1	2.104712000	2.421196000	1.112693000
1	1.766324000	3.917724000	0.216284000
1	-0.807302000	4.686799000	1.367258000
1	-1.955143000	3.804365000	0.364200000
1	-0.545590000	4.554608000	-0.377837000
1	0.207696000	1.124296000	2.148971000
1	-0.390787000	2.625500000	2.871444000
1	-1.480444000	1.596581000	1.948105000
1	5.801478000	0.521397000	0.110193000
1	7.293648000	-1.339506000	0.742098000
1	6.453030000	-3.677898000	0.704242000
1	4.108245000	-4.124408000	0.016870000
1	2.625326000	-2.275951000	-0.621943000
1	-5.698338000	-0.944883000	-1.719122000
1	-6.598834000	-3.014922000	-0.730861000
1	-5.550752000	-3.993047000	1.300761000
1	-3.582130000	-2.879549000	2.328113000
1	-2.667715000	-0.814262000	1.350466000

Zero-point correction= 0.410800 (Hartree/Particle)
Thermal correction to Energy= 0.434332
Thermal correction to Enthalpy= 0.435276
Thermal correction to Gibbs Free Energy= 0.353818
Sum of electronic and zero-point Energies= -983.117589
Sum of electronic and thermal Energies= -983.094058
Sum of electronic and thermal Enthalpies= -983.093114
Sum of electronic and thermal Free Energies= -983.174572

	E (Thermal) KCal/Mol	CV Cal/Mol-Kelvin	S Cal/Mol-Kelvin
Total	272.547	91.406	171.443

#B3LYP/6-311+G**	**190b**

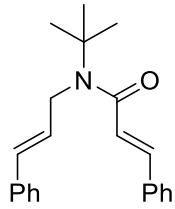

0 1

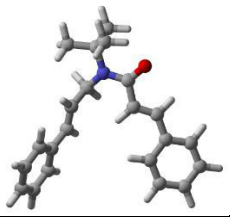

xyz-matrix

6	-1.993483000	-0.553999000	-0.884271000
6	-1.768977000	0.699558000	-0.472368000
6	-0.781160000	1.630022000	-1.131840000
7	0.012048000	2.456690000	-0.199606000
6	1.279840000	2.027556000	0.158590000
6	-0.383597000	3.894869000	0.047622000
6	1.550138000	0.562009000	0.045816000
8	2.145391000	2.789537000	0.580826000
6	2.808859000	0.104999000	0.136827000
6	-1.887310000	4.100338000	-0.224343000
6	-0.149890000	4.248899000	1.531020000
6	0.420556000	4.828534000	-0.877684000
6	-2.953458000	-1.524543000	-0.335897000
6	-3.093819000	-2.768791000	-0.970341000
6	-3.987563000	-3.725756000	-0.495565000
6	-4.761094000	-3.459399000	0.631268000
6	-4.630974000	-2.228030000	1.277124000
6	-3.740180000	-1.273779000	0.801351000
6	3.254113000	-1.290238000	0.103114000
6	4.633203000	-1.556809000	0.091120000
6	5.114942000	-2.862556000	0.055386000
6	4.224370000	-3.933347000	0.036787000
6	2.849372000	-3.686796000	0.055979000
6	2.369643000	-2.383841000	0.089413000
1	-1.414082000	-0.922305000	-1.730640000
1	-2.318380000	1.112350000	0.368088000
1	-0.107702000	1.059878000	-1.774674000
1	-1.311363000	2.305305000	-1.805228000
1	0.715113000	-0.117346000	-0.060459000
1	3.590214000	0.852088000	0.250788000
1	-2.149093000	5.114521000	0.083682000
1	-2.155759000	4.011472000	-1.278749000
1	-2.507960000	3.412282000	0.354133000
1	-0.497346000	5.269332000	1.714686000
1	0.899976000	4.184141000	1.802446000
1	-0.722343000	3.575597000	2.175448000
1	0.242911000	4.576737000	-1.927971000
1	0.110098000	5.866648000	-0.725471000
1	1.487122000	4.748571000	-0.673053000
1	-2.494906000	-2.983742000	-1.849670000
1	-4.078343000	-4.678143000	-1.005894000
1	-5.456998000	-4.201371000	1.005728000
1	-5.226402000	-2.013484000	2.157674000
1	-3.652542000	-0.328046000	1.323291000
1	5.330065000	-0.725443000	0.108829000
1	6.183998000	-3.042860000	0.045015000
1	4.594718000	-4.951937000	0.012096000
1	2.150780000	-4.516128000	0.050153000
1	1.299570000	-2.214640000	0.115732000

Zero-point correction= 0.414419 (Hartree/Particle)
Thermal correction to Energy= 0.437767
Thermal correction to Enthalpy= 0.438712
Thermal correction to Gibbs Free Energy= 0.357551
Sum of electronic and zero-point Energies= -983.201184
Sum of electronic and thermal Energies= -983.177836
Sum of electronic and thermal Enthalpies= -983.176892
Sum of electronic and thermal Free Energies= -983.258053

	E (Thermal) KCal/Mol	CV Cal/Mol-Kelvin	S Cal/Mol-Kelvin
Total	274.703	89.810	170.817

#BU3LYP/6-311+G**	**191b**

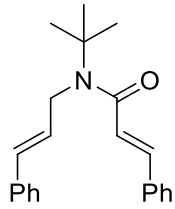

0 3

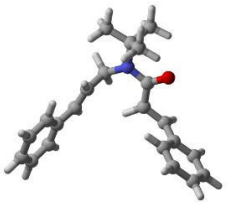

xyz-matrix

6	-2.430898000	0.094596000	-1.015828000
6	-1.784159000	1.105571000	-0.423277000
6	-0.791508000	1.996572000	-1.128293000
7	0.429455000	2.287977000	-0.357991000
6	1.513035000	1.423085000	-0.420942000
6	0.556288000	3.565669000	0.444391000
6	1.344417000	0.131569000	-1.106234000
8	2.605827000	1.688800000	0.088840000
6	2.495924000	-0.734958000	-1.350635000
6	-0.766724000	4.354544000	0.448266000
6	0.891708000	3.222050000	1.911167000
6	1.642279000	4.468759000	-0.175568000
6	-3.439451000	-0.798072000	-0.424778000
6	-3.875985000	-1.908679000	-1.163688000
6	-4.819703000	-2.793585000	-0.648359000
6	-5.352694000	-2.583730000	0.620979000
6	-4.934981000	-1.479495000	1.366771000
6	-3.994028000	-0.596793000	0.850643000
6	2.930969000	-1.780318000	-0.504245000
6	4.059633000	-2.571738000	-0.860777000
6	4.494417000	-3.604317000	-0.049048000
6	3.828466000	-3.893808000	1.148512000
6	2.717437000	-3.128588000	1.521675000
6	2.273224000	-2.092028000	0.718542000
1	-2.195183000	-0.118788000	-2.058335000
1	-1.965257000	1.339567000	0.622215000
1	-0.519176000	1.564442000	-2.093701000
1	-1.269515000	2.945593000	-1.367549000
1	0.362661000	-0.216615000	-1.408113000
1	3.061252000	-0.559541000	-2.265119000
1	-0.643242000	5.205142000	1.121605000
1	-1.022409000	4.760284000	-0.533337000
1	-1.609956000	3.766297000	0.818102000
1	0.979132000	4.144936000	2.491493000
1	1.828947000	2.676036000	1.988071000
1	0.093029000	2.619408000	2.353744000
1	1.390822000	4.706970000	-1.213417000
1	1.701488000	5.408852000	0.381109000
1	2.616773000	3.986067000	-0.151621000
1	-3.464778000	-2.080034000	-2.153333000
1	-5.137934000	-3.645571000	-1.238666000
1	-6.088851000	-3.268786000	1.025713000
1	-5.350060000	-1.304310000	2.353148000
1	-3.694174000	0.260290000	1.442355000
1	4.581734000	-2.350860000	-1.785849000
1	5.357965000	-4.191440000	-0.342119000
1	4.172025000	-4.703053000	1.782335000
1	2.200446000	-3.346745000	2.449855000
1	1.415458000	-1.502221000	1.020999000

Zero-point correction= 0.410393 (Hartree/Particle)
Thermal correction to Energy= 0.433978
Thermal correction to Enthalpy= 0.434922
Thermal correction to Gibbs Free Energy= 0.352383
Sum of electronic and zero-point Energies= -983.121114
Sum of electronic and thermal Energies= -983.097529
Sum of electronic and thermal Enthalpies= -983.096585
Sum of electronic and thermal Free Energies= -983.179124

	E (Thermal) KCal/Mol	CV Cal/Mol-Kelvin	S Cal/Mol-Kelvin
Total	272.325	91.581	173.719

#UB3LYP/6-311+G**	***cis*-193b**

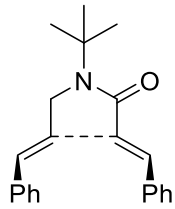

0 3

ν_{imag} = -171.5

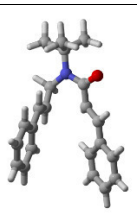

xyz-matrix

1	-2.691259000	1.026965000	1.923653000
1	-4.800448000	0.131722000	2.065473000
1	-2.012506000	-0.522342000	2.358134000
1	2.039818000	1.339891000	1.668125000
1	0.074861000	0.517029000	2.050231000
1	-4.507967000	1.658963000	1.201151000
6	-2.061479000	0.221906000	1.551055000
1	4.127515000	2.543303000	1.229470000
6	-0.665386000	0.762624000	1.295676000
6	2.063514000	2.085531000	0.882711000
6	-4.866324000	0.631838000	1.095726000
1	-5.923262000	0.687066000	0.826135000
6	3.248797000	2.764458000	0.633860000
1	3.872158000	-2.339994000	2.423303000
6	-0.370135000	1.676492000	0.341541000
6	0.907293000	2.345856000	0.120995000
1	-4.762418000	-2.072946000	0.776278000
1	1.547284000	-1.880239000	1.808023000
1	-1.153450000	1.935969000	-0.367700000
7	-2.681791000	-0.342759000	0.343918000
6	-4.131452000	-0.141008000	-0.012758000
6	3.317950000	3.722729000	-0.380143000
6	3.584381000	-2.342861000	1.377234000
1	4.245860000	4.249689000	-0.570746000
1	-0.548500000	-1.838180000	1.167783000
6	0.998798000	3.309349000	-0.901334000
6	2.273801000	-2.080425000	1.030542000
6	-4.815459000	-1.515204000	-0.163304000
6	2.185527000	3.991035000	-1.147710000
6	-4.237532000	0.667299000	-1.321251000
1	-4.347931000	-2.105078000	-0.949552000
1	5.571807000	-2.830477000	0.678282000
1	0.122550000	3.520176000	-1.505769000
6	-0.569354000	-1.501989000	0.137387000
6	4.547149000	-2.620719000	0.395606000
6	-1.864862000	-1.127478000	-0.442501000
1	2.227926000	4.729216000	-1.940809000
1	-5.870452000	-1.376817000	-0.415841000
6	1.854018000	-2.083396000	-0.347024000
6	0.549012000	-1.827067000	-0.751442000
6	4.167592000	-2.632493000	-0.962123000
8	-2.166332000	-1.510482000	-1.579126000
6	2.867864000	-2.374708000	-1.327856000
1	0.309367000	-1.864533000	-1.808054000
1	4.908399000	-2.848558000	-1.724166000
1	2.581575000	-2.386071000	-2.373947000
1	-3.766070000	1.647698000	-1.204595000
1	-5.289381000	0.828653000	-1.575630000
1	-3.754560000	0.141457000	-2.142971000

Zero-point correction= 0.409760 (Hartree/Particle)
Thermal correction to Energy= 0.432699
Thermal correction to Enthalpy= 0.433643
Thermal correction to Gibbs Free Energy= 0.354275
Sum of electronic and zero-point Energies= -983.111250
Sum of electronic and thermal Energies= -983.088311
Sum of electronic and thermal Enthalpies= -983.087366
Sum of electronic and thermal Free Energies= -983.166735

	E (Thermal) KCal/Mol	CV Cal/Mol-Kelvin	S Cal/Mol-Kelvin
Total	271.523	89.973	167.045

#UB3LYP/6-311+G**	***trans*-193b**

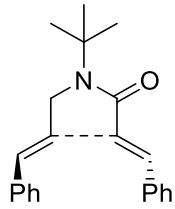

0 3

ν_{imag} = -231.5

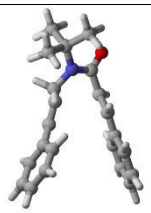

xyz-matrix

6	-0.580357000	1.305856000	-1.552886000
6	0.703071000	0.899540000	-1.355873000
6	0.940554000	-1.517598000	-0.840848000
6	0.040167000	-1.692414000	0.312526000
6	1.577897000	1.111771000	-0.144830000
7	2.586230000	0.046991000	0.010184000
6	2.350176000	-1.133339000	-0.666072000
8	3.237141000	-1.876106000	-1.094949000
6	3.953499000	0.405671000	0.516364000
6	3.829377000	1.533688000	1.561097000
6	4.585334000	-0.802605000	1.235190000
6	4.843575000	0.865782000	-0.653242000
6	-1.596898000	1.840839000	-0.646387000
6	-2.618875000	2.628364000	-1.216332000
6	-3.616981000	3.200097000	-0.437113000
6	-3.636972000	2.985989000	0.940797000
6	-2.653630000	2.184869000	1.521495000
6	-1.650994000	1.617790000	0.743335000
6	-1.315630000	-2.004772000	0.243111000
6	-2.066793000	-2.239070000	1.447115000
6	-3.398728000	-2.584621000	1.406102000
6	-4.065788000	-2.716953000	0.174425000
6	-3.361354000	-2.490200000	-1.018741000
6	-2.026679000	-2.141890000	-0.998462000
1	-0.912760000	1.268695000	-2.588023000
1	1.262367000	0.665555000	-2.257330000
1	0.757272000	-2.103718000	-1.735807000
1	0.495772000	-1.636473000	1.297652000
1	0.997759000	1.247070000	0.767464000
1	2.109195000	2.053716000	-0.316753000
1	4.810333000	1.704732000	2.009640000
1	3.501115000	2.483250000	1.134743000
1	3.139501000	1.255878000	2.362587000
1	4.768020000	-1.631500000	0.556496000
1	3.934486000	-1.148845000	2.043257000
1	5.536221000	-0.494280000	1.677824000
1	4.405175000	1.728480000	-1.164630000
1	5.831113000	1.162717000	-0.287961000
1	4.967392000	0.057891000	-1.375352000
1	-2.614145000	2.798196000	-2.288076000
1	-4.382880000	3.808611000	-0.904964000
1	-4.417007000	3.424782000	1.552364000
1	-2.676569000	1.987730000	2.587582000
1	-0.932184000	0.961975000	1.213527000
1	-1.556621000	-2.149365000	2.400698000
1	-3.937926000	-2.760316000	2.330614000
1	-5.113074000	-2.993017000	0.147034000
1	-3.873512000	-2.589901000	-1.969712000
1	-1.503607000	-1.962729000	-1.929191000

Zero-point correction= 0.410000 (Hartree/Particle)
Thermal correction to Energy= 0.432921
Thermal correction to Enthalpy= 0.433865
Thermal correction to Gibbs Free Energy= 0.354551
Sum of electronic and zero-point Energies= -983.101880
Sum of electronic and thermal Energies= -983.078960
Sum of electronic and thermal Enthalpies= -983.078016
Sum of electronic and thermal Free Energies= -983.157330

	E (Thermal) KCal/Mol	CV Cal/Mol-Kelvin	S Cal/Mol-Kelvin
Total	271.662	89.758	166.931

#UB3LYP/6-311+G**	***cis*-192b**

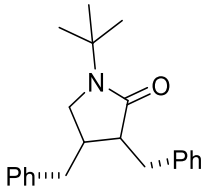

0 3

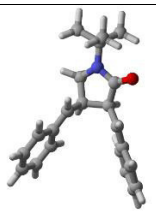

xyz-matrix

1	-3.627731000	-2.971352000	-2.363242000
1	-5.246074000	-3.530195000	-0.563604000
6	-3.370639000	-2.780766000	-1.326740000
6	-4.283968000	-3.097400000	-0.315608000
1	-1.449190000	-1.994556000	-1.822154000
6	-2.138445000	-2.226628000	-1.018564000
6	-3.941930000	-2.851168000	1.020103000
1	-4.643160000	-3.095100000	1.810676000
6	-1.763754000	-1.966898000	0.330762000
6	-2.714103000	-2.300379000	1.339317000
1	0.598354000	-1.719933000	-1.086380000
1	-2.455491000	-2.115824000	2.376532000
6	-0.519082000	-1.409533000	0.699643000
1	4.500191000	-2.164904000	-0.009165000
6	0.562684000	-1.013707000	-0.243785000
1	-2.039711000	1.257283000	-1.678310000
1	-0.117932000	0.431705000	-1.758284000
1	-0.323094000	-1.268406000	1.756835000
1	-4.072221000	2.611713000	-1.669349000
1	2.187891000	0.193709000	-2.254180000
8	2.335854000	-1.870198000	1.211813000
6	1.970905000	-1.066107000	0.370523000
6	0.508831000	0.427819000	-0.866458000
1	4.173333000	-0.635471000	2.055275000
6	4.869261000	-1.297745000	-0.557186000
6	-2.157856000	2.022479000	-0.921405000
1	4.654700000	-1.436009000	-1.621231000
6	1.993507000	0.623815000	-1.261202000
6	-3.313464000	2.786079000	-0.914209000
7	2.734843000	-0.088719000	-0.214952000
1	5.954986000	-1.248523000	-0.436561000
6	4.218239000	-0.002919000	-0.033337000
6	4.536555000	0.200095000	1.459866000
6	0.063880000	1.479865000	0.098312000
1	5.618348000	0.286469000	1.595585000
6	-1.140609000	2.216976000	0.056979000
1	2.261925000	1.679001000	-1.292040000
6	-3.515655000	3.771217000	0.058401000
1	-4.423220000	4.363415000	0.057058000
6	4.769244000	1.197573000	-0.819042000
1	0.745481000	1.696088000	0.917222000
1	4.073124000	1.120131000	1.826920000
6	-1.377808000	3.223603000	1.040056000
6	-2.535559000	3.979683000	1.036866000
1	-0.623956000	3.392473000	1.802031000
1	-2.684332000	4.737972000	1.797893000
1	4.586759000	1.111695000	-1.893055000
1	5.850493000	1.242915000	-0.671662000
1	4.348379000	2.142593000	-0.466410000

Zero-point correction= 0.412924 (Hartree/Particle)
Thermal correction to Energy= 0.435433
Thermal correction to Enthalpy= 0.436377
Thermal correction to Gibbs Free Energy= 0.357934
Sum of electronic and zero-point Energies= -983.160575
Sum of electronic and thermal Energies= -983.138066
Sum of electronic and thermal Enthalpies= -983.137121
Sum of electronic and thermal Free Energies= -983.215565

	E (Thermal) KCal/Mol	CV Cal/Mol-Kelvin	S Cal/Mol-Kelvin
Total	273.238	89.098	165.097

#UB3LYP/6-311+G**	***trans*-192b**

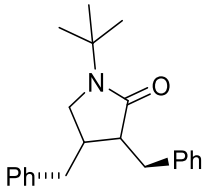

0 3

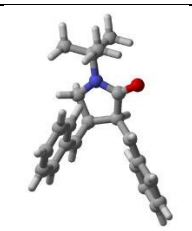

xyz-matrix

1	4.983071000	-2.155232000	1.887572000
6	4.622721000	-1.683789000	0.979520000
1	2.571280000	-1.962172000	1.503258000
1	6.602981000	-1.282627000	0.219145000
6	3.258602000	-1.573578000	0.760666000
6	5.537570000	-1.193962000	0.041551000
1	0.524577000	-2.284843000	0.600633000
1	0.341977000	-0.848995000	2.336703000
1	-3.533487000	-3.252252000	0.941162000
1	-1.894400000	-1.244245000	2.350340000
6	2.749271000	-0.964299000	-0.421228000
6	5.063546000	-0.589802000	-1.129835000
6	0.270213000	-1.290418000	0.208564000
6	-0.094310000	-0.384334000	1.451262000
1	1.294653000	1.185951000	2.081073000
1	5.766067000	-0.209452000	-1.863376000
6	-1.640104000	-0.537180000	1.551670000
6	1.368953000	-0.827975000	-0.690183000
6	3.704244000	-0.475895000	-1.359430000
6	-3.761127000	-2.839895000	-0.046439000
6	-1.057455000	-1.499451000	-0.528066000
1	-4.807945000	-3.062157000	-0.271206000
6	0.441688000	1.020372000	1.430297000
7	-2.086666000	-1.042528000	0.250211000
8	-1.155766000	-2.025436000	-1.625232000
1	-3.135900000	-3.337809000	-0.787968000
1	-2.116359000	0.414579000	1.787721000
6	-3.526139000	-1.317393000	-0.068873000
1	1.078500000	-0.361654000	-1.624859000
1	3.344684000	-0.008471000	-2.269899000
1	-3.258446000	-1.184620000	-2.233089000
6	-4.428261000	-0.645093000	0.978872000
1	1.517483000	3.420417000	1.603863000
6	0.039646000	2.143649000	0.666879000
6	-3.871721000	-0.736990000	-1.453526000
1	-4.924445000	-0.932410000	-1.676453000
6	0.718112000	3.382160000	0.871256000
1	-1.532215000	1.218342000	-0.516415000
6	-0.996882000	2.134575000	-0.309194000
1	-3.721281000	0.346085000	-1.464938000
6	0.382257000	4.519740000	0.160381000
1	0.919512000	5.444420000	0.340790000
6	-1.323627000	3.281319000	-1.016964000
6	-0.644341000	4.482302000	-0.791349000
1	-2.113763000	3.241543000	-1.759135000
1	-0.906420000	5.373233000	-1.349969000
1	-5.469994000	-0.849981000	0.722462000
1	-4.298402000	0.439690000	0.991677000
1	-4.256059000	-1.030548000	1.986303000

Zero-point correction= 0.413485 (Hartree/Particle)
Thermal correction to Energy= 0.435949
Thermal correction to Enthalpy= 0.436893
Thermal correction to Gibbs Free Energy= 0.359210
Sum of electronic and zero-point Energies= -983.154171
Sum of electronic and thermal Energies= -983.131707
Sum of electronic and thermal Enthalpies= -983.130763
Sum of electronic and thermal Free Energies= -983.208447

	E (Thermal) KCal/Mol	CV Cal/Mol-Kelvin	S Cal/Mol-Kelvin
Total	273.562	88.980	163.498

#B3LYP/6-311+G**	***cis*-158g**

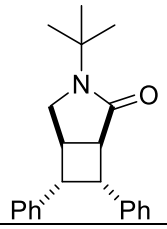

0 1

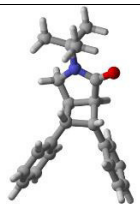

xyz-matrix

6	-0.216676000	0.662055000	0.186028000
6	0.616360000	0.259086000	-1.070251000
6	0.761072000	-1.161375000	-0.491326000
6	-0.363669000	-0.890984000	0.545844000
6	2.031886000	0.831546000	-1.163530000
7	2.812656000	-0.010533000	-0.243223000
6	2.165710000	-1.172524000	0.106332000
8	2.626012000	-2.081174000	0.780650000
6	4.251560000	0.240045000	0.085449000
6	4.664363000	1.636756000	-0.407146000
6	4.445811000	0.183685000	1.612742000
6	5.121749000	-0.822559000	-0.613633000
6	-1.414519000	1.564077000	0.067931000
6	-1.675003000	2.498325000	1.079713000
6	-2.778708000	3.346086000	1.016535000
6	-3.648609000	3.277757000	-0.069726000
6	-3.403261000	2.355866000	-1.085759000
6	-2.299927000	1.508065000	-1.016258000
6	-1.709545000	-1.529304000	0.297333000
6	-2.640849000	-1.560673000	1.344646000
6	-3.905110000	-2.115867000	1.171633000
6	-4.268980000	-2.658569000	-0.060223000
6	-3.354721000	-2.639581000	-1.109940000
6	-2.089509000	-2.079565000	-0.931917000
1	0.458675000	1.096016000	0.928489000
1	0.066544000	0.347394000	-2.006440000
1	0.646709000	-2.035103000	-1.133831000
1	-0.067963000	-1.104584000	1.575141000
1	2.060769000	1.881722000	-0.864148000
1	2.425113000	0.763209000	-2.185805000
1	5.716748000	1.794175000	-0.161231000
1	4.559827000	1.744669000	-1.489248000
1	4.089932000	2.428017000	0.080766000
1	5.490868000	0.393013000	1.858162000
1	4.183185000	-0.796494000	2.006578000
1	3.824429000	0.937961000	2.104023000
1	4.995669000	-0.771273000	-1.699292000
1	6.178002000	-0.650795000	-0.388019000
1	4.853647000	-1.823650000	-0.276093000
1	-0.999948000	2.563272000	1.927636000
1	-2.955674000	4.061202000	1.812444000
1	-4.507654000	3.936863000	-0.125332000
1	-4.074619000	2.293374000	-1.935162000
1	-2.136281000	0.794105000	-1.814376000
1	-2.366502000	-1.147951000	2.310132000
1	-4.604533000	-2.130262000	2.000270000
1	-5.251358000	-3.096182000	-0.197316000
1	-3.621960000	-3.065027000	-2.071187000
1	-1.396854000	-2.084642000	-1.765652000

Zero-point correction= 0.418140 (Hartree/Particle)
Thermal correction to Energy= 0.439494
Thermal correction to Enthalpy= 0.440438
Thermal correction to Gibbs Free Energy= 0.366495
Sum of electronic and zero-point Energies= -983.208379
Sum of electronic and thermal Energies= -983.187026
Sum of electronic and thermal Enthalpies= -983.186082
Sum of electronic and thermal Free Energies= -983.260025

	E (Thermal) KCal/Mol	CV Cal/Mol-Kelvin	S Cal/Mol-Kelvin
Total	275.786	85.424	155.626

#B3LYP/6-311+G**	***trans*-158g**

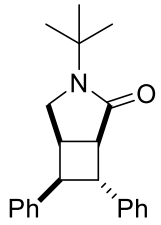

0 1

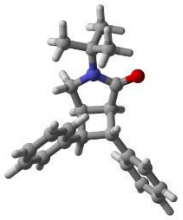

xyz-matrix

6	-0.728938000	0.763936000	-0.893663000
6	0.262868000	-0.192369000	-1.660269000
6	-0.229531000	-1.379321000	-0.804794000
6	-1.139906000	-0.426605000	0.049689000
6	1.774276000	-0.094690000	-1.400820000
7	2.043026000	-1.037435000	-0.302805000
6	0.987586000	-1.880431000	-0.045734000
8	0.999706000	-2.853273000	0.693516000
6	3.422932000	-1.291203000	0.219692000
6	4.347771000	-0.125078000	-0.167919000
6	3.384627000	-1.385614000	1.756681000
6	3.961100000	-2.599996000	-0.390885000
6	-0.240873000	2.064132000	-0.308007000
6	-0.567108000	3.271955000	-0.940043000
6	-0.112738000	4.493020000	-0.446559000
6	0.679680000	4.532037000	0.699101000
6	1.011275000	3.340903000	1.342038000
6	0.557355000	2.121263000	0.842601000
6	-2.609958000	-0.739420000	0.159248000
6	-3.246424000	-0.713727000	1.404899000
6	-4.609100000	-0.984266000	1.523109000
6	-5.362118000	-1.289281000	0.392145000
6	-4.741542000	-1.322034000	-0.856632000
6	-3.380961000	-1.049671000	-0.969666000
1	-1.561881000	0.988042000	-1.563023000
1	0.059043000	-0.232813000	-2.730359000
1	-0.747681000	-2.204786000	-1.290502000
1	-0.735519000	-0.309911000	1.056366000
1	2.077975000	0.918862000	-1.133481000
1	2.333184000	-0.384258000	-2.298733000
1	5.341218000	-0.317828000	0.243208000
1	4.455552000	-0.018060000	-1.249452000
1	3.996093000	0.824075000	0.243735000
1	4.396526000	-1.553081000	2.136299000
1	2.745960000	-2.202294000	2.086989000
1	3.013054000	-0.451237000	2.186985000
1	3.998460000	-2.531905000	-1.482415000
1	4.975255000	-2.795087000	-0.031019000
1	3.327080000	-3.442614000	-0.113949000
1	-1.192352000	3.253671000	-1.827260000
1	-0.383962000	5.413158000	-0.952387000
1	1.030715000	5.480455000	1.089790000
1	1.623460000	3.359895000	2.237142000
1	0.829502000	1.207572000	1.358429000
1	-2.666515000	-0.483249000	2.292491000
1	-5.079700000	-0.959639000	2.499776000
1	-6.421209000	-1.503159000	0.481164000
1	-5.318010000	-1.563145000	-1.743079000
1	-2.916698000	-1.085674000	-1.950463000

Zero-point correction= 0.418328 (Hartree/Particle)
Thermal correction to Energy= 0.439706
Thermal correction to Enthalpy= 0.440651
Thermal correction to Gibbs Free Energy= 0.365797
Sum of electronic and zero-point Energies= -983.209660
Sum of electronic and thermal Energies= -983.188281
Sum of electronic and thermal Enthalpies= -983.187337
Sum of electronic and thermal Free Energies= -983.262191

	E (Thermal) KCal/Mol	CV Cal/Mol-Kelvin	S Cal/Mol-Kelvin
Total	275.920	85.333	157.543

#B3LYP/6-311+G**	**Singulett-153e**

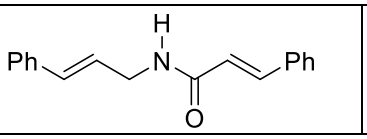

0 1

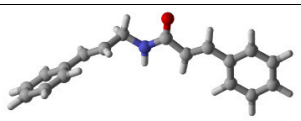

xyz-matrix

6	-3.598643000	0.753141000	-0.615480000
6	-2.449972000	0.954232000	0.042154000
6	-1.321668000	1.794087000	-0.484323000
7	-0.087532000	1.025891000	-0.616621000
6	1.087686000	1.377908000	-0.001588000
6	2.215723000	0.443146000	-0.263828000
8	1.190485000	2.378055000	0.698112000
6	3.426836000	0.676176000	0.262338000
6	-4.759661000	-0.036381000	-0.177809000
6	-5.824870000	-0.225794000	-1.072172000
6	-6.944372000	-0.973336000	-0.715368000
6	-7.025173000	-1.547338000	0.550914000
6	-5.977435000	-1.363121000	1.455644000
6	-4.861150000	-0.616779000	1.098225000
6	4.644299000	-0.123081000	0.110993000
6	5.827184000	0.335688000	0.713506000
6	7.016985000	-0.378229000	0.600659000
6	7.047815000	-1.571170000	-0.117508000
6	5.879722000	-2.044101000	-0.720468000
6	4.693576000	-1.330620000	-0.608120000
1	-3.709298000	1.218264000	-1.594282000
1	-2.276061000	0.500810000	1.014787000
1	-1.595375000	2.238980000	-1.447672000
1	-1.087706000	2.611104000	0.202913000
1	2.023101000	-0.420115000	-0.893982000
1	3.515344000	1.571383000	0.873315000
1	-5.769825000	0.218727000	-2.060776000
1	-7.752691000	-1.105580000	-1.425913000
1	-7.895395000	-2.128259000	0.834359000
1	-6.034995000	-1.799954000	2.446516000
1	-4.065943000	-0.477575000	1.821249000
1	5.806234000	1.264146000	1.274202000
1	7.917787000	-0.003517000	1.073355000
1	7.971741000	-2.131041000	-0.207507000
1	5.897239000	-2.973552000	-1.278616000
1	3.798030000	-1.717004000	-1.080635000
1	-0.114650000	0.180917000	-1.166476000

Zero-point correction= 0.302573 (Hartree/Particle)
Thermal correction to Energy= 0.320687
Thermal correction to Enthalpy= 0.321631
Thermal correction to Gibbs Free Energy= 0.250949
Sum of electronic and zero-point Energies= -826.039754
Sum of electronic and thermal Energies= -826.021640
Sum of electronic and thermal Enthalpies= -826.020696
Sum of electronic and thermal Free Energies= -826.091378

	E (Thermal) KCal/Mol	CV Cal/Mol-Kelvin	S Cal/Mol-Kelvin
Total	201.234	68.519	148.763

#UB3LYP/6-311+G**	**triplet-153e**

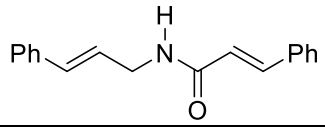

0 3

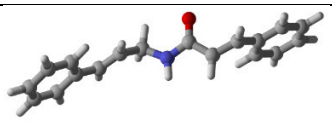

xyz-matrix

6	-3.456144000	-0.846783000	-0.354129000
6	-2.348230000	-0.153694000	-0.645347000
6	-1.024207000	-0.790757000	-0.956828000
7	0.013462000	-0.373586000	-0.019853000
6	1.202142000	0.200255000	-0.420214000
6	2.101827000	0.570162000	0.680060000
8	1.481926000	0.385694000	-1.601561000
6	3.395828000	1.202881000	0.452020000
6	-4.794760000	-0.319141000	-0.050320000
6	-5.799802000	-1.214343000	0.348309000
6	-7.082748000	-0.769745000	0.657853000
6	-7.390946000	0.585553000	0.571125000
6	-6.404737000	1.489229000	0.169853000
6	-5.125025000	1.044087000	-0.138584000
6	4.632080000	0.523920000	0.350840000
6	5.837923000	1.253756000	0.149928000
6	7.057317000	0.607152000	0.055892000
6	7.130079000	-0.787792000	0.156355000
6	5.958028000	-1.527716000	0.350885000
6	4.731577000	-0.892443000	0.446092000
1	-3.381262000	-1.933258000	-0.332770000
1	-2.357561000	0.933190000	-0.664161000
1	-1.119216000	-1.882898000	-0.956952000
1	-0.666715000	-0.490961000	-1.945360000
1	1.758133000	0.413772000	1.703486000
1	3.405199000	2.287544000	0.351945000
1	-5.567848000	-2.272380000	0.416853000
1	-7.840483000	-1.482150000	0.964455000
1	-8.388735000	0.936460000	0.808532000
1	-6.637800000	2.545503000	0.093010000
1	-4.379184000	1.762267000	-0.458533000
1	5.787568000	2.334396000	0.068880000
1	7.961862000	1.185035000	-0.098626000
1	8.086872000	-1.291158000	0.080943000
1	6.009291000	-2.608623000	0.423329000
1	3.828730000	-1.475879000	0.587319000
1	-0.169707000	-0.478796000	0.966372000

Zero-point correction= 0.298589 (Hartree/Particle)
Thermal correction to Energy= 0.317043
Thermal correction to Enthalpy= 0.317987
Thermal correction to Gibbs Free Energy= 0.245356
Sum of electronic and zero-point Energies= -825.958978
Sum of electronic and thermal Energies= -825.940523
Sum of electronic and thermal Enthalpies= -825.939579
Sum of electronic and thermal Free Energies= -826.012210

	E (Thermal) KCal/Mol	CV Cal/Mol-Kelvin	S Cal/Mol-Kelvin
Total	198.948	70.265	152.864

#B3LYP/6-311+G**	**190a**

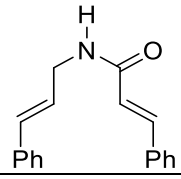

0 1

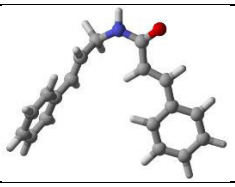

xyz-matrix

6	-2.175549000	0.701964000	-0.874978000
6	-1.813067000	1.901818000	-0.406730000
6	-0.843031000	2.816931000	-1.108678000
7	0.168369000	3.410644000	-0.233729000
6	1.328017000	2.853594000	0.255158000
6	1.554562000	1.411106000	-0.024217000
8	2.119580000	3.540501000	0.891423000
6	2.716464000	0.836915000	0.325365000
6	-3.133581000	-0.244718000	-0.284087000
6	-3.445050000	-1.418833000	-0.987281000
6	-4.345783000	-2.350054000	-0.476153000
6	-4.954576000	-2.127511000	0.756278000
6	-4.652852000	-0.966264000	1.470945000
6	-3.755227000	-0.037445000	0.959109000
6	3.111501000	-0.561263000	0.145459000
6	4.437091000	-0.927990000	0.431012000
6	4.871402000	-2.240796000	0.270226000
6	3.984014000	-3.218586000	-0.173305000
6	2.659403000	-2.873301000	-0.452340000
6	2.227706000	-1.562773000	-0.294787000
1	-1.727567000	0.366597000	-1.810243000
1	-2.227610000	2.290518000	0.519782000
1	-0.369683000	2.297729000	-1.947933000
1	-1.391972000	3.658888000	-1.544024000
1	0.763146000	0.843909000	-0.496580000
1	3.453319000	1.486419000	0.791499000
1	-2.975570000	-1.599364000	-1.949121000
1	-4.570309000	-3.248343000	-1.040355000
1	-5.654993000	-2.849946000	1.159418000
1	-5.118869000	-0.786745000	2.433465000
1	-3.532605000	0.853092000	1.535195000
1	5.129836000	-0.169361000	0.779625000
1	5.900077000	-2.499888000	0.494011000
1	4.316951000	-4.242959000	-0.296104000
1	1.961609000	-3.632378000	-0.787896000
1	1.192760000	-1.317615000	-0.502425000
1	0.087594000	4.394170000	-0.019571000

Zero-point correction= 0.302655 (Hartree/Particle)
Thermal correction to Energy= 0.320665
Thermal correction to Enthalpy= 0.321609
Thermal correction to Gibbs Free Energy= 0.252185
Sum of electronic and zero-point Energies= -826.032923
Sum of electronic and thermal Energies= -826.014914
Sum of electronic and thermal Enthalpies= -826.013969
Sum of electronic and thermal Free Energies= -826.083394

	E (Thermal) KCal/Mol	CV Cal/Mol-Kelvin	S Cal/Mol-Kelvin
Total	201.220	68.518	146.116

#BU3LYP/6-311+G**	**191a**

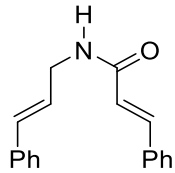

0 3

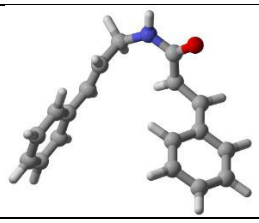

xyz-matrix

6	-2.026644000	1.279308000	-0.661352000
6	-1.445695000	2.165129000	0.156331000
6	-0.575604000	3.301056000	-0.316884000
7	0.705752000	3.409309000	0.378296000
6	1.780945000	2.542109000	0.329257000
6	1.793841000	1.527076000	-0.726298000
8	2.710783000	2.659092000	1.127497000
6	2.875754000	0.551114000	-0.825993000
6	-2.903427000	0.156010000	-0.297466000
6	-3.350876000	-0.706721000	-1.310101000
6	-4.174520000	-1.792191000	-1.022580000
6	-4.571048000	-2.038242000	0.289413000
6	-4.138412000	-1.187249000	1.308725000
6	-3.317550000	-0.103901000	1.020200000
6	2.808882000	-0.785176000	-0.371114000
6	3.934802000	-1.647153000	-0.505277000
6	3.885439000	-2.959591000	-0.071328000
6	2.718871000	-3.471062000	0.511541000
6	1.598809000	-2.643849000	0.653864000
6	1.635281000	-1.327853000	0.225070000
1	-1.840003000	1.377899000	-1.730320000
1	-1.583695000	2.105125000	1.233133000
1	-0.417869000	3.232221000	-1.397796000
1	-1.089432000	4.253409000	-0.148261000
1	1.022964000	1.543821000	-1.492729000
1	3.808715000	0.889703000	-1.273601000
1	-3.044305000	-0.523016000	-2.334841000
1	-4.505032000	-2.444581000	-1.823011000
1	-5.212552000	-2.881534000	0.518279000
1	-4.446062000	-1.368961000	2.332529000
1	-2.999477000	0.546107000	1.826948000
1	4.842394000	-1.255646000	-0.952365000
1	4.757102000	-3.595344000	-0.181705000
1	2.683855000	-4.500133000	0.849783000
1	0.692889000	-3.035251000	1.103630000
1	0.761029000	-0.697060000	0.340098000
1	0.769861000	4.062470000	1.146137000

Zero-point correction= 0.298633 (Hartree/Particle)
Thermal correction to Energy= 0.317006
Thermal correction to Enthalpy= 0.317950
Thermal correction to Gibbs Free Energy= 0.246072
Sum of electronic and zero-point Energies= -825.952917
Sum of electronic and thermal Energies= -825.934545
Sum of electronic and thermal Enthalpies= -825.933600
Sum of electronic and thermal Free Energies= -826.005478

	E (Thermal) KCal/Mol	CV Cal/Mol-Kelvin	S Cal/Mol-Kelvin
Total	198.924	70.280	151.279

#UB3LYP/6-311+G**	***cis*-193a**

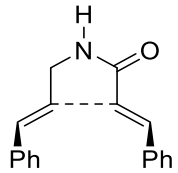

0 3

ν_{imag} = -284.2

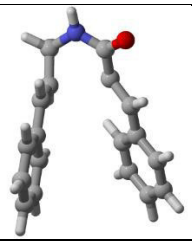

xyz-matrix

1	2.941323000	-2.126598000	2.460453000
1	4.741622000	-2.281778000	0.755257000
6	2.689343000	-2.086291000	1.405996000
6	3.708410000	-2.175723000	0.446871000
1	0.598581000	-1.900291000	1.785651000
6	1.367934000	-1.954787000	1.025530000
6	3.376061000	-2.134477000	-0.921779000
1	-1.474049000	-2.035563000	1.065284000
1	4.160728000	-2.205974000	-1.666935000
6	0.996200000	-1.907206000	-0.363255000
1	-1.140732000	0.316908000	1.978652000
1	0.787343000	1.257655000	1.676171000
1	-3.255336000	-0.675057000	2.301420000
6	2.065931000	-2.006825000	-1.320151000
1	2.828028000	2.561529000	1.313255000
6	-1.494616000	-1.639006000	0.056164000
6	-0.318425000	-1.771264000	-0.801274000
6	-1.863863000	0.531512000	1.199901000
1	1.816077000	-1.976916000	-2.375153000
6	0.799807000	2.012205000	0.899381000
6	-3.259688000	-0.039078000	1.407755000
6	1.958100000	2.748571000	0.693690000
6	-2.813432000	-1.439381000	-0.561708000
8	-3.081510000	-1.804912000	-1.705153000
1	-0.515109000	-1.761292000	-1.867707000
7	-3.714968000	-0.782401000	0.237595000
1	-3.980484000	0.761939000	1.600451000
6	-1.590529000	1.498797000	0.279258000
6	-0.345287000	2.227623000	0.104530000
6	2.011673000	3.722260000	-0.306760000
1	2.918679000	4.294968000	-0.462608000
1	-2.374534000	1.747849000	-0.433731000
6	-0.269221000	3.210258000	-0.903431000
6	0.890397000	3.948676000	-1.105160000
1	-1.136348000	3.388073000	-1.531107000
1	0.921912000	4.699363000	-1.886879000
1	-4.633590000	-0.623898000	-0.147779000

Zero-point correction= 0.297998 (Hartree/Particle)
Thermal correction to Energy= 0.315607
Thermal correction to Enthalpy= 0.316551
Thermal correction to Gibbs Free Energy= 0.248926
Sum of electronic and zero-point Energies= -825.938015
Sum of electronic and thermal Energies= -825.920406
Sum of electronic and thermal Enthalpies= -825.919462
Sum of electronic and thermal Free Energies= -825.987087

	E (Thermal) KCal/Mol	CV Cal/Mol-Kelvin	S Cal/Mol-Kelvin
Total	198.046	68.654	142.330

#UB3LYP/6-311+G**	***trans*-193a**

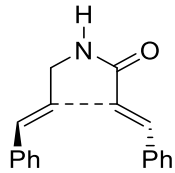

0 3

ν_{imag} = -388.6

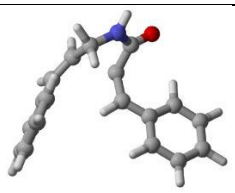

xyz-matrix

1	-0.962135000	2.963750000	-1.158834000
8	2.551190000	2.946395000	-0.029121000
1	1.150722000	1.570290000	-1.896935000
1	-2.272039000	1.319190000	-2.131023000
1	3.544959000	0.694624000	-0.589501000
6	1.432077000	2.460589000	0.064934000
6	-1.211145000	2.113727000	-0.529842000
6	0.928002000	1.376361000	-0.847083000
6	-2.115835000	1.225546000	-1.059109000
1	-3.042761000	-0.877695000	-2.363252000
1	5.475729000	-0.780864000	-0.208737000
7	0.506920000	2.851336000	0.985511000
1	-1.526511000	3.043999000	1.391299000
6	3.385663000	-0.342759000	-0.320329000
6	-0.848785000	2.319958000	0.924866000
6	4.471321000	-1.174877000	-0.098017000
6	-3.265654000	-0.936227000	-1.302994000
6	-2.828935000	0.106656000	-0.456232000
6	0.910134000	-0.025529000	-0.402883000
6	2.055754000	-0.831231000	-0.178870000
1	-0.924876000	1.385430000	1.488133000
1	-4.268775000	-2.822652000	-1.482146000
1	-0.059173000	-0.505512000	-0.287463000
6	-3.956525000	-2.033778000	-0.806947000
6	4.286254000	-2.512231000	0.269318000
6	-3.162563000	0.010654000	0.911624000
1	5.141843000	-3.155094000	0.441332000
1	-2.913111000	0.815140000	1.589748000
6	1.892955000	-2.195776000	0.197357000
6	2.986838000	-3.014252000	0.414972000
6	-4.251856000	-2.120160000	0.554425000
6	-3.858563000	-1.087453000	1.405418000
1	0.888311000	-2.589860000	0.311163000
1	2.836153000	-4.049885000	0.699938000
1	-4.794710000	-2.973433000	0.944265000
1	-4.107255000	-1.131150000	2.460042000
1	0.780841000	3.527891000	1.682713000

Zero-point correction= 0.298915 (Hartree/Particle)
Thermal correction to Energy= 0.316050
Thermal correction to Enthalpy= 0.316994
Thermal correction to Gibbs Free Energy= 0.250884
Sum of electronic and zero-point Energies= -825.935093
Sum of electronic and thermal Energies= -825.917958
Sum of electronic and thermal Enthalpies= -825.917014
Sum of electronic and thermal Free Energies= -825.983124

	E (Thermal) KCal/Mol	CV Cal/Mol-Kelvin	S Cal/Mol-Kelvin
Total	198.324	67.738	139.140

#UB3LYP/6-311+G**	***cis*-192a**

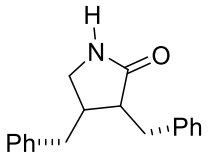

0 3

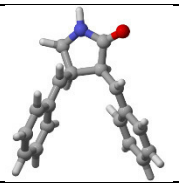

xyz-matrix

6	0.873918000	1.653695000	-0.091879000
6	-0.272278000	1.626681000	0.867568000
6	-1.611408000	1.083838000	0.227133000
6	-1.514916000	-0.064625000	-0.714962000
6	-0.696553000	3.066960000	1.272552000
7	-1.659614000	3.418136000	0.238707000
6	-2.234255000	2.349088000	-0.390733000
8	-3.084273000	2.398293000	-1.256396000
6	2.031959000	0.845378000	-0.056825000
6	3.046115000	1.035767000	-1.042212000
6	4.201469000	0.276042000	-1.046981000
6	4.404512000	-0.711453000	-0.074804000
6	3.424482000	-0.924222000	0.900575000
6	2.263098000	-0.169619000	0.915845000
6	-1.484858000	-1.426491000	-0.339407000
6	-1.381033000	-2.433363000	-1.342605000
6	-1.348184000	-3.776875000	-1.015639000
6	-1.417092000	-4.183464000	0.322773000
6	-1.522208000	-3.217184000	1.328670000
6	-1.554917000	-1.868373000	1.012665000
1	0.799094000	2.371623000	-0.904940000
1	-0.021208000	1.045986000	1.754526000
1	-2.275893000	0.825412000	1.064445000
1	-1.473364000	0.170313000	-1.772766000
1	0.149549000	3.756990000	1.278181000
1	-1.153459000	3.072686000	2.270956000
1	2.896637000	1.797759000	-1.800116000
1	4.953463000	0.446486000	-1.809665000
1	5.309540000	-1.307477000	-0.080294000
1	3.570477000	-1.693269000	1.651271000
1	1.517188000	-0.371187000	1.674463000
1	-1.329320000	-2.126519000	-2.381776000
1	-1.269509000	-4.519442000	-1.802117000
1	-1.391881000	-5.236672000	0.576910000
1	-1.580463000	-3.525368000	2.367097000
1	-1.641623000	-1.142031000	1.812580000
1	-2.014842000	4.350733000	0.091040000

Zero-point correction= 0.301302 (Hartree/Particle)
Thermal correction to Energy= 0.318400
Thermal correction to Enthalpy= 0.319345
Thermal correction to Gibbs Free Energy= 0.252750
Sum of electronic and zero-point Energies= -825.980808
Sum of electronic and thermal Energies= -825.963710
Sum of electronic and thermal Enthalpies= -825.962766
Sum of electronic and thermal Free Energies= -826.029360

	E (Thermal) KCal/Mol	CV Cal/Mol-Kelvin	S Cal/Mol-Kelvin
Total	199.799	67.710	140.160

#UB3LYP/6-311+G**	***trans*-192a**

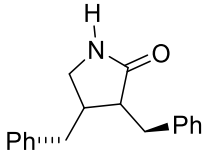

0 3

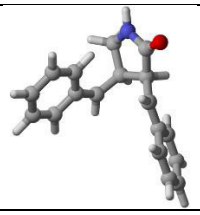

xyz-matrix

1	-4.378078000	-3.125303000	1.289557000
1	-4.101500000	-0.717400000	1.835255000
6	-3.657625000	-2.522827000	0.748810000
1	-2.978002000	-4.147058000	-0.497147000
6	-3.501496000	-1.166994000	1.051532000
6	-2.868972000	-3.095170000	-0.256697000
1	2.208394000	-1.279175000	2.200950000
1	4.302023000	-2.474640000	1.696149000
6	-2.582238000	-0.386146000	0.367378000
1	0.550016000	0.350598000	1.676873000
6	-1.947731000	-2.326915000	-0.944763000
6	2.761369000	-1.045216000	1.297581000
1	-2.479675000	0.655964000	0.637291000
6	3.937594000	-1.715182000	1.013059000
1	-1.338895000	-2.780386000	-1.719945000
6	-1.769234000	-0.939886000	-0.662128000
6	1.045677000	0.622897000	0.751950000
8	-0.404255000	2.953463000	1.876260000
6	2.250407000	-0.039757000	0.426761000
6	4.660831000	-1.417543000	-0.148869000
6	-0.562274000	2.567039000	0.734850000
1	5.582777000	-1.942814000	-0.369281000
6	-0.803991000	-0.218924000	-1.407680000
6	0.404377000	1.688991000	-0.072245000
7	-1.627831000	2.854232000	-0.066630000
1	-0.224060000	-0.809474000	-2.109822000
6	3.005169000	0.242341000	-0.747018000
1	-2.563874000	1.753773000	-1.604672000
6	-0.428182000	1.235275000	-1.348904000
6	4.183401000	-0.433947000	-1.021293000
6	-1.615978000	2.252129000	-1.389887000
1	1.177158000	2.383006000	-0.429777000
1	2.658751000	1.001187000	-1.439302000
1	0.194539000	1.416166000	-2.225611000
1	4.740050000	-0.196619000	-1.921537000
1	-1.446787000	3.007901000	-2.164715000
1	-2.340613000	3.495950000	0.247437000

Zero-point correction= 0.301712 (Hartree/Particle)
Thermal correction to Energy= 0.318797
Thermal correction to Enthalpy= 0.319741
Thermal correction to Gibbs Free Energy= 0.253218
Sum of electronic and zero-point Energies= -825.975247
Sum of electronic and thermal Energies= -825.958162
Sum of electronic and thermal Enthalpies= -825.957218
Sum of electronic and thermal Free Energies= -826.023741

	E (Thermal)	CV	S
	KCal/Mol	Cal/Mol-Kelvin	Cal/Mol-Kelvin
Total	200.048	67.600	140.009

#B3LYP/6-311+G**	***cis*-158e**

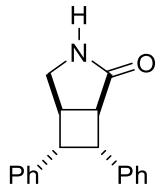

0 1

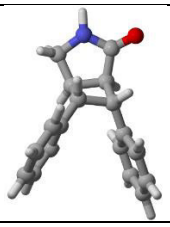

xyz-matrix

6	0.662406000	-0.901471000	-0.270374000
6	1.609851000	-0.710227000	0.953936000
6	2.059599000	0.645687000	0.356840000
6	0.854152000	0.647520000	-0.622747000
6	2.855536000	-1.609300000	1.003177000
7	3.761957000	-0.935235000	0.078632000
6	3.403438000	0.330845000	-0.304085000
8	4.045040000	1.060364000	-1.035300000
6	-0.702257000	-1.514052000	-0.111254000
6	-1.205867000	-2.343830000	-1.122259000
6	-2.469460000	-2.921976000	-1.021757000
6	-3.258409000	-2.682296000	0.101426000
6	-2.772092000	-1.860780000	1.116742000
6	-1.509142000	-1.282243000	1.010138000
6	-0.298493000	1.568544000	-0.300800000
6	-1.253971000	1.820290000	-1.295242000
6	-2.349985000	2.642490000	-1.052196000
6	-2.514964000	3.238555000	0.197587000
6	-1.573432000	3.002147000	1.195358000
6	-0.478202000	2.174452000	0.947614000
1	1.197756000	-1.466758000	-1.038364000
1	1.087032000	-0.663208000	1.907961000
1	2.180364000	1.517120000	1.001155000
1	1.137292000	0.802068000	-1.665919000
1	2.637088000	-2.630381000	0.674415000
1	3.283369000	-1.659568000	2.011433000
1	-0.596227000	-2.541071000	-1.998767000
1	-2.834191000	-3.562397000	-1.817325000
1	-4.241083000	-3.132456000	0.185991000
1	-3.378534000	-1.666324000	1.994497000
1	-1.158176000	-0.639476000	1.808326000
1	-1.131762000	1.368445000	-2.274349000
1	-3.072299000	2.823428000	-1.840562000
1	-3.364535000	3.884496000	0.388173000
1	-1.685732000	3.465388000	2.169597000
1	0.241766000	2.013560000	1.741743000
1	4.651613000	-1.315261000	-0.208656000

Zero-point correction= 0.306479 (Hartree/Particle)
Thermal correction to Energy= 0.322408
Thermal correction to Enthalpy= 0.323352
Thermal correction to Gibbs Free Energy= 0.261146
Sum of electronic and zero-point Energies= -826.029154
Sum of electronic and thermal Energies= -826.013225
Sum of electronic and thermal Enthalpies= -826.012281
Sum of electronic and thermal Free Energies= -826.074487

	E (Thermal) KCal/Mol	CV Cal/Mol-Kelvin	S Cal/Mol-Kelvin
Total	202.314	63.991	130.925

#B3LYP/6-311+G**	***trans*-158e**

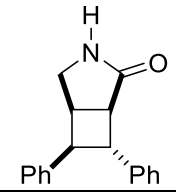

0 1

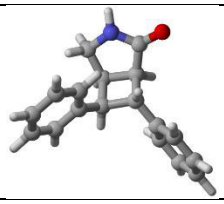

xyz-matrix

6	-0.433122000	-0.143440000	-0.821977000
6	-0.595643000	1.314351000	-1.401012000
6	0.566001000	1.795340000	-0.494367000
6	0.677428000	0.375011000	0.165361000
6	-1.825210000	2.162033000	-1.009091000
7	-1.371206000	2.907798000	0.160880000
6	-0.032707000	2.837405000	0.441589000
8	0.545795000	3.463010000	1.310115000
6	-1.627152000	-0.891064000	-0.285161000
6	-2.165942000	-1.952482000	-1.025052000
6	-3.281501000	-2.655653000	-0.575682000
6	-3.883661000	-2.311110000	0.632767000
6	-3.360317000	-1.258996000	1.382168000
6	-2.245677000	-0.556261000	0.927472000
6	2.010077000	-0.327842000	0.134284000
6	2.529021000	-0.907414000	1.297053000
6	3.754224000	-1.572812000	1.284904000
6	4.486145000	-1.668603000	0.104121000
6	3.983666000	-1.093168000	-1.062942000
6	2.759121000	-0.431103000	-1.046203000
1	0.033164000	-0.763269000	-1.590124000
1	-0.428943000	1.355202000	-2.477206000
1	1.477704000	2.167209000	-0.959474000
1	0.325155000	0.401595000	1.197626000
1	-2.695861000	1.544696000	-0.772181000
1	-2.103033000	2.842996000	-1.821190000
1	-1.698127000	-2.236303000	-1.962548000
1	-3.674394000	-3.476598000	-1.165362000
1	-4.748286000	-2.859284000	0.989422000
1	-3.818695000	-0.984510000	2.325933000
1	-1.858156000	0.259240000	1.527840000
1	1.969010000	-0.831971000	2.223254000
1	4.136577000	-2.012437000	2.199457000
1	5.440553000	-2.182653000	0.091870000
1	4.548243000	-1.157869000	-1.986659000
1	2.389107000	0.014089000	-1.964761000
1	-1.950447000	3.576049000	0.647624000

Zero-point correction= 0.306689 (Hartree/Particle)
Thermal correction to Energy= 0.322650
Thermal correction to Enthalpy= 0.323595
Thermal correction to Gibbs Free Energy= 0.260729
Sum of electronic and zero-point Energies= -826.030579
Sum of electronic and thermal Energies= -826.014618
Sum of electronic and thermal Enthalpies= -826.013674
Sum of electronic and thermal Free Energies= -826.076540

	E (Thermal) KCal/Mol	CV Cal/Mol-Kelvin	S Cal/Mol-Kelvin
Total	202.466	63.880	132.312

#B3LYP-D3/6-311+G**	**Singulett-153e**

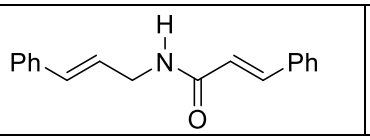

0 1

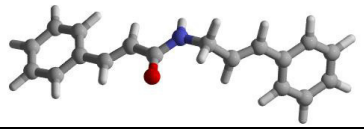

xyz-matrix

6	-3.560948000	-0.887855000	0.563596000
6	-2.389347000	-1.084752000	-0.052184000
6	-1.350635000	-2.064619000	0.416415000
7	-0.080671000	-1.411123000	0.722786000
6	0.998340000	-1.452467000	-0.125606000
6	2.159280000	-0.635780000	0.321491000
8	0.999936000	-2.119293000	-1.153424000
6	3.275278000	-0.580495000	-0.419499000
6	-4.632592000	0.041495000	0.176196000
6	-5.730972000	0.205951000	1.034753000
6	-6.768259000	1.081180000	0.721883000
6	-6.731479000	1.811243000	-0.463657000
6	-5.649437000	1.654106000	-1.332817000
6	-4.615299000	0.780354000	-1.019427000
6	4.503479000	0.164523000	-0.138022000
6	5.535560000	0.144264000	-1.090579000
6	6.724232000	0.837665000	-0.879001000
6	6.907120000	1.565067000	0.294861000
6	5.892396000	1.592606000	1.255015000
6	4.706470000	0.901953000	1.042380000
1	-3.765606000	-1.471331000	1.460712000
1	-2.118668000	-0.519937000	-0.940420000
1	-1.700803000	-2.606774000	1.300152000
1	-1.133026000	-2.796228000	-0.365129000
1	2.068629000	-0.091276000	1.256615000
1	3.263656000	-1.156439000	-1.342074000
1	-5.768701000	-0.359643000	1.960364000
1	-7.604631000	1.190920000	1.403183000
1	-7.537502000	2.491905000	-0.712871000
1	-5.616025000	2.212533000	-2.261775000
1	-3.792347000	0.665055000	-1.714863000
1	5.398042000	-0.422471000	-2.005370000
1	7.506409000	0.808530000	-1.629053000
1	7.831606000	2.105162000	0.464478000
1	6.030597000	2.154215000	2.172144000
1	3.934292000	0.931817000	1.802020000
1	-0.069845000	-0.750461000	1.484995000

Zero-point correction= 0.303064 (Hartree/Particle)
Thermal correction to Energy= 0.321048
Thermal correction to Enthalpy= 0.321992
Thermal correction to Gibbs Free Energy= 0.251757
Sum of electronic and zero-point Energies= -826.067187
Sum of electronic and thermal Energies= -826.049203
Sum of electronic and thermal Enthalpies= -826.048259
Sum of electronic and thermal Free Energies= -826.118493

	E (Thermal) KCal/Mol	CV Cal/Mol-Kelvin	S Cal/Mol-Kelvin
Total	201.461	68.286	147.822

#UB3LYP-D3/6-311+G**	**triplet-153e**

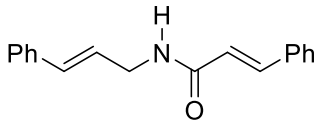

0 3

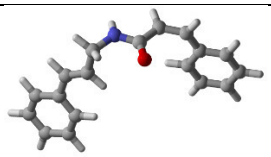

xyz-matrix

6	-3.106954000	1.235744000	-0.031517000
6	-1.858006000	1.392121000	0.421917000
6	-1.091101000	2.683295000	0.341259000
7	0.135586000	2.548865000	-0.444486000
6	1.298519000	2.072363000	0.128417000
6	2.390936000	1.805785000	-0.813164000
8	1.407385000	1.899421000	1.340034000
6	3.675485000	1.280302000	-0.367365000
6	-3.926060000	0.014755000	0.000678000
6	-5.220008000	0.051503000	-0.542127000
6	-6.036375000	-1.077111000	-0.542383000
6	-5.574176000	-2.272527000	0.002642000
6	-4.289444000	-2.326113000	0.548344000
6	-3.476352000	-1.199372000	0.548298000
6	3.978877000	-0.094210000	-0.239455000
6	5.267551000	-0.511993000	0.197928000
6	5.577266000	-1.854434000	0.325610000
6	4.623087000	-2.834872000	0.025070000
6	3.347705000	-2.448505000	-0.403855000
6	3.024923000	-1.108600000	-0.534258000
1	-3.597336000	2.100796000	-0.477165000
1	-1.313764000	0.569177000	0.876432000
1	-1.702174000	3.474228000	-0.101489000
1	-0.786939000	3.005326000	1.339820000
1	2.236299000	2.021921000	-1.870603000
1	4.442801000	2.002466000	-0.093050000
1	-5.588817000	0.978980000	-0.968635000
1	-7.032396000	-1.021496000	-0.967338000
1	-6.205847000	-3.153478000	0.005650000
1	-3.922064000	-3.251776000	0.977464000
1	-2.484812000	-1.264364000	0.980462000
1	6.010146000	0.242344000	0.435541000
1	6.565119000	-2.148457000	0.662812000
1	4.869361000	-3.885277000	0.127333000
1	2.603959000	-3.204265000	-0.631614000
1	2.030299000	-0.819767000	-0.855439000
1	0.032742000	2.467433000	-1.445290000

Zero-point correction= 0.298992 (Hartree/Particle)
Thermal correction to Energy= 0.317307
Thermal correction to Enthalpy= 0.318251
Thermal correction to Gibbs Free Energy= 0.246473
Sum of electronic and zero-point Energies= -825.986909
Sum of electronic and thermal Energies= -825.968594
Sum of electronic and thermal Enthalpies= -825.967650
Sum of electronic and thermal Free Energies= -826.039428

	E (Thermal) KCal/Mol	CV Cal/Mol-Kelvin	S Cal/Mol-Kelvin
Total	199.113	70.064	151.070

#B3LYP-D3/6-311+G**	**190a**

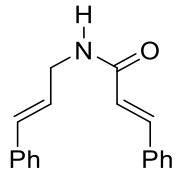

0 1

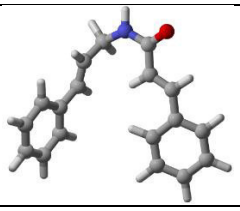

xyz-matrix

6	1.952665000	0.923230000	0.901615000
6	1.659805000	2.122564000	0.386515000
6	0.720383000	3.099555000	1.043320000
7	-0.339387000	3.588671000	0.158088000
6	-1.453063000	2.918652000	-0.298118000
6	-1.531771000	1.468061000	0.012456000
8	-2.313294000	3.512178000	-0.938705000
6	-2.589736000	0.739162000	-0.372067000
6	2.819556000	-0.115868000	0.329611000
6	2.830376000	-1.388183000	0.923118000
6	3.610109000	-2.419290000	0.404823000
6	4.402039000	-2.197140000	-0.719248000
6	4.408950000	-0.934499000	-1.316481000
6	3.630647000	0.093509000	-0.798608000
6	-2.760092000	-0.701672000	-0.170342000
6	-4.041293000	-1.262722000	-0.294236000
6	-4.250990000	-2.624359000	-0.092600000
6	-3.178253000	-3.456303000	0.222000000
6	-1.893997000	-2.916910000	0.328426000
6	-1.685473000	-1.557342000	0.133738000
1	1.477333000	0.649473000	1.843444000
1	2.070393000	2.441419000	-0.567501000
1	0.292598000	2.660995000	1.951549000
1	1.277931000	3.985539000	1.363122000
1	-0.707388000	1.004128000	0.533907000
1	-3.398912000	1.265108000	-0.873010000
1	2.216373000	-1.569054000	1.799878000
1	3.599892000	-3.393913000	0.879823000
1	5.011760000	-2.995941000	-1.125554000
1	5.027737000	-0.751802000	-2.187935000
1	3.658441000	1.068023000	-1.271686000
1	-4.878242000	-0.618845000	-0.543356000
1	-5.249692000	-3.035758000	-0.186018000
1	-3.337026000	-4.518142000	0.372189000
1	-1.051802000	-3.562381000	0.551771000
1	-0.677949000	-1.161327000	0.190822000
1	-0.348550000	4.571687000	-0.071951000

Zero-point correction= 0.303249 (Hartree/Particle)
Thermal correction to Energy= 0.321131
Thermal correction to Enthalpy= 0.322076
Thermal correction to Gibbs Free Energy= 0.252770
Sum of electronic and zero-point Energies= -826.063045
Sum of electronic and thermal Energies= -826.045162
Sum of electronic and thermal Enthalpies= -826.044218
Sum of electronic and thermal Free Energies= -826.113524

#BU3LYP-D3/6-311+G**	**191a**

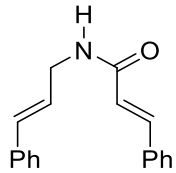

0 3

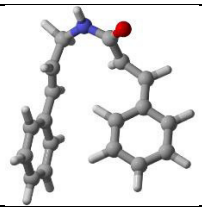

xyz-matrix

6	-0.627640000	2.111960000	-0.678245000
6	0.321337000	2.571092000	0.145322000
6	1.648030000	3.114438000	-0.315409000
7	2.792739000	2.454618000	0.317702000
6	3.061154000	1.095657000	0.305837000
6	2.453298000	0.296744000	-0.759196000
8	3.821579000	0.599473000	1.136185000
6	2.498239000	-1.162542000	-0.738740000
6	-1.905348000	1.487370000	-0.307390000
6	-2.675573000	0.877794000	-1.309569000
6	-3.863533000	0.218270000	-1.005391000
6	-4.309600000	0.156871000	0.312666000
6	-3.558650000	0.765041000	1.321264000
6	-2.373639000	1.423588000	1.016075000
6	1.421437000	-1.977674000	-0.322126000
6	1.532828000	-3.397374000	-0.336288000
6	0.471205000	-4.197539000	0.047943000
6	-0.740717000	-3.625161000	0.458706000
6	-0.872732000	-2.231741000	0.485960000
6	0.184206000	-1.421353000	0.109579000
1	-0.431550000	2.148601000	-1.749128000
1	0.193838000	2.524024000	1.223903000
1	1.727903000	3.052611000	-1.405811000
1	1.731436000	4.176304000	-0.063980000
1	1.994441000	0.802416000	-1.605313000
1	3.421837000	-1.643635000	-1.054231000
1	-2.328437000	0.909125000	-2.337159000
1	-4.436209000	-0.251887000	-1.796713000
1	-5.232568000	-0.357420000	0.554756000
1	-3.899780000	0.724514000	2.349680000
1	-1.808068000	1.888381000	1.814911000
1	2.467220000	-3.847945000	-0.654004000
1	0.578624000	-5.276650000	0.030163000
1	-1.569518000	-4.258528000	0.753325000
1	-1.806497000	-1.776405000	0.797670000
1	0.072652000	-0.345973000	0.135738000
1	3.217063000	2.921705000	1.106809000

Zero-point correction= 0.299266 (Hartree/Particle)
Thermal correction to Energy= 0.317391
Thermal correction to Enthalpy= 0.318335
Thermal correction to Gibbs Free Energy= 0.249252
Sum of electronic and zero-point Energies= -825.986423
Sum of electronic and thermal Energies= -825.968299
Sum of electronic and thermal Enthalpies= -825.967355
Sum of electronic and thermal Free Energies= -826.036438

	E (Thermal) KCal/Mol	CV Cal/Mol-Kelvin	S Cal/Mol-Kelvin
Total	199.166	69.983	145.398

#UB3LYP-D3/6-311+G**	***cis*-193a**

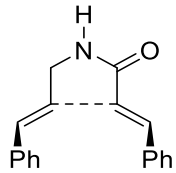

0 3

ν_{imag} = -167.2

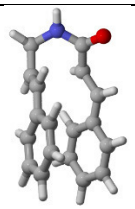

xyz-matrix

1	-2.198115000	-2.375961000	-2.425919000
1	-4.105963000	-2.250665000	-0.839095000
6	-2.016095000	-2.152973000	-1.379900000
6	-3.094512000	-2.083551000	-0.488267000
1	0.094523000	-1.998162000	-1.651586000
6	-0.722761000	-1.936193000	-0.944272000
6	-2.852254000	-1.798790000	0.869637000
1	2.145701000	-1.804257000	-0.843683000
1	-3.684890000	-1.736648000	1.561467000
6	-0.443048000	-1.651791000	0.436055000
1	1.138271000	0.377977000	-2.123680000
1	-0.947715000	0.880659000	-2.049292000
1	3.442962000	-0.048764000	-2.299169000
6	-1.570410000	-1.596429000	1.325013000
1	-3.335889000	1.175703000	-1.597515000
6	2.037497000	-1.276233000	0.096202000
6	0.840924000	-1.415369000	0.920394000
6	1.738869000	0.819269000	-1.335934000
1	-1.391494000	-1.372442000	2.370932000
6	-1.254866000	1.351514000	-1.124612000
6	3.242636000	0.659704000	-1.487244000
6	-2.609025000	1.523306000	-0.872583000
6	3.202152000	-0.573339000	0.650171000
8	3.522603000	-0.650001000	1.834745000
1	0.978193000	-1.234836000	1.981210000
7	3.879501000	0.217239000	-0.247548000
1	3.706924000	1.606824000	-1.782097000
6	1.141690000	1.569820000	-0.377787000
6	-0.286954000	1.771109000	-0.191072000
6	-3.037882000	2.128955000	0.309265000
1	-4.096536000	2.258311000	0.502962000
1	1.778212000	1.999825000	0.393346000
6	-0.738191000	2.385723000	0.993430000
6	-2.093984000	2.562467000	1.241167000
1	-0.009631000	2.711781000	1.728621000
1	-2.416175000	3.033275000	2.163218000
1	4.661568000	0.733528000	0.127176000

Zero-point correction= 0.298635 (Hartree/Particle)
Thermal correction to Energy= 0.316041
Thermal correction to Enthalpy= 0.316985
Thermal correction to Gibbs Free Energy= 0.250674
Sum of electronic and zero-point Energies= -825.975895
Sum of electronic and thermal Energies= -825.958489
Sum of electronic and thermal Enthalpies= -825.957545
Sum of electronic and thermal Free Energies= -826.023857

	E (Thermal) KCal/Mol	CV Cal/Mol-Kelvin	S Cal/Mol-Kelvin
Total	198.319	68.485	139.564

#UB3LYP-D3/6-311+G**	***trans*-193a**

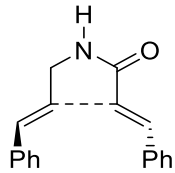

0 3

ν_{imag} = -385.2

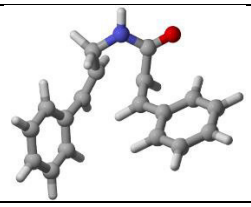

xyz-matrix

1	-0.998924000	3.100483000	-1.058805000
8	2.560962000	2.920705000	-0.052865000
1	1.085543000	1.634728000	-1.922011000
1	-2.329241000	1.485858000	-2.088137000
1	3.450736000	0.660786000	-0.603325000
6	1.432573000	2.461034000	0.058680000
6	-1.227423000	2.211954000	-0.476570000
6	0.868959000	1.427791000	-0.874156000
6	-2.136244000	1.343004000	-1.027917000
1	-2.839817000	-0.833983000	-2.368369000
1	5.328833000	-0.871572000	-0.182790000
7	0.546283000	2.832366000	1.024641000
1	-1.473243000	3.022265000	1.508643000
6	3.255534000	-0.369408000	-0.330493000
6	-0.818416000	2.323570000	0.976953000
6	4.310988000	-1.233441000	-0.086196000
6	-3.070041000	-0.920364000	-1.311623000
6	-2.758893000	0.156773000	-0.454022000
6	0.794805000	0.022571000	-0.450088000
6	1.909181000	-0.817169000	-0.207321000
1	-0.887407000	1.354158000	1.478867000
1	-3.849588000	-2.908608000	-1.505087000
1	-0.191638000	-0.422046000	-0.345073000
6	-3.636016000	-2.091615000	-0.824965000
6	4.078511000	-2.562583000	0.285498000
6	-3.095662000	0.021469000	0.908544000
1	4.910999000	-3.230378000	0.474961000
1	-2.945259000	0.850880000	1.586346000
6	1.697021000	-2.174013000	0.173053000
6	2.761755000	-3.024140000	0.412718000
6	-3.930483000	-2.217459000	0.533885000
6	-3.667583000	-1.150105000	1.392812000
1	0.678534000	-2.535416000	0.273027000
1	2.575229000	-4.053018000	0.700919000
1	-4.374370000	-3.129658000	0.915424000
1	-3.920843000	-1.226360000	2.444417000
1	0.857375000	3.462468000	1.748655000

Zero-point correction= 0.299441 (Hartree/Particle)
Thermal correction to Energy= 0.316422
Thermal correction to Enthalpy= 0.317366
Thermal correction to Gibbs Free Energy= 0.251879
Sum of electronic and zero-point Energies= -825.971139
Sum of electronic and thermal Energies= -825.954158
Sum of electronic and thermal Enthalpies= -825.953213
Sum of electronic and thermal Free Energies= -826.018700

	E (Thermal) KCal/Mol	CV Cal/Mol-Kelvin	S Cal/Mol-Kelvin
Total	198.558	67.486	137.829

#UB3LYP-D3/6-311+G**	***cis*-192a**

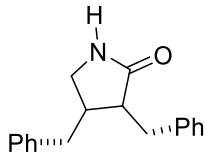

0 3

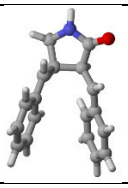

xyz-matrix

6	1.100098000	-1.598486000	0.142411000
6	1.679507000	-0.493155000	0.967079000
6	1.843713000	0.847924000	0.147584000
6	0.743956000	1.202808000	-0.787868000
6	3.152380000	-0.791061000	1.346613000
7	3.883115000	-0.280078000	0.194256000
6	3.210378000	0.664266000	-0.529868000
8	3.624331000	1.249767000	-1.509616000
6	-0.257497000	-1.982041000	0.087840000
6	-0.657073000	-3.030314000	-0.792857000
6	-1.979275000	-3.424081000	-0.891815000
6	-2.966089000	-2.794890000	-0.121931000
6	-2.601377000	-1.764700000	0.751809000
6	-1.280497000	-1.364956000	0.862550000
6	-0.493589000	1.754001000	-0.392119000
6	-1.529486000	1.937582000	-1.351839000
6	-2.768544000	2.432696000	-0.987287000
6	-3.032231000	2.777384000	0.344545000
6	-2.027220000	2.622583000	1.305653000
6	-0.784440000	2.122728000	0.952362000
1	1.788223000	-2.102905000	-0.530903000
1	1.078792000	-0.316001000	1.860018000
1	1.996145000	1.654169000	0.881034000
1	0.898659000	0.978049000	-1.836971000
1	3.332379000	-1.858512000	1.489200000
1	3.433727000	-0.265565000	2.268226000
1	0.099496000	-3.519640000	-1.397639000
1	-2.252631000	-4.222691000	-1.572794000
1	-4.002436000	-3.100712000	-0.205224000
1	-3.359869000	-1.263762000	1.343085000
1	-1.035311000	-0.550623000	1.530547000
1	-1.335804000	1.666310000	-2.384032000
1	-3.541455000	2.552178000	-1.738538000
1	-4.004235000	3.164151000	0.627499000
1	-2.221653000	2.895551000	2.337329000
1	-0.024058000	2.009759000	1.716372000
1	4.857301000	-0.467087000	0.012768000

Zero-point correction= 0.301869 (Hartree/Particle)
Thermal correction to Energy= 0.318753
Thermal correction to Enthalpy= 0.319697
Thermal correction to Gibbs Free Energy= 0.254750
Sum of electronic and zero-point Energies= -826.017094
Sum of electronic and thermal Energies= -826.000210
Sum of electronic and thermal Enthalpies= -825.999266
Sum of electronic and thermal Free Energies= -826.064213

	E (Thermal) KCal/Mol	CV Cal/Mol-Kelvin	S Cal/Mol-Kelvin
Total	200.020	67.476	136.693

#UB3LYP-D3/6-311+G**	***trans*-192a**

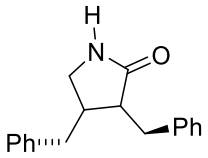

0 3

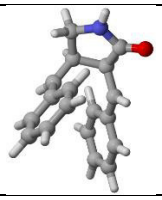

xyz-matrix

6	-0.571852000	-0.195230000	-1.509622000
6	-0.713883000	1.290704000	-1.354143000
6	-0.142399000	1.894946000	-0.003151000
6	0.675796000	0.988908000	0.857527000
6	-2.187736000	1.821576000	-1.419539000
7	-2.418338000	2.434434000	-0.122238000
6	-1.363631000	2.446752000	0.739278000
8	-1.387486000	2.831731000	1.892264000
6	-1.176001000	-1.215201000	-0.737316000
6	-0.879634000	-2.576086000	-1.040184000
6	-1.428212000	-3.615745000	-0.310854000
6	-2.297675000	-3.351791000	0.754444000
6	-2.605465000	-2.025368000	1.074916000
6	-2.062665000	-0.975999000	0.350643000
6	1.940940000	0.474044000	0.502689000
6	2.598035000	-0.448797000	1.365567000
6	3.829969000	-0.986863000	1.038112000
6	4.466260000	-0.629068000	-0.157267000
6	3.846000000	0.281895000	-1.019784000
6	2.610449000	0.823596000	-0.704010000
1	0.123913000	-0.523493000	-2.274242000
1	-0.162078000	1.741543000	-2.178742000
1	0.454451000	2.779302000	-0.266914000
1	0.253755000	0.709738000	1.815761000
1	-2.891886000	1.005249000	-1.597529000
1	-2.301800000	2.552975000	-2.225353000
1	-0.201655000	-2.790839000	-1.859510000
1	-1.179466000	-4.640312000	-0.564819000
1	-2.725142000	-4.166395000	1.327251000
1	-3.272126000	-1.811368000	1.903172000
1	-2.314919000	0.035946000	0.634499000
1	2.110040000	-0.732763000	2.291758000
1	4.305317000	-1.690551000	1.712682000
1	5.431508000	-1.051442000	-0.410960000
1	4.336301000	0.567835000	-1.944160000
1	2.150676000	1.528348000	-1.386866000
1	-3.318415000	2.777711000	0.177695000

Zero-point correction= 0.302100 (Hartree/Particle)
Thermal correction to Energy= 0.319071
Thermal correction to Enthalpy= 0.320015
Thermal correction to Gibbs Free Energy= 0.254552
Sum of electronic and zero-point Energies= -826.012774
Sum of electronic and thermal Energies= -825.995803
Sum of electronic and thermal Enthalpies= -825.994859
Sum of electronic and thermal Free Energies= -826.060322

	E (Thermal) KCal/Mol	CV Cal/Mol-Kelvin	S Cal/Mol-Kelvin
Total	200.220	67.459	137.778

#B3LYP-D3/6-311+G**	***cis*-158e**

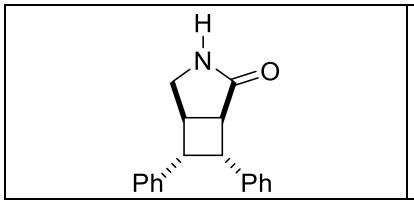

0 1

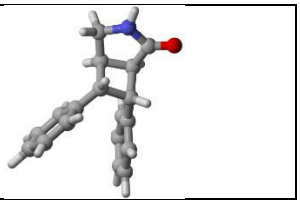

xyz-matrix

6	0.716717000	-0.879675000	-0.244212000
6	1.637625000	-0.607783000	0.984623000
6	2.084935000	0.713396000	0.314246000
6	0.883424000	0.653200000	-0.662459000
6	2.887747000	-1.491302000	1.100608000
7	3.787967000	-0.878975000	0.128090000
6	3.422129000	0.356814000	-0.336335000
8	4.051008000	1.036270000	-1.124252000
6	-0.649594000	-1.478599000	-0.077953000
6	-1.142079000	-2.358144000	-1.050104000
6	-2.423597000	-2.896967000	-0.953186000
6	-3.240184000	-2.563686000	0.125788000
6	-2.763297000	-1.690371000	1.102306000
6	-1.482561000	-1.153550000	1.000133000
6	-0.307001000	1.523857000	-0.348805000
6	-1.338188000	1.606279000	-1.294230000
6	-2.496097000	2.332133000	-1.035750000
6	-2.648127000	2.998339000	0.180537000
6	-1.630371000	2.929975000	1.127916000
6	-0.472363000	2.197308000	0.865045000
1	1.273400000	-1.477050000	-0.971549000
1	1.095877000	-0.509138000	1.923439000
1	2.213394000	1.620235000	0.905573000
1	1.154994000	0.782809000	-1.712067000
1	2.674371000	-2.534094000	0.845308000
1	3.316517000	-1.464073000	2.109059000
1	-0.512811000	-2.621994000	-1.894587000
1	-2.782020000	-3.577079000	-1.718058000
1	-4.238006000	-2.980159000	0.205404000
1	-3.392653000	-1.419877000	1.942900000
1	-1.141364000	-0.459479000	1.757883000
1	-1.232009000	1.084837000	-2.239878000
1	-3.280329000	2.378790000	-1.783129000
1	-3.548323000	3.567059000	0.384167000
1	-1.734008000	3.447398000	2.075439000
1	0.300885000	2.155044000	1.622950000
1	4.673545000	-1.277910000	-0.144484000

Zero-point correction= 0.306947 (Hartree/Particle)
Thermal correction to Energy= 0.322760
Thermal correction to Enthalpy= 0.323705
Thermal correction to Gibbs Free Energy= 0.262215
Sum of electronic and zero-point Energies= -826.067512
Sum of electronic and thermal Energies= -826.051699
Sum of electronic and thermal Enthalpies= -826.050755
Sum of electronic and thermal Free Energies= -826.112244

	E (Thermal) KCal/Mol	CV Cal/Mol-Kelvin	S Cal/Mol-Kelvin
Total	202.535	63.810	129.415

#B3LYP-D3/6-311+G**	**all-*cis*-153e**

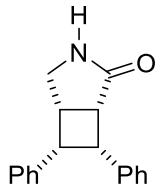

0 1

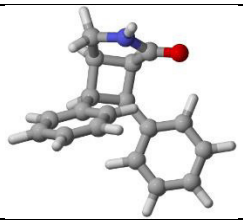

xyz-matrix

6	-0.826627000	0.291158000	-1.458585000
6	-1.316625000	1.776094000	-1.233006000
6	0.101787000	2.170100000	-0.740802000
6	0.648986000	0.820780000	-1.309019000
6	-2.290978000	2.060281000	-0.079968000
7	-1.397499000	2.275633000	1.049491000
6	-0.065310000	2.356486000	0.770193000
8	0.811365000	2.579563000	1.586819000
6	-1.368259000	-0.749088000	-0.507758000
6	-0.923345000	-0.897735000	0.812601000
6	-1.502082000	-1.840982000	1.658795000
6	-2.537484000	-2.657111000	1.206081000
6	-2.987362000	-2.525941000	-0.106356000
6	-2.404446000	-1.582707000	-0.950304000
6	1.736662000	-0.009193000	-0.674152000
6	2.696010000	0.543239000	0.178761000
6	3.723163000	-0.248810000	0.693265000
6	3.807831000	-1.599282000	0.362958000
6	2.856346000	-2.157593000	-0.491073000
6	1.832055000	-1.367657000	-1.004194000
1	-1.037010000	-0.048146000	-2.474479000
1	-1.636653000	2.241353000	-2.164524000
1	0.571962000	3.070723000	-1.140067000
1	0.985270000	1.049986000	-2.326684000
1	-2.962216000	1.216643000	0.103670000
1	-2.896742000	2.952071000	-0.275008000
1	-0.110007000	-0.291381000	1.186614000
1	-1.134883000	-1.941841000	2.674059000
1	-2.983112000	-3.392629000	1.866325000
1	-3.786571000	-3.159187000	-0.475533000
1	-2.758231000	-1.491975000	-1.972918000
1	2.622754000	1.582242000	0.470920000
1	4.453570000	0.194125000	1.361417000
1	4.603795000	-2.213250000	0.769491000
1	2.908180000	-3.208915000	-0.752187000
1	1.087977000	-1.814105000	-1.655037000
1	-1.718426000	2.396112000	1.998340000

Zero-point correction= 0.307520 (Hartree/Particle)
Thermal correction to Energy= 0.323071
Thermal correction to Enthalpy= 0.324015
Thermal correction to Gibbs Free Energy= 0.263655
Sum of electronic and zero-point Energies= -826.064082
Sum of electronic and thermal Energies= -826.048531
Sum of electronic and thermal Enthalpies= -826.047587
Sum of electronic and thermal Free Energies= -826.107947

	E (Thermal) KCal/Mol	CV Cal/Mol-Kelvin	S Cal/Mol-Kelvin
Total	202.730	63.504	127.039

#B3LYP-D3/6-311+G**	***trans*-158e**

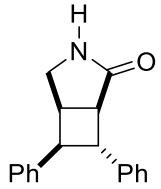

0 1

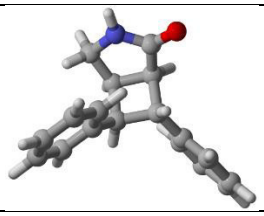

xyz-matrix

6	-0.292797000	-0.286814000	-0.749183000
6	-0.417642000	1.132348000	-1.432825000
6	0.489264000	1.727440000	-0.330064000
6	0.730226000	0.313030000	0.287976000
6	-1.758415000	1.883647000	-1.354058000
7	-1.655824000	2.610959000	-0.094291000
6	-0.435977000	2.592410000	0.520038000
8	-0.158491000	3.136259000	1.572968000
6	-1.550583000	-0.942743000	-0.241546000
6	-2.135568000	-1.973646000	-0.988968000
6	-3.325955000	-2.573644000	-0.583882000
6	-3.957140000	-2.153050000	0.585584000
6	-3.386324000	-1.130464000	1.341467000
6	-2.196860000	-0.530663000	0.931315000
6	2.130038000	-0.235023000	0.201309000
6	2.719135000	-0.851267000	1.309540000
6	4.007126000	-1.381231000	1.235566000
6	4.729967000	-1.301283000	0.047694000
6	4.155258000	-0.687155000	-1.065651000
6	2.868935000	-0.160988000	-0.987396000
1	0.211437000	-0.981196000	-1.422959000
1	-0.016565000	1.135793000	-2.445874000
1	1.381823000	2.287357000	-0.608457000
1	0.391850000	0.250244000	1.322584000
1	-2.610771000	1.198505000	-1.344690000
1	-1.878703000	2.574109000	-2.195995000
1	-1.647754000	-2.312302000	-1.897654000
1	-3.755911000	-3.372902000	-1.177461000
1	-4.880916000	-2.620527000	0.907096000
1	-3.866347000	-0.797602000	2.255129000
1	-1.778603000	0.268187000	1.531209000
1	2.165007000	-0.912409000	2.240325000
1	4.445240000	-1.853131000	2.108073000
1	5.732389000	-1.709822000	-0.011127000
1	4.711132000	-0.616718000	-1.994181000
1	2.436963000	0.316253000	-1.861687000
1	-2.417702000	3.133955000	0.310467000

Zero-point correction= 0.307078 (Hartree/Particle)
Thermal correction to Energy= 0.322939
Thermal correction to Enthalpy= 0.323883
Thermal correction to Gibbs Free Energy= 0.261304
Sum of electronic and zero-point Energies= -826.068072
Sum of electronic and thermal Energies= -826.052212
Sum of electronic and thermal Enthalpies= -826.051267
Sum of electronic and thermal Free Energies= -826.113846

	E (Thermal) KCal/Mol	CV Cal/Mol-Kelvin	S Cal/Mol-Kelvin
Total	202.647	63.701	131.707

#B3LYP-D3/6-311+G**	**all-*trans*-158e**

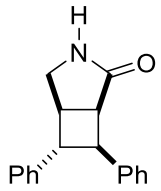

0 1

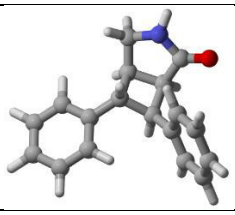

xyz-matrix

6	-0.743168000	0.598310000	0.132851000
6	-0.619105000	2.014160000	-0.504002000
6	0.735081000	1.583428000	-1.126571000
6	0.388362000	0.085979000	-0.816805000
6	-0.312933000	3.173147000	0.455754000
7	1.121952000	3.021848000	0.678571000
6	1.786195000	2.248052000	-0.242257000
8	2.991967000	2.128390000	-0.324749000
6	-2.064126000	-0.124301000	0.120094000
6	-3.275840000	0.571069000	0.179771000
6	-4.492130000	-0.111331000	0.191217000
6	-4.513778000	-1.503700000	0.141732000
6	-3.310899000	-2.207589000	0.083680000
6	-2.097430000	-1.523744000	0.073226000
6	1.416327000	-0.892687000	-0.319174000
6	2.044552000	-0.738400000	0.922568000
6	2.978729000	-1.667692000	1.370251000
6	3.304058000	-2.772739000	0.584137000
6	2.688876000	-2.938367000	-0.654784000
6	1.754070000	-2.004763000	-1.098736000
1	-0.366493000	0.636151000	1.161087000
1	-1.414452000	2.241264000	-1.212603000
1	0.953604000	1.809428000	-2.170507000
1	-0.081872000	-0.324671000	-1.714348000
1	-0.870886000	3.086340000	1.393205000
1	-0.543827000	4.146589000	0.006462000
1	-3.273445000	1.655421000	0.217244000
1	-5.421736000	0.445467000	0.236094000
1	-5.458371000	-2.035673000	0.147123000
1	-3.317451000	-3.291370000	0.045145000
1	-1.166287000	-2.078325000	0.029307000
1	1.815583000	0.119399000	1.544220000
1	3.458502000	-1.526085000	2.332254000
1	4.032129000	-3.496023000	0.933740000
1	2.934894000	-3.792764000	-1.275669000
1	1.277256000	-2.141012000	-2.064493000
1	1.652417000	3.632818000	1.282027000

Zero-point correction= 0.306990 (Hartree/Particle)
Thermal correction to Energy= 0.322818
Thermal correction to Enthalpy= 0.323763
Thermal correction to Gibbs Free Energy= 0.261849
Sum of electronic and zero-point Energies= -826.068258
Sum of electronic and thermal Energies= -826.052429
Sum of electronic and thermal Enthalpies= -826.051485
Sum of electronic and thermal Free Energies= -826.113399

	E (Thermal) KCal/Mol	CV Cal/Mol-Kelvin	S Cal/Mol-Kelvin
Total	202.572	63.709	130.309

#B3LYP-D3/6-311+G**	**Singulett-153g**

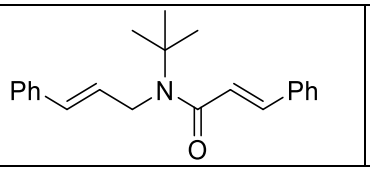

0 1

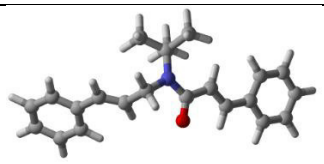

xyz-matrix

6	3.585682000	0.420238000	-0.681476000
6	2.305032000	0.132278000	-0.937736000
6	1.325501000	1.102978000	-1.536990000
7	0.075156000	1.228349000	-0.753054000
6	-0.838815000	0.223304000	-1.024894000
6	-0.032934000	2.256438000	0.346493000
6	-2.208777000	0.266329000	-0.439890000
8	-0.533028000	-0.700142000	-1.781668000
6	-3.026754000	-0.788913000	-0.574302000
6	1.310890000	2.991430000	0.542078000
6	-1.073668000	3.335875000	-0.021043000
6	-0.344502000	1.573518000	1.695974000
6	4.605238000	-0.480268000	-0.122798000
6	5.837636000	0.054702000	0.284349000
6	6.828828000	-0.752504000	0.837740000
6	6.610343000	-2.119558000	0.992042000
6	5.393509000	-2.669667000	0.582578000
6	4.405857000	-1.863389000	0.029404000
6	-4.401450000	-0.908901000	-0.084413000
6	-5.099006000	-2.103947000	-0.326720000
6	-6.408048000	-2.276895000	0.114818000
6	-7.049825000	-1.255080000	0.810792000
6	-6.371167000	-0.059627000	1.061181000
6	-5.065556000	0.111806000	0.620101000
1	3.934567000	1.431972000	-0.887112000
1	1.893964000	-0.851880000	-0.738270000
1	1.775192000	2.084854000	-1.664940000
1	1.037950000	0.743844000	-2.526777000
1	-2.547404000	1.152480000	0.070086000
1	-2.629124000	-1.649432000	-1.105157000
1	1.204983000	3.663528000	1.396166000
1	2.125817000	2.300988000	0.757882000
1	1.581705000	3.605535000	-0.318604000
1	-1.091121000	4.113061000	0.748125000
1	-2.085978000	2.948266000	-0.121908000
1	-0.803204000	3.801575000	-0.971913000
1	0.448414000	0.861942000	1.938845000
1	-0.385706000	2.325131000	2.488960000
1	-1.289049000	1.033409000	1.700291000
1	6.016567000	1.119056000	0.168071000
1	7.771114000	-0.313433000	1.146427000
1	7.379619000	-2.752351000	1.419778000
1	5.218274000	-3.734637000	0.688555000
1	3.475839000	-2.313351000	-0.297378000
1	-4.603750000	-2.902336000	-0.869166000
1	-6.925809000	-3.208204000	-0.085093000
1	-8.069081000	-1.385364000	1.156166000
1	-6.865090000	0.739649000	1.602423000
1	-4.558641000	1.047507000	0.825546000

Zero-point correction= 0.415620 (Hartree/Particle)
Thermal correction to Energy= 0.438659
Thermal correction to Enthalpy= 0.439603
Thermal correction to Gibbs Free Energy= 0.359568
Sum of electronic and zero-point Energies= -983.245002
Sum of electronic and thermal Energies= -983.221963
Sum of electronic and thermal Enthalpies= -983.221019
Sum of electronic and thermal Free Energies= -983.301054

	E (Thermal) KCal/Mol	CV Cal/Mol-Kelvin	S Cal/Mol-Kelvin
Total	275.263	89.210	168.447

#UB3LYP-D3/6-311+G**	**triplet-153g**

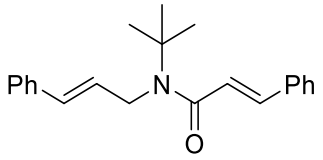

0 3

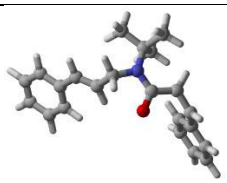

xyz-matrix

6	-3.084259000	0.512642000	0.665744000
6	-1.782122000	0.556297000	0.968100000
6	-1.041665000	1.813384000	1.333995000
7	0.175401000	2.019849000	0.516797000
6	1.262476000	1.280778000	0.970495000
6	0.100300000	2.763930000	-0.791898000
6	2.582977000	1.381690000	0.343063000
8	1.140451000	0.523897000	1.943026000
6	3.661315000	0.495438000	0.775277000
6	-1.342181000	3.235993000	-1.070549000
6	0.974821000	4.034688000	-0.740195000
6	0.486641000	1.837641000	-1.965565000
6	-3.880135000	-0.674319000	0.319410000
6	-5.210615000	-0.504446000	-0.094877000
6	-6.004133000	-1.594377000	-0.445280000
6	-5.482791000	-2.884639000	-0.386830000
6	-4.162360000	-3.071862000	0.028675000
6	-3.372187000	-1.983828000	0.379058000
6	3.916431000	-0.779896000	0.223404000
6	5.011382000	-1.562928000	0.687047000
6	5.273132000	-2.812056000	0.152471000
6	4.459523000	-3.336113000	-0.860351000
6	3.372807000	-2.587913000	-1.328164000
6	3.100306000	-1.336758000	-0.801428000
1	-3.640215000	1.449855000	0.662010000
1	-1.173337000	-0.341915000	0.983581000
1	-1.686575000	2.685291000	1.258119000
1	-0.712786000	1.739352000	2.371955000
1	2.802581000	2.124955000	-0.411464000
1	4.292636000	0.836451000	1.593758000
1	-1.356007000	3.717689000	-2.050441000
1	-2.046632000	2.404873000	-1.096817000
1	-1.685089000	3.974236000	-0.343352000
1	0.871002000	4.595545000	-1.673093000
1	2.033772000	3.827747000	-0.596211000
1	0.648707000	4.674557000	0.083356000
1	-0.182059000	0.973675000	-1.989780000
1	0.387320000	2.375182000	-2.912316000
1	1.510025000	1.471639000	-1.901343000
1	-5.625925000	0.497384000	-0.142581000
1	-7.028831000	-1.434852000	-0.762254000
1	-6.096806000	-3.736428000	-0.656263000
1	-3.749745000	-4.073204000	0.084905000
1	-2.354721000	-2.154324000	0.710444000
1	5.642788000	-1.165188000	1.474523000
1	6.112567000	-3.390046000	0.523188000
1	4.666890000	-4.315711000	-1.274948000
1	2.734767000	-2.993120000	-2.106042000
1	2.246285000	-0.773829000	-1.160346000

Zero-point correction= 0.411675 (Hartree/Particle)
Thermal correction to Energy= 0.434954
Thermal correction to Enthalpy= 0.435898
Thermal correction to Gibbs Free Energy= 0.354848
Sum of electronic and zero-point Energies= -983.166047
Sum of electronic and thermal Energies= -983.142769
Sum of electronic and thermal Enthalpies= -983.141824
Sum of electronic and thermal Free Energies= -983.222874

	E (Thermal) KCal/Mol	CV Cal/Mol-Kelvin	S Cal/Mol-Kelvin
Total	272.937	90.934	170.584

#B3LYP-D3/6-311+G**	**190b**

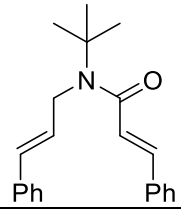

0 1

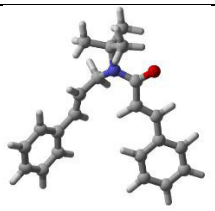

xyz-matrix

6	-0.325956000	-1.873352000	0.893153000
6	0.955067000	-1.678491000	0.559045000
6	1.802026000	-0.582272000	1.146792000
7	2.505004000	0.248669000	0.143660000
6	1.949877000	1.482907000	-0.165852000
6	3.967393000	-0.005598000	-0.100584000
6	0.460785000	1.551589000	-0.101238000
8	2.615660000	2.454633000	-0.507117000
6	-0.175265000	2.731973000	-0.115561000
6	4.246436000	-1.521434000	-0.046302000
6	4.362901000	0.458789000	-1.517301000
6	4.804853000	0.722191000	0.965698000
6	-1.245046000	-2.896050000	0.374400000
6	-2.604843000	-2.818680000	0.714879000
6	-3.523399000	-3.748570000	0.233643000
6	-3.099268000	-4.782089000	-0.598250000
6	-1.748458000	-4.877517000	-0.940577000
6	-0.832990000	-3.949486000	-0.459427000
6	-1.624805000	2.944379000	-0.101981000
6	-2.115637000	4.258036000	-0.027726000
6	-3.483944000	4.516018000	-0.004213000
6	-4.393043000	3.462026000	-0.058543000
6	-3.921980000	2.148791000	-0.138438000
6	-2.557402000	1.891927000	-0.160508000
1	-0.768872000	-1.191796000	1.619006000
1	1.438831000	-2.305688000	-0.182385000
1	1.188835000	0.058353000	1.783985000
1	2.554688000	-1.007429000	1.813686000
1	-0.092672000	0.623134000	-0.086796000
1	0.443638000	3.625632000	-0.139673000
1	5.301929000	-1.687581000	-0.270970000
1	4.054462000	-1.967822000	0.930473000
1	3.658095000	-2.055167000	-0.796500000
1	5.377257000	0.111943000	-1.731042000
1	4.332998000	1.539360000	-1.617511000
1	3.689594000	0.021170000	-2.259428000
1	4.551550000	0.368296000	1.970038000
1	5.871073000	0.538774000	0.804547000
1	4.621280000	1.795586000	0.914383000
1	-2.943208000	-2.016723000	1.363620000
1	-4.568574000	-3.666366000	0.510291000
1	-3.809985000	-5.509460000	-0.973452000
1	-1.408642000	-5.683142000	-1.581958000
1	0.212005000	-4.049032000	-0.728673000
1	-1.411537000	5.082520000	0.012865000
1	-3.838864000	5.538774000	0.054392000
1	-5.459097000	3.658279000	-0.042757000
1	-4.624093000	1.323904000	-0.188765000
1	-2.214817000	0.866215000	-0.232715000

Zero-point correction= 0.415075 (Hartree/Particle)
Thermal correction to Energy= 0.438238
Thermal correction to Enthalpy= 0.439182
Thermal correction to Gibbs Free Energy= 0.359062
Sum of electronic and zero-point Energies= -983.249686
Sum of electronic and thermal Energies= -983.226523
Sum of electronic and thermal Enthalpies= -983.225578
Sum of electronic and thermal Free Energies= -983.305698

	E (Thermal) KCal/Mol	CV Cal/Mol-Kelvin	S Cal/Mol-Kelvin
Total	274.998	89.429	168.626

#UB3LYP-D3/6-311+G**	**191b**

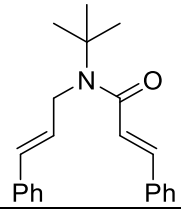

0 3

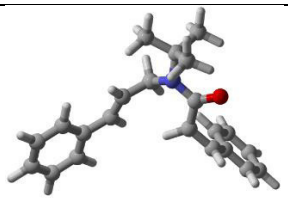

xyz-matrix

6	-2.163888000	-0.638000000	-0.701019000
6	-1.815623000	0.649625000	-0.596391000
6	-0.490778000	1.192076000	-1.060001000
7	0.215725000	2.010913000	-0.055461000
6	1.244646000	1.410961000	0.659544000
6	0.146048000	3.511904000	-0.149179000
6	1.145271000	-0.040176000	0.881855000
8	2.190412000	2.035687000	1.143568000
6	2.284939000	-0.795512000	1.392463000
6	-1.215810000	3.946574000	-0.727353000
6	0.242045000	4.134958000	1.258162000
6	1.277739000	4.023867000	-1.058663000
6	-3.432708000	-1.256730000	-0.290471000
6	-3.529896000	-2.656824000	-0.269448000
6	-4.703727000	-3.292614000	0.127658000
6	-5.811361000	-2.538753000	0.508576000
6	-5.734320000	-1.144479000	0.484085000
6	-4.562786000	-0.511400000	0.086748000
6	3.186809000	-1.523454000	0.584285000
6	4.272352000	-2.235332000	1.170062000
6	5.159598000	-2.954733000	0.389303000
6	5.008665000	-2.998048000	-1.002833000
6	3.951535000	-2.303879000	-1.603167000
6	3.057027000	-1.580868000	-0.832489000
1	-1.434177000	-1.329577000	-1.121570000
1	-2.492155000	1.371335000	-0.150601000
1	0.154554000	0.368820000	-1.374899000
1	-0.628866000	1.800856000	-1.956048000
1	0.180514000	-0.531650000	0.789025000
1	2.460607000	-0.775231000	2.466454000
1	-1.254818000	5.037690000	-0.726972000
1	-1.377366000	3.623663000	-1.756913000
1	-2.043574000	3.585524000	-0.112802000
1	0.061442000	5.210488000	1.183134000
1	1.216555000	3.975399000	1.709817000
1	-0.522214000	3.705439000	1.911693000
1	1.187192000	3.598141000	-2.062994000
1	1.229914000	5.113015000	-1.148880000
1	2.247940000	3.748149000	-0.645989000
1	-2.671225000	-3.252000000	-0.563482000
1	-4.752337000	-4.375704000	0.138467000
1	-6.727727000	-3.029301000	0.816195000
1	-6.594958000	-0.549878000	0.769839000
1	-4.530139000	0.571500000	0.059498000
1	4.397821000	-2.203559000	2.247152000
1	5.979208000	-3.487177000	0.859317000
1	5.706486000	-3.562157000	-1.610497000
1	3.833131000	-2.329925000	-2.681020000
1	2.246149000	-1.040724000	-1.308615000

Zero-point correction= 0.410921 (Hartree/Particle)
Thermal correction to Energy= 0.434404
Thermal correction to Enthalpy= 0.435348
Thermal correction to Gibbs Free Energy= 0.353092
Sum of electronic and zero-point Energies= -983.169631
Sum of electronic and thermal Energies= -983.146148
Sum of electronic and thermal Enthalpies= -983.145203
Sum of electronic and thermal Free Energies= -983.227460

	E (Thermal) KCal/Mol	CV Cal/Mol-Kelvin	S Cal/Mol-Kelvin
Total	272.593	91.182	173.123

#UB3LYP-D3/6-311+G**	***cis*-193b**

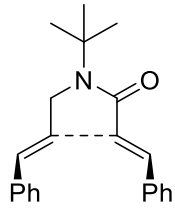

0 3

ν_{imag} = -66.1

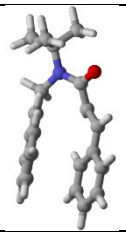

xyz-matrix

1	-2.688534000	0.646241000	2.189058000
1	-4.937531000	-0.104467000	2.019502000
1	-2.082722000	-0.981514000	2.269260000
1	1.999282000	0.883939000	2.035962000
1	-0.004045000	0.135609000	2.258666000
1	-4.390853000	1.565887000	1.741641000
6	-2.104957000	-0.086109000	1.634874000
1	4.268296000	1.632351000	1.504851000
6	-0.689549000	0.431024000	1.470475000
6	2.168855000	1.443516000	1.125286000
6	-4.858041000	0.694288000	1.277252000
1	-5.870913000	0.990094000	0.995798000
6	3.456651000	1.867314000	0.825813000
1	3.500088000	-2.099239000	2.411020000
6	-0.263835000	1.234278000	0.479167000
6	1.099255000	1.710824000	0.252262000
1	-5.127191000	-1.703902000	0.024125000
1	1.180372000	-2.105613000	1.621512000
1	-0.976237000	1.500450000	-0.297698000
7	-2.786948000	-0.372130000	0.362382000
6	-4.122700000	0.225146000	0.009647000
6	3.712473000	2.579722000	-0.346901000
6	3.292022000	-1.940373000	1.358068000
1	4.719896000	2.906261000	-0.578629000
1	-0.895654000	-2.324914000	0.773605000
6	1.374231000	2.430956000	-0.923710000
6	1.983284000	-1.940758000	0.914312000
6	-5.000666000	-0.855069000	-0.653632000
6	2.662985000	2.862811000	-1.219981000
6	-3.928507000	1.429970000	-0.929691000
1	-4.565935000	-1.210667000	-1.584342000
1	5.375407000	-1.732547000	0.822759000
1	0.564834000	2.639561000	-1.615857000
6	-0.838243000	-1.730688000	-0.131080000
6	4.352395000	-1.735641000	0.465684000
6	-2.033105000	-1.016724000	-0.598771000
1	2.849385000	3.413542000	-2.135276000
1	-5.988532000	-0.438845000	-0.868586000
6	1.671086000	-1.745484000	-0.473650000
6	0.367200000	-1.732280000	-0.966543000
6	4.077353000	-1.538849000	-0.900413000
8	-2.299718000	-1.004640000	-1.804615000
6	2.781219000	-1.550125000	-1.363262000
1	0.206280000	-1.626139000	-2.034003000
1	4.894402000	-1.373500000	-1.593956000
1	2.576397000	-1.391309000	-2.416401000
1	-3.323876000	2.200595000	-0.442146000
1	-4.897462000	1.871365000	-1.180937000
1	-3.435205000	1.122307000	-1.850932000

Zero-point correction= 0.410812 (Hartree/Particle)
Thermal correction to Energy= 0.433394
Thermal correction to Enthalpy= 0.434338
Thermal correction to Gibbs Free Energy= 0.357521
Sum of electronic and zero-point Energies= -983.165921
Sum of electronic and thermal Energies= -983.143339
Sum of electronic and thermal Enthalpies= -983.142394
Sum of electronic and thermal Free Energies= -983.219212

	E (Thermal) KCal/Mol	CV Cal/Mol-Kelvin	S Cal/Mol-Kelvin
Total	271.959	89.579	161.677

#UB3LYP-D3/6-311+G**	***trans*-193b**

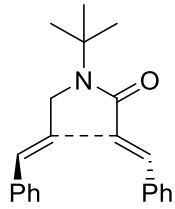

0 3

ν_{imag} = -260.8

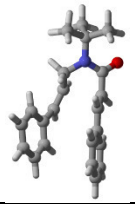

xyz-matrix

6	-0.468237000	0.862477000	-1.796459000
6	0.842037000	0.581308000	-1.545053000
6	0.868604000	-1.611365000	-0.502375000
6	-0.101421000	-1.299969000	0.553091000
6	1.662476000	1.004766000	-0.353089000
7	2.623141000	-0.044043000	0.027367000
6	2.303901000	-1.328585000	-0.375144000
8	3.136466000	-2.203917000	-0.623452000
6	4.006208000	0.325121000	0.463002000
6	3.965794000	1.673676000	1.209028000
6	4.538968000	-0.726017000	1.455890000
6	4.924613000	0.429150000	-0.766960000
6	-1.466929000	1.517890000	-0.962334000
6	-2.815297000	1.133690000	-1.111865000
6	-3.817427000	1.700416000	-0.335292000
6	-3.507633000	2.691904000	0.595046000
6	-2.184239000	3.115032000	0.731800000
6	-1.177880000	2.540931000	-0.036171000
6	-1.469311000	-1.551905000	0.498393000
6	-2.317771000	-1.160884000	1.590876000
6	-3.671073000	-1.409999000	1.574391000
6	-4.266249000	-2.062541000	0.478940000
6	-3.466534000	-2.449944000	-0.607610000
6	-2.108483000	-2.202198000	-0.613212000
1	-0.858536000	0.462364000	-2.729085000
1	1.421705000	0.162612000	-2.362577000
1	0.638601000	-2.385509000	-1.224052000
1	0.289060000	-0.820254000	1.444889000
1	1.020591000	1.269074000	0.489940000
1	2.216417000	1.905449000	-0.628749000
1	4.947310000	1.861875000	1.648967000
1	3.741967000	2.518483000	0.554893000
1	3.230700000	1.654337000	2.018063000
1	4.653217000	-1.701252000	0.990333000
1	3.857519000	-0.821932000	2.305934000
1	5.512049000	-0.400882000	1.833109000
1	4.544134000	1.177676000	-1.469161000
1	5.934420000	0.727678000	-0.470267000
1	4.976377000	-0.534055000	-1.275662000
1	-3.064886000	0.356244000	-1.824151000
1	-4.841082000	1.364639000	-0.453487000
1	-4.288811000	3.139558000	1.198722000
1	-1.938295000	3.907180000	1.430450000
1	-0.168493000	2.920044000	0.051717000
1	-1.868837000	-0.651156000	2.436586000
1	-4.285173000	-1.096948000	2.411546000
1	-5.331257000	-2.261562000	0.472906000
1	-3.921437000	-2.949778000	-1.456279000
1	-1.515692000	-2.501958000	-1.467904000

Zero-point correction= 0.411221 (Hartree/Particle)
Thermal correction to Energy= 0.433664
Thermal correction to Enthalpy= 0.434608
Thermal correction to Gibbs Free Energy= 0.357949
Sum of electronic and zero-point Energies= -983.161616
Sum of electronic and thermal Energies= -983.139172
Sum of electronic and thermal Enthalpies= -983.138228
Sum of electronic and thermal Free Energies= -983.214888

	E (Thermal) KCal/Mol	CV Cal/Mol-Kelvin	S Cal/Mol-Kelvin
Total	272.128	89.135	161.344

#UB3LYP-D3/6-311+G**	***cis*-192b**

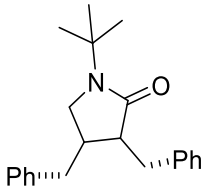

0 3

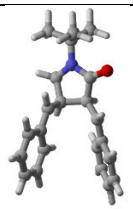

xyz-matrix

1	-3.585554000	-2.735804000	-2.321943000
1	-5.367916000	-2.853240000	-0.594743000
6	-3.359810000	-2.476442000	-1.293087000
6	-4.365074000	-2.545713000	-0.322281000
1	-1.316971000	-2.031590000	-1.724339000
6	-2.076968000	-2.078703000	-0.953176000
6	-4.061456000	-2.218942000	1.005666000
1	-4.834474000	-2.272515000	1.764398000
6	-1.743729000	-1.731499000	0.387322000
6	-2.782712000	-1.825512000	1.356825000
1	0.736186000	-1.860154000	-0.900293000
1	-2.557573000	-1.567595000	2.386067000
6	-0.460302000	-1.286607000	0.770061000
1	4.577758000	-2.059442000	0.426555000
6	0.659091000	-1.034502000	-0.175772000
1	-2.098837000	0.607773000	-1.504679000
1	-0.011669000	0.176198000	-1.890395000
1	-0.275567000	-1.077188000	1.817480000
1	-4.337196000	1.552718000	-1.285321000
1	2.325391000	-0.150357000	-2.294202000
8	2.378047000	-1.604146000	1.469262000
6	2.038257000	-0.961498000	0.490011000
6	0.612812000	0.298814000	-1.004150000
1	4.160890000	-0.188749000	2.155712000
6	4.960832000	-1.304584000	-0.260068000
6	-2.247568000	1.455890000	-0.850471000
1	4.781179000	-1.637079000	-1.286861000
6	2.098444000	0.438438000	-1.394637000
6	-3.519459000	1.987467000	-0.721209000
7	2.811849000	-0.083549000	-0.223957000
1	6.041036000	-1.217794000	-0.114472000
6	4.282674000	0.055066000	-0.007718000
6	4.537331000	0.533097000	1.433316000
6	0.160862000	1.468667000	-0.187522000
1	5.611055000	0.665778000	1.593023000
6	-1.150970000	1.984051000	-0.111215000
1	2.362109000	1.476232000	-1.592727000
6	-3.760475000	3.066050000	0.136999000
1	-4.759391000	3.474800000	0.235085000
6	4.855157000	1.096167000	-0.981345000
1	0.910729000	1.916579000	0.459147000
1	4.043377000	1.493301000	1.606436000
6	-1.424842000	3.084138000	0.754413000
6	-2.698906000	3.609466000	0.872110000
1	-0.609714000	3.507785000	1.332163000
1	-2.876340000	4.444788000	1.540742000
1	4.705366000	0.811256000	-2.025609000
1	5.930858000	1.177347000	-0.811654000
1	4.418819000	2.085100000	-0.820396000

Zero-point correction= 0.414052 (Hartree/Particle)
Thermal correction to Energy= 0.436206
Thermal correction to Enthalpy= 0.437150
Thermal correction to Gibbs Free Energy= 0.360583
Sum of electronic and zero-point Energies= -983.213844
Sum of electronic and thermal Energies= -983.191690
Sum of electronic and thermal Enthalpies= -983.190746
Sum of electronic and thermal Free Energies= -983.267313

	E (Thermal) KCal/Mol	CV Cal/Mol-Kelvin	S Cal/Mol-Kelvin
Total	273.723	88.492	161.150

#UB3LYP-D3/6-311+G**	***trans*-192b**

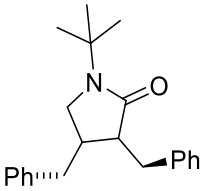

0 3

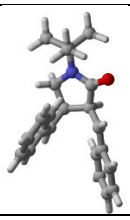

xyz-matrix

1	4.613744000	-2.319037000	1.931069000
6	4.285255000	-1.878666000	0.995700000
1	2.215897000	-2.142594000	1.453330000
1	6.291076000	-1.499066000	0.292024000
6	2.930199000	-1.777438000	0.725069000
6	5.232540000	-1.419697000	0.073611000
1	0.083301000	-2.511691000	0.389722000
1	0.135668000	-1.255488000	2.273058000
1	-4.218723000	-2.801963000	0.317816000
1	-2.125054000	-0.990966000	2.409071000
6	2.463515000	-1.208773000	-0.494004000
6	4.799879000	-0.860431000	-1.135601000
6	-0.024697000	-1.453532000	0.110342000
6	-0.184432000	-0.625654000	1.442977000
1	1.432691000	0.627297000	2.255475000
1	5.527935000	-0.505200000	-1.856716000
6	-1.725866000	-0.417759000	1.567883000
6	1.093568000	-1.074844000	-0.804367000
6	3.449199000	-0.757567000	-1.417757000
6	-4.325856000	-2.066063000	-0.484165000
6	-1.388575000	-1.362384000	-0.576893000
1	-5.390279000	-1.959588000	-0.710509000
6	0.627479000	0.634314000	1.528682000
7	-2.307329000	-0.873110000	0.305166000
8	-1.596882000	-1.690158000	-1.735128000
1	-3.814746000	-2.436901000	-1.370676000
1	-1.956338000	0.634983000	1.742426000
6	-3.753388000	-0.707356000	-0.041292000
1	0.817329000	-0.677680000	-1.774060000
1	3.121851000	-0.321825000	-2.355679000
1	-3.334585000	0.019321000	-2.050474000
6	-4.534058000	-0.224876000	1.191943000
1	2.111251000	2.813659000	1.789155000
6	0.507035000	1.803474000	0.741317000
6	-3.887013000	0.335961000	-1.165991000
1	-4.939328000	0.459224000	-1.436466000
6	1.377553000	2.903112000	0.994900000
1	-1.104433000	1.150645000	-0.566876000
6	-0.432947000	1.958208000	-0.316303000
1	-3.506088000	1.306408000	-0.835824000
6	1.307116000	4.067862000	0.251473000
1	1.985778000	4.885491000	0.468387000
6	-0.495414000	3.129192000	-1.054171000
6	0.368216000	4.194862000	-0.779791000
1	-1.219418000	3.213410000	-1.857491000
1	0.314945000	5.106898000	-1.362727000
1	-5.588420000	-0.136759000	0.921412000
1	-4.200619000	0.755809000	1.537224000
1	-4.462918000	-0.933030000	2.020824000

Zero-point correction= 0.414579 (Hartree/Particle)
Thermal correction to Energy= 0.436743
Thermal correction to Enthalpy= 0.437688
Thermal correction to Gibbs Free Energy= 0.360989
Sum of electronic and zero-point Energies= -983.209913
Sum of electronic and thermal Energies= -983.187748
Sum of electronic and thermal Enthalpies= -983.186804
Sum of electronic and thermal Free Energies= -983.263503

	E (Thermal) KCal/Mol	CV Cal/Mol-Kelvin	S Cal/Mol-Kelvin
Total	274.061	88.427	161.426

#B3LYP-D3/6-311+G**	***cis*-158g**

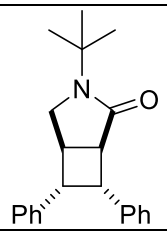

0 1

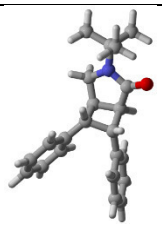

xyz-matrix

6	0.177747000	-0.624039000	0.164893000
6	-0.623014000	-0.157114000	-1.089208000
6	-0.792026000	1.225959000	-0.432060000
6	0.326693000	0.907792000	0.592749000
6	-2.028280000	-0.736291000	-1.236661000
7	-2.817407000	0.021801000	-0.255080000
6	-2.193252000	1.170312000	0.167593000
8	-2.666282000	2.022539000	0.903509000
6	-4.244353000	-0.280688000	0.067030000
6	-4.633319000	-1.646449000	-0.520343000
6	-4.420682000	-0.336695000	1.595721000
6	-5.139888000	0.810967000	-0.547795000
6	1.390082000	-1.498936000	0.033795000
6	1.645677000	-2.474604000	1.005410000
6	2.782588000	-3.277722000	0.941415000
6	3.689993000	-3.118810000	-0.104178000
6	3.449079000	-2.152082000	-1.079617000
6	2.312242000	-1.351000000	-1.010043000
6	1.688405000	1.505446000	0.343725000
6	2.667941000	1.364246000	1.336039000
6	3.963218000	1.832200000	1.141939000
6	4.309456000	2.457231000	-0.056309000
6	3.346766000	2.607306000	-1.050686000
6	2.049587000	2.133110000	-0.851946000
1	-0.515960000	-1.092990000	0.868110000
1	-0.049067000	-0.189701000	-2.013814000
1	-0.697337000	2.139930000	-1.018677000
1	0.042763000	1.089505000	1.631480000
1	-2.042499000	-1.806223000	-1.018942000
1	-2.422800000	-0.591192000	-2.250105000
1	-5.680974000	-1.842032000	-0.281917000
1	-4.531156000	-1.673569000	-1.607594000
1	-4.038854000	-2.456655000	-0.091188000
1	-5.455276000	-0.596358000	1.836750000
1	-4.182759000	0.621745000	2.053045000
1	-3.767169000	-1.102288000	2.023646000
1	-5.019333000	0.835976000	-1.634962000
1	-6.190612000	0.604113000	-0.326276000
1	-4.884176000	1.789733000	-0.142637000
1	0.944064000	-2.604854000	1.823668000
1	2.957598000	-4.027193000	1.705469000
1	4.576006000	-3.741254000	-0.158916000
1	4.151512000	-2.016319000	-1.894518000
1	2.155884000	-0.591859000	-1.766162000
1	2.409511000	0.872237000	2.268054000
1	4.703273000	1.709470000	1.924963000
1	5.317592000	2.824967000	-0.210331000
1	3.602257000	3.094513000	-1.985376000
1	1.321657000	2.256535000	-1.645049000

Zero-point correction= 0.419010 (Hartree/Particle)
Thermal correction to Energy= 0.440149
Thermal correction to Enthalpy= 0.441093
Thermal correction to Gibbs Free Energy= 0.367461
Sum of electronic and zero-point Energies= -983.263833
Sum of electronic and thermal Energies= -983.242694
Sum of electronic and thermal Enthalpies= -983.241750
Sum of electronic and thermal Free Energies= -983.315382

	E (Thermal) KCal/Mol	CV Cal/Mol-Kelvin	S Cal/Mol-Kelvin
Total	276.198	84.924	154.971

#B3LYP-D3/6-311+G**	**all-*cis*-158g**

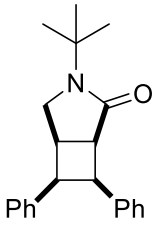

0 1

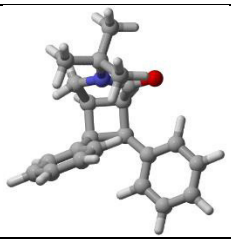

xyz-matrix

6	0.519103000	0.831316000	1.813476000
6	-0.748392000	0.005715000	2.266251000
6	-0.085059000	-1.300408000	1.773952000
6	1.276605000	-0.540811000	1.649183000
6	-2.034569000	0.168350000	1.460069000
7	-1.865772000	-0.743592000	0.323352000
6	-0.873505000	-1.666946000	0.518068000
8	-0.671180000	-2.659675000	-0.168422000
6	-2.900615000	-0.879612000	-0.745467000
6	-3.763920000	0.392019000	-0.784510000
6	-2.222270000	-1.037356000	-2.119097000
6	-3.780474000	-2.102234000	-0.428047000
6	0.322120000	1.761881000	0.641079000
6	0.295473000	1.335093000	-0.692440000
6	0.038759000	2.234284000	-1.725049000
6	-0.201550000	3.579143000	-1.449484000
6	-0.174132000	4.021118000	-0.127856000
6	0.089085000	3.119500000	0.901371000
6	2.300569000	-0.765490000	0.564963000
6	2.373720000	-1.957005000	-0.161926000
6	3.374784000	-2.141019000	-1.117031000
6	4.315708000	-1.142666000	-1.356903000
6	4.252563000	0.047800000	-0.631718000
6	3.254388000	0.231738000	0.319948000
1	0.925228000	1.420718000	2.637818000
1	-0.923353000	0.079132000	3.339122000
1	-0.071148000	-2.174196000	2.427370000
1	1.791051000	-0.708718000	2.602285000
1	-2.168967000	1.197191000	1.123987000
1	-2.914097000	-0.115919000	2.051433000
1	-4.490719000	0.296109000	-1.594073000
1	-4.322251000	0.544681000	0.141833000
1	-3.155420000	1.278127000	-0.980661000
1	-2.992310000	-1.110667000	-2.891999000
1	-1.601512000	-1.929456000	-2.156392000
1	-1.602927000	-0.164788000	-2.336319000
1	-4.266310000	-1.983916000	0.545387000
1	-4.561365000	-2.214526000	-1.185365000
1	-3.176631000	-3.010163000	-0.411806000
1	0.484946000	0.299244000	-0.934392000
1	0.030797000	1.880376000	-2.750129000
1	-0.399813000	4.276206000	-2.255910000
1	-0.351987000	5.065880000	0.102109000
1	0.112657000	3.474272000	1.927428000
1	1.632120000	-2.729126000	-0.006052000
1	3.411722000	-3.068672000	-1.677697000
1	5.089408000	-1.287069000	-2.102825000
1	4.976658000	0.834787000	-0.812143000
1	3.203724000	1.166573000	0.867918000

Zero-point correction= 0.420087 (Hartree/Particle)
Thermal correction to Energy= 0.440752
Thermal correction to Enthalpy= 0.441696
Thermal correction to Gibbs Free Energy= 0.370696
Sum of electronic and zero-point Energies= -983.262367
Sum of electronic and thermal Energies= -983.241702
Sum of electronic and thermal Enthalpies= -983.240758
Sum of electronic and thermal Free Energies= -983.311759

	E (Thermal) KCal/Mol	CV Cal/Mol-Kelvin	S Cal/Mol-Kelvin
Total	276.576	84.424	149.434

#B3LYP-D3/6-311+G**	***trans*-158g**

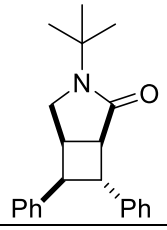

0 1

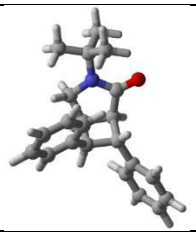

xyz-matrix

6	-0.731569000	0.813920000	-0.772650000
6	-0.052388000	-0.346416000	-1.600195000
6	-0.571216000	-1.370496000	-0.572125000
6	-1.344844000	-0.256450000	0.206301000
6	1.473083000	-0.459216000	-1.575875000
7	1.767113000	-1.205457000	-0.345451000
6	0.668868000	-1.843995000	0.171316000
8	0.660064000	-2.639025000	1.099536000
6	3.160534000	-1.498953000	0.106081000
6	4.142091000	-0.548794000	-0.598307000
6	3.275560000	-1.268360000	1.624423000
6	3.500716000	-2.957697000	-0.249594000
6	0.165738000	1.894395000	-0.227952000
6	0.291784000	3.098732000	-0.933633000
6	1.166590000	4.096353000	-0.509114000
6	1.936049000	3.908645000	0.638408000
6	1.817599000	2.718535000	1.353797000
6	0.942149000	1.722829000	0.924249000
6	-2.847813000	-0.341723000	0.208224000
6	-3.567212000	-0.128391000	1.388121000
6	-4.960732000	-0.182227000	1.399280000
6	-5.660008000	-0.453666000	0.225666000
6	-4.955077000	-0.671502000	-0.958618000
6	-3.564219000	-0.615292000	-0.965047000
1	-1.519407000	1.282491000	-1.365039000
1	-0.445361000	-0.420871000	-2.613969000
1	-1.164222000	-2.222857000	-0.901936000
1	-0.999605000	-0.158683000	1.235906000
1	1.947892000	0.522907000	-1.563185000
1	1.842046000	-1.004152000	-2.453570000
1	5.151750000	-0.763437000	-0.241178000
1	4.141520000	-0.679464000	-1.682722000
1	3.919472000	0.495988000	-0.368765000
1	4.299530000	-1.479065000	1.945299000
1	2.595327000	-1.914207000	2.175609000
1	3.051850000	-0.226524000	1.865762000
1	3.423186000	-3.117164000	-1.329288000
1	4.523970000	-3.192736000	0.056028000
1	2.819170000	-3.641654000	0.256920000
1	-0.305498000	3.254801000	-1.826666000
1	1.243976000	5.020615000	-1.071064000
1	2.616210000	4.683383000	0.973763000
1	2.408375000	2.562136000	2.249837000
1	0.877104000	0.801690000	1.488012000
1	-3.029906000	0.077482000	2.308012000
1	-5.498079000	-0.015256000	2.326287000
1	-6.743146000	-0.498575000	0.232251000
1	-5.490146000	-0.887403000	-1.876915000
1	-3.030408000	-0.790416000	-1.894056000

Zero-point correction= 0.419620 (Hartree/Particle)
Thermal correction to Energy= 0.440588
Thermal correction to Enthalpy= 0.441532
Thermal correction to Gibbs Free Energy= 0.368229
Sum of electronic and zero-point Energies= -983.265675
Sum of electronic and thermal Energies= -983.244707
Sum of electronic and thermal Enthalpies= -983.243763
Sum of electronic and thermal Free Energies= -983.317066

	E (Thermal) KCal/Mol	CV Cal/Mol-Kelvin	S Cal/Mol-Kelvin
Total	276.473	84.614	154.281

#B3LYP-D3/6-311+G**	**all-*trans*-158g**

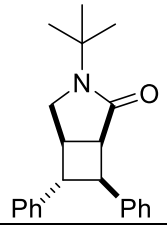

0 1

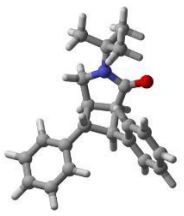

xyz-matrix

6	-0.992033000	-0.660321000	0.122897000
6	-0.060070000	-1.497587000	1.048949000
6	0.473688000	-0.183555000	1.661100000
6	-0.714890000	0.601914000	1.003161000
6	1.136299000	-2.166460000	0.373393000
7	2.089488000	-1.063935000	0.181582000
6	1.839291000	0.002342000	1.018159000
8	2.581673000	0.948111000	1.222419000
6	3.398175000	-1.240523000	-0.515746000
6	3.340993000	-2.486585000	-1.413550000
6	3.670154000	-0.013797000	-1.406017000
6	4.512217000	-1.412365000	0.533290000
6	-2.422814000	-1.079107000	-0.088363000
6	-2.794464000	-2.427259000	-0.086551000
6	-4.118038000	-2.804768000	-0.311498000
6	-5.092775000	-1.835930000	-0.542093000
6	-4.733039000	-0.488315000	-0.548072000
6	-3.410161000	-0.114038000	-0.323527000
6	-0.518935000	1.947816000	0.361093000
6	0.279597000	2.112828000	-0.777415000
6	0.439740000	3.365017000	-1.362649000
6	-0.196668000	4.481270000	-0.820267000
6	-0.992135000	4.333303000	0.313757000
6	-1.149429000	3.076637000	0.895998000
1	-0.511299000	-0.539617000	-0.854096000
1	-0.597399000	-2.159434000	1.727118000
1	0.567465000	-0.076200000	2.741761000
1	-1.506550000	0.679514000	1.753120000
1	0.855256000	-2.618174000	-0.579967000
1	1.573125000	-2.951349000	1.004715000
1	4.294293000	-2.584216000	-1.937400000
1	3.184017000	-3.403731000	-0.841258000
1	2.553774000	-2.403562000	-2.167353000
1	4.616211000	-0.150806000	-1.937023000
1	3.727846000	0.897807000	-0.814995000
1	2.876179000	0.097971000	-2.150096000
1	4.312341000	-2.283422000	1.164562000
1	5.475724000	-1.565022000	0.039311000
1	4.579735000	-0.527373000	1.165763000
1	-2.045604000	-3.191796000	0.092151000
1	-4.387151000	-3.855384000	-0.304094000
1	-6.122716000	-2.127416000	-0.713982000
1	-5.484136000	0.273318000	-0.726833000
1	-3.138855000	0.936187000	-0.331469000
1	0.794895000	1.260948000	-1.204952000
1	1.067662000	3.471155000	-2.240372000
1	-0.070936000	5.456823000	-1.276290000
1	-1.490384000	5.194227000	0.745751000
1	-1.771522000	2.969106000	1.779201000

Zero-point correction= 0.419235 (Hartree/Particle)
Thermal correction to Energy= 0.440278
Thermal correction to Enthalpy= 0.441222
Thermal correction to Gibbs Free Energy= 0.367831
Sum of electronic and zero-point Energies= -983.265532
Sum of electronic and thermal Energies= -983.244489
Sum of electronic and thermal Enthalpies= -983.243545
Sum of electronic and thermal Free Energies= -983.316937

	E (Thermal) KCal/Mol	CV Cal/Mol-Kelvin	S Cal/Mol-Kelvin
Total	276.279	84.763	154.465

4 References

[1] V. V. Pavlishchuk, A. W. Addison, *Inorg. Chim. Acta* **2000**, *298*, 97–102.

[2] a) M.-A. Haga, E. S. Dodsworth, G. Eryavec, P. Seymour, A. B. P. Lever, *Inorg. Chem.* **1985**, *24*, 1901–1906; b) R. J. Crutchley, A. B. P. Lever, *J. Am. Chem. Soc.* **1980**, *102*, 7128–7129.

[3] M. Pirtsch, S. Paria, T. Matsuno, H. Isobe, O. Reiser, *Chem. Eur. J.* **2012**, *18*, 7336–7340.

[4] J. Sun, W. Wu, J. Zhao, *Chem. Eur. J.* **2012**, *18*, 8100–8112.

[5] J. D. Slinker, A. A. Gorodetsky, M. S. Lowry, J. Wang, S. Parker, R. Rohl, S. Bernhard, G. G. Malliaras, *J. Am. Chem. Soc.* **2004**, *126*, 2763–2767.

[6] M. Lee, S. Neukirchen, C. Cabrele, O. Reiser, *J. Pept. Sci.* **2017**, *23*, 556–562.

[7] D.-J. Barrios Antúnez, M. D. Greenhalgh, C. Fallan, A. M. Z. Slawin, A. D. Smith, *Org. Biomol. Chem.* **2016**, *14*, 7268–7274.

[8] S. Zhao, J.-B. Lin, Y.-Y. Zhao, Y.-M. Liang, P.-F. Xu, *Org. Lett.* **2014**, *16*, 1802–1805.

[9] P. Blaney, R. Grigg, Z. Rankovic, M. Thornton-Pett, J. Xu, *Tetrahedron* **2002**, *58*, 1719–1737.

[10] J. D. More, N. S. Finney, *Org. Lett.* **2002**, *4*, 3001–3003.

[11] B. P. Zavesky, N. R. Babij, J. A. Fritz, J. P. Wolfe, *Org. Lett.* **2013**, *15*, 5420–5423.

[12] H. Alinezhad, M. Tajbakhsh, N. Mahdavi, *Synth. Commun.* **2010**, *40*, 951–956.

[13] O. S. Nayal, V. Bhatt, S. Sharma, N. Kumar, *J. Org. Chem.* **2015**, *80*, 5912–5918.

[14] A. A. Nagarkar, M. Yasir, A. Crochet, K. M. Fromm, A. F. M. Kilbinger, *Angew. Chem., Int. Ed.* **2016**, *55*, 12343–12346.

[15] J. Penjisevic, V. Sukalovic, D. Andric, S. Kostic-Rajacic, V. Soskic, G. Roglic, *Archiv der Pharmazie* **2007**, *340*, 456–465.

[16] M. D. Kosobokov, V. V. Levin, A. A. Zemtsov, M. I. Struchkova, A. A. Korlyukov, D. E. Arkhipov, A. D. Dilman, *Org. Lett.* **2014**, *16*, 1438–1441.

[17] M. Sietzen, S. Batke, L. Merz, H. Wadepohl, J. Ballmann, *Organometallics* **2015**, *34*, 1118–1128.

[18] X. Huang, N. Jiao, *Org. Biomol. Chem.* **2014**, *12*, 4324–4328.

[19] N. J. Gesmundo, J.-M. M. Grandjean, D. A. Nicewicz, *Org. Lett.* **2015**, *17*, 1316–1319.

[20] G. W. Langley, A. Brinko, M. Munzel, L. J. Walport, C. J. Schofield, R. J. Hopkinson, *ACS Chem. Biol.* **2016**, *11*, 755–762.

[21] S. P. Raillard, R. A. Scheuerman, S. K. Manthati, PCT/US2014/041406, **2014**.

[22] P. Zhang, H.-R. Hu, Z.-H. Huang, J.-Y. Lei, Y. Chu, D.-Y. Ye, *Bioorg. Med. Chem.* **2012**, *22*, 7232–7236.

[23] P. Kancharla, J. X. Kelly, K. A. Reynolds, *J. Med. Chem.* **2015**, *58*, 7286–7309.

[24] K. Naresh, B. Madhava Reddy, V. Harinadha Babu, *Eur. J. Pharm. Sci.* **2014**, *1*, 446–451.

[25] S. Yamazaki, Y. Iwata, Y. Fukushima, *Org. Biomol. Chem.* **2009**, *7*, 655–659.

[26] A. G. Chittiboyina, C. S. Mizuno, P. V. Desai, A. Patny, T. W. Kurtz, H. A. Pershadsingh, R. C. Speth, V. Karamyan, M. A. Avery, *Med. Chem. Res.* **2009**, *18*, 589–610.

[27] T. Vilaivan, *Tetrahedron Lett.* **2006**, *47*, 6739–6742.

[28] M. Chen, A. Maetzke, Knak Jensen, Svend J., K. V. Gothelf, *Eur. J. Org. Chem.* **2007**, *2007*, 5826–5833.

[29] R. Buchholz, H. Martin R. Hoffmann, *Helv. Chim. Acta* **1991**, *1991*, 1213–1220.

[30] N. de Kimpe, E. Stanoeva, R. Verhé, N. Schamp, *Synthesis* **1988**, *8*, 587–592.

[31] S. G. Davies, D. Diez, S. H. Dominguez, N. M. Garrido, D. Kruchinin, P. D. Price, A. D. Smith, *Org. Biomol. Chem.* **2005**, *3*, 1284–1301.

[32] M. Porel, D. N. Thornlow, N. N. Phan, C. A. Alabi, *Nat. Chem.* **2016**, *8*, 590–596.

[33] B. Emayavaramban, M. Roy, B. Sundararaju, *Chem. Eur. J.* **2016**, *22*, 3952–3955.

[34] S. G. Davies, M. E. C. Polywka, D. R. Fenwick, Frank, R. WO Patent WO/1995/018134, **1995**.

[35] A. Acharya, J. Eickhoff, C. Jeffrey, *Synthesis* **2013**, *45*, 1825–1836.

[36] H. You, H.-S. Youn, I. Im, M.-H. Bae, S.-K. Lee, H. Ko, S. H. Eom, Y.-C. Kim, *Eur. J. Med. Chem.* **2011**, *46*, 1153–1164.

[37] M. Beugelmans-Verrier, J. Royer, *Tetrahedron Lett.* **1976**, *18*, 1499–1502.

[38] W. Oppolzer, R. Achini, E. Pfenninger, H. P. Weber, *Helvetica Chimica Acta* **1976**, *59*, 1186–1202.

[39] a) E. Ciganek, *Org. React. (Hoboken, NJ, U. S.)* **1984**, *32*, 1–374; b) L. H. Klemm, T. M. McGuire, *J. Heterocycl. Chem.* **1972**, *9*, 1215–1218.

[40] R. Hunter, D. Macfarlane, R. Whitby, *Synlett* **2006**, *2006*, 3314–3318.

[41] J. S. Bryans, D. C. Horwell, C. O. Kneen, D. J. Wustrow, A. J. Thorpe, WO 9817627, **1998**.

[42] A. Leyva-Pérez, P. García-García, A. Corma, *Angew. Chem.* **2014**, *126*, 8831–8834.

[43] X.-T. G. F. Sha, X.-Y. Wu, *Synthesis* **2017**, *49*, 647–656.

[44] M. J. Frisch, G. W. Trucks, H. B. Schlegel, G. E. Scuseria, M. A. Robb, J. R. Cheeseman, G. Scalmani, V. Barone, B. Mennucci, G. A. Petersson, H. Nakatsuji, M. Caricato, X. Li, H. P. Hratchian, A. F. Izmaylov, J. Bloino, G. Zheng, J. L. Sonnenberg, M. Hada, M. Ehara, K. Toyota, R. Fukuda, J. Hasegawa, M. Ishida, T. Nakajima, Y. Honda, O. Kitao, H. Nakai, T. Vreven, J. A. Montgomery, Jr., J. E. Peralta, F. Ogliaro, M. Bearpark, J. J. Heyd, E. Brothers, K. N. Kudin, V. N. Staroverov, T. Keith, R. Kobayashi, J. Normand, K. Raghavachari, A. Rendell, J. C. Burant, S. S. Iyengar, J. Tomasi, M. Cossi, N. Rega, J. M. Millam, M. Klene, J. E. Knox, J. B. Cross, V. Bakken, C. Adamo, J. Jaramillo, R. Gomperts, R. E. Stratmann, O. Yazyev, A. J. Austin, R. Cammi, C. Pomelli, J. W. Ochterski, R. L. Martin, K. Morokuma, V. G. Zakrzewski, G. A. Voth, P. Salvador, J. J. Dannenberg, S. Dapprich, A. D. Daniels, O. Farkas, J. B. Foresman, J. V. Ortiz, J. Cioslowski, D. J. Fox, *Gaussian 09, Revision E.01, Gaussian, Inc., Wallingford CT*, **2013**.

[45] A. D. McLean and G. S. Chandler, *J. Chem. Phys.* **1980**, *72,* 5639-5648.

[46] K. Raghavachari, J. S. Binkley, R. Seeger, J. A. Pople, *J. Chem. Phys.* **1980**, *72*, 650-654.

[47] A. D. Becke. *J. Chem. Phys.* 98 **1993** 5648-5652.

[48] C. Lee, W. Yang, R. G. Parr, *Phys. Rev. B* **1988**, *37*, 785-789.

[49] B. Miehlich, A. Savin, H. Stoll, H. Preuss, *Chem. Phys. Lett.* **1989**, *157*, 200-206.

[50] S. Grimme, J. Antony, S. Ehrlich, H. Krieg, *J. Chem. Phys*. **2010,** 154104.

[51] E. R. Johnson, S. Keinan, P. Mori-Sanchez, J. Contreras-Garcia, A. J. Cohen, W. Yang, *J. Am. Chem. Soc*. **2010**, *132*, 6498-6506.

[52] J. Contreras-Garcia, E. R. Johnson, S. Keinan, R. Chaudret, J-P. Piquemal, D. N. Beratan, W. Yang. *J. Chem. Theory Comput*. **2011**, 7, 625-632.

F Appendix

1 NMR spectra

^{1}H-NMR spectra: upper image

^{13}C-NMR spectra (DEPT135 integrated): lower image

Solvent and frequency are stated in each spectrum.

2-Hydroxyethyl (*E*)-4-oxo-4-phenylbut-2-enoate (131)

(400 MHz, $CDCl_3$)

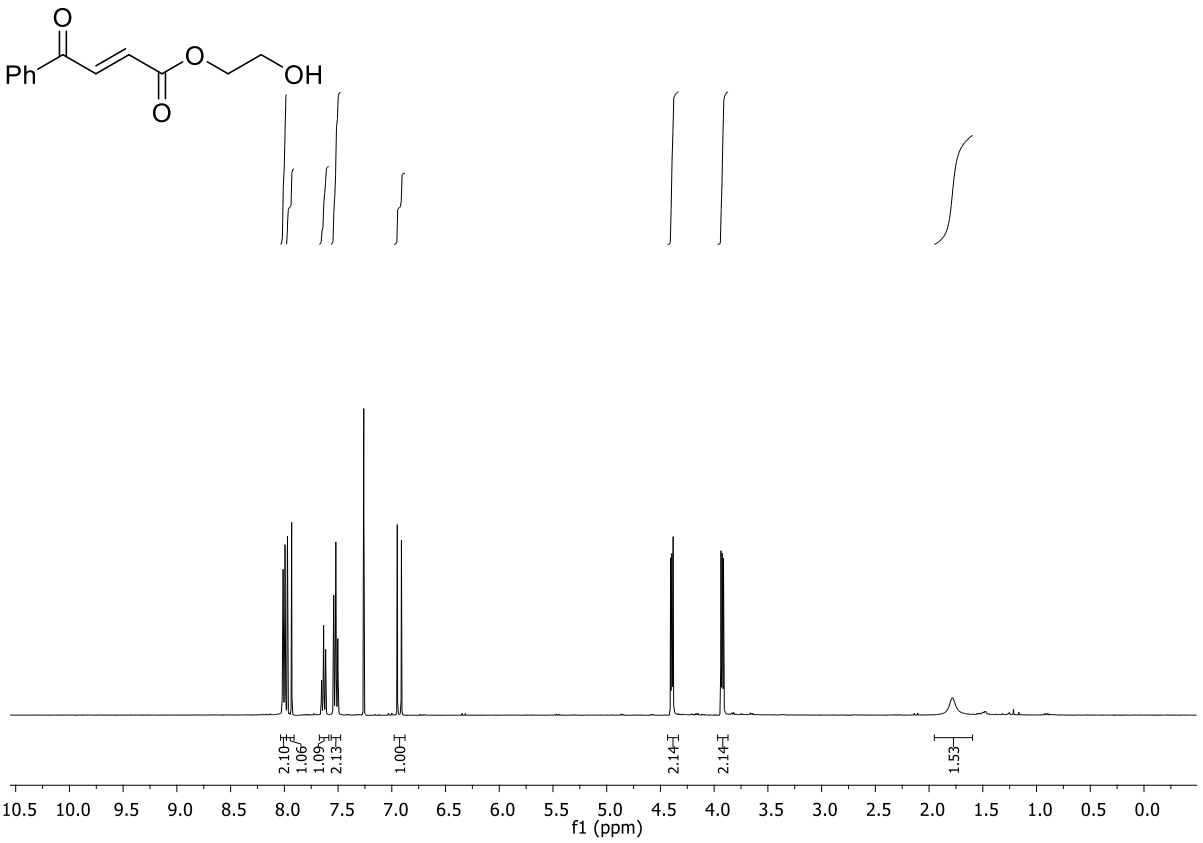

(75 MHz, $CDCl_3$)

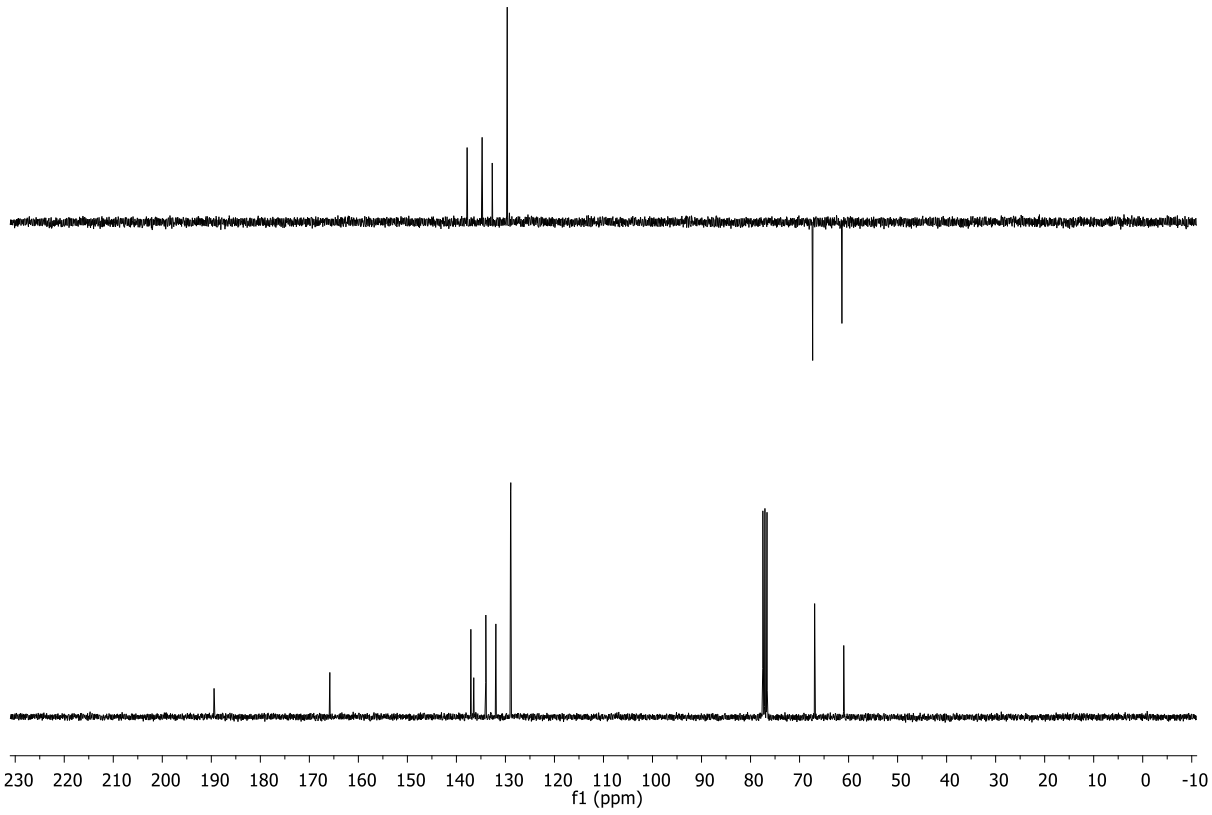

(*E*)-4-Oxo-4-phenylbut-2-en-1-yl (*Z*)-4-oxo-4-phenylbut-2-enoate (136)

(300 MHz, $CDCl_3$)

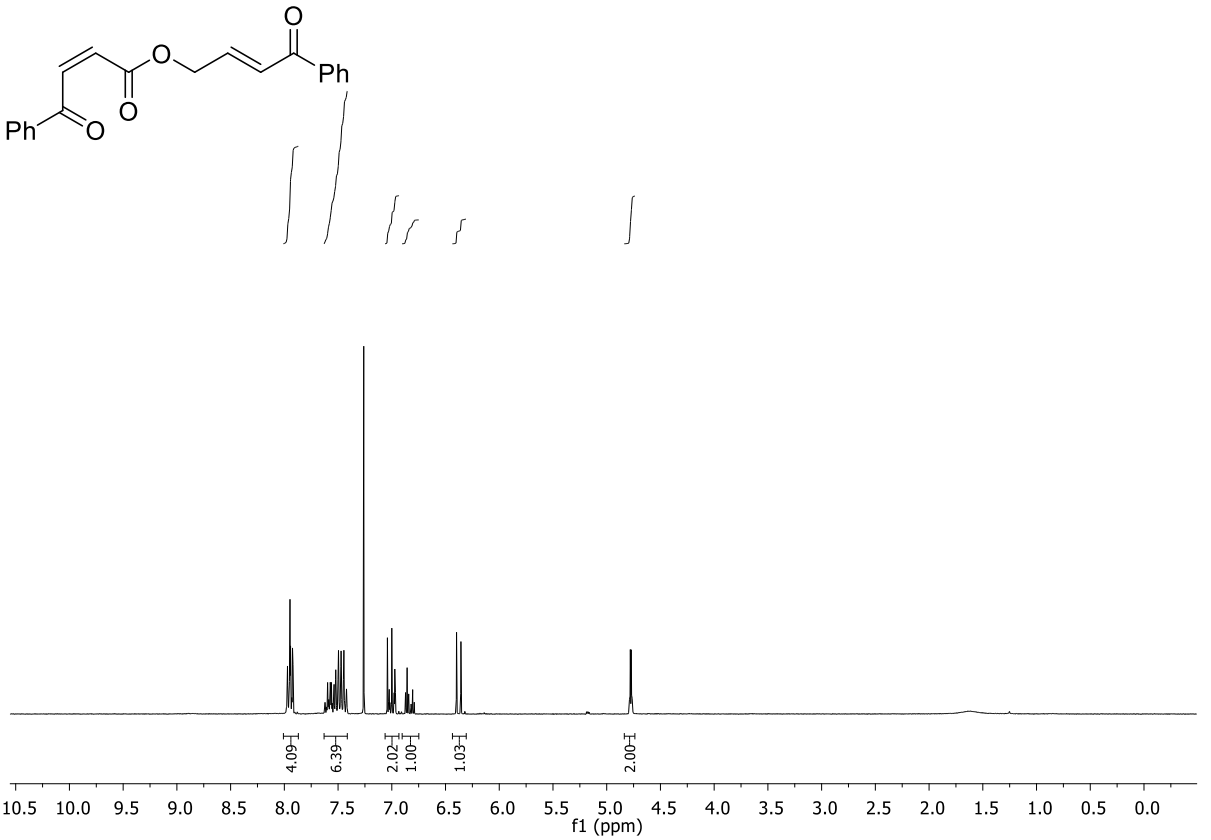

(101 MHz, $CDCl_3$)

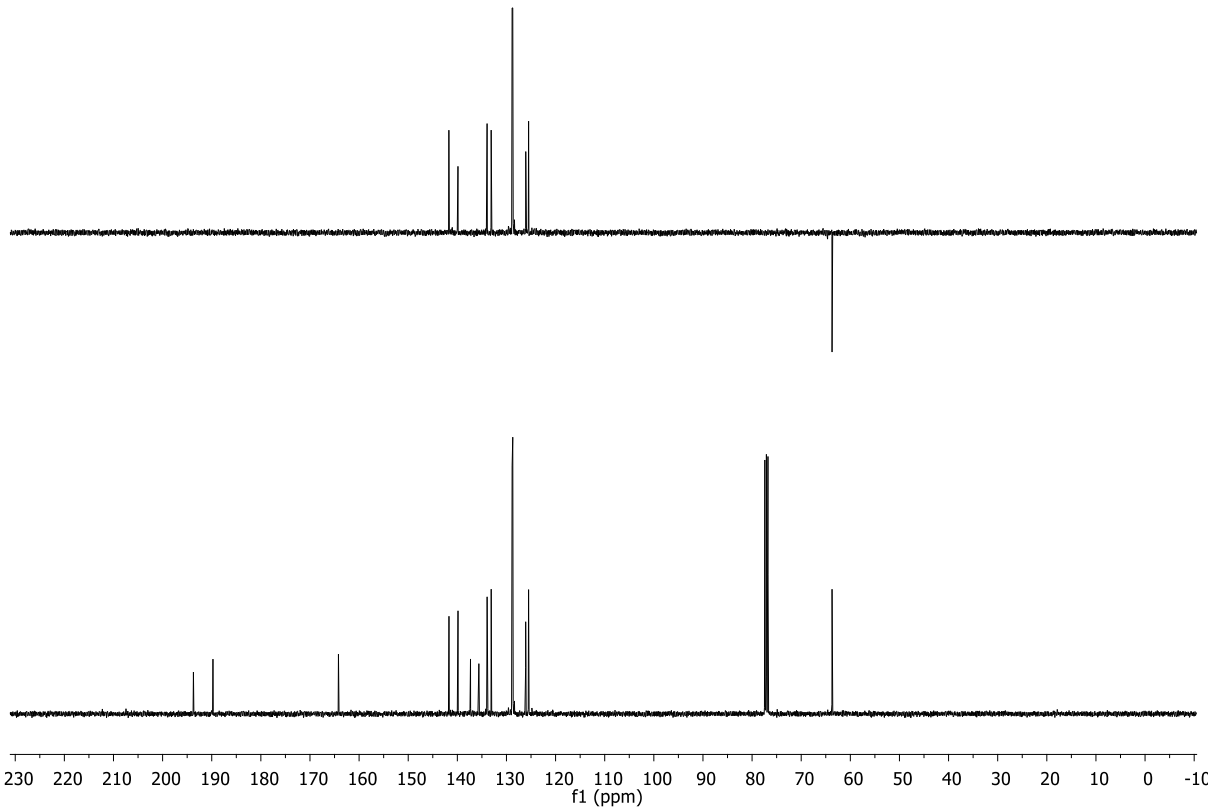

2-((*tert*-Butyldimethylsilyl)oxy)-*N*-methylethan-1-amine (140)

(400 MHz, $CDCl_3$)

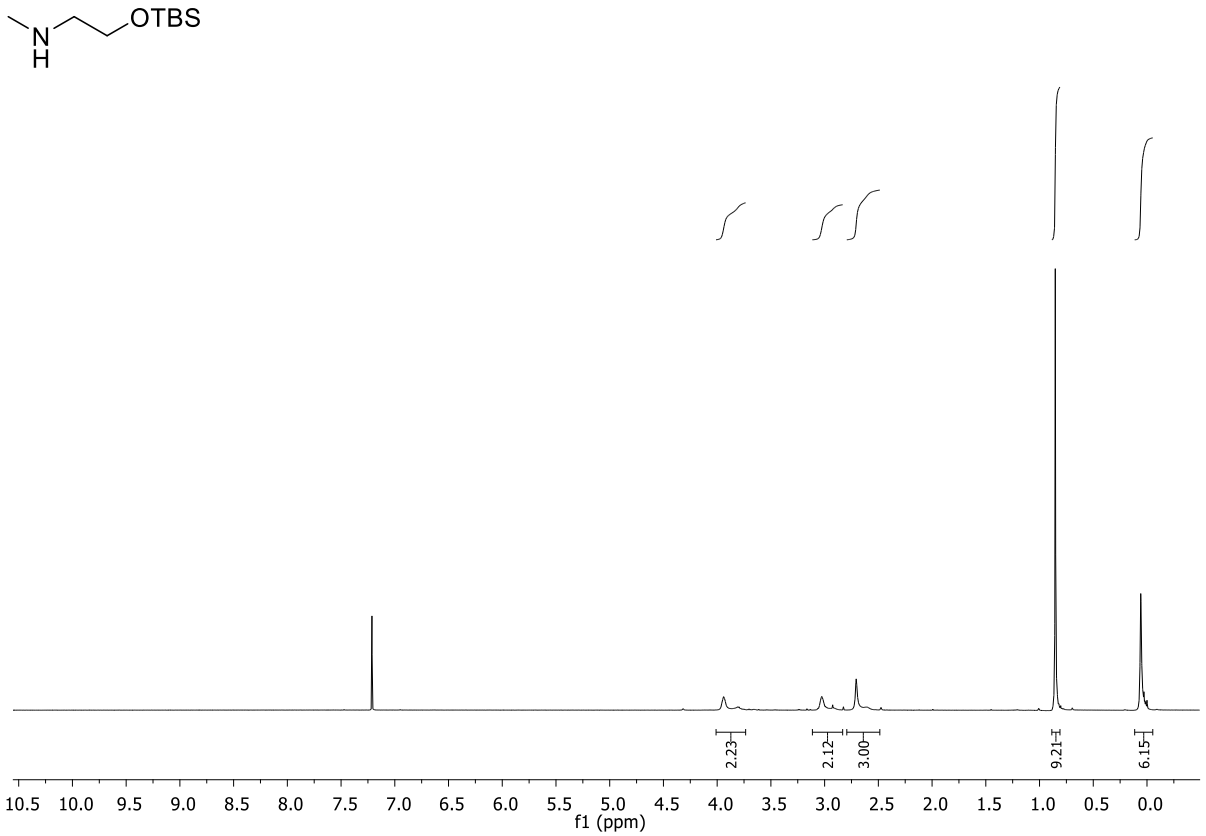

(75 MHz, $CDCl_3$)

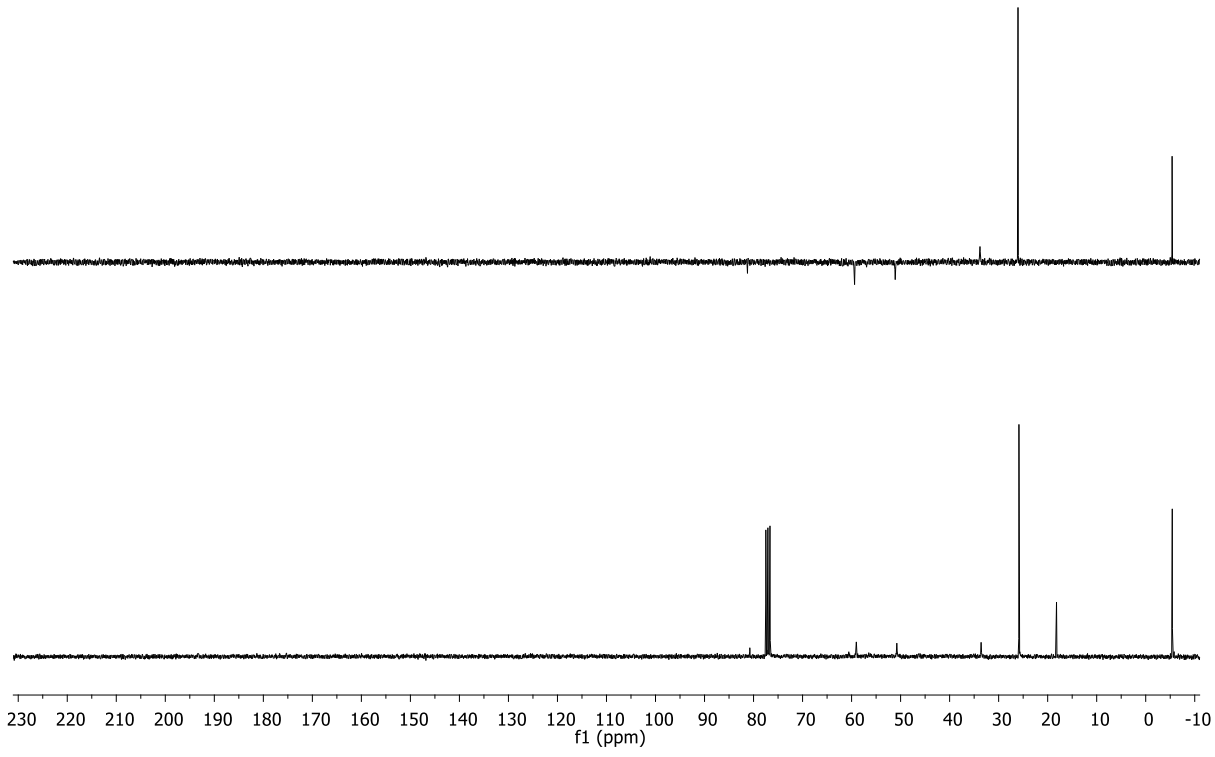

(*E*)-*N*-(2-((*tert*-Butyldimethylsilyl)oxy)ethyl)-N-methyl-4-oxo-4-phenylbut-2-enamide (141)

(400 MHz, $CDCl_3$)

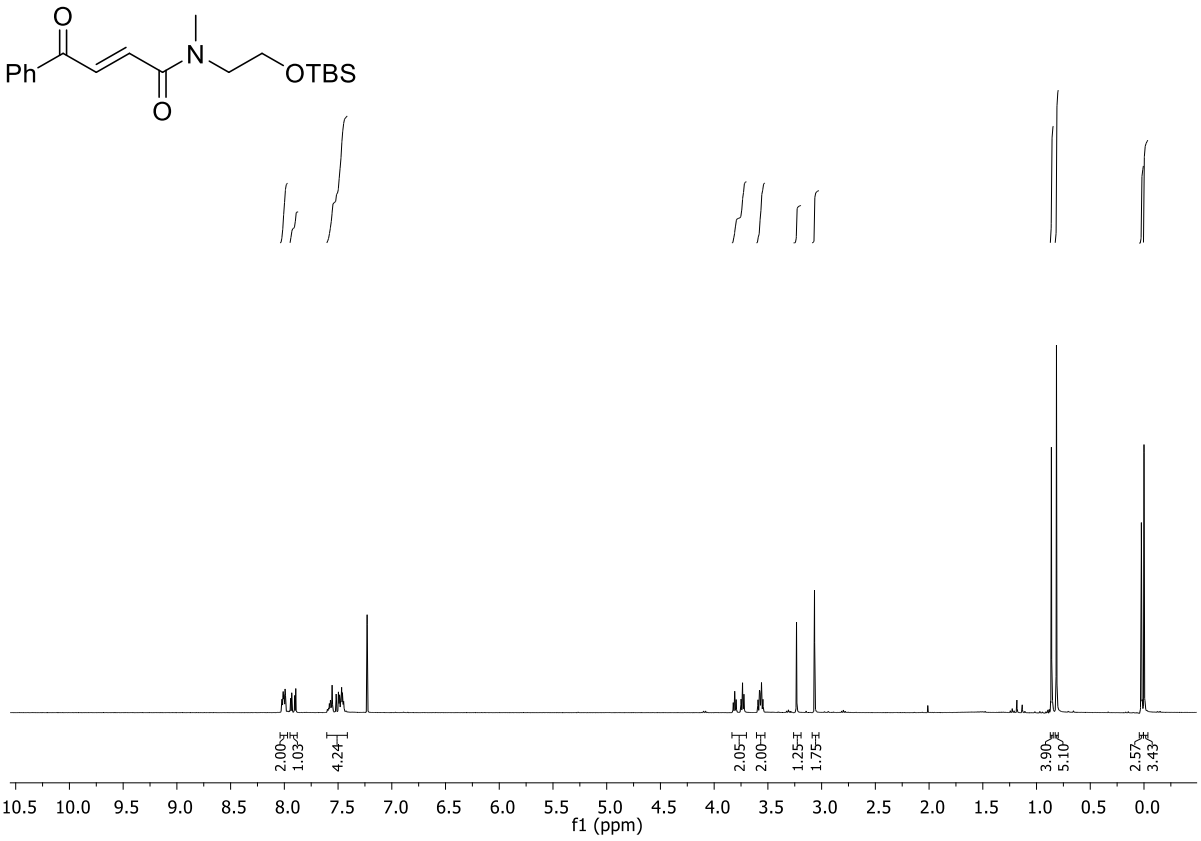

(101 MHz, $CDCl_3$)

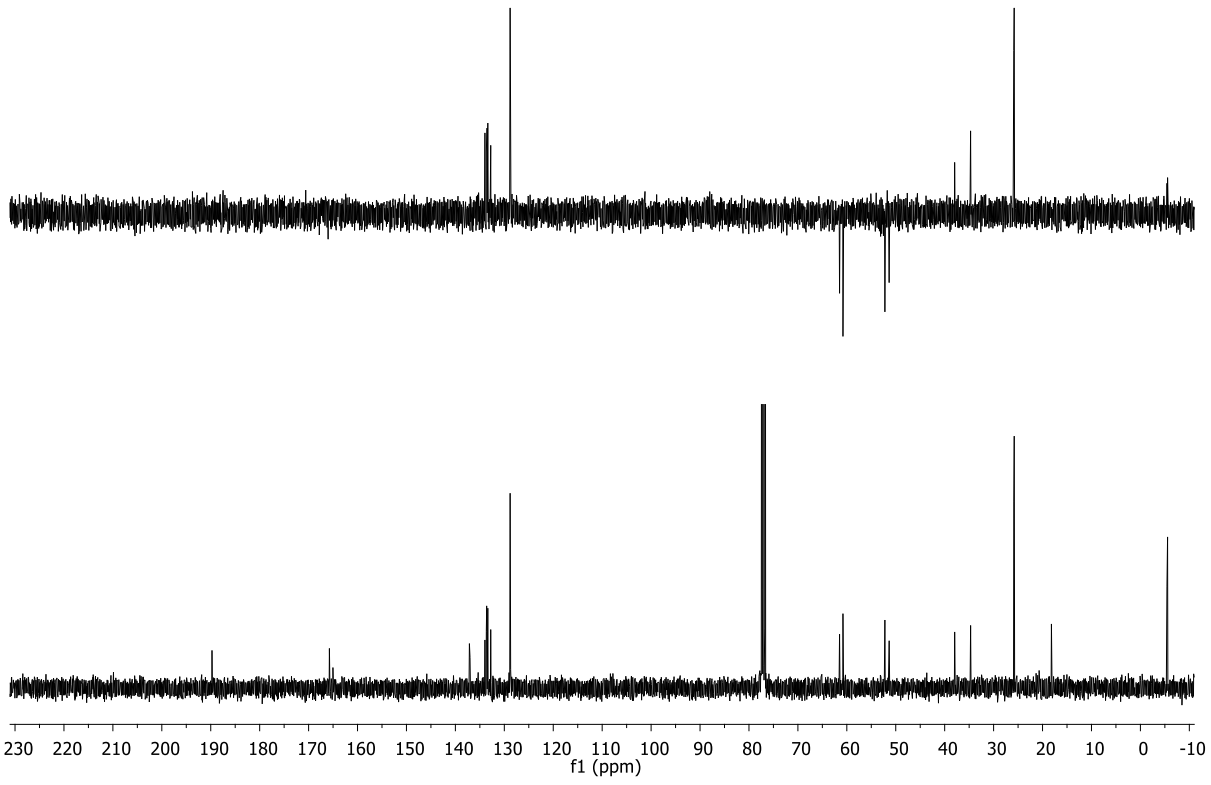

4-Methyl-2-(2-oxo-2-phenylethyl)morpholin-3-one (143)

(300 MHz, $CDCl_3$)

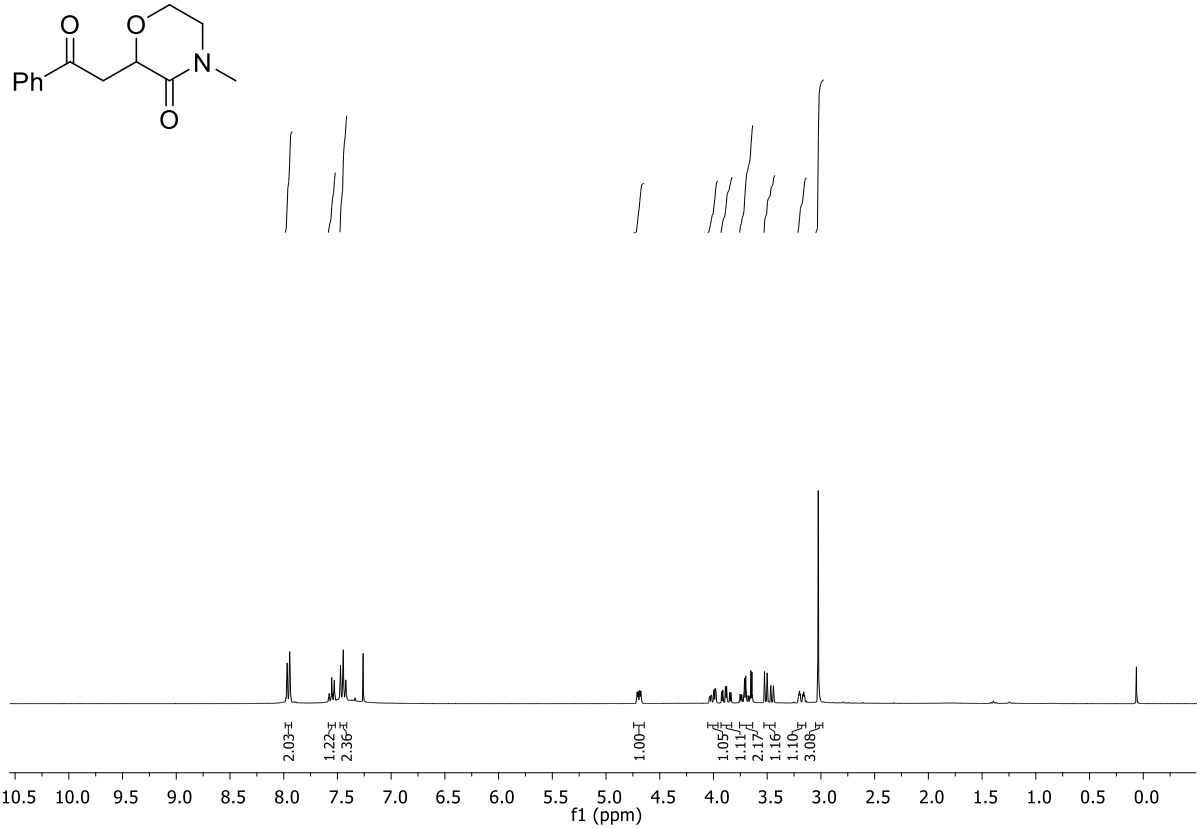

(101 MHz, $CDCl_3$)

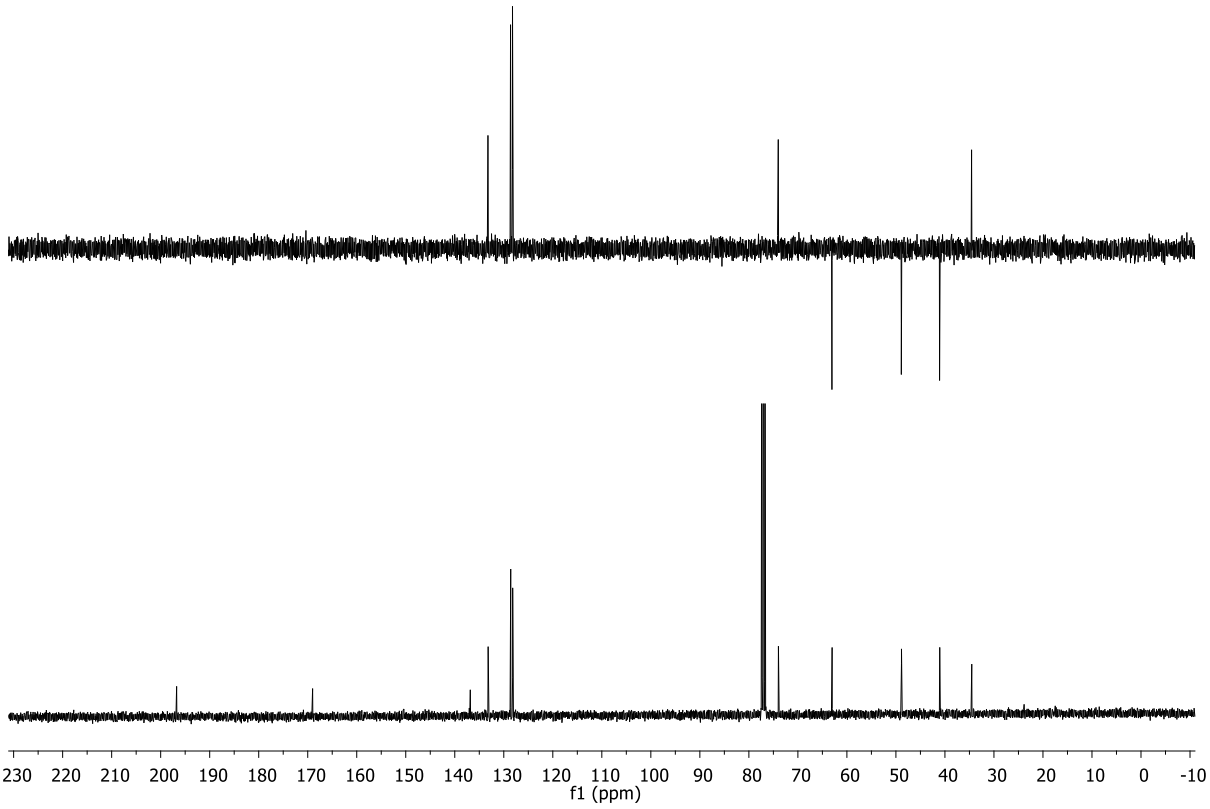

tert-Butyl (2-hydroxyethyl)(methyl)carbamate (146a)

(400 MHz, $CDCl_3$)

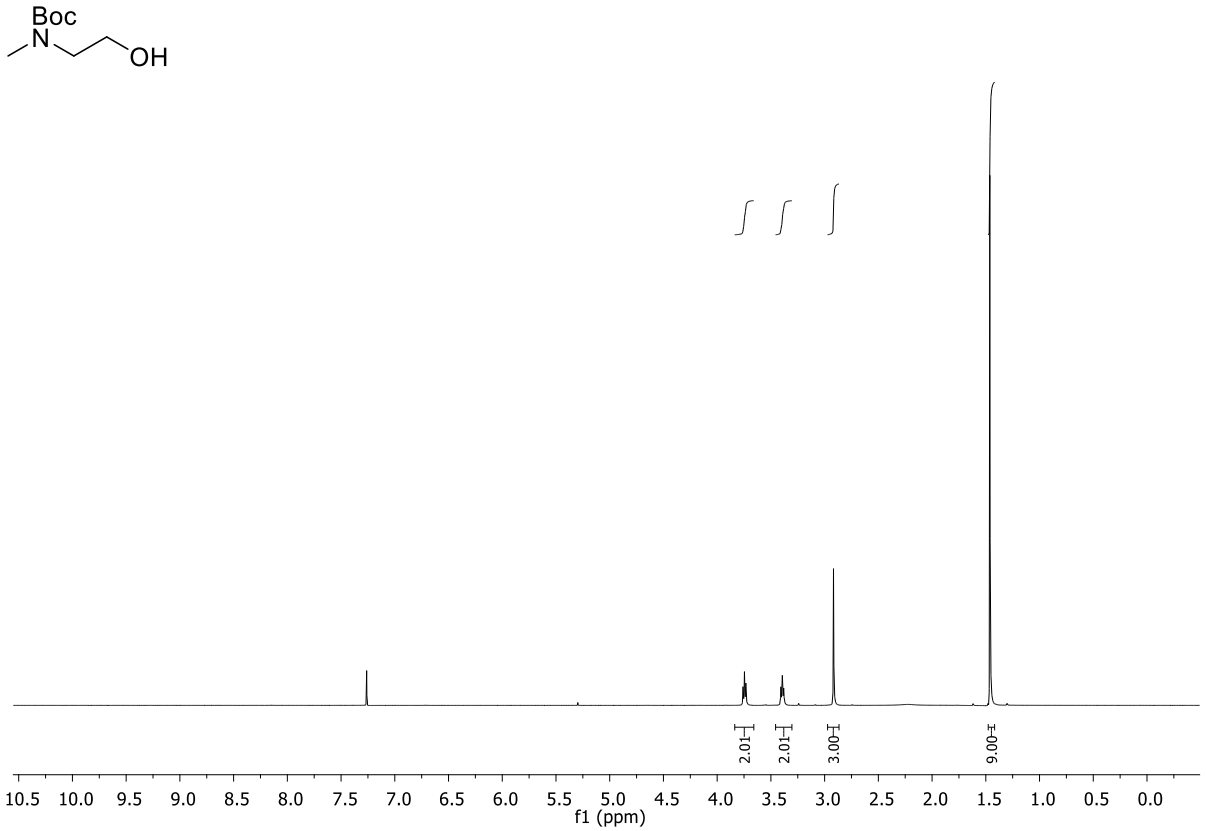

(101 MHz, $CDCl_3$)

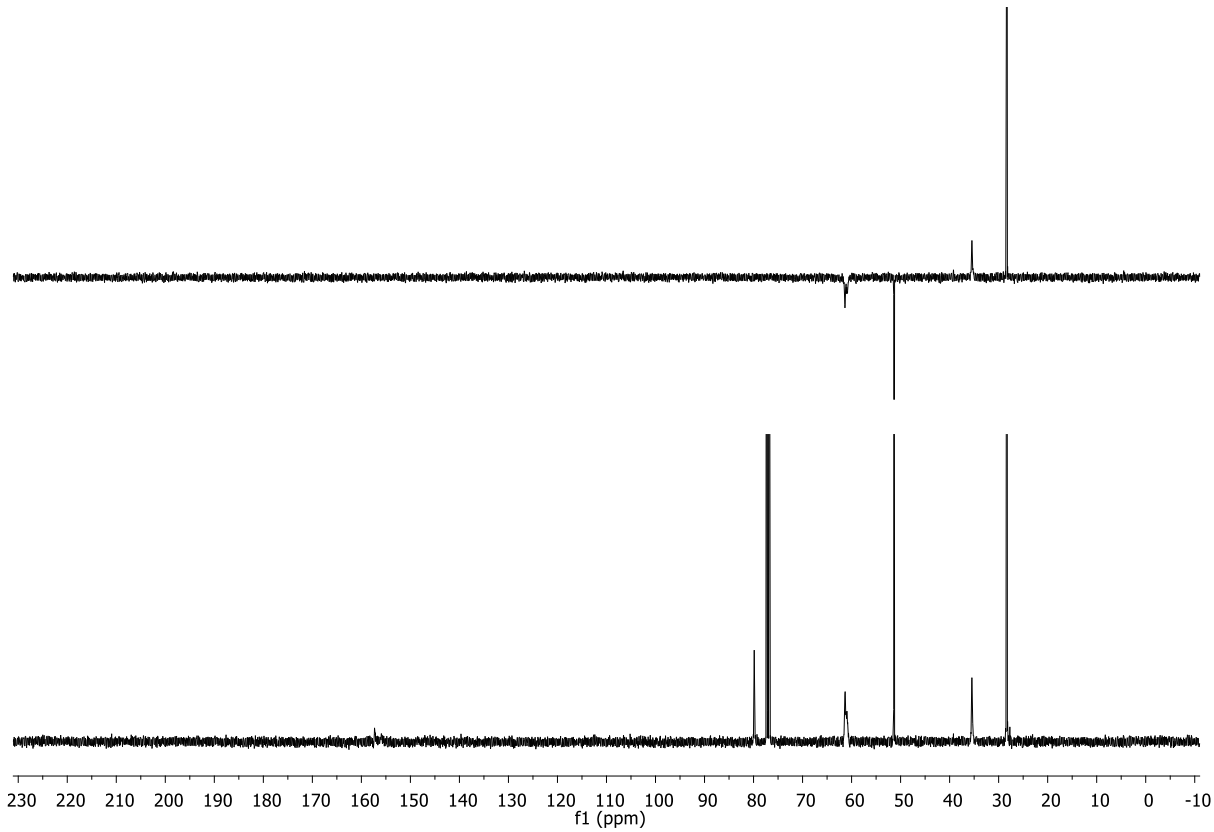

tert-Butyl (2-hydroxyethyl)(phenyl)carbamate (146b)

(300 MHz, $CDCl_3$)

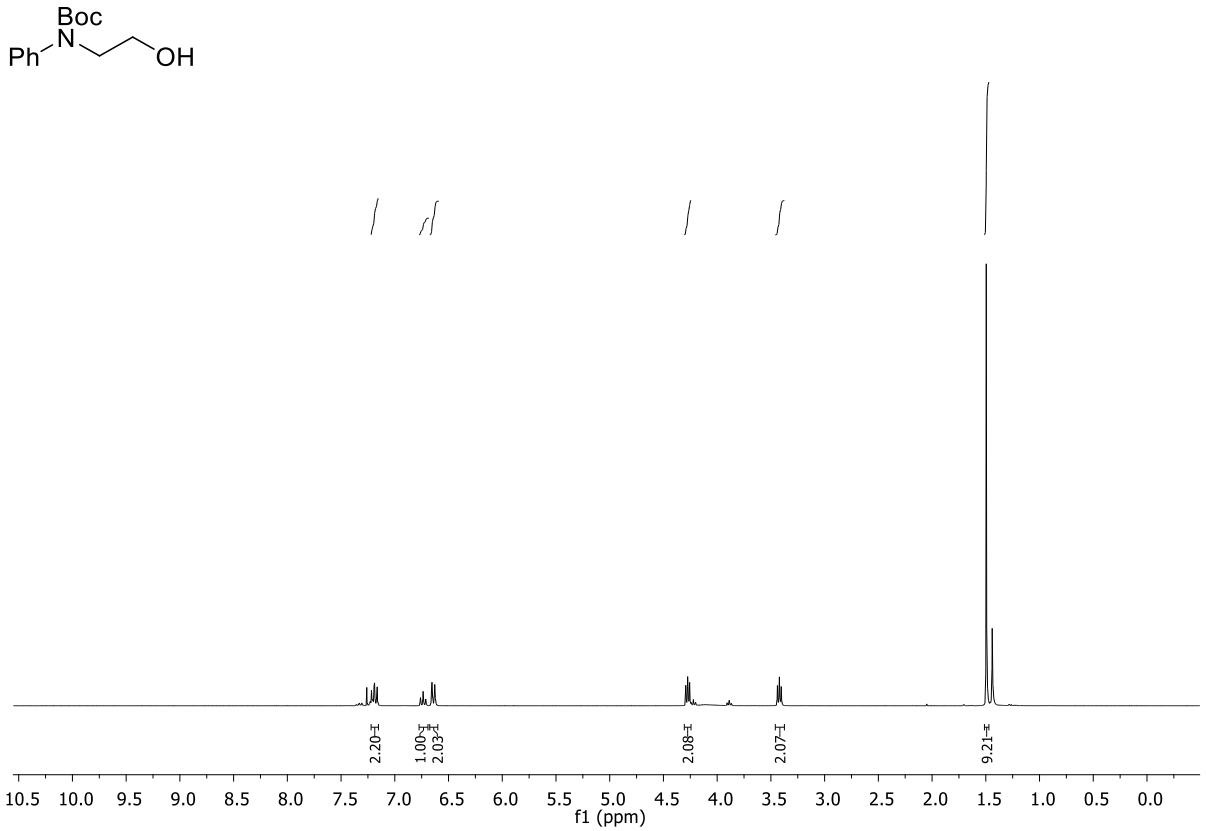

(101 MHz, $CDCl_3$)

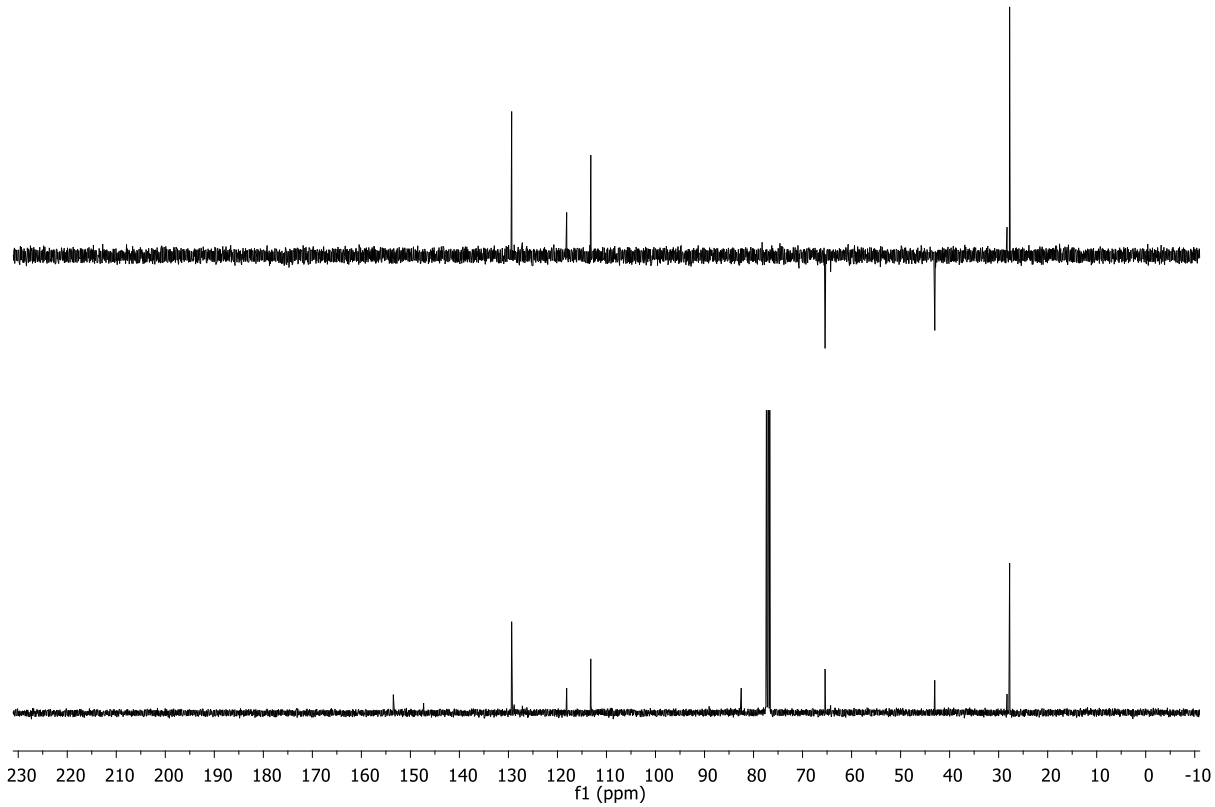

(9*H*-Fluoren-9-yl)methyl (2-hydroxyethyl)(methyl)carbamate (146c)

(300 MHz, $CDCl_3$)

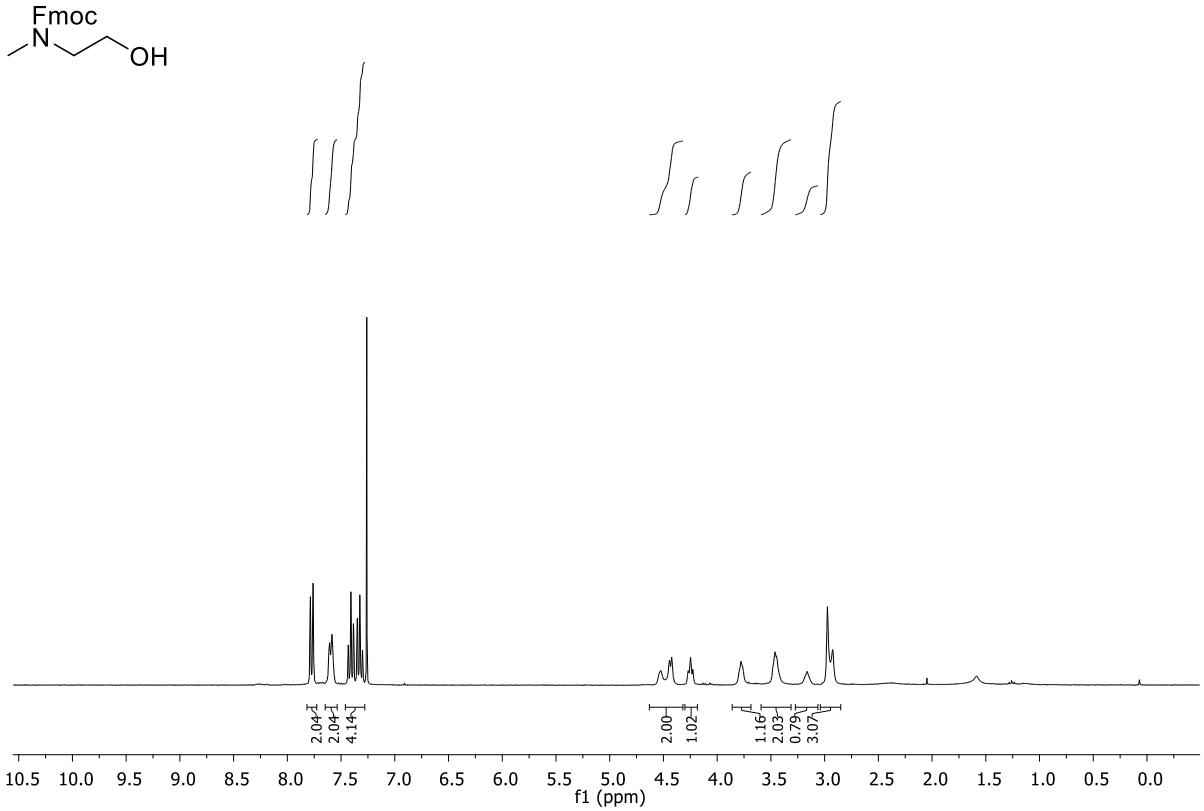

(101 MHz, $CDCl_3$)

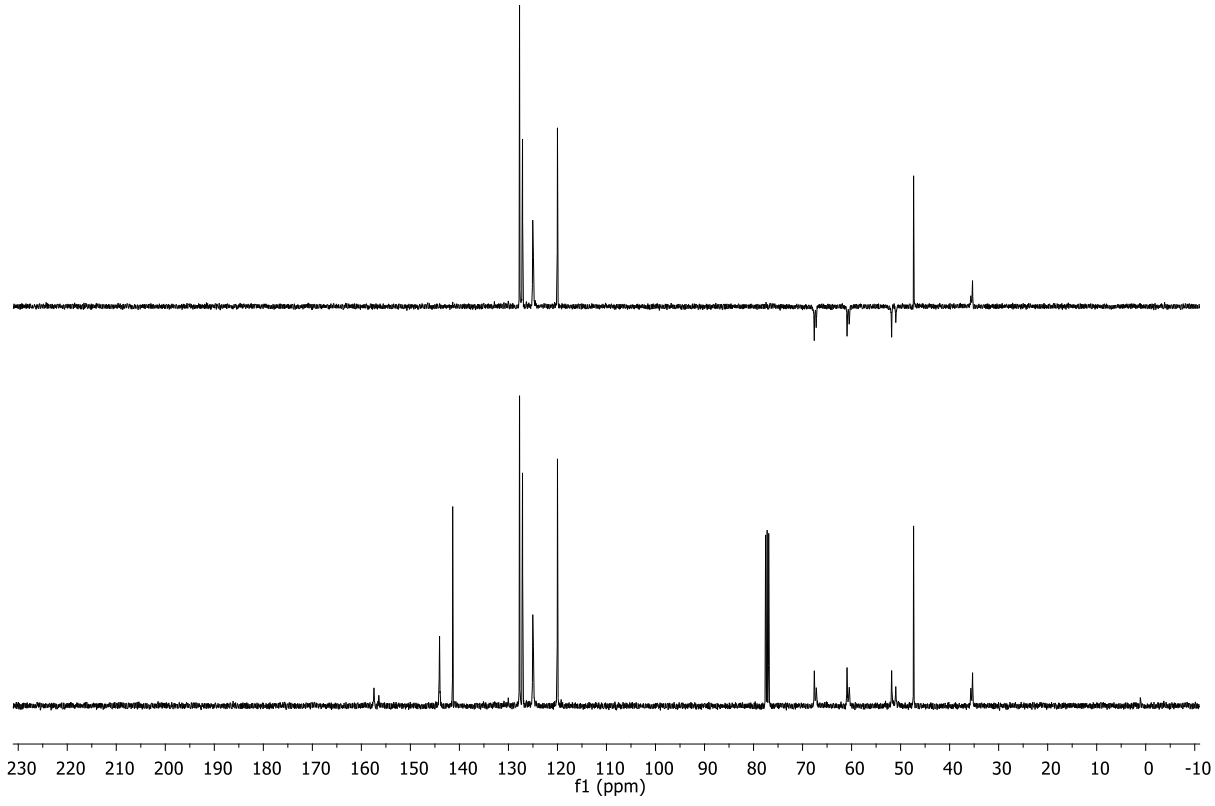

tert-Butyl (_E_)-methyl(4-oxo-4-phenylbut-2-en-1-yl)carbamate (147a)

(300 MHz, $CDCl_3$)

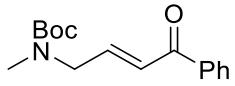

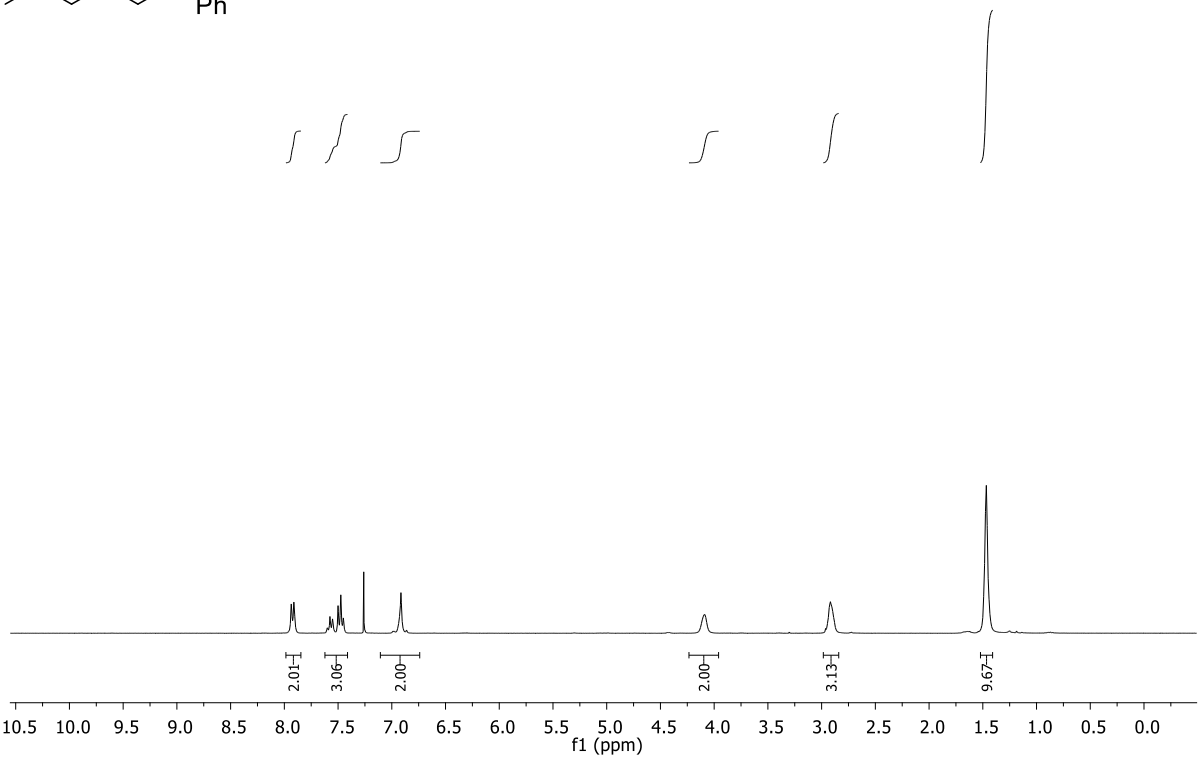

(101 MHz, $CDCl_3$)

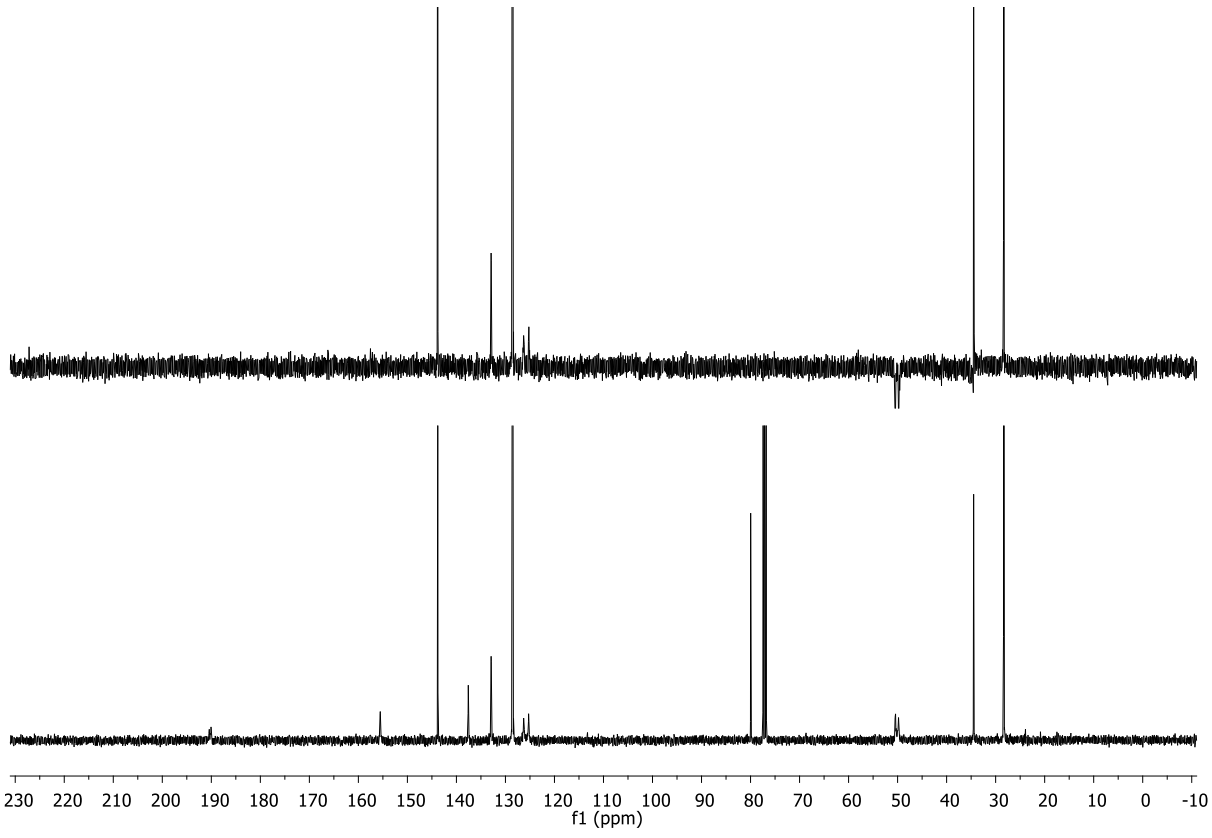

(9*H*-Fuoren-9-yl)methyl (*E*)-methyl(4-oxo-4-phenylbut-2-en-1-yl)carbamate (147b)

(300 MHz, $CDCl_3$)

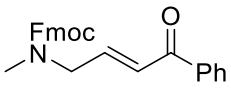

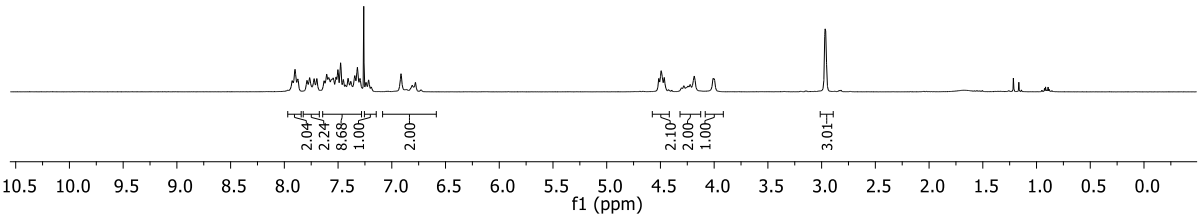

(75 MHz, $CDCl_3$)

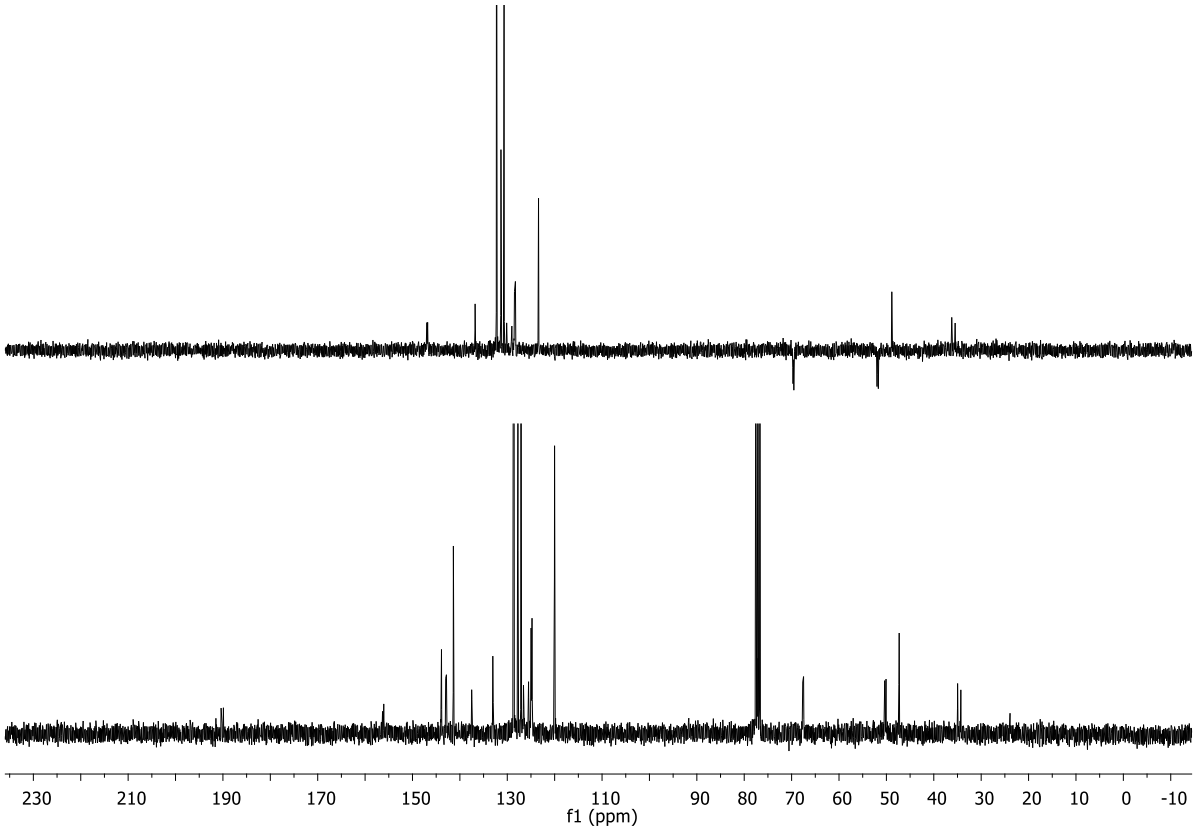

(*E*)-*N*-(*tert*-Butyl)-3-phenylprop-2-en-1-amine (170b)

(400 MHz, $CDCl_3$)

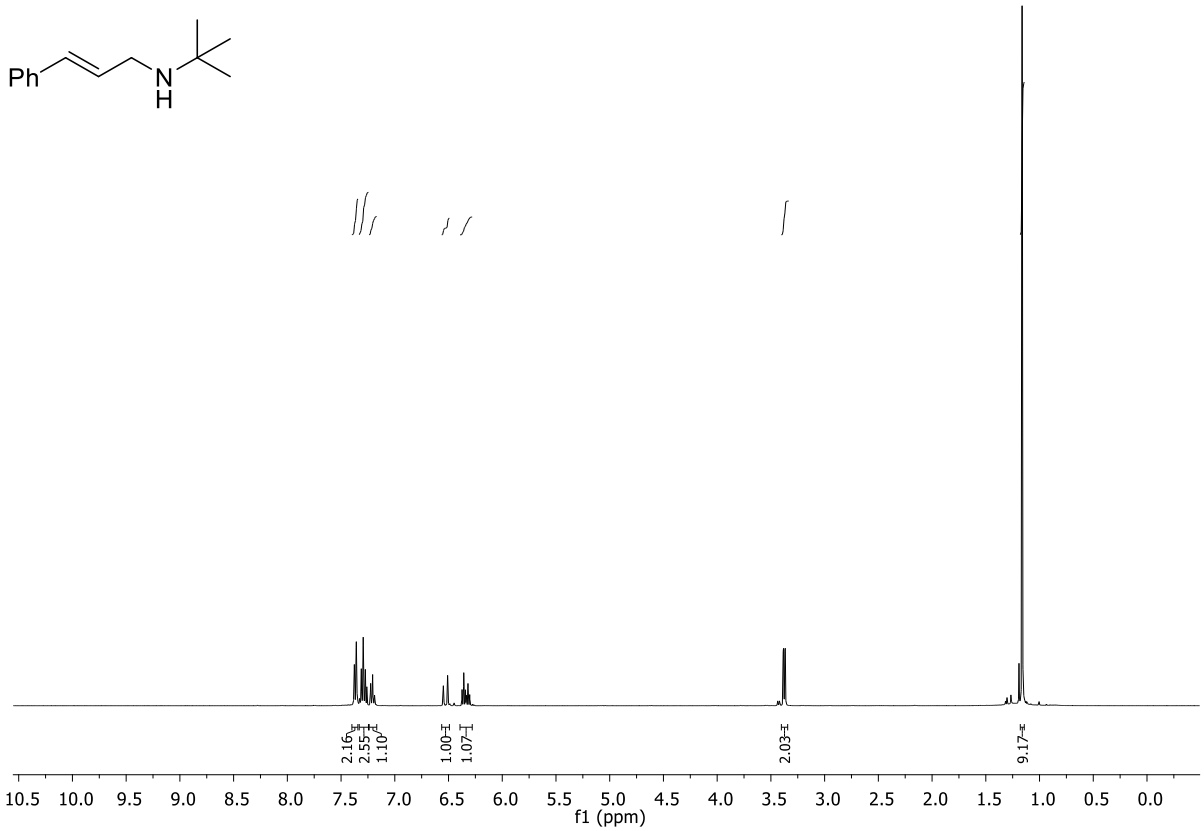

(101 MHz, $CDCl_3$)

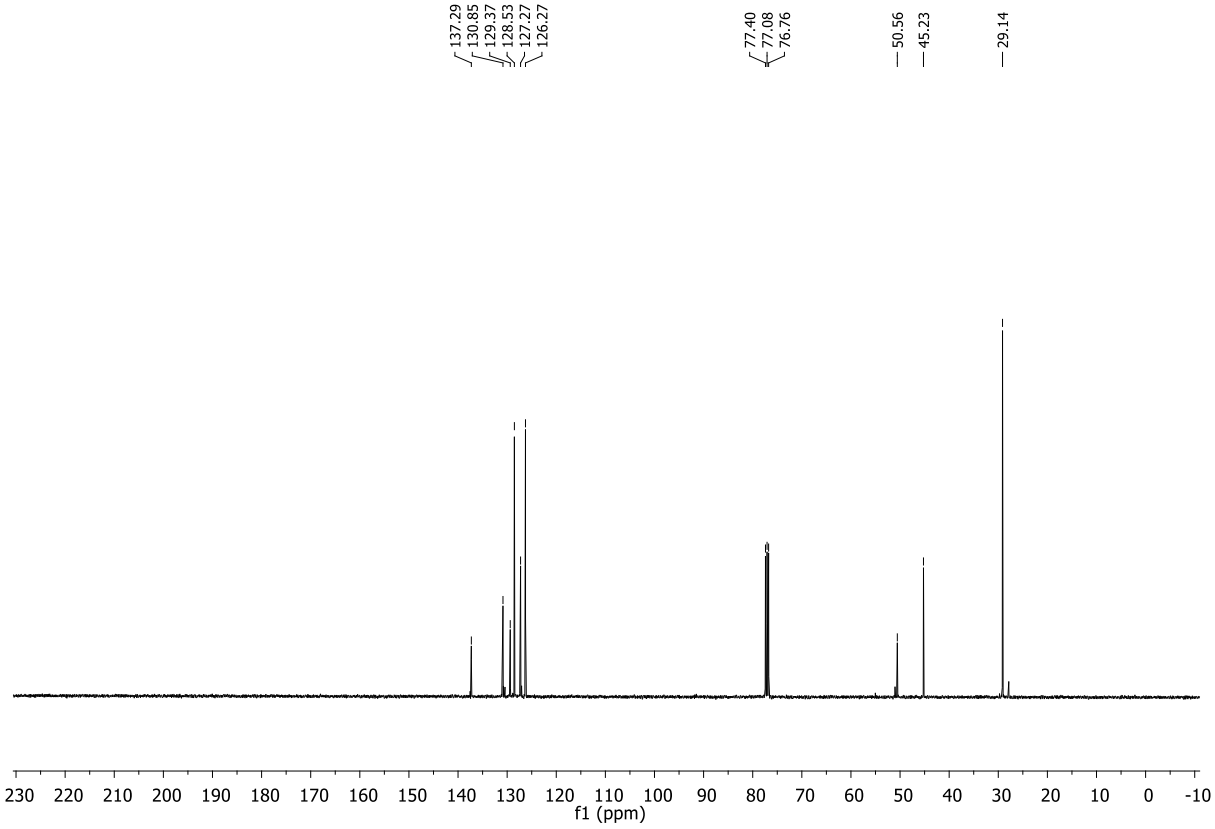

(*E*)-*N*-(*tert*-Butyl)-3-(4-methoxyphenyl)prop-2-en-1-amine (157)

(300 MHz, $CDCl_3$)

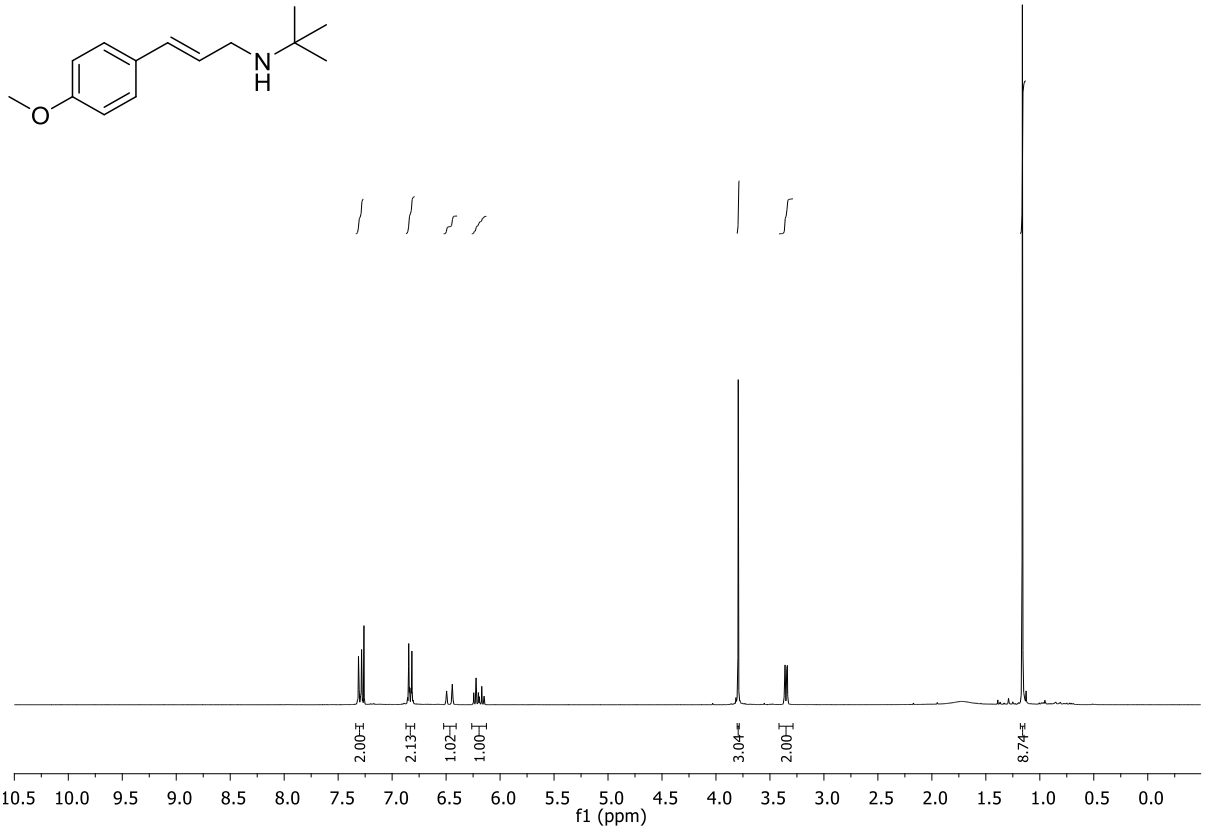

(75 MHz, $CDCl_3$)

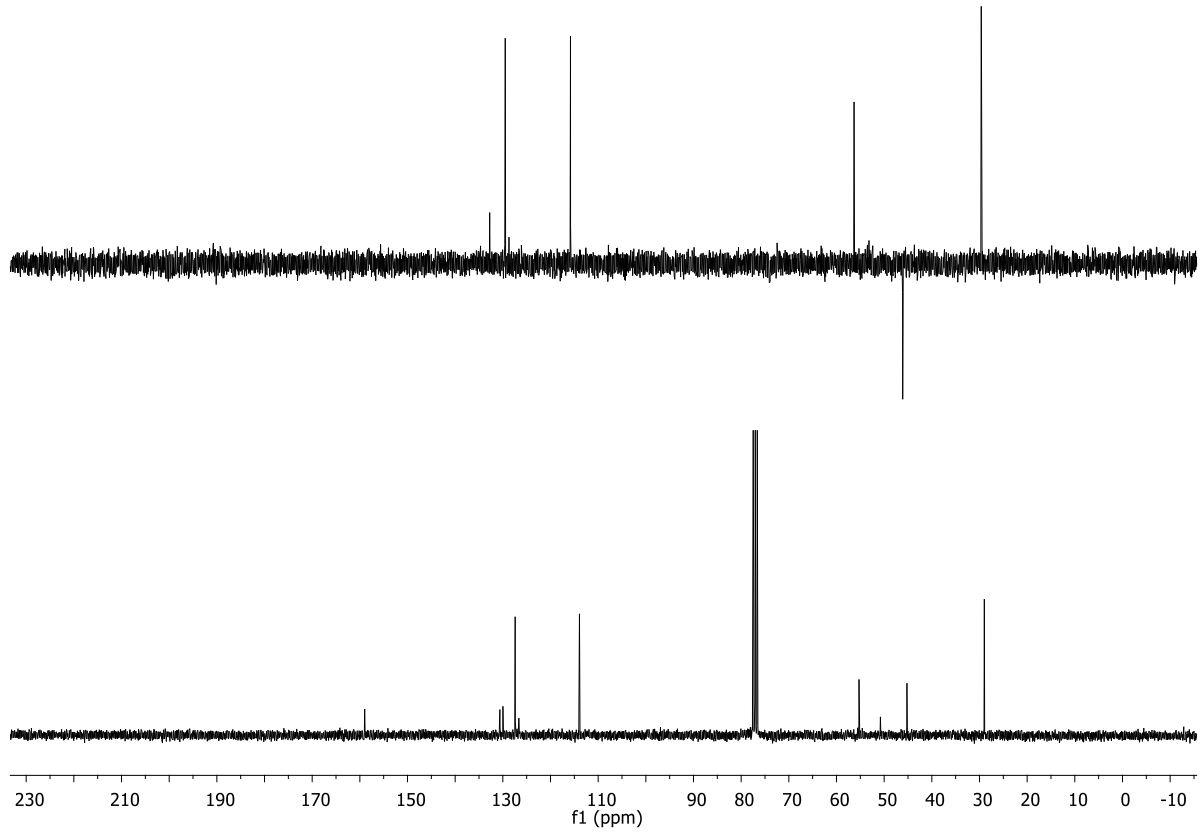

Methyl (*E*)-4-(*tert*-butylamino)but-2-enoate (170c)

(300 MHz, $CDCl_3$)

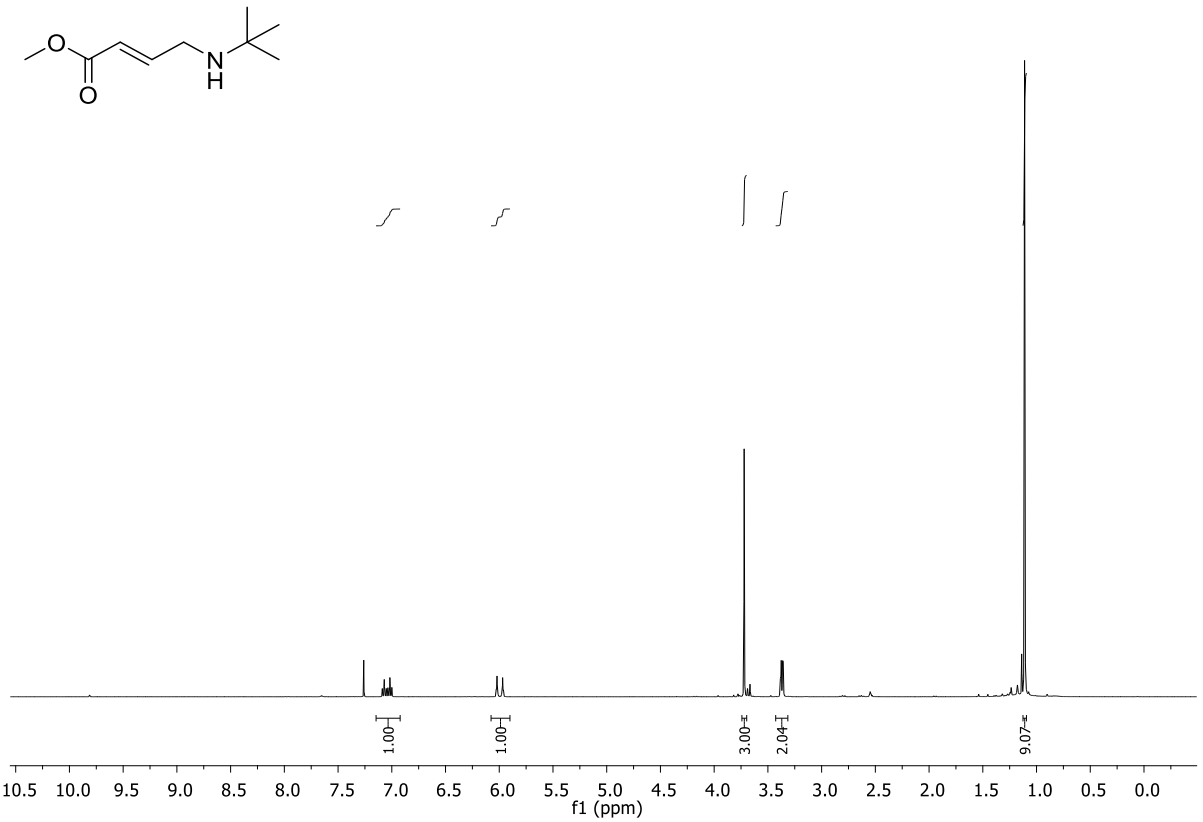

(101 MHz, $CDCl_3$)

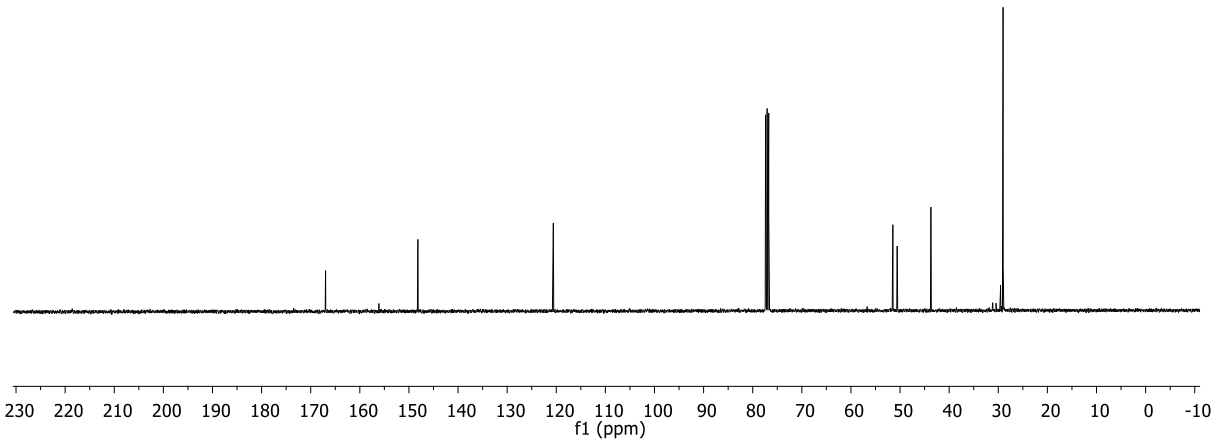

_N_-Benzylprop-2-en-1-amine (170d)

(300 MHz, $CDCl_3$)

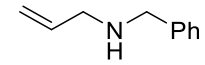

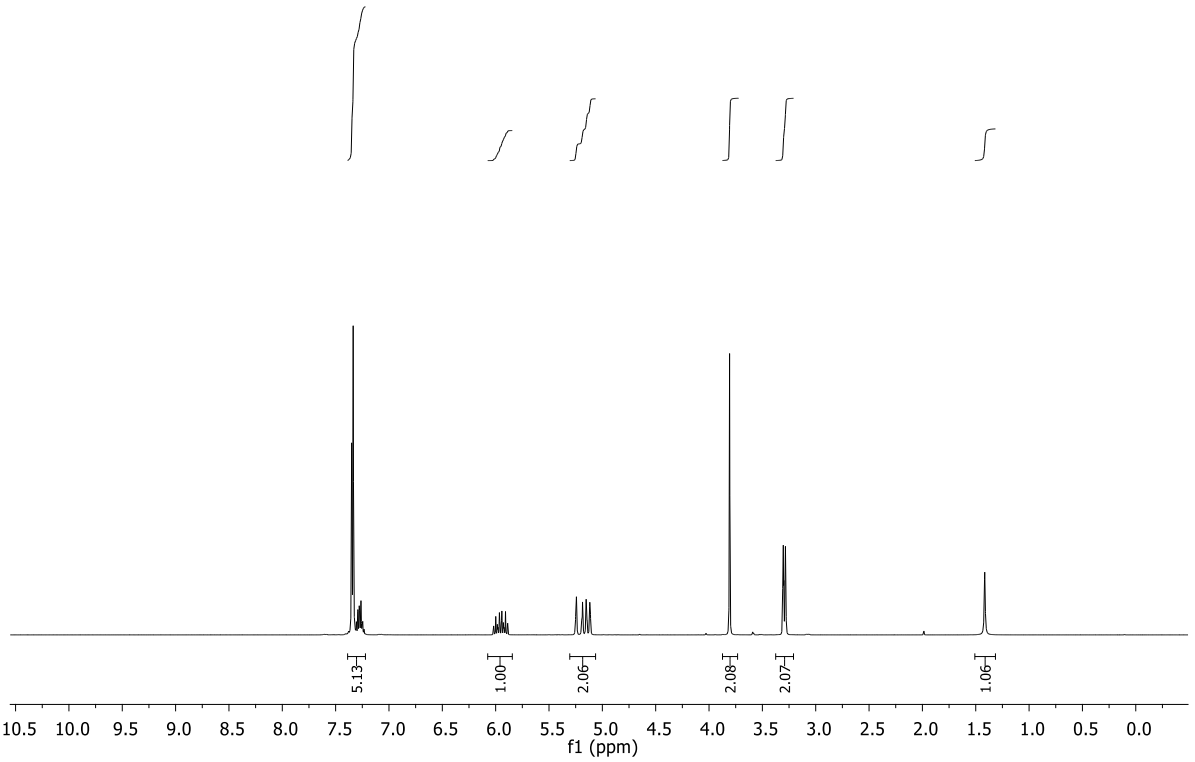

(75 MHz, $CDCl_3$)

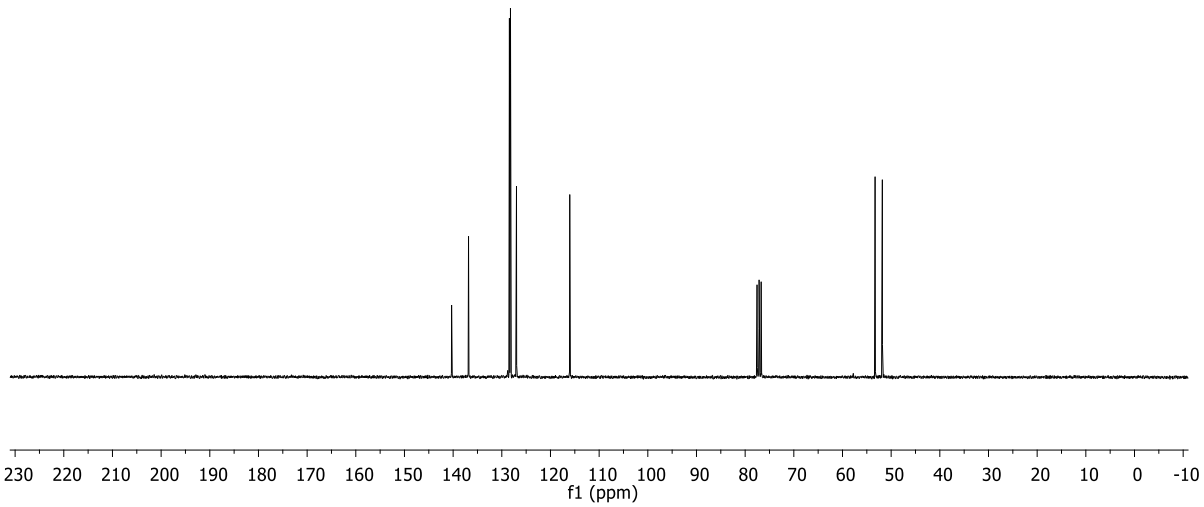

(*E*)-*N*-Benzyl-3-phenylprop-2-en-1-amine (170e)

(300 MHz, $CDCl_3$)

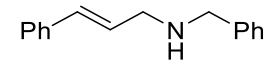

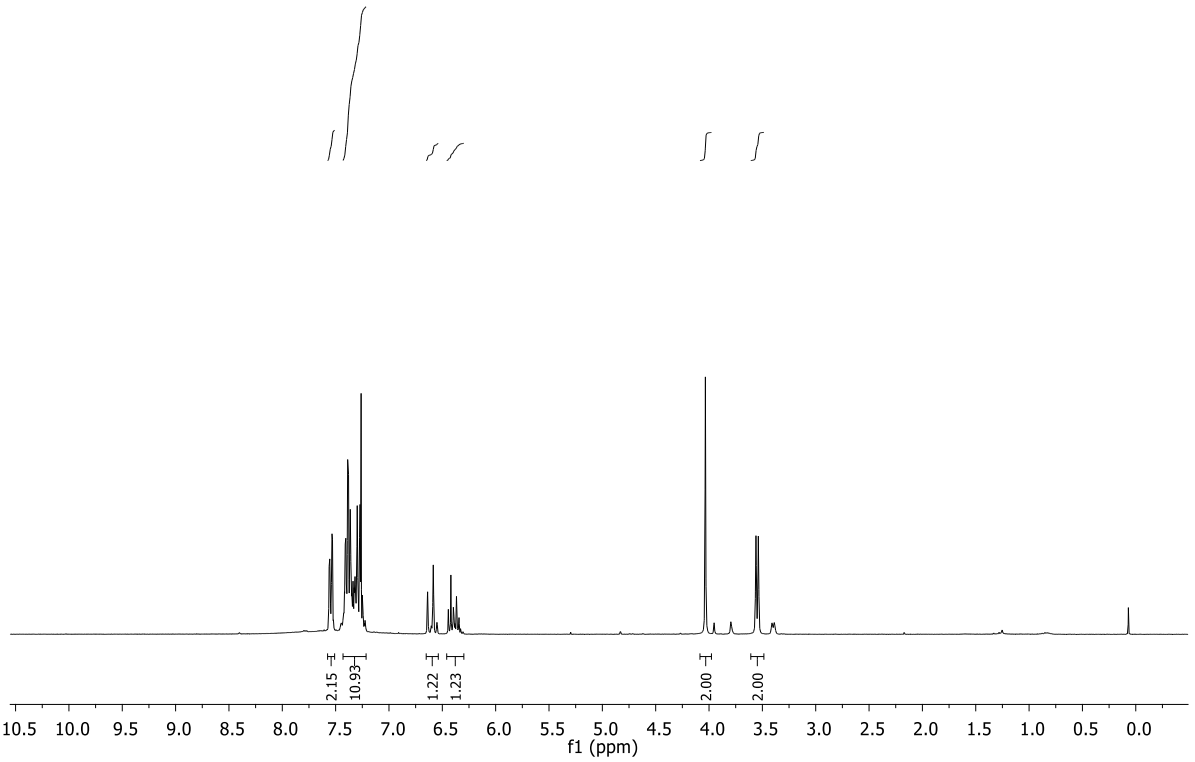

(101 MHz, $CDCl_3$)

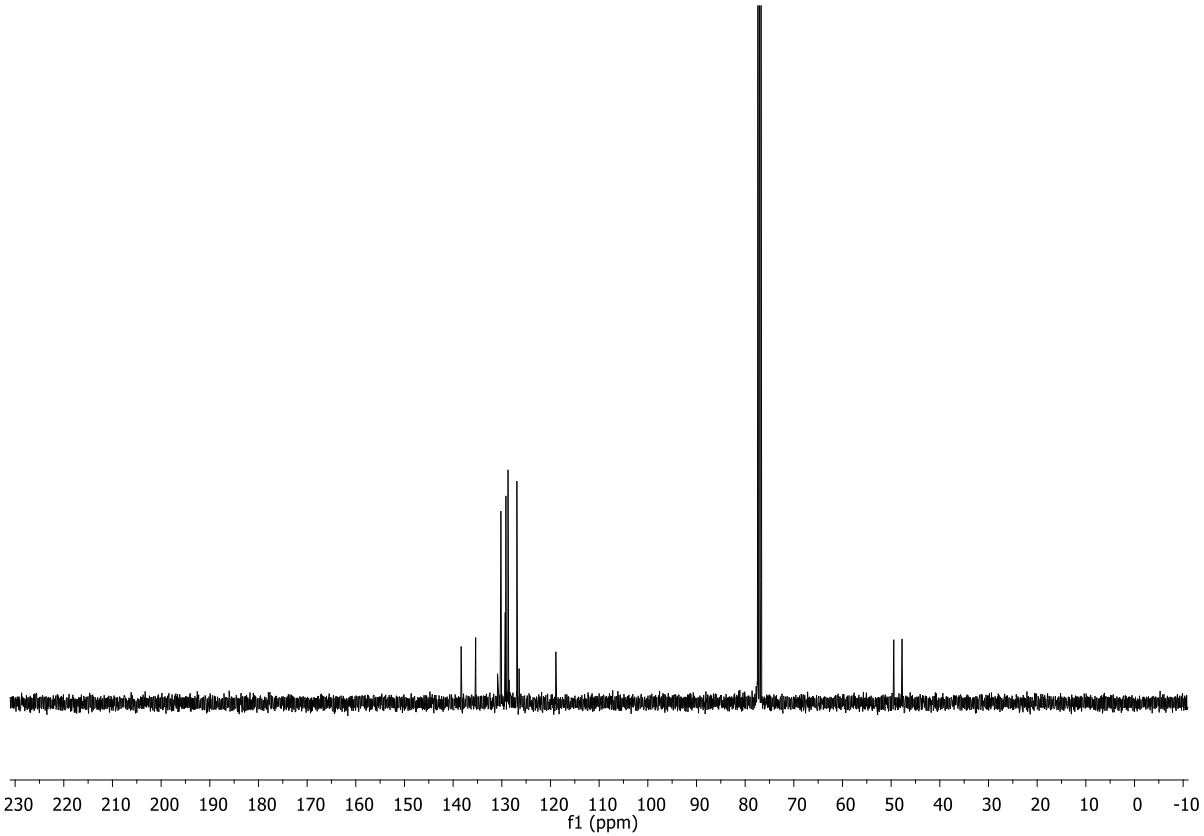

(*S,E*)-3-Phenyl-*N*-(1-phenylethyl)prop-2-en-1-amine (248)

(300 MHz, $CDCl_3$)

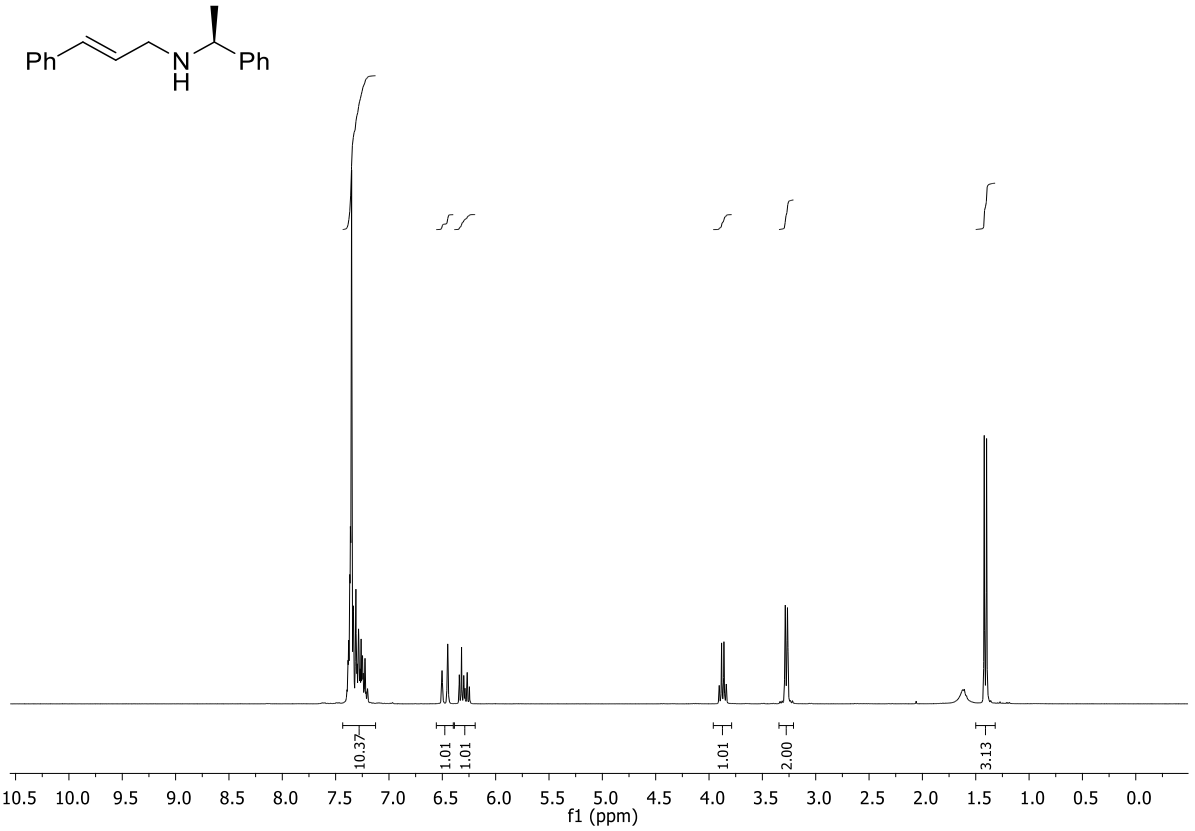

(75 MHz, $CDCl_3$)

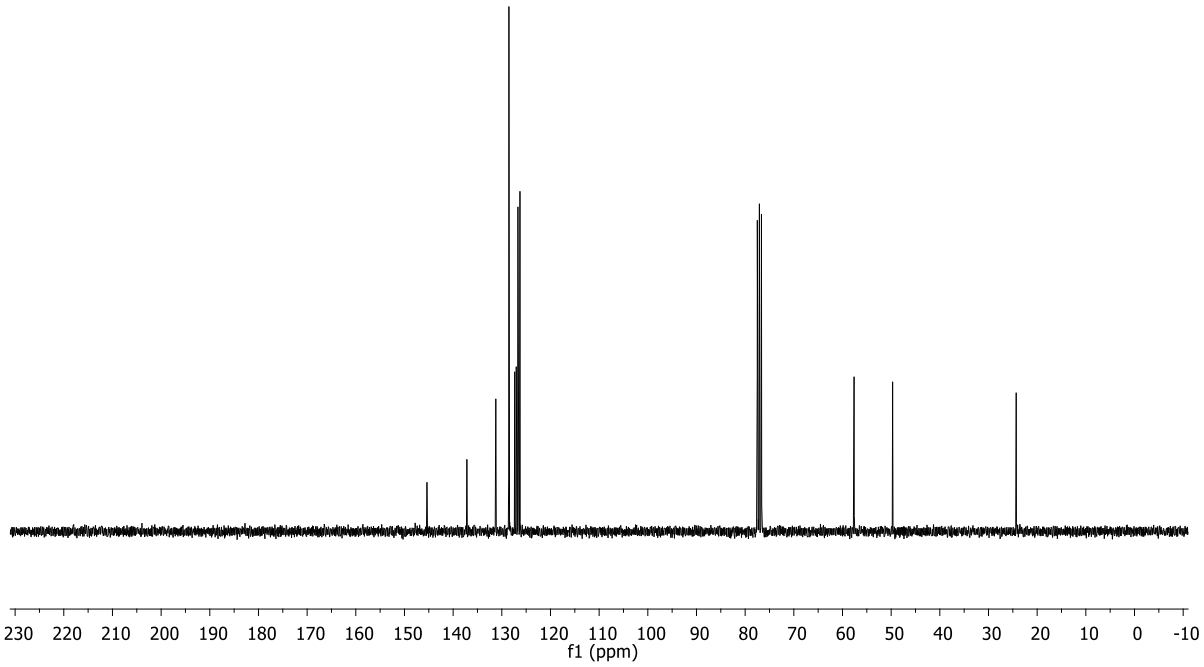

(*S*)-*N*-(1-Phenylethyl)prop-2-en-1-amine (260)

(300 MHz, $CDCl_3$)

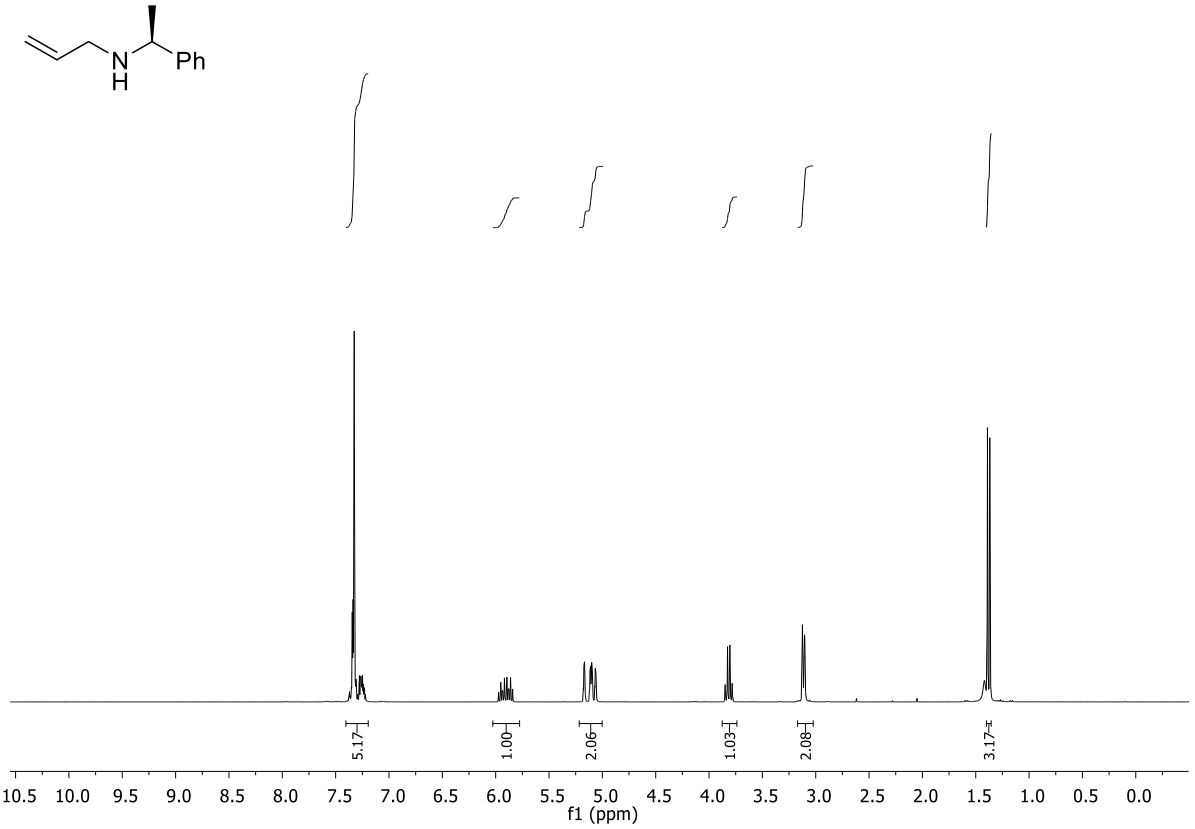

(101 MHz, $CDCl_3$)

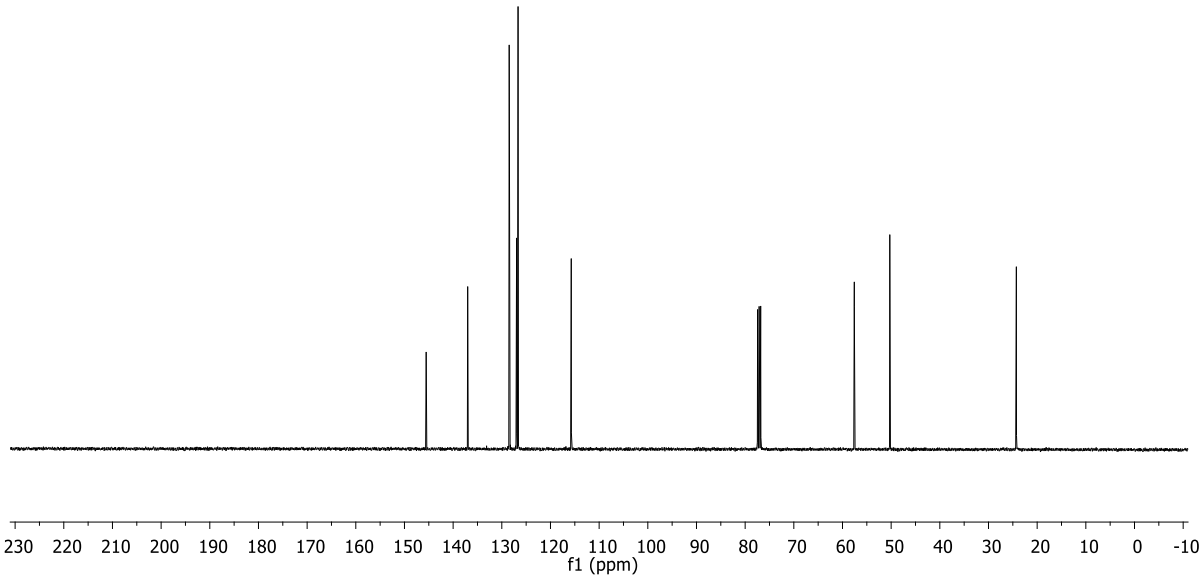

tert-Butyl (_E_)-2-(3-ethoxy-3-oxoprop-1-en-1-yl)-1_H_-pyrrole-1-carboxylate (183a)

(300 MHz, $CDCl_3$)

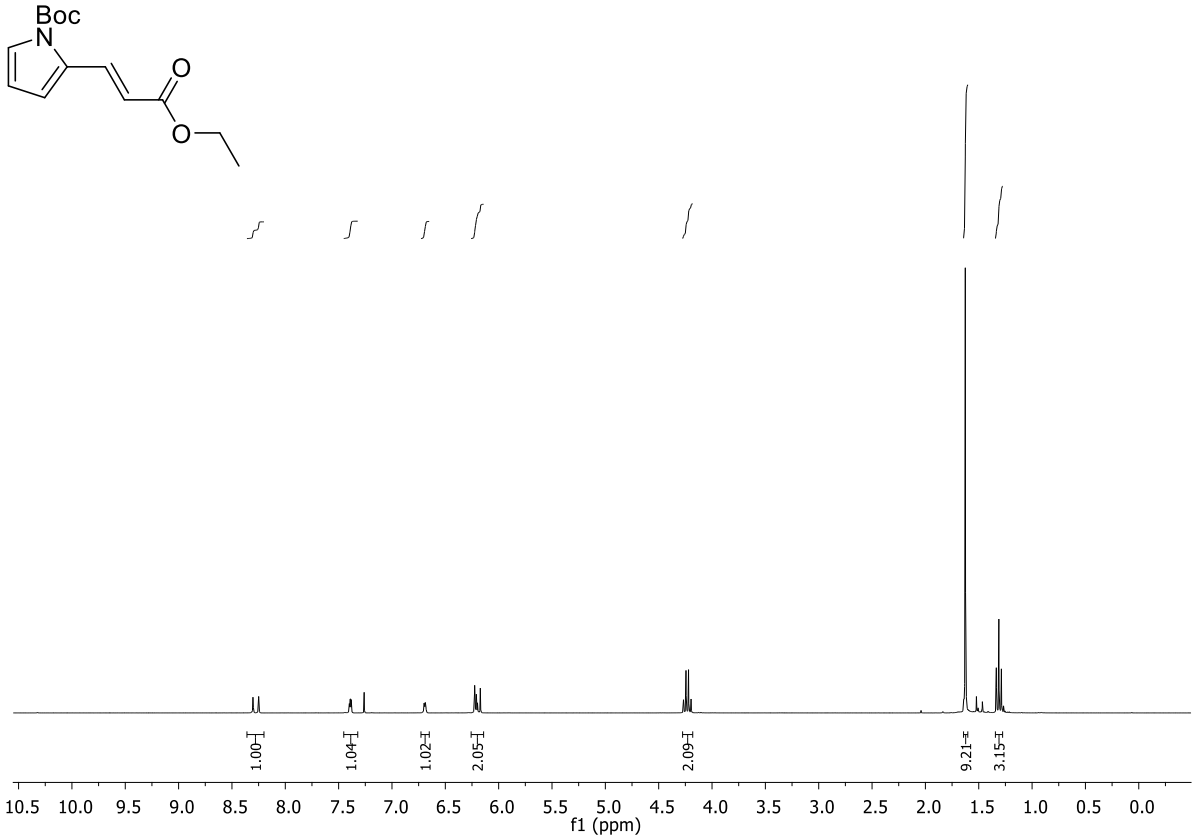

(75 MHz, $CDCl_3$)

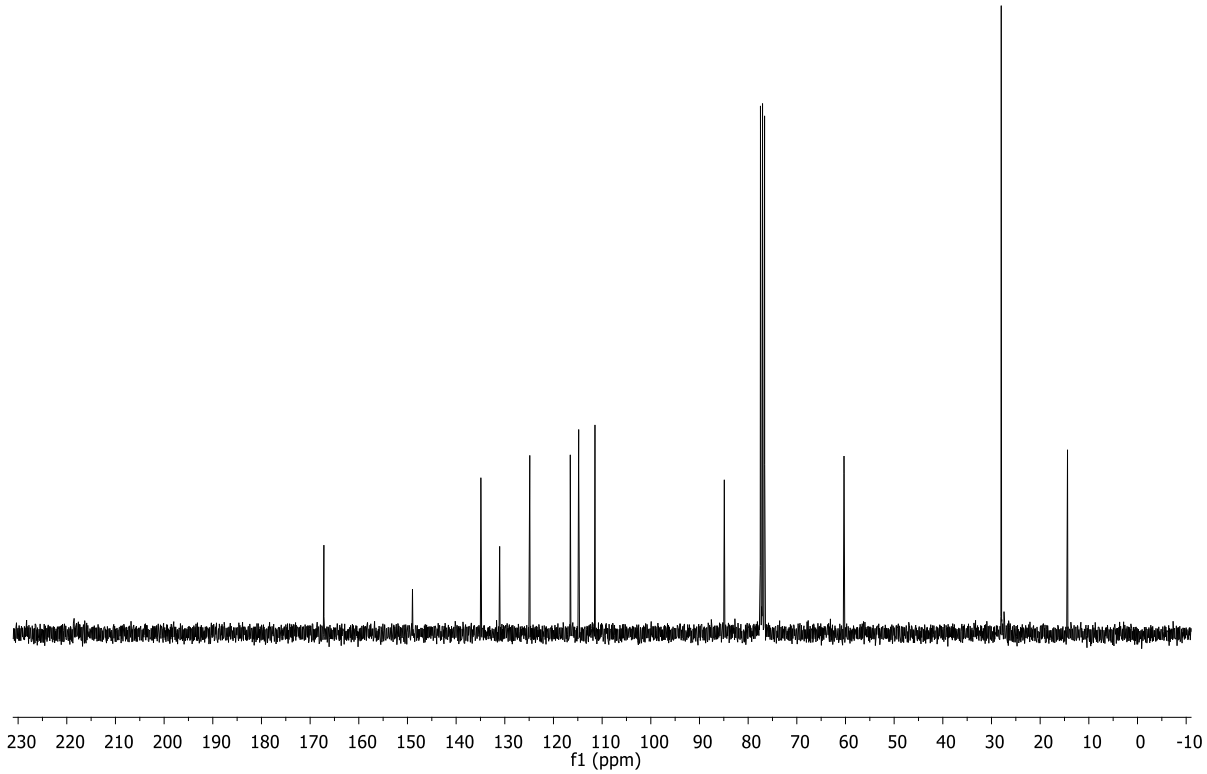

tert-Butyl (_E_)-2-(3-methoxy-3-oxoprop-1-en-1-yl)-1H-pyrrole-1-carboxylate (183b)

(300 MHz, $CDCl_3$)

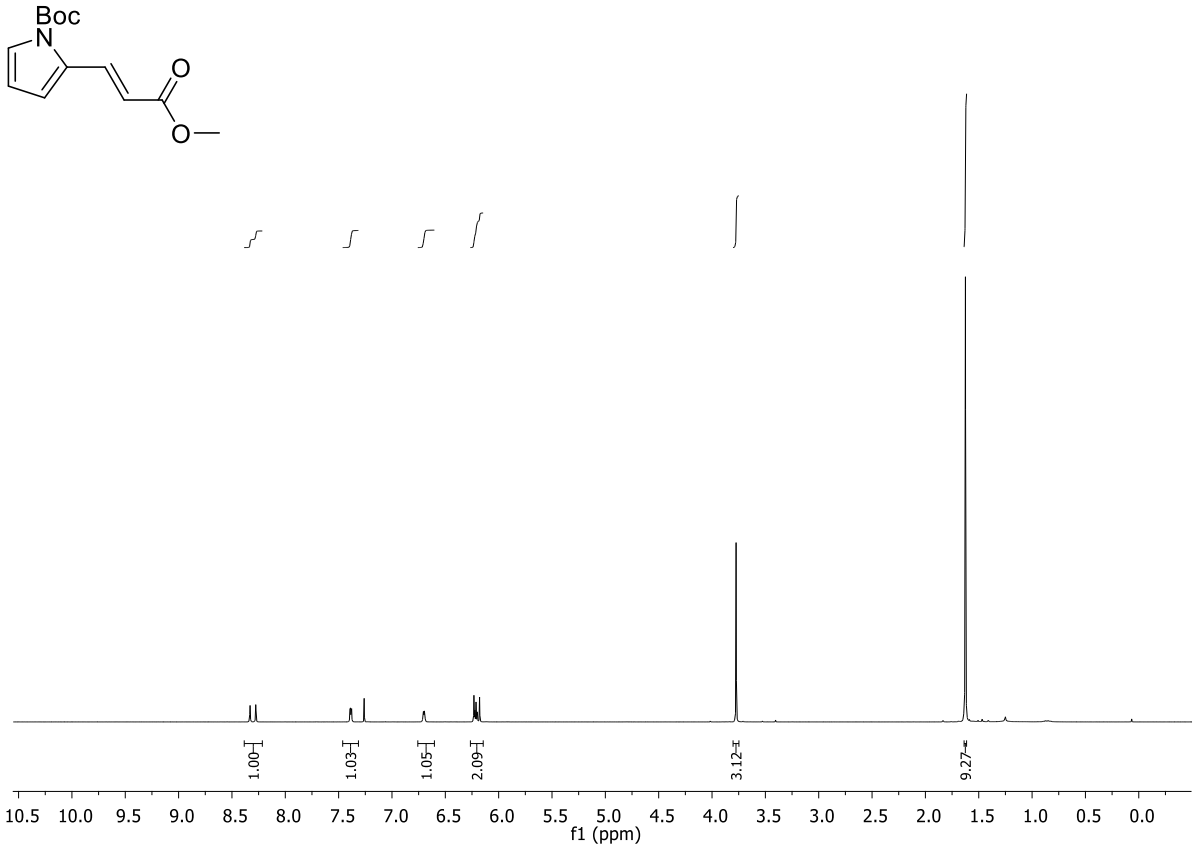

(75 MHz, $CDCl_3$)

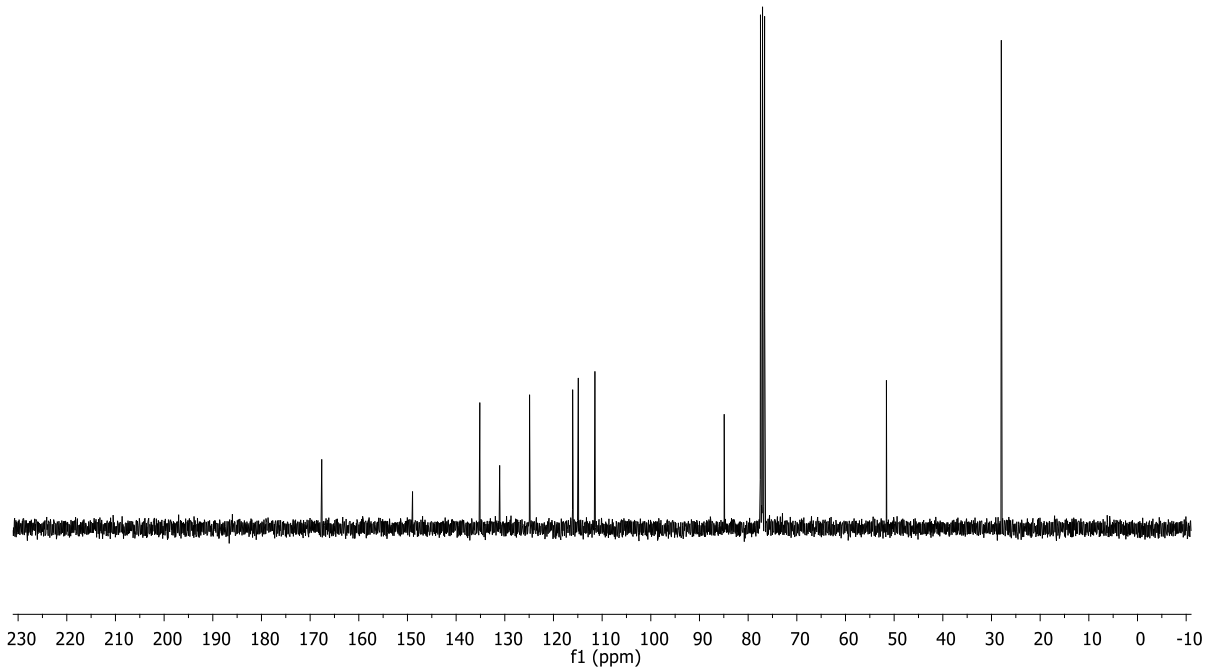

(*E*)-3-(1-Acetyl-1*H*-pyrrol-2-yl)acrylic acid (184a)

(300 MHz, $CDCl_3$)

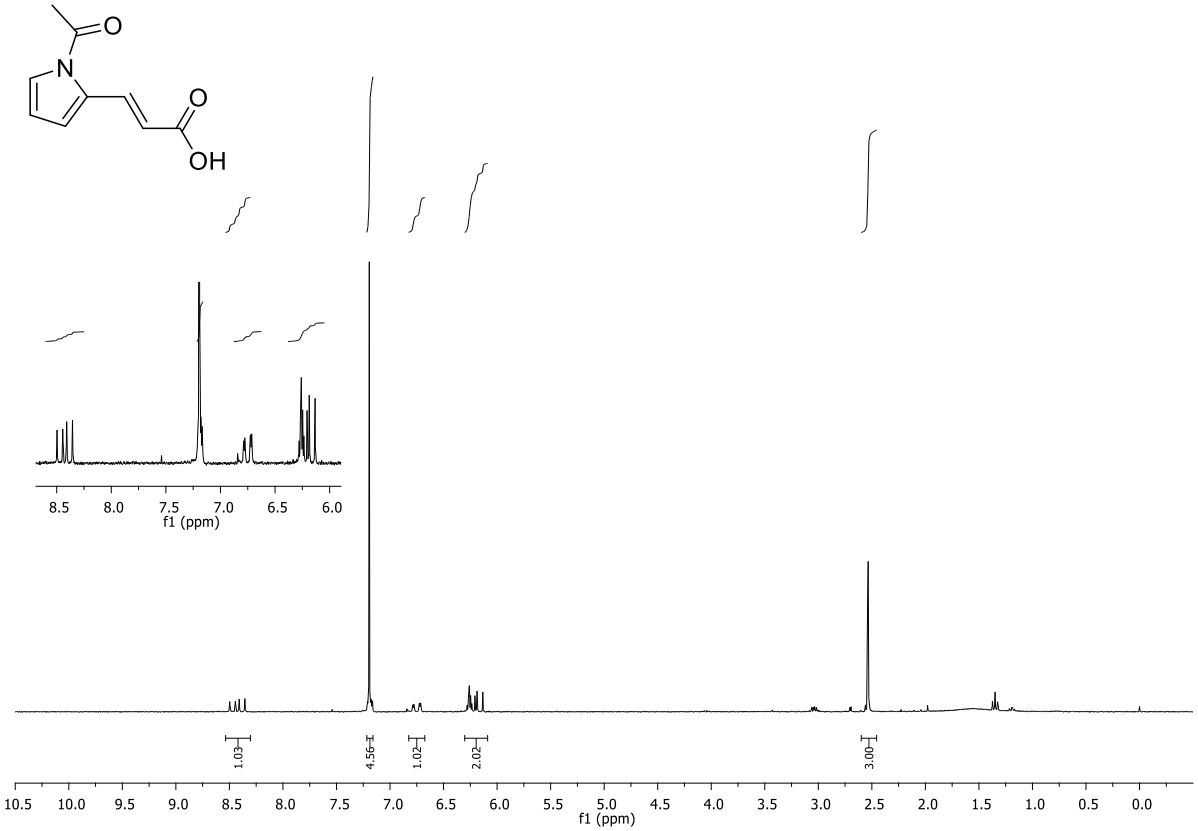

(75 MHz, $CDCl_3$)

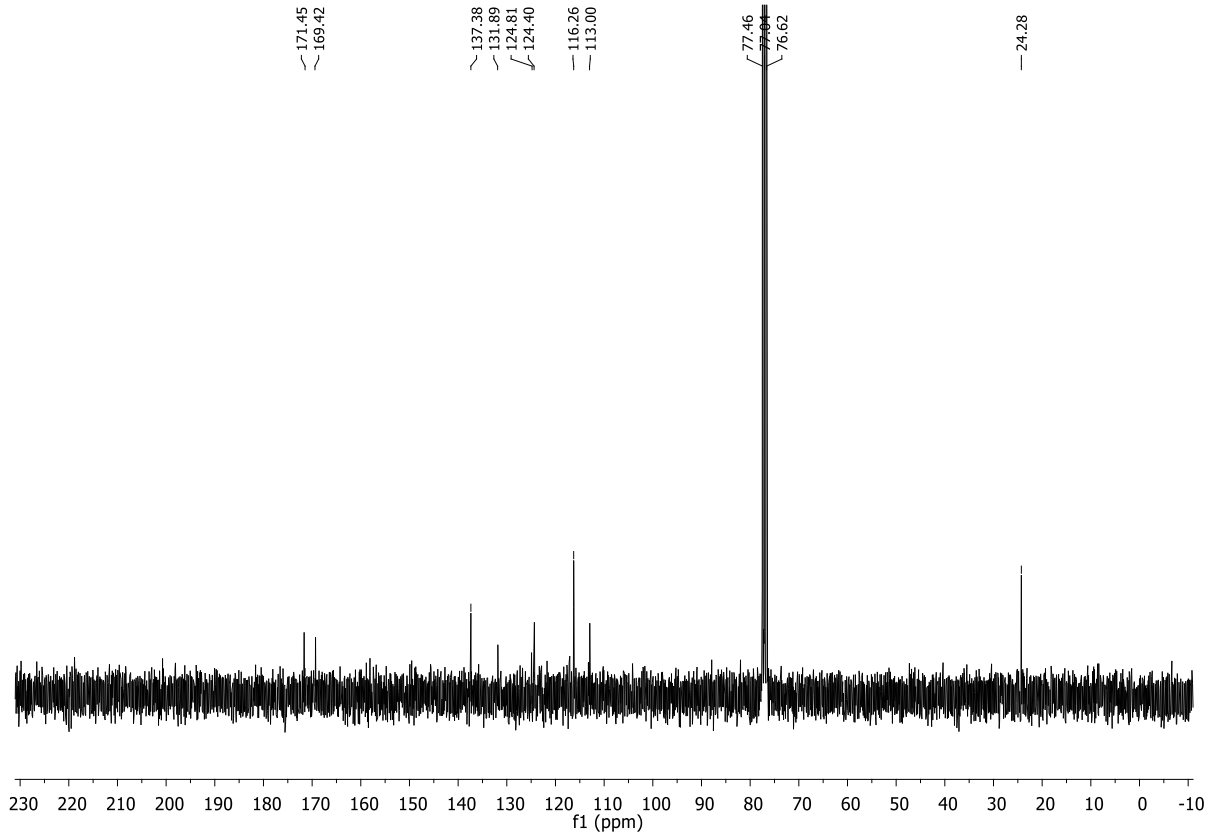

(*E*)-3-(1-Acetyl-1*H*-indol-3-yl)acrylic acid (184b)

(300 MHz, $CDCl_3$)

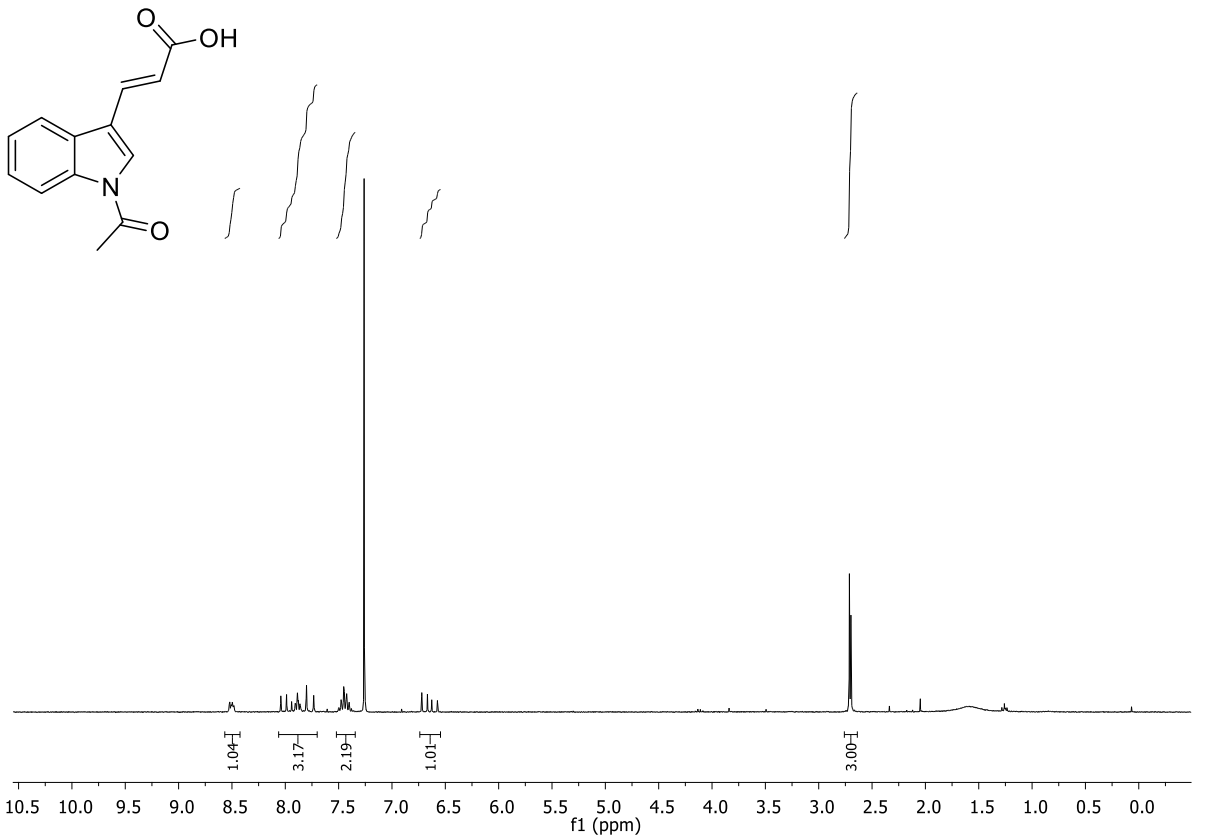

(101 MHz, $CDCl_3$)

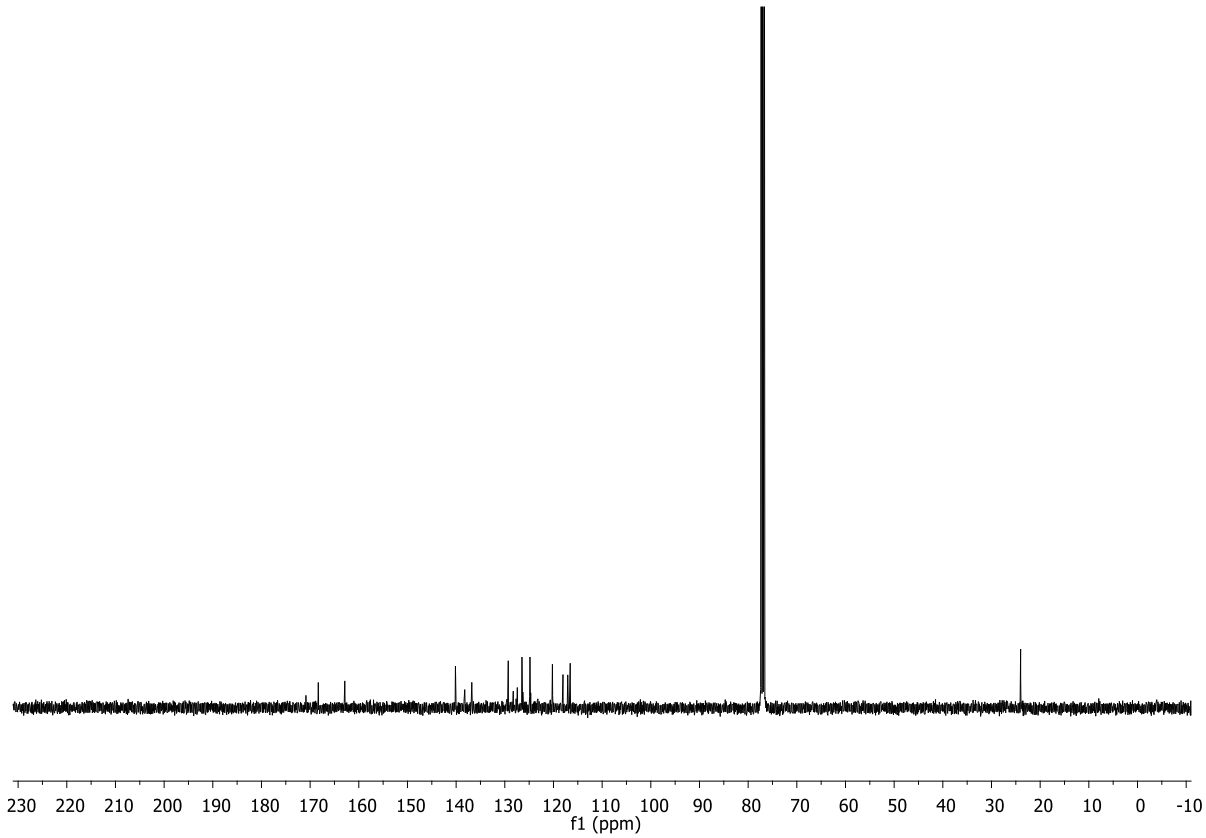

_N_-Cinnamyl-_N_-methylcinnamamide (153a)

(400 MHz, $CDCl_3$)

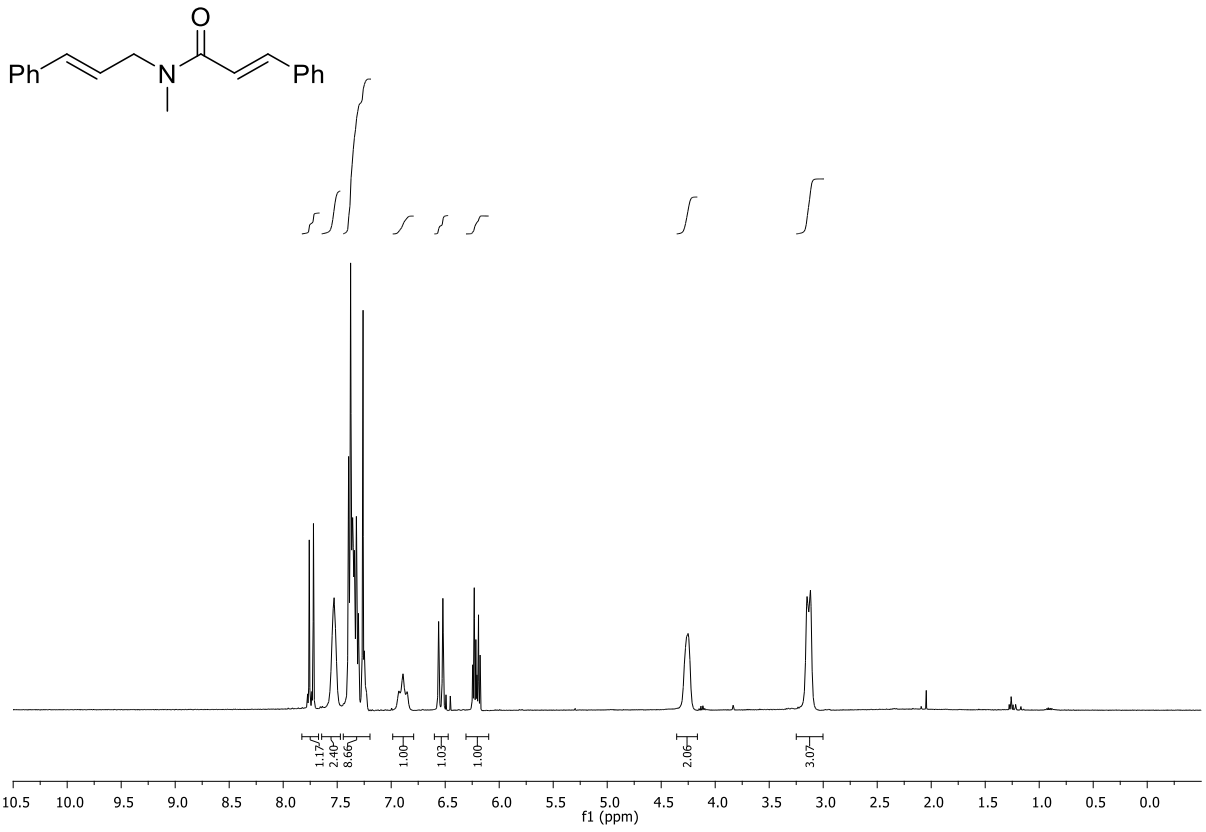

(75 MHz, $CDCl_3$)

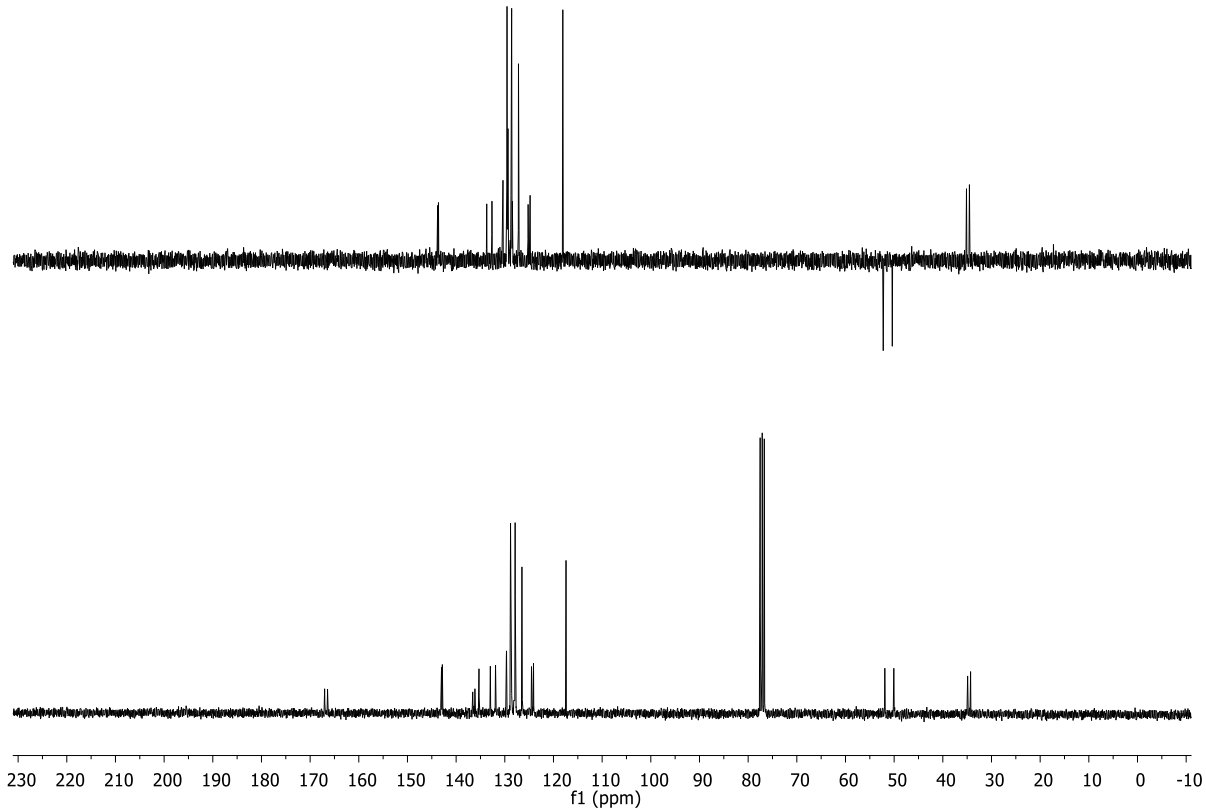

_N_-Cinnamyl-_N_-phenylcinnamamide (153b)

(300 MHz, $CDCl_3$)

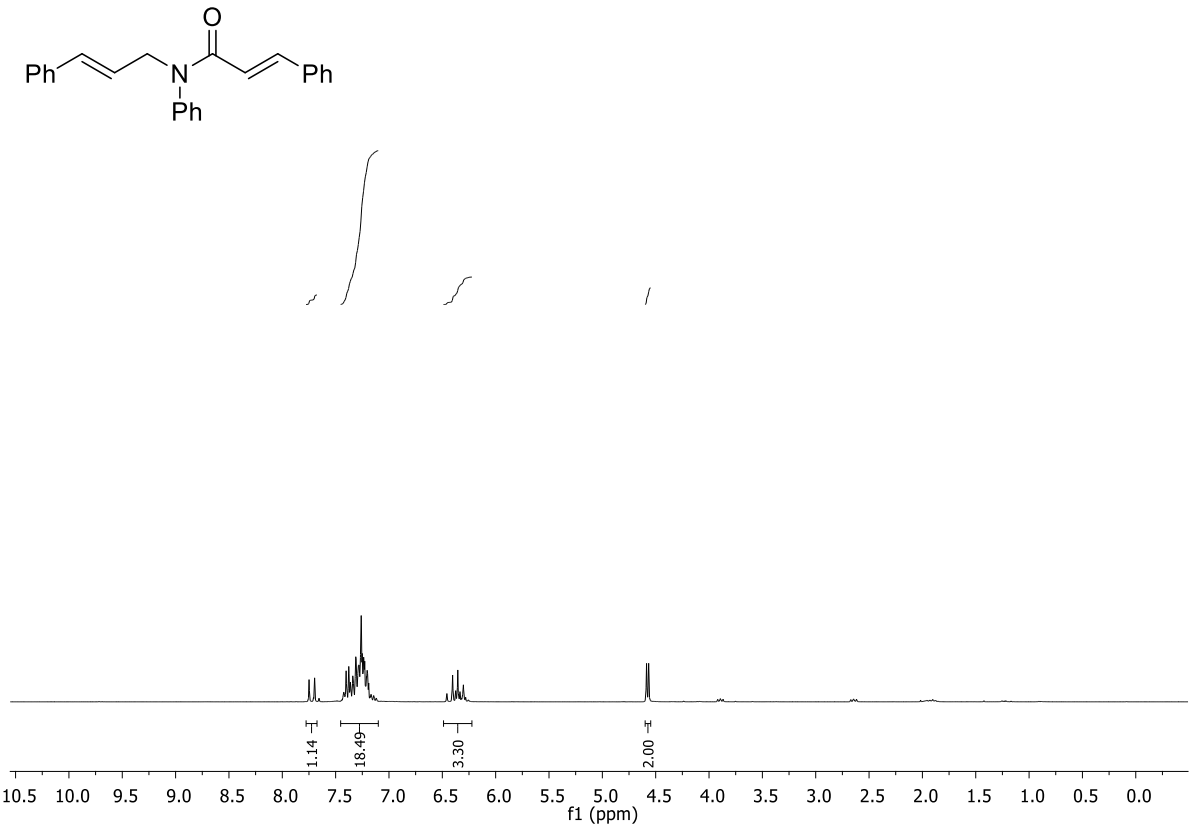

(75 MHz, $CDCl_3$)

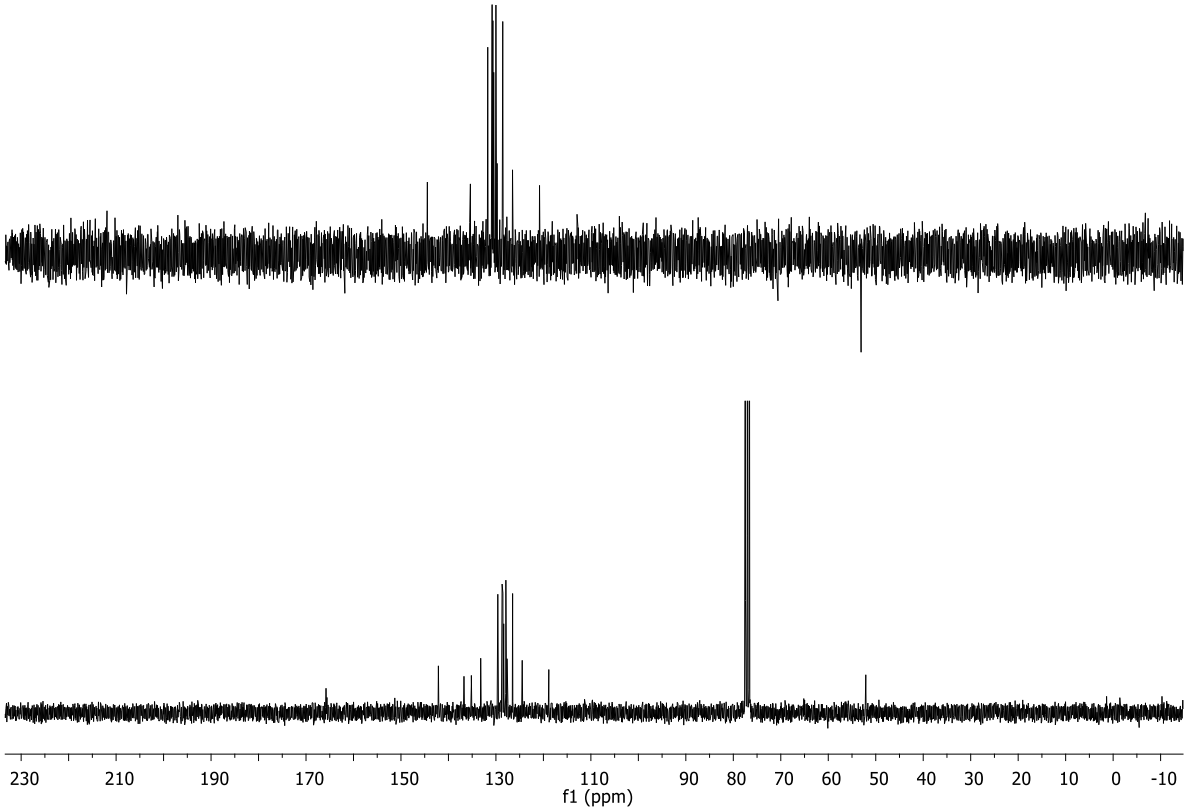

_N_-((_E_)-3-(4-Methoxyphenyl)allyl)-_N_-phenylcinnamamide (153c)

(300 MHz, $CDCl_3$)

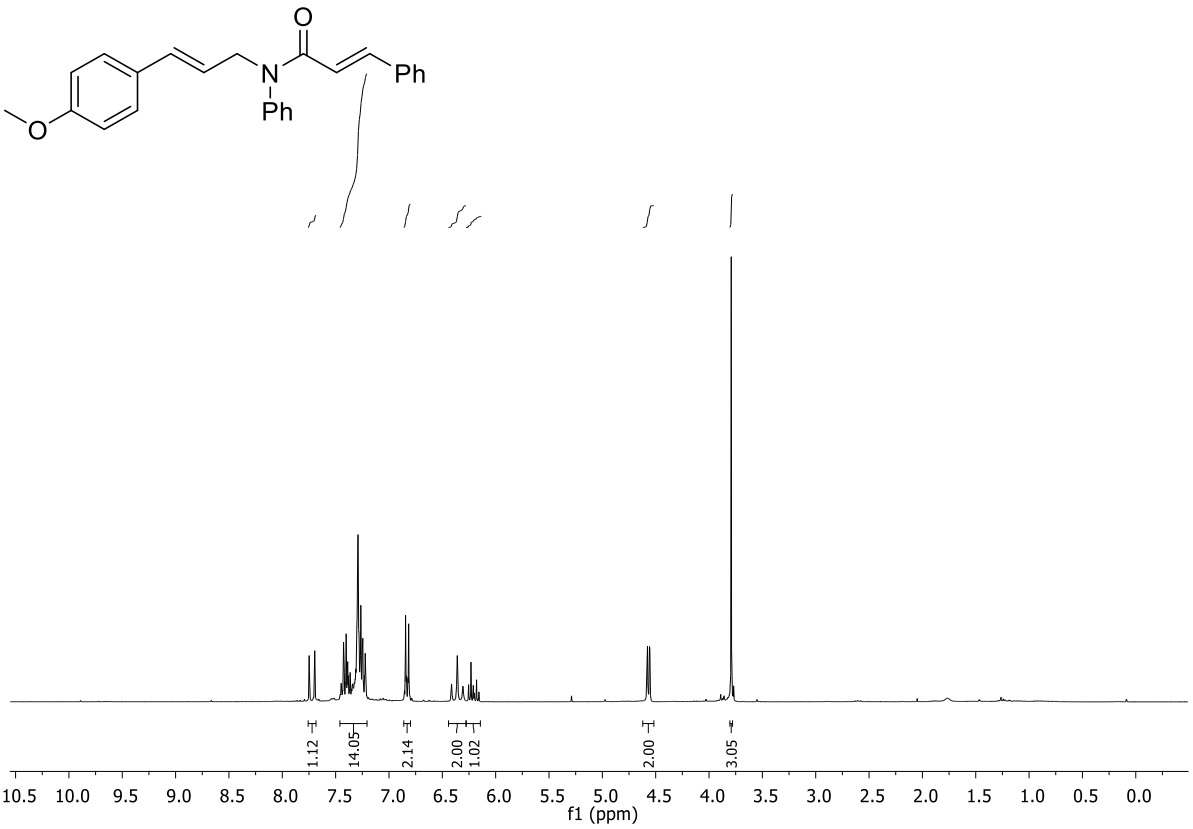

(75 MHz, $CDCl_3$)

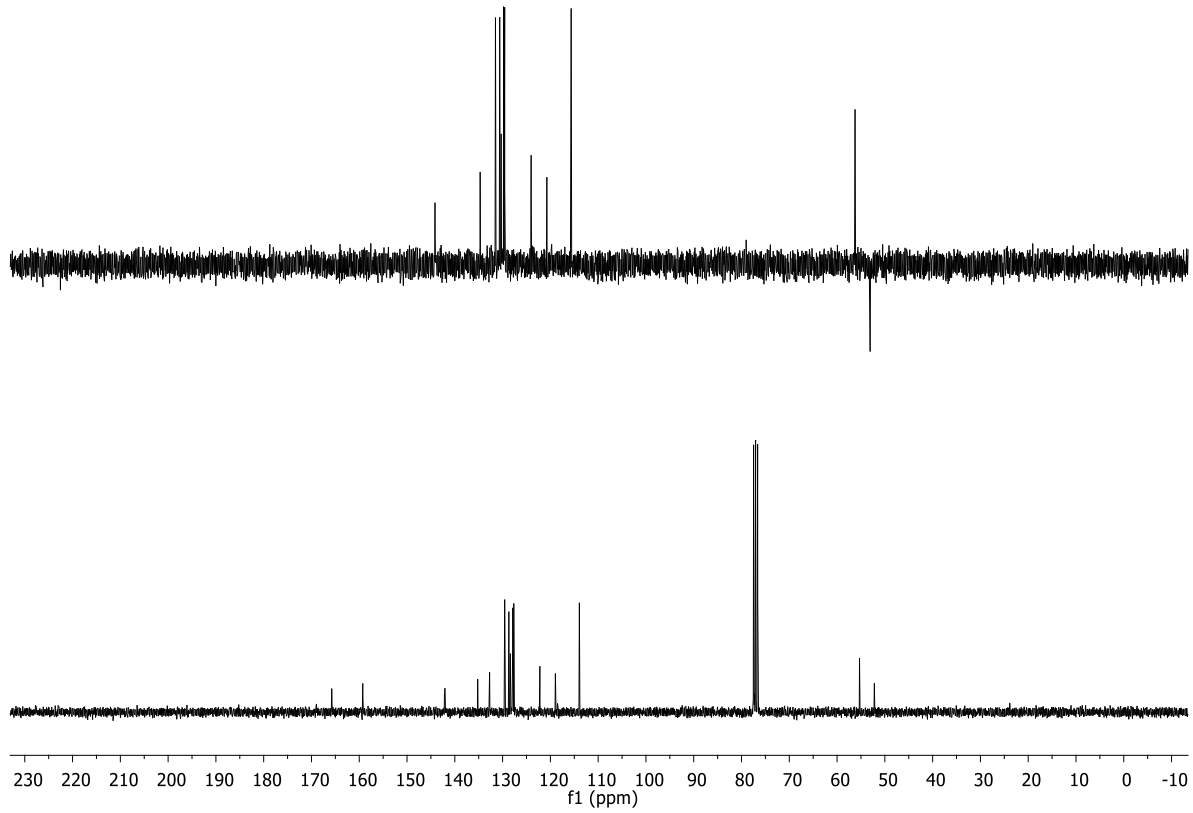

_N_-(_tert_-Butyl)-_N_-((_E_)-3-(4-methoxyphenyl)allyl)cinnamamide (153d)

(300 MHz, $CDCl_3$)

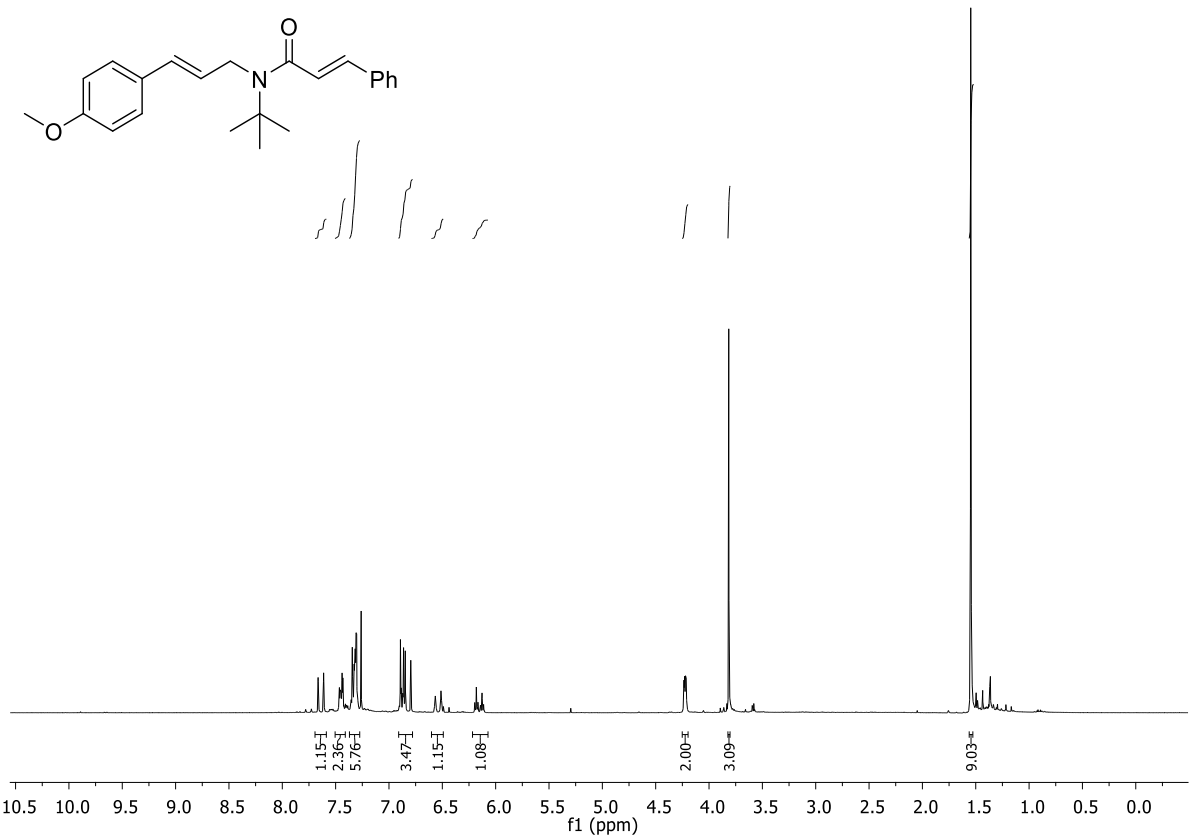

(75 MHz, $CDCl_3$)

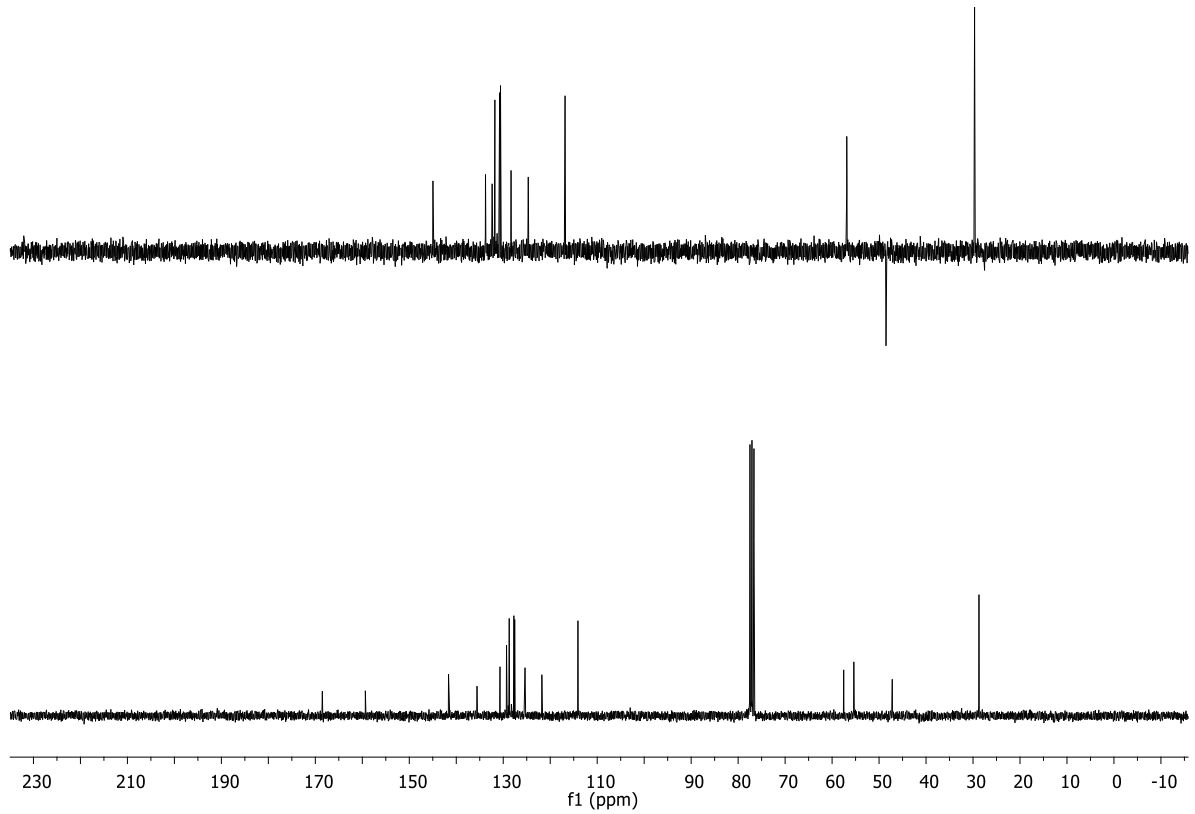

_N_-(_tert_-Butyl)-_N_-cinnamylcinnamamide (153g)

(300 MHz, $CDCl_3$)

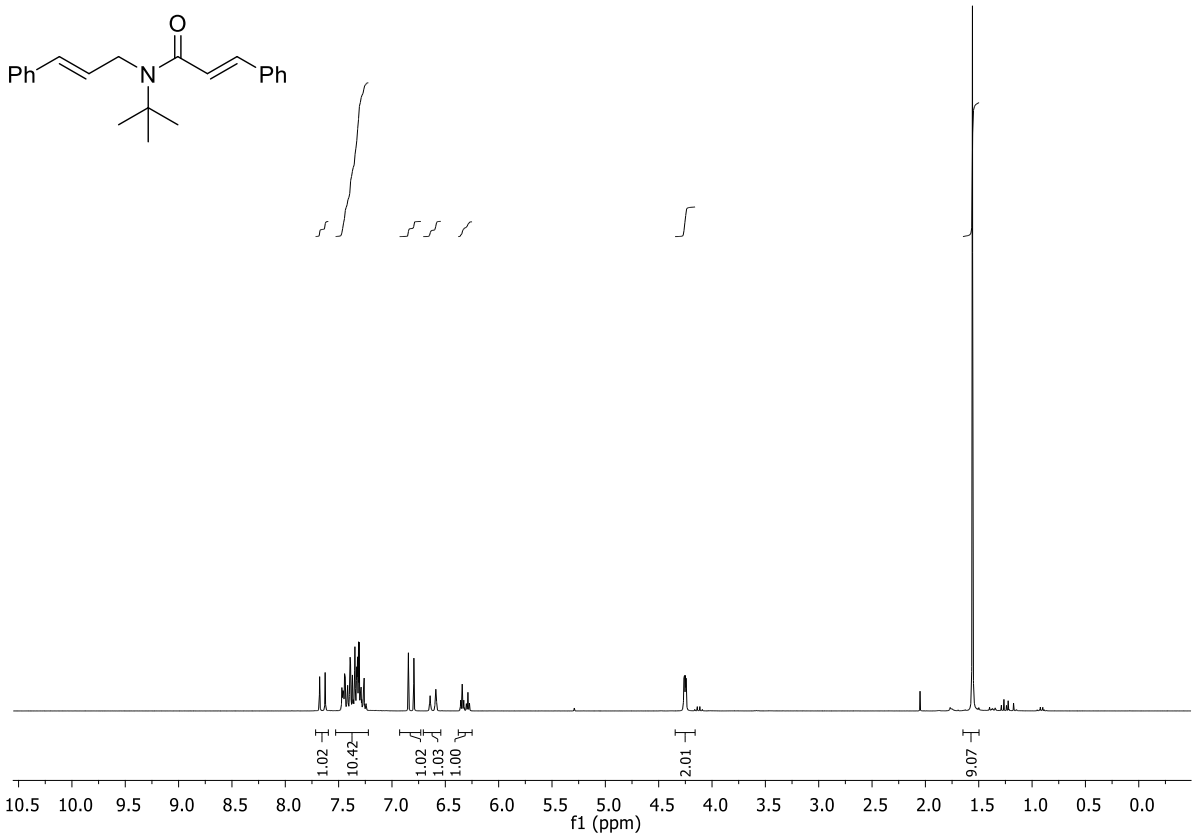

(75 MHz, $CDCl_3$)

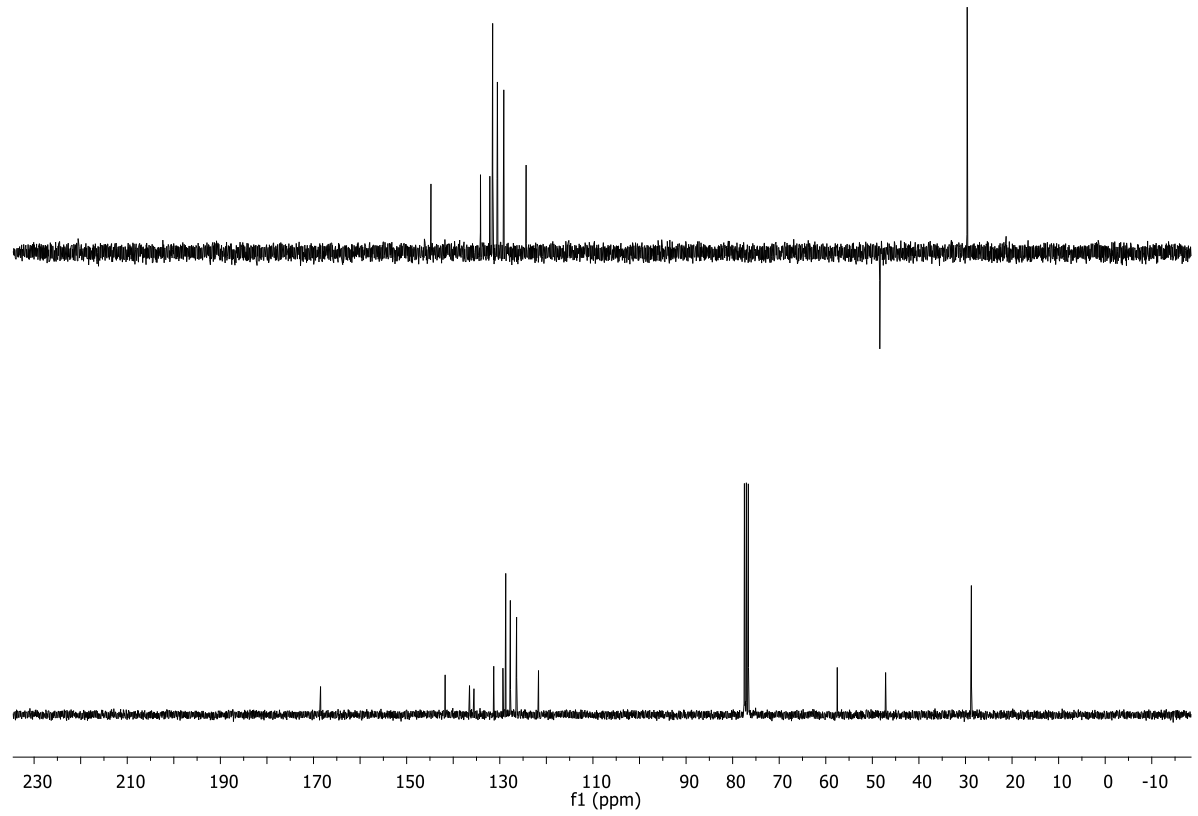

N-Cinnamylcinnamamide (153e)

(300 MHz, $CDCl_3$)

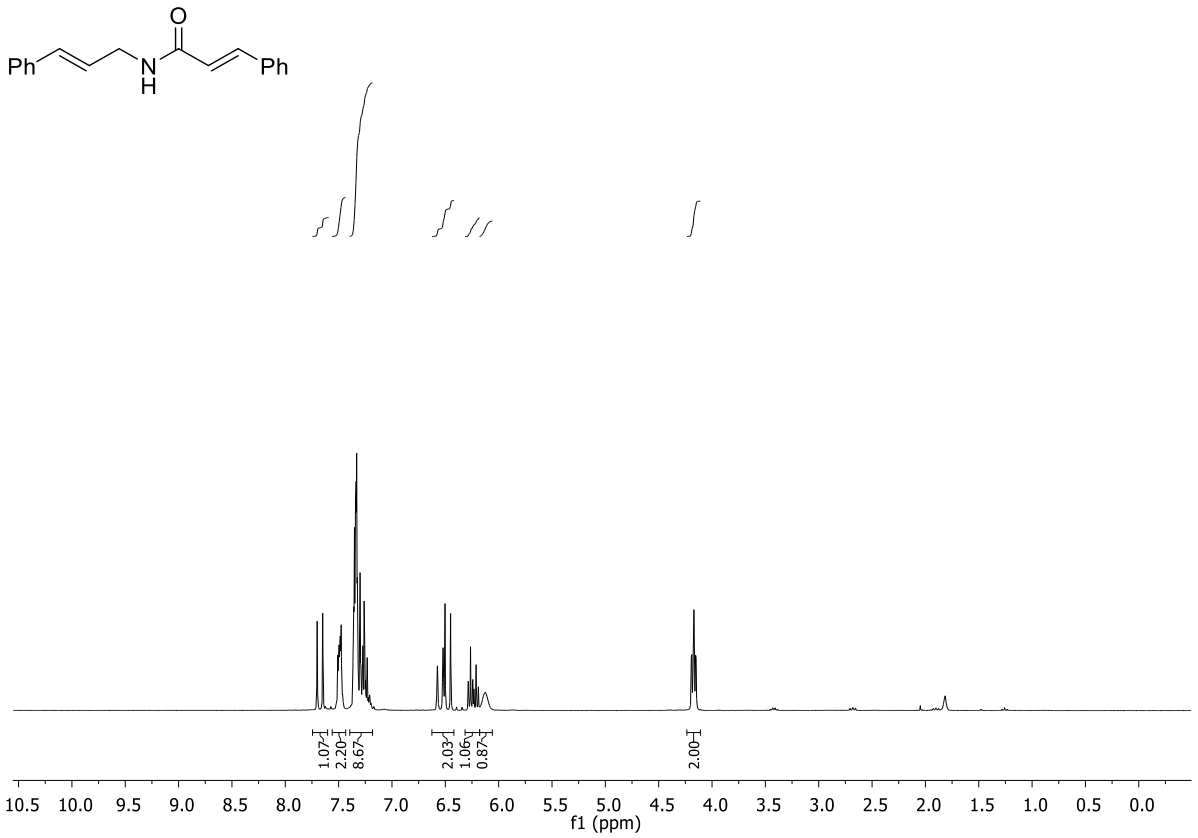

(75 MHz, $CDCl_3$)

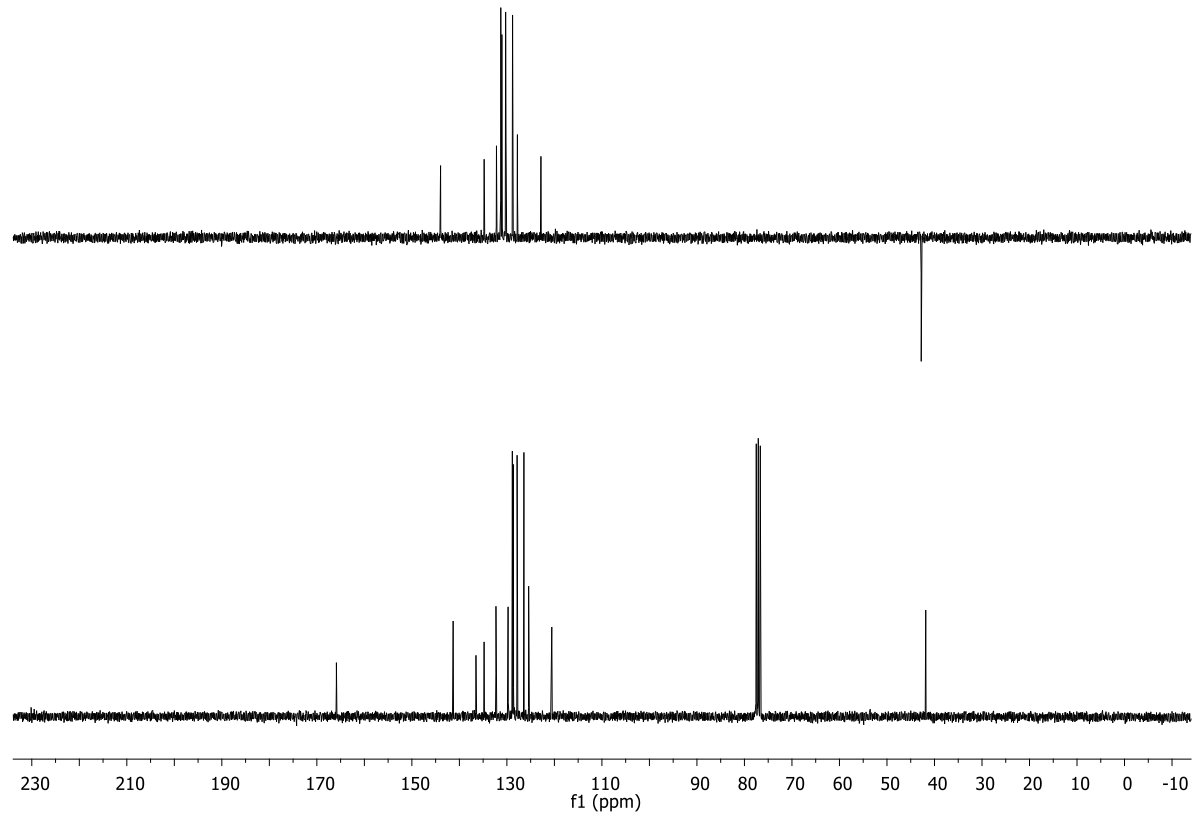

_N_-Benzyl-_N_-cinnamylcinnamamide (153q)

(300 MHz, $CDCl_3$)

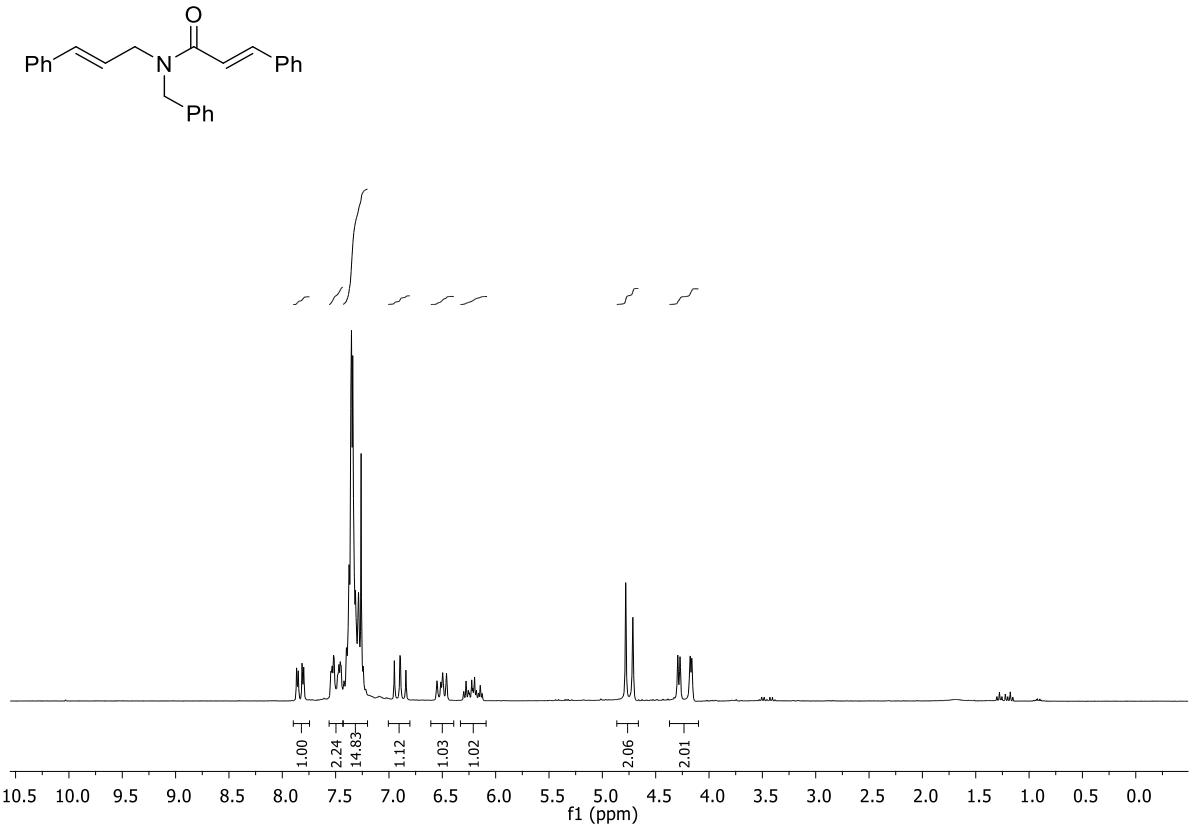

(75 MHz, $CDCl_3$)

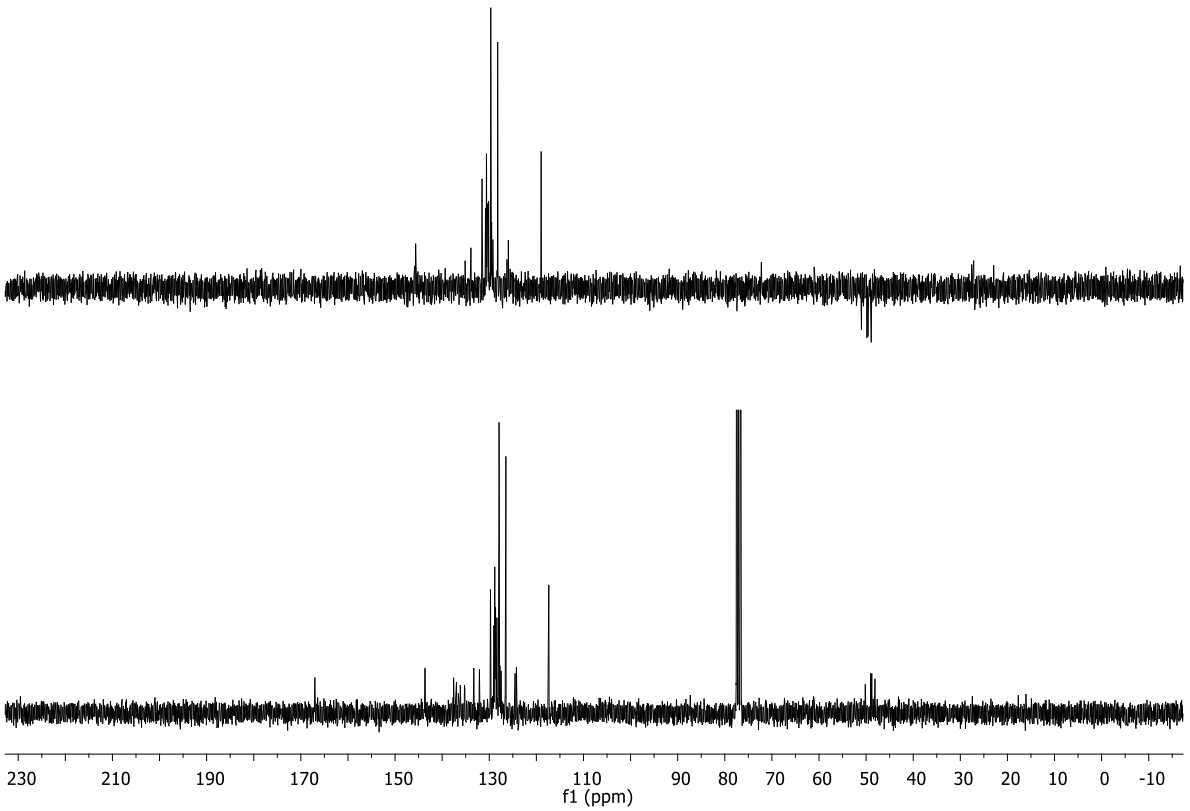

tert-Butyl cinnamoyl(cinnamyl)carbamate (153t)

(300 MHz, $CDCl_3$)

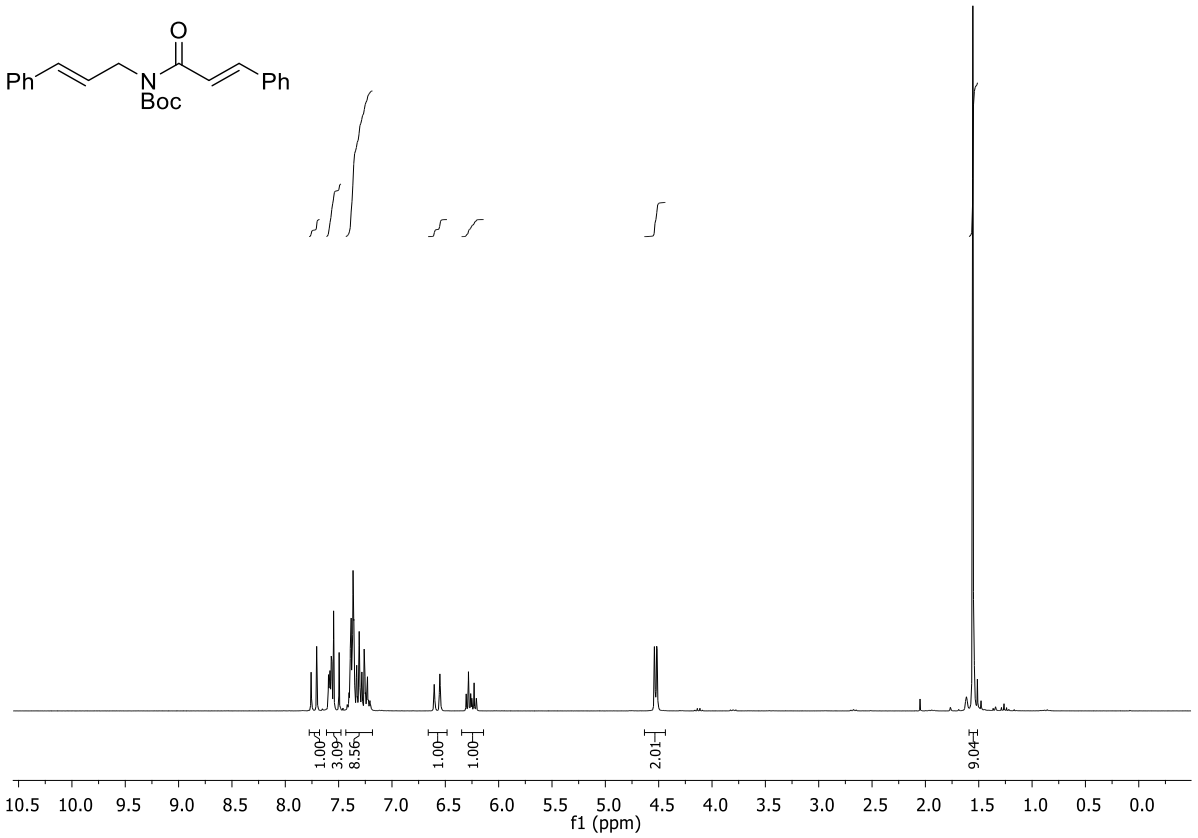

(75 MHz, $CDCl_3$)

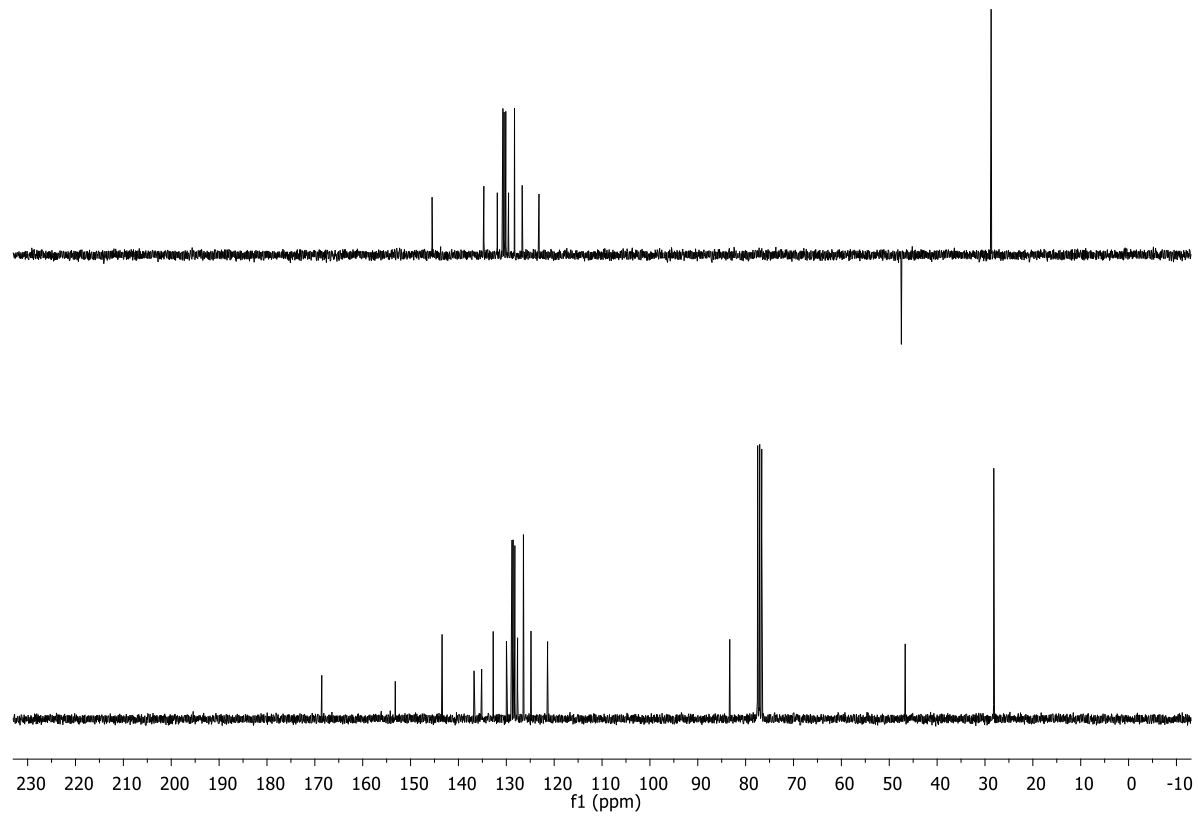

_N_-(_tert_-Butyl)-_N_-cinnamylacrylamide (153i)

(300 MHz, $CDCl_3$)

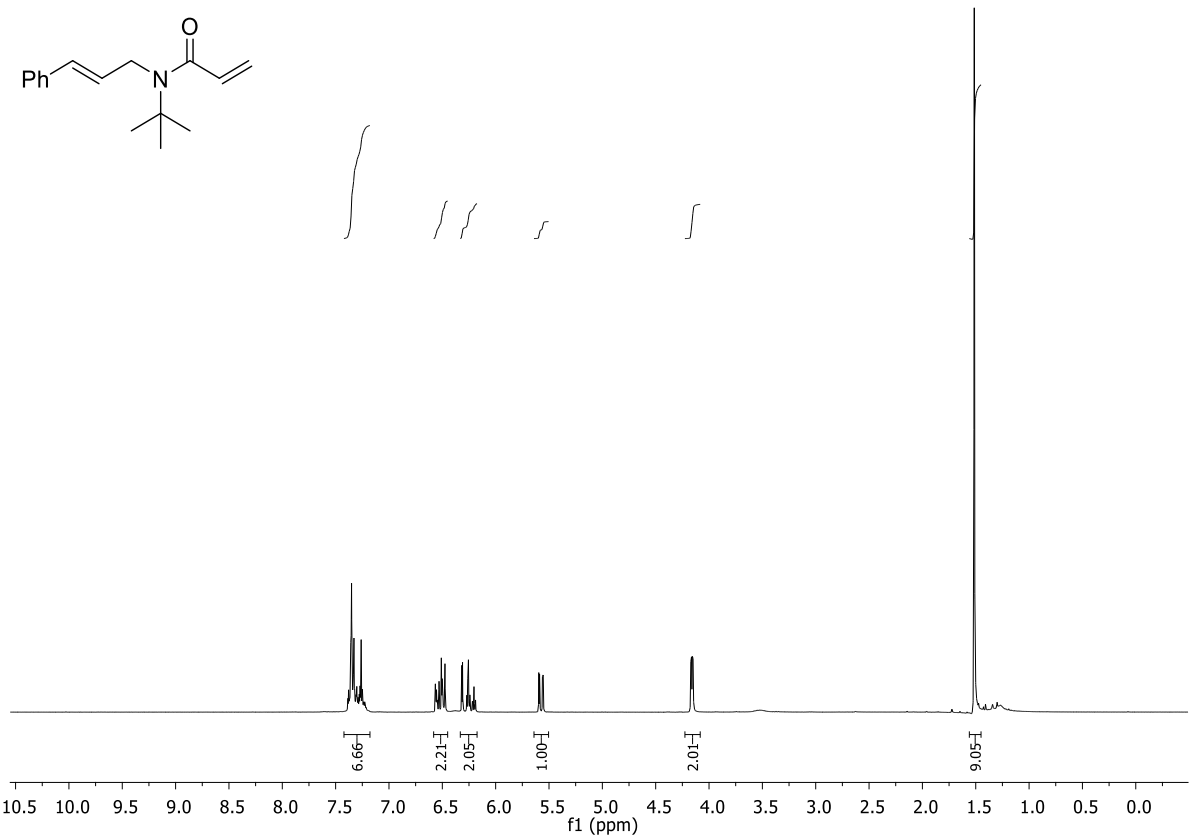

(101 MHz, $CDCl_3$)

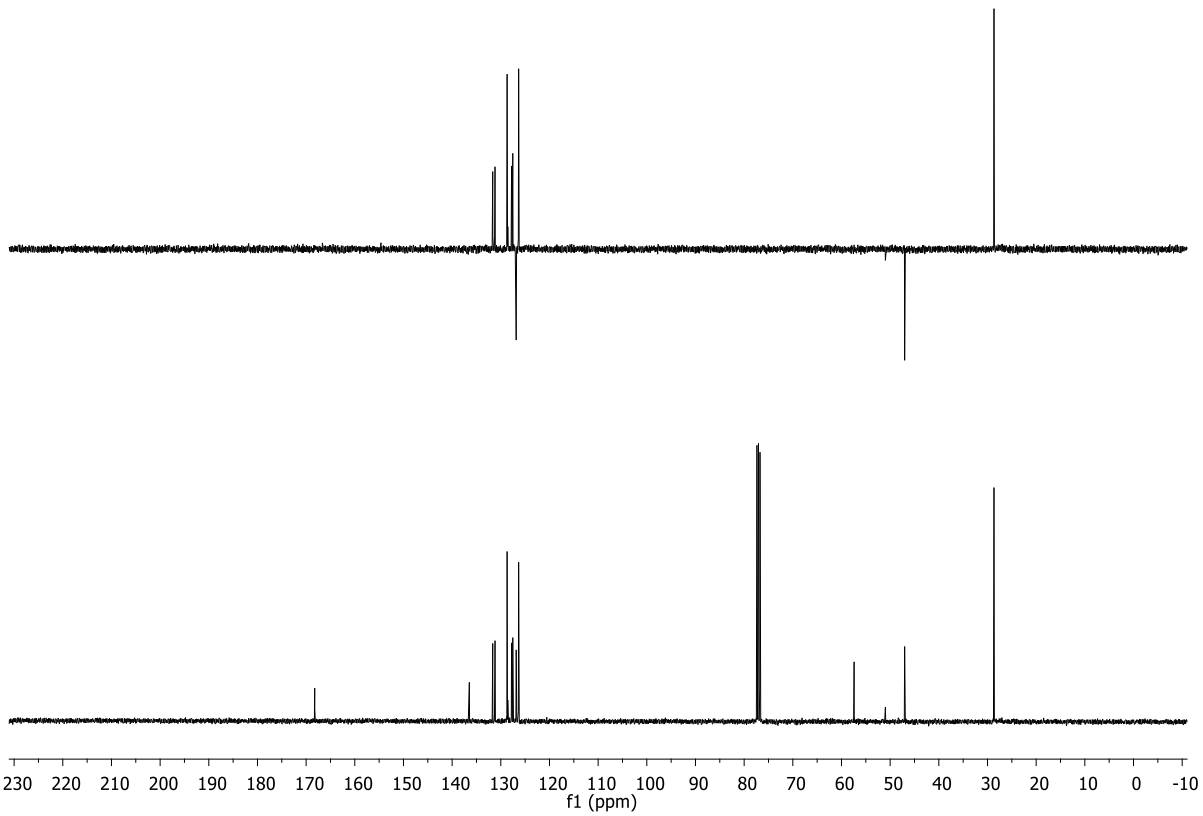

_N_-Benzyl-_N_-cinnamylacrylamide (153s)

(400 MHz, $CDCl_3$)

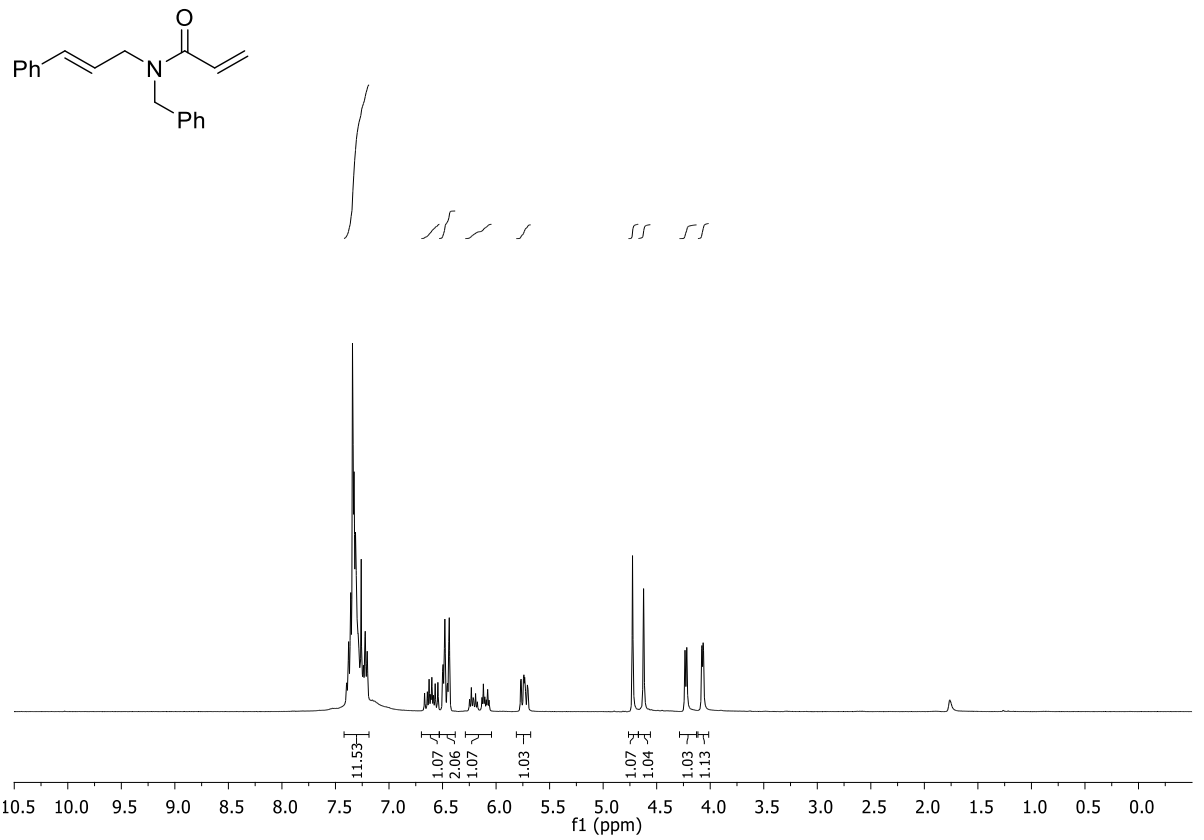

(101 MHz, $CDCl_3$)

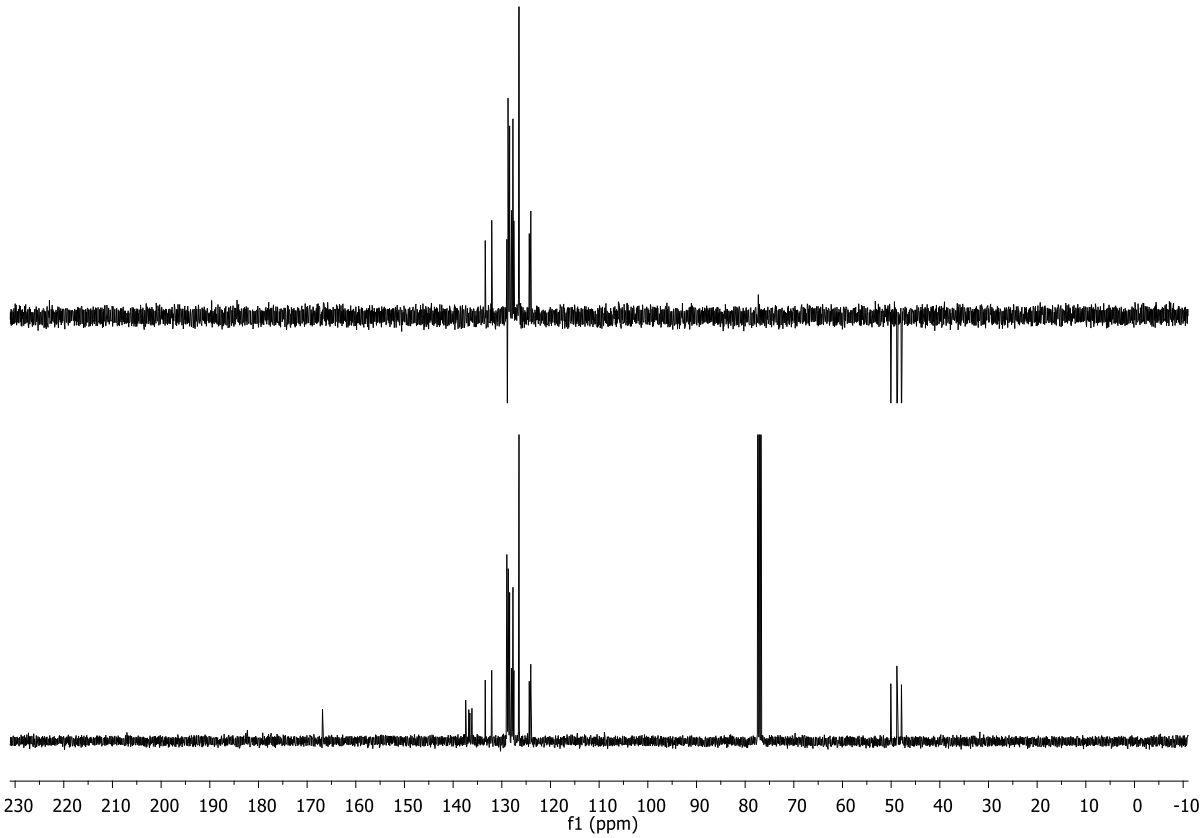

N-Cinnamylacrylamide (153f)

(300 MHz, $CDCl_3$)

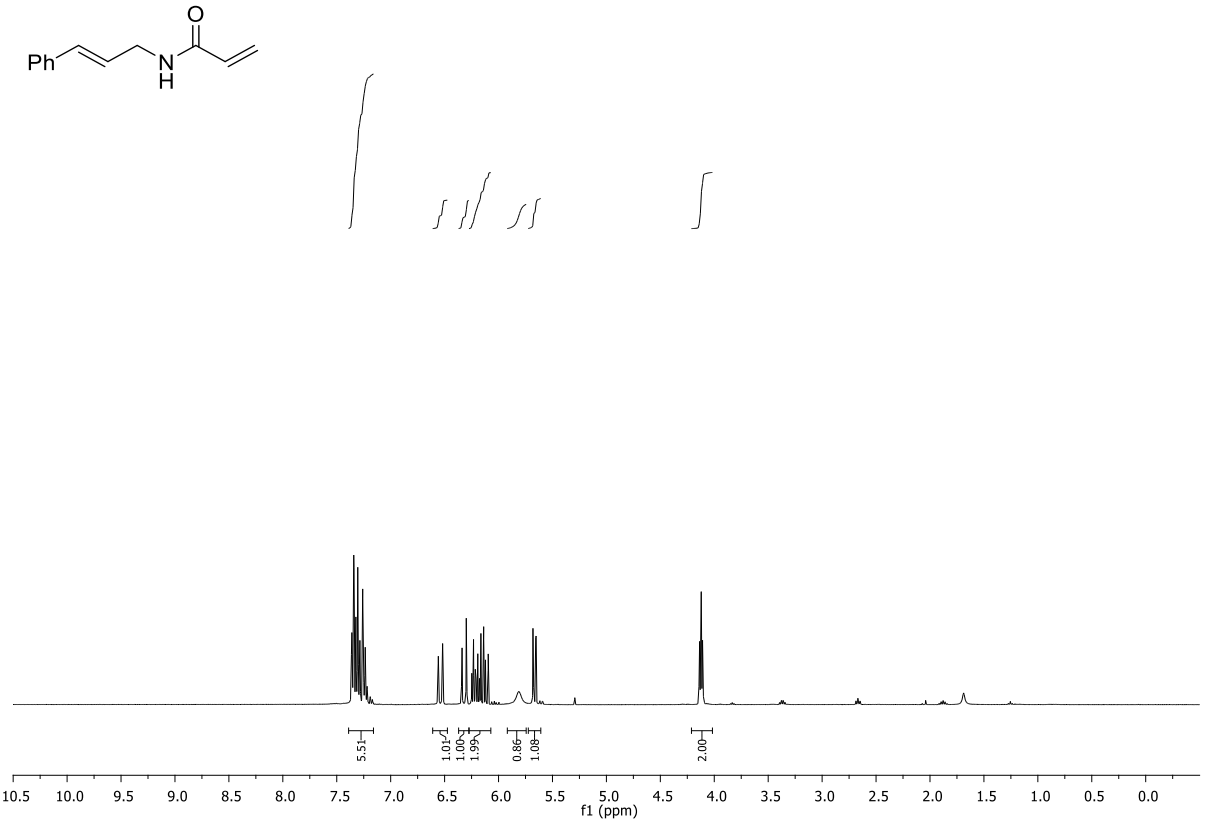

(101 MHz, $CDCl_3$)

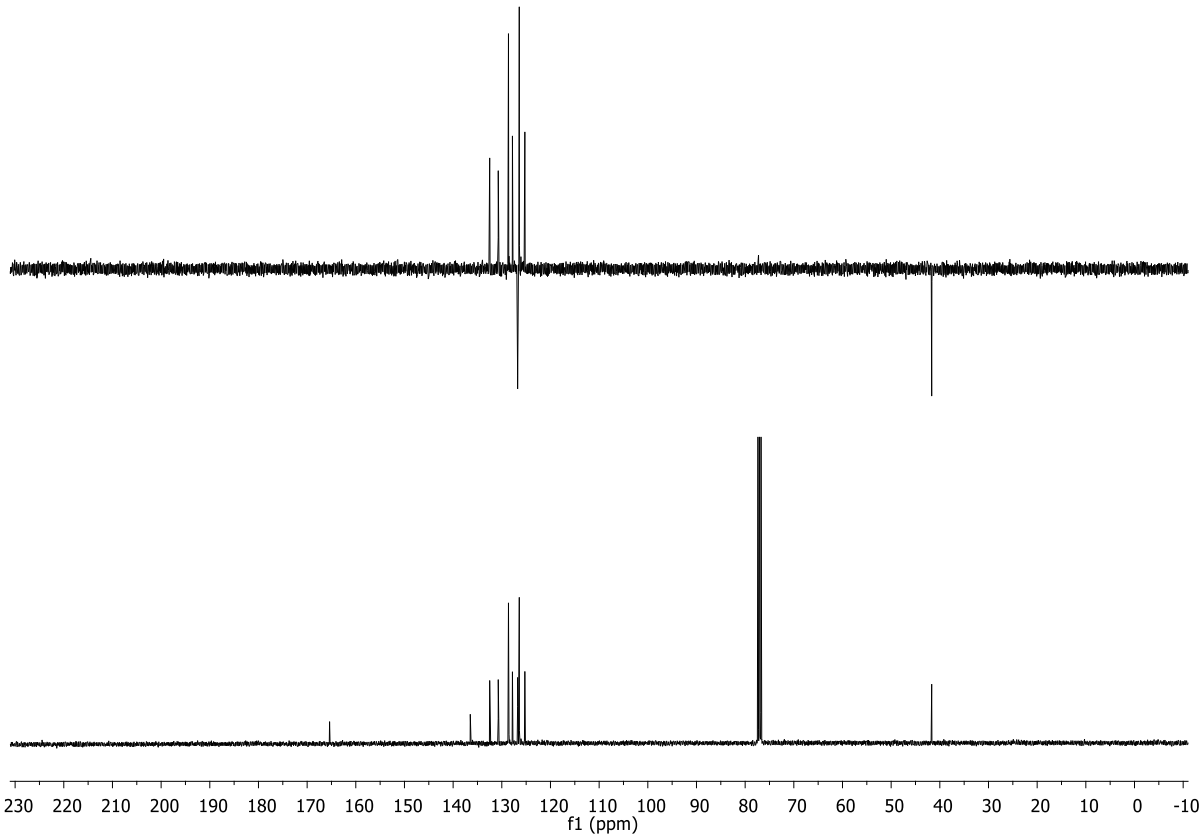

tert-Butyl allyl(cinnamoyl)carbamate (153u)

(400 MHz, $CDCl_3$)

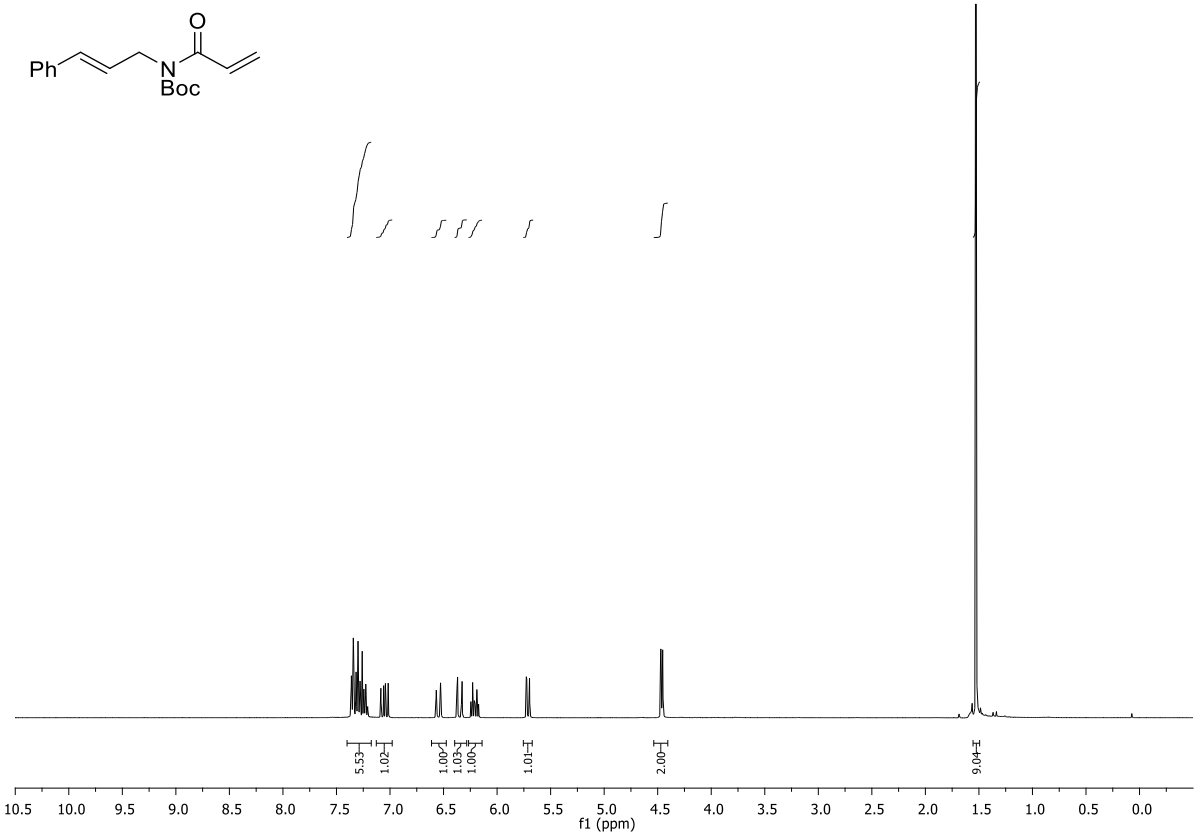

(101 MHz, $CDCl_3$)

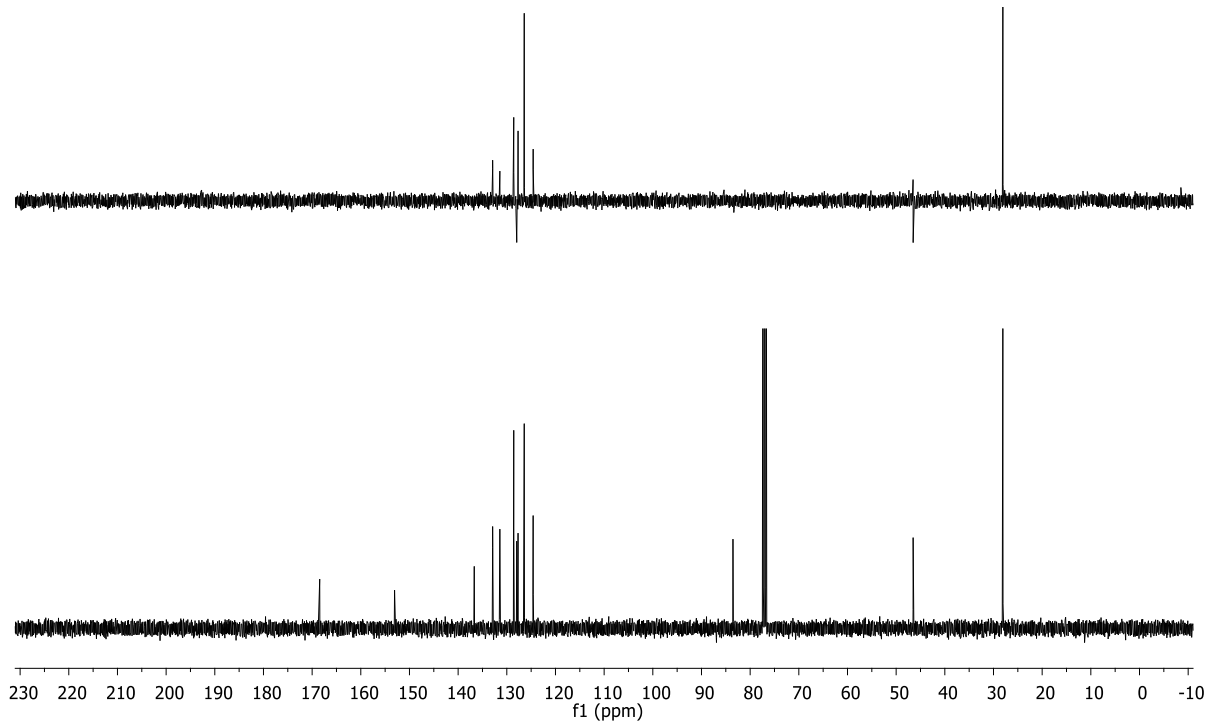

Methyl (*E*)-4-(*N*-(*tert*-butyl)cinnamamido)but-2-enoate (153o)

(400 MHz, $CDCl_3$)

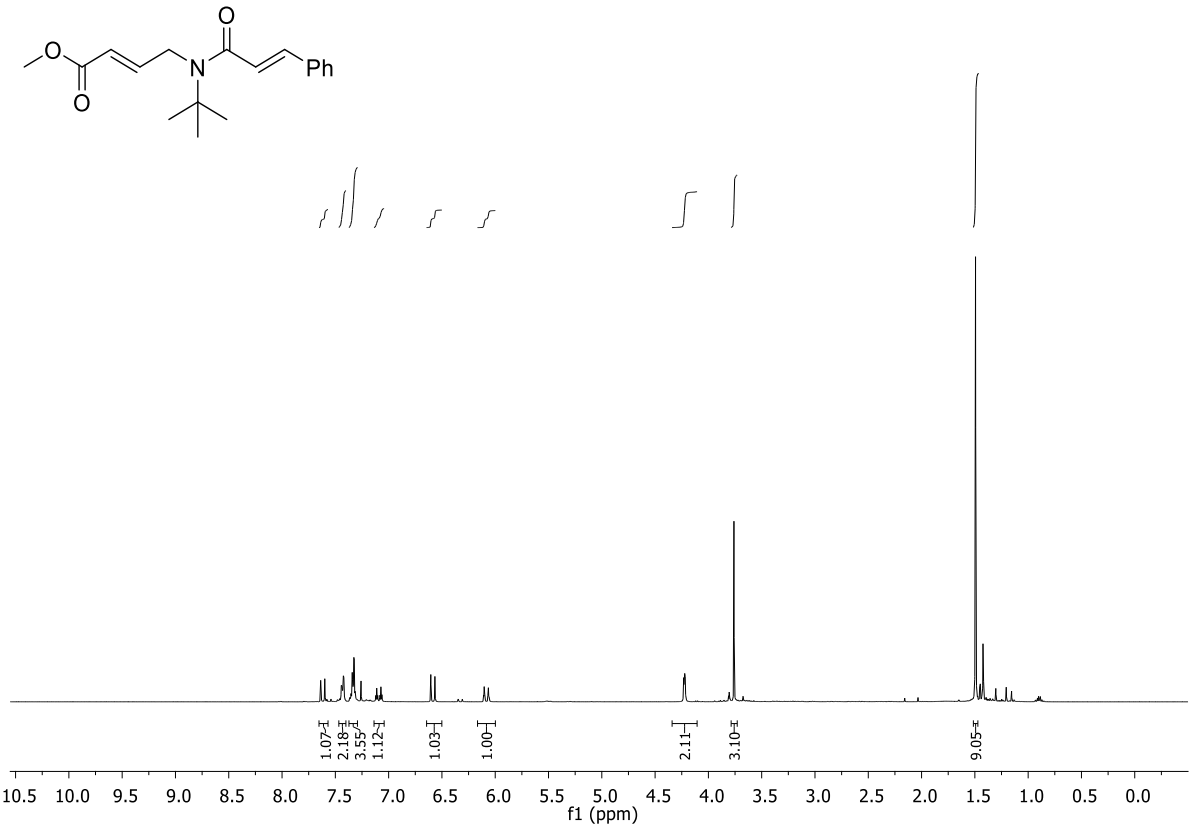

(101 MHz, $CDCl_3$)

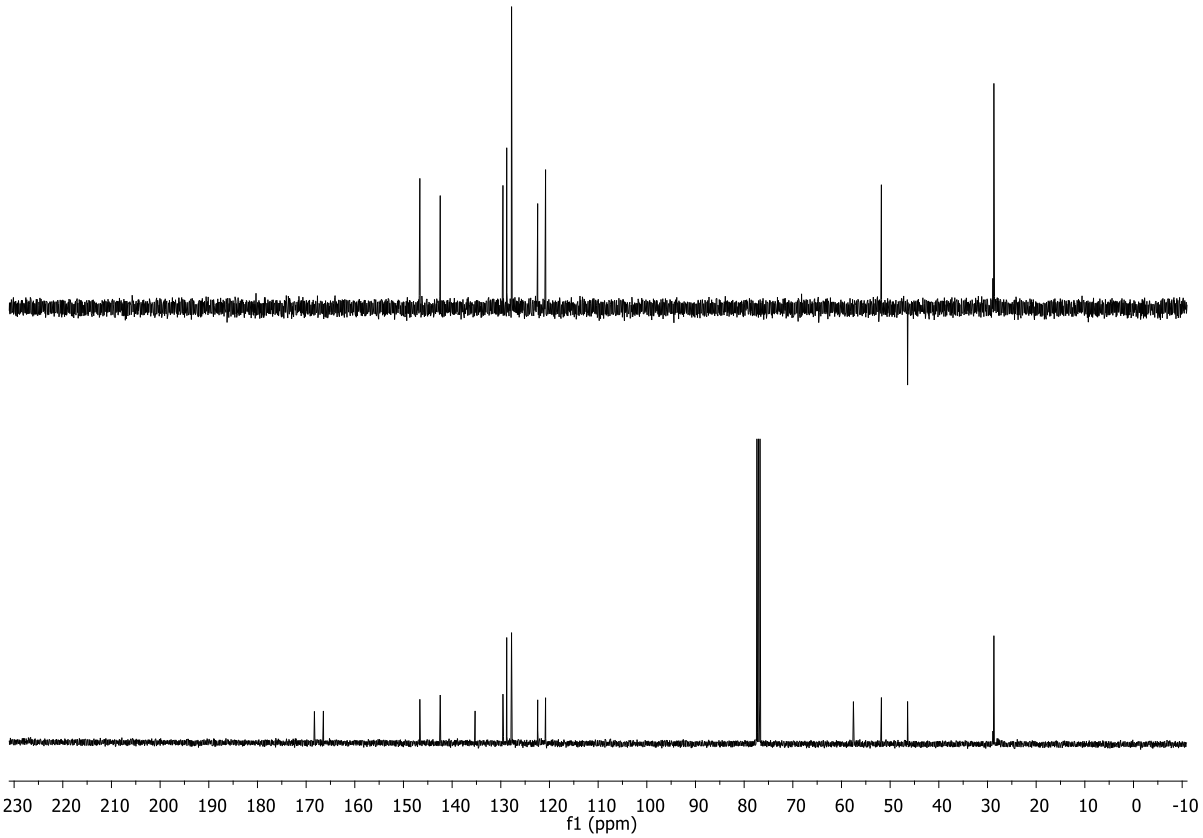

Methyl 2-(*tert*-butyl)-3-oxo-2,3,3a,4,9,9a-hexahydro-1H-benzo[f]isoindole-4-carboxylate (189) (300 MHz, $CDCl_3$)

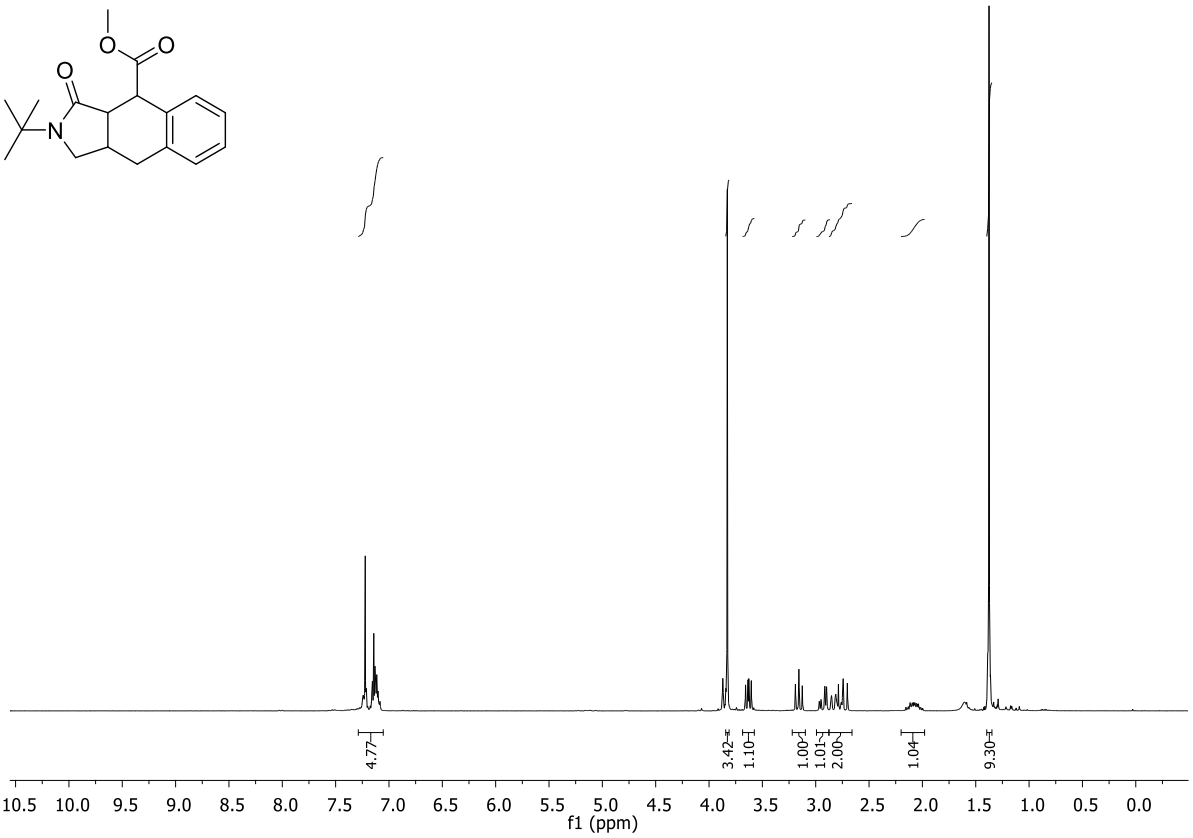

(75 MHz, $CDCl_3$)

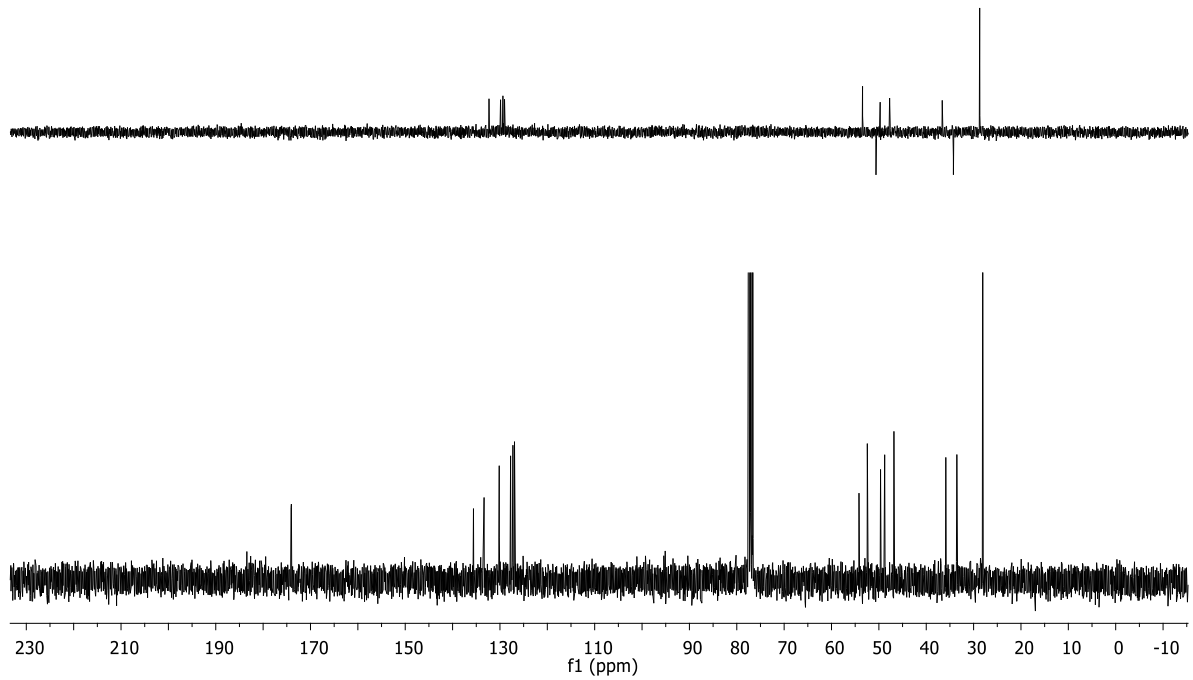

_N_-Allyl-_N_-(_tert_-butyl)cinnamamide (153h)

(300 MHz, $CDCl_3$)

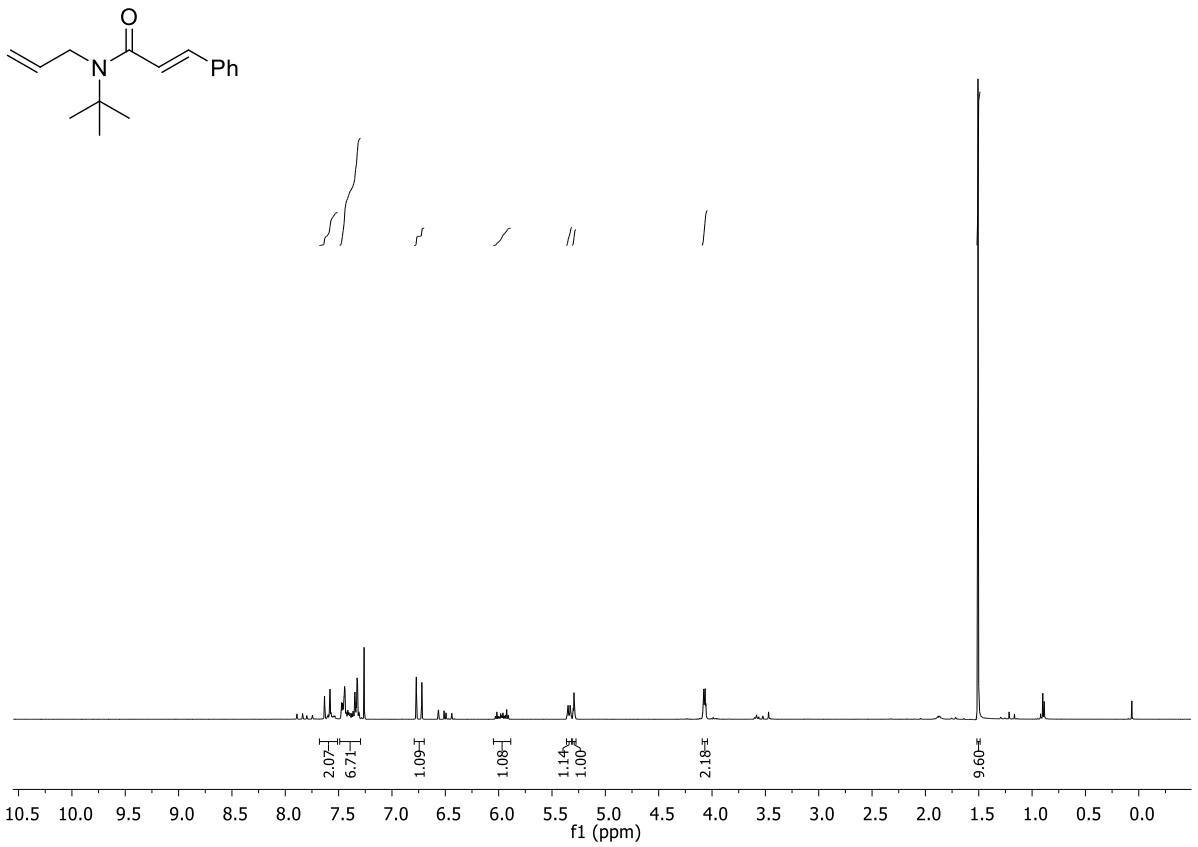

(101 MHz, $CDCl_3$)

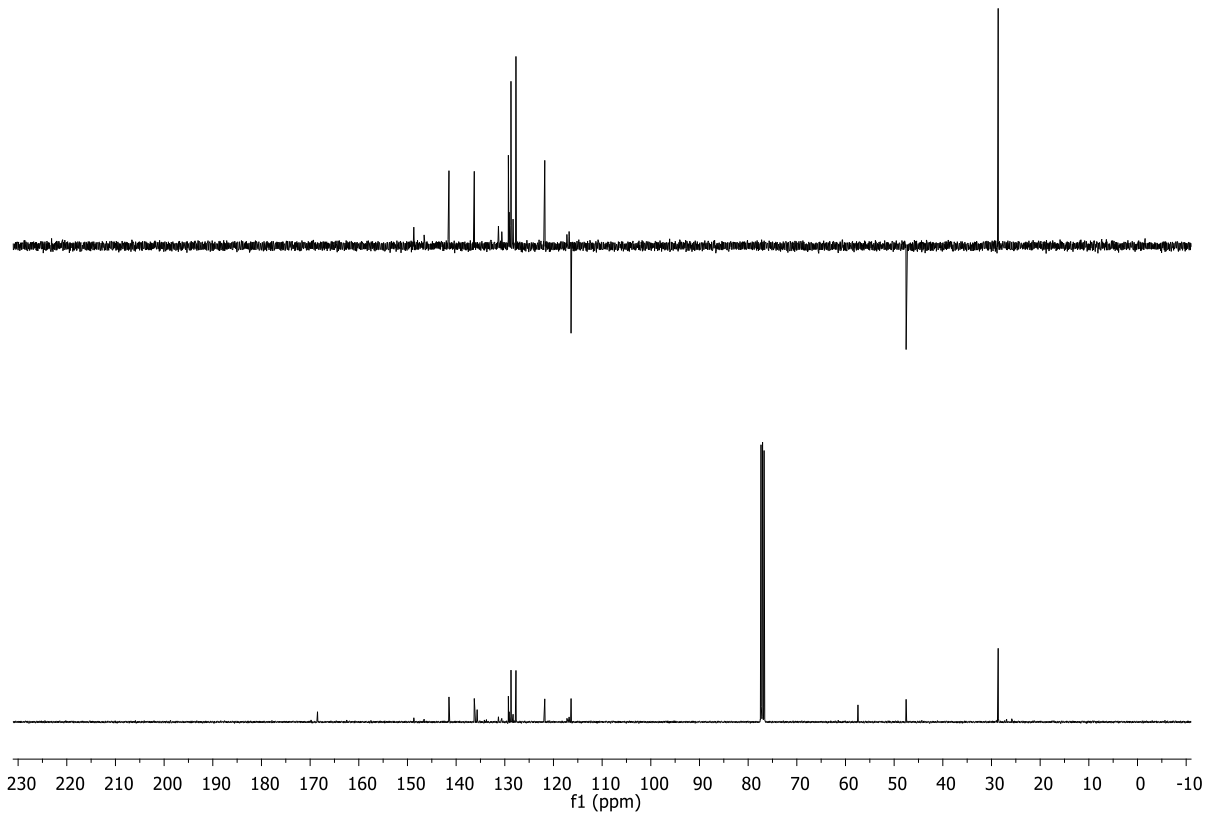

_N_-Allyl-_N_-benzylcinnamamide (153r)

(400 MHz, $CDCl_3$)

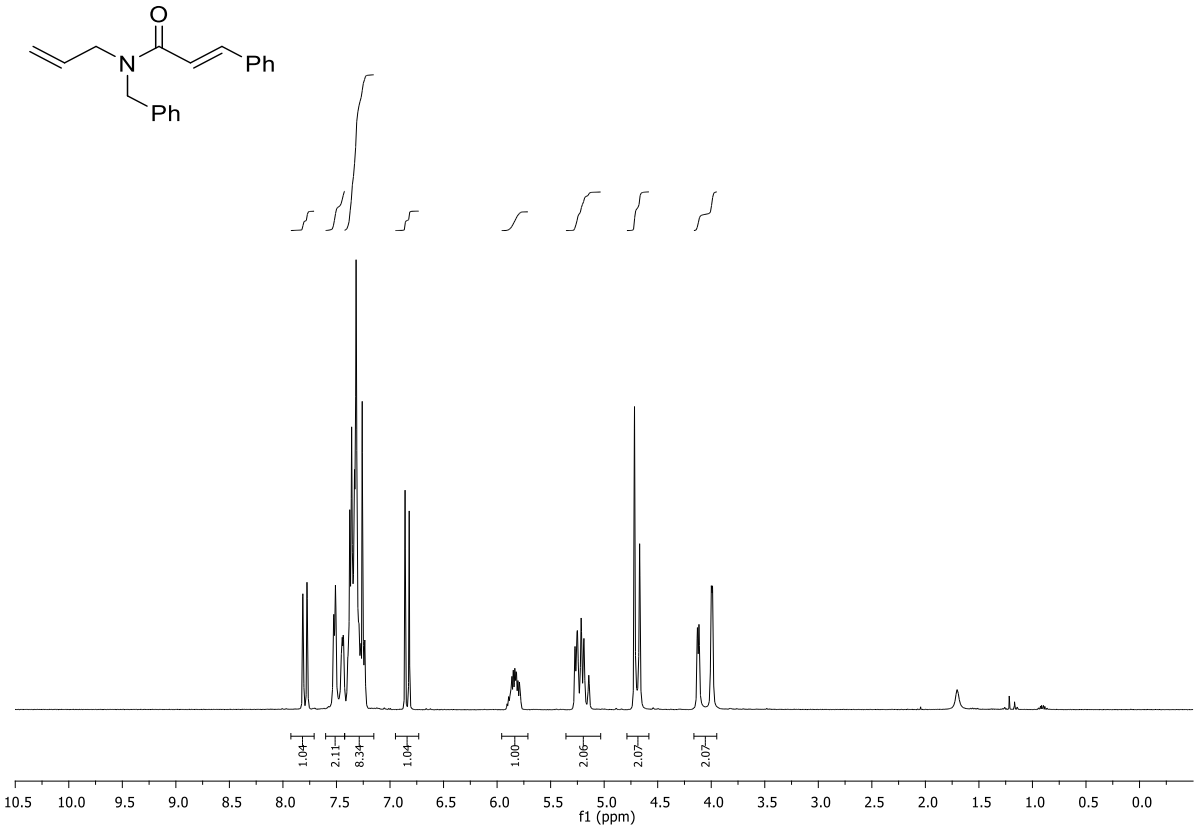

(101 MHz, $CDCl_3$)

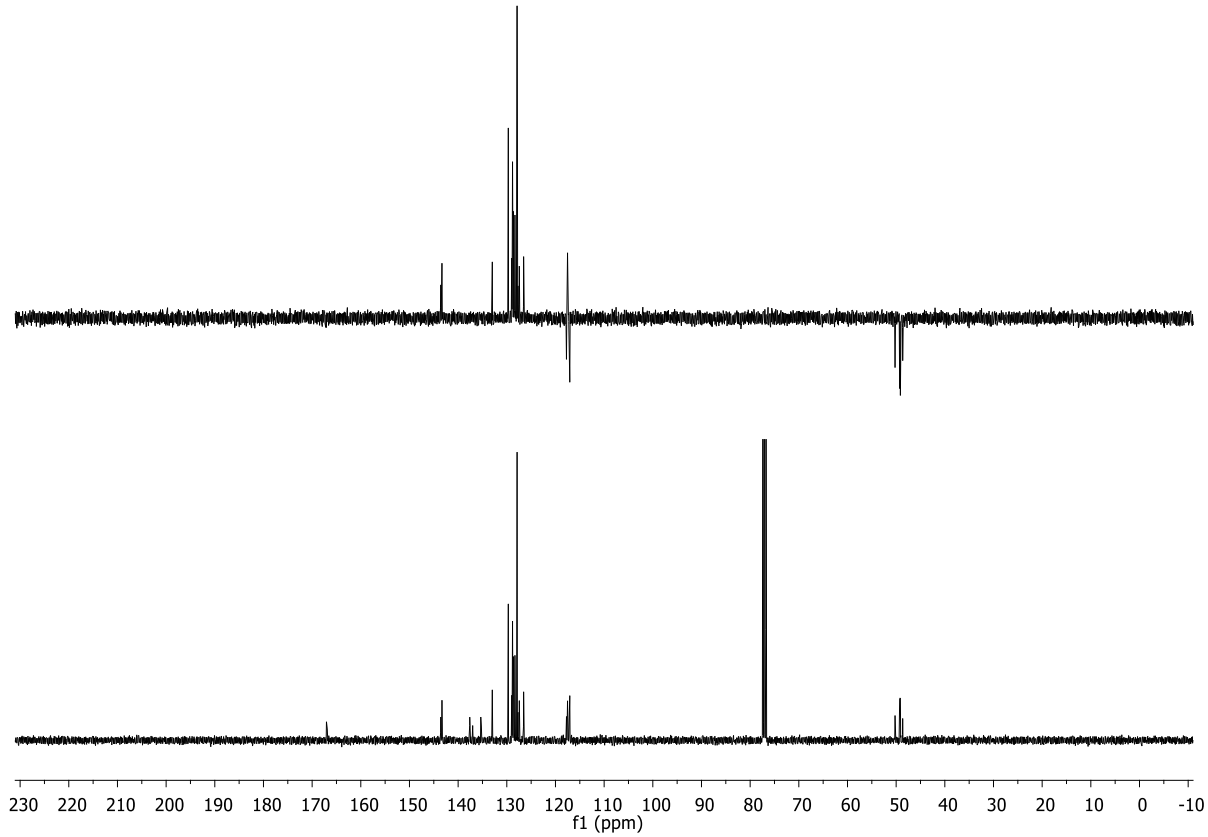

***tert*-Butyl acryloyl(cinnamyl)carbamate (153v)**

(300 MHz, $CDCl_3$)

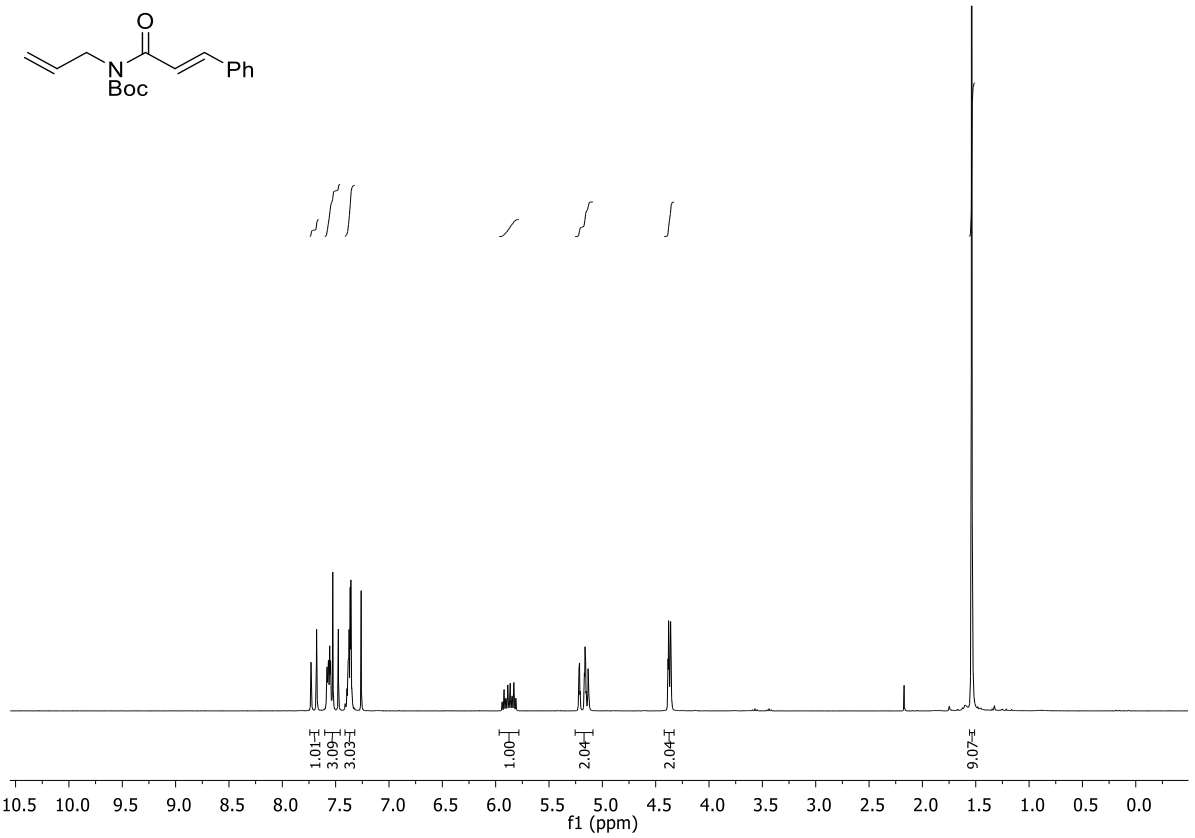

(101 MHz, $CDCl_3$)

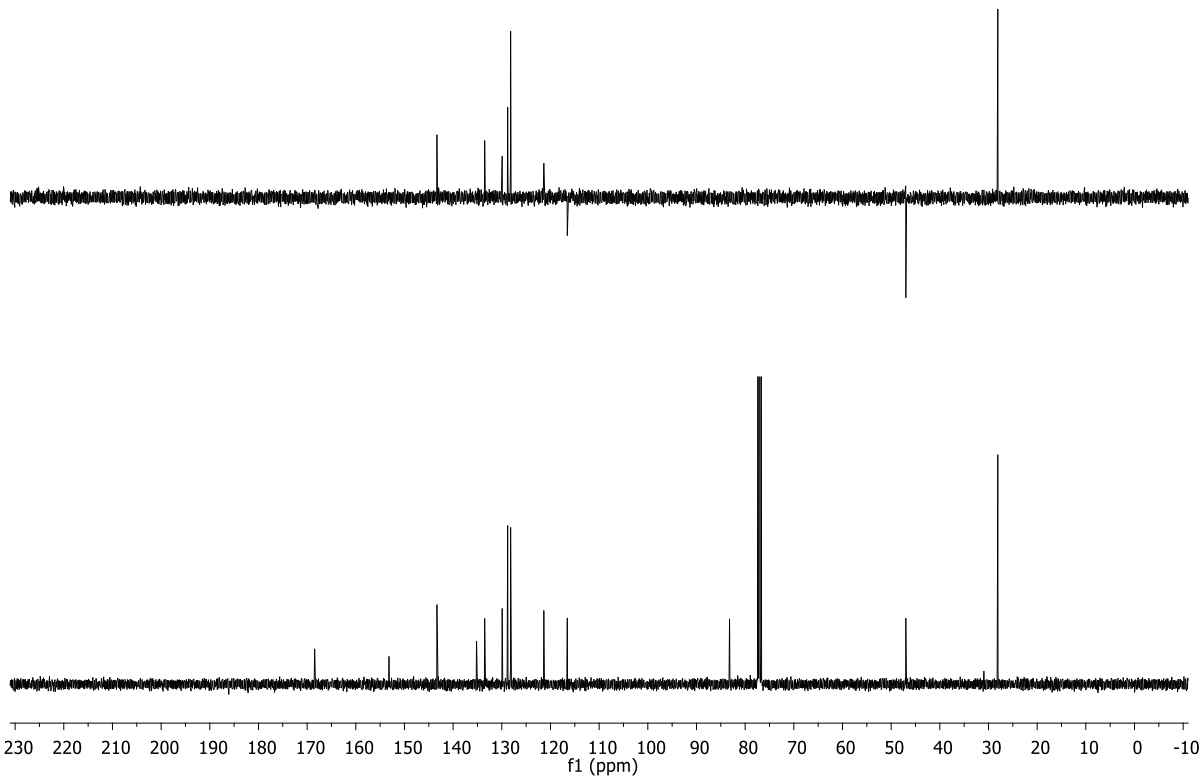

(*E*)-*N*-Allyl-*N*-(*tert*-butyl)-3-(furan-2-yl)acrylamide (153k)

(300 MHz, $CDCl_3$)

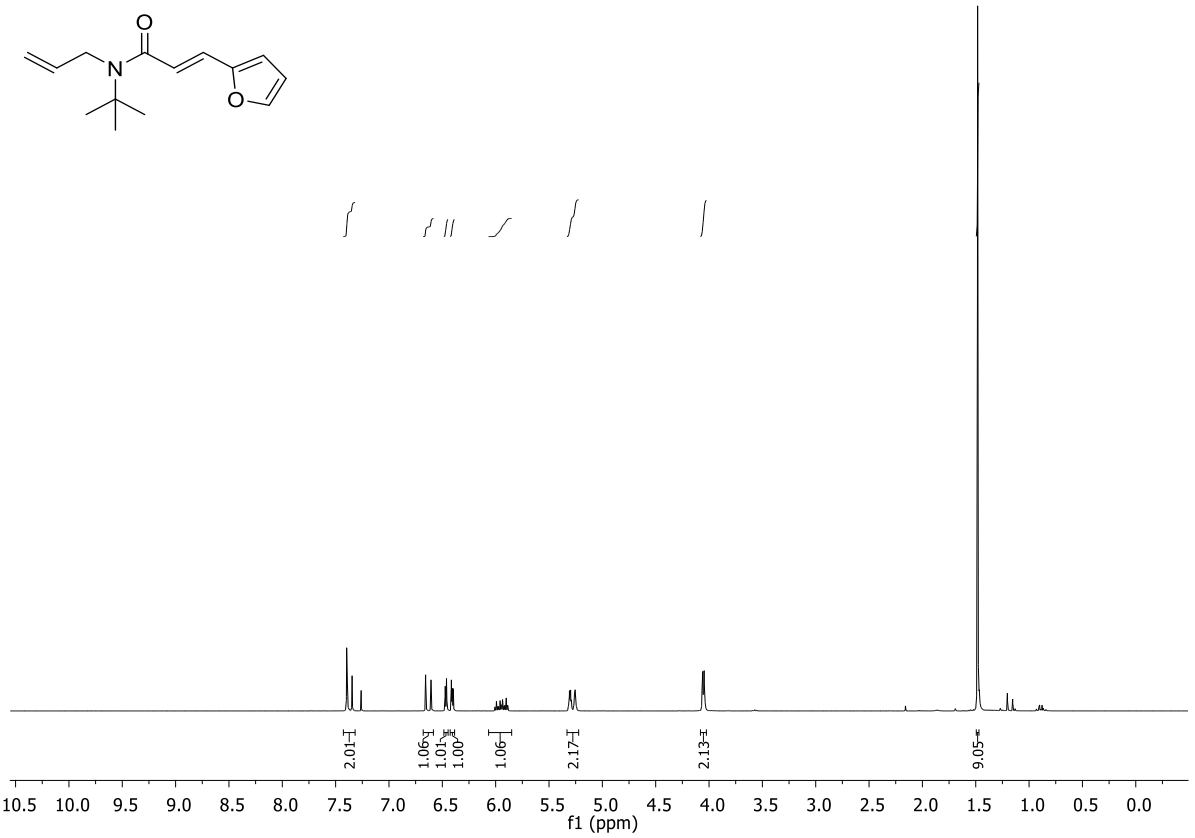

(75 MHz, $CDCl_3$)

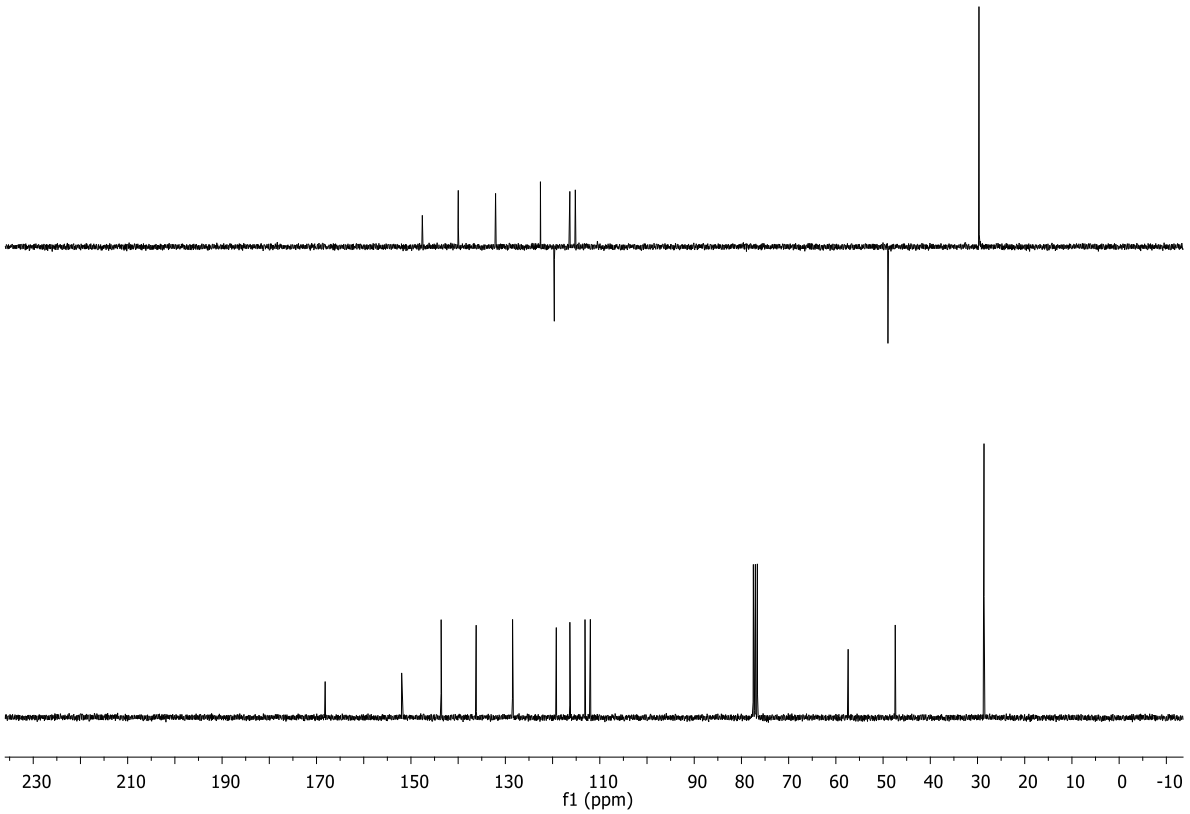

(*E*)-*N*-Allyl-*N*-(*tert*-butyl)-3-(thiophen-2-yl)acrylamide (153l)

(300 MHz, $CDCl_3$)

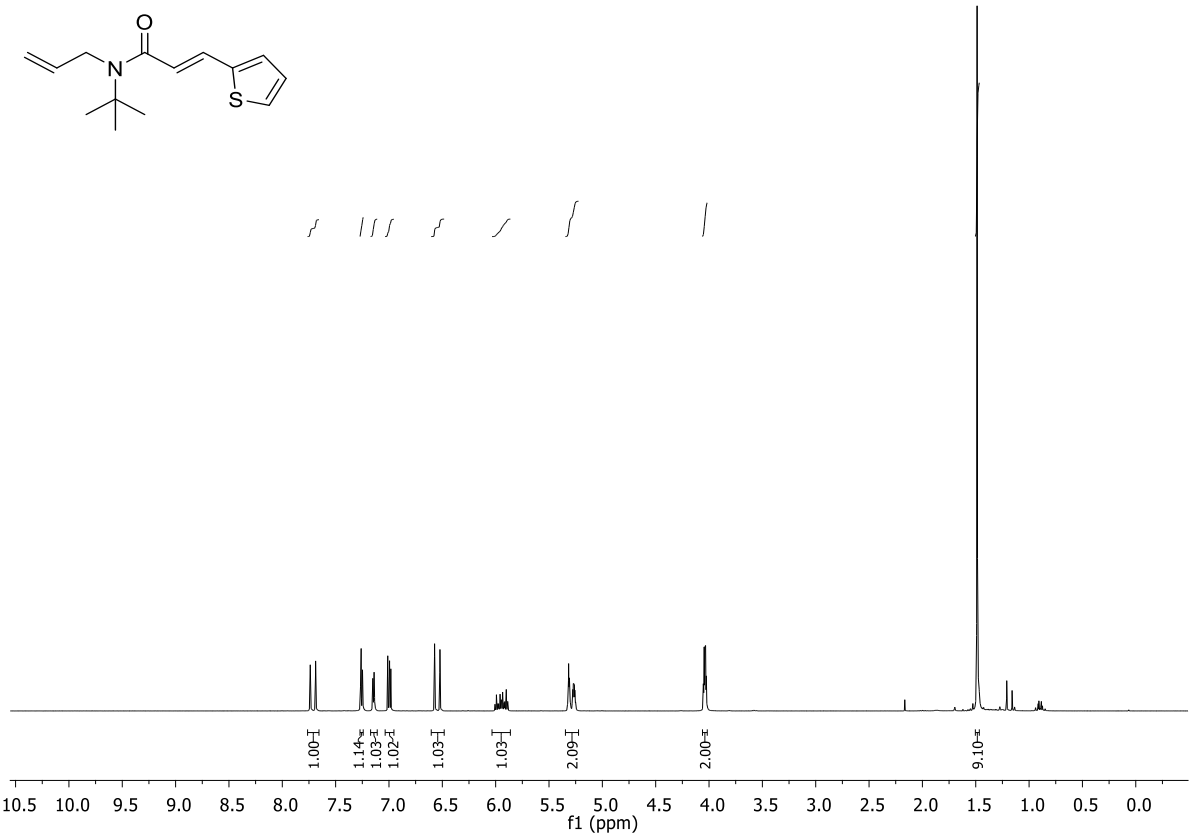

(75 MHz, $CDCl_3$)

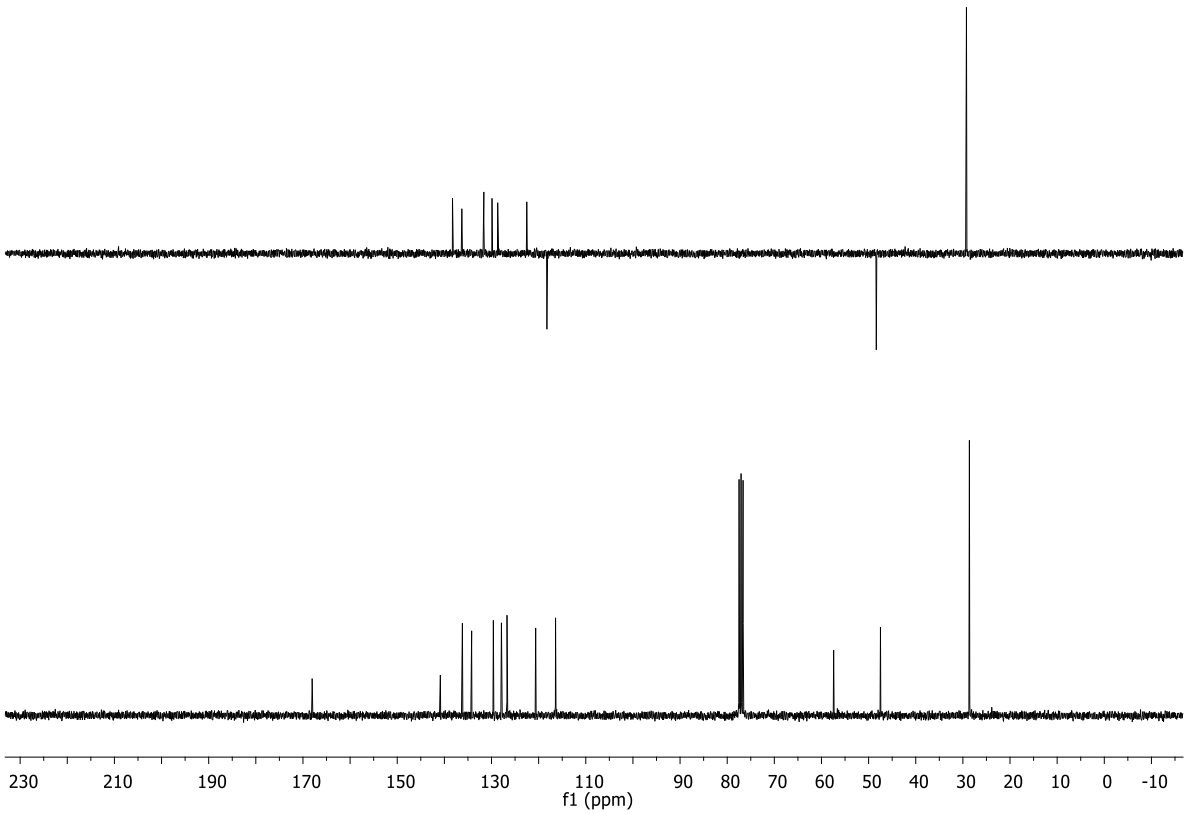

(*E*)-3-(1-Acetyl-1*H*-indol-3-yl)-*N*-allyl-*N*-(*tert*-butyl)acrylamide (153m)

(300 MHz, $CDCl_3$)

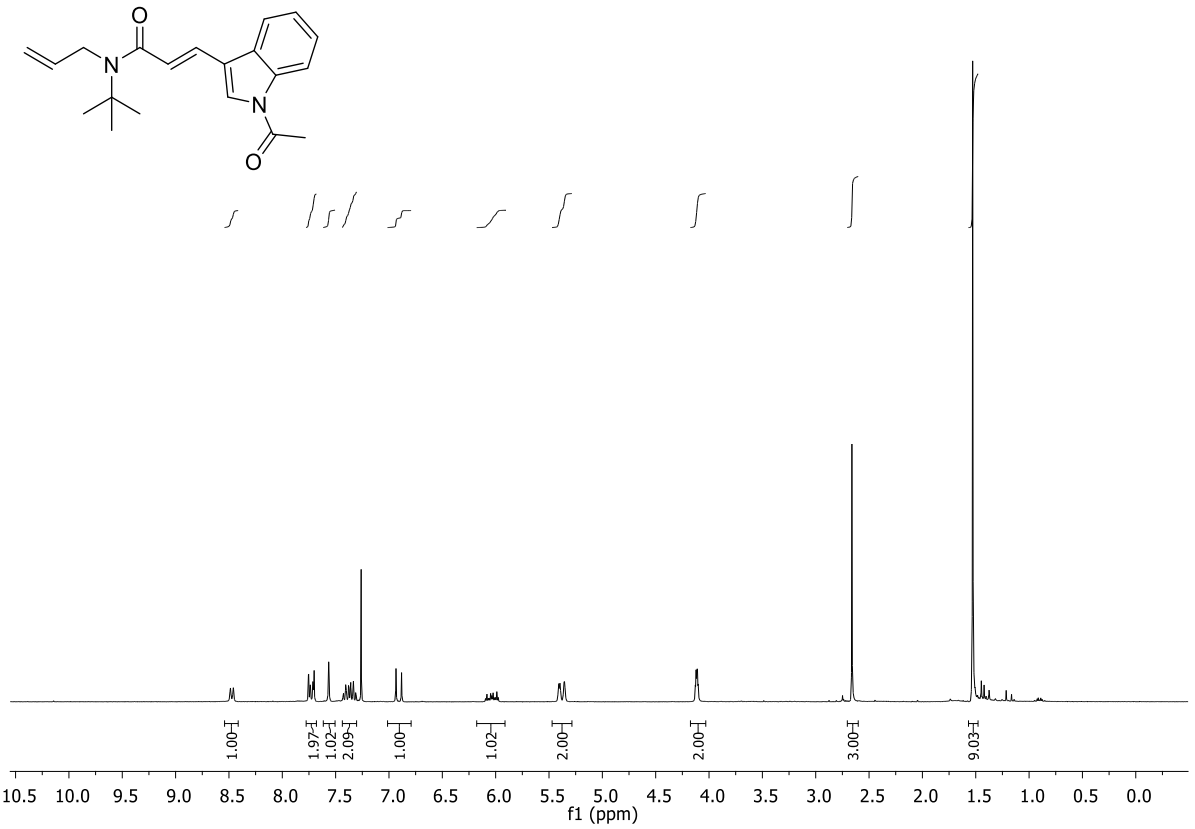

(101 MHz, $CDCl_3$)

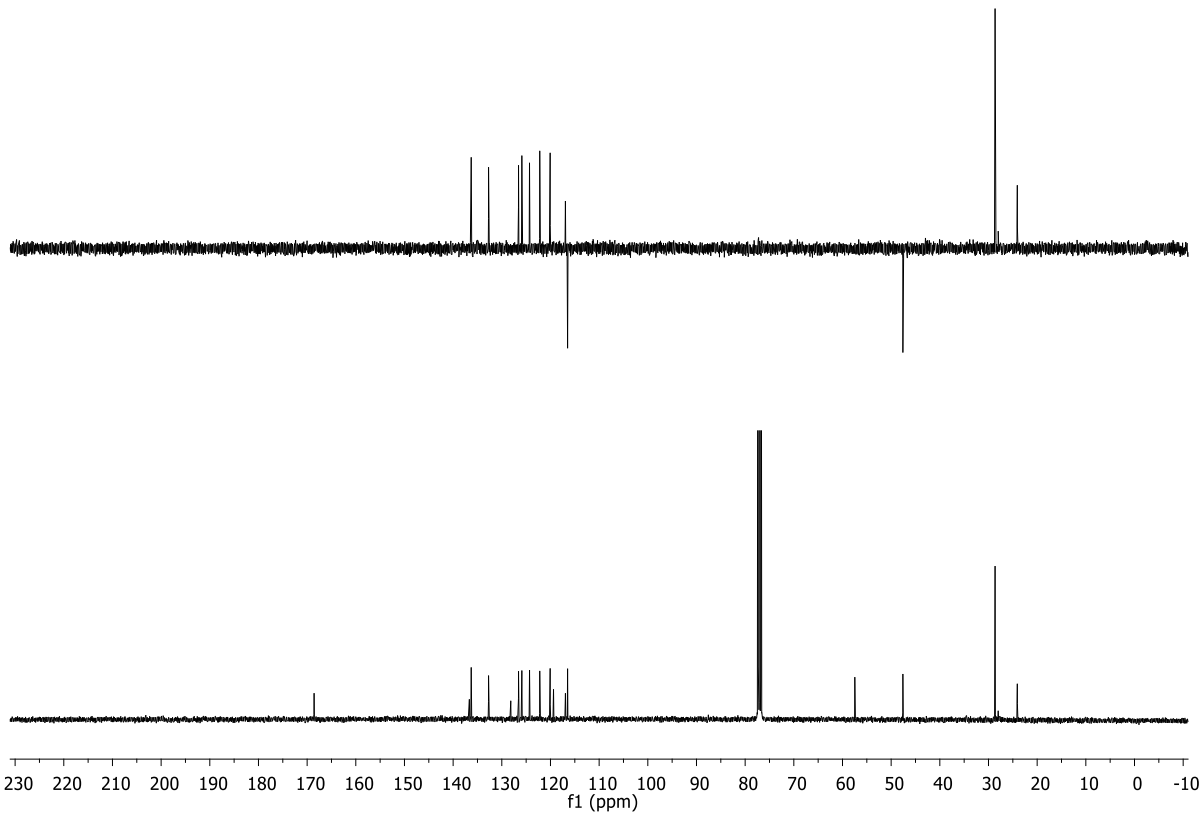

_N_-Allyl-_N_-(_tert_-butyl)acrylamide (153j)

(300 MHz, $CDCl_3$)

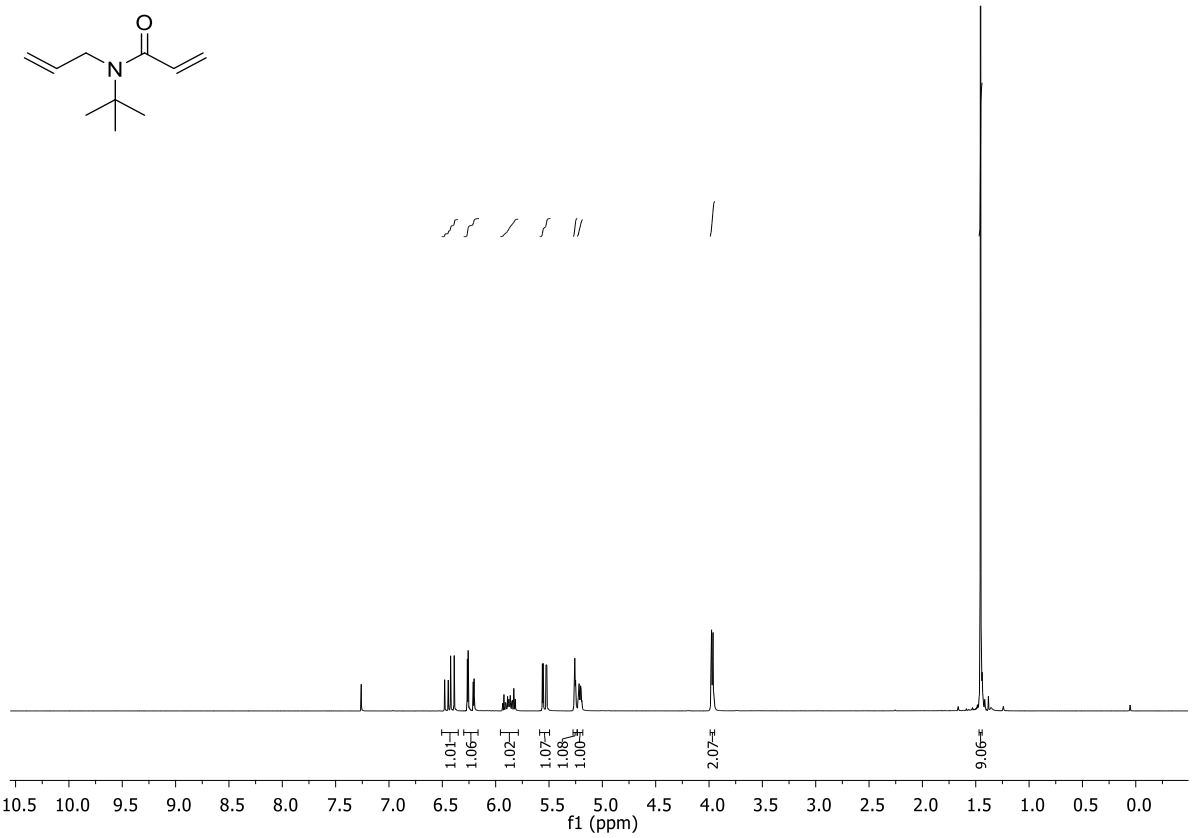

(75 MHz, $CDCl_3$)

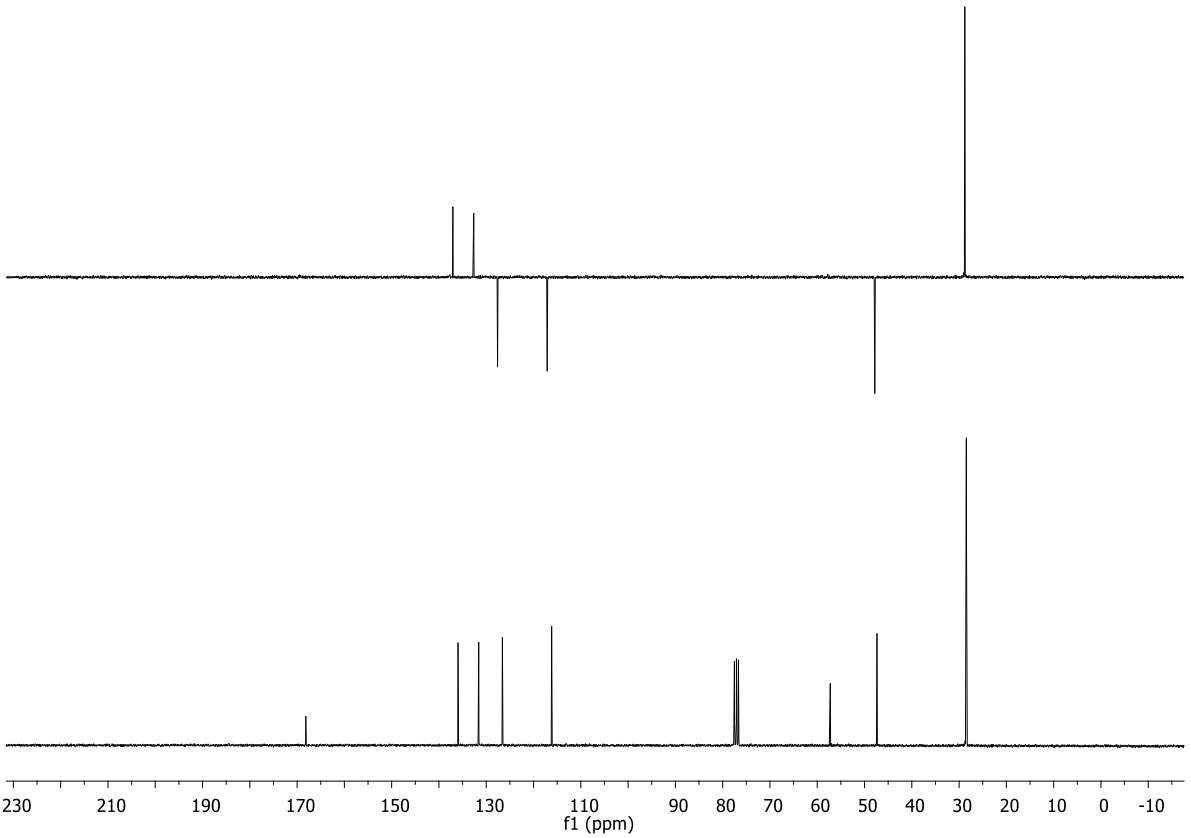

Cinnamyl cinnamate (153w)

(300 MHz, $CDCl_3$)

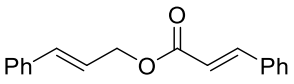

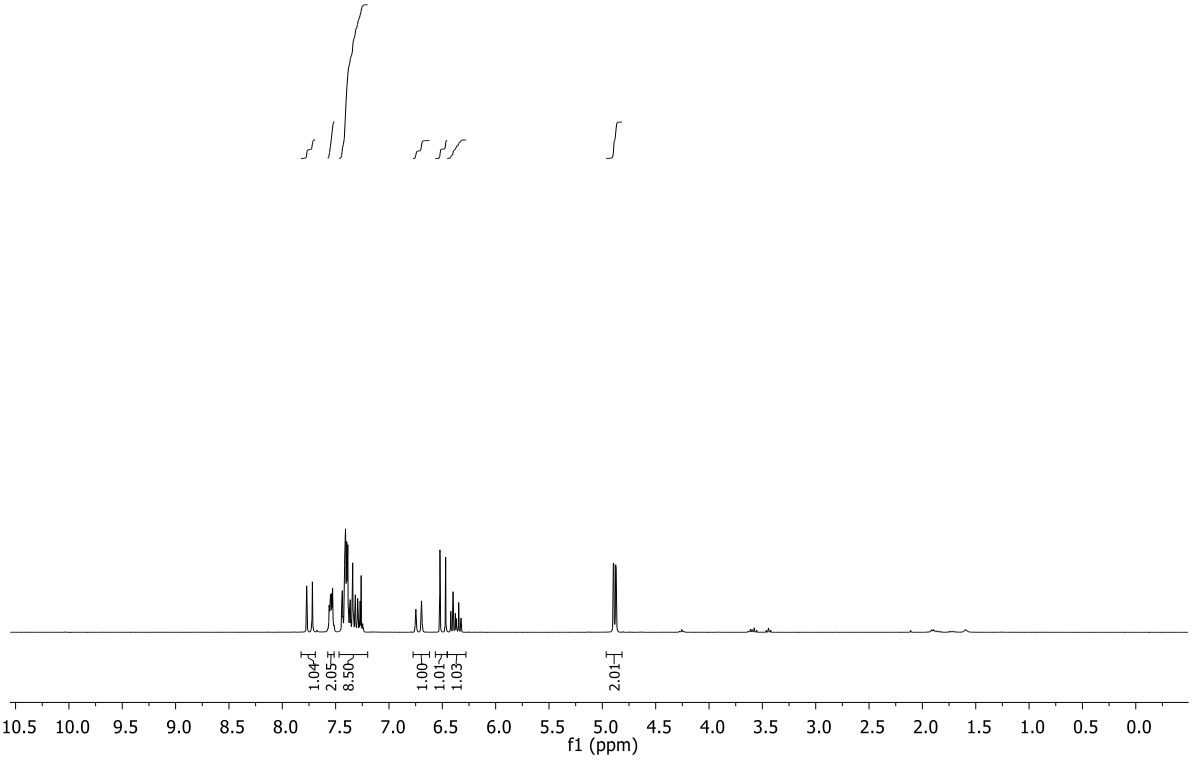

(75 MHz, $CDCl_3$)

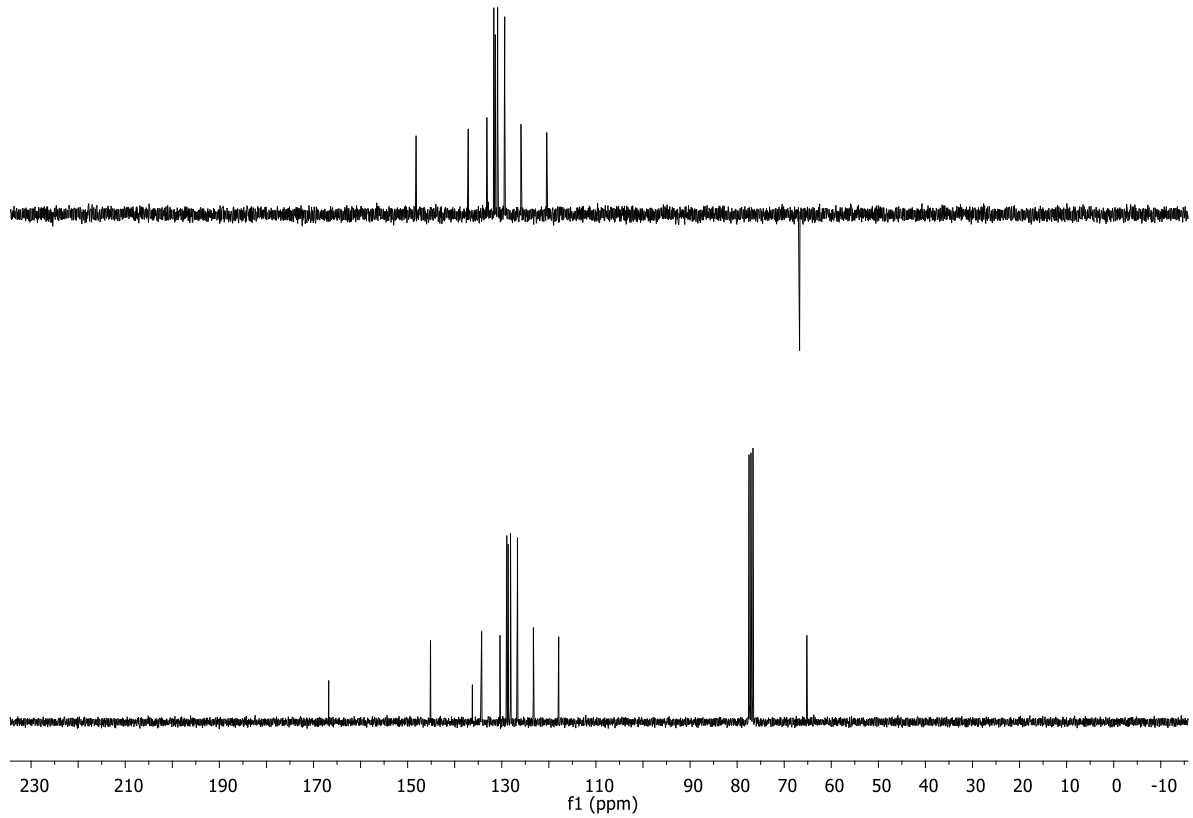

(*S*)-*N*-Cinnamyl-*N*-(1-phenylethyl)acrylamide (153x)

(300 MHz, $CDCl_3$)

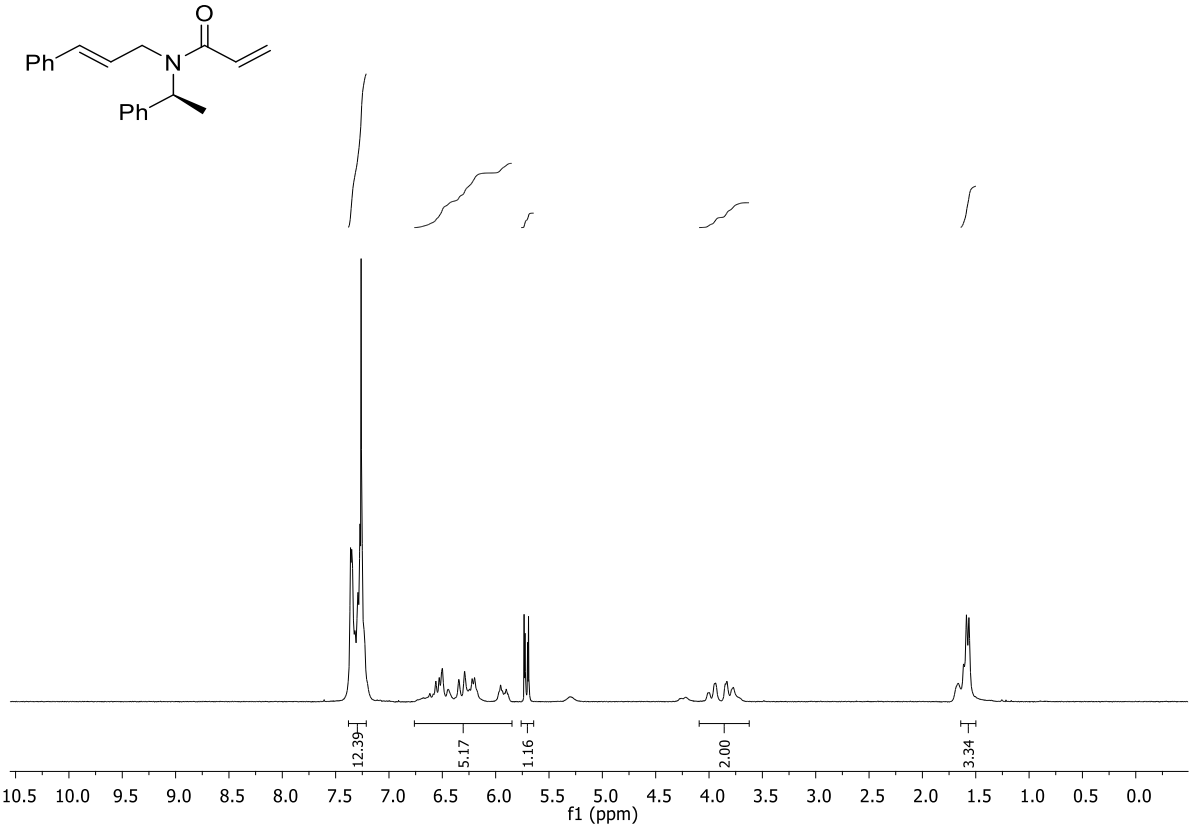

(75 MHz, $CDCl_3$)

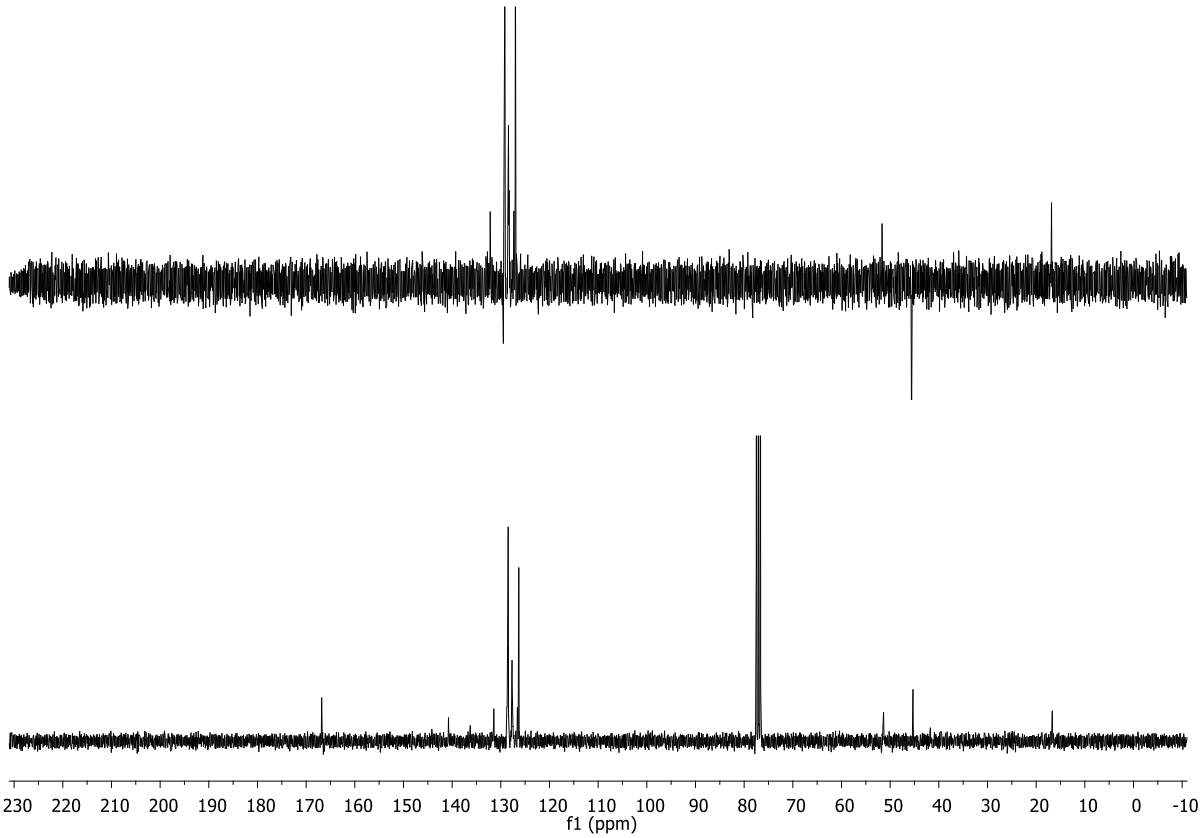

(*S*)-*N*-Allyl-*N*-(1-phenylethyl)cinnamamide (153y)

(400 MHz, $CDCl_3$)

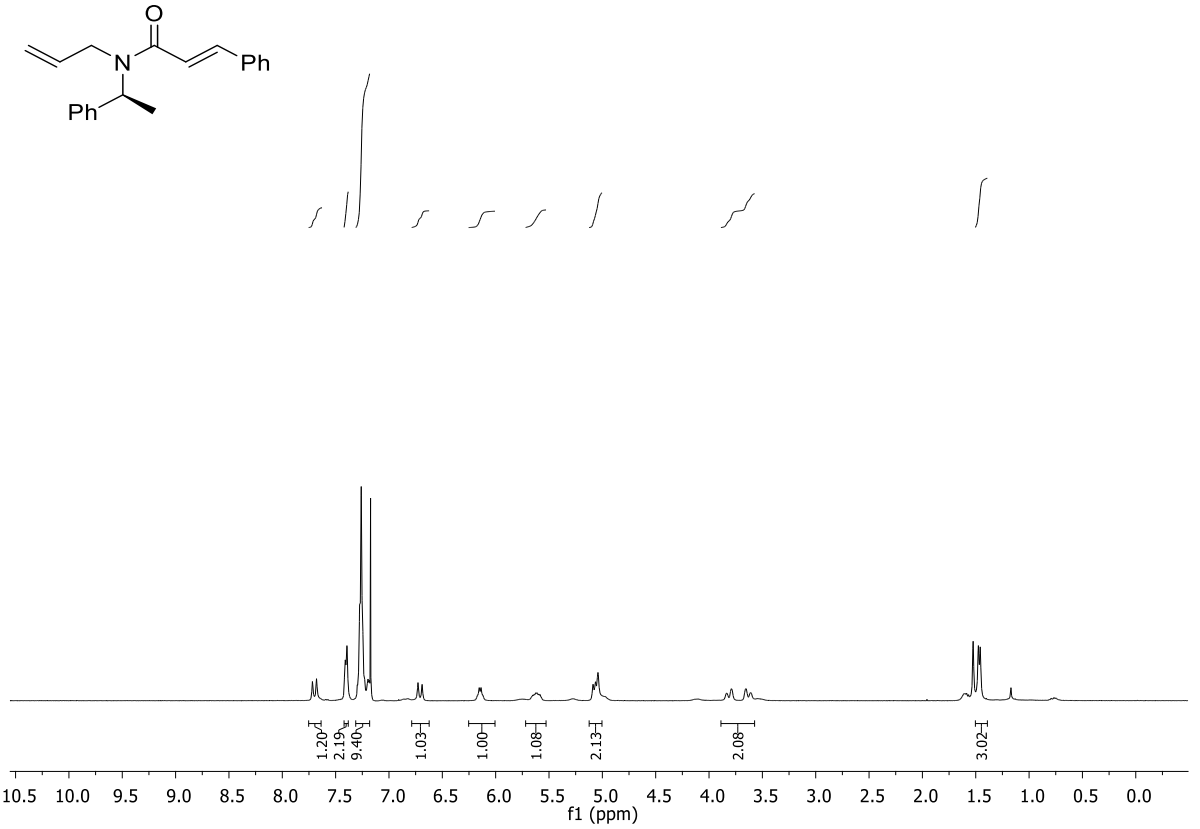

(101 MHz, $CDCl_3$)

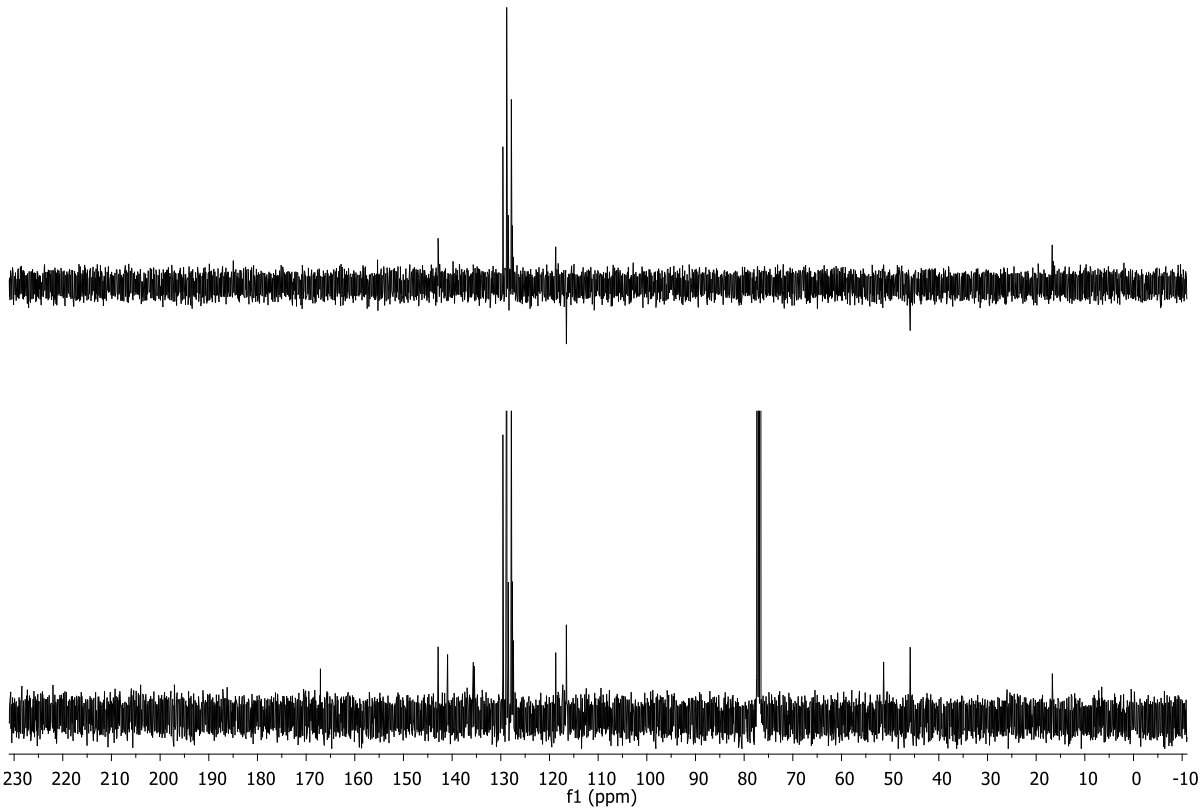

(±)-3-(*tert*-Butyl)-6,7-diphenyl-3-azabicyclo[3.2.0]heptan-2-one (158g)

(400 MHz, $CDCl_3$)

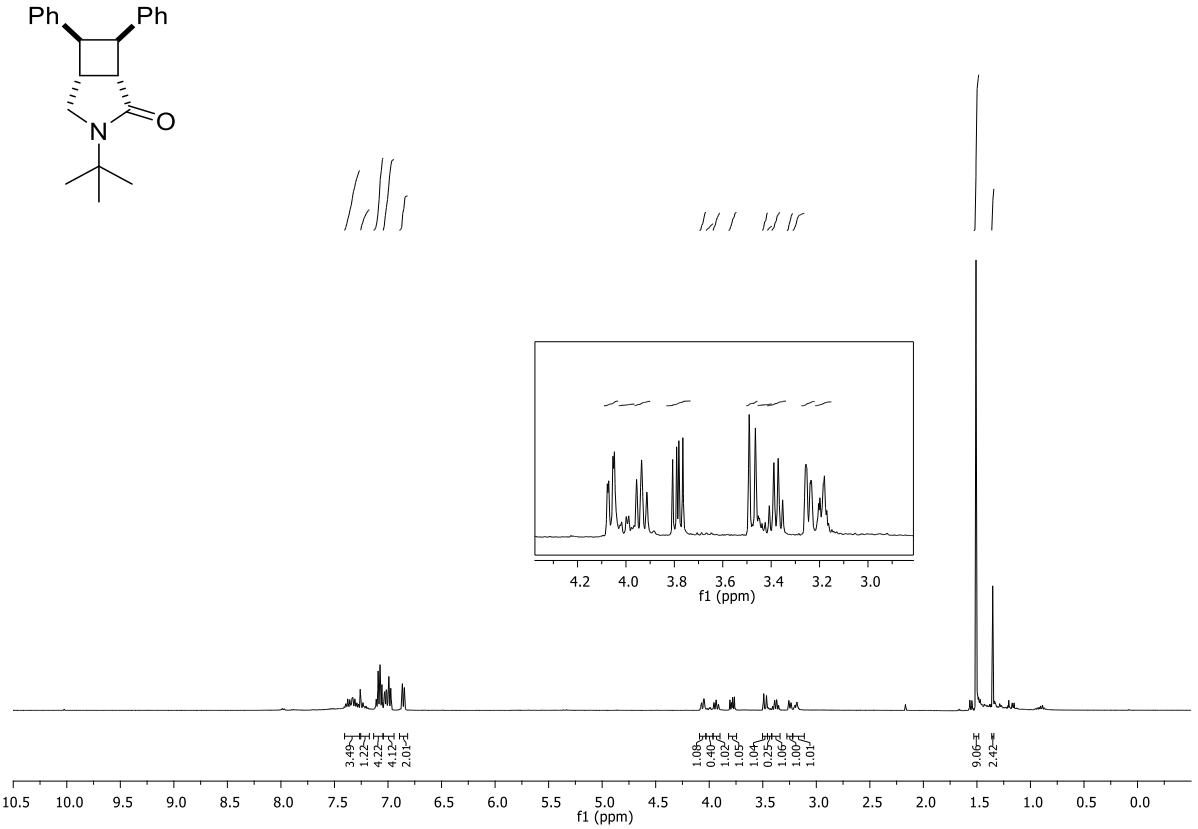

(75 MHz, $CDCl_3$)

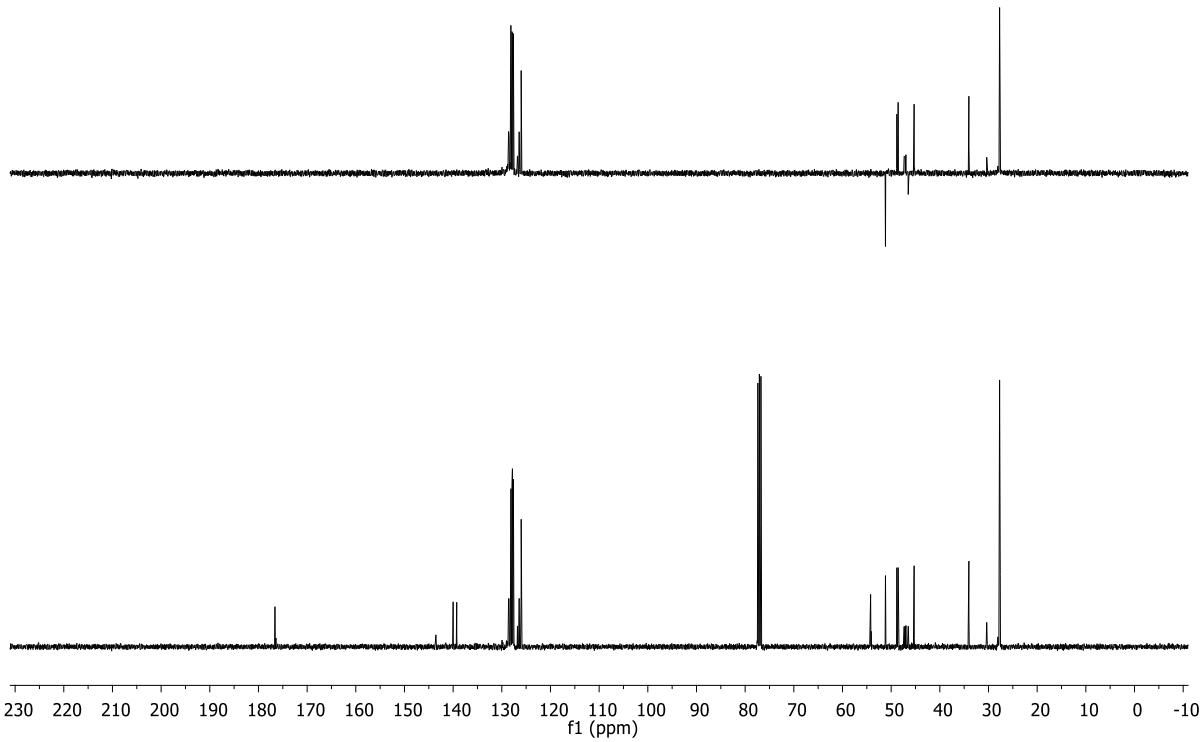

(±)-3-(*tert*-Butyl)-6-(4-methoxyphenyl)-7-phenyl-3-azabicyclo[3.2.0]heptan-2-one (158d)

(300 MHz, $CDCl_3$)

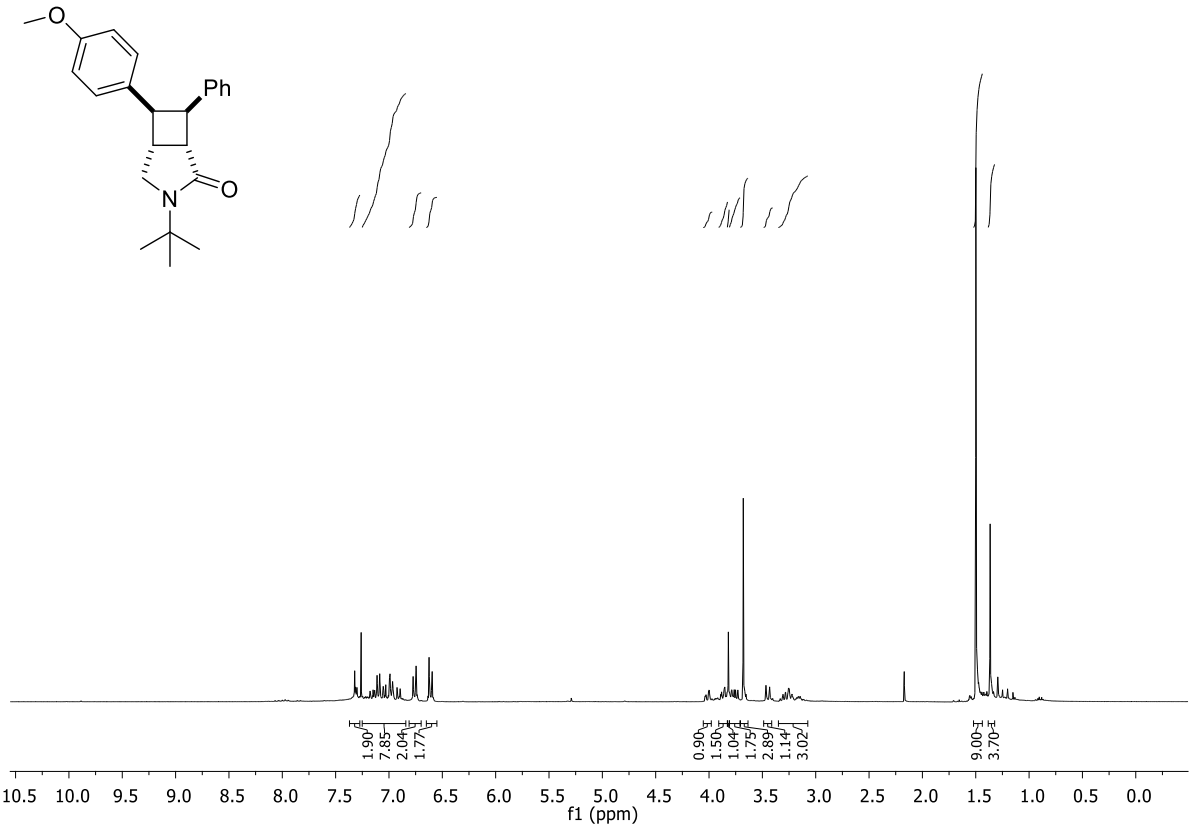

(75 MHz, $CDCl_3$)

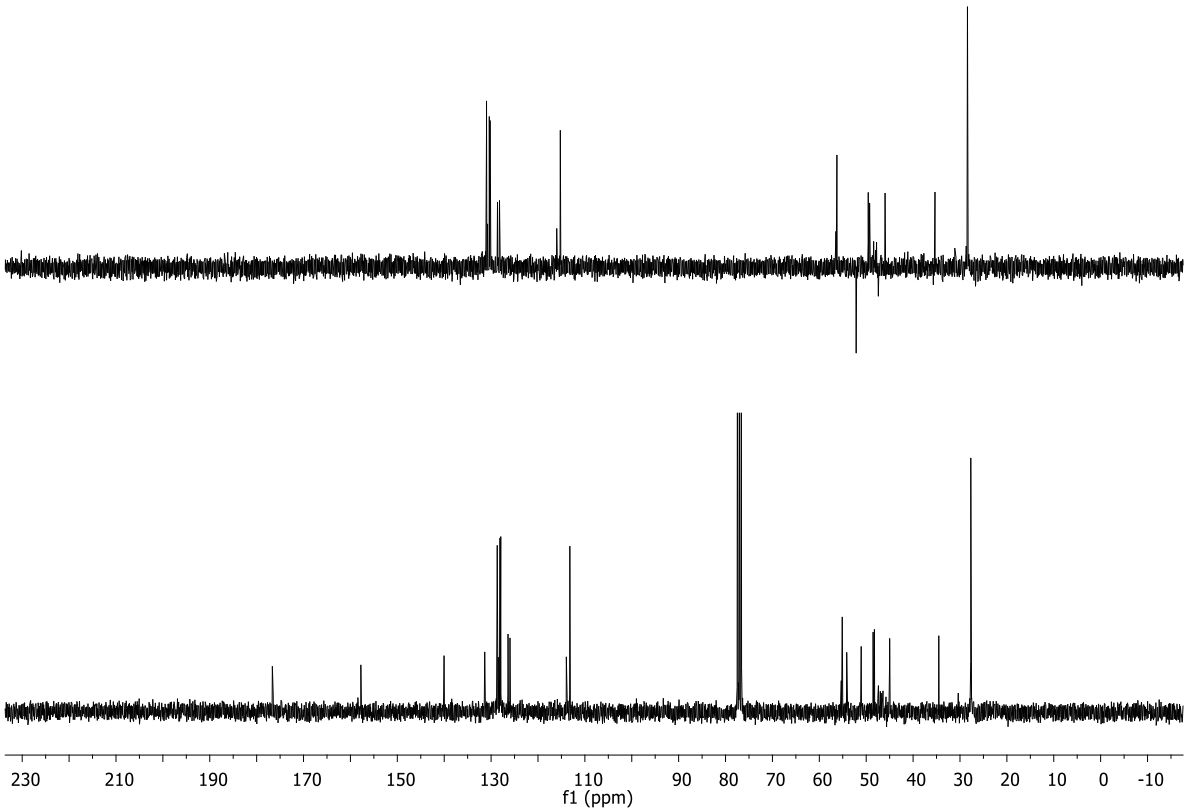

(±)-3-Benzyl-6,7-diphenyl-3-azabicyclo[3.2.0]heptan-2-one (158f)

(300 MHz, $CDCl_3$)

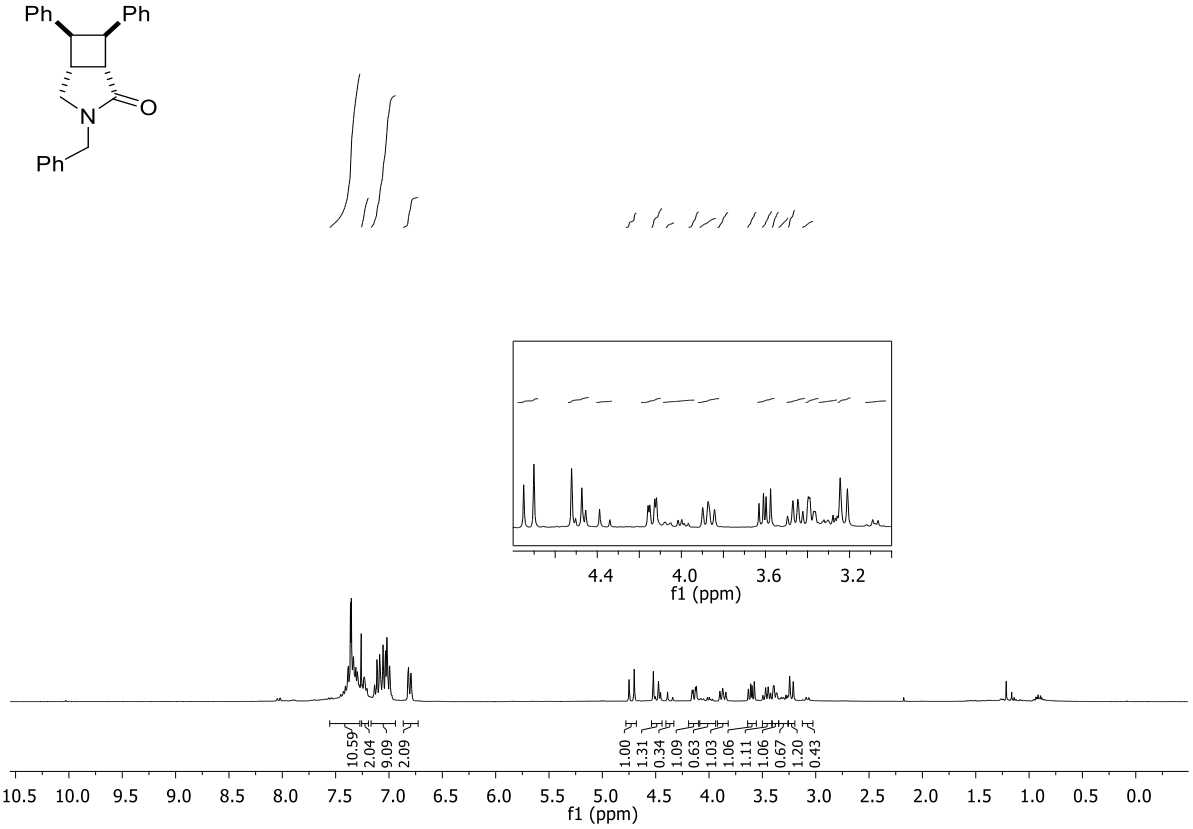

(75 MHz, $CDCl_3$)

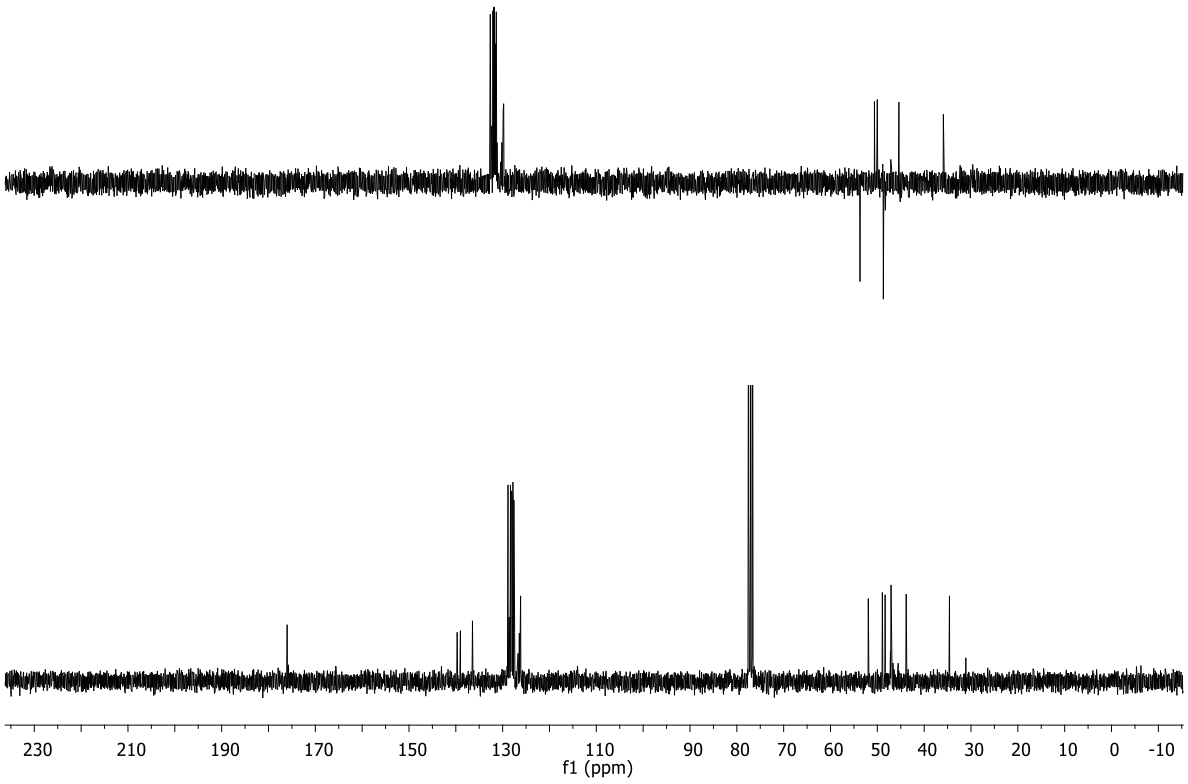

(±)-*tert*-Butyl -2-oxo-6,7-diphenyl-3-azabicyclo[3.2.0]heptane-3-carboxylate (158h)

(300 MHz, $CDCl_3$)

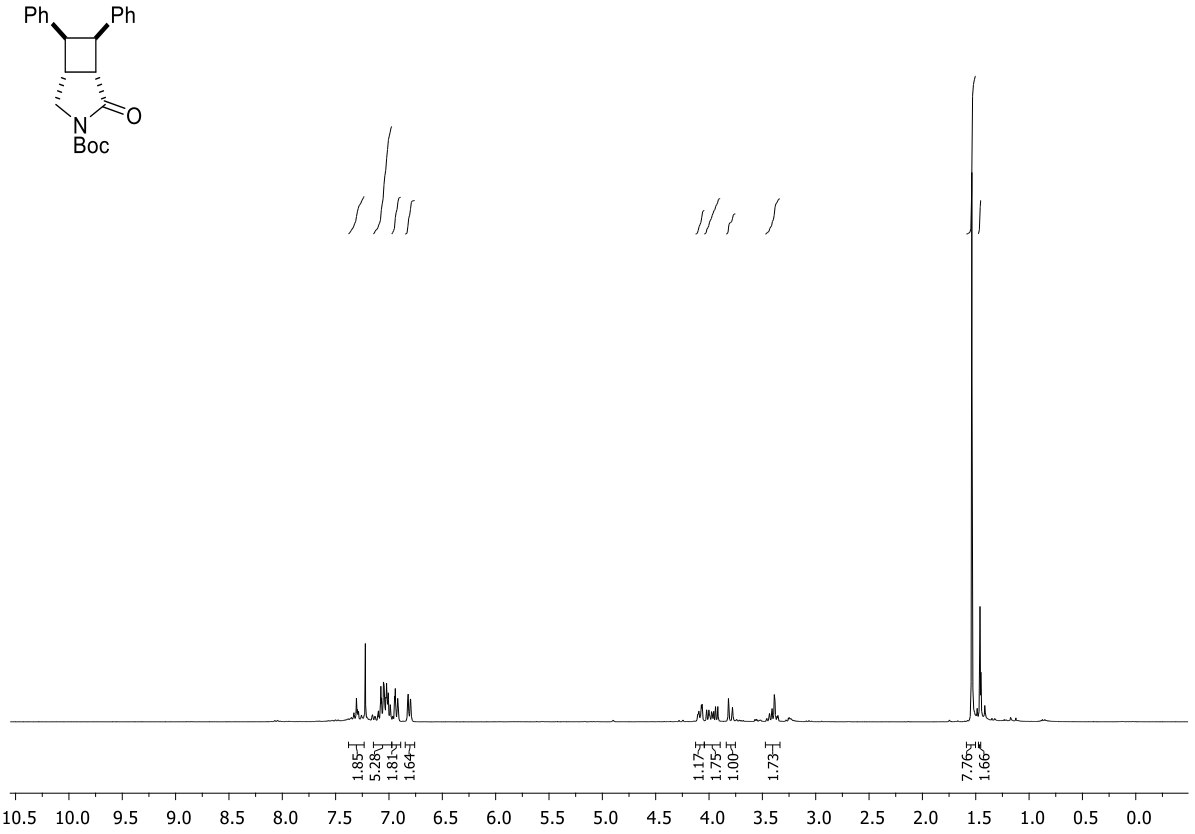

(101 MHz, $CDCl_3$)

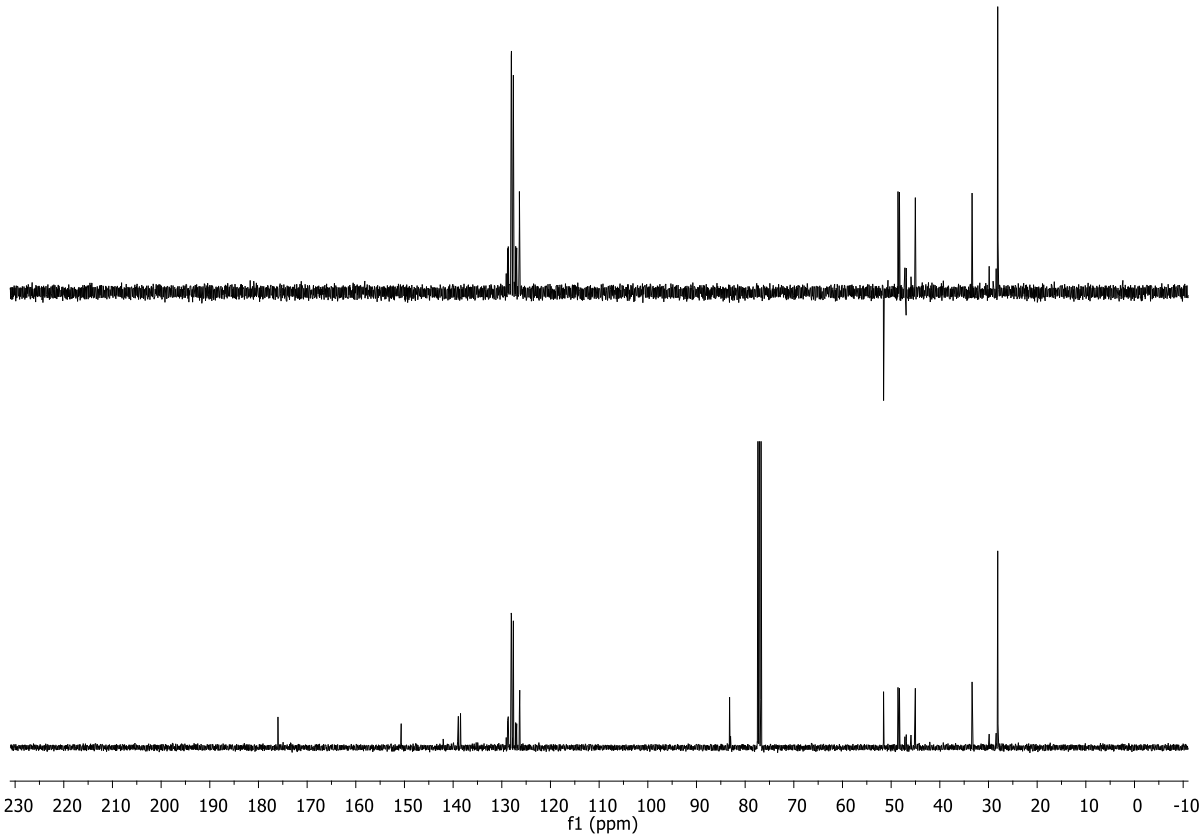

(±)-*trans*-3-(*tert*-Butyl)-6-phenyl-3-azabicyclo[3.2.0]heptan-2-one (158ia)

(400 MHz, $CDCl_3$)

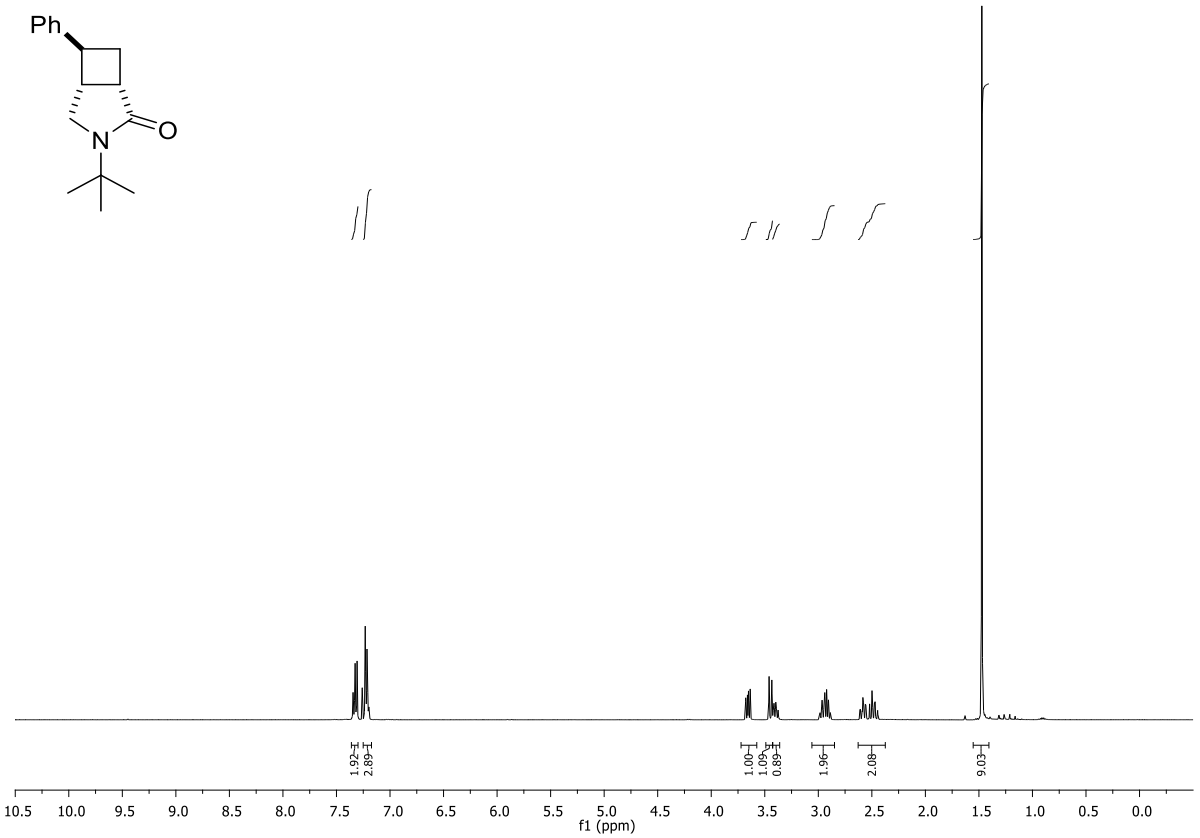

(75 MHz, $CDCl_3$)

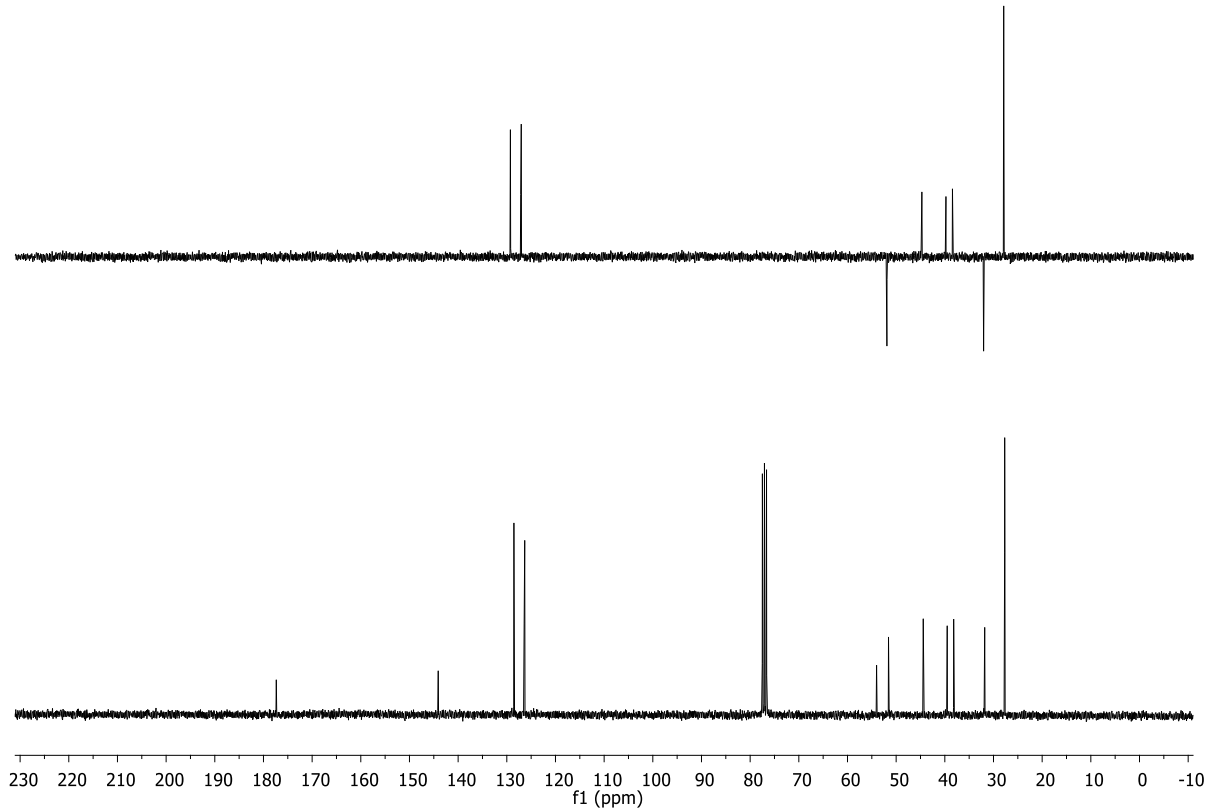

(±)-*cis*-3-(*tert*-Butyl)-6-phenyl-3-azabicyclo[3.2.0]heptan-2-one (158ib)

(400 MHz, $CDCl_3$)

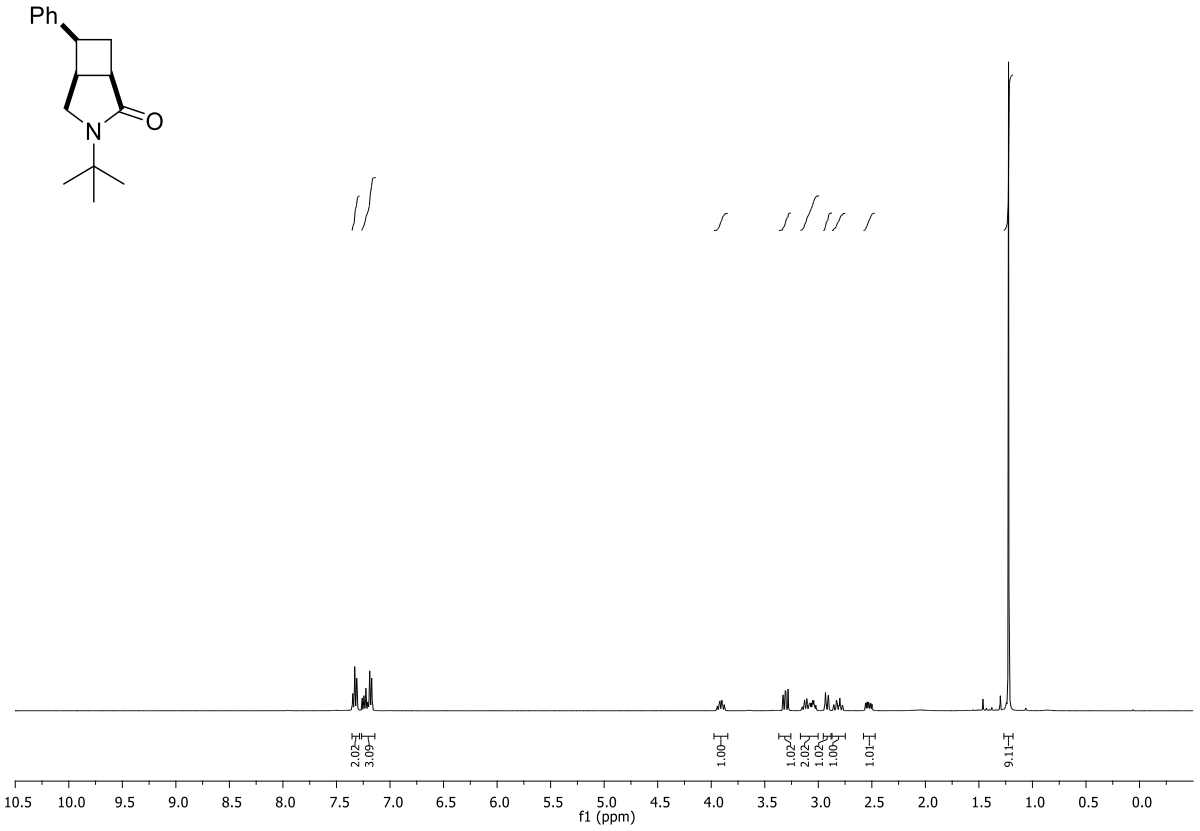

(101 MHz, $CDCl_3$)

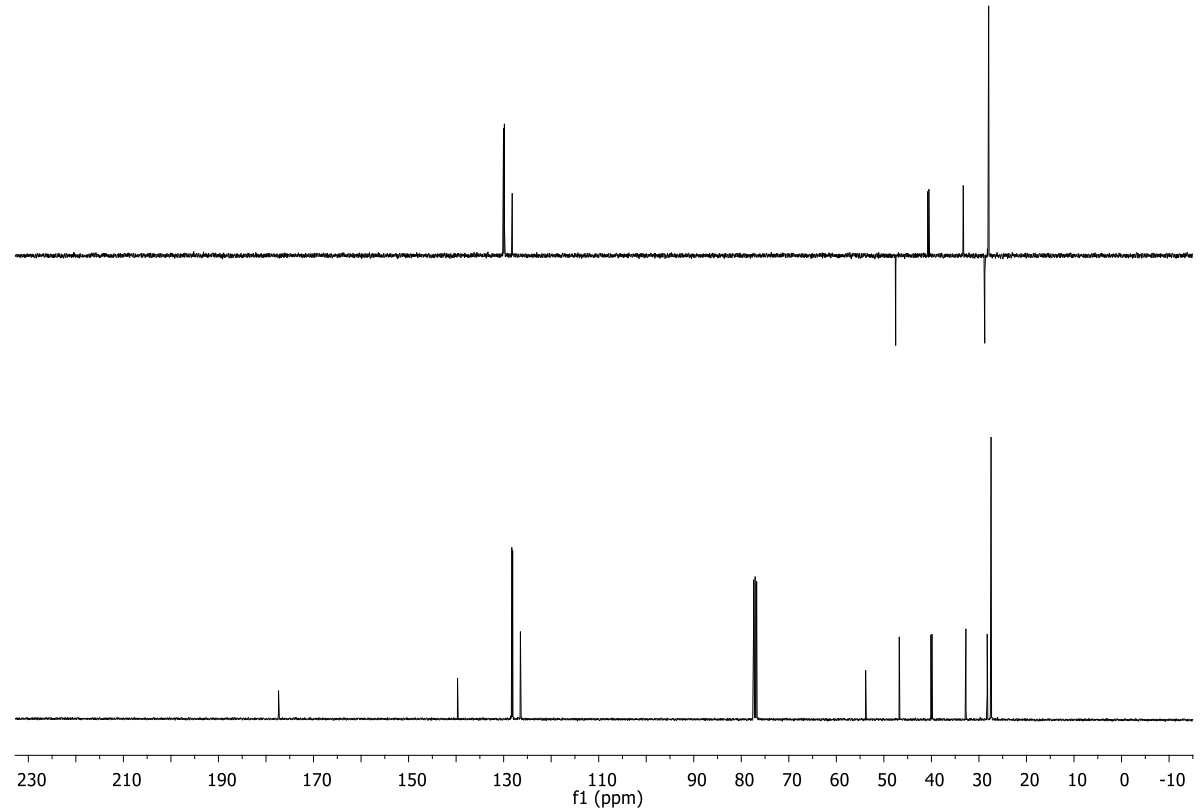

(±)-*trans*-3-Benzyl-6-phenyl-3-azabicyclo[3.2.0]heptan-2-on (158ja)

(400 MHz, $CDCl_3$)

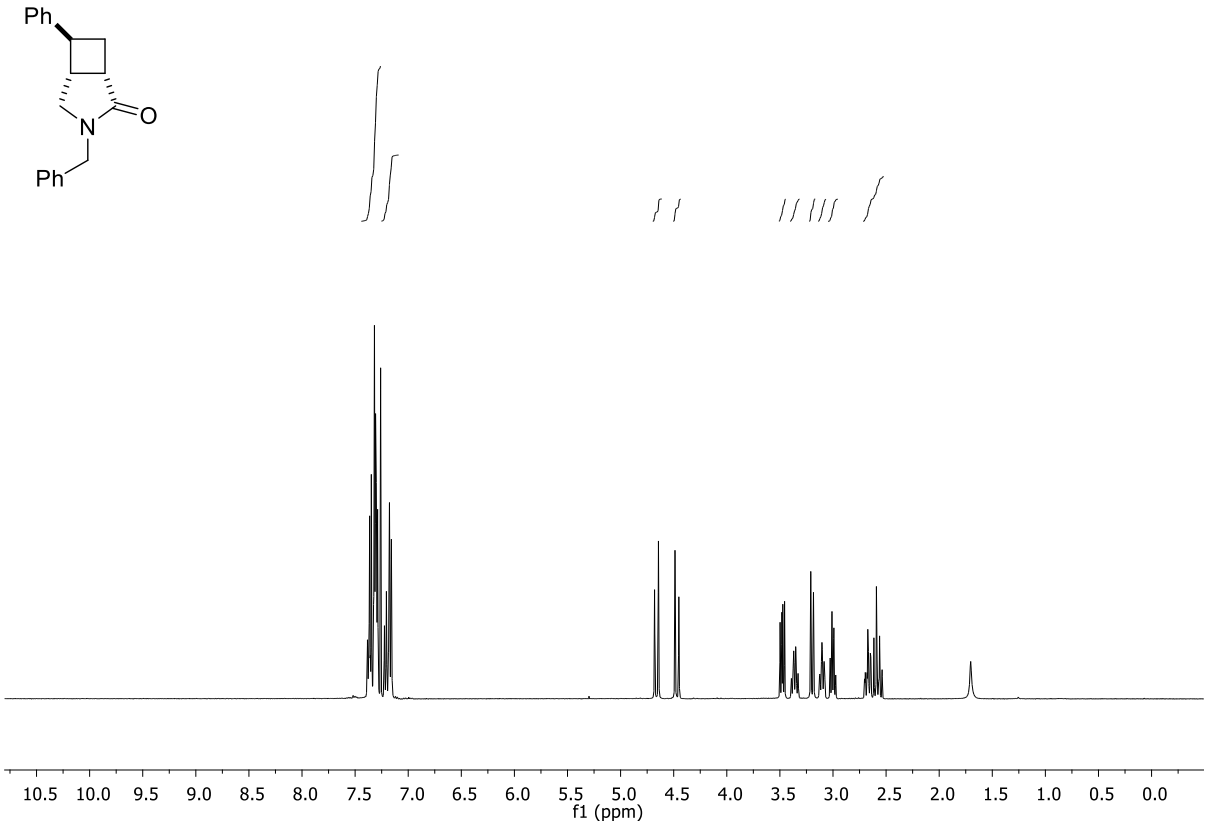

(101 MHz, $CDCl_3$)

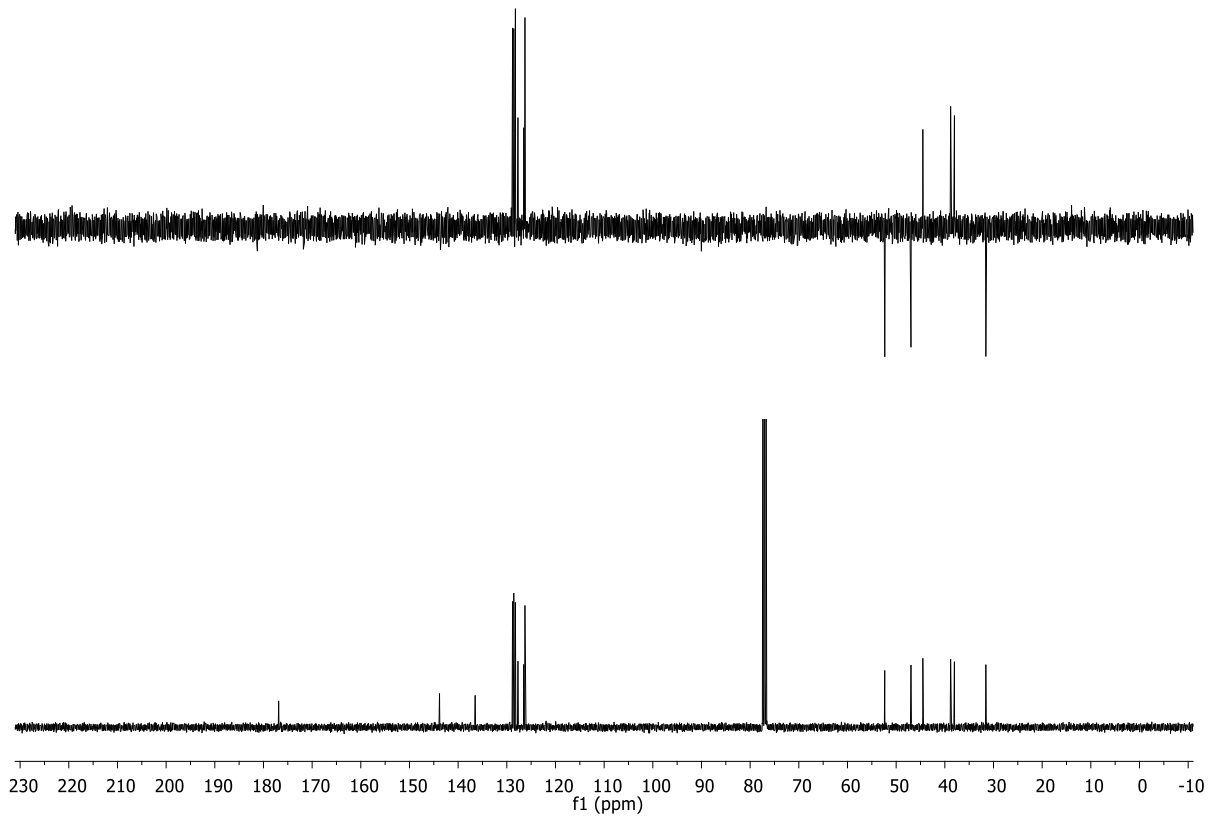

(±)-*cis*-3-Benzyl-6-phenyl-3-azabicyclo[3.2.0]heptan-2-on (158jb)

(400 MHz, $CDCl_3$)

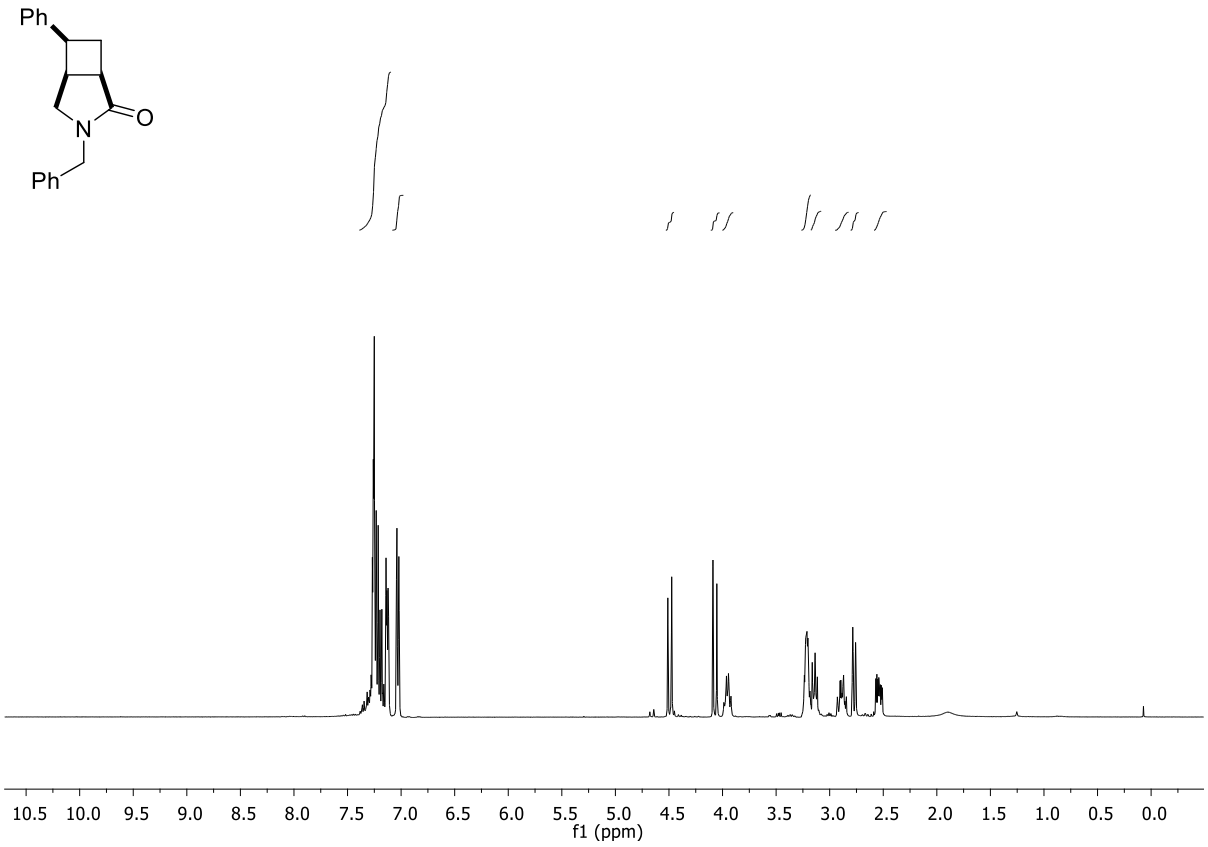

(101 MHz, $CDCl_3$)

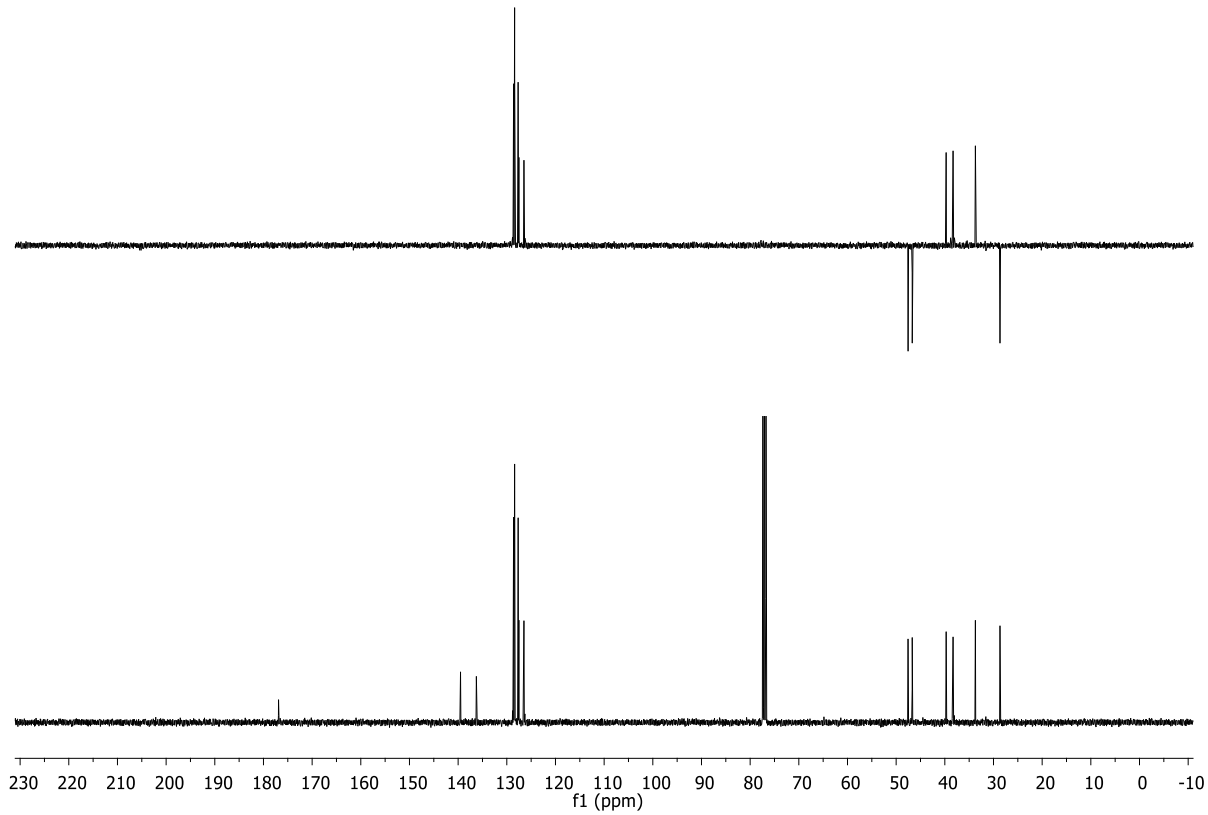

(±)-*trans*-*tert*-Butyl-2-oxo-6-phenyl-3-azabicyclo[3.2.0]heptane-3-carboxylate (158ka)

(300 MHz, $CDCl_3$)

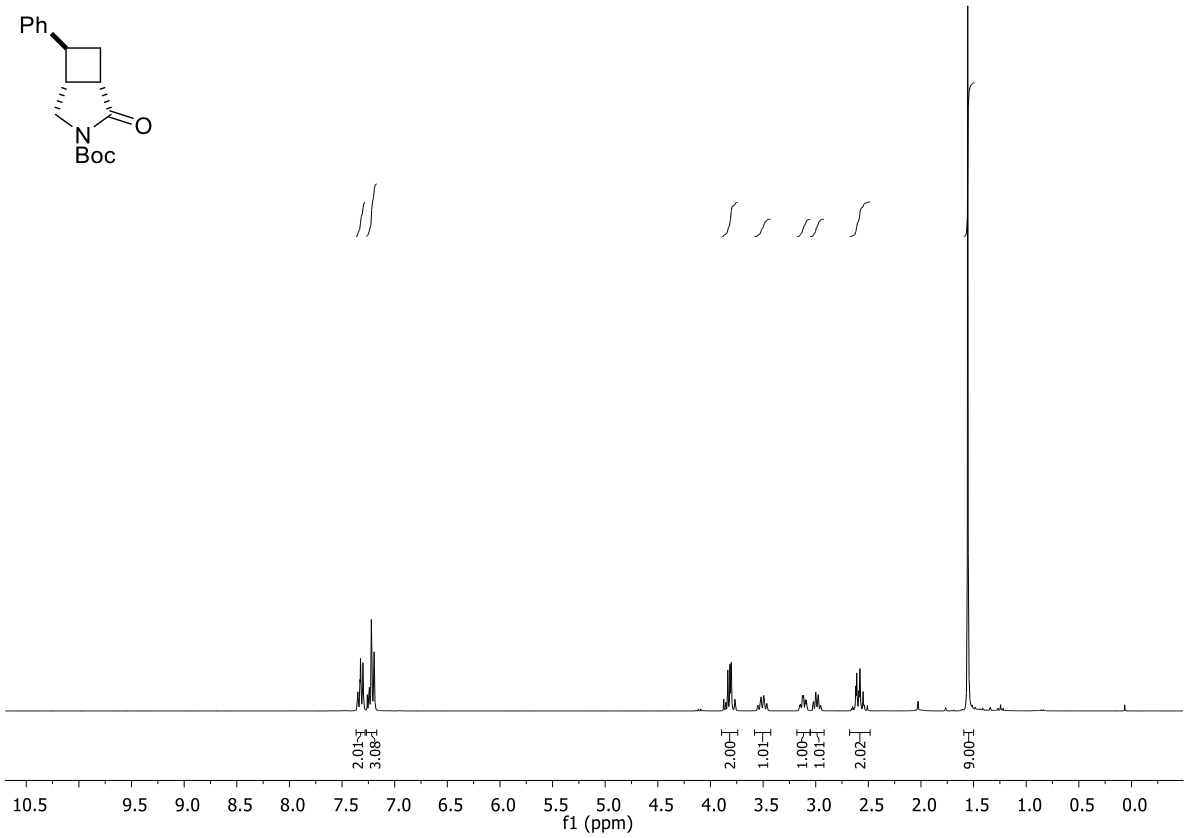

(75 MHz, $CDCl_3$)

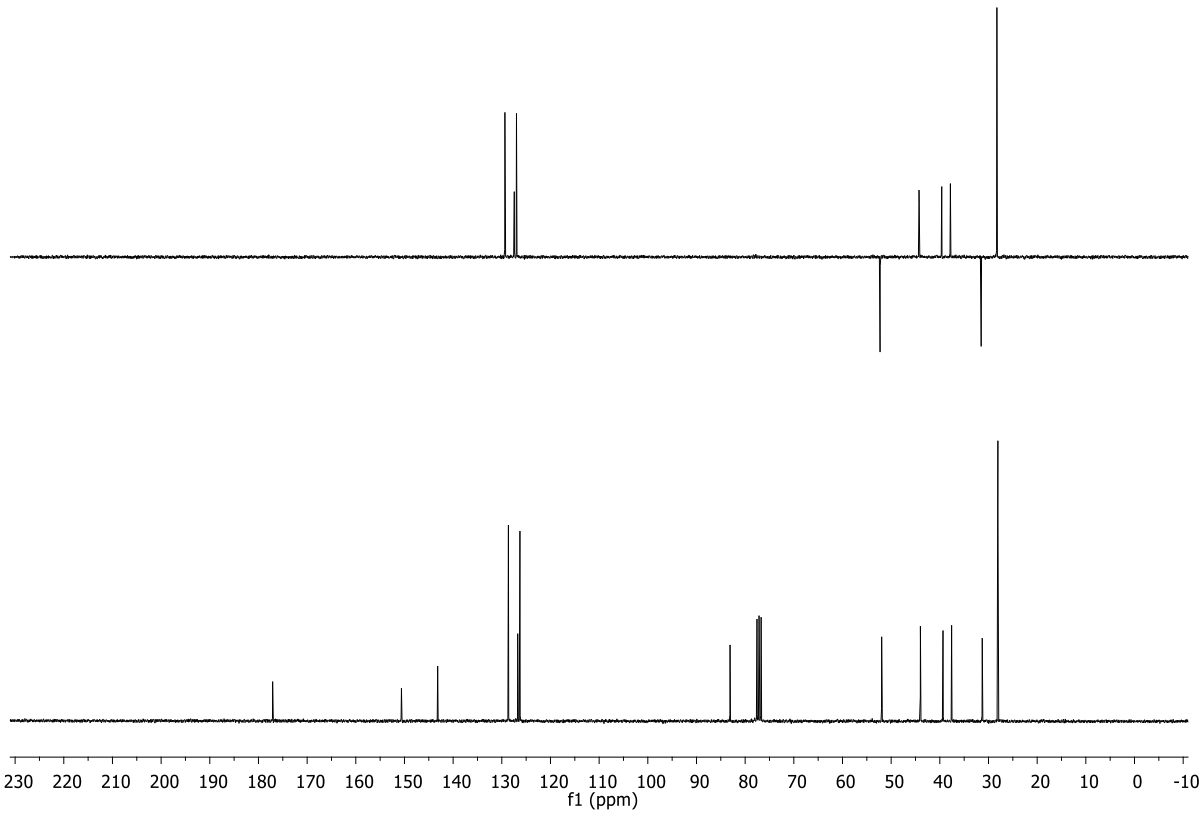

(±)-*cis*-*tert*-Butyl-2-oxo-6-phenyl-3-azabicyclo[3.2.0]heptane-3-carboxylate (158kb)

(300 MHz, $CDCl_3$)

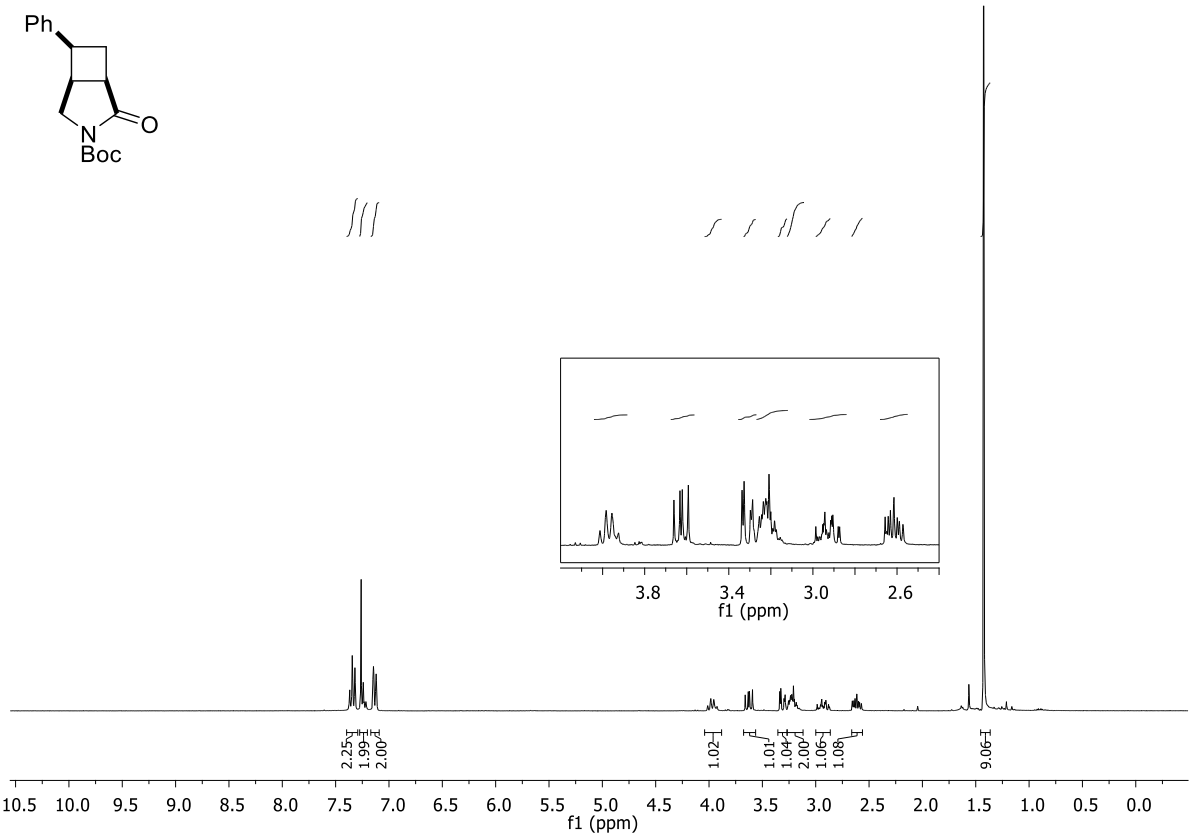

(101 MHz, $CDCl_3$)

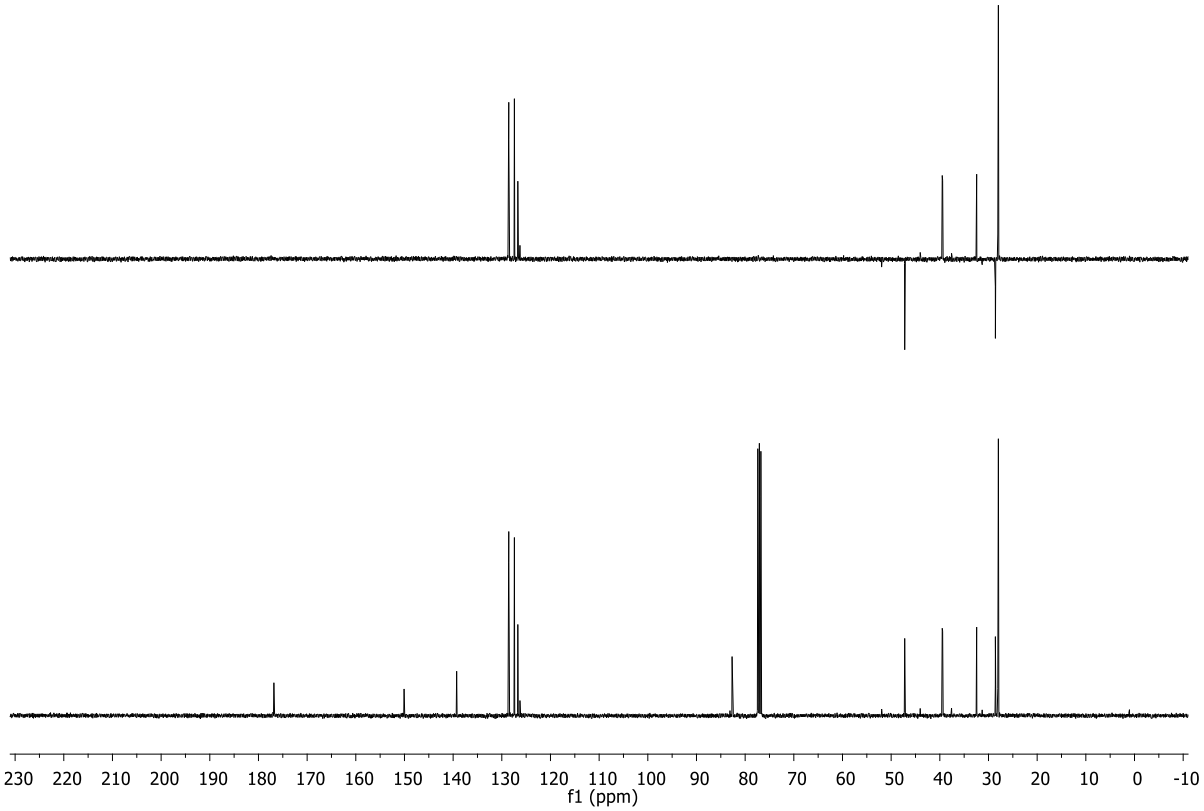

(±)-Methyl-3-(*tert*-butyl)-2-oxo-7-phenyl-3-azabicyclo[3.2.0]heptane-6-carboxylate (158l)

(400 MHz, $CDCl_3$)

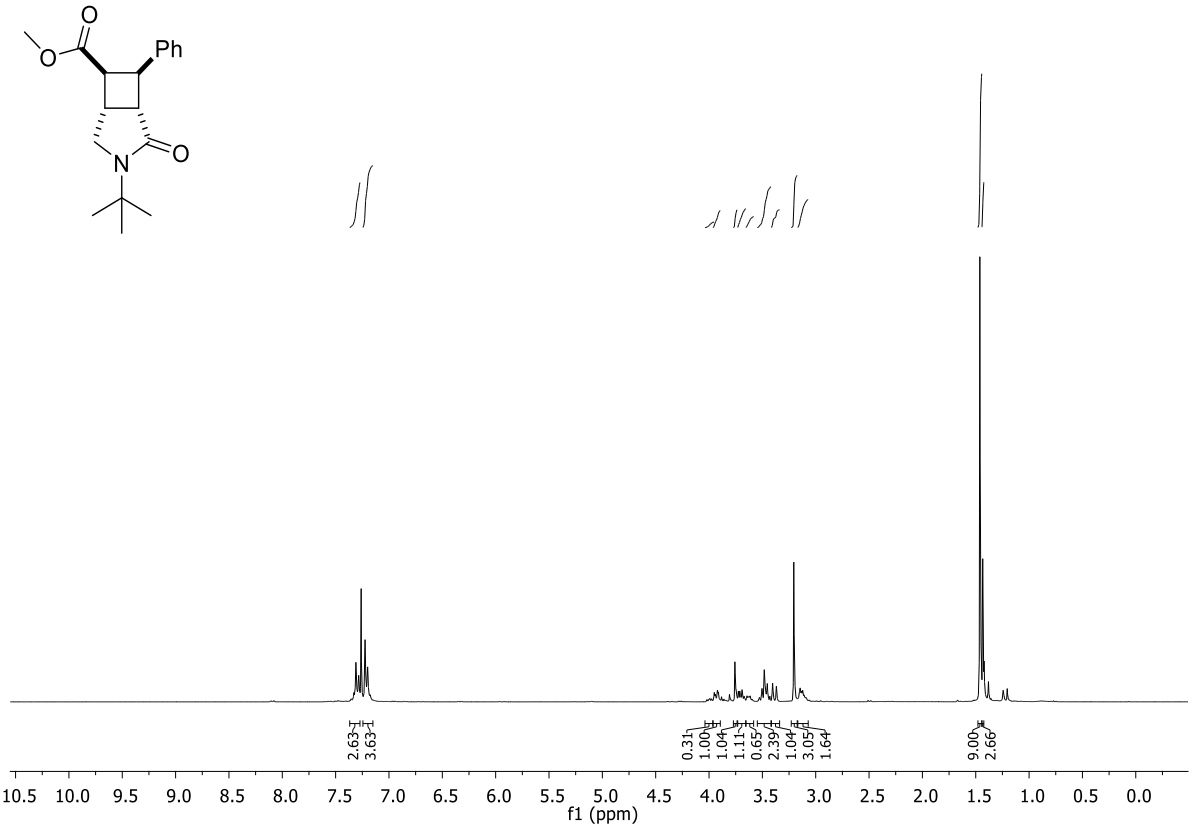

(101 MHz, $CDCl_3$)

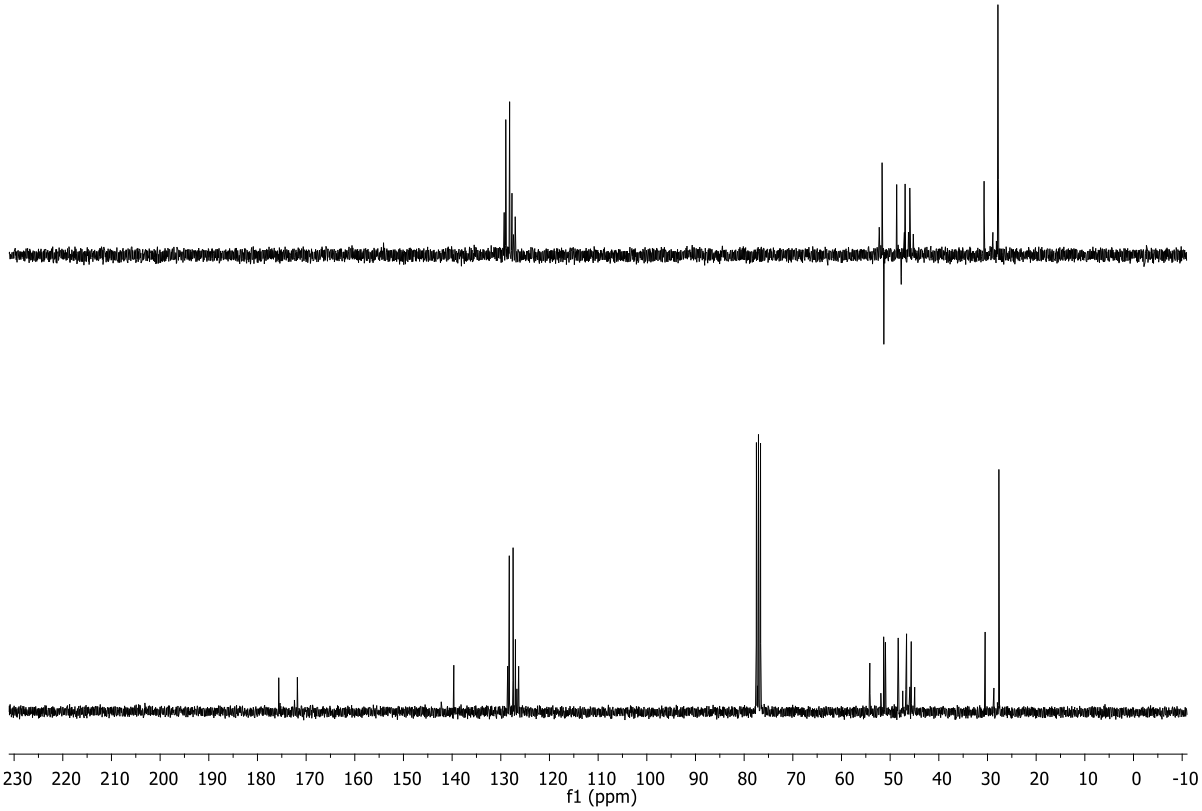

(±)-3-(*tert*-Butyl)-7-phenyl-3-azabicyclo[3.2.0]heptan-2-one (158m)

(300 MHz, $CDCl_3$)

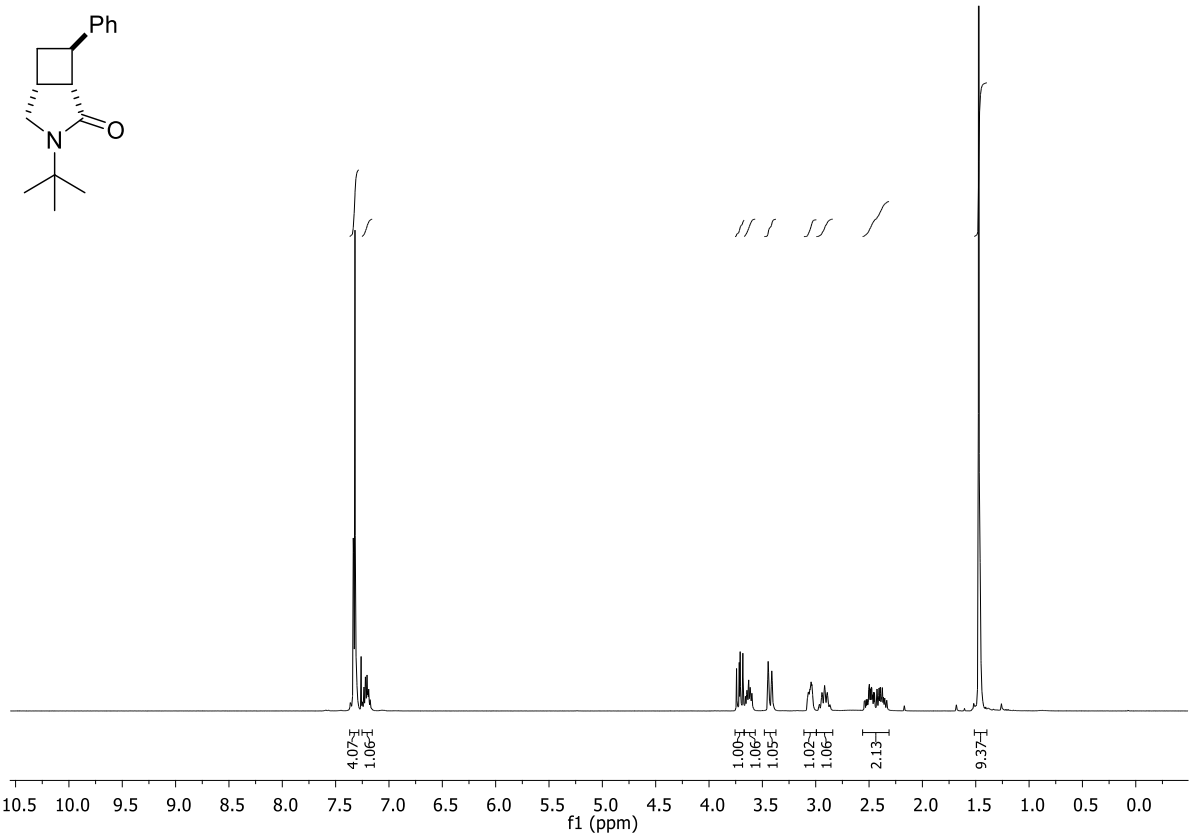

(75 MHz, $CDCl_3$)

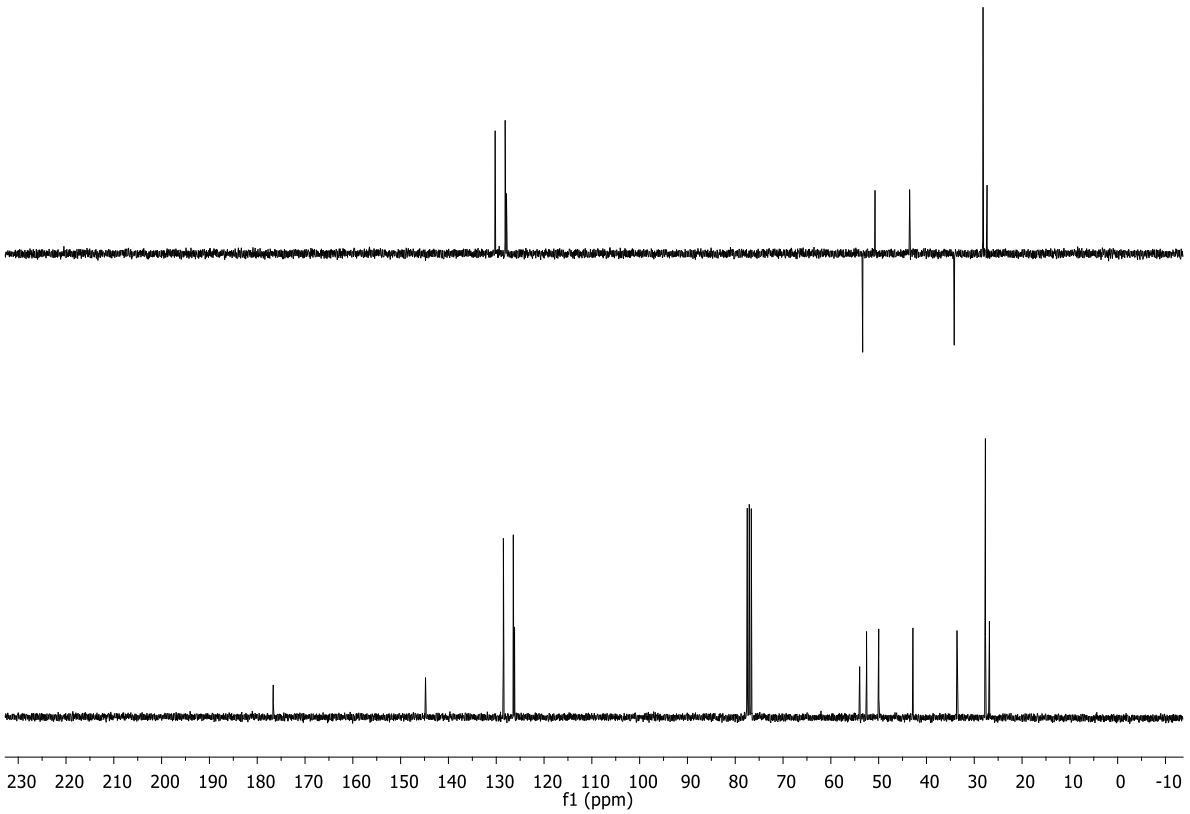

(±)-3-Benzyl-7-phenyl-3-azabicyclo[3.2.0]heptan-2-one (158n)

(300 MHz, $CDCl_3$)

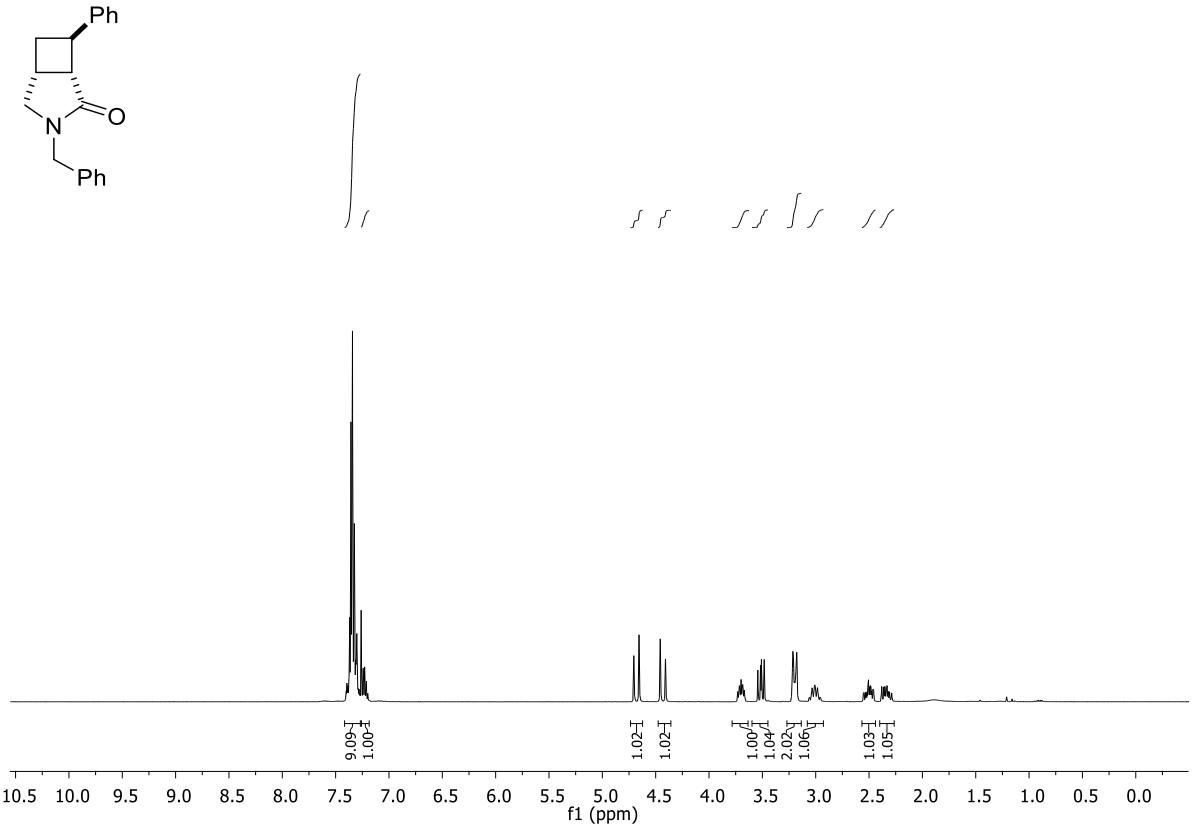

(101 MHz, $CDCl_3$)

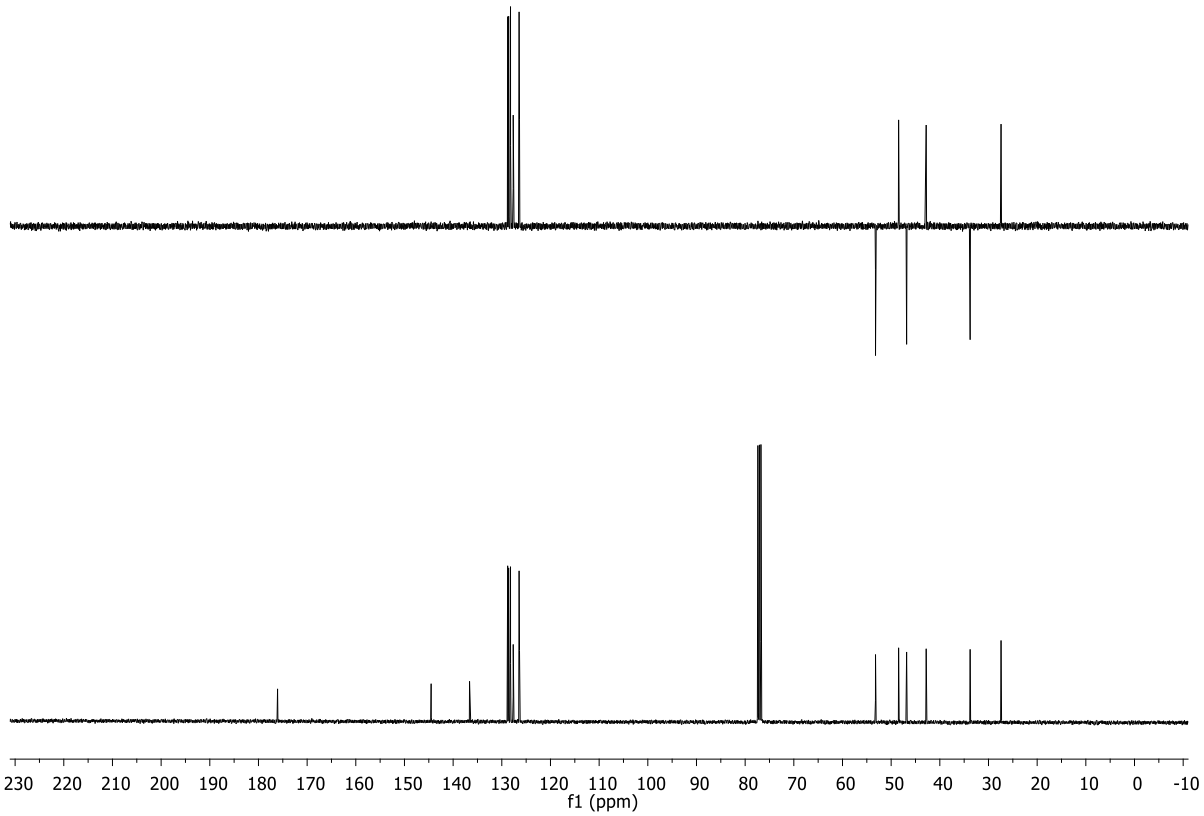

(±)-*tert*-Butyl-2-oxo-7-phenyl-3-azabicyclo[3.2.0]heptane-3-carboxylate (158o)

(400 MHz, $CDCl_3$)

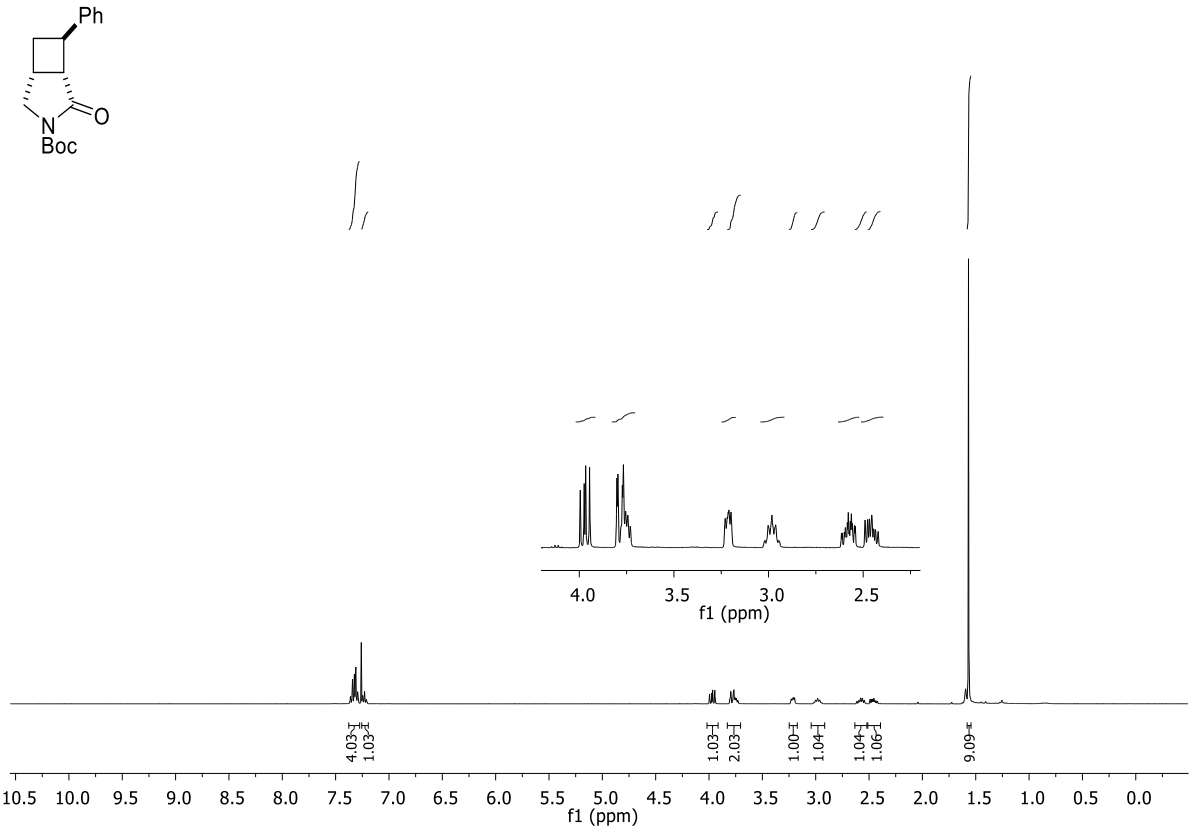

(101 MHz, $CDCl_3$)

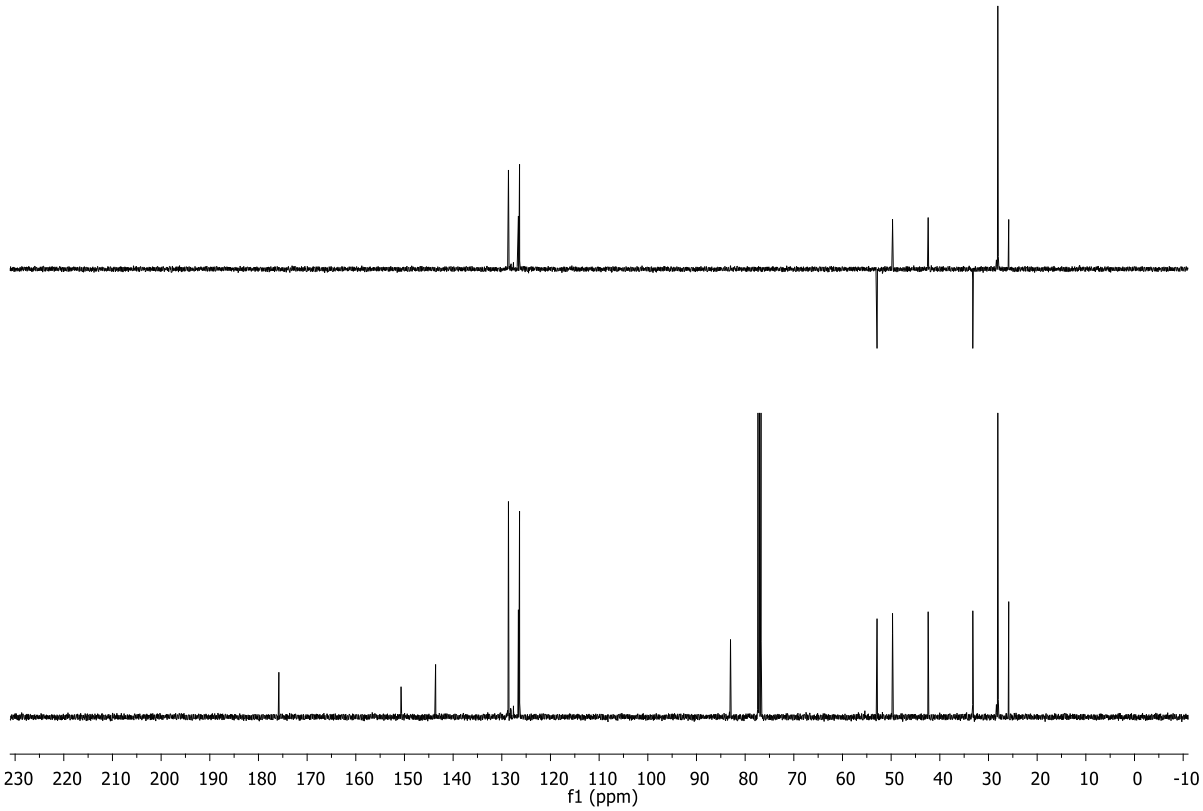

(±)-3-(*tert*-Butyl)-7-(furan-2-yl)-3-azabicyclo[3.2.0]heptan-2-one (158p)

(300 MHz, $CDCl_3$)

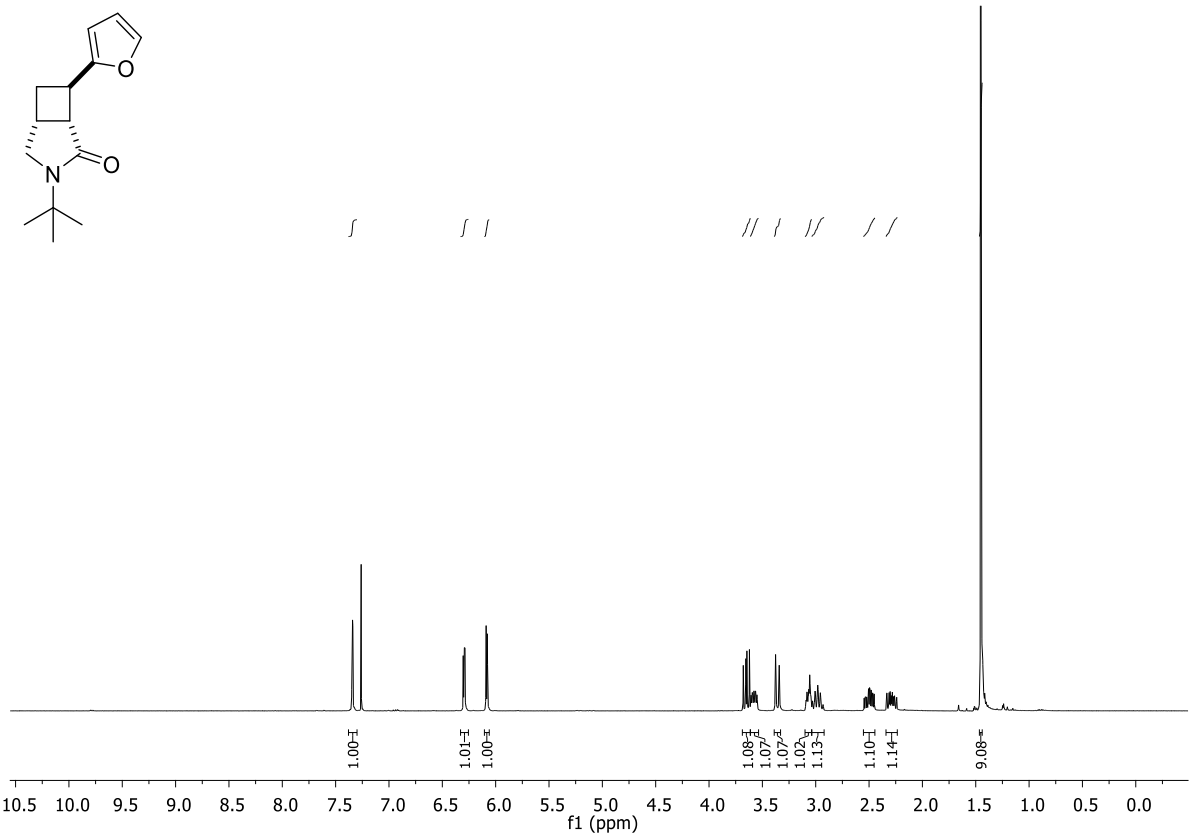

(75 MHz, $CDCl_3$)

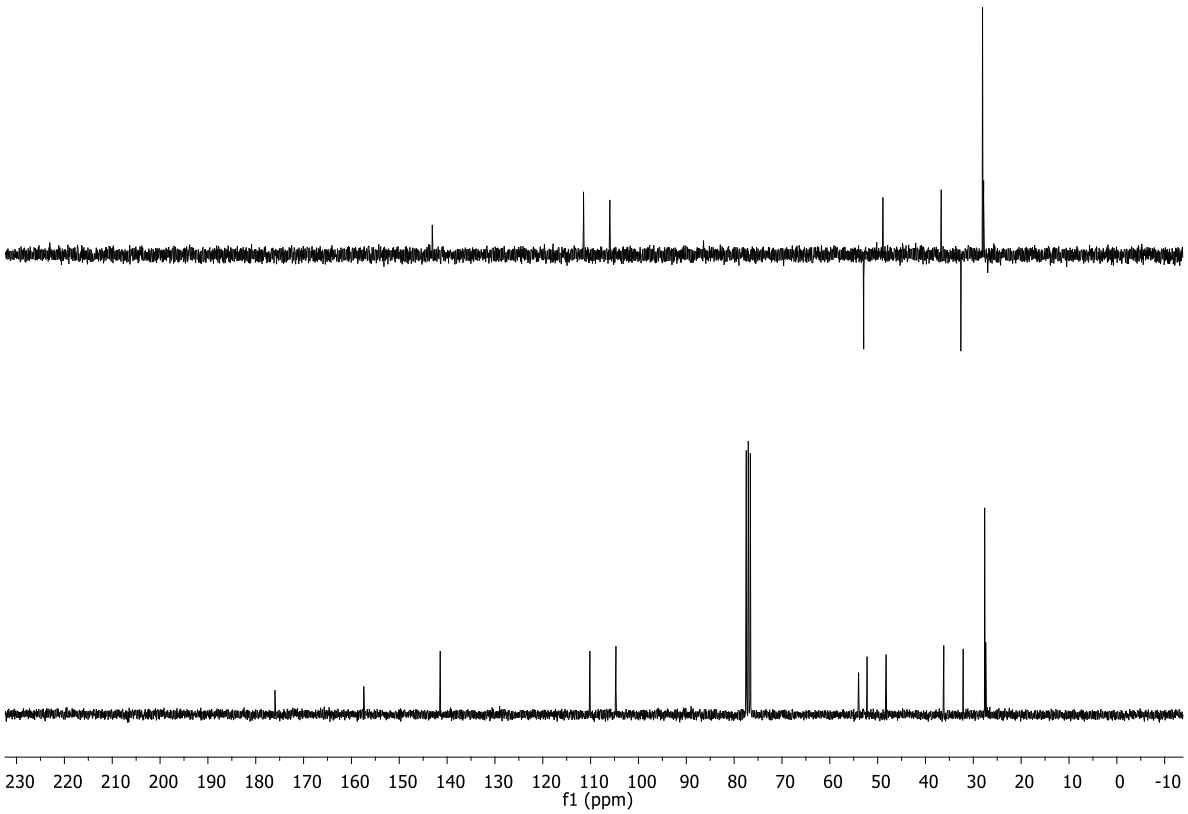

(±)-3-(*tert*-Butyl)-7-(thiophen-2-yl)-3-azabicyclo[3.2.0]heptan-2-one (158q)

(300 MHz, $CDCl_3$)

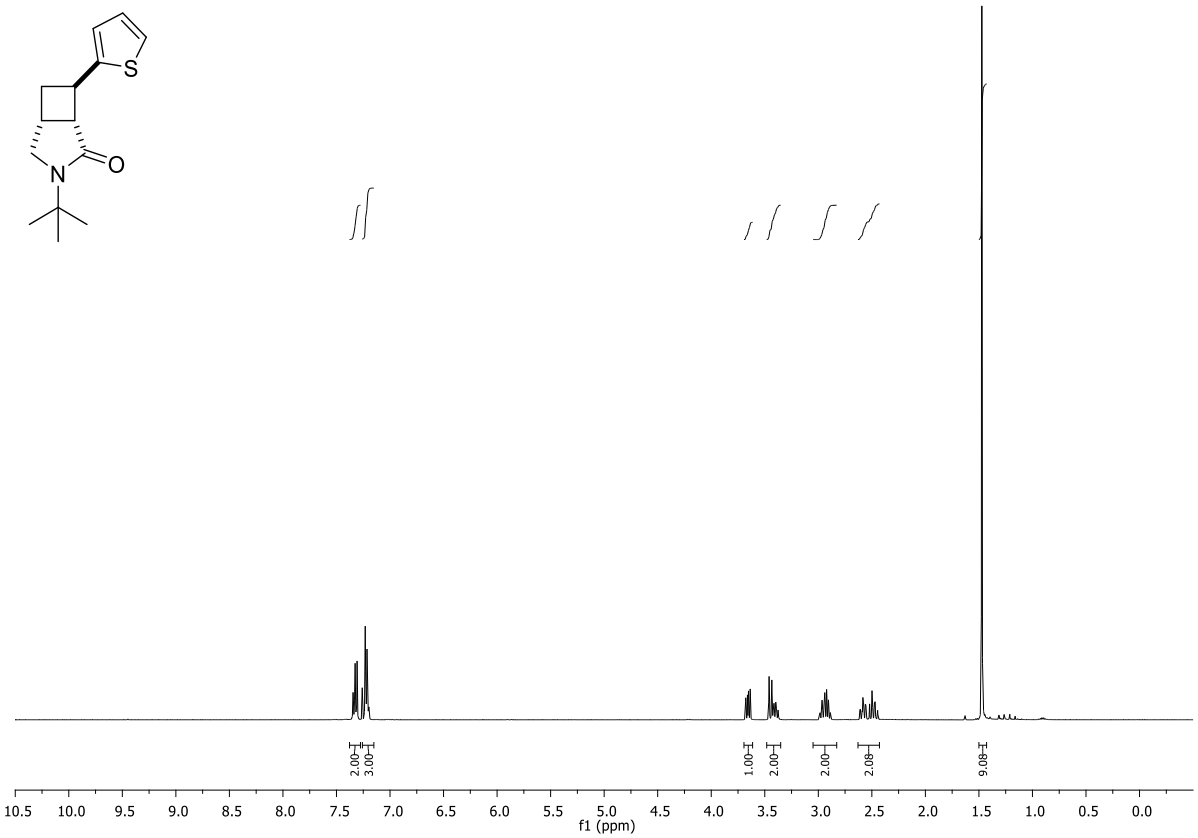

(75 MHz, $CDCl_3$)

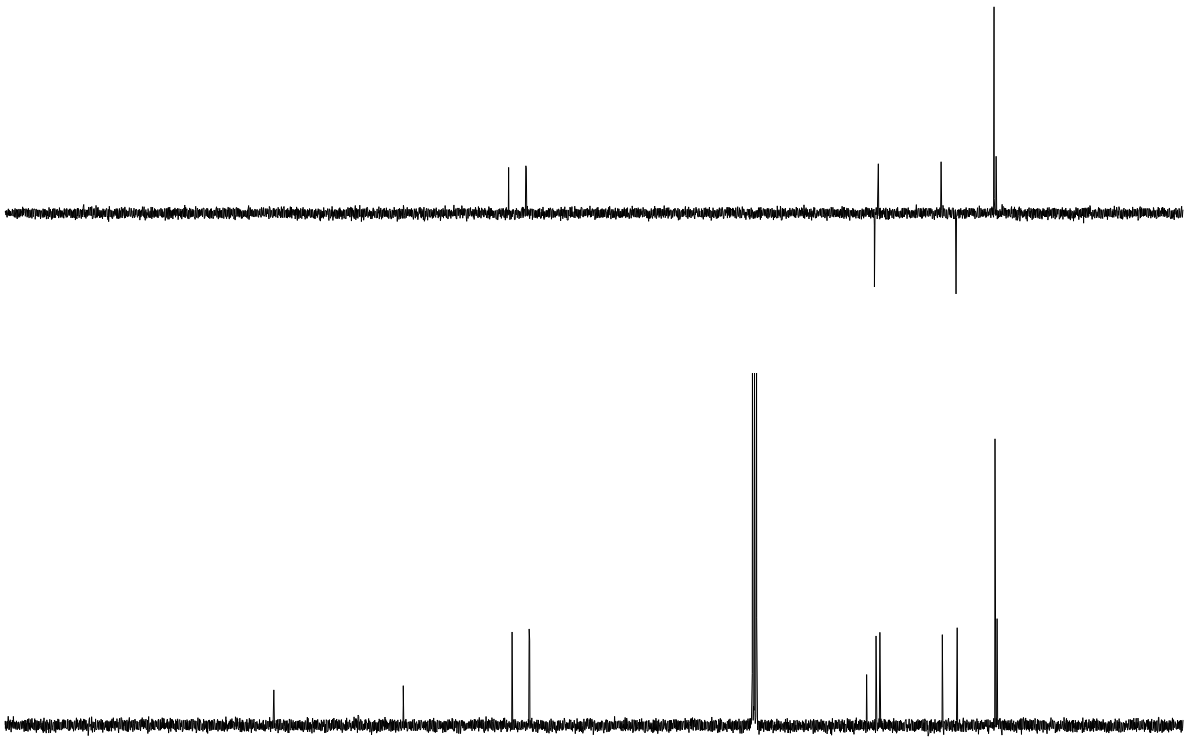

(±)-7-(1-Acetyl-1*H*-indol-3-yl)-3-(*tert*-butyl)-3-azabicyclo[3.2.0]heptan-2-one (158r)

(300 MHz, $CDCl_3$)

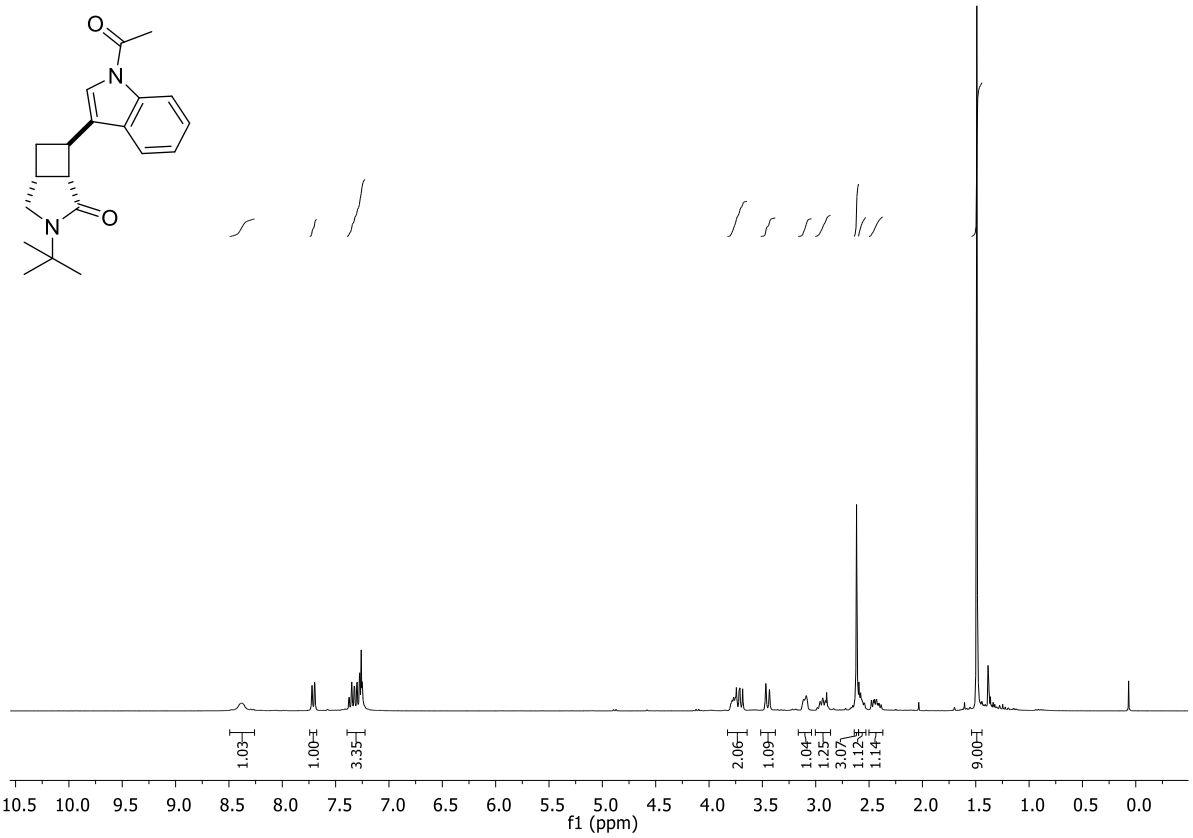

(75 MHz, $CDCl_3$)

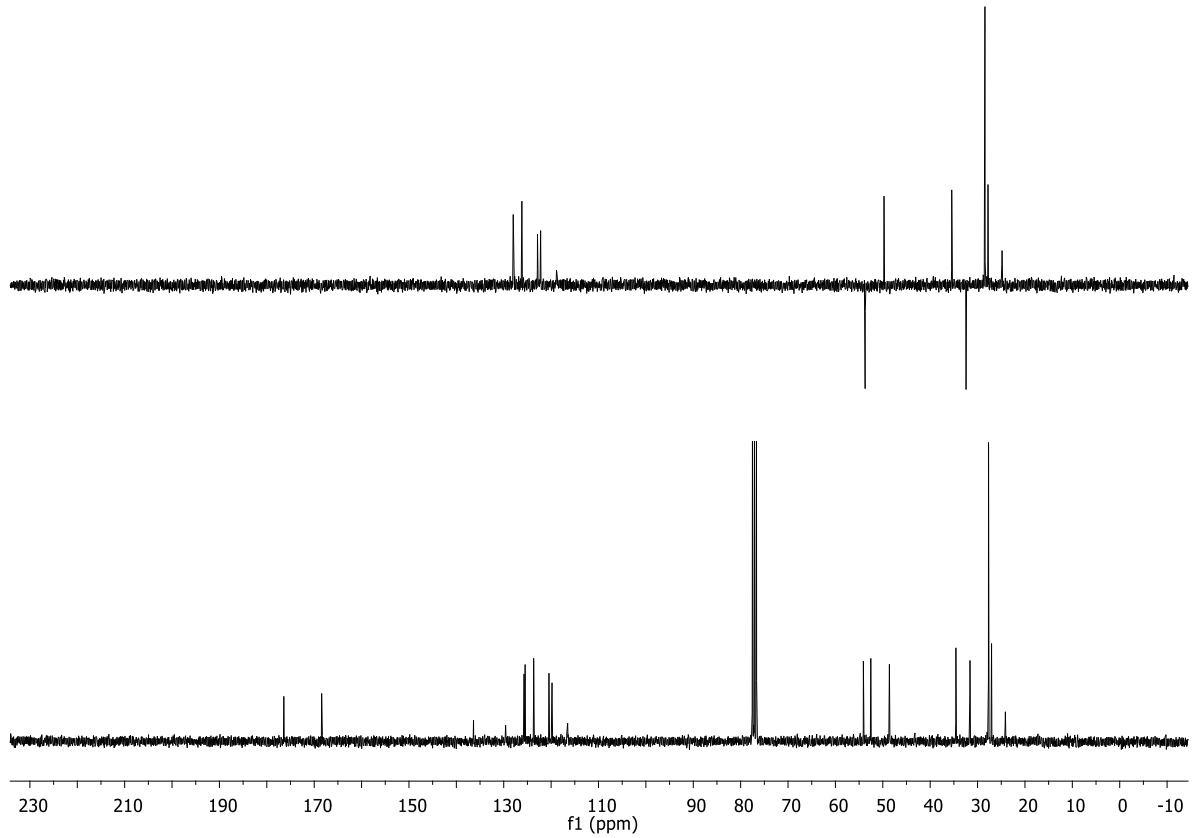

(±)-6,7-Diphenyl-3-oxabicyclo[3.2.0]heptan-2-one (158t)

(300 MHz, $CDCl_3$)

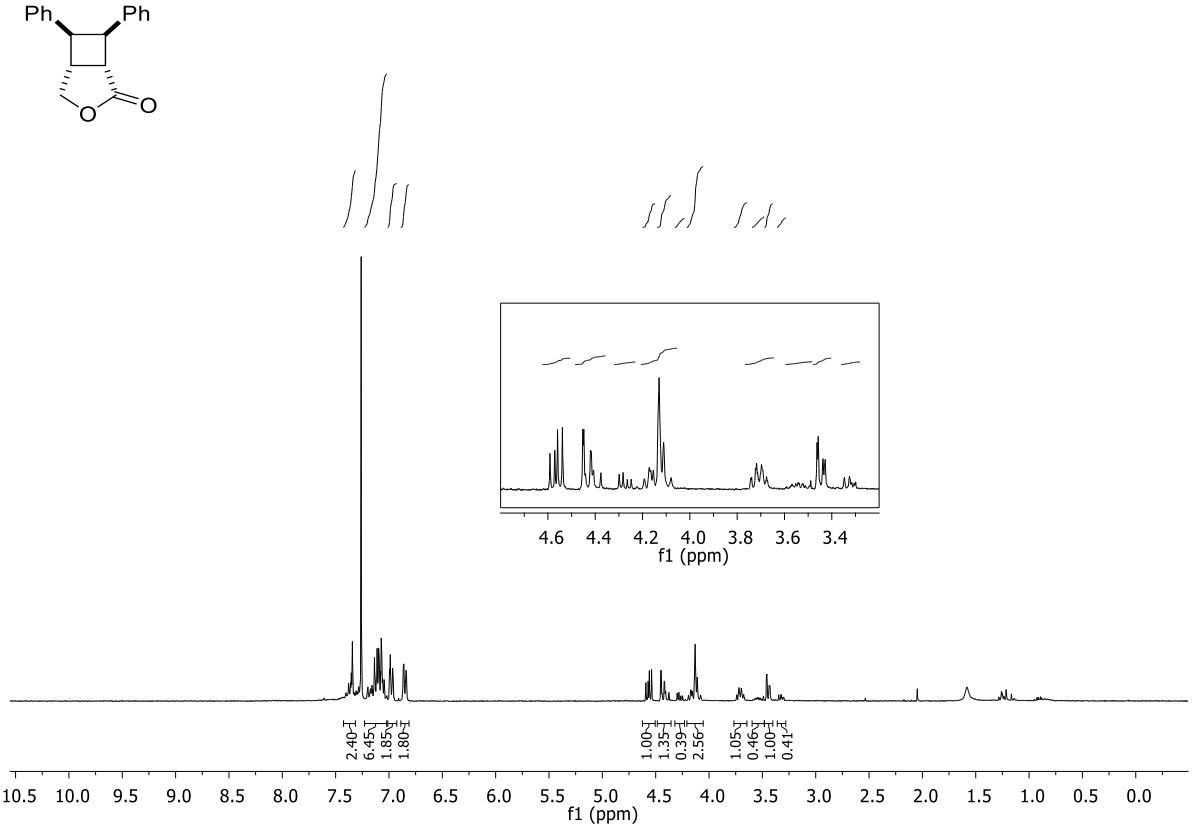

(101 MHz, $CDCl_3$)

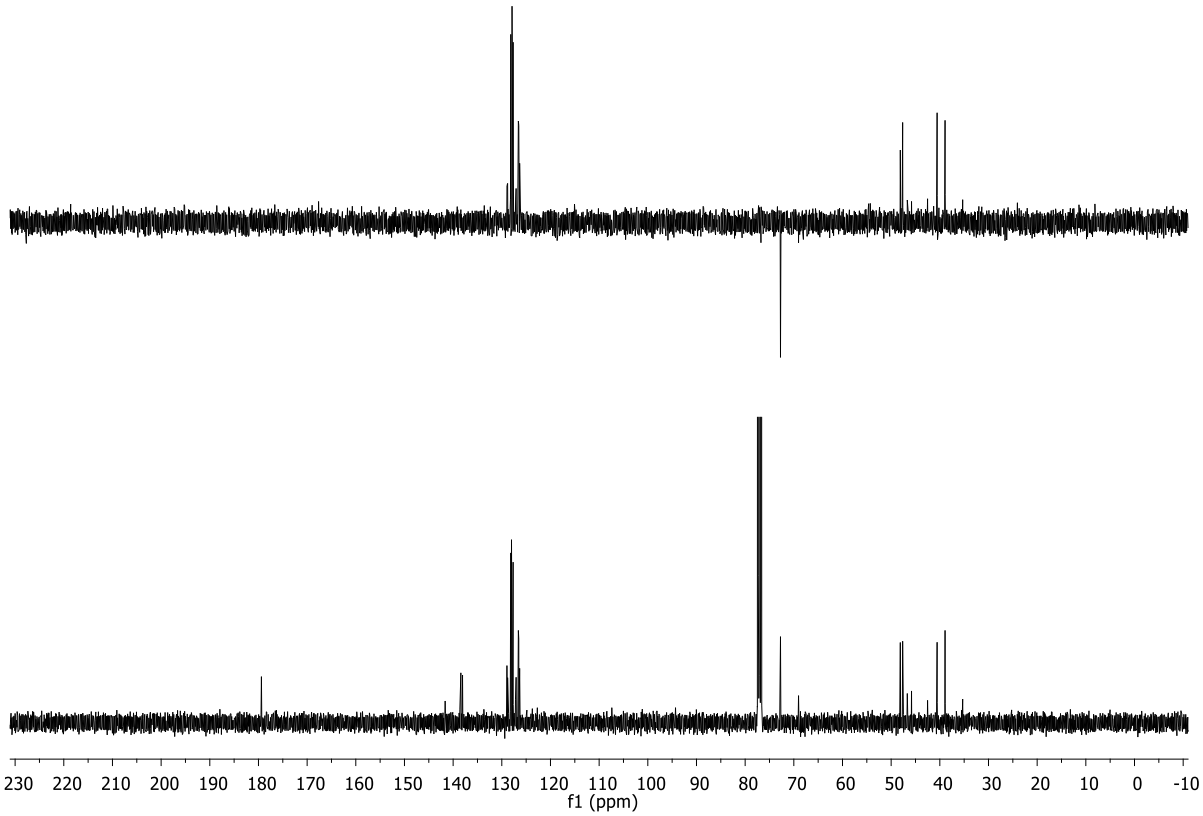

(1*R*,5*S*,6*R*)-6-Phenyl-3-((*S*)-1-phenylethyl)-3-azabicyclo[3.2.0]heptan-2-one (158va)

(400 MHz, $CDCl_3$)

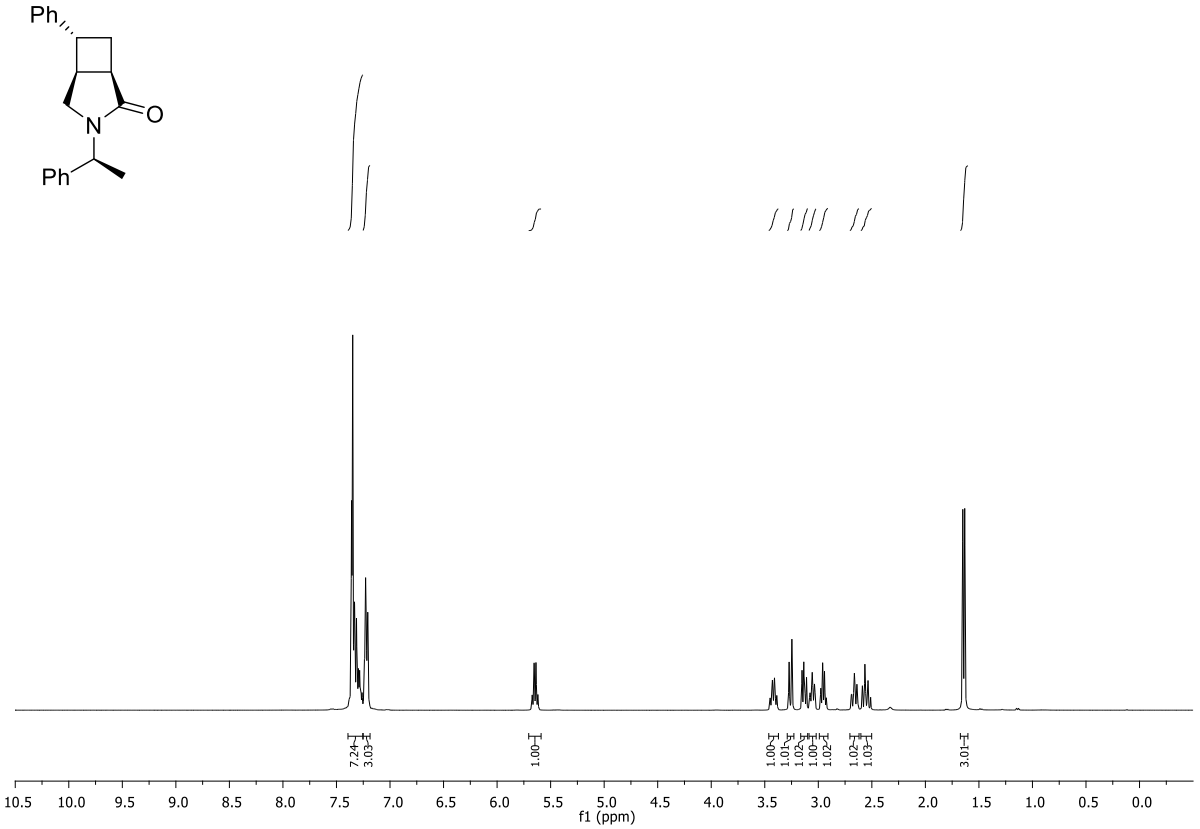

(101 MHz, $CDCl_3$)

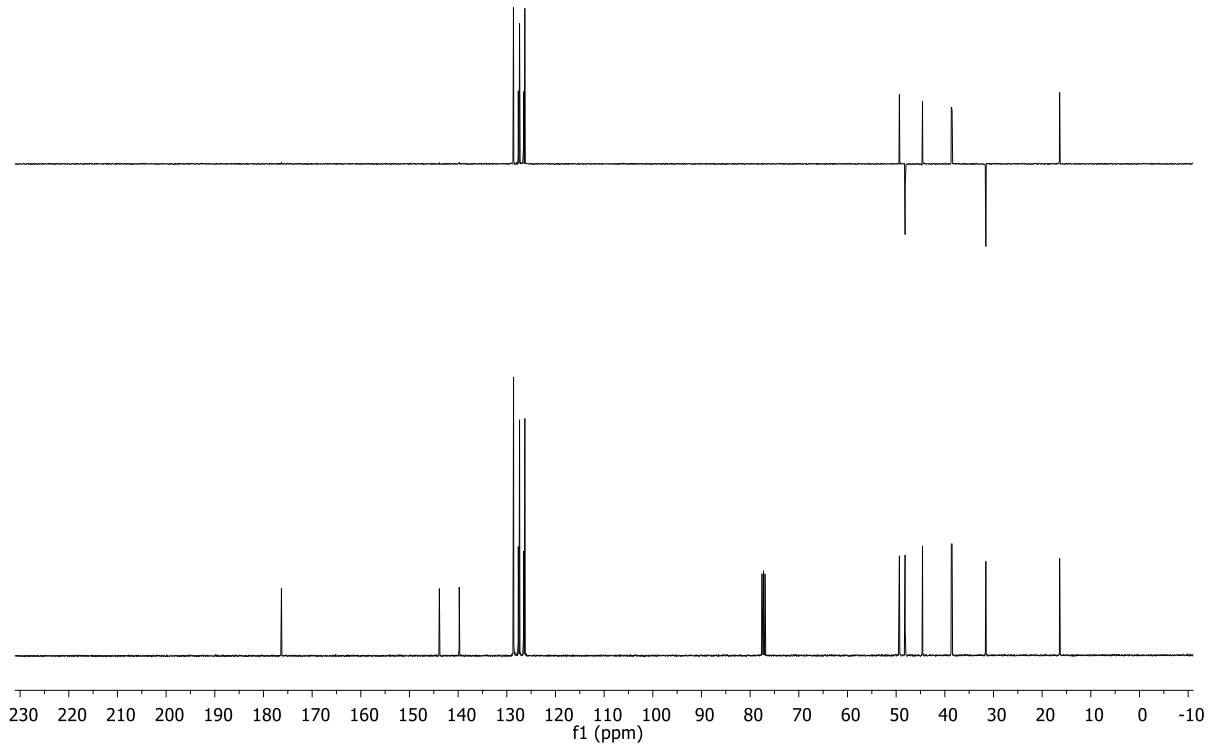

(1*S*,5*R*,6*S*)-6-Phenyl-3-((*S*)-1-phenylethyl)-3-azabicyclo[3.2.0]heptan-2-one (158vb)

(300 MHz, $CDCl_3$)

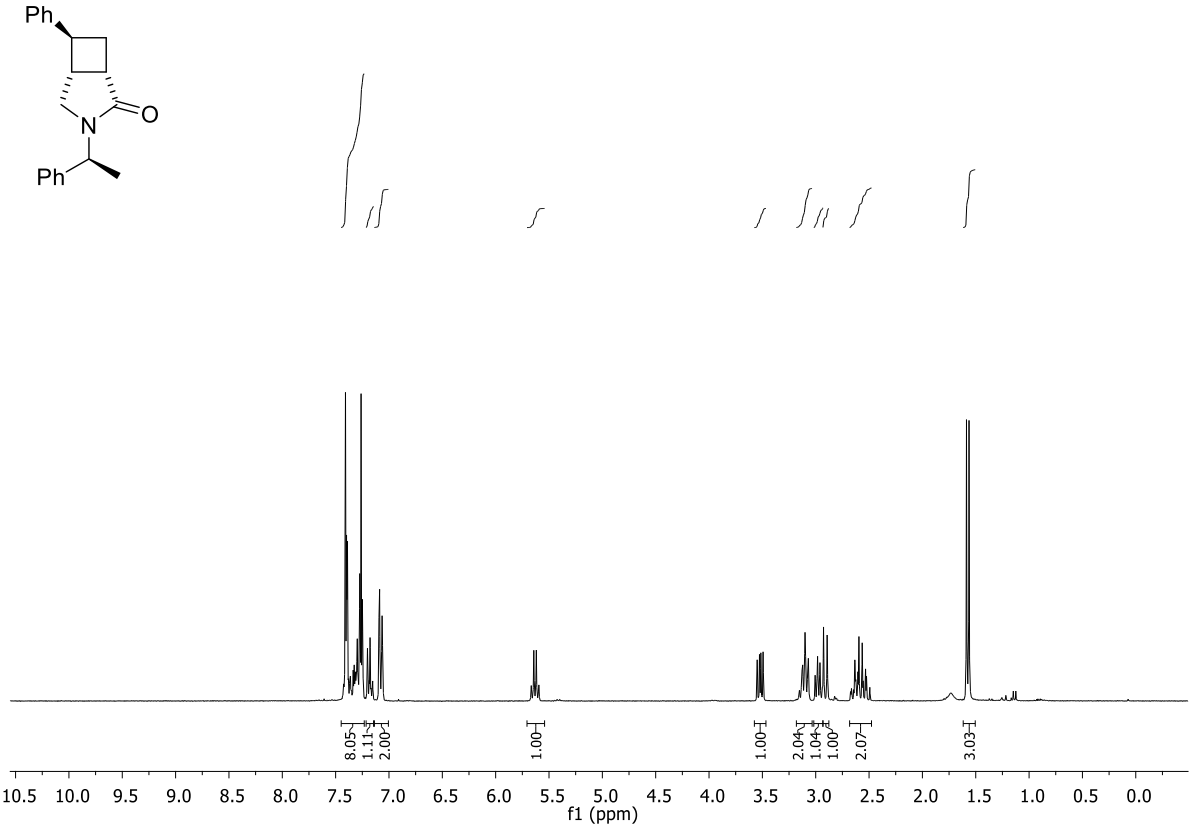

(101 MHz, $CDCl_3$)

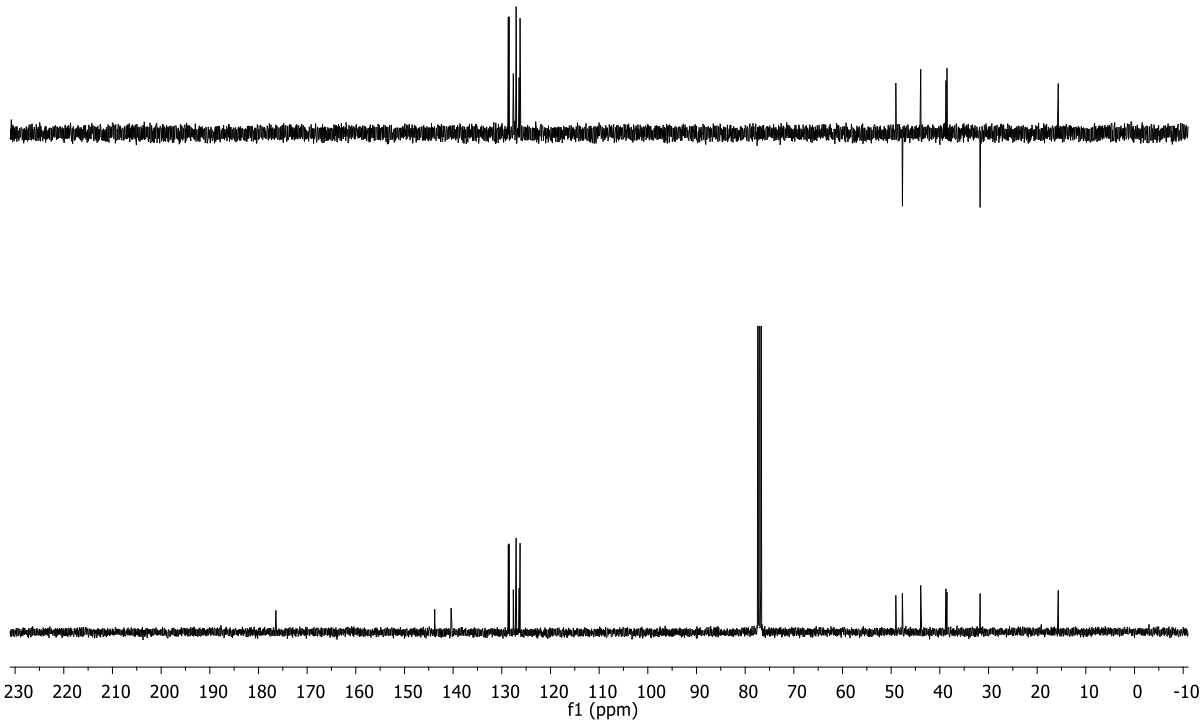

(1*R*,5*S*,7*S*)-7-Phenyl-3-((*S*)-1-phenylethyl)-3-azabicyclo[3.2.0]heptan-2-one (158wa)

(400 MHz, $CDCl_3$)

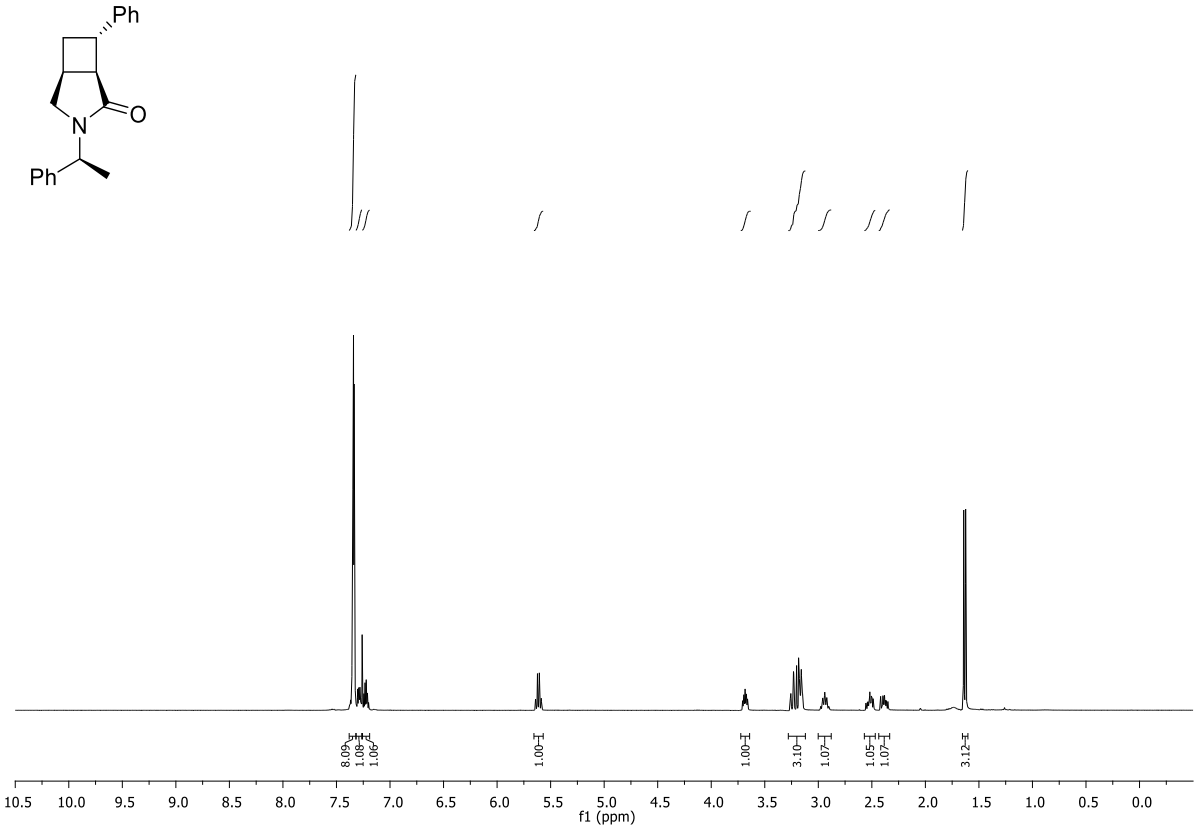

(101 MHz, $CDCl_3$)

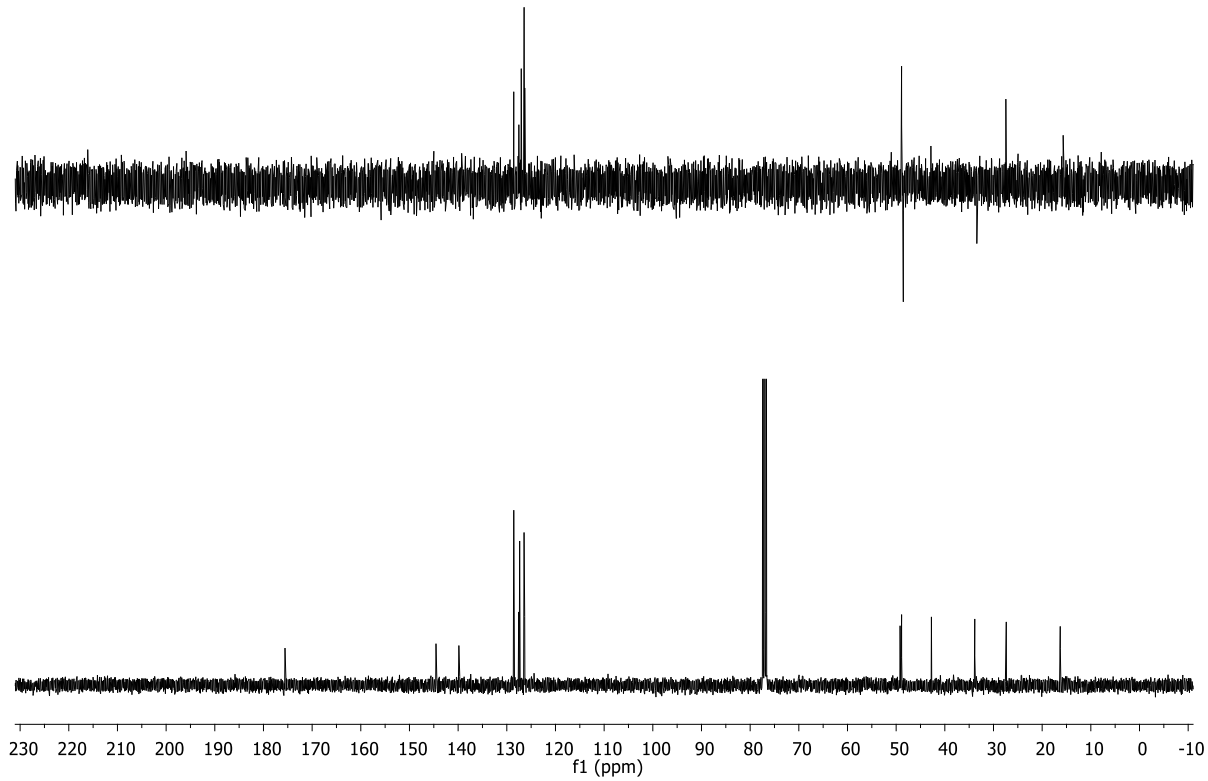

(1*S*,5*R*,7*R*)-7-Phenyl-3-((*S*)-1-phenylethyl)-3-azabicyclo[3.2.0]heptan-2-one (158wb)

(400 MHz, $CDCl_3$)

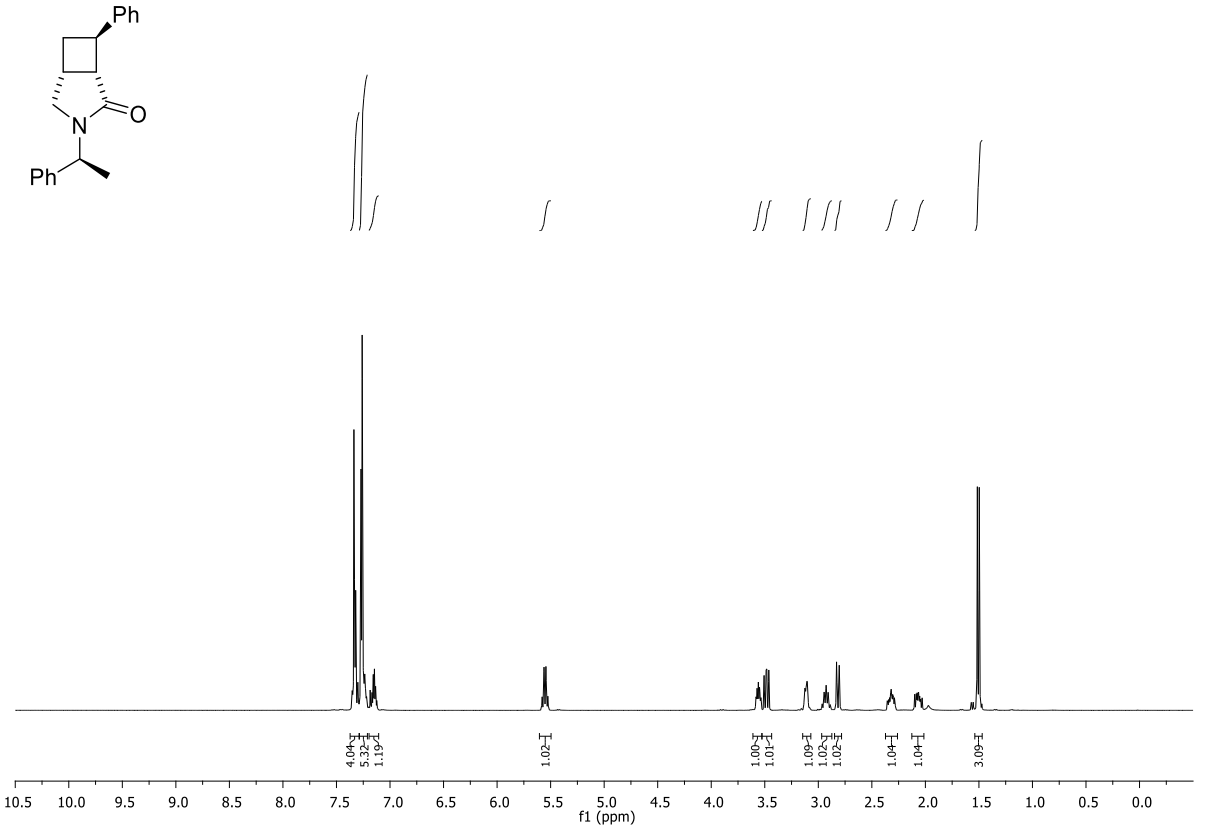

(101 MHz, $CDCl_3$)

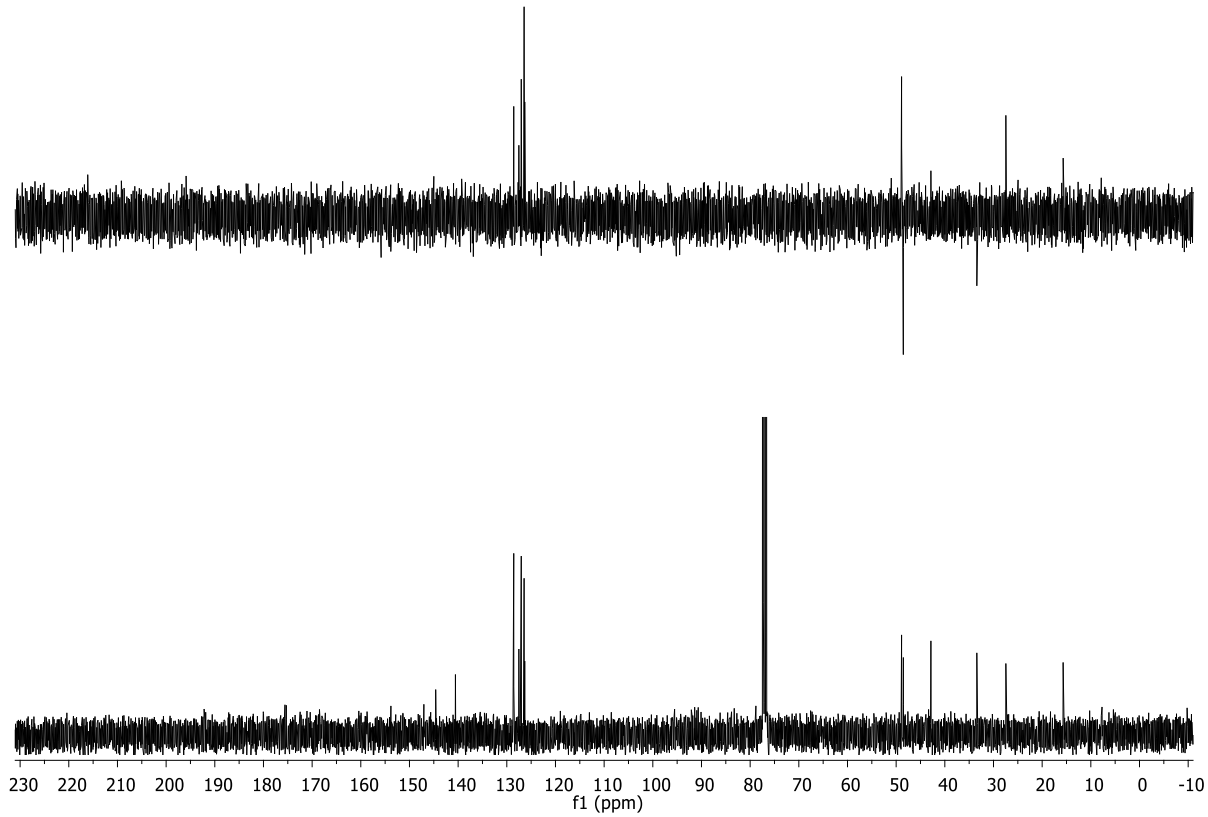

(±)-2-(Aminomethyl)-3,4-diphenylcyclobutane-1-carboxylic acid (198)

(300 MHz, MeOD)

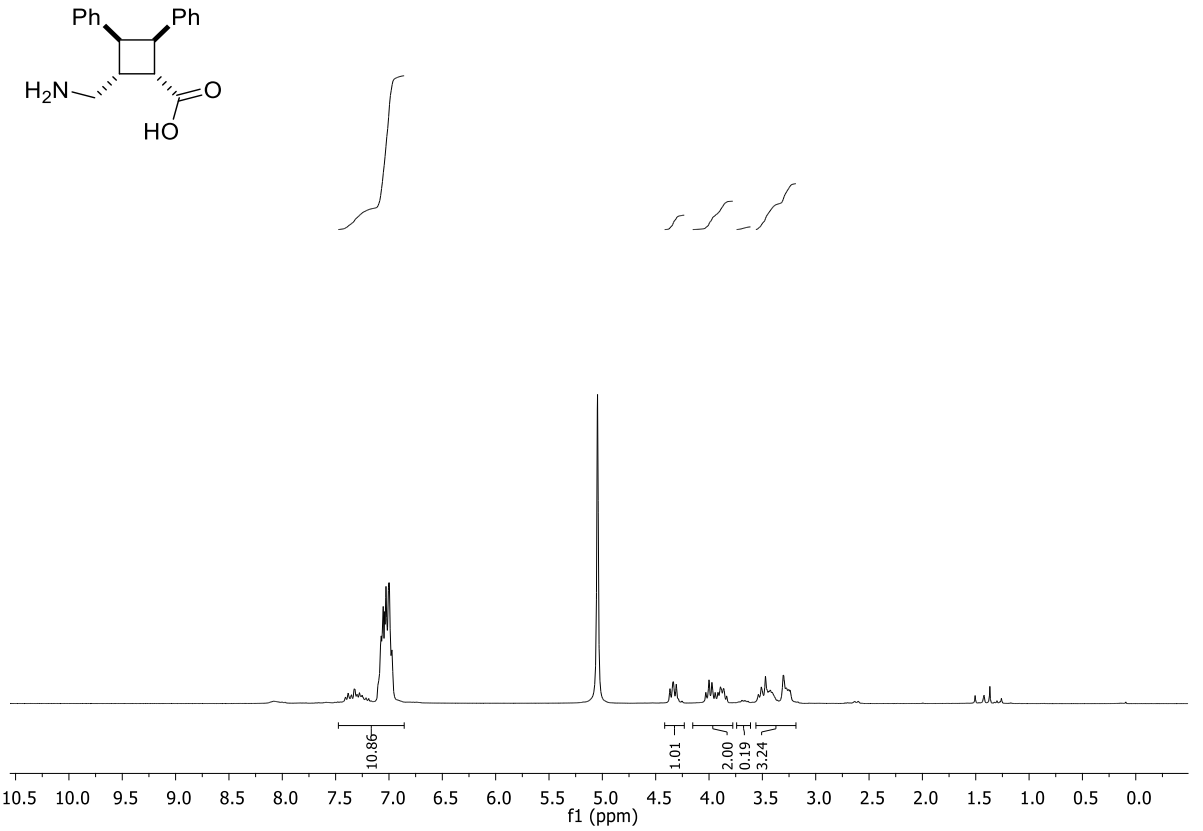

(75 MHz, MeOD)

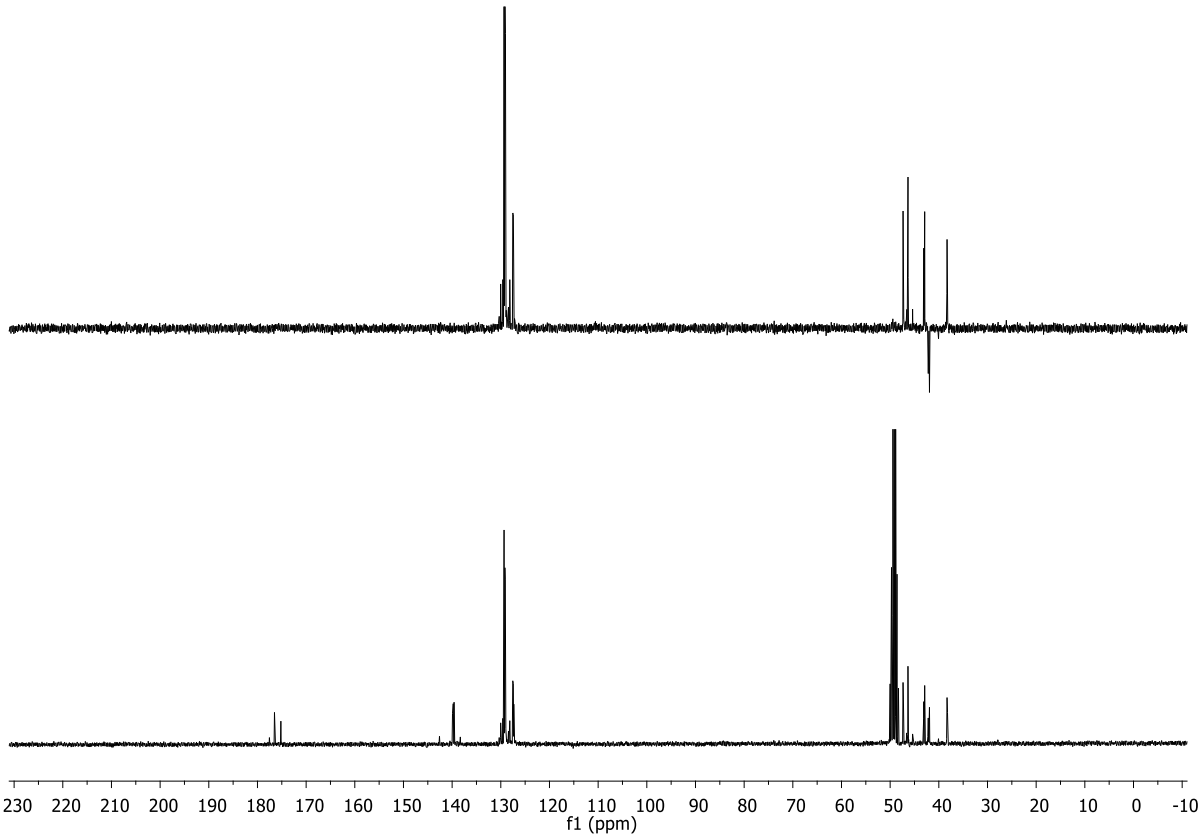

(±)-2-(Aminomethyl)-3-phenylcyclobutane-1-carboxylic acid (200)

(300 MHz, MeOD)

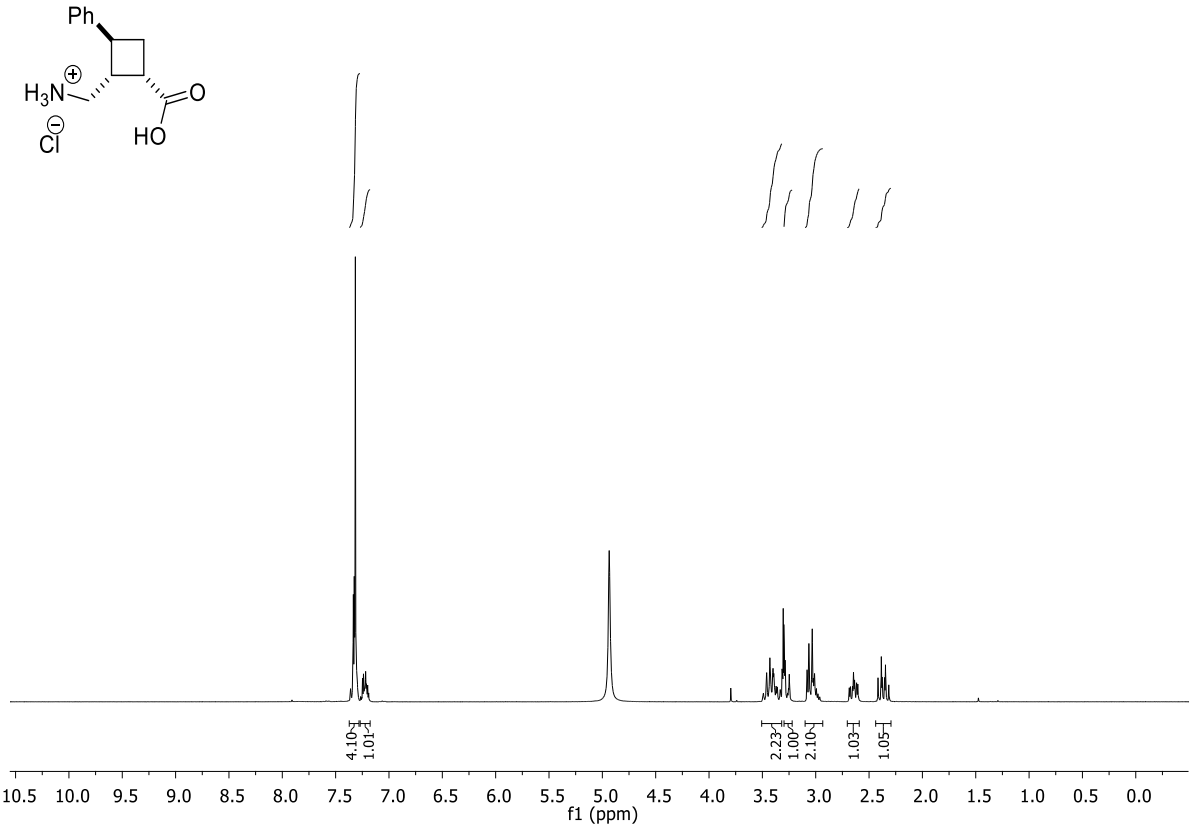

(75 MHz, MeOD)

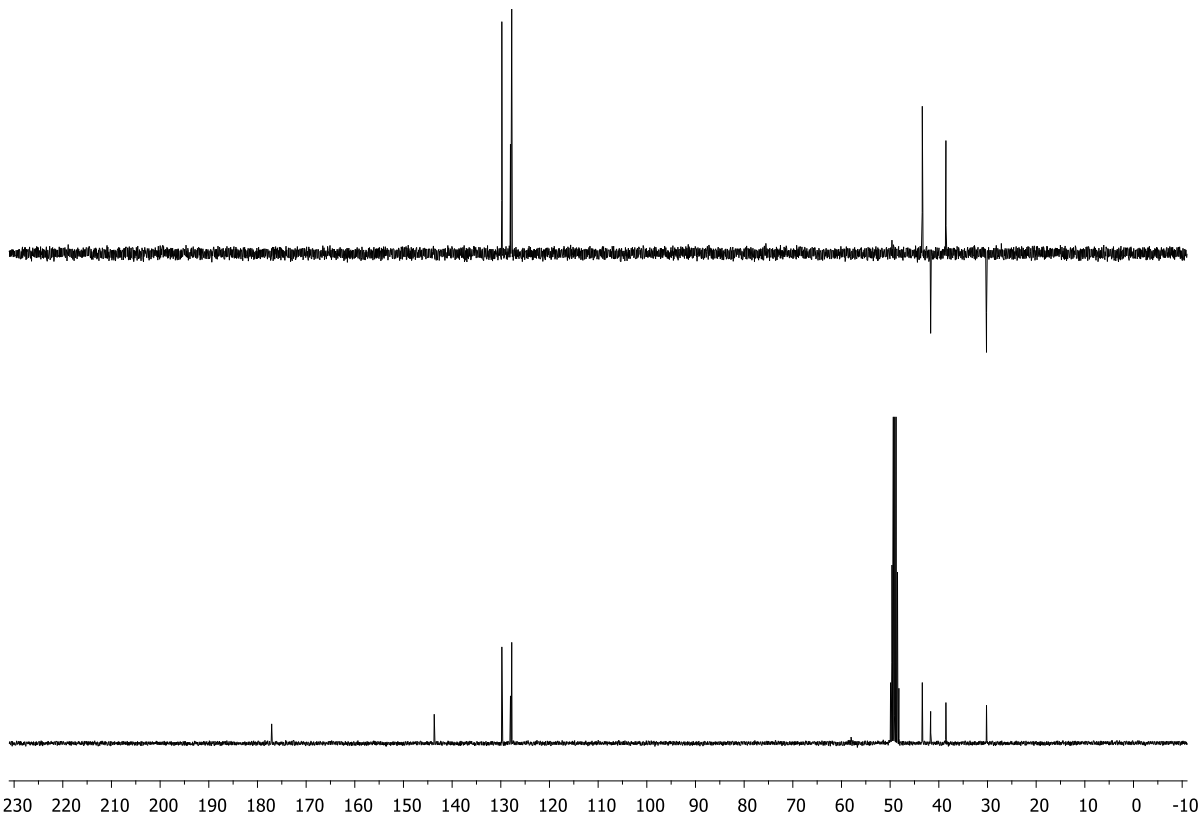

(±)-2-(Aminomethyl)-3-phenylcyclobutane-1-carboxylic acid (201)

(300 MHz, MeOD)

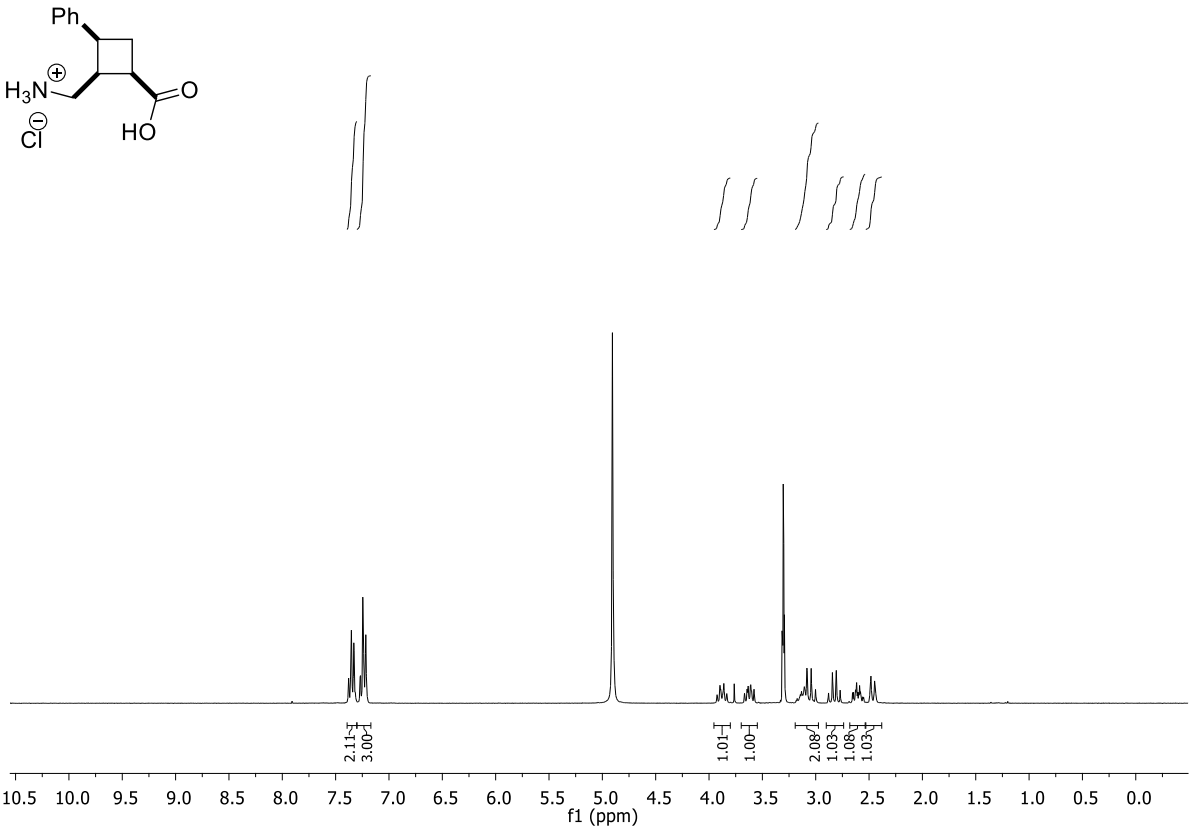

(75 MHz, MeOD)

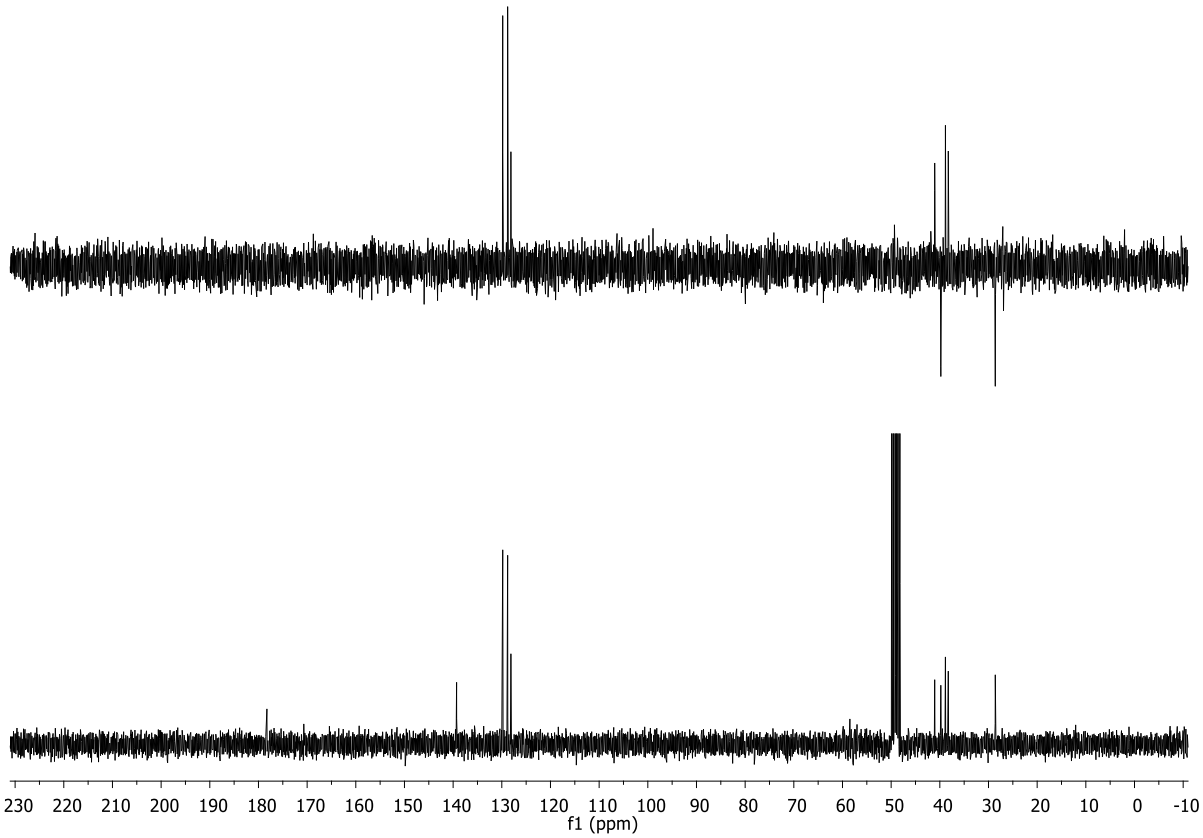

(±)-2-(Aminomethyl)-4-phenylcyclobutane-1,3-dicarboxylic acid (203)

(400 MHz, MeOD)

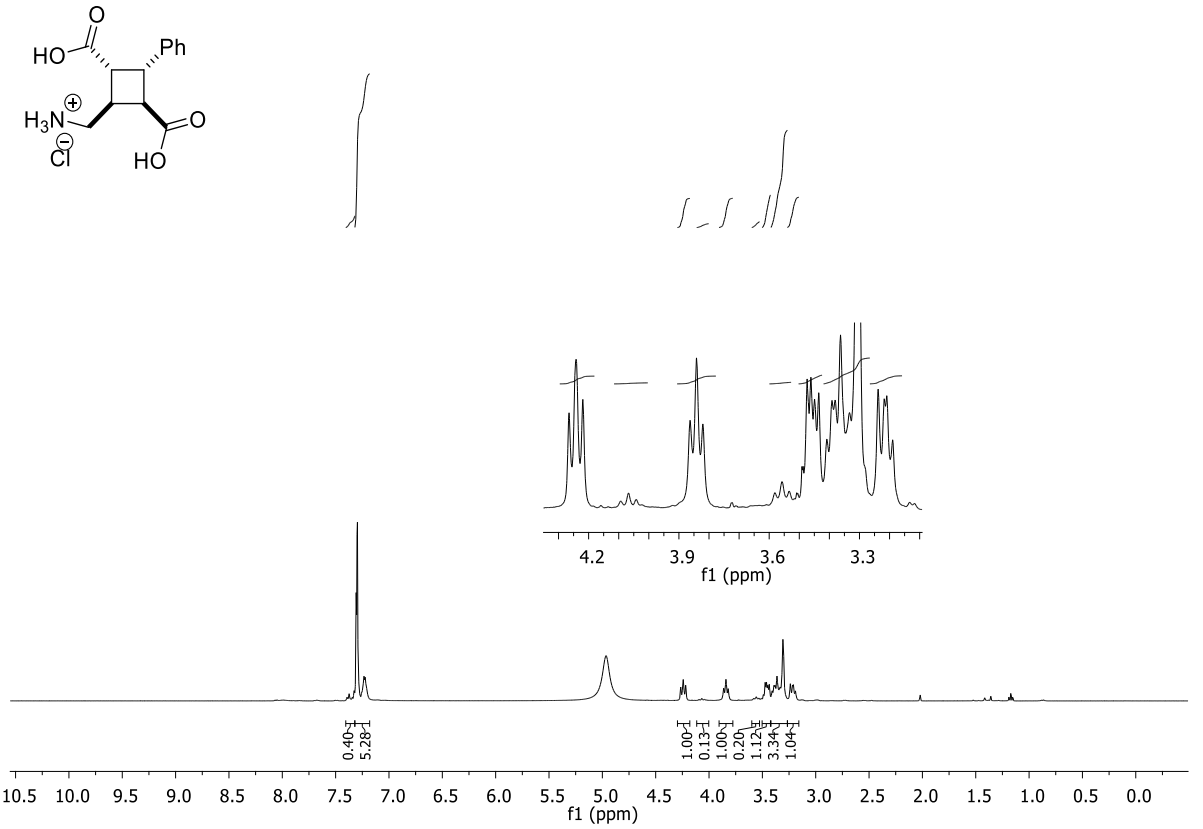

(101 MHz, MeOD)

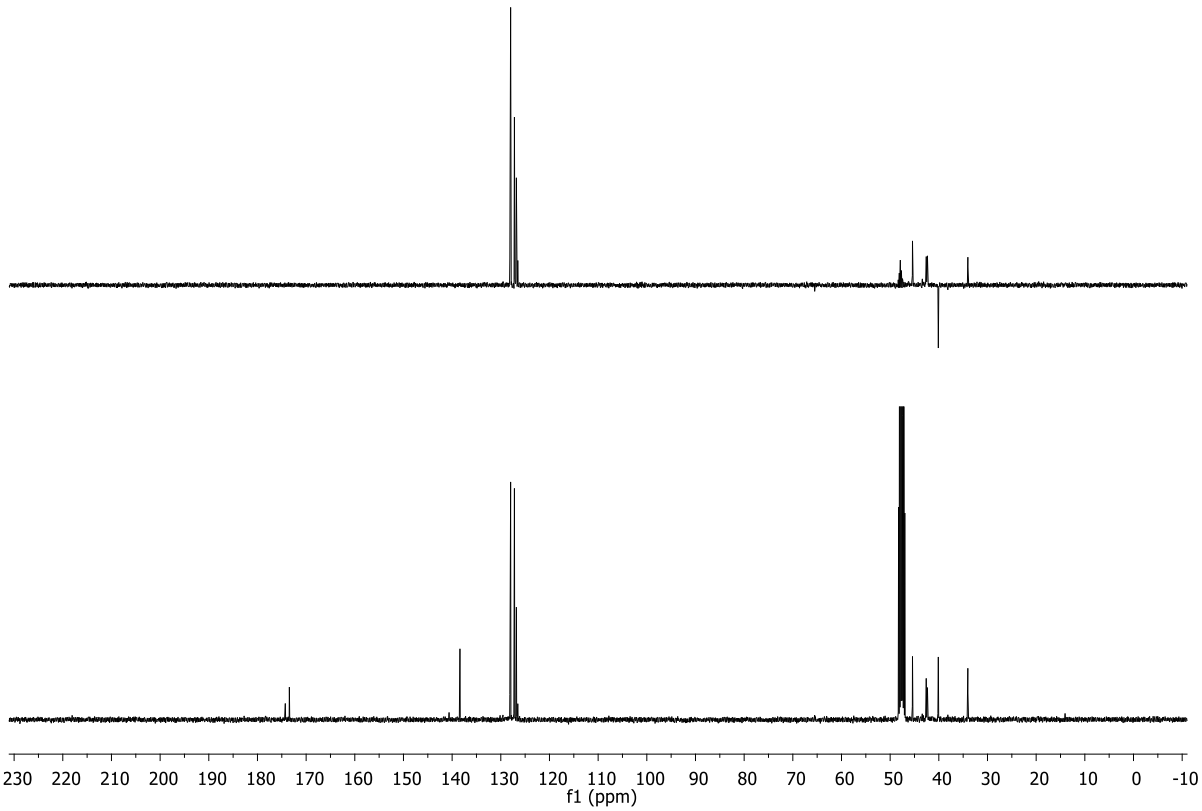

(±)-2-(Aminomethyl)-4-phenylcyclobutane-1-carboxylic acid (202)

(400 MHz, MeOD)

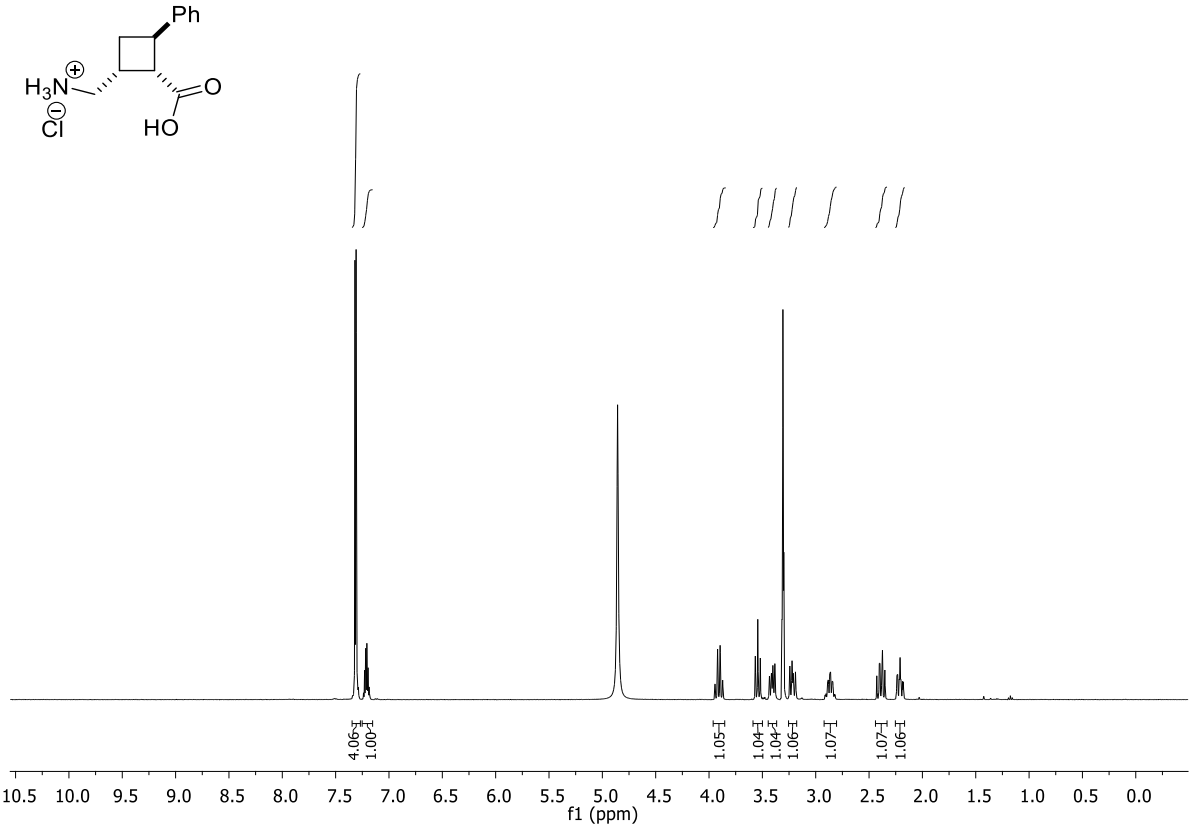

(101 MHz, MeOD)

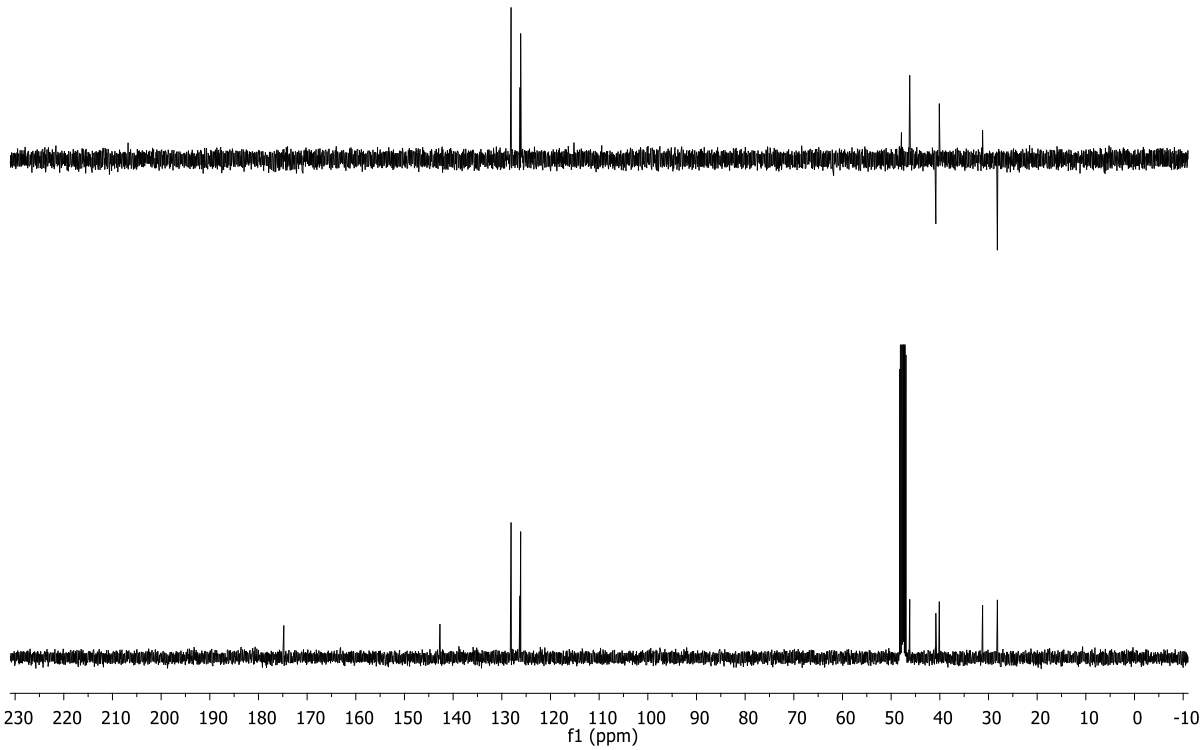

(±)-2-(((*tert*-Butoxycarbonyl)amino)methyl)-3,4-diphenylcyclobutane-1-carboxylic acid (225) (300 MHz, $CDCl_3$)

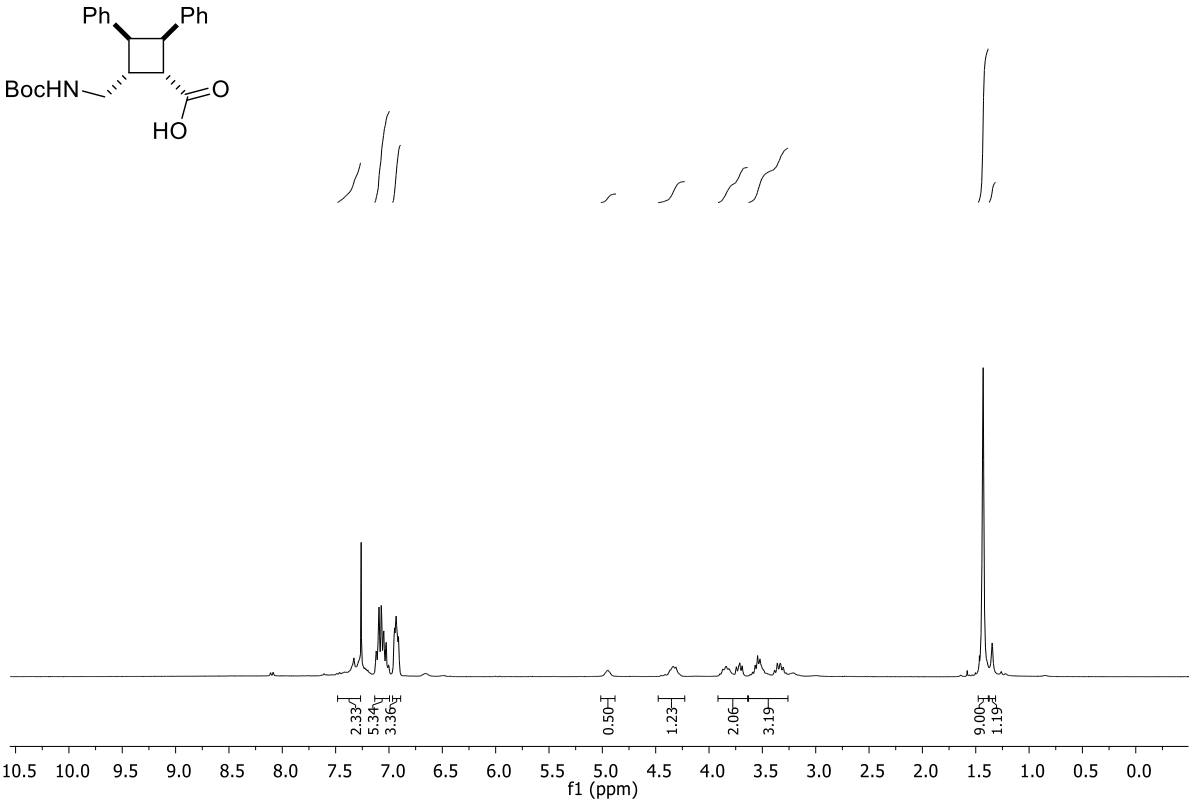

(75 MHz, MeOD)

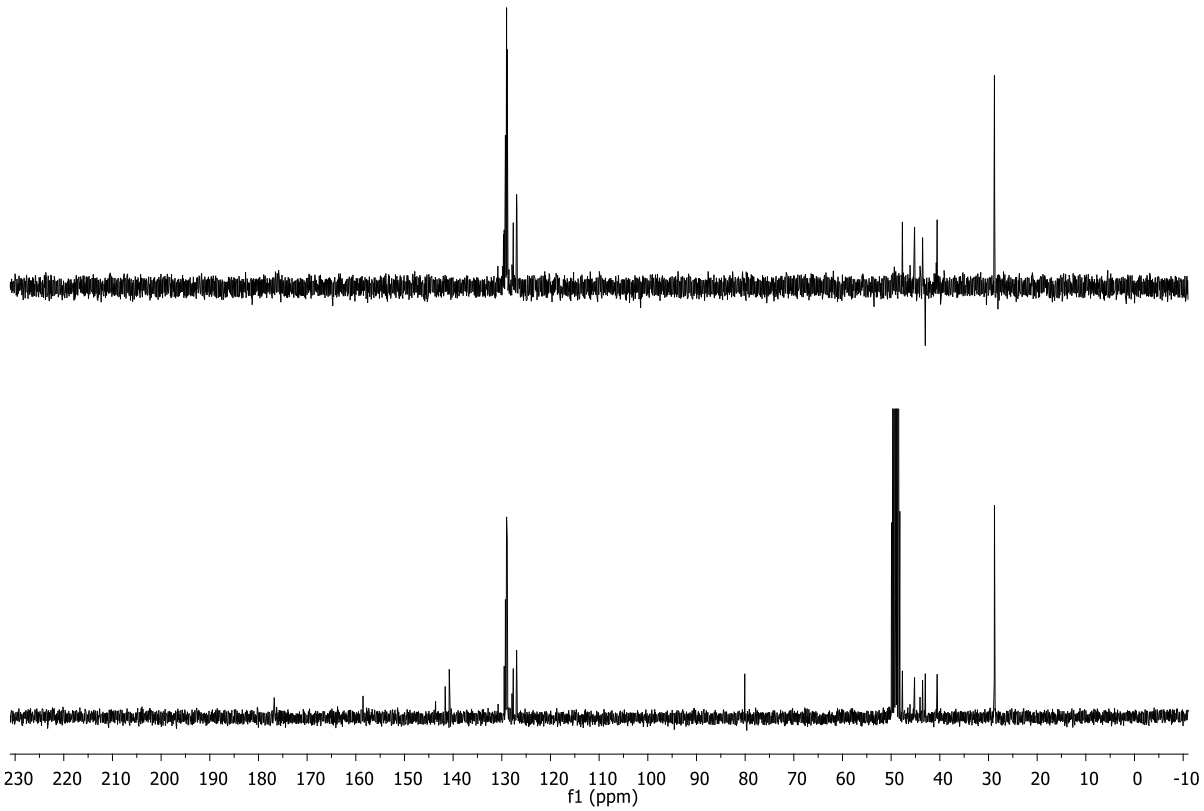

(±)-2-(((*tert*-Butoxycarbonyl)amino)methyl)-3-phenylcyclobutane-1-carboxylic acid ((±)-226) (400 MHz, $CDCl_3$)

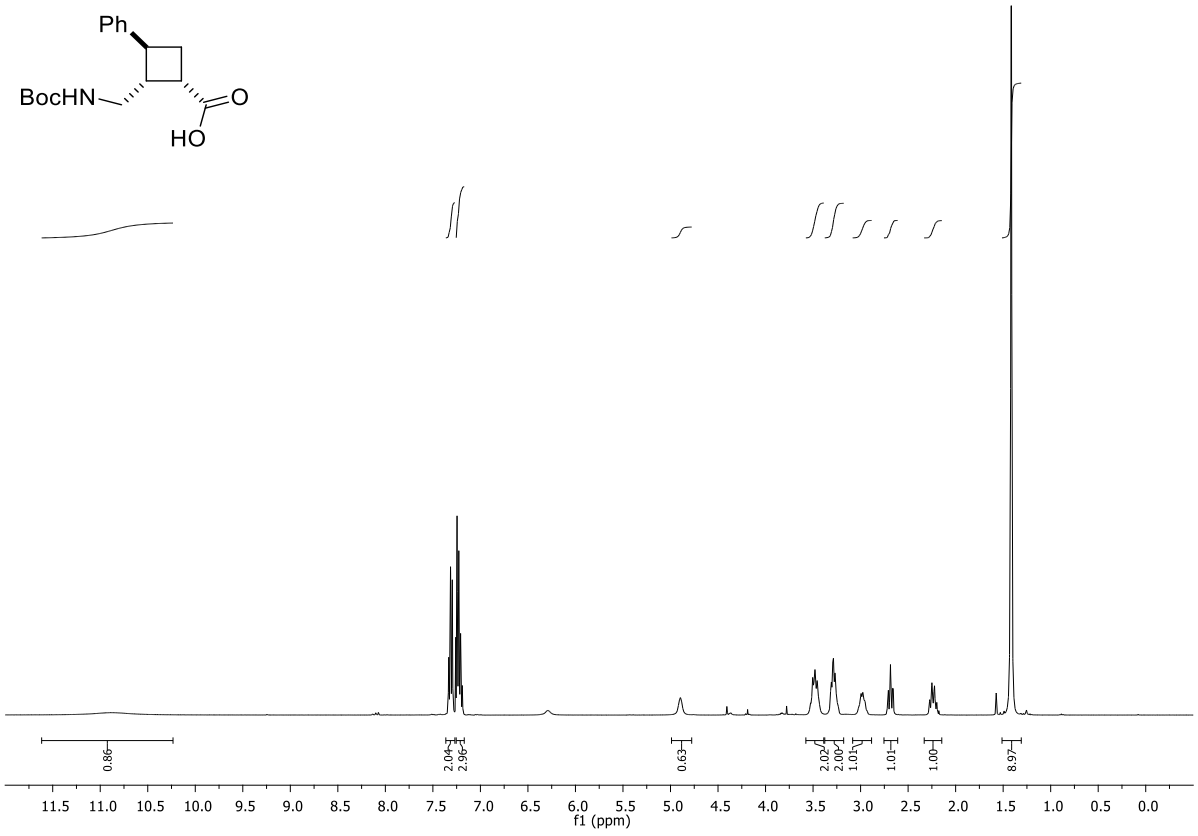

(101 MHz, $CDCl_3$)

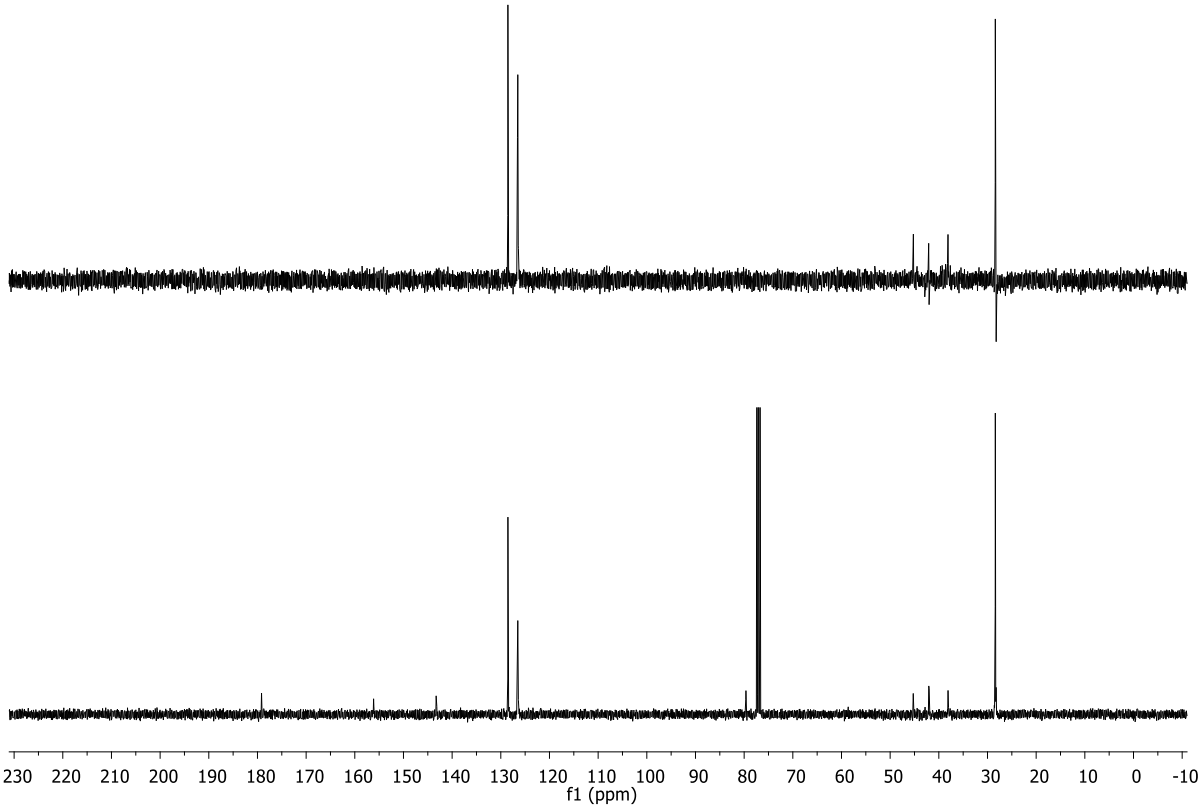

(±)-*cis*-2-(((*tert*-Butoxycarbonyl)amino)methyl)-3-phenylcyclobutane-1-carboxylic acid (227) (300 MHz, MeOD)

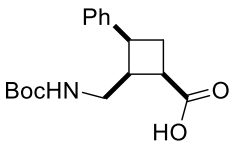

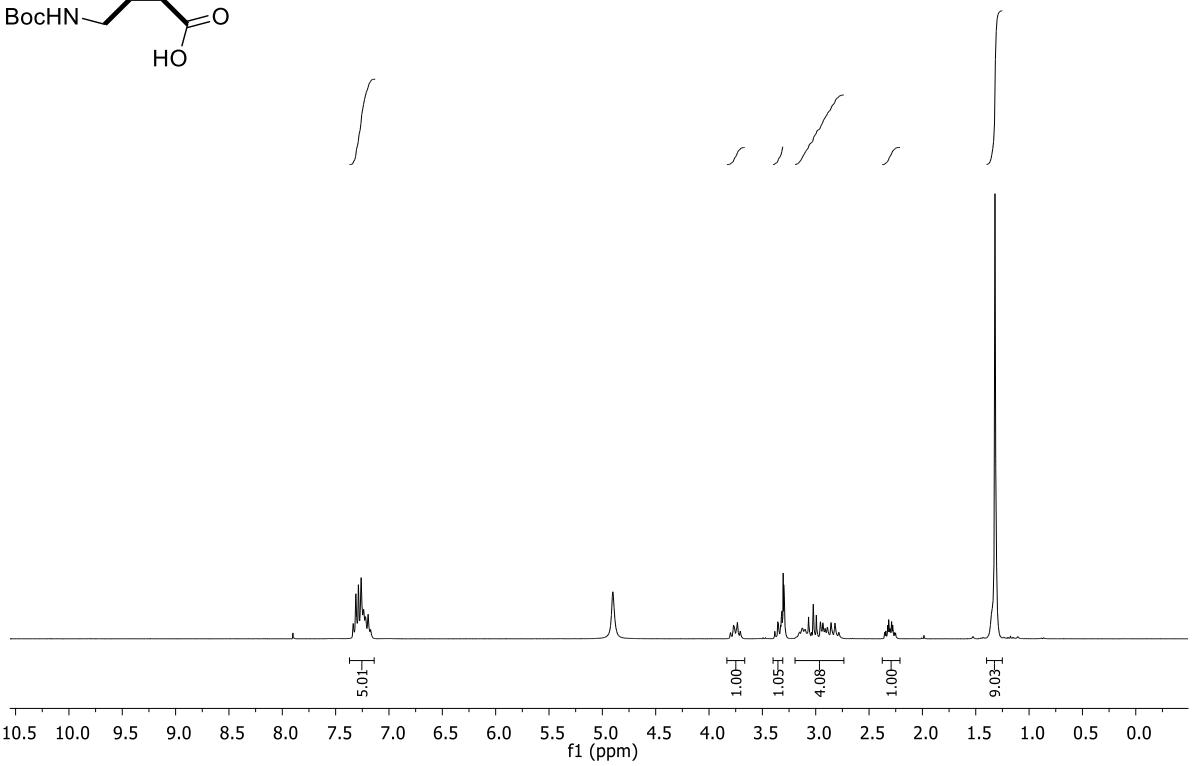

(101 MHz, MeOD)

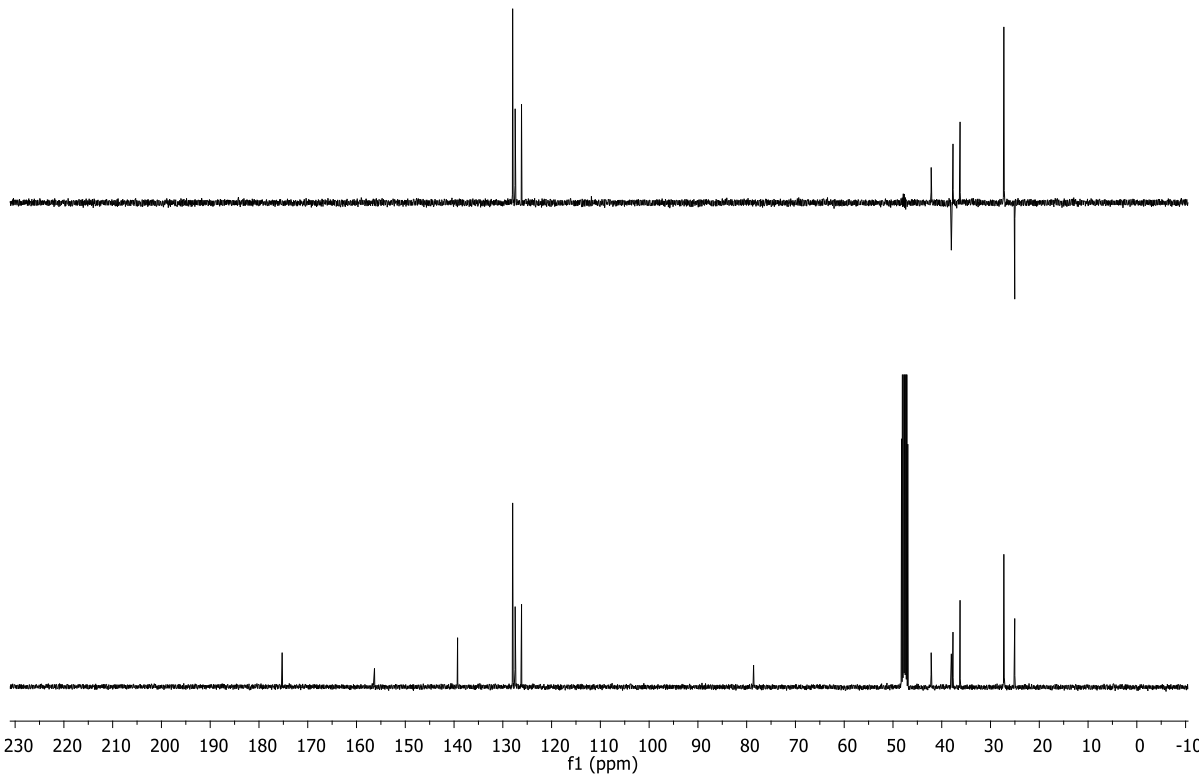

***tert*-Butyl(((1*R*,2*S*,4*S*)-2-((4*S*,5*R*)-4-methyl-2-oxo-5-phenyloxazolidine-3-carbonyl)-4-phenylcyclobutyl)methyl)carbamate (237a)** (400 MHz, $CDCl_3$)

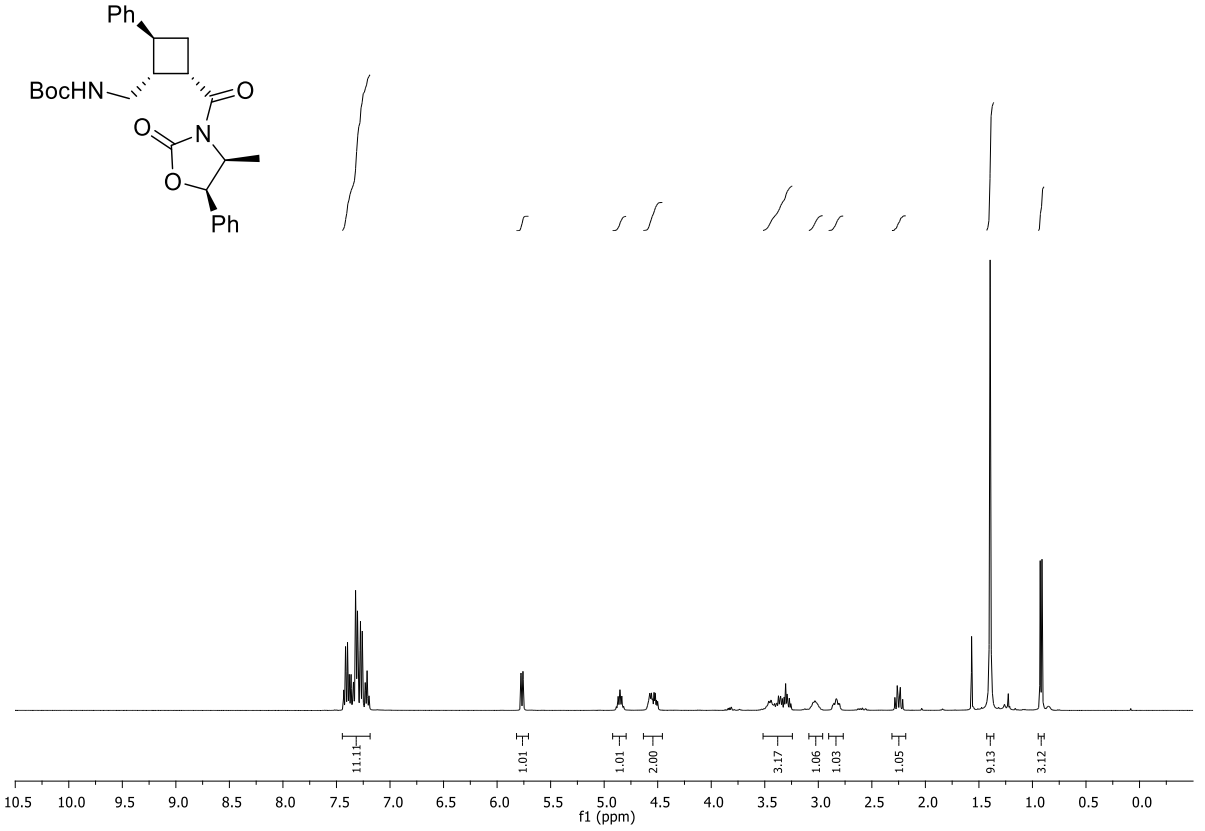

(101 MHz, $CDCl_3$)

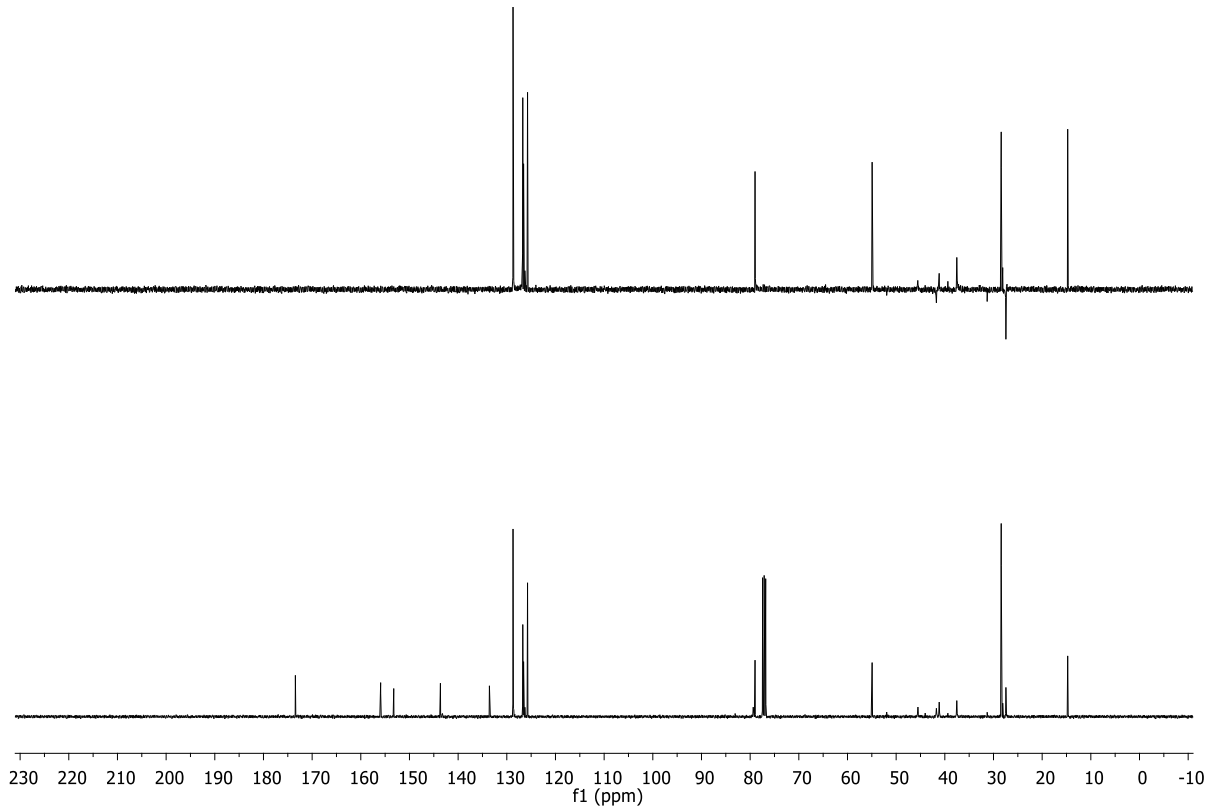

***tert*-Butyl(((1*S*,2*R*,4*R*)-2-((4*S*,5*R*)-4-methyl-2-oxo-5-phenyloxazolidine-3-carbonyl)-4-phenylcyclobutyl)methyl)carbamate (237b)** (300 MHz, $CDCl_3$)

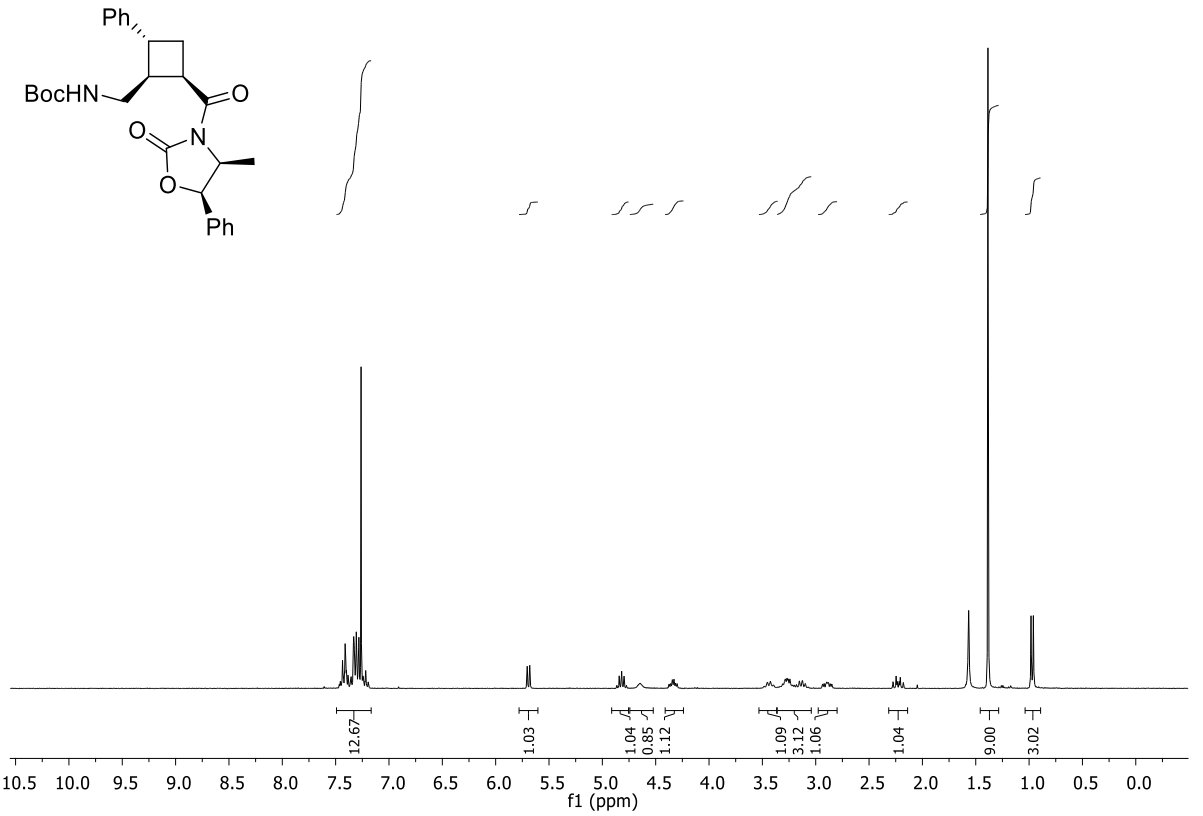

(101 MHz, $CDCl_3$)

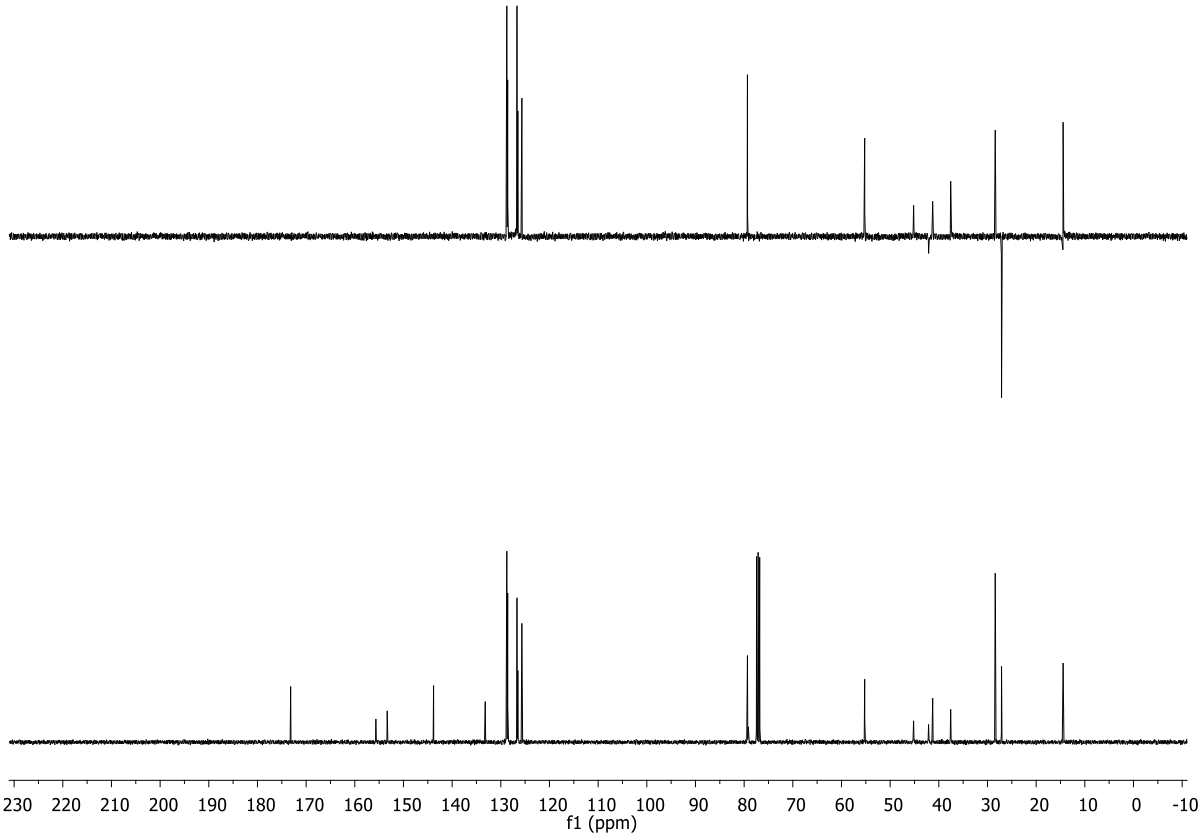

(±)-2-(((((9*H*-Fluoren-9-yl)methoxy)carbonyl)amino)methyl)-3-phenylcyclobutane-1-carboxylic acid ((±)-264) (400 MHz)

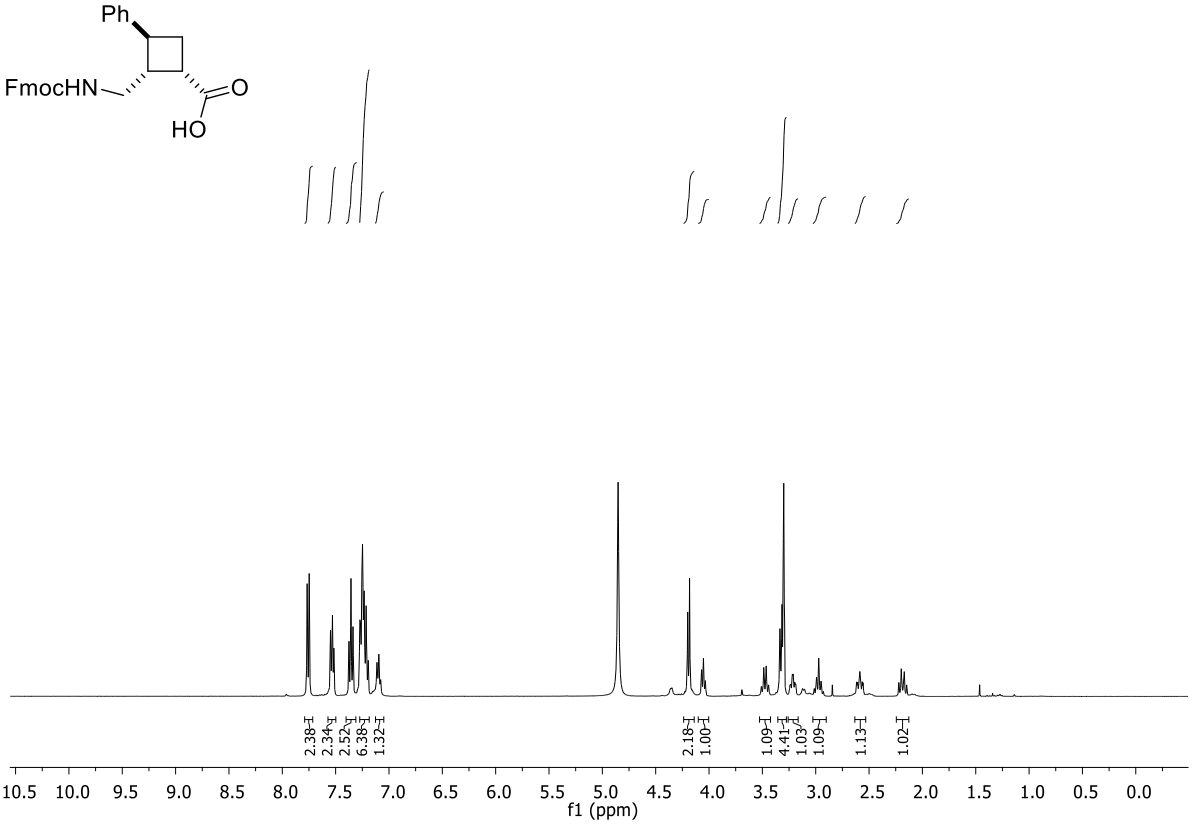

(101 MHz, MeOD)

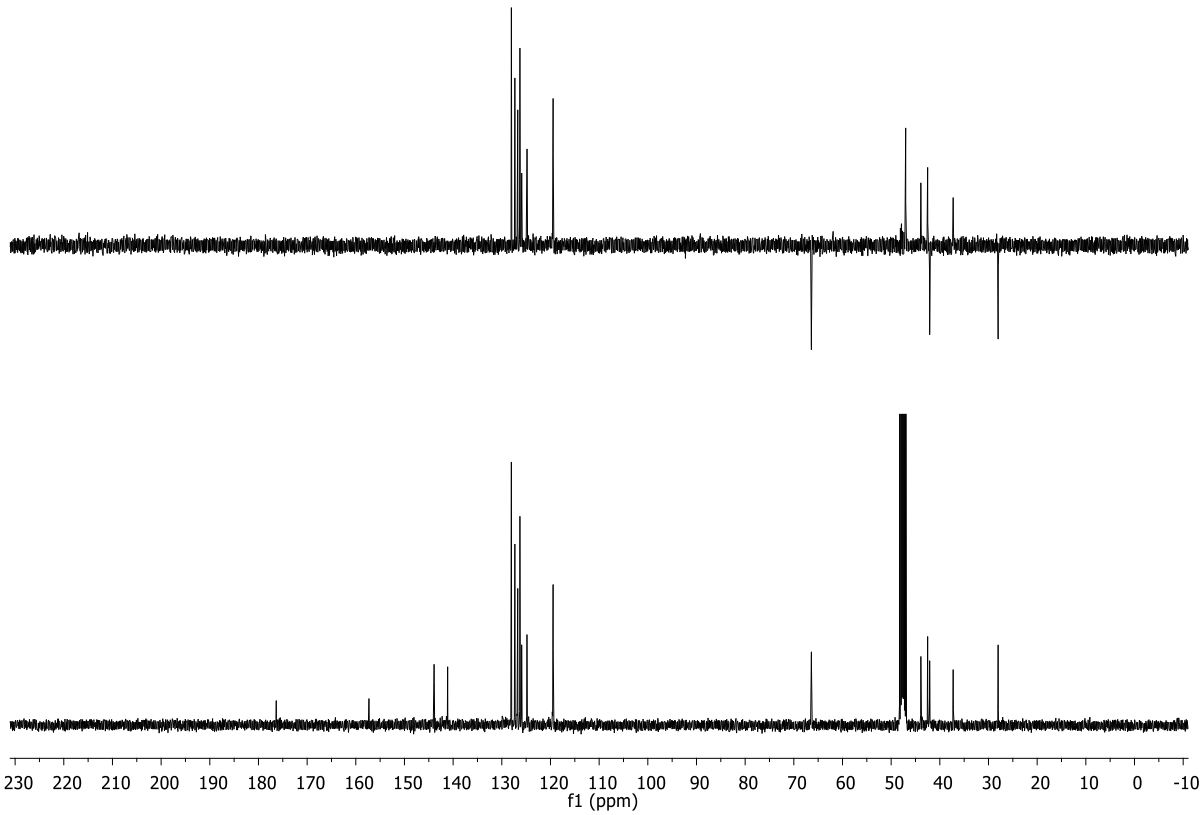

(1*R*,5*S*,6*R*)-6-Phenyl-3-azabicyclo[3.2.0]heptan-2-one ((1*R*,5*S*,6*R*)-158u)

(300 MHz, $CDCl_3$)

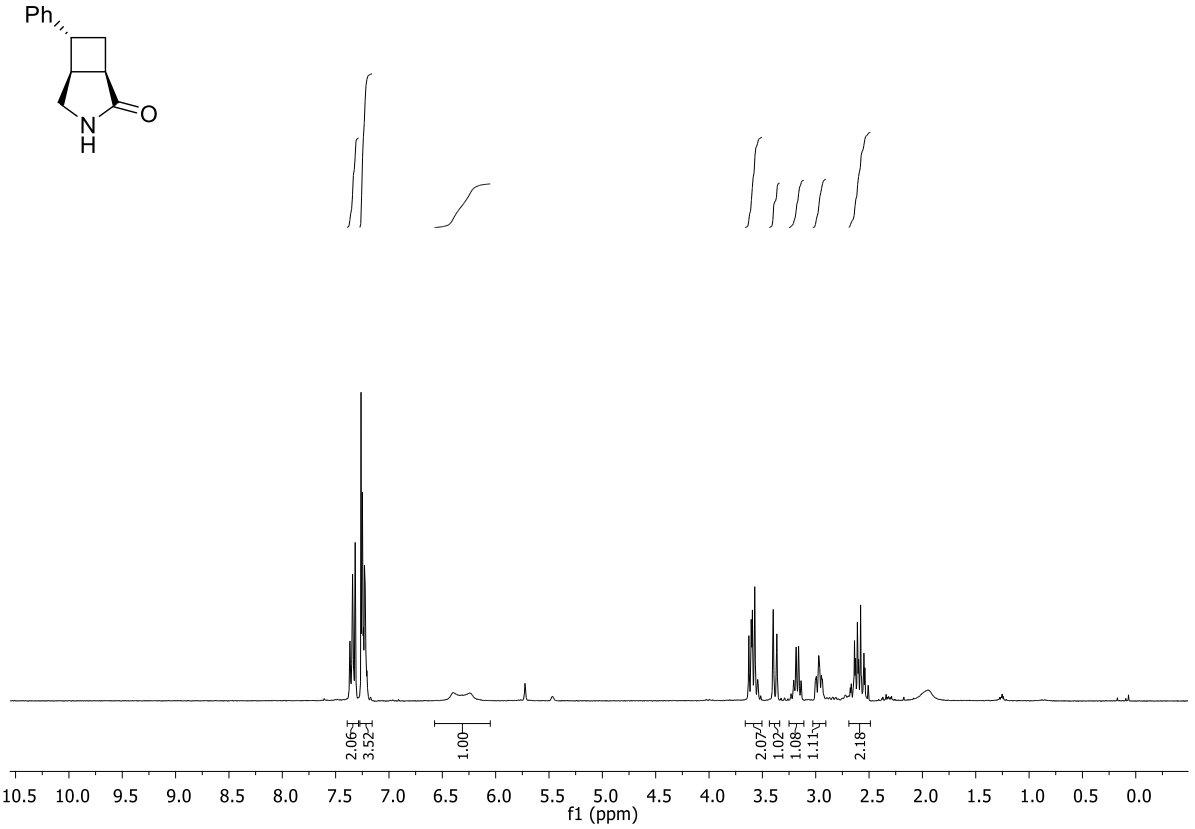

(75 MHz, $CDCl_3$)

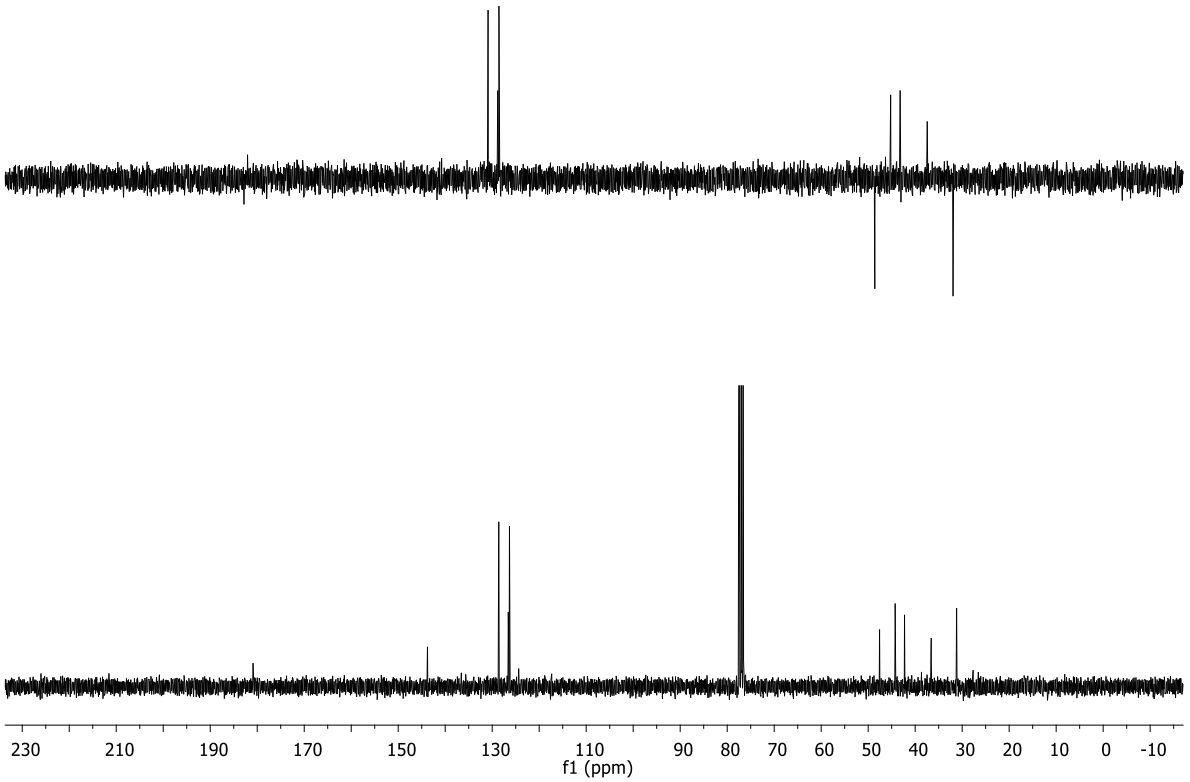

(±)-4-Phenethylpyrrolidin-2-one ((±)-215)

(300 MHz, $CDCl_3$)

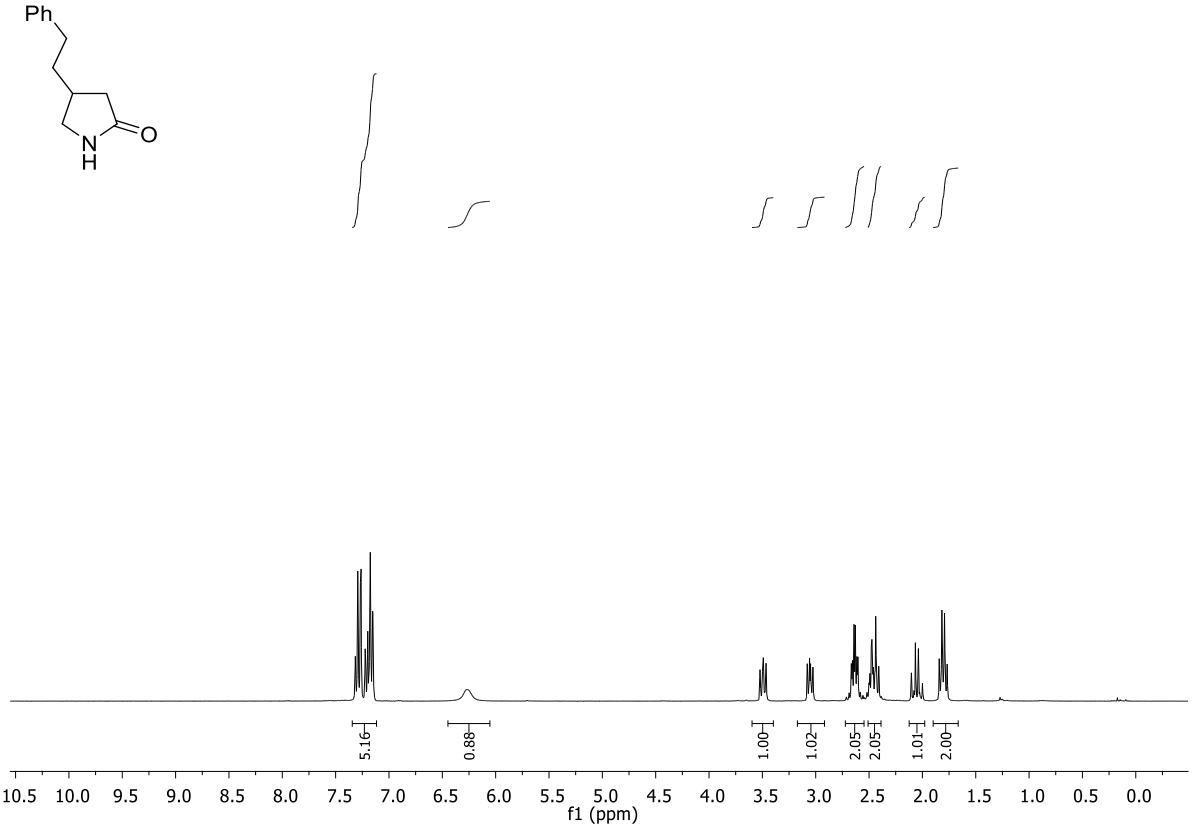

(101 MHz, $CDCl_3$)

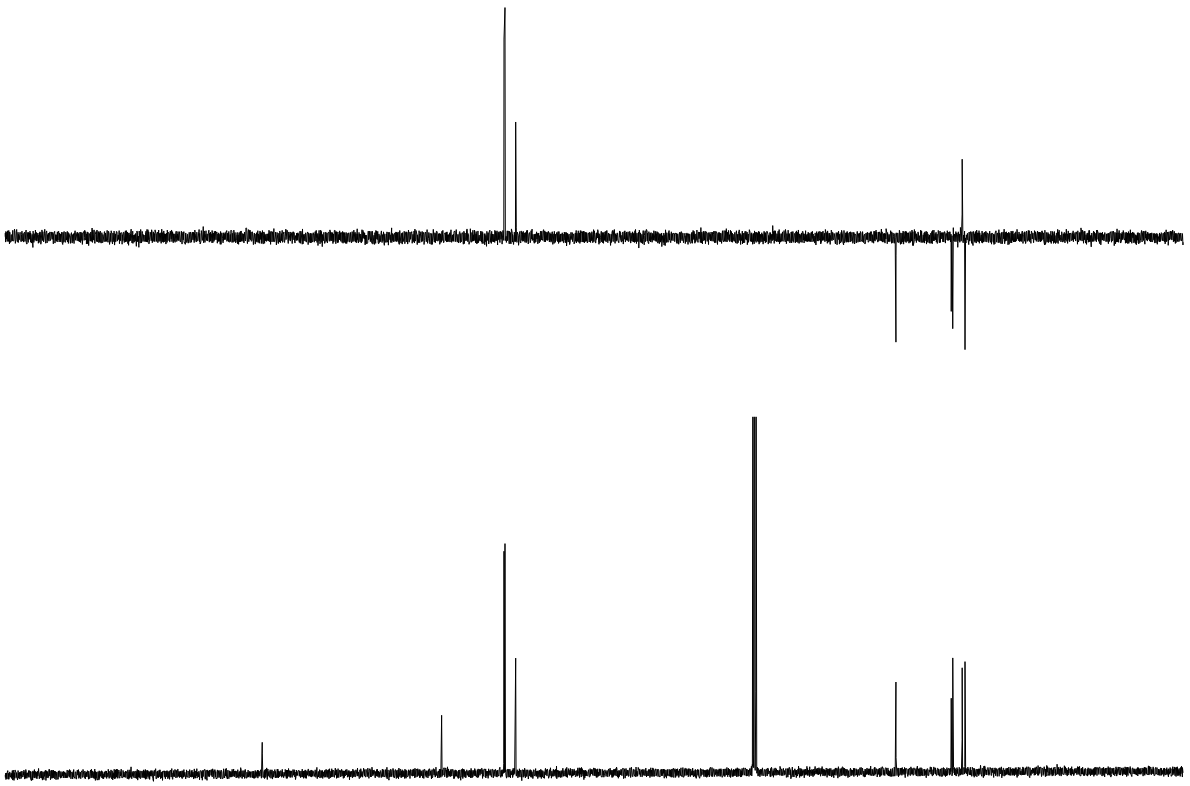

(±)-3-(Aminomethyl)-5-phenylpentanoic acid hydrochloride ((±)-257)

(300 MHz, MeOD)

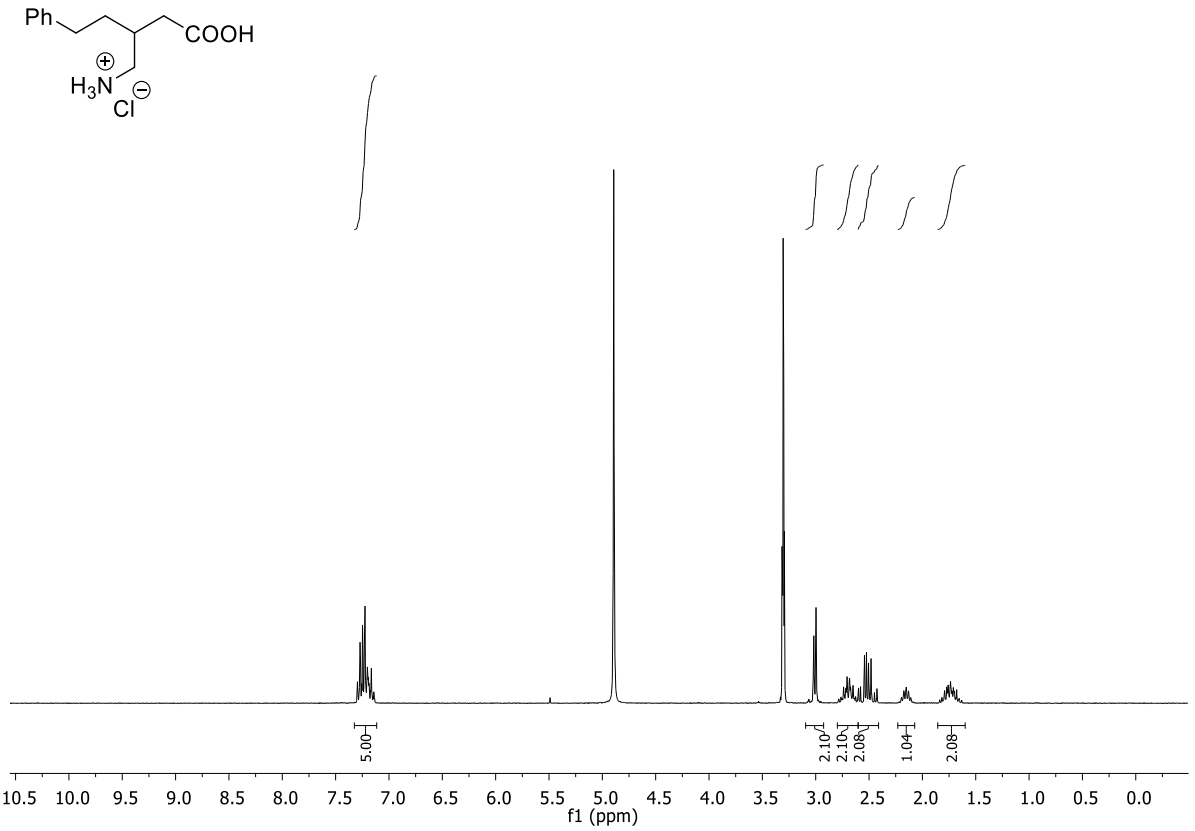

(101 MHz, MeOD)

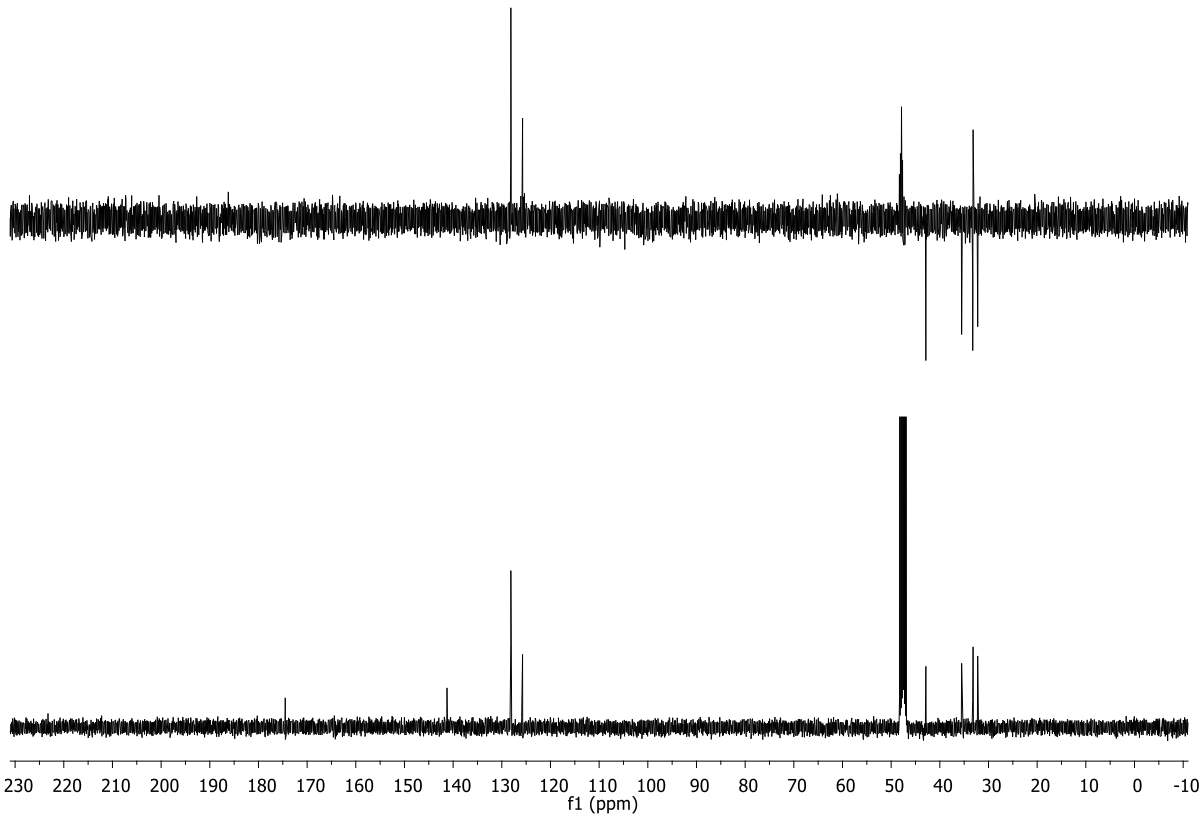

2 HPLC-chromatograms

(±)-(*E*)-3-Phenyl-*N*-(1-phenylethyl)prop-2-en-1-amine

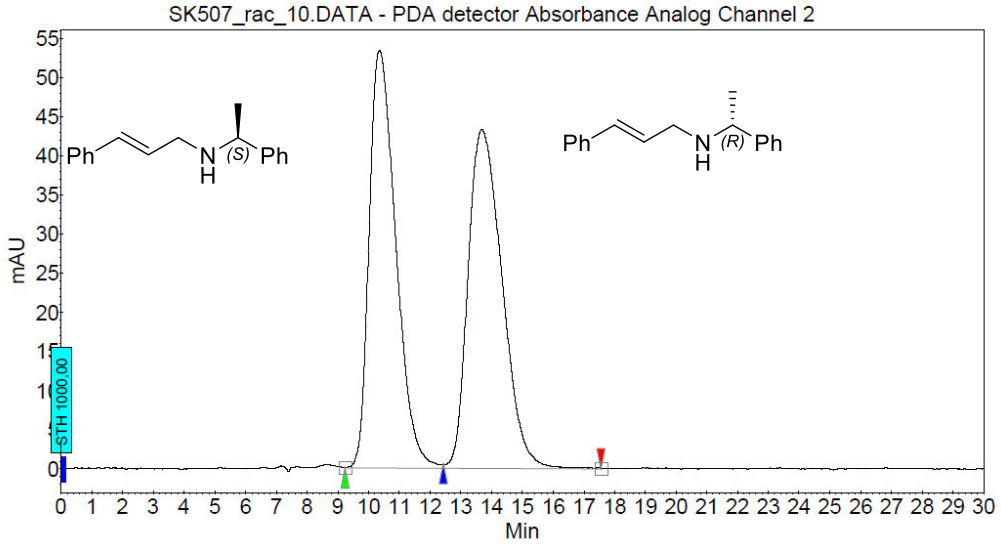

Peak Results :

Index	Name	Time [Min]	Quantity [% Area]	Height [mAU]	Area [mAU.Min]	Area % [%]
1	UNKNOWN	10.35	49.13	53.4	53.8	49.125
2	UNKNOWN	13.68	50.87	43.4	55.7	50.875
Total			100.00	96.8	109.5	100.000

(*S*,*E*)-3-Phenyl-*N*-(1-phenylethyl)prop-2-en-1-amine (248)

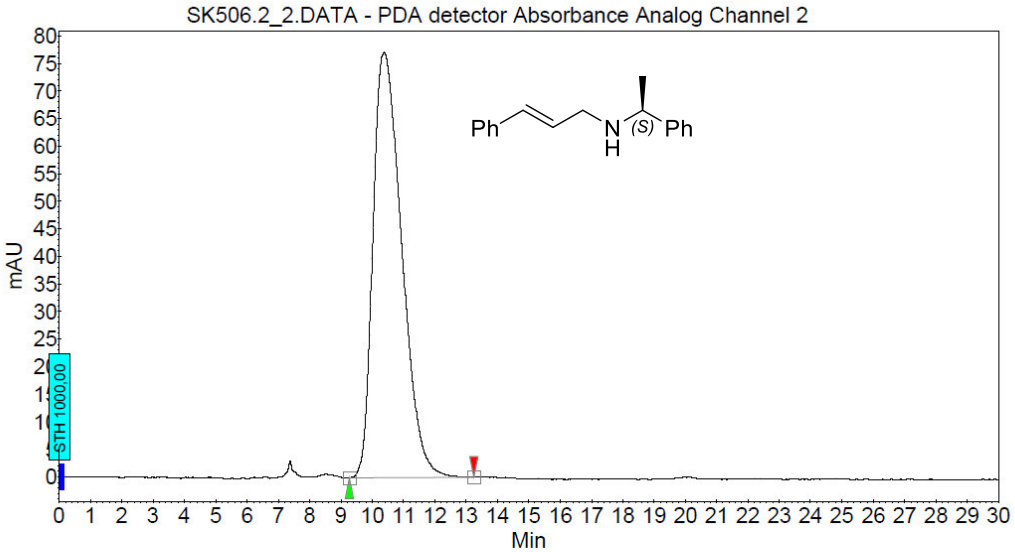

Peak Results :

Index	Name	Time [Min]	Quantity [% Area]	Height [mAU]	Area [mAU.Min]	Area % [%]
1	UNKNOWN	10.37	100.00	77.2	82.1	100.000
Total			100.00	77.2	82.1	100.000

(±)-*N*-Cinnamyl-*N*-(1-phenylethyl)acrylamide

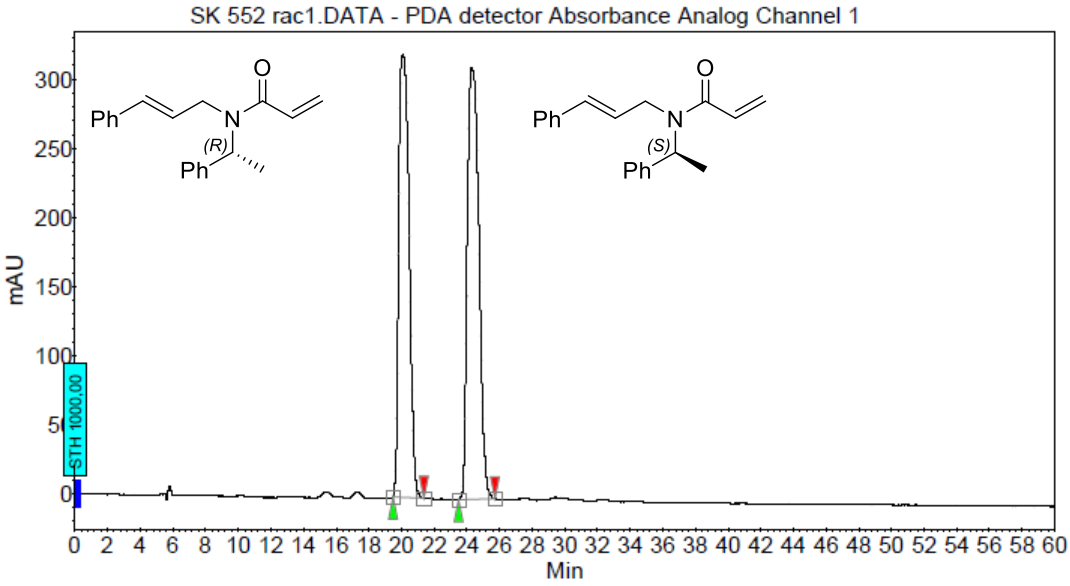

Peak Results :

Index	Name	Time [Min]	Quantity [% Area]	Height [mAU]	Area [mAU.Min]	Area % [%]
1	UNKNOWN	20,08	47,94	320,8	237,2	47,938
2	UNKNOWN	24,32	52,06	312,8	257,6	52,062
Total			100,00	633,6	494,7	100,000

(*S*)-*N*-Cinnamyl-*N*-(1-phenylethyl)acrylamide (153x)

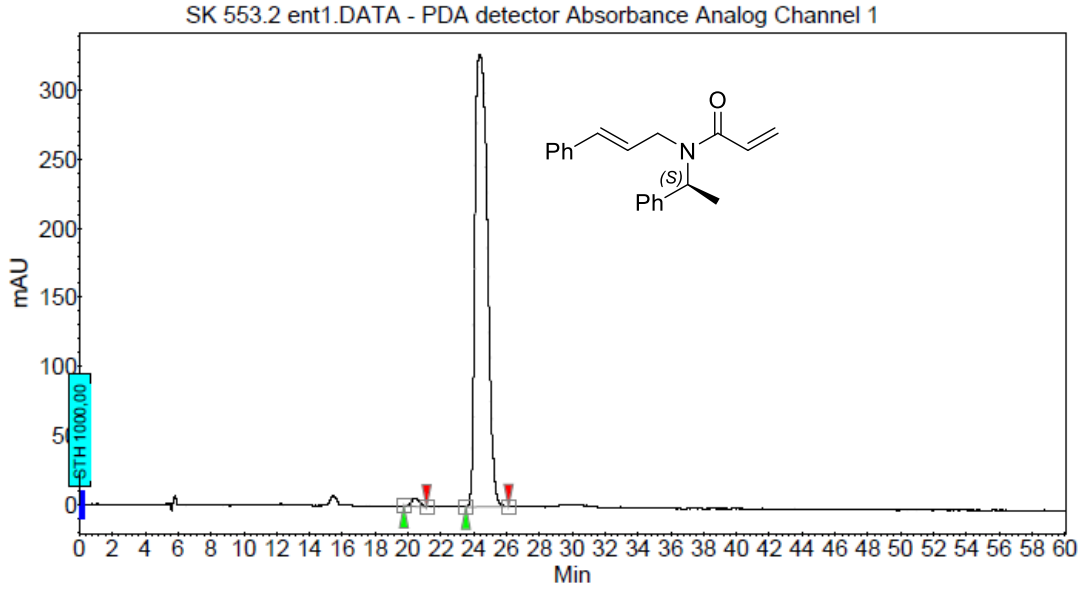

Peak Results :

Index	Name	Time [Min]	Quantity [% Area]	Height [mAU]	Area [mAU.Min]	Area % [%]
2	UNKNOWN	20,47	1,19	6,2	3,4	1,188
1	UNKNOWN	24,38	98,81	327,6	286,8	98,812
Total			100,00	333,8	290,3	100,000

(±)-*N*-Allyl-*N*-(1-phenylethyl)cinnamamide

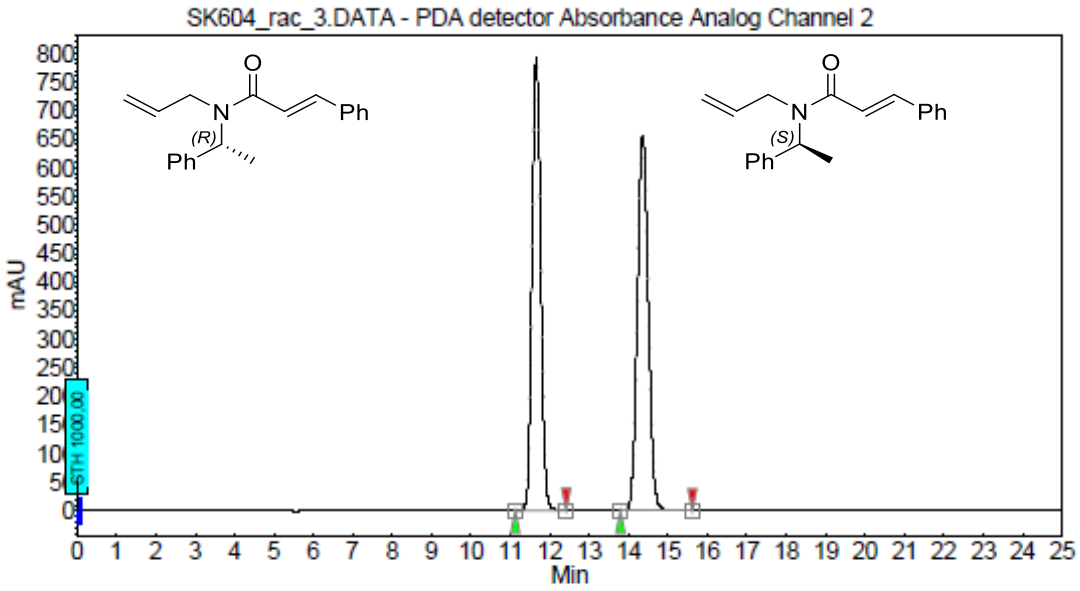

Peak Results :

Index	Name	Time [Min]	Quantity [% Area]	Height [mAU]	Area [mAU.Min]	Area % [%]
1	UNKNOWN	11,66	49,08	792,2	204,3	49,080
2	UNKNOWN	14,36	50,92	655,1	212,0	50,920
Total			100,00	1447,3	416,3	100,000

(*S*)-*N*-Allyl-*N*-(1-phenylethyl)cinnamamide (153y)

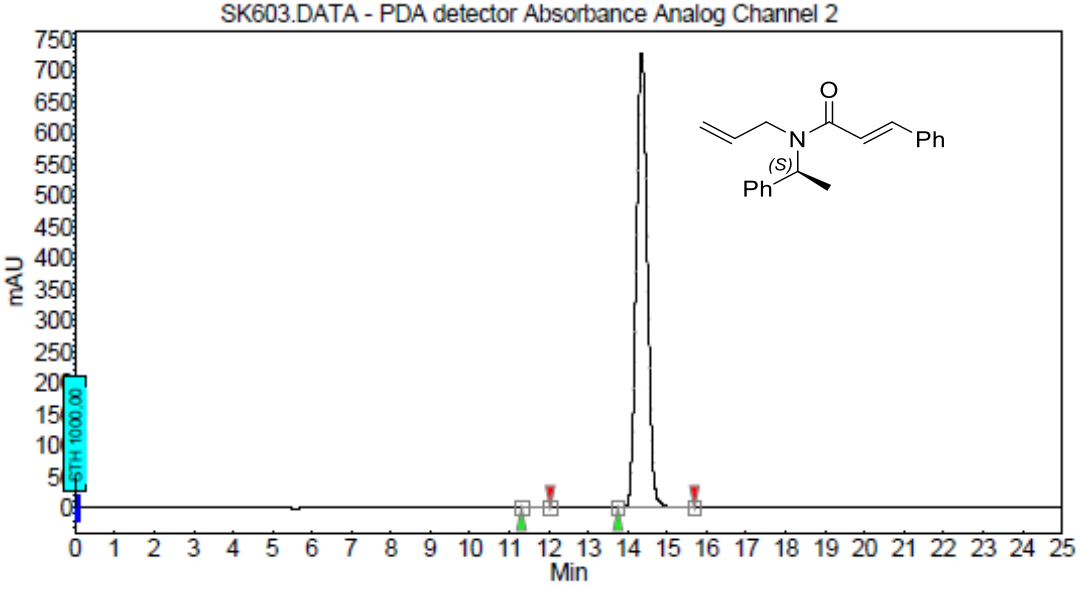

Peak Results :

Index	Name	Time [Min]	Quantity [% Area]	Height [mAU]	Area [mAU.Min]	Area % [%]
1	UNKNOWN	11,66	0,19	1,8	0,5	0,189
2	UNKNOWN	14,35	99,81	728,0	238,9	99,811
Total			100,00	729,9	239,3	100,000

(±)-6-Phenyl-3-((*S*)-1-phenylethyl)-3-azabicyclo[3.2.0]heptan-2-one

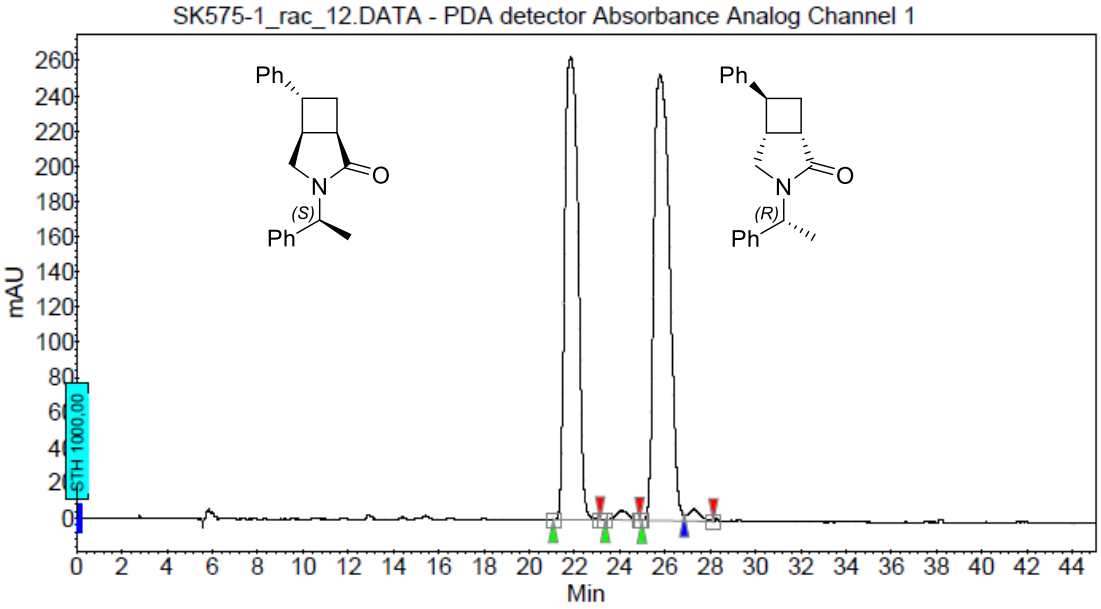

Peak Results :

Index	Name	Time [Min]	Quantity [% Area]	Height [mAU]	Area [mAU.Min]	Area % [%]
1	UNKNOWN	21,83	45,84	262,8	178,2	45,843
2	UNKNOWN	24,10	0,81	5,2	3,2	0,810
3	UNKNOWN	25,78	52,27	253,3	203,2	52,275
4	UNKNOWN	27,30	1,07	6,6	4,2	1,072
Total			100,00	527,9	388,8	100,000

(1*R*,5*S*,6*R*)-6-Phenyl-3-((*S*)-1-phenylethyl)-3-azabicyclo[3.2.0]heptan-2-one (158va)

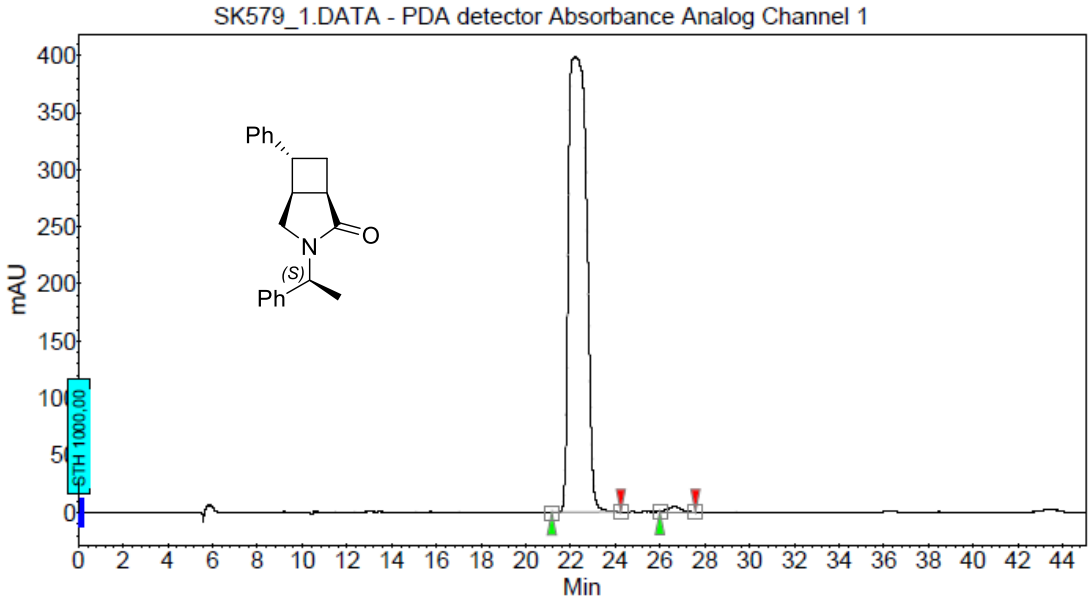

Peak Results :

Index	Name	Time [Min]	Quantity [% Area]	Height [mAU]	Area [mAU.Min]	Area % [%]
1	UNKNOWN	22,20	99,23	397,8	368,6	99,230
2	UNKNOWN	26,67	0,77	4,3	2,9	0,770
Total			100,00	402,1	371,4	100,000

(±)-6-Phenyl-3-((*S*)-1-phenylethyl)-3-azabicyclo[3.2.0]heptan-2-one

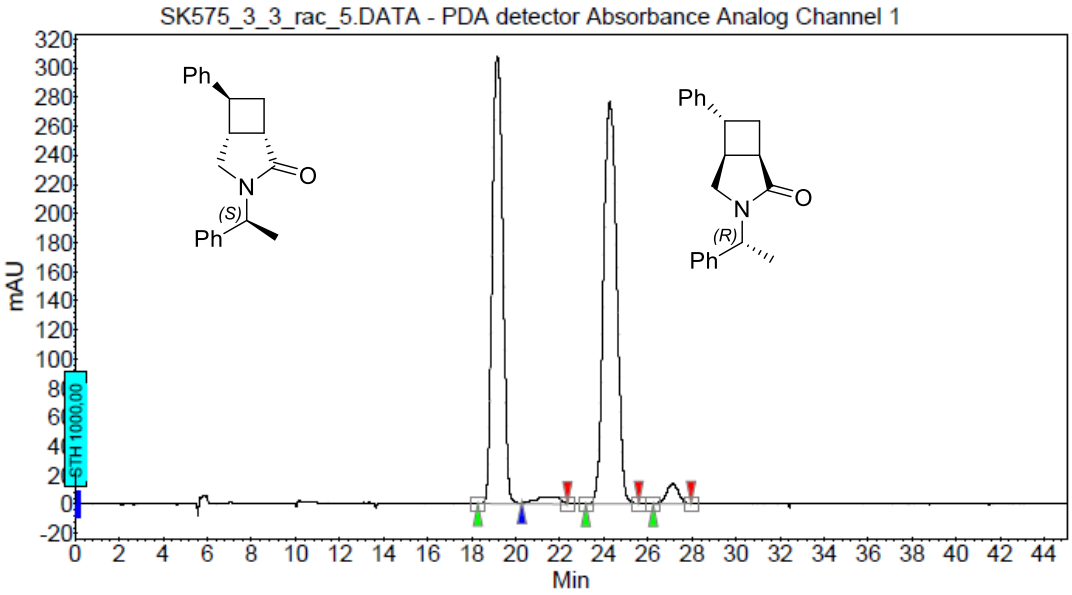

Peak Results :

Index	Name	Time [Min]	Quantity [% Area]	Height [mAU]	Area [mAU.Min]	Area % [%]
1	UNKNOWN	19,17	45,32	307,2	171,2	45,320
2	UNKNOWN	21,36	1,61	4,7	6,1	1,612
3	UNKNOWN	24,27	50,74	276,3	191,6	50,743
4	UNKNOWN	27,12	2,32	14,1	8,8	2,324
Total			100,00	602,2	377,7	100,000

(1*S*,5*R*,6*S*)-6-Phenyl-3-((*S*)-1-phenylethyl)-3-azabicyclo[3.2.0]heptan-2-one (158vb)

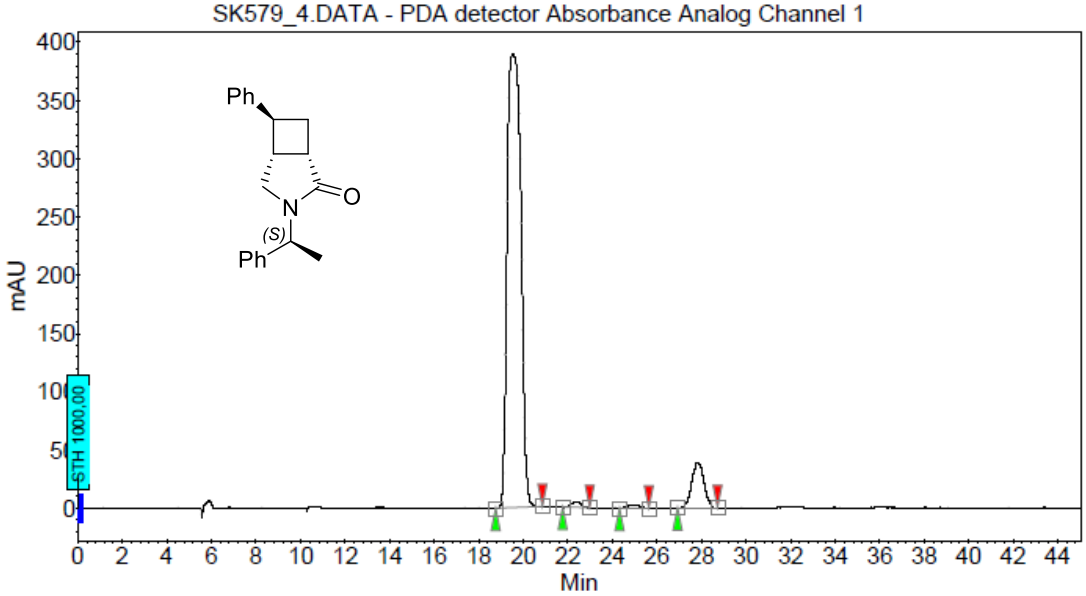

Peak Results :

Index	Name	Time [Min]	Quantity [% Area]	Height [mAU]	Area [mAU.Min]	Area % [%]
1	UNKNOWN	19,53	90,74	388,8	279,8	90,739
2	UNKNOWN	22,44	0,85	5,0	2,6	0,846
3	UNKNOWN	24,94	0,54	2,5	1,7	0,536
4	UNKNOWN	27,83	7,88	38,9	24,3	7,879
Total			100,00	435,3	308,4	100,000

(±)-7-Phenyl-3-((*S*)-1-phenylethyl)-3-azabicyclo[3.2.0]heptan-2-one

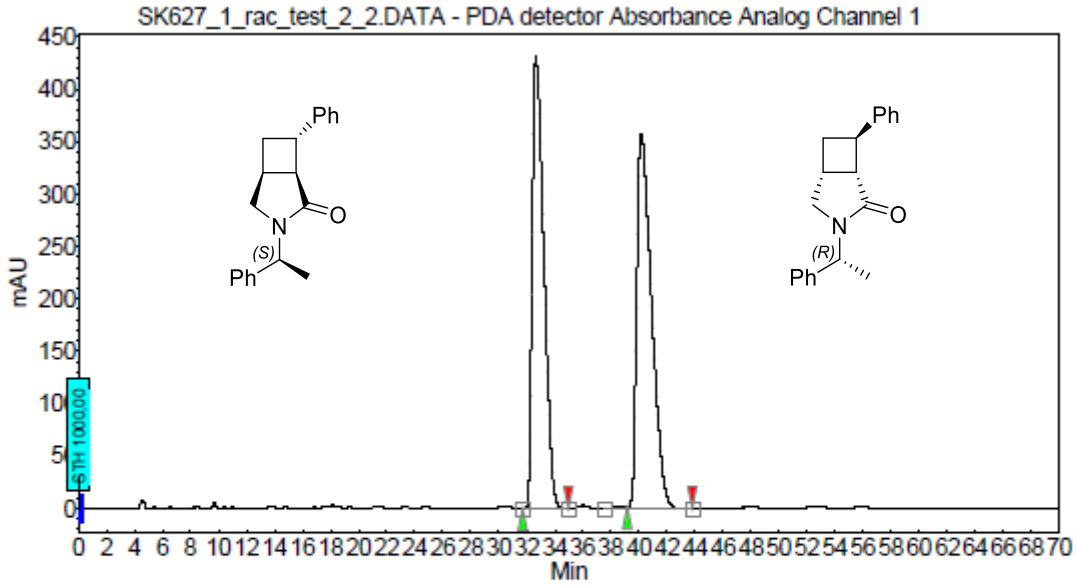

Peak Results :

Index	Name	Time [Min]	Quantity [% Area]	Height [mAU]	Area [mAU.Min]	Area % [%]
1	UNKNOWN	32,65	48,60	431,8	415,3	48,602
2	UNKNOWN	40,16	51,40	357,5	439,1	51,398
Total			100,00	789,4	854,4	100,000

(1*R*,5*S*,7*S*)-7-Phenyl-3-((*S*)-1-phenylethyl)-3-azabicyclo[3.2.0]heptan-2-one (158wa)

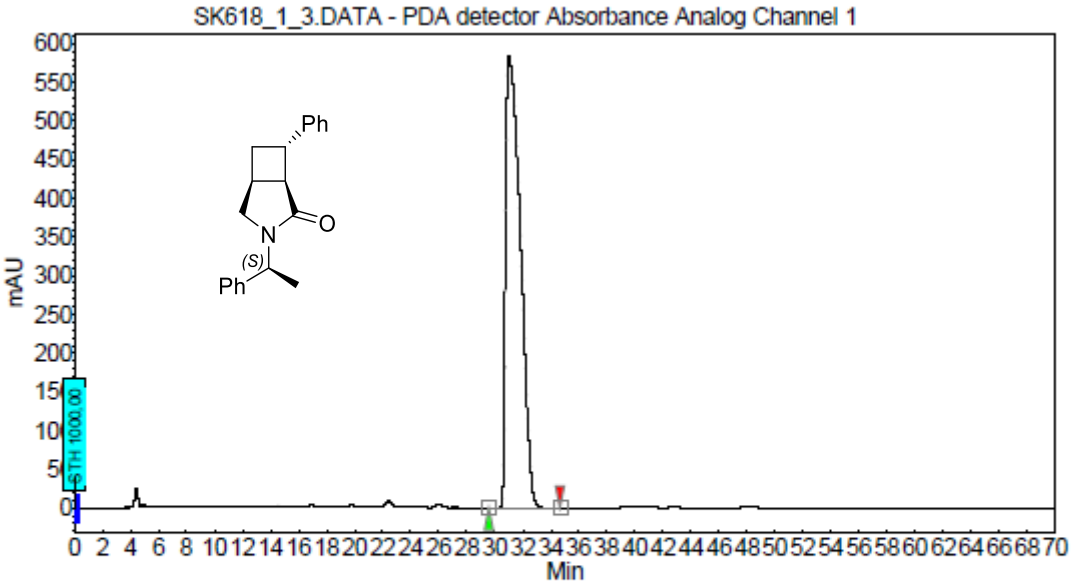

Peak Results :

Index	Name	Time [Min]	Quantity [% Area]	Height [mAU]	Area [mAU.Min]	Area % [%]
1	UNKNOWN	31,01	100,00	584,4	716,4	100,000
Total			100,00	584,4	716,4	100,000

(±)-7-Phenyl-3-((*S*)-1-phenylethyl)-3-azabicyclo[3.2.0]heptan-2-one

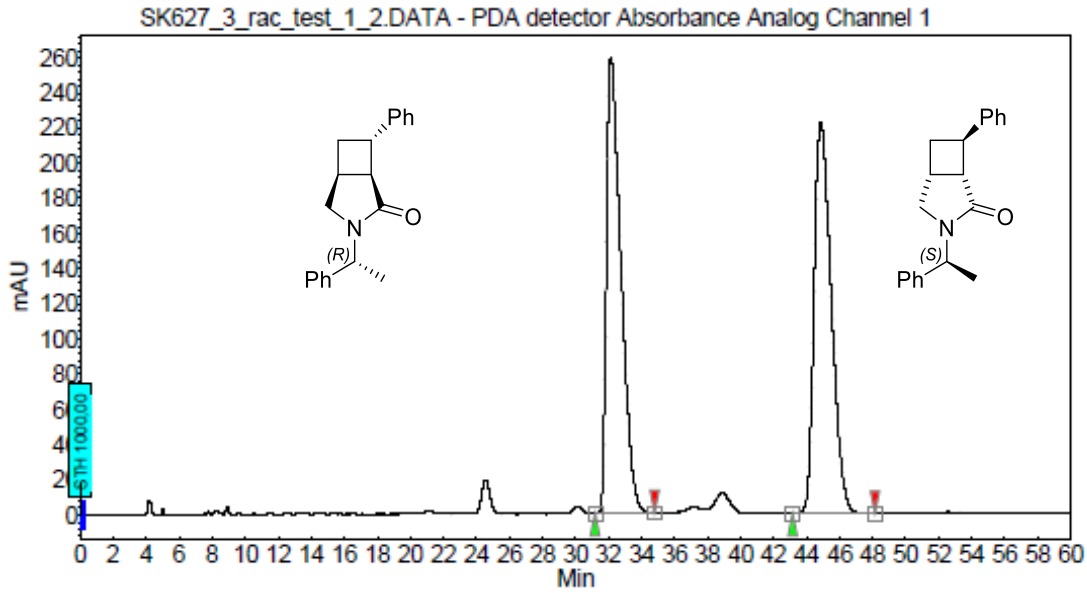

Peak Results :

Index	Name	Time [Min]	Quantity [% Area]	Height [mAU]	Area [mAU.Min]	Area % [%]
1	UNKNOWN	32,14	49,68	259,1	264,9	49,685
2	UNKNOWN	44,85	50,32	221,8	268,3	50,315
Total			100,00	480,9	533,2	100,000

(1*S*,5*R*,7*R*)-7-Phenyl-3-((*S*)-1-phenylethyl)-3-azabicyclo[3.2.0]heptan-2-one (158wb)

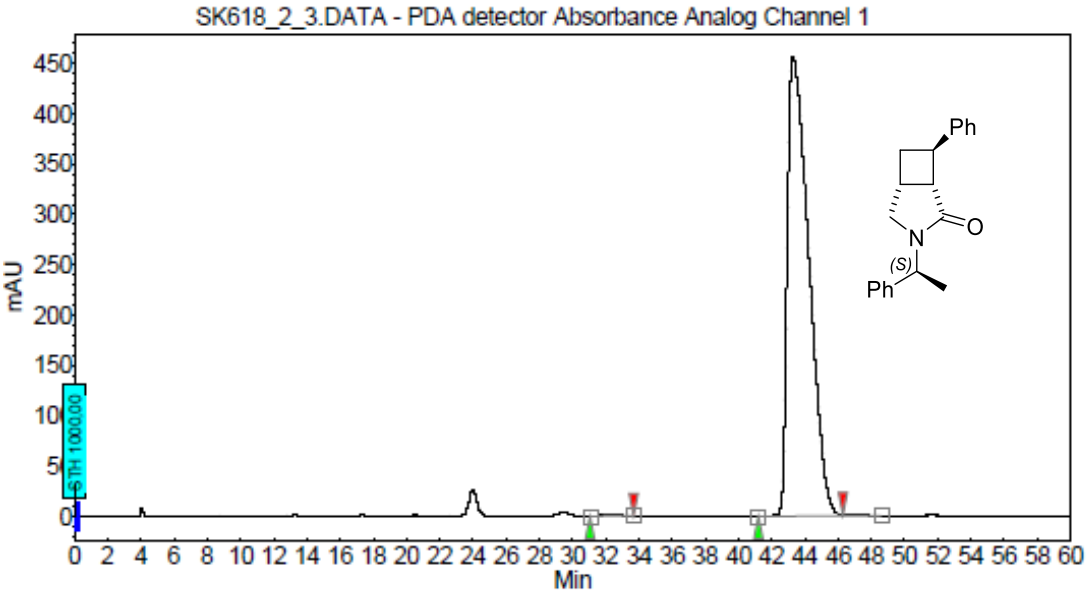

Peak Results :

Index	Name	Time [Min]	Quantity [% Area]	Height [mAU]	Area [mAU.Min]	Area % [%]
1	UNKNOWN	32,15	0,30	1,9	2,1	0,301
2	UNKNOWN	43,29	99,70	455,9	680,9	99,699
Total			100,00	457,8	683,0	100,000

(±)-*tert*-Butyl-2-oxo-6-phenyl-3-azabicyclo[3.2.0]heptane-3-carboxylate ((±)-158ka)

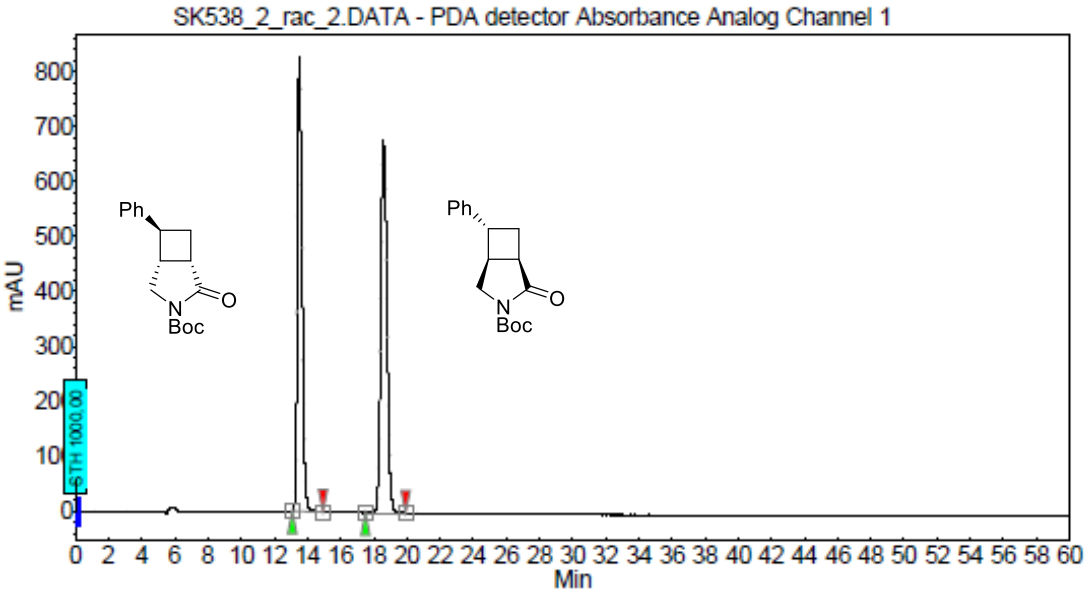

Peak Results :

Index	Name	Time [Min]	Quantity [% Area]	Height [mAU]	Area [mAU.Min]	Area % [%]
1	UNKNOWN	13,51	48,05	826,3	274,4	48,051
2	UNKNOWN	18,59	51,95	678,4	296,6	51,949
Total			100,00	1504,7	571,0	100,000

***tert*-Butyl-(1*S*,5*R*,6*S*)-2-oxo-6-phenyl-3-azabicyclo[3.2.0]heptane-3-carboxylate ((1*S*,5*R*,6*S*)-158ka)**

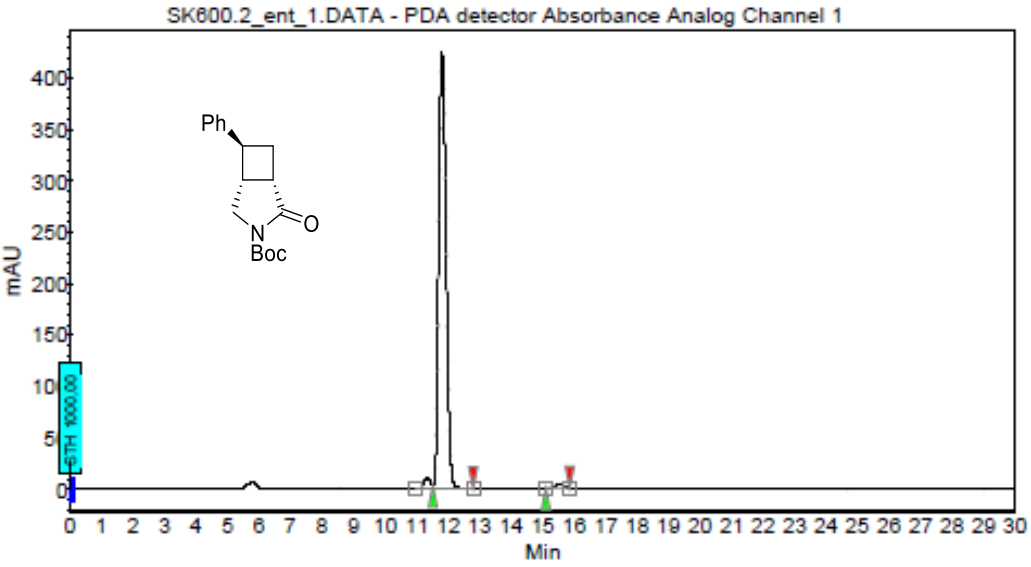

Peak Results :

Index	Name	Time [Min]	Quantity [% Area]	Height [mAU]	Area [mAU.Min]	Area % [%]
2	UNKNOWN	11,81	98,96	424,4	115,2	98,958
1	UNKNOWN	15,52	1,04	3,6	1,2	1,042
Total			100,00	428,0	116,5	100,000

***tert*-Butyl-(1*R*,5*S*,6*R*)-2-oxo-6-phenyl-3-azabicyclo[3.2.0]heptane-3-carboxylate ((1*R*,5*S*,6*R*)-158ka)**

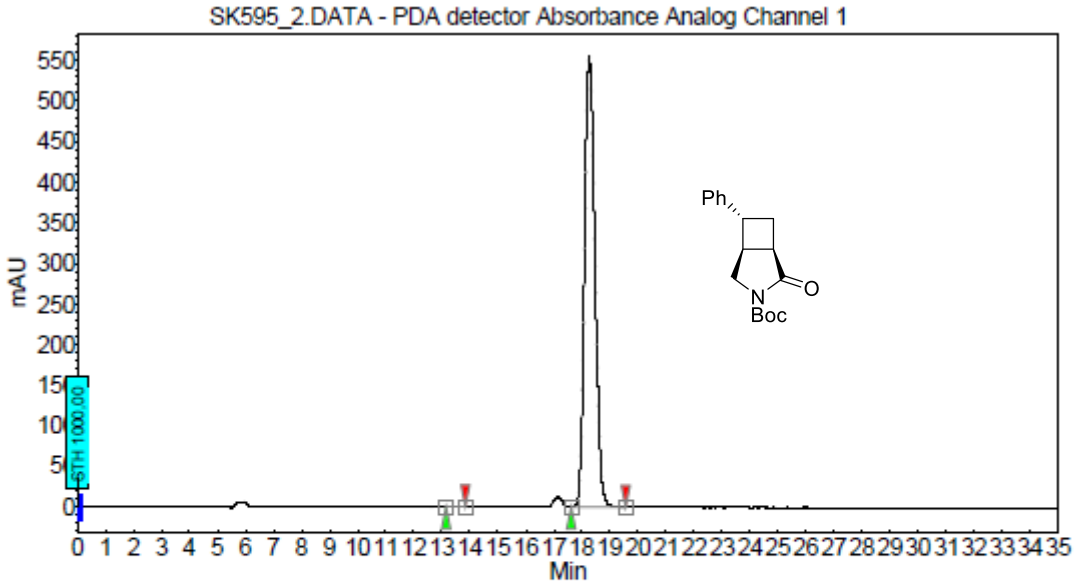

Peak Results :

Index	Name	Time [Min]	Quantity [% Area]	Height [mAU]	Area [mAU.Min]	Area % [%]
1	UNKNOWN	13,46	0,19	1,5	0,4	0,188
2	UNKNOWN	18,26	99,81	556,0	237,6	99,812
Total			100,00	557,6	238,0	100,000

(±)-6-Phenyl-3-azabicyclo[3.2.0]heptan-2-one ((±)-158u)

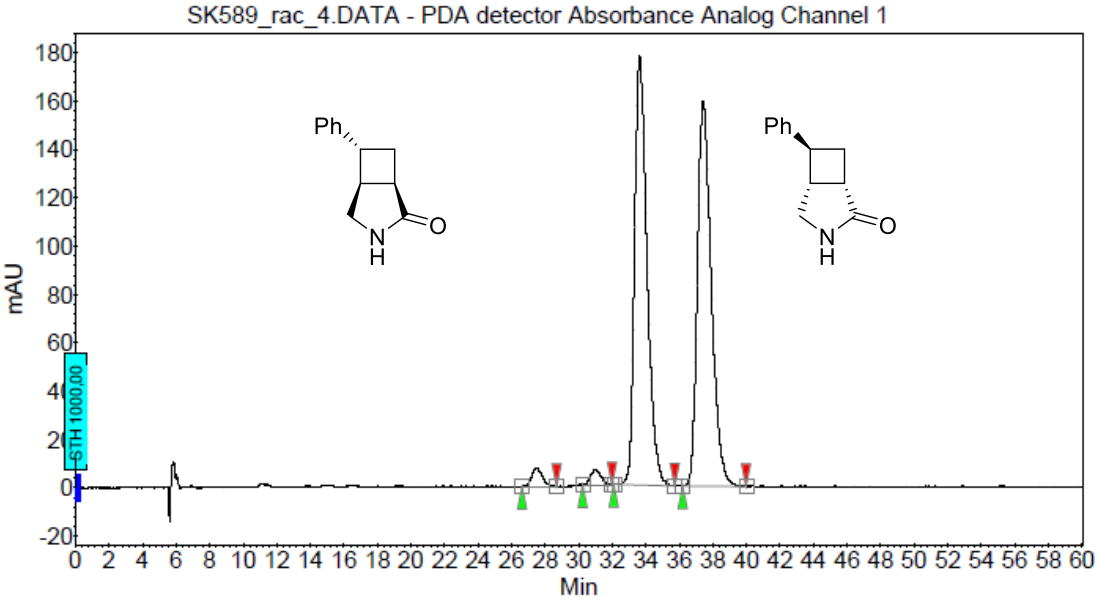

Peak Results :

Index	Name	Time [Min]	Quantity [% Area]	Height [mAU]	Area [mAU.Min]	Area % [%]
1	UNKNOWN	27,52	1,71	7,5	5,4	1,712
2	UNKNOWN	31,05	1,40	6,2	4,4	1,402
3	UNKNOWN	33,64	48,44	177,6	152,0	48,436
4	UNKNOWN	37,43	48,45	159,3	152,0	48,451
Total			100,00	350,6	313,8	100,000

(1*R*,5*S*,6*R*)-6-Phenyl-3-azabicyclo[3.2.0]heptan-2-one ((1*R*,5*S*,6*R*)-158u)

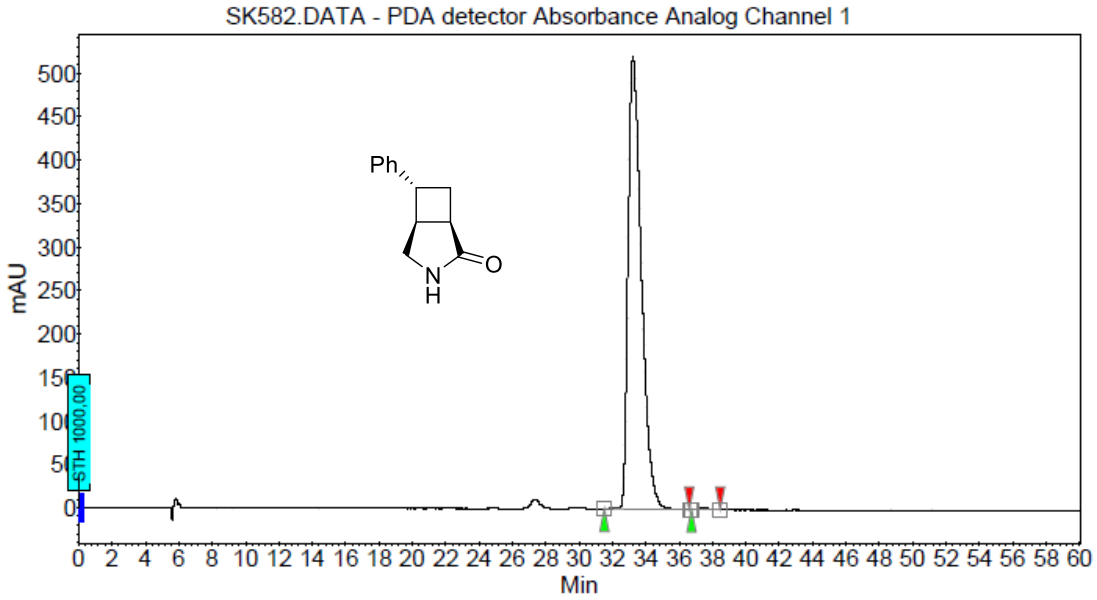

Peak Results :

Index	Name	Time [Min]	Quantity [% Area]	Height [mAU]	Area [mAU.Min]	Area % [%]
1	UNKNOWN	33,23	99,81	520,3	480,4	99,815
2	UNKNOWN	37,47	0,19	1,3	0,9	0,185
Total			100,00	521,5	481,3	100,000

(1*S*,5*R*,6*S*)-6-Phenyl-3-azabicyclo[3.2.0]heptan-2-one ((1*S*,5*R*,6*S*)-158u)

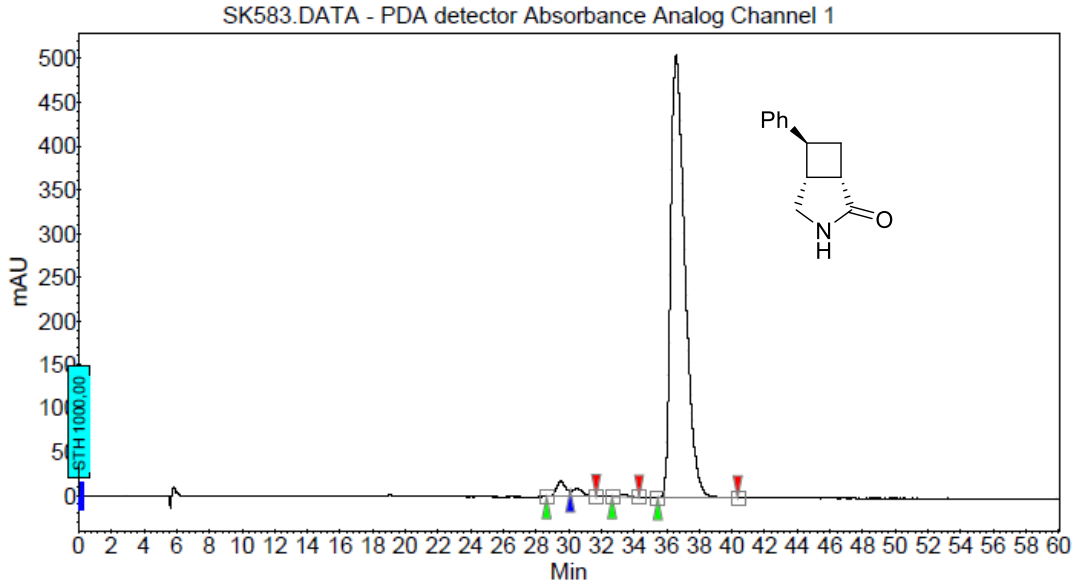

Peak Results :

Index	Name	Time [Min]	Quantity [% Area]	Height [mAU]	Area [mAU.Min]	Area % [%]
3	UNKNOWN	29,51	2,29	17,5	12,2	2,286
4	UNKNOWN	30,54	1,30	9,2	6,9	1,301
2	UNKNOWN	33,36	0,37	2,8	2,0	0,367
1	UNKNOWN	36,57	96,05	505,9	512,1	96,045
Total			100,00	535,4	533,2	100,000

(±)-4-Phenethylpyrrolidin-2-one ((±)-215)

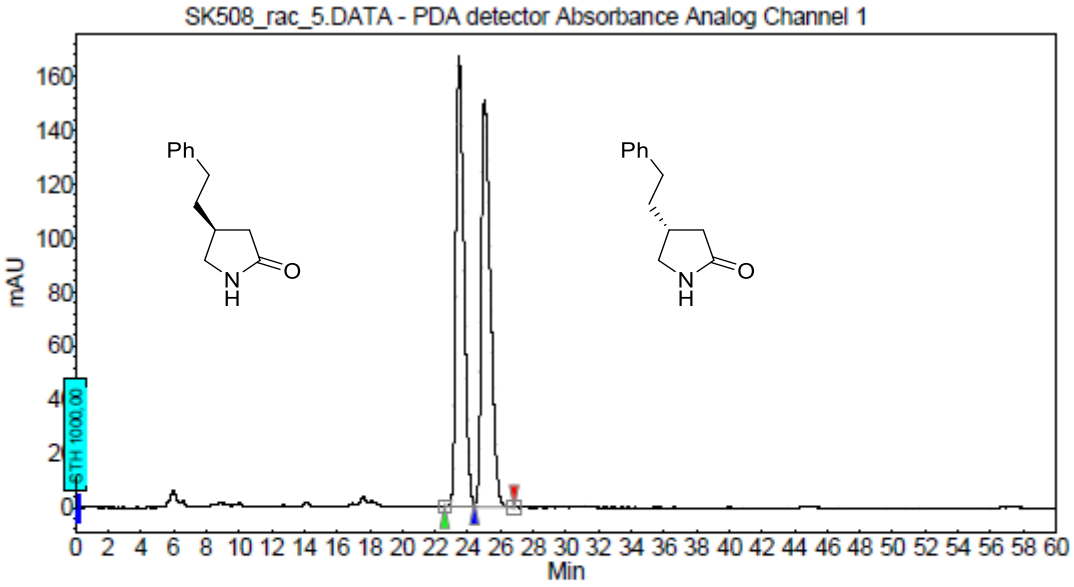

Peak Results :

Index	Name	Time [Min]	Quantity [% Area]	Height [mAU]	Area [mAU.Min]	Area % [%]
1	UNKNOWN	23,46	49,14	167,2	95,3	49,135
2	UNKNOWN	25,03	50,86	150,7	98,7	50,865
Total			100,00	317,9	194,0	100,000

(*S*)-4-Phenethylpyrrolidin-2-one ((*S*)-215)

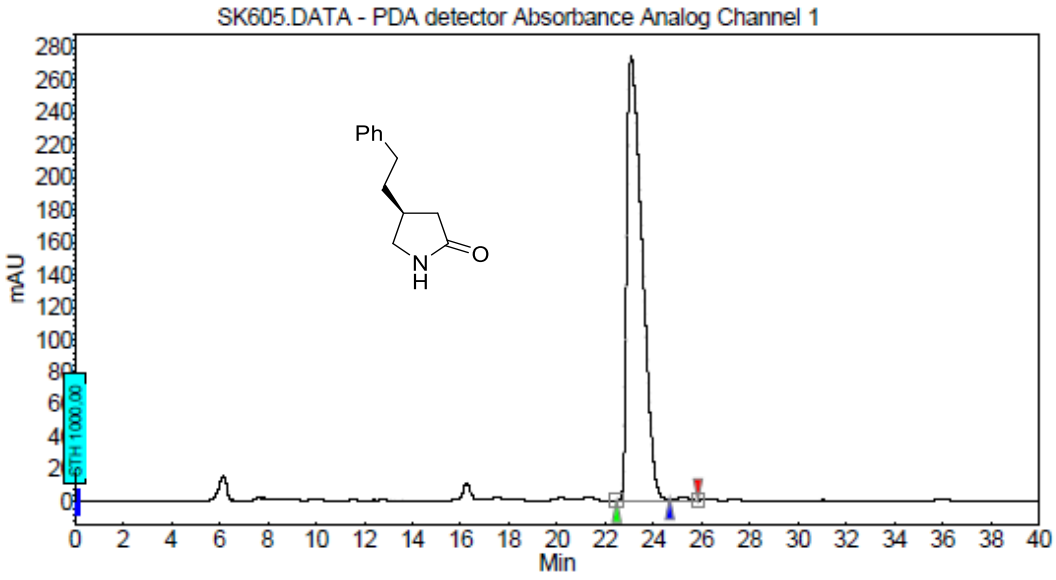

Peak Results :

Index	Name	Time [Min]	Quantity [% Area]	Height [mAU]	Area [mAU.Min]	Area % [%]
1	UNKNOWN	23,07	99,41	274,6	202,4	99,407
2	UNKNOWN	25,25	0,59	2,0	1,2	0,593
Total			100,00	276,6	203,6	100,000

(*R*)-4-Phenethylpyrrolidin-2-one ((*R*)-215)

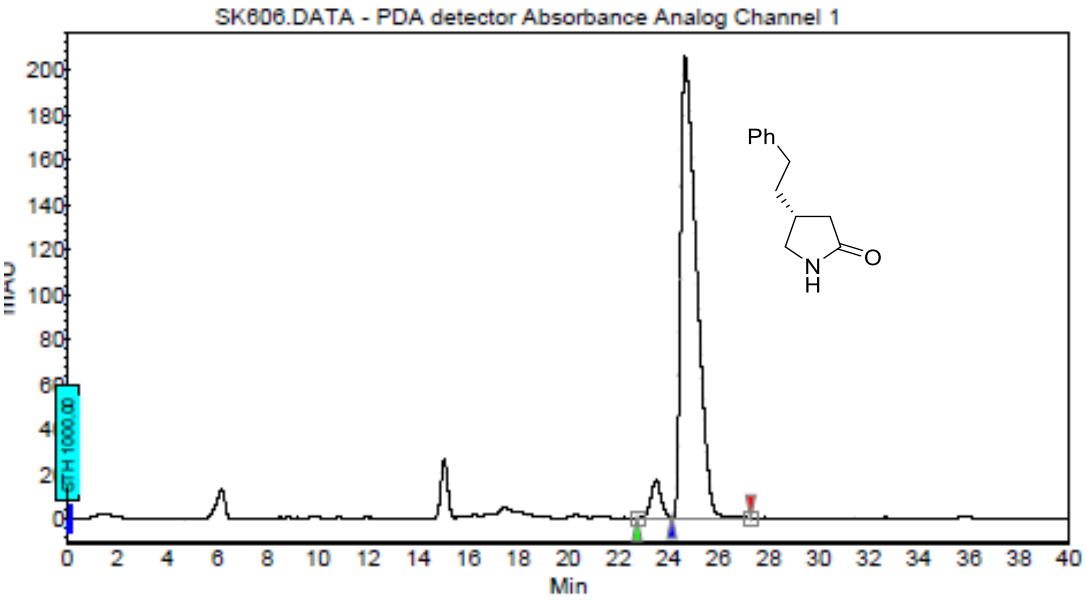

Peak Results :

Index	Name	Time [Min]	Quantity [% Area]	Height [mAU]	Area [mAU.Min]	Area % [%]
1	UNKNOWN	23,50	4,94	16,6	7,9	4,943
2	UNKNOWN	24,67	95,06	205,4	151,4	95,057
Total			100,00	222,0	159,3	100,000

(±)-2-(((*tert*-Butoxycarbonyl)amino)methyl)-3-phenylcyclobutane-1-carboxylic acid ((±)-226)

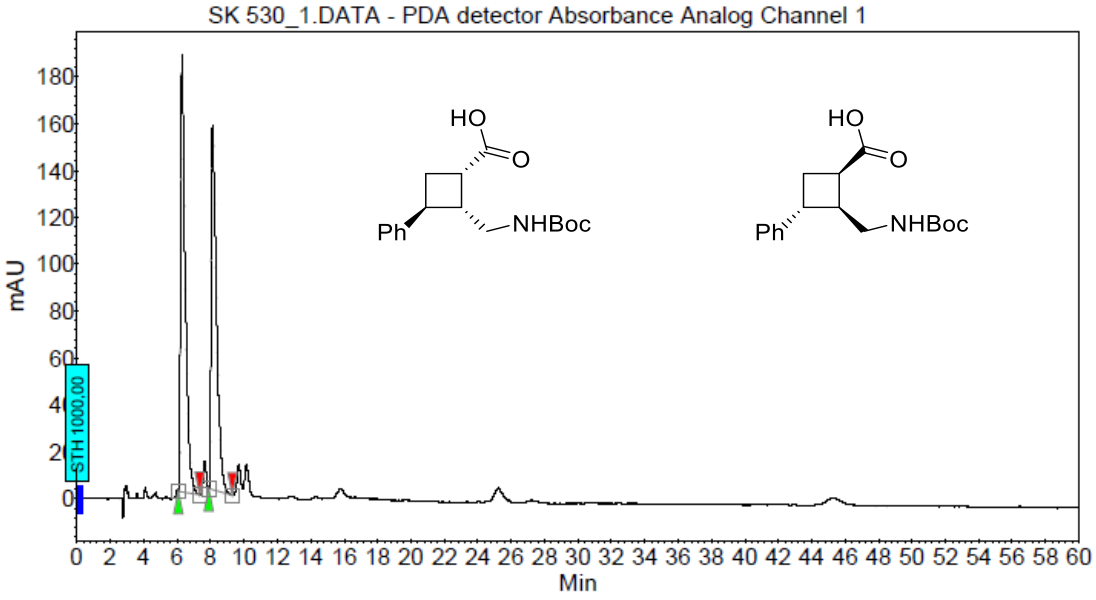

Peak Results :

Index	Name	Time [Min]	Quantity [% Area]	Height [mAU]	Area [mAU.Min]	Area % [%]
2	UNKNOWN	6,28	50,74	186,7	59,1	50,738
1	UNKNOWN	8,12	49,26	155,8	57,4	49,262
Total			100,00	342,5	116,4	100,000

(1*S*,2*R*,3*S*)-2-(((*tert*-Butoxycarbonyl)amino)methyl)-3-phenylcyclobutane-1-carboxylic acid ((1*S*,2*R*,3*S*)-226)

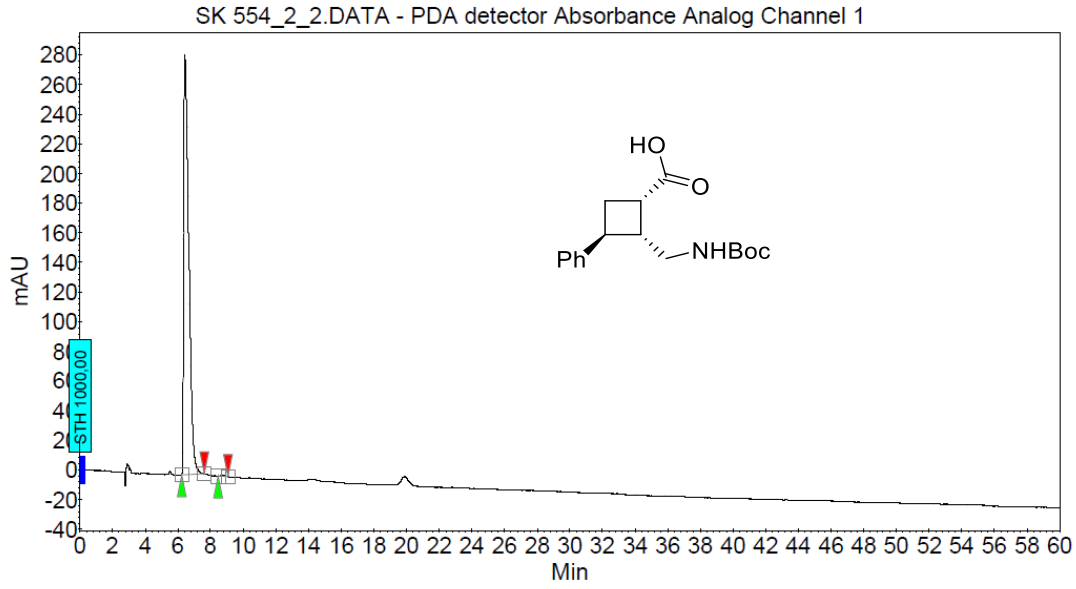

Peak Results :

Index	Name	Time [Min]	Quantity [% Area]	Height [mAU]	Area [mAU.Min]	Area % [%]
1	UNKNOWN	6,43	99,77	283,3	102,7	99,773
2	UNKNOWN	8,78	0,23	0,8	0,2	0,227
Total			100,00	284,2	102,9	100,000

(1*R*,2*S*,3*R*)-2-(((*tert*-Butoxycarbonyl)amino)methyl)-3-phenylcyclobutane-1-carboxylic acid ((1*R*,2*S*,3*R*)-226)

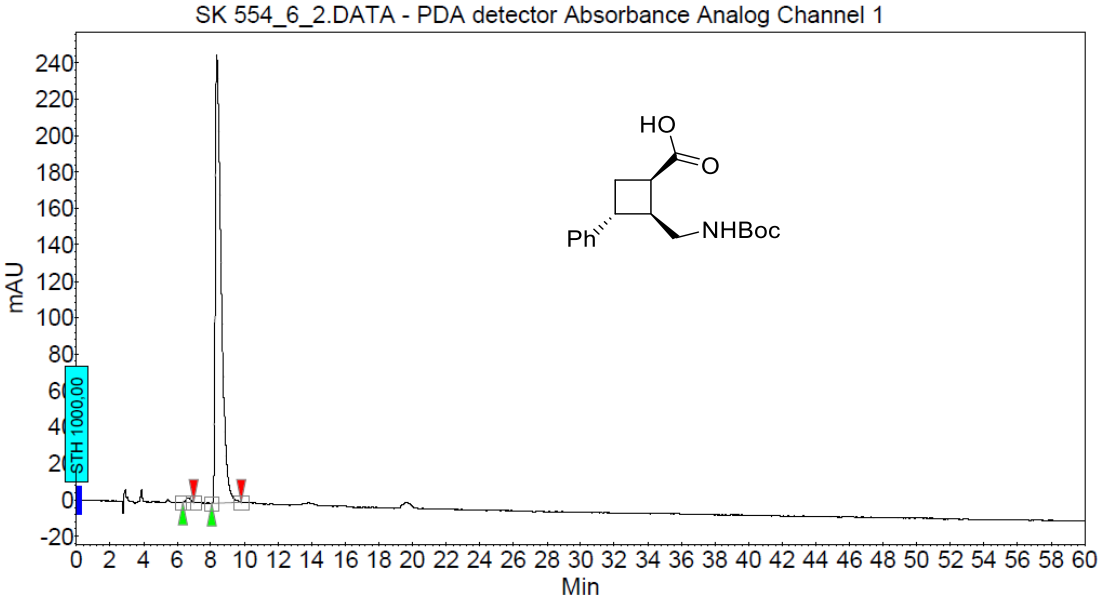

Peak Results :

Index	Name	Time [Min]	Quantity [% Area]	Height [mAU]	Area [mAU.Min]	Area % [%]
1	UNKNOWN	6,69	0,71	2,5	0,7	0,705
2	UNKNOWN	8,35	99,29	246,2	102,9	99,295
Total			100,00	248,8	103,6	100,000

(±)-2-(((((9H-Fluoren-9-yl)methoxy)carbonyl)amino)methyl)-3-phenylcyclobutane-1-carboxylic acid ((±)-264)

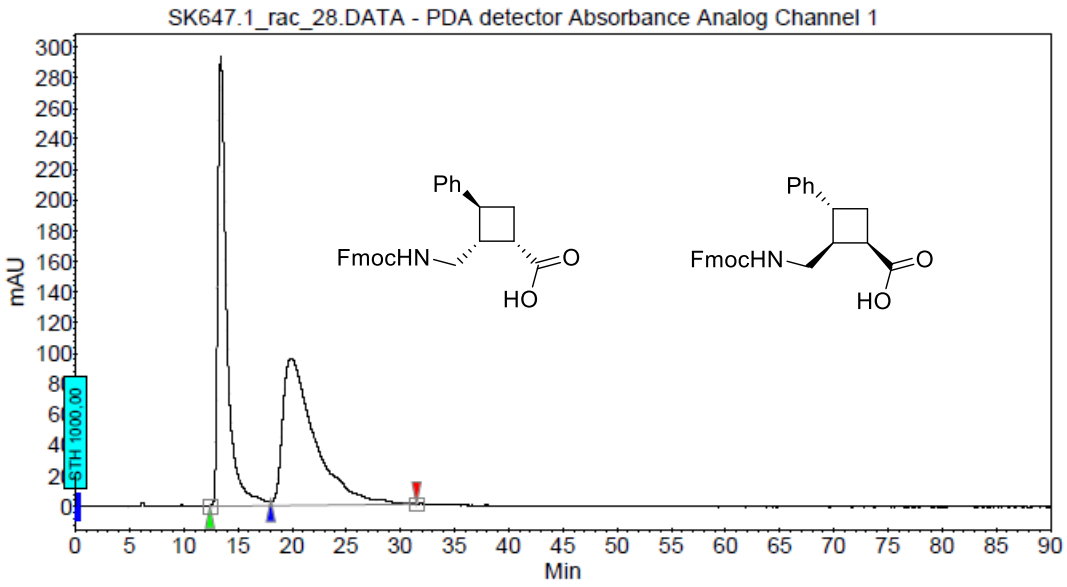

Peak Results :

Index	Name	Time [Min]	Quantity [% Area]	Height [mAU]	Area [mAU.Min]	Area % [%]
1	UNKNOWN	13.44	46.76	293.6	290.9	46.758
2	UNKNOWN	19.96	53.24	95.8	331.2	53.242
Total			100.00	389.4	622.1	100.000

(1*S*,2*R*,3*S*)-2-(((((9H-Fluoren-9-yl)methoxy)carbonyl)amino)methyl)-3-phenylcyclobutane-1-carboxylic acid ((1*S*,2*R*,3*S*)-264)

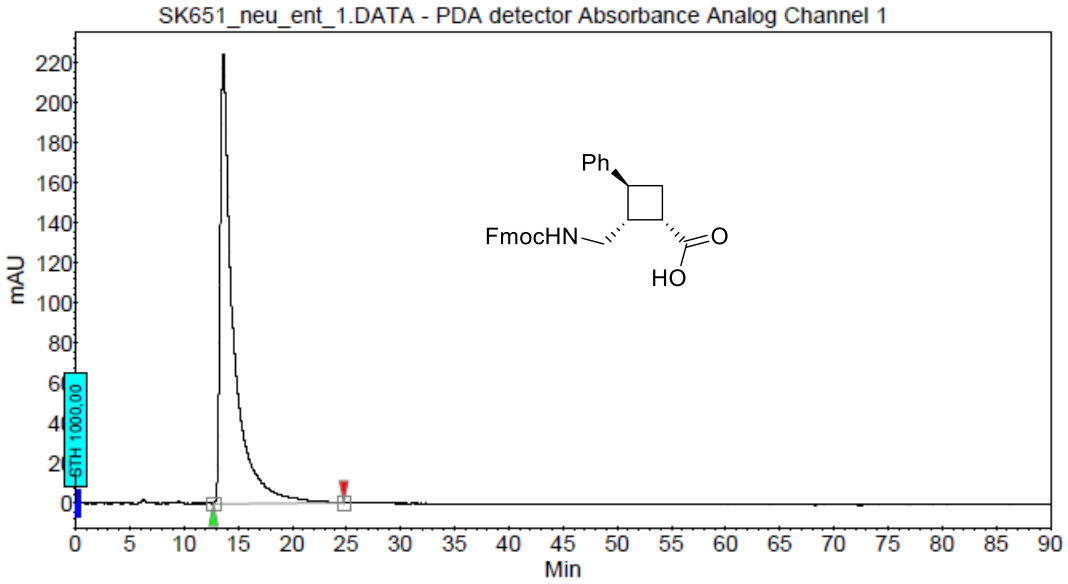

Peak Results :

Index	Name	Time [Min]	Quantity [% Area]	Height [mAU]	Area [mAU.Min]	Area % [%]
1	UNKNOWN	13,66	100,00	224,3	316,9	100,000
Total			100,00	224,3	316,9	100,000

(1*R*,2*S*,3*R*)-2-(((((9H-Fluoren-9-yl)methoxy)carbonyl)amino)methyl)-3-phenylcyclobutane-1-carboxylic acid ((1*R*,2*S*,3*R*)-264)

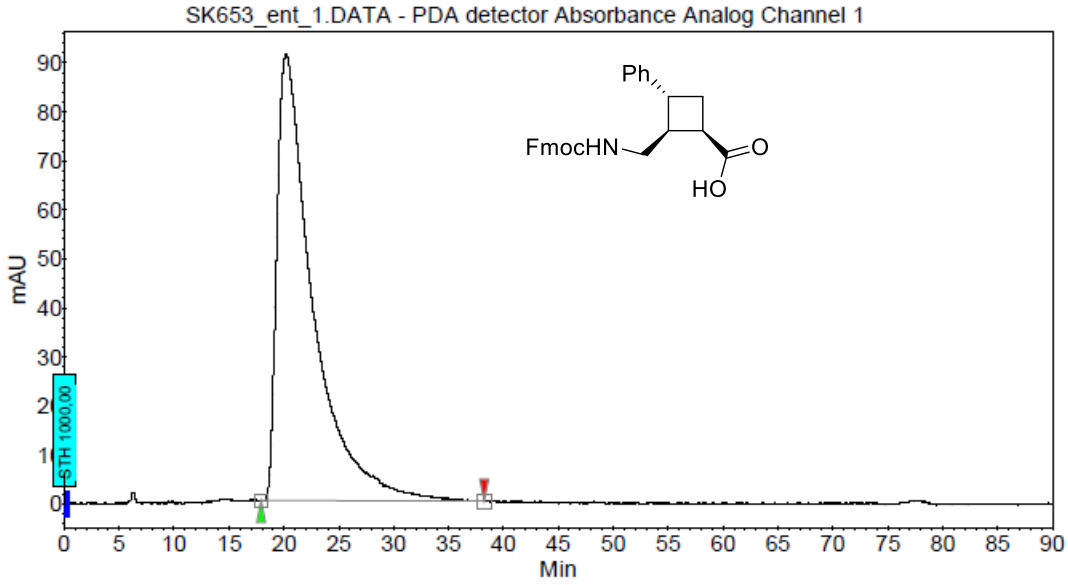

Peak Results :

Index	Name	Time [Min]	Quantity [% Area]	Height [mAU]	Area [mAU.Min]	Area % [%]
1	UNKNOWN	20,20	100,00	91,2	345,2	100,000
Total			100,00	91,2	345,2	100,000

Analytical HPLC of NPY-analoga (267-270)

Ac-[Tyr-Arg-(1*S*,2*R*,3*S*)-Ph-ACBC-Arg-Tyr]-CONH$_2$ (267)

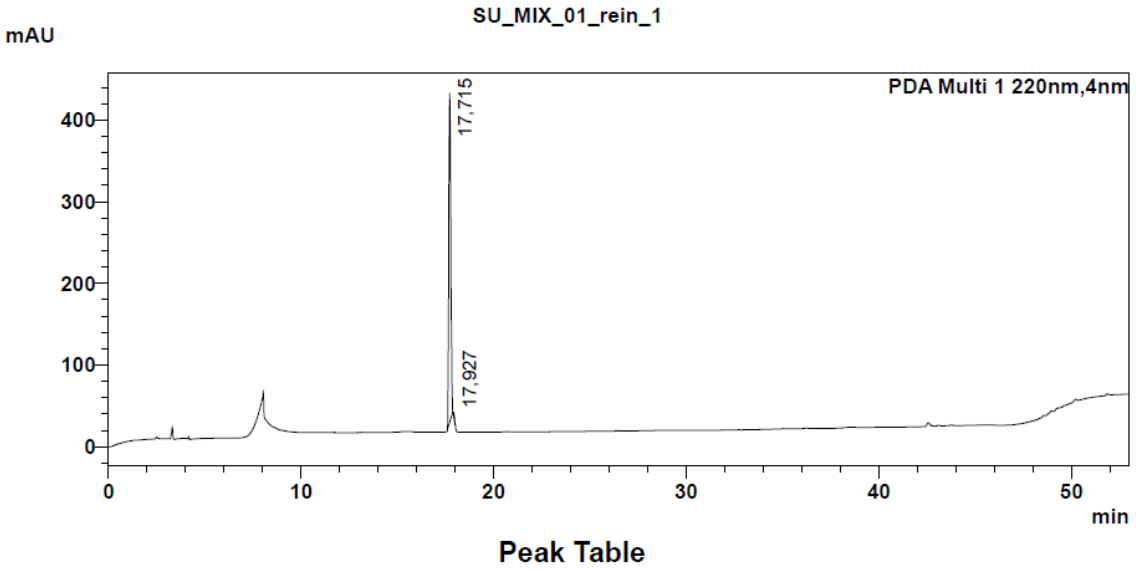

Peak Table

PDA Ch1 220nm

Peak#	Ret. Time	Area%
1	17,715	99,371
2	17,927	0,629
Total		100,000

Ac-[Tyr-Arg-(1*R*,2*S*,3*R*)-Ph-ACBC-Arg-Tyr]-CONH$_2$ (268)

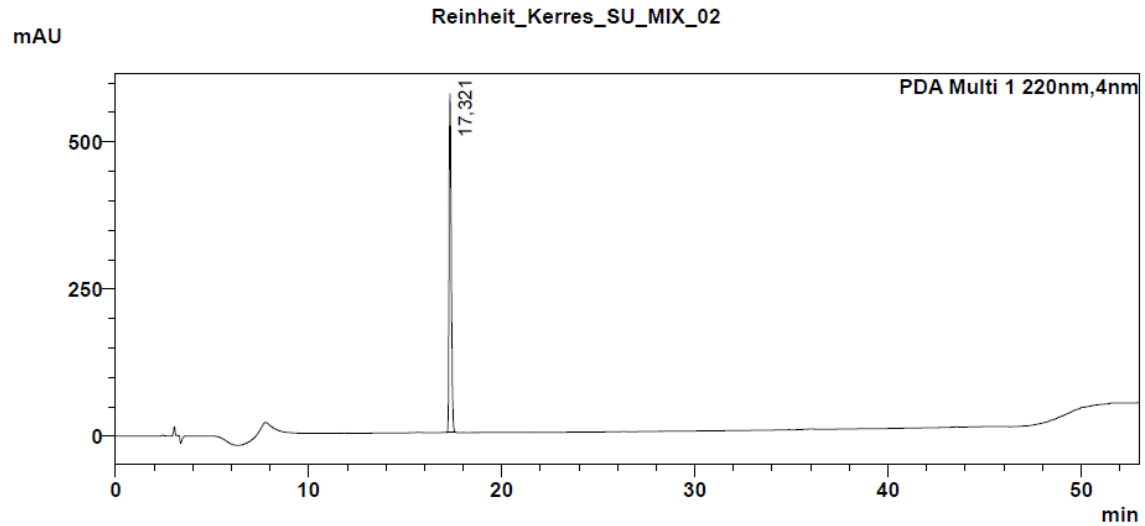

Peak Table

PDA Ch1 220nm

Peak#	Ret. Time	Area%
1	17,321	100,000
Total		100,000

Ac-[Arg-(1*S*,2*R*,3*S*)-Ph-ACBC-Arg-(1*S*,2*R*,3*S*)-Ph-ACBC-Arg-Tyr]-CONH$_2$ (269)

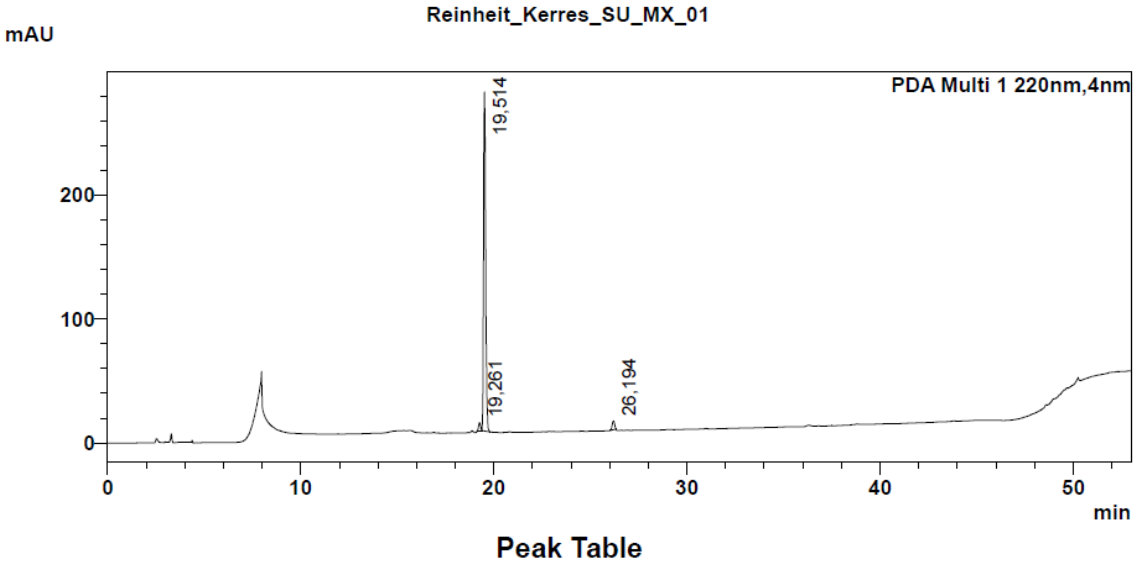

Peak Table

PDA Ch1 220nm

Peak#	Ret. Time	Area%
1	19,261	1,993
2	19,514	95,189
3	26,194	2,818
Total		100,000

Ac-[Arg-(1R*S*,2*S*,3*R*)-Ph-ACBC-Arg-(1*R*,2*S*,3*R*)-Ph-ACBC-Arg-Tyr]-CONH$_2$ (270)

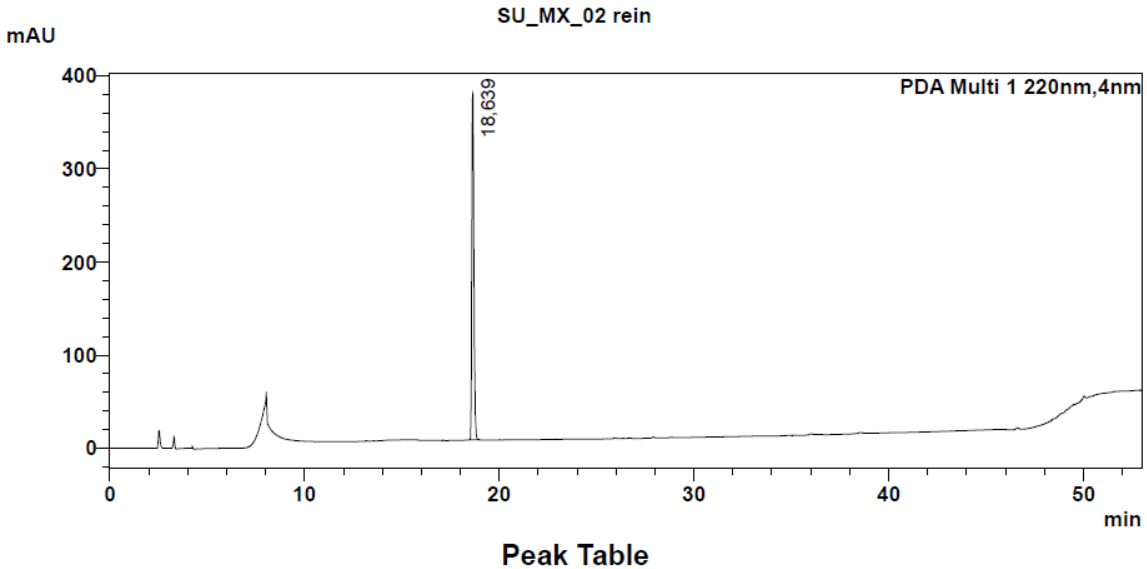

Peak Table

PDA Ch1 220nm

Peak#	Ret. Time	Area%
1	18,639	100,000
Total		100,000

3 X-ray crystallographic data

(±)-Methyl 2-(*tert*-butyl)-3-oxo-2,3,3a,4,9,9a-hexahydro-1H-benzo[f]isoindole-4-carboxylate (189)

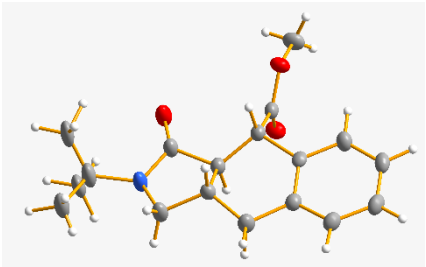

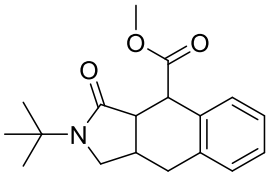

Table 1: Crystal data and structure refinement for **189**.

Chemical formula	$C_{18}H_{23}NO_3$
M_r	301.37
Crystal system, space group	Orthorhombic, *Pnma*
Temperature (K)	123
a, *b*, *c* (Å)	19.4261 (6), 7.7504 (3), 10.7507 (3)
V (Å^3)	1618.63 (9)
Z	4
Radiation type	Cu *K*α
μ (mm^{-1})	0.67
Crystal size (mm)	0.18 × 0.05 × 0.04
F(000)	648
Diffractometer	SuperNova, Single source at offset, Atlas
Absorption correction	Gaussian *CrysAlis PRO* 1.171.38.42b (Rigaku Oxford Diffraction, 2015) Numerical absorption correction based on gaussian integration over a multifaceted crystal model Empirical absorption correction using spherical harmonics, implemented in SCALE3 ABSPACK scaling algorithm.

T_{min}, T_{max}	0.924, 0.980
No. of measured, independent and observed [$I > 2\sigma(I)$] reflections	18337, 1748, 1555
R_{int}	0.042
$(\sin \theta/\lambda)_{max}$ (Å^{-1})	0.622
$R[F^2 > 2\sigma(F^2)]$, $wR(F^2)$, S	0.047, 0.130, 1.04
No. of reflections	1748
No. of parameters	239
No. of restraints	25
H-atom treatment	All H-atom parameters refined
$\Delta\rho_{max}$, $\Delta\rho_{min}$ (e Å^{-3})	0.33, −0.35

Table 2: Fractional Atomic Coordinates (×10^4) and Equivalent Isotropic Displacement Parameters (Å^2×10^3) for **189**. U_{eq} is defined as 1/3 of the trace of the orthogonalized U_{ij}.

Atom	x	y	z	U_{eq}
O(3)	3015.2(7)	7500	2780.2(12)	40.0(4)
N(1)	2886.4(10)	7253(17)	4915.7(18)	33(2)
C(1)	5292.0(9)	7500	5325.9(17)	26.1(4)
C(9)	3245.5(9)	7500	3836.2(18)	29.8(4)
C(3)	6540.6(10)	7500	5190(2)	33.2(5)
C(2)	5942.9(10)	7500	5880(2)	31.2(4)
C(12)	4665(1)	7500	6164.2(18)	32.1(5)
C(10)	3328.3(10)	7500	6020.0(18)	34.1(5)
C(8)	3992.6(12)	7747(14)	4192(2)	25(2)
C(17)	4683.0(13)	7500	-59.4(19)	35.6(5)
C(6)	5251.7(12)	7218(5)	4031(2)	21.2(11)
C(4)	6503.6(13)	7252(10)	3908(3)	29.0(16)
O(2)	4656.2(10)	6745(2)	1179.3(16)	28.2(4)
C(15A)	1822(3)	9095(7)	4506(4)	46.8(6)
C(5)	5861.6(13)	7154(4)	3344(2)	30.7(11)
C(16)	4568.3(12)	7895(3)	2100(2)	24.0(8)
C(7)	4551.9(12)	7028(3)	3360(2)	23.2(6)
C(11)	4031.0(13)	6983(3)	5486(2)	25.8(6)
C(13)	2119.2(11)	7500	4976(2)	47.9(5)
C(14)	1884.7(15)	7983(6)	6327(3)	49.8(6)
C(15)	1878(3)	9165(7)	4213(4)	46.2(6)
O(1)	4525.5(10)	9430(2)	1925.8(17)	31.0(4)

Table 3: Anisotropic Displacement Parameters (×10^4) **for 189**. The anisotropic displacement factor exponent takes the form: $-2\pi^2[h^2a^{*2} \times U_{11} + ... + 2hka^* \times b^* \times U_{12}]$

Atom	U_{11}	U_{22}	U_{33}	U_{23}	U_{13}	U_{12}
O(3)	23.4(7)	71.9(11)	24.7(7)	0	-1.1(5)	0
N(1)	18.8(8)	57(7)	23.7(9)	0.0(14)	1.0(6)	-1.9(14)
C(1)	23.4(9)	25.5(9)	29.4(9)	0	-1.5(7)	0
C(9)	20.4(9)	43.5(11)	25.5(9)	0	1.6(7)	0
C(3)	21.9(9)	32.2(10)	45.6(12)	0	-5.5(8)	0
C(2)	25.6(9)	33.6(10)	34.4(10)	0	-5.8(8)	0
C(12)	26(1)	45.5(12)	24.9(9)	0	-1.8(7)	0
C(10)	23.2(9)	56.9(14)	22.2(9)	0	1.3(7)	0
C(8)	20.2(10)	29(7)	24.2(10)	0.3(12)	0.0(7)	0.1(12)
C(17)	46.0(13)	38.8(12)	22.0(9)	0	3.8(8)	0
C(6)	20.6(9)	14(3)	29.5(10)	0.4(9)	-0.7(8)	-1.0(9)
C(4)	21.5(10)	24(5)	42.1(12)	3.7(13)	4.5(9)	-0.8(12)
O(2)	36.8(10)	28.0(8)	19.8(9)	-1.5(7)	3.7(7)	1.5(7)
C(15A)	20.6(9)	82.0(13)	37.8(13)	-7.6(8)	10.5(10)	1.2(7)
C(5)	24.4(11)	36(3)	31.8(12)	2.5(11)	3.6(9)	-1.5(10)
C(16)	17.9(9)	25(3)	28.8(12)	-0.9(9)	1.8(8)	-1.0(8)
C(7)	21.1(10)	23.8(17)	24.6(11)	0.3(8)	0.7(9)	-2.4(8)
C(11)	23.1(11)	32.1(16)	22.2(11)	-1.5(9)	1.0(9)	0.0(8)
C(13)	21.3(7)	86.1(12)	36.2(10)	0	7.8(7)	0
C(14)	23.9(9)	88.0(16)	37.6(11)	0.0(9)	8.1(9)	1.2(9)
C(15)	20.4(9)	81.6(13)	36.7(13)	-7.1(8)	10.2(10)	1.1(7)
O(1)	39.2(10)	25.6(11)	28.3(9)	1.9(8)	3.5(8)	0.5(8)

Table 4: Bond Lengths in Å for **189**.

Atom	Atom	Length/Å
O(3)	C(9)	1.220(2)
N(1)	N(1)^1	0.38(3)
N(1)	C(9)	1.367(3)
N(1)	C(10)	1.478(3)
N(1)	C(13)^1	1.504(3)
N(1)	C(13)	1.504(3)
C(1)	C(2)	1.398(3)
C(1)	C(12)	1.515(3)
C(1)	C(6)^1	1.411(3)
C(1)	C(6)	1.411(3)
C(9)	N(1)^1	1.367(3)
C(9)	C(8)^1	1.513(3)
C(9)	C(8)	1.513(3)
C(3)	C(2)	1.378(3)
C(3)	C(4)	1.394(4)
C(3)	C(4)^1	1.394(4)
C(12)	C(11)	1.486(3)
C(12)	C(11)^1	1.486(3)
C(10)	N(1)^1	1.478(3)
C(10)	C(11)^1	1.534(3)
C(10)	C(11)	1.534(3)
C(8)	C(8)^1	0.38(2)
C(8)	C(7)	1.514(5)
C(8)	C(11)	1.514(5)
C(17)	O(2)^1	1.456(2)
C(17)	O(2)	1.456(2)
C(6)	C(5)	1.397(3)
C(6)	C(5)^1	1.479(3)
C(6)	C(7)	1.546(3)
C(6)	C(7)^1	1.646(3)
C(4)	C(4)^1	0.384(16)
C(4)	C(5)	1.389(3)
O(2)	C(16)	1.343(3)
O(2)	O(1)^1	1.240(3)
C(15A)	C(13)^1	1.455(5)
C(15A)	C(13)	1.455(5)
C(5)	C(4)^1	1.461(4)
C(16)	O(2)^1	1.042(3)
C(16)	C(7)	1.512(3)
C(16)	O(1)	1.207(3)

Atom	Atom	Length/Å
C(16)	O(1)[1]	1.814(3)
C(7)	C(8)[1]	1.419(3)
C(7)	C(16)[1]	1.356(3)
C(7)	O(1)[1]	1.912(3)
C(11)	C(8)[1]	1.409(4)
C(13)	N(1)[1]	1.504(3)
C(13)	C(15A)[1]	1.455(5)
C(13)	C(13)[1]	0.000(5)
C(13)	C(14)	1.567(4)
C(13)	C(14)[1]	1.567(4)
C(13)	C(15)[1]	1.599(5)
C(13)	C(15)	1.599(5)
C(14)	C(14)[1]	0.748(9)
C(15)	C(13)[1]	1.599(5)
O(1)	O(2)[1]	1.240(3)
O(1)	C(16)[1]	1.814(3)
O(1)	C(7)[1]	1.912(3)

Table 5: Bond Angles in ° for **189**.

Atom	Atom	Atom	Angle/°
N(1)[1]	N(1)	C(9)	81.9(5)
N(1)[1]	N(1)	C(10)	82.5(5)
N(1)[1]	N(1)	C(13)	82.7(5)
N(1)[1]	N(1)	C(13)[1]	82.7(5)
C(9)	N(1)	C(10)	111.6(3)
C(9)	N(1)	C(13)[1]	121.6(3)
C(9)	N(1)	C(13)	121.6(3)
C(10)	N(1)	C(13)[1]	121.6(3)
C(10)	N(1)	C(13)	121.6(3)
C(13)	N(1)	C(13)[1]	0.00(18)
C(2)	C(1)	C(12)	118.27(17)
C(2)	C(1)	C(6)	118.09(18)
C(2)	C(1)	C(6)[1]	118.09(18)
C(6)	C(1)	C(12)	122.82(17)
C(6)[1]	C(1)	C(12)	122.82(17)
C(6)	C(1)	C(6)[1]	17.8(3)
O(3)	C(9)	N(1)[1]	127.05(19)
O(3)	C(9)	N(1)	127.04(19)
O(3)	C(9)	C(8)[1]	125.96(18)
O(3)	C(9)	C(8)	125.96(18)
N(1)[1]	C(9)	N(1)	16.1(11)
N(1)	C(9)	C(8)[1]	104.9(2)
N(1)[1]	C(9)	C(8)[1]	106.99(19)
N(1)	C(9)	C(8)	106.99(19)
N(1)[1]	C(9)	C(8)	104.9(2)
C(8)	C(9)	C(8)[1]	14.5(8)
C(2)	C(3)	C(4)[1]	119.3(2)
C(2)	C(3)	C(4)	119.3(2)
C(4)[1]	C(3)	C(4)	15.8(7)
C(3)	C(2)	C(1)	122.19(19)
C(11)[1]	C(12)	C(1)	112.01(17)
C(11)	C(12)	C(1)	112.01(17)
C(11)	C(12)	C(11)[1]	31.3(2)
N(1)[1]	C(10)	N(1)	14.9(10)
N(1)[1]	C(10)	C(11)[1]	100.5(2)
N(1)	C(10)	C(11)	100.5(2)
N(1)	C(10)	C(11)[1]	104.5(2)
N(1)[1]	C(10)	C(11)	104.5(2)
C(11)[1]	C(10)	C(11)	30.3(2)
C(9)	C(8)	C(7)	119.5(4)
C(9)	C(8)	C(11)	103.3(3)
C(8)[1]	C(8)	C(9)	82.7(4)
C(8)[1]	C(8)	C(7)	68.4(4)
C(8)[1]	C(8)	C(11)	67.0(4)
C(11)	C(8)	C(7)	111.4(5)
O(2)[1]	C(17)	O(2)	47.43(16)
C(1)	C(6)	C(5)[1]	113.4(2)
C(1)	C(6)	C(7)	121.61(19)
C(1)	C(6)	C(7)[1]	115.1(2)
C(5)	C(6)	C(1)	118.7(2)
C(5)	C(6)	C(5)[1]	21.3(2)
C(5)	C(6)	C(7)	119.7(2)
C(5)	C(6)	C(7)[1]	118.7(2)
C(5)[1]	C(6)	C(7)	120.2(2)
C(5)[1]	C(6)	C(7)[1]	109.0(2)
C(7)	C(6)	C(7)[1]	26.24(17)
C(4)[1]	C(4)	C(3)	82.1(3)
C(4)[1]	C(4)	C(5)	93.2(4)
C(5)	C(4)	C(3)	119.1(2)
C(16)	O(2)	C(17)	114.32(17)
O(1)[1]	O(2)	C(17)	153.48(19)
O(1)[1]	O(2)	C(16)	89.12(17)
C(13)[1]	C(15A)	C(13)	0.00(17)
C(6)	C(5)	C(4)[1]	119.5(2)
C(4)	C(5)	C(6)	121.9(2)
C(4)	C(5)	C(4)[1]	15.2(6)
O(2)[1]	C(16)	O(2)	57.1(2)
O(2)[1]	C(16)	C(7)	166.6(2)
O(2)	C(16)	C(7)	111.58(18)
O(2)	C(16)	O(1)[1]	43.13(12)

Atom	Atom	Atom	Angle/°
O(2)[1]	C(16)	O(1)	66.43(19)
O(2)[1]	C(16)	O(1)[1]	100.1(2)
C(7)	C(16)	O(1)[1]	69.51(14)
O(1)	C(16)	O(2)	123.3(2)
O(1)	C(16)	C(7)	125.1(2)
O(1)	C(16)	O(1)[1]	163.8(3)
C(8)[1]	C(7)	C(8)	14.5(8)
C(8)[1]	C(7)	C(6)	111.5(2)
C(8)	C(7)	C(6)	108.6(2)
C(8)[1]	C(7)	C(16)	121.8(3)
C(8)	C(7)	O(1)[1]	132.5(3)
C(8)[1]	C(7)	O(1)[1]	124.1(3)
C(6)	C(7)	O(1)[1]	117.14(19)
C(16)[1]	C(7)	C(8)[1]	130.0(2)
C(16)	C(7)	C(8)	112.4(3)
C(16)[1]	C(7)	C(8)	126.3(3)
C(16)	C(7)	C(6)	110.9(2)
C(16)[1]	C(7)	C(6)	116.2(2)
C(16)[1]	C(7)	C(16)	23.86(17)
C(16)[1]	C(7)	O(1)[1]	38.88(13)
C(16)	C(7)	O(1)[1]	62.69(13)
C(12)	C(11)	C(10)	118.94(19)
C(12)	C(11)	C(8)	112.7(3)
C(8)[1]	C(11)	C(12)	119.2(3)
C(8)[1]	C(11)	C(10)	106.5(2)
C(8)	C(11)	C(10)	101.4(2)
C(8)[1]	C(11)	C(8)	14.5(8)
N(1)	C(13)	N(1)[1]	14.6(10)
N(1)	C(13)	C(14)[1]	107.3(2)
N(1)	C(13)	C(14)	111.0(2)
N(1)[1]	C(13)	C(14)[1]	111.0(2)
N(1)[1]	C(13)	C(14)	107.3(2)
N(1)[1]	C(13)	C(15)	99.5(5)
N(1)	C(13)	C(15)[1]	99.5(5)

Atom	Atom	Atom	Angle/°
N(1)[1]	C(13)	C(15)[1]	111.8(5)
N(1)	C(13)	C(15)	111.8(5)
C(15A)	C(13)	N(1)[1]	105.7(5)
C(15A)[1]	C(13)	N(1)	105.7(5)
C(15A)[1]	C(13)	N(1)[1]	119.1(5)
C(15A)	C(13)	N(1)	119.1(5)
C(15A)[1]	C(13)	C(15A)	116.3(5)
C(15A)	C(13)	C(14)[1]	114.2(2)
C(15A)	C(13)	C(14)	90.2(2)
C(15A)[1]	C(13)	C(14)	114.2(2)
C(15A)[1]	C(13)	C(14)[1]	90.2(2)
C(13)[1]	C(13)	N(1)	0(10)
C(13)[1]	C(13)	N(1)[1]	0(10)
C(13)[1]	C(13)	C(15A)	0(10)
C(13)[1]	C(13)	C(15A)[1]	0(10)
C(13)[1]	C(13)	C(14)[1]	0(10)
C(13)[1]	C(13)	C(14)	0(10)
C(13)[1]	C(13)	C(15)[1]	0(10)
C(13)[1]	C(13)	C(15)	0(10)
C(14)	C(13)	C(14)[1]	27.6(3)
C(14)	C(13)	C(15)	101.4(2)
C(14)[1]	C(13)	C(15)[1]	101.4(2)
C(14)	C(13)	C(15)[1]	125.6(2)
C(14)[1]	C(13)	C(15)	125.6(2)
C(15)[1]	C(13)	C(15)	107.6(5)
C(14)[1]	C(14)	C(13)	76.19(16)
C(13)[1]	C(15)	C(13)	0.00(14)
O(2)[1]	O(1)	C(16)[1]	47.76(13)
O(2)[1]	O(1)	C(7)[1]	94.71(15)
C(16)	O(1)	O(2)[1]	50.39(16)
C(16)	O(1)	C(16)[1]	3.28(6)
C(16)[1]	O(1)	C(7)[1]	47.79(12)
C(16)	O(1)	C(7)[1]	44.82(15)

Table 6: Torsion Angles in ° for **189**.

Atom	Atom	Atom	Atom	Angle/°
O(3)	C(9)	C(8)	C(8)[1]	-95.3(3)
O(3)	C(9)	C(8)	C(7)	-35.2(9)
O(3)	C(9)	C(8)	C(11)	-159.5(2)
N(1)[1]	N(1)	C(9)	O(3)	-96.1(4)
N(1)[1]	N(1)	C(9)	C(8)	84.8(4)
N(1)[1]	N(1)	C(9)	C(8)[1]	99.8(4)
N(1)[1]	N(1)	C(10)	C(11)	-106.98(15)
N(1)[1]	N(1)	C(10)	C(11)[1]	-76.21(17)
N(1)[1]	N(1)	C(13)	C(15A)	24.6(3)
N(1)[1]	N(1)	C(13)	C(15A)[1]	157.8(2)

Atom	Atom	Atom	Atom	Angle/°
N(1)[1]	N(1)	C(13)	C(13)[1]	0.00(11)
N(1)[1]	N(1)	C(13)	C(14)[1]	-107.0(2)
N(1)[1]	N(1)	C(13)	C(14)	-78.0(3)
N(1)[1]	N(1)	C(13)	C(15)[1]	147.8(2)
N(1)[1]	N(1)	C(13)	C(15)	34.4(3)
N(1)	C(9)	C(8)	C(8)[1]	83.8(6)
N(1)[1]	C(9)	C(8)	C(8)[1]	100.4(6)
N(1)	C(9)	C(8)	C(7)	143.9(7)
N(1)[1]	C(9)	C(8)	C(7)	160.5(7)
N(1)[1]	C(9)	C(8)	C(11)	36.2(8)

Atom	Atom	Atom	Atom	Angle/°
N(1)	C(9)	C(8)	C(11)	19.6(8)
N(1)[1]	C(10)	C(11)	C(12)	148.1(5)
N(1)	C(10)	C(11)	C(12)	162.8(5)
N(1)	C(10)	C(11)	C(8)[1]	24.7(7)
N(1)[1]	C(10)	C(11)	C(8)[1]	10.0(7)
N(1)[1]	C(10)	C(11)	C(8)	23.9(6)
N(1)	C(10)	C(11)	C(8)	38.7(6)
N(1)[1]	C(13)	C(14)	C(14)[1]	-102.4(5)
N(1)	C(13)	C(14)	C(14)[1]	-87.4(5)
N(1)[1]	C(13)	C(15)	C(13)[1]	0(39)
N(1)	C(13)	C(15)	C(13)[1]	0(80)
C(1)	C(12)	C(11)	C(10)	-158.81(14)
C(1)	C(12)	C(11)	C(8)	-40.4(4)
C(1)	C(12)	C(11)	C(8)[1]	-26.0(5)
C(1)	C(6)	C(5)	C(4)[1]	-13.5(6)
C(1)	C(6)	C(5)	C(4)	4.0(6)
C(1)	C(6)	C(7)	C(8)	17.9(5)
C(1)	C(6)	C(7)	C(8)[1]	2.7(6)
C(1)	C(6)	C(7)	C(16)[1]	167.4(2)
C(1)	C(6)	C(7)	C(16)	141.9(3)
C(1)	C(6)	C(7)	O(1)[1]	-148.9(2)
C(9)	N(1)	C(10)	N(1)[1]	78.2(8)
C(9)	N(1)	C(10)	C(11)	-28.7(9)
C(9)	N(1)	C(10)	C(11)[1]	2.0(9)
C(9)	N(1)	C(13)	N(1)[1]	-75.8(9)
C(9)	N(1)	C(13)	C(15A)	-51.2(11)
C(9)	N(1)	C(13)	C(15A)[1]	81.9(10)
C(9)	N(1)	C(13)	C(13)[1]	0.00(14)
C(9)	N(1)	C(13)	C(14)[1]	177.2(8)
C(9)	N(1)	C(13)	C(14)	-153.8(7)
C(9)	N(1)	C(13)	C(15)[1]	72.0(10)
C(9)	N(1)	C(13)	C(15)	-41.4(11)
C(9)	C(8)	C(7)	C(8)[1]	-67.7(6)
C(9)	C(8)	C(7)	C(6)	-171.7(5)
C(9)	C(8)	C(7)	C(16)[1]	42.7(9)
C(9)	C(8)	C(7)	C(16)	65.2(7)
C(9)	C(8)	C(7)	O(1)[1]	-7.7(9)
C(9)	C(8)	C(11)	C(12)	-164.3(3)
C(9)	C(8)	C(11)	C(10)	-36.0(5)
C(9)	C(8)	C(11)	C(8)[1]	76.0(5)
C(3)	C(4)	C(5)	C(6)	-2.9(8)
C(3)	C(4)	C(5)	C(4)[1]	82.7(6)
C(2)	C(1)	C(12)	C(11)[1]	163.10(11)
C(2)	C(1)	C(12)	C(11)	-163.10(11)
C(2)	C(1)	C(6)	C(5)[1]	-30.3(3)
C(2)	C(1)	C(6)	C(5)	-7.3(4)
C(2)	C(1)	C(6)	C(7)[1]	-156.78(15)
C(2)	C(1)	C(6)	C(7)	174.2(2)

Atom	Atom	Atom	Atom	Angle/°
C(2)	C(3)	C(4)	C(4)[1]	94.47(19)
C(2)	C(3)	C(4)	C(5)	5.3(8)
C(12)	C(1)	C(2)	C(3)	180.000(0)
C(12)	C(1)	C(6)	C(5)	-176.8(2)
C(12)	C(1)	C(6)	C(5)[1]	160.27(17)
C(12)	C(1)	C(6)	C(7)[1]	33.8(3)
C(12)	C(1)	C(6)	C(7)	4.8(4)
C(10)	N(1)	C(9)	O(3)	-174.8(3)
C(10)	N(1)	C(9)	N(1)[1]	-78.7(7)
C(10)	N(1)	C(9)	C(8)[1]	21.1(10)
C(10)	N(1)	C(9)	C(8)	6.2(10)
C(10)	N(1)	C(13)	N(1)[1]	76.6(9)
C(10)	N(1)	C(13)	C(15A)[1]	-125.7(8)
C(10)	N(1)	C(13)	C(15A)	101.2(8)
C(10)	N(1)	C(13)	C(13)[1]	0.00(13)
C(10)	N(1)	C(13)	C(14)[1]	-30.4(10)
C(10)	N(1)	C(13)	C(14)	-1.4(11)
C(10)	N(1)	C(13)	C(15)[1]	-135.6(9)
C(10)	N(1)	C(13)	C(15)	111.0(8)
C(8)[1]	C(9)	C(8)	C(7)	60.1(6)
C(8)[1]	C(9)	C(8)	C(11)	-64.2(5)
C(8)[1]	C(8)	C(7)	C(6)	-104.0(2)
C(8)[1]	C(8)	C(7)	C(16)[1]	110.4(4)
C(8)[1]	C(8)	C(7)	C(16)	132.9(2)
C(8)[1]	C(8)	C(7)	O(1)[1]	60.0(4)
C(8)[1]	C(8)	C(11)	C(12)	119.7(2)
C(8)[1]	C(8)	C(11)	C(10)	-112.04(17)
C(17)	O(2)	C(16)	O(2)[1]	-7.6(3)
C(17)	O(2)	C(16)	C(7)	-179.45(19)
C(17)	O(2)	C(16)	O(1)[1]	167.2(2)
C(17)	O(2)	C(16)	O(1)	-1.1(3)
C(6)[1]	C(1)	C(2)	C(3)	-10.11(18)
C(6)	C(1)	C(2)	C(3)	10.11(18)
C(6)	C(1)	C(12)	C(11)[1]	-27.5(2)
C(6)	C(1)	C(12)	C(11)	6.3(2)
C(6)[1]	C(1)	C(12)	C(11)	27.5(2)
C(6)[1]	C(1)	C(12)	C(11)[1]	-6.3(2)
C(6)[1]	C(1)	C(6)	C(5)	87.4(3)
C(6)[1]	C(1)	C(6)	C(5)[1]	64.5(3)
C(6)[1]	C(1)	C(6)	C(7)[1]	-62.0(2)
C(6)[1]	C(1)	C(6)	C(7)	-91.0(3)
C(4)[1]	C(3)	C(2)	C(1)	9.1(4)
C(4)	C(3)	C(2)	C(1)	-9.1(4)
C(4)[1]	C(3)	C(4)	C(5)	-89.2(6)
C(4)[1]	C(4)	C(5)	C(6)	-85.6(4)
O(2)[1]	C(17)	O(2)	C(16)	6.2(2)
O(2)[1]	C(17)	O(2)	O(1)[1]	156.4(4)
O(2)[1]	C(16)	C(7)	C(8)	-168.1(11)

Atom	Atom	Atom	Atom	Angle/°
O(2)	C(16)	C(7)	C(8)[1]	-124.7(4)
O(2)	C(16)	C(7)	C(8)	-137.2(4)
O(2)[1]	C(16)	C(7)	C(8)[1]	-155.6(11)
O(2)[1]	C(16)	C(7)	C(6)	70.0(11)
O(2)	C(16)	C(7)	C(6)	100.9(2)
O(2)[1]	C(16)	C(7)	C(16)[1]	-37.6(11)
O(2)	C(16)	C(7)	C(16)[1]	-6.8(2)
O(2)	C(16)	C(7)	O(1)[1]	-9.72(16)
O(2)[1]	C(16)	C(7)	O(1)[1]	-40.6(11)
O(2)	C(16)	O(1)	O(2)[1]	-5.92(15)
O(2)[1]	C(16)	O(1)	C(16)[1]	35.7(9)
O(2)	C(16)	O(1)	C(16)[1]	29.8(7)
O(2)	C(16)	O(1)	C(7)[1]	-175.6(3)
O(2)[1]	C(16)	O(1)	C(7)[1]	-169.7(3)
C(15A)	C(13)	C(14)	C(14)[1]	151.1(3)
C(15A)[1]	C(13)	C(14)	C(14)[1]	31.9(3)
C(5)[1]	C(6)	C(5)	C(4)	85.0(5)
C(5)[1]	C(6)	C(5)	C(4)[1]	67.5(4)
C(5)[1]	C(6)	C(7)	C(8)[1]	-151.1(5)
C(5)[1]	C(6)	C(7)	C(8)	-135.9(5)
C(5)	C(6)	C(7)	C(8)[1]	-175.7(5)
C(5)	C(6)	C(7)	C(8)	-160.5(5)
C(5)	C(6)	C(7)	C(16)[1]	-11.0(4)
C(5)[1]	C(6)	C(7)	C(16)[1]	13.6(4)
C(5)	C(6)	C(7)	C(16)	-36.5(4)
C(5)[1]	C(6)	C(7)	C(16)	-11.9(4)
C(5)[1]	C(6)	C(7)	O(1)[1]	57.3(4)
C(5)	C(6)	C(7)	O(1)[1]	32.7(4)
C(7)	C(8)	C(11)	C(12)	66.2(6)
C(7)	C(8)	C(11)	C(10)	-165.5(4)
C(7)	C(8)	C(11)	C(8)[1]	-53.5(5)
C(7)	C(6)	C(5)	C(4)[1]	165.0(4)
C(7)	C(6)	C(5)	C(4)	-177.5(5)
C(7)[1]	C(6)	C(5)	C(4)[1]	134.8(4)
C(7)[1]	C(6)	C(5)	C(4)	152.3(5)
C(7)[1]	C(6)	C(7)	C(8)[1]	-80.2(5)
C(7)[1]	C(6)	C(7)	C(8)	-65.0(4)
C(7)[1]	C(6)	C(7)	C(16)[1]	84.5(2)
C(7)[1]	C(6)	C(7)	C(16)	59.04(17)
C(7)[1]	C(6)	C(7)	O(1)[1]	128.20(15)
C(7)	C(16)	O(1)	O(2)[1]	172.2(3)
C(7)	C(16)	O(1)	C(16)[1]	-152.1(11)
C(7)	C(16)	O(1)	C(7)[1]	2.46(10)
C(11)[1]	C(12)	C(11)	C(10)	-62.32(19)
C(11)[1]	C(12)	C(11)	C(8)	56.1(4)
C(11)[1]	C(12)	C(11)	C(8)[1]	70.5(5)
C(11)[1]	C(10)	C(11)	C(12)	62.06(19)
C(11)[1]	C(10)	C(11)	C(8)	-62.1(4)

Atom	Atom	Atom	Atom	Angle/°
C(11)[1]	C(10)	C(11)	C(8)[1]	-76.1(4)
C(11)	C(8)	C(7)	C(8)[1]	52.7(5)
C(11)	C(8)	C(7)	C(6)	-51.3(6)
C(11)	C(8)	C(7)	C(16)	-174.5(4)
C(11)	C(8)	C(7)	C(16)[1]	163.1(3)
C(11)	C(8)	C(7)	O(1)[1]	112.7(3)
C(13)[1]	N(1)	C(9)	O(3)	-19.9(13)
C(13)	N(1)	C(9)	O(3)	-19.9(13)
C(13)	N(1)	C(9)	N(1)[1]	76.2(9)
C(13)[1]	N(1)	C(9)	N(1)[1]	76.2(9)
C(13)	N(1)	C(9)	C(8)[1]	176.0(8)
C(13)[1]	N(1)	C(9)	C(8)[1]	176.0(8)
C(13)	N(1)	C(9)	C(8)	161.0(8)
C(13)[1]	N(1)	C(9)	C(8)	161.0(8)
C(13)[1]	N(1)	C(10)	N(1)[1]	-76.6(9)
C(13)	N(1)	C(10)	N(1)[1]	-76.6(9)
C(13)	N(1)	C(10)	C(11)[1]	-152.8(7)
C(13)[1]	N(1)	C(10)	C(11)[1]	-152.8(7)
C(13)	N(1)	C(10)	C(11)	176.4(8)
C(13)[1]	N(1)	C(10)	C(11)	176.4(8)
C(13)[1]	N(1)	C(13)	N(1)[1]	0(100)
C(13)[1]	N(1)	C(13)	C(15A)	0(100)
C(13)[1]	N(1)	C(13)	C(15A)[1]	0(100)
C(13)[1]	N(1)	C(13)	C(14)	0(100)
C(13)[1]	N(1)	C(13)	C(14)[1]	0(100)
C(13)[1]	N(1)	C(13)	C(15)	0(100)
C(13)[1]	N(1)	C(13)	C(15)[1]	0(100)
C(13)[1]	C(15A)	C(13)	N(1)[1]	0(100)
C(13)[1]	C(15A)	C(13)	N(1)	0(100)
C(13)[1]	C(15A)	C(13)	C(15A)[1]	0(100)
C(13)[1]	C(15A)	C(13)	C(14)[1]	0(100)
C(13)[1]	C(15A)	C(13)	C(14)	0(100)
C(13)[1]	C(13)	C(14)	C(14)[1]	0.0(5)
C(14)[1]	C(13)	C(15)	C(13)[1]	0(100)
C(14)	C(13)	C(15)	C(13)[1]	0(100)
C(15)[1]	C(13)	C(14)	C(14)[1]	32.2(3)
C(15)	C(13)	C(14)	C(14)[1]	153.8(3)
C(15)[1]	C(13)	C(15)	C(13)[1]	0(100)
O(1)[1]	O(2)	C(16)	O(2)[1]	-174.75(13)
O(1)[1]	O(2)	C(16)	C(7)	13.4(2)
O(1)[1]	O(2)	C(16)	O(1)	-168.3(3)
O(1)[1]	C(16)	C(7)	C(8)	-127.5(3)
O(1)[1]	C(16)	C(7)	C(8)[1]	-115.0(4)
O(1)	C(16)	C(7)	C(8)	44.5(4)
O(1)	C(16)	C(7)	C(8)[1]	57.0(5)
O(1)	C(16)	C(7)	C(6)	-77.4(3)
O(1)[1]	C(16)	C(7)	C(6)	110.6(2)
O(1)[1]	C(16)	C(7)	C(16)[1]	2.95(11)

Atom	Atom	Atom	Atom	Angle/°
O(1)	C(16)	C(7)	C(16)[1]	174.92(19)
O(1)	C(16)	C(7)	O(1)[1]	172.0(3)
O(1)[1]	C(16)	O(1)	O(2)[1]	-35.7(8)

Atom	Atom	Atom	Atom	Angle/°
O(1)[1]	C(16)	O(1)	C(16)[1]	0.01(3)
O(1)[1]	C(16)	O(1)	C(7)[1]	154.6(9)

Table 7: Hydrogen Fractional Atomic Coordinates ($\times 10^4$) and Equivalent Isotropic Displacement Parameters ($Å^2 \times 10^3$) for **189**. U_{eq} is defined as 1/3 of the trace of the orthogonalized U_{ij}.

Atom	x	y	z	U_{eq}
H(4)	6918(13)	7190(50)	3400(20)	30(9)
H(5)	5820(14)	6990(30)	2410(20)	23(7)
H(2)	5958(14)	7500	6800(30)	50(7)
H(10)	3239(10)	8500(30)	6536(19)	52(5)
H(11)	4047(16)	5680(50)	5410(30)	33(8)
H(17A)	4886(18)	8460(40)	-390(30)	111(10)
H(17B)	4230(20)	7500	-290(30)	72(10)
H(15A)	1964(9)	9270(20)	3543(19)	43(5)
H(15B)	1323(12)	9140(30)	4384(19)	62(6)
H(15C)	2039(14)	10290(40)	4890(30)	103(9)
H(14A)	2021(15)	8990(40)	6630(30)	20(7)
H(14B)	2090(20)	7500	6910(40)	95(13)
H(14C)	1360(20)	7500	6340(40)	99(13)
H(8)	4064(19)	9000(50)	4280(30)	44(10)
H(12A)	4742(10)	7900(30)	7080(20)	5(6)
H(7)	4466(15)	5760(50)	3210(30)	25(7)
H(12B)	4610(17)	8780(50)	6520(30)	40(9)
H(3)	6991(14)	7500	5590(20)	43(7)

Table 8: Atomic Occupancies for all atoms that are not fully occupied in **189**.

Atom	Occupancy
N(1)	0.5
C(8)	0.5
C(6)	0.5
C(4)	0.5
O(2)	0.5
C(15A)	0.5
C(5)	0.5
C(16)	0.5
C(7)	0.5
C(11)	0.5
C(14)	0.5
C(15)	0.5
H(4)	0.5
H(5)	0.5
H(11)	0.5
H(14A)	0.5
H(8)	0.5
H(12A)	0.5
O(1)	0.5

Atom	Occupancy
H(7)	0.5
H(12B)	0.5

(±)-*tert*-Butyl-2-oxo-6,7-diphenyl-3-azabicyclo[3.2.0]heptane-3-carboxylate (225)

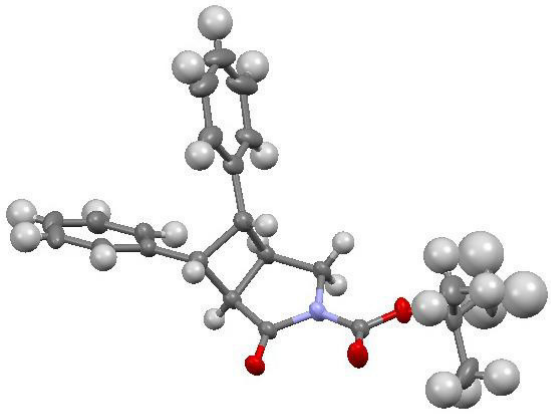

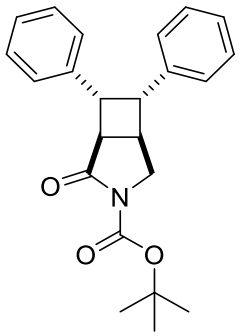

Table 1: Crystal data and structure refinement for **225**.

Chemical formula	$C_{23}H_{25}NO_3$
M_r	363.44
Crystal system, space group	Monoclinic, $P2_1/n$
Temperature (K)	123
a, b, c (Å)	14.0383 (7), 6.5220 (3), 22.5569 (11)
β (°)	100.806 (4)
V (Å^3)	2028.64 (17)
Z	4
Radiation type	Cu $K\alpha$
μ (mm^{-1})	0.63
Crystal size (mm)	0.23 × 0.21 × 0.08
F(000)	776
Diffractometer	SuperNova, Single source at offset, Atlas
Absorption correction	Gaussian *CrysAlis PRO* 1.171.38.42b (Rigaku Oxford Diffraction, 2015) Numerical absorption correction based on gaussian integration over a multifaceted crystal model Empirical absorption correction using spherical harmonics, implemented in SCALE3 ABSPACK scaling algorithm.

T_{min}, T_{max}	0.763, 1.000
No. of measured, independent and observed [$I > 2\sigma(I)$] reflections	6395, 6395, 5371
R_{int}	-1.0
$(\sin \theta/\lambda)_{max}$ (Å^{-1})	0.622
$R[F^2 > 2\sigma(F^2)]$, $wR(F^2)$, S	0.048, 0.138, 1.05
No. of reflections	6395
No. of parameters	248
H-atom treatment	H-atom parameters constrained
$\Delta\rho_{max}$, $\Delta\rho_{min}$ (e Å^{-3})	0.27, −0.23

Table 2: Fractional Atomic Coordinates (×10^4) and Equivalent Isotropic Displacement Parameters (Å^2×10^3) for **225**. U_{eq} is defined as 1/3 of the trace of the orthogonalized U_{ij}.

Atom	**x**	**y**	**z**	U_{eq}
O(3)	2943.6(7)	1916.4(16)	7079.5(5)	33.7(3)
O(1)	136.6(7)	3688.2(16)	6307.8(6)	35.3(3)
O(2)	1081.8(8)	856.8(17)	6469.6(6)	44.1(3)
N(1)	1716.8(8)	4105.7(19)	6616.3(6)	29.7(3)
C(6)	2661.3(10)	3599(2)	6900.5(7)	28.5(3)
C(7)	3270.9(10)	5529(2)	6945.2(7)	28.0(3)
C(5)	969.4(10)	2677(2)	6464.1(6)	29.3(3)
C(8)	2610.5(10)	7092(2)	6553.2(7)	29.3(3)
C(9)	1573.8(10)	6322(2)	6491.1(8)	31.1(3)
C(10)	3132.3(11)	6526(2)	6027.7(7)	33.6(3)
C(11)	3981.8(10)	5514(2)	6492.4(7)	32.5(3)
C(12)	4877.8(11)	6802(3)	6686.4(8)	34.8(4)
C(18)	3328.9(12)	8081(3)	5574.7(8)	38.4(4)
C(13)	5783.5(12)	5999(3)	6648.4(8)	44.1(4)
C(2)	-768(1)	2578(3)	6053.2(8)	42.3(4)
C(17)	4840.5(12)	8785(3)	6914.0(9)	43.6(4)
C(19)	2961.4(15)	10045(3)	5559.6(9)	48.1(4)
C(23)	3844.4(14)	7480(4)	5132.0(8)	53.1(5)
C(16)	5681.2(13)	9933(3)	7089.4(9)	51.1(5)
C(14)	6622.3(12)	7161(4)	6826.7(8)	56.9(6)
C(15)	6573.8(13)	9119(4)	7042.7(9)	56.9(6)
C(20)	3106.4(19)	11397(4)	5102.4(10)	63.9(6)
C(21)	3614(2)	10784(4)	4666.9(10)	73.0(8)
C(22)	3982.2(18)	8838(4)	4681.9(10)	67.0(7)
C(3)	-1022.9(15)	1057(4)	6504.1(11)	65.0(7)
C(4)	-644.7(17)	1566(4)	5474.3(10)	63.0(6)
C(1)	-1490.1(15)	4327(4)	5946(2)	105.7(14)

Table 3: Anisotropic Displacement Parameters ($\times 10^4$) **225**. The anisotropic displacement factor exponent takes the form: $-2p^2[h^2a^{*2} \times U_{11} + ... + 2hka^* \times b^* \times U_{12}]$

Atom	U_{11}	U_{22}	U_{33}	U_{23}	U_{13}	U_{12}
O(3)	30.5(5)	28.1(5)	39.0(6)	8.0(4)	-2.7(5)	0.5(4)
O(1)	23.1(5)	34.2(6)	44.6(7)	-6.4(5)	-4.1(5)	-1.7(4)
O(2)	33.7(5)	27.2(6)	65.7(9)	7.2(5)	-5.3(5)	-5.0(4)
N(1)	25.8(6)	25.9(6)	33.7(7)	4.6(5)	-4.2(5)	-1.9(4)
C(6)	26.3(6)	28.6(7)	28.3(8)	4.3(5)	-1.0(6)	-0.9(5)
C(7)	26.8(6)	26.2(7)	28.3(7)	3.1(5)	-1.9(6)	-2.6(5)
C(5)	26.7(6)	30.1(8)	28.7(7)	2.4(6)	-1.0(6)	-3.1(5)
C(8)	28.0(6)	25.2(6)	31.4(8)	4.4(5)	-2.8(6)	-2.6(5)
C(9)	26.9(6)	25.2(7)	37.6(9)	5.7(6)	-3.4(6)	-0.7(5)
C(10)	32.8(7)	33.9(8)	30.7(8)	0.8(6)	-2.5(6)	-7.2(6)
C(11)	30.2(7)	31.1(8)	34.8(8)	1.7(6)	2.5(6)	-1.9(5)
C(12)	28.2(7)	41.7(9)	31.9(9)	10.5(6)	-0.8(6)	-3.6(6)
C(18)	38.0(7)	45.7(9)	26.0(8)	3.5(6)	-8.3(6)	-17.1(7)
C(13)	34.5(8)	66.9(12)	30.6(9)	10.3(8)	5.5(7)	3.2(7)
C(2)	24.3(6)	47.3(10)	51.2(10)	-13.0(9)	-3.7(7)	-6.0(6)
C(17)	34.0(8)	41.2(9)	50.3(11)	6.3(7)	-6.0(7)	-8.1(7)
C(19)	60.7(10)	45.9(10)	30.7(9)	8.3(7)	-9.9(8)	-15.8(8)
C(23)	49.5(9)	71.0(14)	36.2(10)	-0.1(10)	1.5(8)	-21.9(10)
C(16)	45.3(9)	54.0(11)	47.0(11)	11.3(9)	-9.2(8)	-19.3(8)
C(14)	27.7(7)	110.6(18)	31.6(9)	13.1(11)	3.1(7)	-4.5(9)
C(15)	37.9(9)	96.7(17)	32.6(10)	8.8(10)	-2.2(8)	-30.5(10)
C(20)	84.0(15)	54.4(12)	41.7(12)	17.4(9)	-18.1(11)	-26.0(11)
C(21)	89.1(16)	90.1(18)	31.3(11)	18.8(11)	-10.5(11)	-52.1(15)
C(22)	69.0(13)	95.2(19)	34.9(11)	2.8(11)	5(1)	-40.6(13)
C(3)	46.5(10)	92.6(17)	58.3(14)	-15.6(12)	16(1)	-35.0(11)
C(4)	57.5(11)	87.0(17)	39.0(11)	-15.2(10)	-5.2(9)	-19.5(10)
C(1)	27.4(9)	76.9(18)	194(4)	-33(2)	-28.7(15)	10.9(10)

Table 4: Bond Lengths in Å for **225**.

Atom	Atom	Length/Å
O(3)	C(6)	1.2103(18)
O(1)	C(5)	1.3310(17)
O(1)	C(2)	1.4808(17)
O(2)	C(5)	1.1972(19)
N(1)	C(6)	1.3998(18)
N(1)	C(5)	1.3972(18)
N(1)	C(9)	1.4790(18)
C(6)	C(7)	1.5147(19)
C(7)	C(8)	1.540(2)
C(7)	C(11)	1.5560(19)
C(8)	C(9)	1.5210(18)
C(8)	C(10)	1.550(2)
C(10)	C(11)	1.577(2)
C(10)	C(18)	1.501(2)
C(11)	C(12)	1.508(2)

Atom	Atom	Length/Å
C(12)	C(13)	1.392(2)
C(12)	C(17)	1.396(3)
C(18)	C(19)	1.379(3)
C(18)	C(23)	1.395(3)
C(13)	C(14)	1.395(3)
C(2)	C(3)	1.511(3)
C(2)	C(4)	1.502(3)
C(2)	C(1)	1.515(3)
C(17)	C(16)	1.391(2)
C(19)	C(20)	1.400(3)
C(23)	C(22)	1.388(3)
C(16)	C(15)	1.383(3)
C(14)	C(15)	1.373(3)
C(20)	C(21)	1.376(4)
C(21)	C(22)	1.368(4)

Table 5: Bond Angles in ° for **225**.

Atom	Atom	Atom	Angle/°
C(5)	O(1)	C(2)	120.48(12)
C(6)	N(1)	C(9)	113.64(11)
C(5)	N(1)	C(6)	123.94(12)
C(5)	N(1)	C(9)	122.42(12)
O(3)	C(6)	N(1)	126.13(13)
O(3)	C(6)	C(7)	125.86(12)
N(1)	C(6)	C(7)	108.02(12)
C(6)	C(7)	C(8)	103.88(11)
C(6)	C(7)	C(11)	112.02(12)
C(8)	C(7)	C(11)	91.06(11)
O(1)	C(5)	N(1)	108.45(12)
O(2)	C(5)	O(1)	126.98(13)
O(2)	C(5)	N(1)	124.56(13)
C(7)	C(8)	C(10)	87.79(11)
C(9)	C(8)	C(7)	107.27(11)
C(9)	C(8)	C(10)	115.60(13)
N(1)	C(9)	C(8)	102.24(11)
C(8)	C(10)	C(11)	89.90(11)
C(18)	C(10)	C(8)	122.22(14)
C(18)	C(10)	C(11)	121.49(13)
C(7)	C(11)	C(10)	86.30(10)
C(12)	C(11)	C(7)	114.14(13)
C(12)	C(11)	C(10)	116.45(13)
C(13)	C(12)	C(11)	119.64(16)
C(13)	C(12)	C(17)	117.94(16)
C(17)	C(12)	C(11)	122.41(14)
C(19)	C(18)	C(10)	121.91(16)
C(19)	C(18)	C(23)	119.02(17)
C(23)	C(18)	C(10)	118.94(17)
C(12)	C(13)	C(14)	120.6(2)
O(1)	C(2)	C(3)	110.74(15)
O(1)	C(2)	C(4)	108.77(14)
O(1)	C(2)	C(1)	101.16(14)
C(3)	C(2)	C(1)	111.5(2)
C(4)	C(2)	C(3)	112.13(18)
C(4)	C(2)	C(1)	112.0(2)
C(16)	C(17)	C(12)	120.99(18)
C(18)	C(19)	C(20)	119.9(2)
C(22)	C(23)	C(18)	120.4(2)
C(15)	C(16)	C(17)	120.3(2)
C(15)	C(14)	C(13)	120.83(18)
C(14)	C(15)	C(16)	119.34(17)
C(21)	C(20)	C(19)	120.6(2)
C(22)	C(21)	C(20)	119.73(19)
C(21)	C(22)	C(23)	120.4(2)

Table 6: Torsion Angles in ° for **225**

Atom	Atom	Atom	Atom	Angle/°
O(3)	C(6)	C(7)	C(8)	170.17(15)
O(3)	C(6)	C(7)	C(11)	73.25(19)
N(1)	C(6)	C(7)	C(8)	-9.82(15)
N(1)	C(6)	C(7)	C(11)	-106.74(14)
C(6)	N(1)	C(5)	O(1)	168.48(13)
C(6)	N(1)	C(5)	O(2)	-12.4(2)
C(6)	N(1)	C(9)	C(8)	16.81(17)
C(6)	C(7)	C(8)	C(9)	20.08(16)
C(6)	C(7)	C(8)	C(10)	-96.07(12)
C(6)	C(7)	C(11)	C(10)	88.78(13)
C(6)	C(7)	C(11)	C(12)	-153.82(13)
C(7)	C(8)	C(9)	N(1)	-22.11(16)
C(7)	C(8)	C(10)	C(11)	-16.70(10)
C(7)	C(8)	C(10)	C(18)	-144.74(14)
C(7)	C(11)	C(12)	C(13)	133.49(15)
C(7)	C(11)	C(12)	C(17)	-45.6(2)
C(5)	O(1)	C(2)	C(3)	62.2(2)
C(5)	O(1)	C(2)	C(4)	-61.5(2)
C(5)	O(1)	C(2)	C(1)	-179.5(2)
C(5)	N(1)	C(6)	O(3)	-4.2(2)
C(5)	N(1)	C(6)	C(7)	175.78(13)
C(5)	N(1)	C(9)	C(8)	-163.45(13)
C(8)	C(7)	C(11)	C(10)	-16.66(11)
C(8)	C(7)	C(11)	C(12)	100.74(14)
C(8)	C(10)	C(11)	C(7)	16.55(11)
C(8)	C(10)	C(11)	C(12)	-98.64(14)
C(8)	C(10)	C(18)	C(19)	-7.4(2)
C(8)	C(10)	C(18)	C(23)	176.86(14)
C(9)	N(1)	C(6)	O(3)	175.53(15)
C(9)	N(1)	C(6)	C(7)	-4.48(17)
C(9)	N(1)	C(5)	O(1)	-11.23(19)
C(9)	N(1)	C(5)	O(2)	167.86(16)
C(9)	C(8)	C(10)	C(11)	-124.81(13)
C(9)	C(8)	C(10)	C(18)	107.14(16)
C(10)	C(8)	C(9)	N(1)	73.87(15)
C(10)	C(11)	C(12)	C(13)	-128.23(16)
C(10)	C(11)	C(12)	C(17)	52.7(2)
C(10)	C(18)	C(19)	C(20)	-175.47(16)
C(10)	C(18)	C(23)	C(22)	175.61(17)
C(11)	C(7)	C(8)	C(9)	133.09(13)
C(11)	C(7)	C(8)	C(10)	16.93(11)
C(11)	C(10)	C(18)	C(19)	-120.00(18)
C(11)	C(10)	C(18)	C(23)	64.3(2)
C(11)	C(12)	C(13)	C(14)	-179.84(16)
C(11)	C(12)	C(17)	C(16)	179.97(17)
C(12)	C(13)	C(14)	C(15)	-0.1(3)
C(12)	C(17)	C(16)	C(15)	-0.2(3)

Atom	Atom	Atom	Atom	Angle/°
C(18)	C(10)	C(11)	C(7)	145.17(15)
C(18)	C(10)	C(11)	C(12)	30.0(2)
C(18)	C(19)	C(20)	C(21)	0.0(3)
C(18)	C(23)	C(22)	C(21)	0.0(3)
C(13)	C(12)	C(17)	C(16)	0.9(3)
C(13)	C(14)	C(15)	C(16)	0.7(3)
C(2)	O(1)	C(5)	O(2)	-6.5(2)
C(2)	O(1)	C(5)	N(1)	172.59(13)
C(17)	C(12)	C(13)	C(14)	-0.7(2)
C(17)	C(16)	C(15)	C(14)	-0.6(3)
C(19)	C(18)	C(23)	C(22)	-0.2(3)
C(19)	C(20)	C(21)	C(22)	-0.2(3)
C(23)	C(18)	C(19)	C(20)	0.2(3)
C(20)	C(21)	C(22)	C(23)	0.2(3)

Table 7: Hydrogen Fractional Atomic Coordinates ($\times 10^4$) and Equivalent Isotropic Displacement Parameters ($Å^2 \times 10^3$) for **225**. U_{eq} is defined as 1/3 of the trace of the orthogonalized U_{ij}.

Atom	x	y	z	U_{eq}
H(7)	3548	5982	7356	34
H(8)	2705	8515	6691	35
H(9A)	1244	6973	6782	37
H(9B)	1208	6558	6088	37
H(10)	2763	5409	5802	40
H(11)	4133	4123	6374	39
H(13)	5829	4676	6503	53
H(17)	4245	9347	6949	52
H(19)	2618	10471	5852	58
H(23)	4097	6161	5138	64
H(16)	5643	11254	7239	61
H(14)	7222	6603	6799	68
H(15)	7136	9891	7157	68
H(20)	2858	12721	5093	77
H(21)	3705	11688	4364	88
H(22)	4327	8424	4389	80
H(3A)	-549	-22	6566	98
H(3B)	-1652	486	6353	98
H(3C)	-1030	1739	6880	98
H(4A)	-432	2562	5214	95
H(4B)	-1253	995	5278	95
H(4C)	-171	493	5560	95
H(1A)	-1475	5064	6316	159
H(1B)	-2129	3788	5807	159
H(1C)	-1323	5236	5647	159

(±)-*cis*-3-(*tert*-Butyl)-6-phenyl-3-azabicyclo[3.2.0]heptan-2-one (158ib)

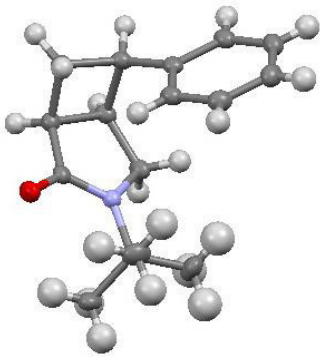

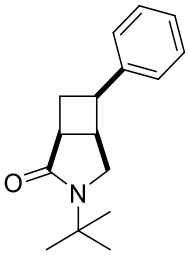

Table 1: Crystal data and structure refinement for **158ib**.

Chemical formula	$C_{16}H_{21}NO$
M_r	243.34
Crystal system, space group	Monoclinic, $P2_1/c$
Temperature (K)	123
a, b, c (Å)	9.89130 (17), 24.3530 (4), 11.16173 (17)
β (°)	90.4878 (14)
V (Å^3)	2688.57 (8)
Z	8
Radiation type	Cu $K\alpha$
μ (mm^{-1})	0.57
Crystal size (mm)	0.20 × 0.14 × 0.04
F(000)	1056
Diffractometer	SuperNova, Single source at offset, Atlas
Absorption correction	Gaussian *CrysAlis PRO* 1.171.38.42b (Rigaku Oxford Diffraction, 2015) Numerical absorption correction based on gaussian integration over a multifaceted crystal model Empirical absorption correction using spherical harmonics, implemented in SCALE3 ABSPACK scaling algorithm.

T_{min}, T_{max}	0.991, 0.997
No. of measured, independent and observed [$I > 2\sigma(I)$] reflections	28853, 5625, 4815
R_{int}	0.032
$(\sin \theta/\lambda)_{max}$ (Å^{-1})	0.630
$R[F^2 > 2\sigma(F^2)]$, $wR(F^2)$, S	0.040, 0.108, 1.03
No. of reflections	5625
No. of parameters	331
H-atom treatment	H-atom parameters constrained
$\Delta\rho_{max}$, $\Delta\rho_{min}$ (e Å^{-3})	0.26, −0.19

Table 2: Fractional Atomic Coordinates (×10^4) and Equivalent Isotropic Displacement Parameters (Å^2×10^3) for **158ib**. U_{eq} is defined as 1/3 of the trace of the orthogonalized U_{ij}.

Atom	**x**	**y**	**z**	U_{eq}
O(2)	5081.4(9)	3179.8(4)	6974.6(7)	27.25(19)
O(1)	67.4(9)	1794.1(4)	5343.8(8)	27.77(19)
N(2)	7252.7(10)	3429.9(4)	6475.8(8)	21.6(2)
N(1)	2189(1)	1539.3(4)	6019.1(8)	22.1(2)
C(5)	1086.9(11)	1870.8(5)	5960.8(10)	21.4(2)
C(21)	6129.3(12)	3112.4(5)	6409.3(10)	21.2(2)
C(10)	1704.5(12)	1533.7(5)	9102.9(10)	22.8(2)
C(25)	6738.0(12)	3530.7(5)	3270.4(10)	23.6(2)
C(22)	6358.8(12)	2653.5(5)	5517.9(10)	23.1(2)
C(6)	1296.2(12)	2359.1(5)	6783.4(10)	23.1(2)
C(7)	2610.4(12)	2228.8(5)	7471(1)	23.4(2)
C(8)	3261.8(11)	1749.1(5)	6819.1(10)	24.6(2)
C(9)	1753.6(12)	2113.3(5)	8635.2(10)	22.9(2)
C(26)	7474.8(12)	3695.1(5)	2266.3(11)	27.3(3)
C(11)	914.0(12)	1127.1(5)	8561.6(10)	25.3(2)
C(16)	480.1(12)	2335.9(5)	7958.9(10)	24.4(2)
C(15)	2487.5(12)	1385.6(5)	10106(1)	25.5(2)
C(18)	7411.0(12)	3895.3(5)	7333.8(11)	25.2(2)
C(24)	6808.3(12)	2945.1(5)	3702.3(10)	23.6(2)
C(32)	8287.3(11)	3285.7(5)	5593.3(10)	24.9(2)
C(23)	5538.8(12)	2706.1(5)	4336.6(10)	24.4(2)
C(30)	5959.4(13)	3926.6(5)	3850.5(11)	26.2(2)
C(14)	2496.3(13)	846.9(6)	10523.9(11)	30.3(3)
C(31)	7667.7(12)	2815.0(5)	4872.5(10)	23.8(2)
C(2)	2388.7(13)	1059.1(5)	5210.6(11)	27.1(3)
C(13)	1717.9(14)	447.8(5)	9969.7(12)	31.8(3)
C(12)	915.4(14)	590.7(5)	8988.6(12)	30.1(3)

Atom	x	y	z	U_{eq}
C(29)	5920.0(14)	4466.6(5)	3452.0(12)	31.6(3)
C(27)	7449.4(14)	4236.8(6)	1875.7(11)	32.3(3)
C(28)	6670.2(15)	4623.9(6)	2465.5(12)	34.8(3)
C(19)	6390.8(16)	4343.1(6)	7019.9(13)	37.3(3)
C(3)	1203.6(17)	660.7(6)	5322.3(14)	39.4(3)
C(1)	2509.1(16)	1270.3(6)	3925.5(12)	36.3(3)
C(17)	7202.1(17)	3688.3(6)	8609.4(12)	39.6(3)
C(20)	8840.8(15)	4128.6(6)	7253.1(15)	41.0(3)
C(4)	3685.2(17)	756.6(7)	5571.9(15)	45.2(4)

Table 3: Anisotropic Displacement Parameters ($\times 10^4$) **158ib**. The anisotropic displacement factor exponent takes the form: $-2p^2[h^2a^{*2} \times U_{11} + ... + 2hka^* \times b^* \times U_{12}]$

Atom	U_{11}	U_{22}	U_{33}	U_{23}	U_{13}	U_{12}
O(2)	23.8(4)	35.1(5)	22.9(4)	-0.4(3)	4.2(3)	-2.6(4)
O(1)	23.6(4)	34.7(5)	24.9(4)	-0.8(3)	-3.9(3)	2.3(3)
N(2)	21.4(5)	22.0(5)	21.4(5)	0.0(4)	0.7(4)	-0.6(4)
N(1)	21.8(5)	24.8(5)	19.9(5)	-0.5(4)	-0.4(3)	1.9(4)
C(5)	22.4(5)	24.0(5)	17.7(5)	3.4(4)	2.1(4)	0.4(4)
C(21)	23.5(5)	22.8(5)	17.4(5)	3.1(4)	-0.6(4)	0.0(4)
C(10)	22.7(5)	26.7(6)	19.1(5)	-0.4(4)	5.5(4)	-0.8(4)
C(25)	23.1(5)	27.5(6)	20.2(5)	-1.3(4)	-4.1(4)	1.0(5)
C(22)	26.3(6)	20.7(5)	22.3(6)	1.4(4)	-1.6(4)	0.3(4)
C(6)	25.2(6)	22.1(5)	21.9(5)	2.0(4)	2.5(4)	-0.2(4)
C(7)	23.7(5)	25.9(6)	20.5(5)	0.6(4)	1.6(4)	-5.0(4)
C(8)	19.1(5)	33.0(6)	21.6(5)	0.9(5)	0.5(4)	-1.1(5)
C(9)	25.2(6)	24.4(6)	19.1(5)	-1.8(4)	2.0(4)	-3.0(4)
C(26)	24.7(6)	34.6(6)	22.4(6)	-1.7(5)	-2.2(4)	-0.6(5)
C(11)	25.6(6)	28.7(6)	21.6(5)	-0.4(4)	2.6(4)	-2.3(5)
C(16)	26.4(6)	23.7(6)	23.0(6)	-1.3(4)	3.6(4)	0.7(4)
C(15)	22.5(5)	32.7(6)	21.3(5)	-0.7(5)	3.0(4)	-1.1(5)
C(18)	28.3(6)	23.1(6)	24.3(6)	-2.0(4)	-3.4(4)	-0.4(5)
C(24)	25.0(6)	26.0(6)	19.8(5)	-2.9(4)	-0.3(4)	4.2(4)
C(32)	18.8(5)	32.9(6)	23.1(5)	0.7(5)	0.1(4)	0.8(5)
C(23)	25.5(6)	25.1(6)	22.5(6)	-2.5(4)	-2.1(4)	0.0(5)
C(30)	28.9(6)	28.8(6)	21.0(5)	-1.0(5)	-1.7(4)	3.6(5)
C(14)	29.5(6)	36.6(7)	24.7(6)	5.1(5)	2.9(5)	4.2(5)
C(31)	23.8(6)	26.8(6)	20.9(5)	0.3(4)	0.1(4)	5.9(5)
C(2)	31.8(6)	26.7(6)	22.9(6)	-2.2(5)	1.8(5)	5.2(5)
C(13)	35.7(7)	27.5(6)	32.3(6)	6.1(5)	7.7(5)	2.7(5)
C(12)	32.5(6)	27.3(6)	30.7(6)	-1.4(5)	5.7(5)	-4.9(5)
C(29)	39.4(7)	28.3(6)	27.2(6)	-2.8(5)	-6.0(5)	6.5(5)
C(27)	36.6(7)	36.8(7)	23.4(6)	3.2(5)	-2.3(5)	-7.8(6)
C(28)	49.0(8)	26.2(6)	29.1(6)	3.6(5)	-8.8(6)	-3.9(6)
C(19)	44.9(8)	27.5(6)	39.3(7)	-6.9(5)	-11.2(6)	8.0(6)
C(3)	51.8(9)	27.9(7)	38.6(7)	-6.6(6)	8.2(6)	-6.1(6)
C(1)	49.2(8)	35.8(7)	24.1(6)	-1.7(5)	8.4(5)	7.2(6)
C(17)	59.7(9)	36.3(7)	22.5(6)	-1.7(5)	-6.7(6)	-8.7(7)
C(20)	35.8(7)	35.8(7)	51.3(9)	-9.1(6)	-3.3(6)	-10.2(6)

Atom	U_{11}	U_{22}	U_{33}	U_{23}	U_{13}	U_{12}
C(4)	49.6(9)	41.1(8)	44.9(8)	-9.2(7)	-6.5(7)	21.5(7)

Table 4: Bond Lengths in Å for **158ib**.

Atom	Atom	Length/Å	Atom	Atom	Length/Å
O(2)	C(21)	1.2290(15)	C(7)	C(8)	1.5224(17)
O(1)	C(5)	1.2305(15)	C(7)	C(9)	1.5826(15)
N(2)	C(21)	1.3553(15)	C(9)	C(16)	1.5602(16)
N(2)	C(18)	1.4912(15)	C(26)	C(27)	1.3896(19)
N(2)	C(32)	1.4691(15)	C(11)	C(12)	1.3904(18)
N(1)	C(5)	1.3576(15)	C(15)	C(14)	1.3923(18)
N(1)	C(8)	1.4724(14)	C(18)	C(19)	1.5246(17)
N(1)	C(2)	1.4914(15)	C(18)	C(17)	1.5261(18)
C(5)	C(6)	1.5155(16)	C(18)	C(20)	1.5274(18)
C(21)	C(22)	1.5146(16)	C(24)	C(23)	1.5595(17)
C(10)	C(9)	1.5060(16)	C(24)	C(31)	1.5843(15)
C(10)	C(11)	1.3960(17)	C(32)	C(31)	1.5260(17)
C(10)	C(15)	1.4031(17)	C(30)	C(29)	1.3886(18)
C(25)	C(26)	1.4004(17)	C(14)	C(13)	1.383(2)
C(25)	C(24)	1.5068(17)	C(2)	C(3)	1.5275(19)
C(25)	C(30)	1.3966(17)	C(2)	C(1)	1.5294(17)
C(22)	C(23)	1.5475(16)	C(2)	C(4)	1.5300(19)
C(22)	C(31)	1.5380(16)	C(13)	C(12)	1.3913(19)
C(6)	C(7)	1.5370(16)	C(29)	C(28)	1.387(2)
C(6)	C(16)	1.5474(16)	C(27)	C(28)	1.387(2)

Table 5: Bond Angles in ° for **158ib**.

Atom	Atom	Atom	Angle/°	Atom	Atom	Atom	Angle/°
C(21)	N(2)	C(18)	123.40(10)	C(21)	C(22)	C(31)	104.51(9)
C(21)	N(2)	C(32)	113.73(9)	C(31)	C(22)	C(23)	90.97(9)
C(32)	N(2)	C(18)	122.84(10)	C(5)	C(6)	C(7)	104.54(9)
C(5)	N(1)	C(8)	113.40(10)	C(5)	C(6)	C(16)	114.55(10)
C(5)	N(1)	C(2)	123.21(10)	C(7)	C(6)	C(16)	90.81(9)
C(8)	N(1)	C(2)	122.71(10)	C(6)	C(7)	C(9)	89.44(9)
O(1)	C(5)	N(1)	126.19(11)	C(8)	C(7)	C(6)	106.22(9)
O(1)	C(5)	C(6)	124.42(11)	C(8)	C(7)	C(9)	119.20(10)
N(1)	C(5)	C(6)	109.39(10)	N(1)	C(8)	C(7)	104.49(9)
O(2)	C(21)	N(2)	126.17(11)	C(10)	C(9)	C(7)	118.05(10)
O(2)	C(21)	C(22)	124.59(11)	C(10)	C(9)	C(16)	117.72(10)
N(2)	C(21)	C(22)	109.24(10)	C(16)	C(9)	C(7)	88.67(8)
C(11)	C(10)	C(9)	122.30(11)	C(27)	C(26)	C(25)	120.94(12)
C(11)	C(10)	C(15)	117.80(11)	C(12)	C(11)	C(10)	121.27(12)
C(15)	C(10)	C(9)	119.89(11)	C(6)	C(16)	C(9)	89.89(9)
C(26)	C(25)	C(24)	120.24(11)	C(14)	C(15)	C(10)	120.76(12)
C(30)	C(25)	C(26)	117.81(11)	N(2)	C(18)	C(19)	109.29(10)
C(30)	C(25)	C(24)	121.95(11)	N(2)	C(18)	C(17)	109.50(10)
C(21)	C(22)	C(23)	114.73(10)	N(2)	C(18)	C(20)	109.70(10)

Atom	Atom	Atom	Angle/°
C(19)	C(18)	C(17)	110.86(12)
C(19)	C(18)	C(20)	109.37(11)
C(17)	C(18)	C(20)	108.10(12)
C(25)	C(24)	C(23)	117.61(10)
C(25)	C(24)	C(31)	118.43(10)
C(23)	C(24)	C(31)	88.82(9)
N(2)	C(32)	C(31)	104.72(9)
C(22)	C(23)	C(24)	89.97(9)
C(29)	C(30)	C(25)	121.29(12)
C(13)	C(14)	C(15)	120.70(12)
C(22)	C(31)	C(24)	89.40(9)
C(32)	C(31)	C(22)	106.33(9)

Atom	Atom	Atom	Angle/°
C(32)	C(31)	C(24)	119.64(10)
N(1)	C(2)	C(3)	110.06(10)
N(1)	C(2)	C(1)	108.39(10)
N(1)	C(2)	C(4)	109.46(11)
C(3)	C(2)	C(1)	110.86(12)
C(3)	C(2)	C(4)	108.34(12)
C(1)	C(2)	C(4)	109.71(12)
C(14)	C(13)	C(12)	119.21(12)
C(11)	C(12)	C(13)	120.25(12)
C(28)	C(29)	C(30)	120.14(12)
C(28)	C(27)	C(26)	120.33(12)
C(29)	C(28)	C(27)	119.48(12)

Table 6: Torsion Angles in ° for **158ib**.

Atom	Atom	Atom	Atom	Angle/°
O(2)	C(21)	C(22)	C(23)	70.53(15)
O(2)	C(21)	C(22)	C(31)	168.49(11)
O(1)	C(5)	C(6)	C(7)	172.53(11)
O(1)	C(5)	C(6)	C(16)	74.79(14)
N(2)	C(21)	C(22)	C(23)	-109.42(11)
N(2)	C(21)	C(22)	C(31)	-11.46(12)
N(2)	C(32)	C(31)	C(22)	-8.35(12)
N(2)	C(32)	C(31)	C(24)	90.51(12)
N(1)	C(5)	C(6)	C(7)	-7.41(12)
N(1)	C(5)	C(6)	C(16)	-105.14(11)
C(5)	N(1)	C(8)	C(7)	9.75(12)
C(5)	N(1)	C(2)	C(3)	-57.46(15)
C(5)	N(1)	C(2)	C(1)	63.93(15)
C(5)	N(1)	C(2)	C(4)	-176.43(12)
C(5)	C(6)	C(7)	C(8)	12.97(12)
C(5)	C(6)	C(7)	C(9)	-107.38(9)
C(5)	C(6)	C(16)	C(9)	98.02(11)
C(21)	N(2)	C(18)	C(19)	-65.48(14)
C(21)	N(2)	C(18)	C(17)	56.13(15)
C(21)	N(2)	C(18)	C(20)	174.61(11)
C(21)	N(2)	C(32)	C(31)	1.27(13)
C(21)	C(22)	C(23)	C(24)	99.43(10)
C(21)	C(22)	C(31)	C(24)	-108.94(9)
C(21)	C(22)	C(31)	C(32)	11.87(12)
C(10)	C(9)	C(16)	C(6)	-113.12(10)
C(10)	C(11)	C(12)	C(13)	-0.30(19)
C(10)	C(15)	C(14)	C(13)	-0.95(19)
C(25)	C(26)	C(27)	C(28)	-1.13(19)
C(25)	C(24)	C(23)	C(22)	-114.93(10)
C(25)	C(24)	C(31)	C(22)	114.18(11)
C(25)	C(24)	C(31)	C(32)	5.67(16)
C(25)	C(30)	C(29)	C(28)	-0.50(19)
C(6)	C(7)	C(8)	N(1)	-13.70(12)
C(6)	C(7)	C(9)	C(10)	112.77(11)
C(6)	C(7)	C(9)	C(16)	-8.21(9)
C(7)	C(6)	C(16)	C(9)	-8.39(9)
C(7)	C(9)	C(16)	C(6)	8.15(9)
C(8)	N(1)	C(5)	O(1)	178.62(11)
C(8)	N(1)	C(5)	C(6)	-1.45(13)
C(8)	N(1)	C(2)	C(3)	132.60(12)
C(8)	N(1)	C(2)	C(1)	-106.00(13)
C(8)	N(1)	C(2)	C(4)	13.64(16)
C(8)	C(7)	C(9)	C(10)	4.44(15)
C(8)	C(7)	C(9)	C(16)	-116.54(11)
C(9)	C(10)	C(11)	C(12)	178.09(11)
C(9)	C(10)	C(15)	C(14)	-177.50(11)
C(9)	C(7)	C(8)	N(1)	84.98(12)
C(26)	C(25)	C(24)	C(23)	-150.01(11)
C(26)	C(25)	C(24)	C(31)	105.11(12)
C(26)	C(25)	C(30)	C(29)	-0.35(18)
C(26)	C(27)	C(28)	C(29)	0.3(2)
C(11)	C(10)	C(9)	C(7)	-76.14(14)
C(11)	C(10)	C(9)	C(16)	28.35(16)
C(11)	C(10)	C(15)	C(14)	1.58(17)
C(16)	C(6)	C(7)	C(8)	128.62(9)
C(16)	C(6)	C(7)	C(9)	8.27(9)
C(15)	C(10)	C(9)	C(7)	102.90(12)
C(15)	C(10)	C(9)	C(16)	-152.62(10)
C(15)	C(10)	C(11)	C(12)	-0.96(17)
C(15)	C(14)	C(13)	C(12)	-0.34(19)
C(18)	N(2)	C(21)	O(2)	4.63(18)
C(18)	N(2)	C(21)	C(22)	-175.42(10)
C(18)	N(2)	C(32)	C(31)	-176.72(10)
C(24)	C(25)	C(26)	C(27)	-178.27(11)
C(24)	C(25)	C(30)	C(29)	179.06(11)
C(32)	N(2)	C(21)	O(2)	-173.35(11)
C(32)	N(2)	C(21)	C(22)	6.60(13)
C(32)	N(2)	C(18)	C(19)	112.32(13)
C(32)	N(2)	C(18)	C(17)	-126.07(12)
C(32)	N(2)	C(18)	C(20)	-7.59(15)
C(23)	C(22)	C(31)	C(24)	6.94(9)
C(23)	C(22)	C(31)	C(32)	127.76(9)
C(23)	C(24)	C(31)	C(22)	-6.89(9)
C(23)	C(24)	C(31)	C(32)	-115.40(11)
C(30)	C(25)	C(26)	C(27)	1.16(17)
C(30)	C(25)	C(24)	C(23)	30.58(16)
C(30)	C(25)	C(24)	C(31)	-74.30(15)
C(30)	C(29)	C(28)	C(27)	0.6(2)
C(14)	C(13)	C(12)	C(11)	0.96(19)
C(31)	C(22)	C(23)	C(24)	-7.05(9)
C(31)	C(24)	C(23)	C(22)	6.85(9)
C(2)	N(1)	C(5)	O(1)	7.84(18)
C(2)	N(1)	C(5)	C(6)	-172.23(10)
C(2)	N(1)	C(8)	C(7)	-179.42(10)

Table 7: Hydrogen Fractional Atomic Coordinates ($\times 10^4$) and Equivalent Isotropic Displacement Parameters ($Å^2 \times 10^3$) for **158ib**. U_{eq} is defined as 1/3 of the trace of the orthogonalized U_{ij}.

Atom	x	y	z	U_{eq}
H(22)	6367	2284	5867	28
H(6)	1286	2717	6380	28
H(7)	3211	2547	7553	28
H(8A)	4036	1871	6363	30
H(8B)	3552	1468	7381	30
H(9)	2020	2367	9277	27
H(26)	7988	3438	1855	33
H(11)	376	1217	7903	30
H(16A)	-267	2078	7933	29
H(16B)	183	2693	8238	29
H(15)	3007	1650	10496	31
H(24)	7084	2703	3047	28
H(32A)	9116	3170	5989	30
H(32B)	8484	3596	5079	30
H(23A)	4791	2963	4384	29
H(23B)	5241	2357	4012	29
H(30)	5458	3827	4517	31
H(14)	3031	755	11183	36
H(31)	8289	2506	4769	29
H(13)	1731	88	10249	38
H(12)	378	327	8617	36
H(29)	5389	4723	3847	38
H(27)	7957	4340	1216	39
H(28)	6651	4986	2201	42
H(19A)	6555	4474	6223	56
H(19B)	6483	4641	7577	56
H(19C)	5492	4196	7062	56
H(3A)	1127	544	6140	59
H(3B)	1356	347	4820	59
H(3C)	384	841	5077	59
H(1A)	1707	1471	3712	54
H(1B)	2615	965	3390	54
H(1C)	3281	1507	3868	54
H(17A)	6312	3535	8677	59
H(17B)	7299	3988	9161	59
H(17C)	7863	3412	8793	59
H(20A)	9485	3847	7446	61
H(20B)	8940	4427	7808	61
H(20C)	8996	4259	6454	61
H(4A)	4444	999	5491	68
H(4B)	3804	443	5062	68
H(4C)	3621	638	6390	68

(±)-*trans-tert*-Butyl-2-oxo-6-phenyl-3-azabicyclo[3.2.0]heptane-3-carboxylate (158ka)

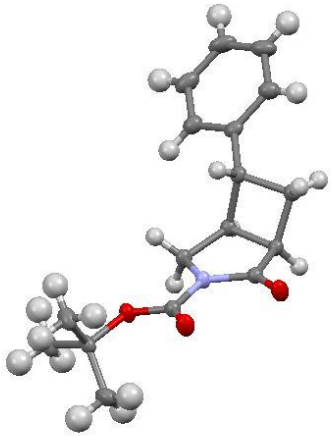

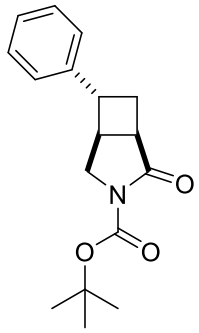

Table 1: Crystal data and structure refinement for **158ka**.

Chemical formula	$C_{17}H_{21}NO_3$
M_r	287.35
Crystal system, space group	Monoclinic, $P2_1/c$
Temperature (K)	123
a, b, c (Å)	9.3829 (2), 26.3989 (5), 6.1630 (1)
β (°)	94.269 (2)
V (Å^3)	1522.33 (5)
Z	4
Radiation type	Cu $K\alpha$
μ (mm^{-1})	0.69
Crystal size (mm)	0.23 × 0.07 × 0.04
F(000)	616
Diffractometer	GV1000, TitanS2
Absorption correction	Gaussian *CrysAlis PRO* 1.171.38.46 (Rigaku Oxford Diffraction, 2015) Numerical absorption correction based on gaussian integration over a multifaceted crystal model Empirical absorption correction using spherical harmonics, implemented in SCALE3 ABSPACK scaling algorithm.

T_{min}, T_{max}	0.777, 1.000
No. of measured, independent and observed [$I > 2\sigma(I)$] reflections	32136, 3039, 2705
R_{int}	0.051
$(\sin \theta/\lambda)_{max}$ (Å^{-1})	0.622
$R[F^2 > 2\sigma(F^2)]$, $wR(F^2)$, S	0.034, 0.090, 1.04
No. of reflections	3039
No. of parameters	193
H-atom treatment	H-atom parameters constrained
$\Delta\rho_{max}$, $\Delta\rho_{min}$ (e Å^{-3})	0.23, −0.18

Table 2: Fractional Atomic Coordinates (×10^4) and Equivalent Isotropic Displacement Parameters (Å^2×10^3) for **158ka**. U_{eq} is defined as 1/3 of the trace of the orthogonalized U_{ij}.

Atom	x	y	z	U_{eq}
O(3)	3614.8(8)	4397.9(3)	7361.0(12)	24.27(18)
O(2)	3418.3(9)	4120.5(3)	10822.3(13)	29.5(2)
O(1)	4790.2(9)	3186.8(3)	11455.3(13)	29.6(2)
N(1)	4850.3(9)	3720.3(3)	8461.0(14)	20.2(2)
C(13)	3886.6(11)	4090.3(4)	9070.3(17)	21.2(2)
C(2)	6092.8(11)	2946.8(4)	8358.3(17)	20.5(2)
C(1)	5173.8(11)	3282.2(4)	9668.1(17)	20.6(2)
C(3)	6501.3(11)	3284.7(4)	6461.0(17)	20.1(2)
C(4)	7994.2(11)	3371.5(4)	7700.8(17)	20.8(2)
C(5)	7674.5(11)	2932.1(4)	9270.7(17)	22.5(2)
C(6)	9296.8(11)	3337.4(4)	6422.1(18)	23.2(2)
C(12)	5446.5(11)	3724.0(4)	6309.1(17)	22.1(2)
C(14)	2548.2(12)	4807.6(4)	7407.3(18)	24.9(2)
C(7)	9301.9(13)	3572.9(4)	4394.6(19)	27.8(2)
C(11)	10516.6(12)	3079.4(5)	7220(2)	30.1(3)
C(15)	3127.4(14)	5224.7(4)	8922(2)	33.7(3)
C(8)	10500.9(14)	3554.5(5)	3211(2)	35.5(3)
C(17)	1127.2(13)	4602.4(5)	8034(2)	37.2(3)
C(10)	11714.6(13)	3058.5(5)	6017(2)	37.7(3)
C(16)	2456.4(15)	4981.9(5)	5054(2)	35.1(3)
C(9)	11711.4(13)	3296.7(5)	4016(2)	38.2(3)

Table 3: Anisotropic Displacement Parameters (×10^4) **158ka**. The anisotropic displacement factor exponent takes the form: $-2p^2[h^2a^{*2} \times U_{11} + ... + 2hka^* \times b^* \times U_{12}]$

Atom	U_{11}	U_{22}	U_{33}	U_{23}	U_{13}	U_{12}
O(3)	27.9(4)	22.3(4)	22.9(4)	2.2(3)	3.6(3)	7.3(3)
O(2)	36.3(4)	29.0(4)	24.2(4)	0.3(3)	10.0(3)	8.4(3)
O(1)	33.6(4)	32.0(4)	24.4(4)	8.2(3)	10.9(3)	8.4(3)

Atom	U_{11}	U_{22}	U_{33}	U_{23}	U_{13}	U_{12}
N(1)	23.3(4)	19.6(4)	18.1(4)	1.0(3)	4.6(3)	2.2(3)
C(13)	22.1(5)	19.6(5)	22.1(5)	-0.4(4)	2.2(4)	0.6(4)
C(2)	22.3(5)	17.9(5)	21.7(5)	0.0(4)	4.0(4)	-0.4(4)
C(1)	19.9(5)	21.1(5)	20.9(5)	1.1(4)	2.1(4)	0.0(4)
C(3)	22.5(5)	19.8(5)	18.2(5)	-1.1(4)	3.8(4)	0.7(4)
C(4)	22.8(5)	19.9(5)	20.0(5)	-2.0(4)	3.0(4)	-0.7(4)
C(5)	22.2(5)	23.5(5)	22.1(5)	1.8(4)	3.6(4)	1.7(4)
C(6)	23.3(5)	22.1(5)	24.7(5)	-5.3(4)	4.9(4)	-5.3(4)
C(12)	25.7(5)	23.0(5)	18.1(5)	1.8(4)	5.2(4)	2.8(4)
C(14)	25.6(5)	20.1(5)	28.3(6)	-3.1(4)	-2.4(4)	6.4(4)
C(7)	30.3(6)	26.7(5)	27.0(6)	-1.8(4)	6.1(5)	-4.8(4)
C(11)	24.6(5)	35.6(6)	30.3(6)	-2.5(5)	4.1(5)	-1.5(5)
C(15)	40.7(7)	24.4(6)	34.5(7)	-5.7(5)	-8.3(5)	4.8(5)
C(8)	39.0(7)	39.0(7)	29.9(6)	-4.9(5)	12.3(5)	-13.1(5)
C(17)	24.8(6)	35.1(7)	51.0(8)	-4.2(6)	-0.3(5)	4.3(5)
C(10)	22.2(5)	47.1(7)	44.3(7)	-8.5(6)	5.0(5)	-1.5(5)
C(16)	45.3(7)	28.5(6)	30.0(6)	0.5(5)	-7.1(5)	10.5(5)
C(9)	28.0(6)	49.6(8)	39.0(7)	-13.4(6)	16.3(5)	-11.7(5)

Table 4: Bond Lengths in Å for **158ka**.

Atom	Atom	Length/Å
O(3)	C(13)	1.3395(13)
O(3)	C(14)	1.4752(12)
O(2)	C(13)	1.1984(13)
O(1)	C(1)	1.2104(13)
N(1)	C(13)	1.4010(13)
N(1)	C(1)	1.3963(13)
N(1)	C(12)	1.4772(13)
C(2)	C(1)	1.5109(14)
C(2)	C(3)	1.5415(14)
C(2)	C(5)	1.5479(14)
C(3)	C(4)	1.5618(14)
C(3)	C(12)	1.5231(14)
C(4)	C(5)	1.5540(14)
C(4)	C(6)	1.5055(15)
C(6)	C(7)	1.3960(16)
C(6)	C(11)	1.3900(16)
C(14)	C(15)	1.5180(15)
C(14)	C(17)	1.5154(17)
C(14)	C(16)	1.5180(16)
C(7)	C(8)	1.3867(17)
C(11)	C(10)	1.3929(17)
C(8)	C(9)	1.384(2)
C(10)	C(9)	1.384(2)

Table 5: Bond Angles in ° for **158ka**

Atom	Atom	Atom	Angle/°
C(13)	O(3)	C(14)	121.26(8)
C(13)	N(1)	C(12)	122.08(8)
C(1)	N(1)	C(13)	123.62(9)
C(1)	N(1)	C(12)	113.70(8)
O(3)	C(13)	N(1)	107.50(9)
O(2)	C(13)	O(3)	127.38(10)
O(2)	C(13)	N(1)	125.12(10)
C(1)	C(2)	C(3)	104.49(8)
C(1)	C(2)	C(5)	112.99(9)
C(3)	C(2)	C(5)	90.24(8)
O(1)	C(1)	N(1)	126.13(10)
O(1)	C(1)	C(2)	125.76(9)
N(1)	C(1)	C(2)	108.11(8)
C(2)	C(3)	C(4)	88.76(8)
C(12)	C(3)	C(2)	106.86(8)
C(12)	C(3)	C(4)	118.25(8)
C(5)	C(4)	C(3)	89.28(8)
C(6)	C(4)	C(3)	117.94(9)
C(6)	C(4)	C(5)	118.89(9)
C(2)	C(5)	C(4)	88.82(8)
C(7)	C(6)	C(4)	119.93(10)
C(11)	C(6)	C(4)	121.55(10)
C(11)	C(6)	C(7)	118.52(11)
N(1)	C(12)	C(3)	103.16(8)
O(3)	C(14)	C(15)	109.36(9)
O(3)	C(14)	C(17)	110.73(9)
O(3)	C(14)	C(16)	101.19(9)
C(17)	C(14)	C(15)	112.59(10)
C(17)	C(14)	C(16)	111.30(10)
C(16)	C(14)	C(15)	111.09(10)
C(8)	C(7)	C(6)	120.82(12)
C(6)	C(11)	C(10)	120.46(12)
C(9)	C(8)	C(7)	120.33(12)
C(9)	C(10)	C(11)	120.53(12)
C(8)	C(9)	C(10)	119.34(11)

Table 6: Hydrogen Fractional Atomic Coordinates ($\times 10^4$) and Equivalent Isotropic Displacement Parameters ($Å^2 \times 10^3$) for **158ka**. U_{eq} is defined as 1/3 of the trace of the orthogonalized U_{ij}.

Atom	x	y	z	U_{eq}
H(2)	5674.83	2617.91	7935.76	25
H(3)	6550.2	3100.16	5088.69	24
H(4)	7996.37	3694.83	8482.63	25
H(5A)	8160.71	2618.26	8972.31	27
H(5B)	7815.5	3021.38	10798.39	27
H(12A)	5927	4041.68	6057.96	26
H(12B)	4704.3	3669.79	5150.96	26
H(7)	8491.03	3744.36	3831.09	33
H(11)	10533.01	2919.61	8566.67	36
H(15A)	3275.73	5094.09	10374.93	51
H(15B)	2454.2	5498.88	8900.42	51
H(15C)	4018.54	5345.12	8448.58	51
H(8)	10491.6	3716.1	1868.82	43
H(17A)	872.27	4309.62	7165.94	56
H(17B)	404.53	4857.7	7786.98	56
H(17C)	1204.53	4510.05	9544.27	56
H(10)	12523.06	2883.19	6563.32	45
H(16A)	3387.73	5081.94	4666.1	53
H(16B)	1814.4	5264.5	4878.99	53
H(16C)	2109.1	4709.34	4128.05	53
H(9)	12514.82	3283.7	3220.07	46

(1*S*,5*R*,6*S*)-6-Phenyl-3-((*S*)-1-phenylethyl)-3-azabicyclo[3.2.0]heptan-2-one (158vb)

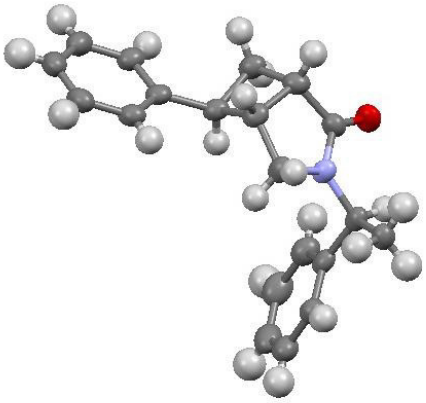

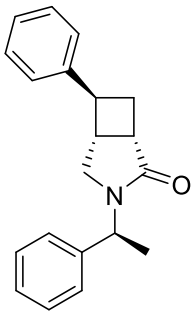

Table 1: Crystal data and structure refinement for **158vb**.

Chemical formula	$C_{20}H_{21}NO$
M_r	291.38
Crystal system, space group	Monoclinic, *C*2
Temperature (K)	123
a, *b*, *c* (Å)	15.9956 (4), 6.5511 (2), 30.3071 (6)
β (°)	91.187 (2)
V (Å^3)	3175.16 (14)
Z	8
Radiation type	Cu *K*α
μ (mm^{-1})	0.58
Crystal size (mm)	0.17 × 0.16 × 0.09
F(000)	1248
Diffractometer	GV1000, TitanS2
Absorption correction	Gaussian *CrysAlis PRO* 1.171.38.46 (Rigaku Oxford Diffraction, 2015) Numerical absorption correction based on gaussian integration over a multifaceted crystal model Empirical absorption correction using spherical harmonics, implemented in SCALE3 ABSPACK scaling algorithm.

T_{min}, T_{max}	0.912, 1.000
No. of measured, independent and observed [$I > 2\sigma(I)$] reflections	32743, 6285, 5766
R_{int}	0.074
$(\sin \theta/\lambda)_{max}$ (Å^{-1})	0.624
$R[F^2 > 2\sigma(F^2)]$, $wR(F^2)$, S	0.047, 0.129, 1.05
No. of reflections	6285
No. of parameters	442
No. of restraints	169
H-atom treatment	H-atom parameters constrained
$\Delta\rho_{max}$, $\Delta\rho_{min}$ (e Å^{-3})	0.17, −0.20
Absolute structure	Flack x determined using 2313 quotients [(I+)-(I-)]/[(I+)+(I-)] (Parsons, Flack and Wagner, Acta Cryst. B69 (2013) 249-259).
Absolute structure parameter	0.00 (16)

Table 2: Fractional Atomic Coordinates (×10^4) and Equivalent Isotropic Displacement Parameters (Å^2×10^3) for **158vb**. U_{eq} is defined as 1/3 of the trace of the orthogonalized U_{ij}.

Atom	x	y	z	U_{eq}
O(1)	4124.4(15)	12786(3)	3413.6(6)	52.0(5)
O(2)	4092.5(15)	-2795(3)	1566.6(7)	52.4(5)
N(1)	4047.4(15)	9349(3)	3547.4(6)	37.8(5)
N(2)	4130.7(15)	682(3)	1501.9(7)	39.2(5)
C(34)	2909.2(18)	1669(4)	1934.5(7)	41.0(6)
C(32)	4255.2(17)	-1237(4)	1359.0(8)	39.5(6)
C(14)	2864.4(18)	8031(4)	3107.3(7)	39.4(6)
C(33)	3824.2(18)	1115(4)	1946.9(7)	39.0(6)
C(22)	4505.6(17)	1074(4)	766.8(8)	40.6(6)
C(23)	3729.5(18)	400(4)	489.0(8)	41.5(6)
C(4)	3502.4(17)	9454(4)	5022.8(8)	40.2(6)
C(13)	3761.3(18)	8763(4)	3102.2(7)	39.1(6)
C(5)	3637.6(19)	7456(4)	5160.9(9)	45.7(6)
C(12)	4219.2(17)	11297(4)	3658.3(8)	39.1(6)
C(40)	4386.7(18)	2661(4)	2179.6(8)	42.3(6)
C(2)	4373.8(17)	9201(4)	4303.1(8)	41.0(6)
C(3)	3618.7(17)	10077(4)	4550.1(8)	39.2(6)
C(1)	4199.3(19)	7854(4)	3898.9(8)	42.0(6)
C(15)	2618.0(19)	6060(4)	2991.1(8)	46.2(6)
C(10)	3944.1(19)	12262(4)	4461.5(9)	44.8(6)

Atom	x	y	z	U_{eq}
C(9)	3245.9(18)	10871(5)	5336.1(8)	45.7(6)
C(20)	4378.2(19)	7296(4)	2894.7(9)	43.0(6)
C(8)	3159(2)	10308(5)	5774.4(10)	52.5(7)
C(24)	3602(7)	1347(16)	38(2)	46.5(6)
C(21)	4358(2)	2278(4)	1187.2(8)	44.4(7)
C(35)	2624(2)	3637(5)	1851.0(9)	51.2(7)
C(25)	3863(6)	3348(15)	-44(2)	47.0(6)
C(31)	4632.2(19)	-1170(4)	905.7(9)	43.4(6)
C(11)	4551.8(18)	11359(4)	4127.8(9)	43.8(6)
C(6)	3551(2)	6893(5)	5597.5(10)	54.6(7)
C(39)	2326(2)	148(6)	2014.4(10)	59.6(8)
C(7)	3314(2)	8334(5)	5905.8(9)	55.7(8)
C(16)	1783(2)	5525(6)	2978.3(9)	55.1(8)
C(17)	1180(2)	6906(7)	3089.4(10)	62.0(9)
C(19)	2246(2)	9413(5)	3222.7(9)	53.1(7)
C(30)	4036(2)	-1843(4)	529.8(10)	47.4(6)
C(29)	3195(5)	319(13)	-309(3)	47.6(7)
C(36)	1781(2)	4076(7)	1844.3(10)	66.1(9)
C(38)	1483(3)	602(8)	2009.6(13)	77.6(12)
C(26)	3736(5)	4278(13)	-448(2)	47.6(7)
C(28)	3077(5)	1216(16)	-722(2)	48.0(7)
C(37)	1206(2)	2569(8)	1920.9(11)	75.5(12)
C(18)	1413(2)	8862(7)	3216.7(11)	64.8(9)
C(27)	3339(5)	3208(14)	-790(2)	48.0(7)
C(0AA)	3236(5)	-198(12)	-278(2)	47.4(7)
C(1AA)	3059(4)	464(14)	-705.2(19)	48.1(7)
C(2AA)	3213(4)	2479(14)	-822.0(15)	48.0(7)
C(XD)	3544(5)	3832(11)	-511(2)	47.7(7)
C(XE)	3722(5)	3169(13)	-84(2)	47.0(7)
C(XF)	3568(6)	1154(14)	32.9(18)	46.6(6)

Table 3: Anisotropic Displacement Parameters ($\times 10^4$) **158vb** The anisotropic displacement factor exponent takes the form: $-2p^2[h^2a^{*2} \times U_{11} + ... + 2hka^* \times b^* \times U_{12}]$

Atom	U_{11}	U_{22}	U_{33}	U_{23}	U_{13}	U_{12}
O(1)	76.3(15)	30.7(10)	49.3(10)	5.5(8)	5.7(9)	-2.9(9)
O(2)	69.8(15)	27.0(9)	60.4(11)	7.3(8)	3.5(10)	-0.6(9)
N(1)	51.9(13)	27.4(10)	34.1(9)	2.0(8)	-3.3(8)	4.7(9)
N(2)	56.0(14)	25.7(10)	35.9(10)	2.2(8)	2.3(9)	-7.2(9)
C(34)	49.5(16)	46.9(15)	26.5(10)	1.6(10)	-1.9(9)	-9.3(12)
C(32)	42.0(15)	27.9(12)	48.7(13)	2.4(10)	0.9(10)	0(1)
C(14)	51.9(16)	39.1(12)	27.1(10)	0.9(9)	-2.3(9)	7.1(11)
C(33)	54.2(16)	31.5(12)	31.2(10)	4.4(9)	-1.3(10)	-7.5(11)
C(22)	48.4(16)	33.4(13)	40.3(12)	-1.4(10)	6.1(10)	-9.5(11)
C(23)	48.1(16)	35.5(13)	41.3(12)	-7.9(10)	7.4(10)	-3.6(11)
C(4)	40.1(14)	40.5(13)	39.4(12)	-3.5(10)	-9.9(10)	-3.1(11)
C(13)	57.4(17)	29.3(12)	30.6(10)	3.5(9)	0.7(10)	4.0(11)
C(5)	50.6(16)	39.9(14)	46.0(14)	-2.0(11)	-9.1(11)	-5.5(12)
C(12)	43.9(15)	29.9(12)	43.6(12)	1.6(10)	2.4(10)	-0.6(10)

Atom	U_{11}	U_{22}	U_{33}	U_{23}	U_{13}	U_{12}
C(40)	50.4(16)	38.6(14)	37.6(11)	0(1)	-5.3(10)	-7.3(11)
C(2)	44.7(16)	38.9(13)	38.9(11)	1.2(10)	-8.4(10)	8.2(11)
C(3)	42.1(15)	36.6(13)	38.6(12)	-2.3(10)	-8.9(10)	3.9(10)
C(1)	58.7(17)	30.3(13)	36.8(12)	5.6(9)	-3.5(10)	8.8(11)
C(15)	53.9(17)	44.0(15)	40.5(12)	-1.8(11)	-1.1(11)	0.6(12)
C(10)	54.2(18)	38.6(14)	41.3(13)	-4.4(10)	-5.3(11)	4.2(11)
C(9)	44.6(16)	48.5(16)	43.8(13)	-7.2(12)	-6.3(11)	0.2(12)
C(20)	51.5(17)	35.9(13)	42.0(12)	0(1)	7.7(11)	2.2(11)
C(8)	49.9(18)	61.9(19)	45.7(14)	-9.6(13)	2.6(12)	-8.9(14)
C(24)	47.2(11)	46.2(17)	46.1(9)	-6.6(10)	2.5(8)	6.2(12)
C(21)	68(2)	28.8(12)	36.0(12)	2.1(10)	3.4(11)	-15.2(12)
C(35)	52.8(18)	55.0(18)	45.9(14)	9.5(12)	5.1(12)	-0.9(14)
C(25)	48.2(12)	46.4(16)	46.6(10)	-6.4(10)	2.0(9)	6.6(12)
C(31)	43.9(16)	35.1(13)	51.4(14)	-2.3(11)	6.0(11)	0.4(11)
C(11)	41.9(15)	39.1(14)	50.0(14)	-3.4(11)	-6.2(11)	-1.7(11)
C(6)	59(2)	49.3(17)	54.7(16)	7.4(13)	-9.4(13)	-15.2(14)
C(39)	62(2)	62(2)	55.4(16)	3.3(14)	-1.8(14)	-25.1(16)
C(7)	57.8(19)	66(2)	43.7(14)	3.2(14)	-1.5(12)	-20.8(15)
C(16)	54.2(19)	68(2)	42.8(13)	-2.6(13)	-1.3(12)	-7.5(15)
C(17)	51(2)	90(3)	44.1(15)	5.2(16)	-8.0(13)	-5.3(17)
C(19)	58(2)	51.0(17)	49.9(14)	-3.2(13)	-2.0(12)	13.4(14)
C(30)	56.6(18)	34.6(13)	51.5(14)	-10.8(11)	10.1(12)	-6.2(12)
C(29)	48.3(11)	46.8(18)	47.7(9)	-6.1(11)	0.8(8)	5.9(13)
C(36)	57(2)	88(3)	53.2(16)	11.4(17)	2.3(14)	10.7(19)
C(38)	58(2)	105(3)	70(2)	-2(2)	2.1(16)	-36(2)
C(26)	48.6(13)	46.8(17)	47.5(10)	-6.3(11)	1.4(9)	6.3(13)
C(28)	49.1(11)	46.8(18)	48.1(9)	-6.0(12)	-0.2(8)	5.8(14)
C(37)	46(2)	130(4)	50.1(16)	1(2)	-2.3(13)	-6(2)
C(18)	55(2)	83(3)	56.3(16)	-0.4(17)	0.2(14)	23.0(18)
C(27)	49.2(12)	46.9(18)	47.8(10)	-6.1(12)	0.6(9)	5.9(13)
C(0AA)	48.3(11)	46.6(18)	47.3(9)	-5.9(11)	0.7(8)	5.9(13)
C(1AA)	49.1(12)	46.9(18)	48.3(10)	-6.0(12)	-0.1(9)	5.8(14)
C(2AA)	49.2(12)	46.9(18)	47.8(10)	-6.1(12)	0.0(9)	5.8(14)
C(XD)	48.8(12)	46.7(17)	47.6(10)	-6.1(11)	0.9(9)	6.2(13)
C(XE)	48.0(12)	46.4(17)	46.6(10)	-6.5(10)	2.1(9)	6.6(12)
C(XF)	47.3(11)	46.3(17)	46.2(9)	-6.5(10)	2.5(8)	6.3(12)

Table 4: Bond Lengths in Å for **158vb**.

Atom	Atom	Length/Å
O(1)	C(12)	1.233(3)
O(2)	C(32)	1.229(3)
N(1)	C(13)	1.467(3)
N(1)	C(12)	1.347(3)
N(1)	C(1)	1.464(3)
N(2)	C(32)	1.345(3)
N(2)	C(33)	1.472(3)
N(2)	C(21)	1.466(3)

Atom	Atom	Length/Å
C(34)	C(33)	1.507(4)
C(34)	C(35)	1.389(4)
C(34)	C(39)	1.389(4)
C(32)	C(31)	1.512(4)
C(14)	C(13)	1.513(4)
C(14)	C(15)	1.393(4)
C(14)	C(19)	1.392(4)
C(33)	C(40)	1.519(3)

Atom	Atom	Length/Å
C(22)	C(23)	1.550(4)
C(22)	C(21)	1.521(4)
C(22)	C(31)	1.542(4)
C(23)	C(24)	1.512(7)
C(23)	C(30)	1.553(4)
C(23)	C(XF)	1.486(5)
C(4)	C(5)	1.390(4)
C(4)	C(3)	1.505(4)
C(4)	C(9)	1.396(4)
C(13)	C(20)	1.523(4)
C(5)	C(6)	1.383(4)
C(12)	C(11)	1.509(3)
C(2)	C(3)	1.545(4)
C(2)	C(1)	1.530(3)
C(2)	C(11)	1.539(4)
C(3)	C(10)	1.549(4)
C(15)	C(16)	1.380(4)
C(10)	C(11)	1.536(4)
C(9)	C(8)	1.389(4)
C(8)	C(7)	1.374(5)
C(24)	C(25)	1.399(9)
C(24)	C(29)	1.398(8)
C(35)	C(36)	1.378(5)
C(25)	C(26)	1.378(8)
C(31)	C(30)	1.535(4)
C(6)	C(7)	1.387(5)
C(39)	C(38)	1.382(6)
C(16)	C(17)	1.369(5)
C(17)	C(18)	1.387(6)
C(19)	C(18)	1.379(5)
C(29)	C(28)	1.391(8)
C(36)	C(37)	1.372(6)
C(38)	C(37)	1.387(7)
C(26)	C(27)	1.395(8)
C(28)	C(27)	1.387(9)
C(0AA)	C(1AA)	1.3900
C(0AA)	C(XF)	1.3900
C(1AA)	C(2AA)	1.3900
C(2AA)	C(XD)	1.3900
C(XD)	C(XE)	1.3900
C(XE)	C(XF)	1.3900

Table 5: Bond Angles in ° for **158vb**.

Atom	Atom	Atom	Angle/°
C(12)	N(1)	C(13)	122.4(2)
C(12)	N(1)	C(1)	115.0(2)
C(1)	N(1)	C(13)	122.61(19)
C(32)	N(2)	C(33)	122.0(2)
C(32)	N(2)	C(21)	114.6(2)
C(21)	N(2)	C(33)	123.4(2)
C(35)	C(34)	C(33)	122.9(2)
C(39)	C(34)	C(33)	118.5(3)
C(39)	C(34)	C(35)	118.6(3)
O(2)	C(32)	N(2)	125.2(2)
O(2)	C(32)	C(31)	125.5(2)
N(2)	C(32)	C(31)	109.3(2)
C(15)	C(14)	C(13)	123.7(2)
C(19)	C(14)	C(13)	118.4(3)
C(19)	C(14)	C(15)	117.9(3)
N(2)	C(33)	C(34)	111.41(19)
N(2)	C(33)	C(40)	110.4(2)
C(34)	C(33)	C(40)	114.6(2)
C(21)	C(22)	C(23)	117.8(2)
C(21)	C(22)	C(31)	106.7(2)
C(31)	C(22)	C(23)	88.60(19)
C(22)	C(23)	C(30)	88.8(2)
C(24)	C(23)	C(22)	117.8(5)
C(24)	C(23)	C(30)	119.8(4)
C(XF)	C(23)	C(22)	122.2(4)
C(XF)	C(23)	C(30)	115.9(4)
C(5)	C(4)	C(3)	121.4(2)
C(5)	C(4)	C(9)	117.9(2)
C(9)	C(4)	C(3)	120.7(2)
N(1)	C(13)	C(14)	110.6(2)
N(1)	C(13)	C(20)	110.6(2)
C(14)	C(13)	C(20)	115.3(2)
C(6)	C(5)	C(4)	121.4(3)
O(1)	C(12)	N(1)	125.3(2)
O(1)	C(12)	C(11)	125.6(2)
N(1)	C(12)	C(11)	109.1(2)
C(1)	C(2)	C(3)	118.1(2)
C(1)	C(2)	C(11)	106.6(2)
C(11)	C(2)	C(3)	88.7(2)
C(4)	C(3)	C(2)	118.3(2)
C(4)	C(3)	C(10)	117.7(2)
C(2)	C(3)	C(10)	89.5(2)
N(1)	C(1)	C(2)	102.8(2)
C(16)	C(15)	C(14)	120.7(3)
C(11)	C(10)	C(3)	88.7(2)
C(8)	C(9)	C(4)	120.7(3)

Atom	Atom	Atom	Angle/°
C(7)	C(8)	C(9)	120.4(3)
C(25)	C(24)	C(23)	120.6(7)
C(29)	C(24)	C(23)	122.3(7)
C(29)	C(24)	C(25)	117.0(5)
N(2)	C(21)	C(22)	102.7(2)
C(36)	C(35)	C(34)	120.9(3)
C(26)	C(25)	C(24)	122.2(6)
C(32)	C(31)	C(22)	102.9(2)
C(32)	C(31)	C(30)	114.4(2)
C(30)	C(31)	C(22)	89.7(2)
C(12)	C(11)	C(2)	103.7(2)
C(12)	C(11)	C(10)	114.6(2)
C(10)	C(11)	C(2)	90.1(2)
C(5)	C(6)	C(7)	119.8(3)
C(38)	C(39)	C(34)	120.2(4)
C(8)	C(7)	C(6)	119.7(3)
C(17)	C(16)	C(15)	120.7(3)
C(16)	C(17)	C(18)	119.5(3)

Atom	Atom	Atom	Angle/°
C(18)	C(19)	C(14)	121.2(3)
C(31)	C(30)	C(23)	88.7(2)
C(28)	C(29)	C(24)	121.6(6)
C(37)	C(36)	C(35)	120.4(4)
C(39)	C(38)	C(37)	120.6(4)
C(25)	C(26)	C(27)	119.7(6)
C(27)	C(28)	C(29)	119.8(5)
C(36)	C(37)	C(38)	119.3(4)
C(19)	C(18)	C(17)	120.0(3)
C(28)	C(27)	C(26)	119.7(6)
C(1AA)	C(0AA)	C(XF)	120.0
C(2AA)	C(1AA)	C(0AA)	120.0
C(XD)	C(2AA)	C(1AA)	120.0
C(XE)	C(XD)	C(2AA)	120.0
C(XD)	C(XE)	C(XF)	120.0
C(0AA)	C(XF)	C(23)	118.3(5)
C(XE)	C(XF)	C(23)	121.6(5)
C(XE)	C(XF)	C(0AA)	120.0

Table 6: Hydrogen Fractional Atomic Coordinates ($\times 10^4$) and Equivalent Isotropic Displacement Parameters ($Å^2 \times 10^3$) for **158vb**. U_{eq} is defined as 1/3 of the trace of the orthogonalized U_{ij}.

Atom	x	y	z	U_{eq}
H(33)	3873.85	-159.47	2114.73	47
H(22)	4960.31	1616.95	589.52	49
H(23)	3223.75	582.06	661.81	50
H(23A)	3225.33	578.11	663.25	50
H(13)	3764.79	10009.32	2923.24	47
H(5)	3789.75	6476.23	4955.42	55
H(40A)	4951.2	2161.9	2187.95	63
H(40B)	4199.99	2863.95	2475.39	63
H(40C)	4364.69	3932.75	2022.62	63
H(2)	4816.59	8669.73	4499.76	49
H(3)	3102.25	9833.51	4378.6	47
H(1A)	4676.48	6997.5	3835.24	50
H(1B)	3713.05	6997.05	3941.14	50
H(15)	3020.33	5093.96	2921.35	55
H(10A)	3527.56	13166.08	4330.58	54
H(10B)	4218.28	12893.64	4715.3	54
H(9)	3132.16	12207.05	5250.33	55
H(20A)	4927.11	7889.4	2903.43	65
H(20B)	4211.33	7038.89	2593.76	65
H(20C)	4385.15	6035.51	3056.22	65
H(8)	2994.56	11272.46	5980.38	63
H(21A)	4860.46	2991.7	1284.16	53
H(21B)	3908.33	3256.55	1145.86	53
H(35)	3007.25	4673.19	1799.05	61
H(25)	4131.21	4073.61	181.32	56

Atom	x	y	z	U_{eq}
H(31)	5206.23	-1682.54	888.47	52
H(11)	5133.12	11814	4162.41	53
H(6)	3650.77	5551.03	5683.97	65
H(39)	2504.64	-1179.32	2071.35	72
H(7)	3260.49	7965.96	6200.28	67
H(16)	1628.22	4212.27	2893.38	66
H(17)	619.16	6535.02	3079.5	74
H(19)	2396.14	10732.42	3305.37	64
H(30A)	3607.57	-2791.9	621.02	57
H(30B)	4318.84	-2339.85	270.82	57
H(29)	2998.57	-998.11	-262.77	57
H(36)	1600.93	5401.47	1787.47	79
H(38)	1096.49	-421.36	2066.46	93
H(26)	3913.6	5612.58	-491.48	57
H(28)	2824.45	483.05	-950.84	58
H(37)	637.19	2863.55	1913.37	91
H(18)	1008.57	9800.95	3297.91	78
H(27)	3249.44	3827.48	-1063.39	58
H(0AA)	3132.96	-1546.2	-199.53	57
H(1AA)	2836.72	-440.79	-913.02	58
H(2AA)	3093.98	2922.12	-1108.05	58
H(XD)	3647.48	5179.65	-589.6	57
H(XE)	3943.72	4074.28	123.89	56

Table 7: Atomic Occupancies for all atoms that are not fully occupied in **158vb**.

Atom	Occupancy
H(23)	0.518(12)
H(23A)	0.482(12)
C(24)	0.518(12)
C(25)	0.518(12)
H(25)	0.518(12)
C(29)	0.518(12)
H(29)	0.518(12)
C(26)	0.518(12)
H(26)	0.518(12)
C(28)	0.518(12)
H(28)	0.518(12)
C(27)	0.518(12)
H(27)	0.518(12)
C(0AA)	0.482(12)
H(0AA)	0.482(12)
C(1AA)	0.482(12)
H(1AA)	0.482(12)
C(2AA)	0.482(12)
H(2AA)	0.482(12)
C(XD)	0.482(12)
(XD)	0.482(12)

Atom	Occupancy
C(XE)	0.482(12)
H(XE)	0.482(12)
C(XF)	0.482(12)

(1*S*,5*R*,7*R*)-7-Phenyl-3-((*S*)-1-phenylethyl)-3-azabicyclo[3.2.0]heptan-2-one (158wb)

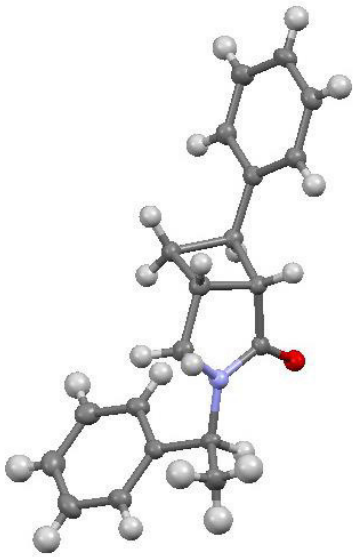

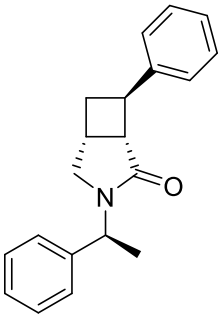

Table 1: Crystal data and structure refinement for **158wb**.

Chemical formula	$C_{20}H_{21}NO$
*M*r	291.38
Crystal system, space group	Orthorhombic, *P*212121
Temperature (K)	123
a, *b*, *c* (Å)	6.1125 (3), 9.5571 (6), 53.180 (3)
V (Å3)	3106.7 (3)
Z	8
Radiation type	Cu *Kα*
μ (mm−1)	0.59
Crystal size (mm)	0.20 × 0.12 × 0.06
F(000)	1248
Diffractometer	GV1000, TitanS2
Absorption correction	Gaussian *CrysAlis PRO* 1.171.38.42b (Rigaku Oxford Diffraction, 2015) Numerical absorption correction based on gaussian integration over a multifaceted crystal model Empirical absorption correction using spherical harmonics, implemented in SCALE3 ABSPACK scaling algorithm.

*T*min, *T*max	0.824, 1.000
No. of measured, independent and observed [$I > 2\sigma(I)$] reflections	25558, 6266, 5570
*R*int	0.063
(sin θ/λ)max (Å−1)	0.631
$R[F2 > 2\sigma(F2)]$, $wR(F2)$, S	0.041, 0.099, 1.07
No. of reflections	6266
No. of parameters	399
H-atom treatment	H-atom parameters constrained
$\Delta\rho$max, $\Delta\rho$min (e Å^{-3})	0.15, −0.17
Absolute structure	Flack x determined using 2086 quotients [(I+)-(I-)]/[(I+)+(I-)] (Parsons, Flack and Wagner, Acta Cryst. B69 (2013) 249-259).
Absolute structure parameter	−0.1 (2)

Table 2: Fractional Atomic Coordinates (×10^4) and Equivalent Isotropic Displacement Parameters (Å^2×10^3) for **158wb**. U_{eq} is defined as 1/3 of the trace of the orthogonalized U_{ij}.

Atom	x	y	z	U_{eq}
O2	9849(3)	2537(2)	3104.4(3)	27.3(4)
O1	5882(3)	8845(2)	4353.2(4)	28.9(4)
N1	9272(3)	8035(2)	4239.0(4)	21.4(4)
N2	8629(4)	321(2)	3014.3(4)	21.9(4)
C23	4721(4)	2534(3)	3680.1(4)	21.2(5)
C9	7533(4)	8150(3)	4395.2(4)	21.2(5)
C26	8851(4)	1469(3)	3160.4(4)	21.8(5)
C3	4202(4)	4368(3)	4895.4(5)	22.4(5)
C13	9404(4)	8762(3)	3996.9(4)	22.8(5)
C4	6036(4)	5231(3)	4874.5(4)	20.4(5)
C22	2723(4)	3235(3)	3693.2(5)	24.2(5)
C34	7981(4)	295(3)	2558.3(4)	22.5(5)
C10	10046(4)	6439(3)	4558.8(4)	23.0(5)
C14	9435(4)	7695(3)	3783.9(4)	24.0(5)
C24	5526(4)	2114(3)	3421.7(4)	21.6(5)

Atom	x	y	z	U_{eq}
C25	7631(4)	1223(3)	3405.7(4)	21.7(5)
C11	11084(4)	7189(3)	4334.2(5)	23.1(5)
C20	11289(5)	9791(3)	3996.5(5)	27.7(6)
C5	7385(5)	5370(3)	5085.1(5)	26.0(6)
C28	4264(4)	847(3)	3305.8(4)	23.5(5)
C27	6268(4)	-104(3)	3352.2(4)	23.4(5)
C33	9682(4)	202(3)	2767.8(4)	23.3(5)
C30	5850(5)	2277(3)	3901.7(4)	25.8(6)
C8	7946(4)	7254(3)	4626.3(4)	21.8(5)
C35	6213(5)	1207(3)	2581.9(4)	26.1(6)
C2	3709(5)	3680(3)	5118.1(5)	28.1(6)
C21	1885(5)	3678(3)	3921.4(5)	28.3(6)
C6	6918(5)	4671(3)	5307.1(5)	28.5(6)
C29	7310(5)	-803(3)	3121.7(5)	25.2(6)
C39	8171(5)	-477(3)	2338.0(5)	27.7(6)
C7	6591(4)	5878(3)	4623.9(4)	22.8(5)
C32	3027(5)	3418(3)	4142.4(5)	29.1(6)
C1	5069(5)	3832(3)	5324.6(5)	28.3(6)
C12	8608(5)	5158(3)	4496.7(5)	26.1(6)
C15	7631(5)	6822(3)	3753.3(5)	31.3(6)
C31	4986(5)	2708(3)	4132.9(5)	28.5(6)
C19	11184(5)	7561(3)	3619.6(5)	29.2(6)
C36	4667(5)	1333(3)	2393.0(5)	32.8(6)
C38	6619(5)	-358(4)	2147.7(5)	35.0(7)
C40	11110(5)	-1102(3)	2758.4(5)	31.8(6)
C16	7597(6)	5837(3)	3559.3(6)	41.7(8)
C37	4870(5)	535(4)	2174.6(5)	36.6(7)
C18	11138(6)	6567(4)	3426.5(5)	38.1(7)
C17	9348(6)	5717(3)	3396.2(6)	42.1(8)

Table 3: Anisotropic Displacement Parameters ($\times 10^4$) **158wb**. The anisotropic displacement factor exponent takes the form: $-2p^2[h^2a^{*2} \times U_{11} + ... + 2hka^* \times b^* \times U_{12}]$

Atom	U_{11}	U_{22}	U_{33}	U_{23}	U_{13}	U_{12}
O2	30(1)	24.0(11)	27.9(8)	-3.2(7)	4.3(8)	-6.4(8)
O1	20.2(9)	26.6(11)	40(1)	5.4(8)	0.8(8)	7.3(8)
N1	19.5(10)	20.7(12)	24.0(9)	3.7(8)	0.8(8)	4.0(9)
N2	23.7(11)	20.2(11)	21.9(9)	-0.6(8)	0.3(8)	-1.1(9)
C23	23.8(12)	17.2(13)	22.6(11)	1.9(9)	0.2(10)	-1.3(10)
C9	19.4(12)	17.1(13)	27.2(11)	-0.5(9)	0(1)	-1.3(10)
C26	20.4(12)	23.8(14)	21.3(10)	-0.9(10)	-2.2(10)	0(1)
C3	20.7(13)	21.4(14)	25.1(11)	2(1)	-1.8(10)	-1.7(10)
C13	23.8(13)	20.4(13)	24.1(11)	4.4(10)	-0.7(10)	1.3(11)
C4	20.9(12)	18.0(13)	22.3(10)	-0.3(9)	2.9(10)	-0.2(10)
C22	25.9(13)	21.1(14)	25.6(11)	1(1)	-3(1)	2.6(11)
C34	25.0(13)	20.5(13)	22.0(11)	0.3(9)	2.8(10)	-2.6(11)
C10	21.3(13)	22.2(14)	25.5(11)	2.8(10)	1.5(10)	1.7(10)
C14	27.8(14)	19.1(14)	25.0(11)	4.6(10)	-6.4(10)	-1.5(11)

Atom	U_{11}	U_{22}	U_{33}	U_{23}	U_{13}	U_{12}
C24	21.7(12)	22.9(14)	20.1(10)	3.0(9)	-1.0(9)	1.4(10)
C25	19.9(12)	26.6(14)	18.7(10)	2.0(9)	-0.7(9)	-0.4(11)
C11	20.2(12)	21.6(14)	27.4(11)	5(1)	1.7(10)	3.9(11)
C20	38.0(15)	21.8(14)	23.5(11)	3.6(10)	-1.1(11)	-5.8(12)
C5	25.2(14)	26.3(15)	26.6(11)	-1.6(10)	0.6(10)	-5.2(12)
C28	21.3(13)	28.1(15)	21(1)	-0.7(10)	-0.8(10)	-1.6(11)
C27	23.8(13)	23.0(14)	23.5(11)	4.6(10)	0.5(10)	1.7(11)
C33	22.2(13)	23.6(14)	24.0(11)	-3.7(9)	5.6(10)	-0.5(11)
C30	26.2(14)	27.9(15)	23.4(11)	-0.5(10)	-1.5(10)	2.3(12)
C8	22.2(12)	20.3(14)	23(1)	-0.1(9)	1.5(9)	0.3(10)
C35	29.4(14)	26.4(15)	22.6(11)	0.7(10)	3.7(10)	3.9(12)
C2	27.1(14)	24.6(15)	32.5(12)	3.1(11)	2.0(11)	-5.8(12)
C21	28.3(14)	25.5(15)	31.1(12)	-2.6(11)	2.0(11)	4.0(12)
C6	31.9(14)	29.9(16)	23.8(11)	-1.5(11)	-2.2(11)	-4.5(12)
C29	26.2(14)	19.3(14)	30.0(12)	1.6(10)	2.5(11)	-0.6(11)
C39	31.0(15)	26.7(16)	25.4(12)	-0.5(10)	2.8(11)	1.6(12)
C7	21.6(13)	23.4(15)	23.5(11)	1.8(10)	1.1(10)	-1.7(10)
C32	35.4(15)	27.6(16)	24.4(11)	-6.1(10)	4.9(11)	0.0(12)
C1	38.6(16)	23.2(14)	23.1(11)	3(1)	0.7(11)	-6.7(12)
C12	29.7(14)	21.9(14)	26.7(11)	-0.8(10)	6.9(11)	-1.6(11)
C15	31.5(15)	25.5(16)	36.9(14)	5.8(11)	-9.9(12)	-4.3(12)
C31	32.8(15)	30.6(15)	22.0(11)	0.5(10)	-4.1(11)	-1.1(12)
C19	32.6(15)	27.7(16)	27.2(12)	2.7(11)	-1.4(11)	1.9(12)
C36	31.1(15)	38.2(18)	29.2(12)	8.0(12)	2.4(11)	5.5(13)
C38	45.6(18)	35.6(18)	23.8(12)	-2.3(12)	-2.5(12)	-2.9(14)
C40	27.5(14)	34.1(17)	33.8(13)	-7.5(12)	-2.4(12)	5.8(13)
C16	52(2)	23.0(16)	50.0(17)	3.9(13)	-25.7(16)	-5.8(15)
C37	36.8(16)	47(2)	26.3(12)	6.9(12)	-4.9(12)	-2.3(15)
C18	50.9(19)	33.4(18)	30.0(13)	-2.4(12)	-4.6(14)	14.1(15)
C17	66(2)	25.3(17)	34.7(14)	-6.4(12)	-21.5(16)	13.2(16)

Table 4: Bond Lengths in Å for **158wb**.

Atom	Atom	Length/Å
O2	C26	1.226(3)
O1	C9	1.229(3)
N1	C9	1.354(3)
N1	C13	1.466(3)
N1	C11	1.462(3)
N2	C26	1.351(3)
N2	C33	1.465(3)
N2	C29	1.459(3)
C23	C22	1.395(4)
C23	C24	1.513(3)
C23	C30	1.388(3)
C9	C8	1.519(3)
C26	C25	1.521(3)

Atom	Atom	Length/Å
C3	C4	1.396(4)
C3	C2	1.387(4)
C13	C14	1.524(4)
C13	C20	1.515(4)
C4	C5	1.397(4)
C4	C7	1.508(3)
C22	C21	1.384(4)
C34	C33	1.526(4)
C34	C35	1.394(4)
C34	C39	1.390(4)
C10	C11	1.530(3)
C10	C8	1.544(4)
C10	C12	1.543(4)

Atom	Atom	Length/Å
C14	C15	1.392(4)
C14	C19	1.387(4)
C24	C25	1.546(4)
C24	C28	1.563(4)
C25	C27	1.544(4)
C5	C6	1.386(4)
C28	C27	1.545(4)
C27	C29	1.534(4)
C33	C40	1.522(4)
C30	C31	1.400(4)
C8	C7	1.554(4)
C35	C36	1.385(4)

Atom	Atom	Length/Å
C2	C1	1.385(4)
C21	C32	1.389(4)
C6	C1	1.389(4)
C39	C38	1.392(4)
C7	C12	1.566(4)
C32	C31	1.377(4)
C15	C16	1.397(4)
C19	C18	1.399(4)
C36	C37	1.395(4)
C38	C37	1.375(5)
C16	C17	1.382(5)
C18	C17	1.372(5)

Table 5: Bond Angles in ° for **158wb.**

Atom	Atom	Atom	Angle/°
C9	N1	C13	122.9(2)
C9	N1	C11	115.3(2)
C11	N1	C13	121.7(2)
C26	N2	C33	122.2(2)
C26	N2	C29	115.3(2)
C29	N2	C33	122.4(2)
C22	C23	C24	117.2(2)
C30	C23	C22	118.5(2)
C30	C23	C24	124.2(2)
O1	C9	N1	125.3(2)
O1	C9	C8	126.0(2)
N1	C9	C8	108.7(2)
O2	C26	N2	125.9(2)
O2	C26	C25	125.5(2)
N2	C26	C25	108.6(2)
C2	C3	C4	121.5(2)
N1	C13	C14	109.6(2)
N1	C13	C20	110.5(2)
C20	C13	C14	115.1(2)
C3	C4	C5	117.8(2)
C3	C4	C7	119.6(2)
C5	C4	C7	122.4(2)
C21	C22	C23	121.0(2)
C35	C34	C33	119.9(2)
C39	C34	C33	121.8(2)
C39	C34	C35	118.2(2)
C11	C10	C8	106.9(2)
C11	C10	C12	116.1(2)
C12	C10	C8	88.7(2)
C15	C14	C13	118.6(2)
C19	C14	C13	122.6(3)
C19	C14	C15	118.8(3)
C23	C24	C25	117.8(2)
C23	C24	C28	113.8(2)
C25	C24	C28	87.82(19)
C26	C25	C24	111.7(2)
C26	C25	C27	103.5(2)
C27	C25	C24	90.77(19)
N1	C11	C10	102.4(2)
C6	C5	C4	121.0(3)
C27	C28	C24	90.10(19)
C25	C27	C28	88.5(2)
C29	C27	C25	106.3(2)
C29	C27	C28	117.2(2)
N2	C33	C34	110.4(2)
N2	C33	C40	110.2(2)
C40	C33	C34	114.5(2)
C23	C30	C31	120.4(3)
C9	C8	C10	103.55(19)
C9	C8	C7	112.4(2)
C10	C8	C7	90.8(2)
C36	C35	C34	121.2(2)
C1	C2	C3	119.8(3)
C22	C21	C32	120.1(3)
C5	C6	C1	120.2(2)
N2	C29	C27	102.8(2)
C34	C39	C38	120.8(3)
C4	C7	C8	117.4(2)
C4	C7	C12	112.2(2)
C8	C7	C12	87.47(19)
C31	C32	C21	119.6(2)
C2	C1	C6	119.8(2)
C10	C12	C7	90.4(2)
C14	C15	C16	120.1(3)
C32	C31	C30	120.3(2)
C14	C19	C18	120.6(3)
C35	C36	C37	119.8(3)
C37	C38	C39	120.3(3)
C17	C16	C15	120.5(3)
C38	C37	C36	119.7(3)
C17	C18	C19	120.3(3)
C18	C17	C16	119.6(3)

Table 6: Hydrogen Fractional Atomic Coordinates ($\times 10^4$) and Equivalent Isotropic Displacement Parameters ($Å^2 \times 10^3$) for **158wb**. U_{eq} is defined as 1/3 of the trace of the orthogonalized U_{ij}.

Atom	x	y	z	U_{eq}
H3	3290.1	4251.19	4757.02	27
H13	8056.39	9308.71	3978.63	27
H22	1942.53	3408.04	3546.36	29
H10	11043.82	6296.35	4700.73	28
H24	5571.38	2913.43	3306.31	26

Atom	x	y	z	U_{eq}
H25	8533.7	1198.42	3557.99	26
H11A	12301.05	7771.02	4386.44	28
H11B	11586.71	6525.95	4208.7	28
H20A	11076.04	10467.87	4127.73	42
H20B	11349.96	10259.92	3837.02	42
H20C	12635.25	9298.48	4024.69	42
H5	8616.37	5939.52	5076.12	31
H28A	2979.74	574.99	3401.18	28
H28B	3909.45	965.89	3129.32	28
H27	6112.11	-726.74	3497.5	28
H33	10654.91	1010.71	2749.45	28
H30	7189.04	1815.23	3896.63	31
H8	7978.84	7756.52	4786.92	26
H35	6069.06	1740.76	2727.23	31
H2	2469.99	3117.82	5128.63	34
H21	555.5	4150.9	3926.91	34
H6	7844.4	4764.5	5444.8	34
H29A	8214.42	-1591.38	3170.39	30
H29B	6203.29	-1118.6	3003.99	30
H39	9350.83	-1081.35	2317.47	33
H7	5323.02	5931.73	4511.5	27
H32	2471.78	3721.4	4295.79	35
H1	4744.51	3374.95	5474.35	34
H12A	9072.63	4307.5	4580.73	31
H12B	8422.73	5000.21	4317.8	31
H15	6446.65	6895.28	3862.24	38
H31	5738.72	2513.72	4280.84	34
H19	12399.85	8137.27	3637.99	35
H36	3498.07	1946.42	2411.59	39
H38	6764.08	-885.79	2001.64	42
H40A	12004.72	-1143.22	2906.53	48
H40B	12027.71	-1067.08	2612.07	48
H40C	10196.33	-1918.09	2750.63	48
H16	6386.48	5257.84	3539.64	50
H37	3828.98	607.56	2047.76	44
H18	12325.19	6482.01	3318.25	46
H17	9313.23	5062.98	3266.67	50

(±)-*cis*-2-(((*tert*-Butoxycarbonyl)amino)methyl)-3-phenylcyclobutane-1-carboxylic acid (227)

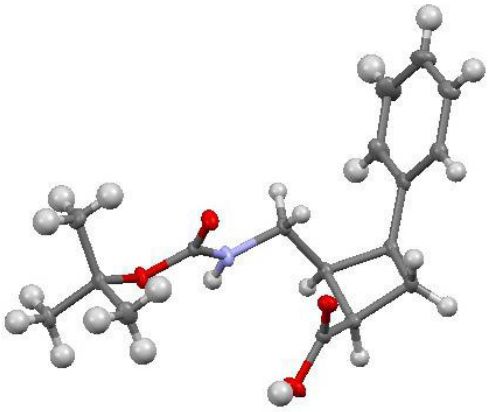

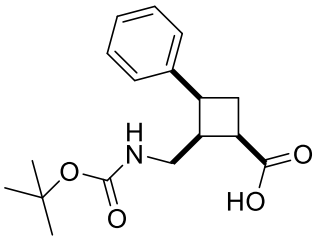

Table 1: Crystal data and structure refinement for **227**.

Chemical formula	$C_{17}H_{23}NO_4$
M_r	305.36
Crystal system, space group	Monoclinic, $P2_1/c$
Temperature (K)	123
a, b, c (Å)	11.4168 (1), 14.3790 (1), 10.0058 (1)
β (°)	99.937 (1)
V (Å^3)	1617.93 (2)
Z	4
Radiation type	Cu $K\alpha$
μ (mm^{-1})	0.73
Crystal size (mm)	0.28 × 0.11 × 0.08
F(000)	656
Diffractometer	GV1000, TitanS2
Absorption correction	Gaussian *CrysAlis PRO* 1.171.38.46 (Rigaku Oxford Diffraction, 2015) Numerical absorption correction based on gaussian integration over a multifaceted crystal model Empirical absorption correction using spherical harmonics, implemented in SCALE3 ABSPACK scaling algorithm.

T_{min}, T_{max}	0.724, 1.000
No. of measured, independent and observed [$I > 2\sigma(I)$] reflections	41835, 3281, 3078
R_{int}	0.057
$(\sin \theta/\lambda)_{max}$ (Å^{-1})	0.624
$R[F^2 > 2\sigma(F^2)]$, $wR(F^2)$, S	0.038, 0.100, 1.02
No. of reflections	3281
No. of parameters	203
H-atom treatment	H-atom parameters constrained
$\Delta\rho_{max}$, $\Delta\rho_{min}$ (e Å^{-3})	0.21, −0.22

Table 2: Fractional Atomic Coordinates (×10^4) and Equivalent Isotropic Displacement Parameters (Å^2×10^3) for **227**. U_{eq} is defined as 1/3 of the trace of the orthogonalized U_{ij}.

Atom	**x**	**y**	**z**	U_{eq}
O(4)	7730.3(6)	8063.7(6)	4719.3(7)	17.47(18)
O(2)	4155.8(7)	9075.3(5)	5011.4(7)	19.07(18)
O(3)	6450.8(7)	7833.9(6)	6211.7(7)	19.42(18)
O(1)	4740.5(7)	9713.3(6)	3196.0(8)	23.9(2)
N(1)	5958.2(8)	7475.5(7)	3966.2(9)	16.6(2)
C(13)	6687.8(9)	7792.6(7)	5070.6(10)	13.9(2)
C(3)	3928.3(9)	7379.7(7)	2775(1)	14.8(2)
C(1)	4159.7(9)	9086.9(7)	3788.9(11)	16.0(2)
C(5)	2341.4(9)	6180.8(8)	3423.9(10)	16.4(2)
C(4)	2607.4(9)	7055.8(7)	2709.3(10)	15.9(2)
C(12)	4801.7(9)	7059.2(7)	4012.1(10)	15.2(2)
C(2)	3470.1(9)	8405.8(7)	2825.5(10)	16.8(2)
C(6)	1709.1(9)	6184.6(8)	4493.4(11)	18.3(2)
C(14)	8662.3(9)	8506.2(7)	5711.6(10)	15.7(2)
C(11)	2321.8(9)	8019.7(8)	3246.1(11)	18.9(2)
C(15)	9629.0(9)	8690.2(8)	4874.3(12)	22.0(2)
C(7)	1486.1(11)	5359.7(9)	5134.4(12)	25.2(3)
C(17)	9111.7(10)	7847.4(9)	6871.8(13)	26.0(3)
C(10)	2729.3(11)	5329.1(9)	3002.2(14)	28.1(3)
C(16)	8210.1(11)	9414.7(8)	6205.7(13)	26.4(3)
C(8)	1903.8(12)	4523.7(9)	4724.5(14)	31.5(3)
C(9)	2521.8(13)	4508.8(9)	3646.8(17)	36.8(3)

Table 3: Anisotropic Displacement Parameters (×10^4) **227**. The anisotropic displacement factor exponent takes the form: $-2p^2[h^2a^{*2} \times U_{11} + ... + 2hka^* \times b^* \times U_{12}]$

Atom	U_{11}	U_{22}	U_{33}	U_{23}	U_{13}	U_{12}
O(4)	10.4(3)	26.8(4)	15.2(3)	-3.5(3)	2.2(3)	-4.3(3)
O(2)	22.2(4)	16.6(4)	18.3(4)	-0.1(3)	3.3(3)	-3.5(3)
O(3)	16.5(4)	28.7(4)	13.2(3)	-0.4(3)	3.2(3)	-2.4(3)
O(1)	28.0(4)	23.1(4)	21.6(4)	-2.4(3)	7.1(3)	-13.0(3)
N(1)	12.0(4)	24.8(5)	13.3(4)	-2.6(3)	3.2(3)	-3.6(3)
C(13)	11.1(4)	15.2(5)	15.5(5)	1.5(4)	2.3(4)	0.9(4)
C(3)	13.0(5)	18.2(5)	13.4(4)	-2.0(4)	2.4(4)	-3.5(4)
C(1)	13.4(5)	14.2(5)	20.4(5)	1.9(4)	2.8(4)	0.4(4)
C(5)	10.7(4)	17.8(5)	19.6(5)	-1.9(4)	-0.5(4)	-3.1(4)
C(4)	12.4(5)	18.8(5)	15.8(5)	-1.2(4)	0.3(4)	-2.9(4)
C(12)	12.1(5)	17.2(5)	16.6(5)	-0.6(4)	2.9(4)	-2.0(4)
C(2)	14.3(5)	17.7(5)	17.5(5)	1.9(4)	0.2(4)	-2.8(4)
C(6)	16.7(5)	19.7(5)	17.6(5)	-1.7(4)	0.6(4)	-2.2(4)
C(14)	11.5(4)	17.2(5)	17.4(5)	-2.3(4)	-0.4(4)	-2.6(4)
C(11)	12.4(5)	17.7(5)	26.2(5)	0.8(4)	2.9(4)	-1.3(4)
C(15)	14.4(5)	24.9(6)	27.2(6)	-3.5(4)	5.4(4)	-4.4(4)
C(7)	26.6(6)	27.8(6)	20.6(5)	2.1(4)	2.6(4)	-8.2(5)
C(17)	16.9(5)	29.3(6)	28.4(6)	6.9(5)	-5.8(4)	-3.2(4)
C(10)	26.9(6)	21.9(6)	39.2(7)	-5.1(5)	15.8(5)	-2.5(4)
C(16)	25.9(6)	20.9(6)	34.6(6)	-7.0(5)	11.0(5)	-1.2(5)
C(8)	35.3(7)	19.6(6)	38.6(7)	7.1(5)	3.2(5)	-7.3(5)
C(9)	38.7(7)	16.7(6)	57.8(9)	-3.0(6)	16.1(6)	0.7(5)

Table 4: Bond Lengths in Å for **227**.

Atom	Atom	Length/Å
O(4)	C(13)	1.3551(12)
O(4)	C(14)	1.4691(12)
O(2)	C(1)	1.2240(13)
O(3)	C(13)	1.2194(13)
O(1)	C(1)	1.3186(13)
N(1)	C(13)	1.3436(13)
N(1)	C(12)	1.4576(13)
C(3)	C(4)	1.5688(13)
C(3)	C(12)	1.5208(14)
C(3)	C(2)	1.5692(15)
C(1)	C(2)	1.4988(14)
C(5)	C(4)	1.5037(14)

Atom	Atom	Length/Å
C(5)	C(6)	1.3903(15)
C(5)	C(10)	1.3923(16)
C(4)	C(11)	1.5415(15)
C(2)	C(11)	1.5474(14)
C(6)	C(7)	1.3927(16)
C(14)	C(15)	1.5195(14)
C(14)	C(17)	1.5175(15)
C(14)	C(16)	1.5184(15)
C(7)	C(8)	1.3814(19)
C(10)	C(9)	1.3843(19)
C(8)	C(9)	1.387(2)

Table 5: Bond Angles in ° for **227**.

Atom	Atom	Atom	Angle/°
C(13)	O(4)	C(14)	121.03(8)
C(13)	N(1)	C(12)	123.36(8)
O(3)	C(13)	O(4)	125.14(9)
O(3)	C(13)	N(1)	125.48(9)
N(1)	C(13)	O(4)	109.38(8)
C(4)	C(3)	C(2)	87.54(7)
C(12)	C(3)	C(4)	115.77(8)
C(12)	C(3)	C(2)	115.73(8)
O(2)	C(1)	O(1)	123.21(10)
O(2)	C(1)	C(2)	122.80(9)
O(1)	C(1)	C(2)	113.96(9)
C(6)	C(5)	C(4)	122.48(10)
C(6)	C(5)	C(10)	118.12(10)
C(10)	C(5)	C(4)	119.40(10)
C(5)	C(4)	C(3)	120.00(9)
C(5)	C(4)	C(11)	120.96(9)
C(11)	C(4)	C(3)	88.75(8)
N(1)	C(12)	C(3)	108.67(8)
C(1)	C(2)	C(3)	119.61(8)
C(1)	C(2)	C(11)	115.80(9)
C(11)	C(2)	C(3)	88.52(8)
C(5)	C(6)	C(7)	120.77(11)
O(4)	C(14)	C(15)	102.30(8)
O(4)	C(14)	C(17)	110.88(9)
O(4)	C(14)	C(16)	110.21(9)
C(17)	C(14)	C(15)	110.40(9)
C(17)	C(14)	C(16)	112.15(10)
C(16)	C(14)	C(15)	110.48(9)
C(4)	C(11)	C(2)	89.30(8)
C(8)	C(7)	C(6)	120.31(11)
C(9)	C(10)	C(5)	121.29(11)
C(7)	C(8)	C(9)	119.49(11)
C(10)	C(9)	C(8)	120.00(12)

Table 6: Hydrogen Fractional Atomic Coordinates ($\times 10^4$) and Equivalent Isotropic Displacement Parameters ($Å^2 \times 10^3$) for **227**. U_{eq} is defined as 1/3 of the trace of the orthogonalized U_{ij}.

Atom	x	y	z	U_{eq}
H(1)	5087.67	10070.97	3769.54	36
H(1A)	6185.08	7520.48	3192.59	20
H(3)	4218.91	7248.61	1928.3	18
H(4)	2231.39	7009.91	1754.19	19
H(12A)	4524.57	7248.46	4834.33	18
H(12B)	4865.43	6386.47	4012.72	18
H(2)	3295.84	8669.23	1909.39	20
H(6)	1431.85	6744.59	4784.13	22
H(11A)	2329.14	8034.69	4216.7	23
H(11B)	1598.23	8294.99	2754.28	23
H(15A)	9881.33	8111.86	4537.5	33
H(15B)	10293.32	8986.44	5431.49	33
H(15C)	9323	9088.43	4125.09	33
H(7)	1054.03	5371.73	5841.59	30
H(17A)	8488.39	7729.81	7382.49	39
H(17B)	9778.15	8123.34	7452.83	39
H(17C)	9352.89	7272.4	6514.13	39
H(10)	3135.85	5311	2273.2	34
H(16A)	7876.33	9789.35	5439.98	40
H(16B)	8857.55	9742.77	6744.09	40
H(16C)	7610.64	9286.49	6745.37	40
H(8)	1771.71	3975.03	5167.86	38
H(9)	2796.72	3947.64	3357.14	44

***tert*-Butyl (((1*R*,2*S*,4*S*)-2-((4*S*,5*R*)-4-methyl-2-oxo-5-phenyloxazolidine-3-carbonyl)-4-phenylcyclobutyl)methyl)carbamate (237a)**

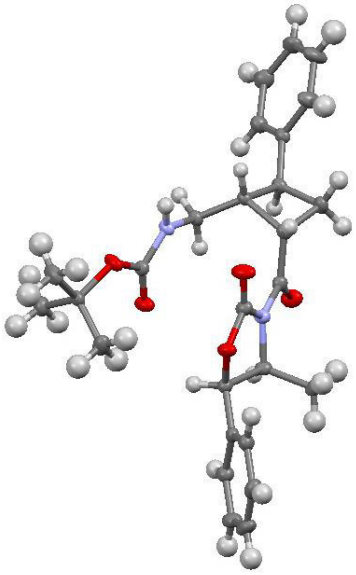

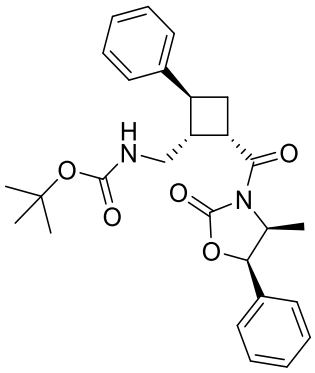

Table 1: Crystal data and structure refinement for **237a**.

Chemical formula	$C_{27}H_{32}N_2O_5$
M_r	464.54
Crystal system, space group	Orthorhombic, $P2_12_12_1$
Temperature (K)	123
a, *b*, *c* (Å)	9.6101 (1), 11.1874 (1), 23.1811 (3)
V (Å^3)	2492.25 (5)
Z	4
Radiation type	Cu *K*α
μ (mm^{-1})	0.69
Crystal size (mm)	0.19 × 0.06 × 0.04
F(000)	992
Diffractometer	SuperNova, Single source at offset, Atlas
Absorption correction	Gaussian *CrysAlis PRO* 1.171.38.42b (Rigaku Oxford Diffraction, 2015) Numerical absorption correction based on gaussian integration over a multifaceted crystal model Empirical absorption correction using spherical harmonics, implemented in SCALE3 ABSPACK scaling algorithm.

T_{min}, T_{max}	0.976, 0.994
No. of measured, independent and observed [$I > 2\sigma(I)$] reflections	29493, 4992, 4717
R_{int}	0.042
$(\sin \theta/\lambda)_{max}$ (Å^{-1})	0.622
$R[F^2 > 2\sigma(F^2)]$, $wR(F^2)$, S	0.028, 0.070, 1.06
No. of reflections	4992
No. of parameters	312
H-atom treatment	H-atom parameters constrained
$\Delta\rho_{max}$, $\Delta\rho_{min}$ (e Å^{-3})	0.15, −0.16
Absolute structure	Refined as an inversion twin.
Absolute structure parameter	−0.07 (17)

Table 2: Fractional Atomic Coordinates (×10^4) and Equivalent Isotropic Displacement Parameters (Å^2×10^3) for **237a**. U_{eq} is defined as 1/3 of the trace of the orthogonalized U_{ij}.

Atom	x	y	z	U_{eq}
O(3)	4947.4(12)	4041.2(11)	4282.7(5)	23.7(3)
O(1)	7336.2(13)	5765.3(12)	5688.3(6)	28.6(3)
O(4)	6682.9(13)	6884.6(12)	3942.6(6)	27.9(3)
O(2)	3582.3(13)	5292.5(13)	4777.2(6)	32.2(3)
O(5)	4556.8(12)	7345.5(12)	3558.9(5)	26.9(3)
N(1)	5906.0(14)	4967.8(12)	5034.3(6)	19.2(3)
N(2)	5020.8(14)	7904.1(13)	4444.7(6)	20.3(3)
C(23)	5534.7(16)	7340.2(15)	3979.1(7)	19.0(3)
C(1)	5849.2(17)	8213.7(15)	4947.8(7)	19.0(3)
C(22)	4696.9(18)	4836.3(15)	4709.9(7)	21.9(3)
C(12)	6166.0(17)	5759.0(15)	5484.4(7)	20.2(3)
C(15)	6674.2(18)	2544.2(15)	4037.2(7)	21.1(3)
C(3)	5009.7(18)	6544.5(14)	5701.8(7)	20.4(3)
C(6)	5582.5(16)	9327.1(15)	6402.4(7)	19.7(3)
C(14)	6430.1(17)	3794.6(15)	4248.2(7)	20.3(3)
C(13)	6948.4(17)	4072.1(15)	4862.4(7)	20.7(3)
C(5)	5869.3(17)	8179.6(15)	6083.8(7)	19.5(3)
C(24)	4846.8(18)	6918.7(15)	2972.1(7)	21.2(3)
C(4)	5305(2)	6983.6(15)	6324.4(7)	24.9(4)
C(7)	6505.4(19)	10282.3(16)	6362.3(8)	25.8(4)
C(16)	5601.2(19)	1718.3(16)	3979.6(8)	25.7(4)
C(20)	8025.3(19)	2207.2(17)	3900.5(8)	26.1(4)
C(2)	5118.2(16)	7887.6(14)	5505.4(7)	16.9(3)
C(8)	6311(2)	11313.1(17)	6686.4(9)	30.0(4)

Atom	x	y	z	U_{eq}
C(19)	8297(2)	1049.3(18)	3711.8(9)	32.5(4)
C(25)	5154(2)	5587.3(16)	2971.9(8)	32.2(4)
C(18)	7231(2)	233.0(17)	3658.2(9)	34.4(4)
C(27)	6030(2)	7618.6(17)	2705.3(8)	28.7(4)
C(17)	5882(2)	565.1(17)	3789.2(8)	31.2(4)
C(21)	6919(2)	3020.2(17)	5277.8(8)	28.4(4)
C(11)	4438(2)	9456.2(18)	6764.6(10)	35.7(5)
C(9)	5201(2)	11415.4(17)	7058.9(8)	33.2(4)
C(26)	3485(2)	7186(2)	2664.7(8)	32.8(4)
C(10)	4260(2)	10487(2)	7092.9(10)	43.4(5)

Table 3: Anisotropic Displacement Parameters ($\times 10^4$) **237a**. The anisotropic displacement factor exponent takes the form: $-2p^2[h^2a^{*2} \times U_{11} + ... + 2hka^* \times b^* \times U_{12}]$

Atom	U_{11}	U_{22}	U_{33}	U_{23}	U_{13}	U_{12}
O(3)	21.8(6)	25.5(6)	23.7(6)	-7.4(5)	-5.5(5)	6.5(5)
O(1)	21.2(6)	29.4(7)	35.4(7)	-7.5(6)	-7.7(5)	-2.0(5)
O(4)	23.4(6)	36.1(7)	24.1(6)	-7.4(5)	-4.5(5)	9.8(5)
O(2)	21.5(6)	37.6(7)	37.4(7)	-15.2(6)	-9.2(5)	10.2(6)
O(5)	21.0(6)	43.8(7)	16.1(6)	-7.3(5)	-2.8(4)	7.6(5)
N(1)	16.6(6)	19.8(6)	21.1(6)	-2.0(5)	-1.7(5)	1.4(5)
N(2)	15.9(6)	28.1(7)	16.9(6)	-2.7(5)	-1.5(5)	0.8(5)
C(23)	18.5(8)	21.0(7)	17.5(7)	-0.2(6)	-2.3(6)	-0.5(6)
C(1)	17.4(7)	21.6(8)	17.8(7)	-2.1(6)	-0.3(6)	-2.7(6)
C(22)	21.4(8)	21.5(8)	22.8(8)	-2.5(7)	-5.0(6)	2.1(6)
C(12)	20.2(8)	18.6(7)	21.6(8)	-0.1(6)	-1.1(6)	-2.9(6)
C(15)	26.6(8)	20.1(8)	16.5(7)	1.5(6)	0.4(6)	3.6(7)
C(3)	21.2(8)	20.6(8)	19.4(7)	-2.5(6)	2.0(6)	-3.2(6)
C(6)	17.4(7)	25.0(8)	16.5(7)	-3.1(6)	-2.2(6)	0.0(6)
C(14)	19.3(8)	20.0(8)	21.5(8)	0.2(6)	0.2(6)	1.7(6)
C(13)	16.4(7)	21.2(8)	24.4(8)	-3.1(7)	-1.1(6)	1.7(6)
C(5)	18.3(7)	23.5(8)	16.8(7)	-3.5(6)	-1.2(6)	-0.3(6)
C(24)	23.2(8)	25.8(8)	14.5(7)	-2.1(6)	-0.6(6)	-0.2(7)
C(4)	34.2(9)	23.8(8)	16.7(8)	-1.5(7)	0.1(7)	-1.1(7)
C(7)	24.4(9)	27.5(9)	25.6(8)	-1.7(7)	1.7(7)	-2.3(7)
C(16)	28.1(9)	25.3(9)	23.7(8)	2.3(7)	3.3(7)	0.9(7)
C(20)	24.9(9)	27.9(9)	25.6(9)	-1.0(7)	-1.1(7)	3.6(7)
C(2)	14.8(7)	19.6(7)	16.2(7)	-2.6(6)	-0.2(6)	-0.9(6)
C(8)	31.1(10)	25.5(9)	33.6(10)	-3.9(8)	-7.5(8)	-4.9(8)
C(19)	33.2(10)	33.1(10)	31.1(10)	-3.5(8)	-3.0(8)	14.8(8)
C(25)	47.0(11)	24.1(9)	25.4(8)	-1.4(7)	-5.4(8)	-4.4(8)
C(18)	49.3(12)	22.1(9)	31.7(10)	-3.7(8)	-8.3(9)	11.8(8)
C(27)	31.4(10)	29.9(9)	24.9(8)	4.9(8)	0.9(7)	-3.0(8)
C(17)	41.7(11)	21.7(8)	30.2(9)	2.8(7)	-4.4(8)	-2.3(8)
C(21)	35.1(10)	26.0(9)	24.2(9)	-0.3(7)	-7.6(7)	8.4(8)
C(11)	27.9(10)	31.1(10)	48.0(12)	-10.3(9)	15.3(9)	-6.0(8)
C(9)	45.6(11)	27.9(9)	26.1(9)	-10.2(8)	-3.3(9)	5.5(9)
C(26)	27.3(9)	52.2(12)	19.0(8)	-4.6(8)	-5.2(7)	3.9(9)
C(10)	44.9(12)	38.3(11)	47.2(13)	-11(1)	24.2(10)	1.6(10)

Table 4: Bond Lengths in Å for **237a**.

Atom	Atom	Length/Å
O(3)	C(22)	1.353(2)
O(3)	C(14)	1.454(2)
O(1)	C(12)	1.220(2)
O(4)	C(23)	1.218(2)
O(2)	C(22)	1.197(2)
O(5)	C(23)	1.354(2)
O(5)	C(24)	1.4683(19)
N(1)	C(22)	1.392(2)
N(1)	C(12)	1.391(2)
N(1)	C(13)	1.472(2)
N(2)	C(23)	1.344(2)
N(2)	C(1)	1.454(2)
C(1)	C(2)	1.516(2)
C(12)	C(3)	1.504(2)
C(15)	C(14)	1.500(2)
C(15)	C(16)	1.391(3)
C(15)	C(20)	1.389(2)
C(3)	C(4)	1.551(2)
C(3)	C(2)	1.573(2)
C(6)	C(5)	1.506(2)
C(6)	C(7)	1.392(2)
C(6)	C(11)	1.391(2)
C(14)	C(13)	1.540(2)
C(13)	C(21)	1.521(2)
C(5)	C(4)	1.548(2)
C(5)	C(2)	1.558(2)
C(24)	C(25)	1.519(2)
C(24)	C(27)	1.513(2)
C(24)	C(26)	1.520(2)
C(7)	C(8)	1.389(3)
C(16)	C(17)	1.390(3)
C(20)	C(19)	1.392(3)
C(8)	C(9)	1.377(3)
C(19)	C(18)	1.378(3)
C(18)	C(17)	1.383(3)
C(11)	C(10)	1.392(3)
C(9)	C(10)	1.379(3)

Table 5: Bond Angles in ° for **237a**.

Atom	Atom	Atom	Angle/°
C(22)	O(3)	C(14)	109.84(13)
C(23)	O(5)	C(24)	122.24(13)
C(22)	N(1)	C(13)	110.48(13)
C(12)	N(1)	C(22)	128.50(15)
C(12)	N(1)	C(13)	120.94(14)
C(23)	N(2)	C(1)	123.69(13)
O(4)	C(23)	O(5)	125.49(15)
O(4)	C(23)	N(2)	125.79(15)
N(2)	C(23)	O(5)	108.71(13)
N(2)	C(1)	C(2)	111.89(13)
O(3)	C(22)	N(1)	108.45(14)
O(2)	C(22)	O(3)	122.35(15)
O(2)	C(22)	N(1)	129.17(16)
O(1)	C(12)	N(1)	117.38(16)
O(1)	C(12)	C(3)	123.23(15)
N(1)	C(12)	C(3)	119.38(14)
C(16)	C(15)	C(14)	122.33(15)
C(20)	C(15)	C(14)	118.27(16)
C(20)	C(15)	C(16)	119.40(16)
C(12)	C(3)	C(4)	111.22(14)
C(12)	C(3)	C(2)	114.34(13)
C(4)	C(3)	C(2)	87.40(12)
C(7)	C(6)	C(5)	120.33(15)
C(11)	C(6)	C(5)	121.94(16)
C(11)	C(6)	C(7)	117.67(16)
O(3)	C(14)	C(15)	110.37(14)
O(3)	C(14)	C(13)	103.18(13)
C(15)	C(14)	C(13)	116.02(14)
N(1)	C(13)	C(14)	99.64(13)
N(1)	C(13)	C(21)	110.05(14)
C(21)	C(13)	C(14)	115.05(14)
C(6)	C(5)	C(4)	119.74(14)
C(6)	C(5)	C(2)	121.07(14)
C(4)	C(5)	C(2)	88.07(12)
O(5)	C(24)	C(25)	110.86(14)
O(5)	C(24)	C(27)	110.68(14)
O(5)	C(24)	C(26)	101.94(13)
C(25)	C(24)	C(26)	111.12(16)
C(27)	C(24)	C(25)	111.19(15)
C(27)	C(24)	C(26)	110.72(15)
C(5)	C(4)	C(3)	90.16(12)
C(8)	C(7)	C(6)	121.04(17)
C(17)	C(16)	C(15)	120.22(17)
C(15)	C(20)	C(19)	119.99(18)
C(1)	C(2)	C(3)	120.49(13)
C(1)	C(2)	C(5)	117.96(13)

Atom	Atom	Atom	Angle/°
C(5)	C(2)	C(3)	88.96(12)
C(9)	C(8)	C(7)	120.81(18)
C(18)	C(19)	C(20)	120.37(18)
C(19)	C(18)	C(17)	119.96(18)
C(18)	C(17)	C(16)	120.06(18)
C(6)	C(11)	C(10)	120.88(18)
C(8)	C(9)	C(10)	118.76(18)
C(9)	C(10)	C(11)	120.78(18)

Table 6: Hydrogen Fractional Atomic Coordinates ($\times 10^4$) and Equivalent Isotropic Displacement Parameters ($Å^2 \times 10^3$) for **237a**. U_{eq} is defined as 1/3 of the trace of the orthogonalized U_{ij}.

Atom	x	y	z	U_{eq}
H(2)	4153.2	8092.38	4445.08	24
H(1A)	6036.78	9065.66	4944.45	23
H(1B)	6733.89	7798.18	4928.85	23
H(3)	4080.66	6198.85	5651.37	24
H(14)	6859.24	4358.14	3977.77	24
H(13)	7878.88	4429.74	4850.24	25
H(5)	6875.63	8104.4	6025.79	23
H(4A)	4473.18	7072.8	6557.54	30
H(4B)	6000.52	6512.85	6525.1	30
H(7)	7264.11	10229.48	6114.54	31
H(16)	4693.13	1938.54	4068.67	31
H(20)	8748.4	2755	3934.95	31
H(2A)	4188.55	8247.6	5508.52	20
H(8)	6938.5	11941.94	6651.56	36
H(19)	9203.22	825.44	3621.32	39
H(25A)	6020.56	5443.11	3165.84	48
H(25B)	5215.2	5306.31	2581.44	48
H(25C)	4420.42	5170.69	3168.38	48
H(18)	7419.25	-540.84	3534.12	41
H(27A)	5848.36	8458.86	2742.4	43
H(27B)	6110.13	7415.26	2304.33	43
H(27C)	6882.94	7425.76	2899.88	43
H(17)	5160.93	16.33	3749.78	37
H(21A)	7097.69	3299.05	5662.38	43
H(21B)	7620.53	2452.08	5169.15	43
H(21C)	6021.16	2645.6	5263.99	43
H(11)	3783.66	8845.85	6787.76	43
H(9)	5087.27	12097.75	7283.15	40
H(26A)	2747.12	6738.34	2841.51	49
H(26B)	3562.78	6963.7	2266.04	49
H(26C)	3284.94	8024.74	2692.5	49
H(10)	3497.34	10550.25	7338.05	52

(±)-4-Phenethylpyrrolidin-2-one ((±)-215)

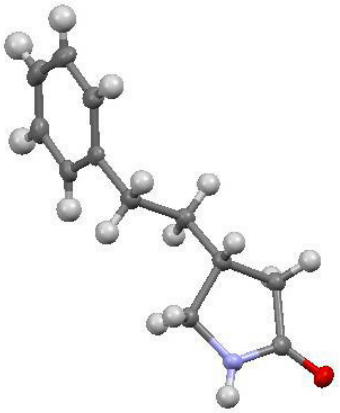

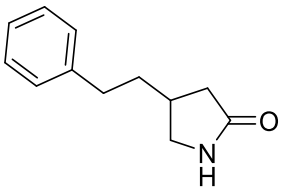

Table 1: Crystal data and structure refinement for **(±)-215**.

Chemical formula	$C_{12}H_{15}NO$
M_r	189.25
Crystal system, space group	Monoclinic, *P*21/*c*
Temperature (K)	123
a, *b*, *c* (Å)	13.2652 (6), 8.1381 (3), 10.0280 (4)
β (°)	109.190 (5)
V (Å^3)	1022.40 (8)
Z	4
Radiation type	Cu *Kα*
μ (mm^{-1})	0.61
Crystal size (mm)	0.22 × 0.12 × 0.08
F(000)	408
Diffractometer	SuperNova, Single source at offset, Atlas
Absorption correction	Gaussian *CrysAlis PRO* 1.171.38.42b (Rigaku Oxford Diffraction, 2015) Numerical absorption correction based on gaussian integration over a multifaceted crystal model Empirical absorption correction using spherical harmonics, implemented in SCALE3 ABSPACK scaling algorithm .

T_{min}, T_{max}	0.759, 0.899
No. of measured, independent and observed [$I > 2\sigma(I)$] reflections	19680, 1787, 1480
R_{int}	0.070
$(\sin \theta/\lambda)_{max}$ (Å^{-1})	0.595
$R[F^2 > 2\sigma(F^2)]$, $wR(F^2)$, S	0.035, 0.096, 1.03
No. of reflections	1787
No. of parameters	127
H-atom treatment	H-atom parameters constrained
$\Delta\rho_{max}$, $\Delta\rho_{min}$ (e Å^{-3})	0.17, −0.17

Table 2: Fractional Atomic Coordinates (×10^4) and Equivalent Isotropic Displacement Parameters (Å^2×10^3) for **(±)-215**. U_{eq} is defined as 1/3 of the trace of the orthogonalized U_{ij}.

Atom	x	y	z	U_{eq}
O(001)	5496.1(7)	2678.0(12)	3186.9(10)	29.5(3)
N(002)	4200.0(9)	4610.0(14)	2994.5(11)	25.6(3)
C(003)	1555.7(11)	4792.6(16)	6617.9(14)	25.7(3)
C(004)	4190.3(10)	2393.3(17)	4430.7(14)	24.4(3)
C(005)	3149.7(10)	3348.2(16)	4203.0(14)	23.9(3)
C(006)	4713.3(11)	3205.9(16)	3469.5(13)	24.0(3)
C(007)	3329.3(10)	4982.0(16)	3527.0(14)	24.5(3)
C(008)	1833.3(11)	4594.6(18)	5284.2(15)	27.2(3)
C(009)	2859.4(11)	3600.0(17)	5532.5(14)	25.0(3)
C(00A)	2202.2(12)	5732.9(17)	7741.3(16)	29.9(3)
C(00B)	689.3(11)	3970.6(18)	6798.2(15)	30.1(3)
C(00C)	472.3(12)	4077(2)	8057.5(16)	36.5(4)
C(00D)	1997.1(13)	5820.1(18)	9009.2(16)	35.0(4)
C(00E)	1130.8(13)	4994(2)	9167.8(17)	38.2(4)

Table 3: Anisotropic Displacement Parameters (×10^4) **(±)-215**. The anisotropic displacement factor exponent takes the form: $-2p^2[h^2a^{*2} \times U_{11} + ... + 2hka^* \times b^* \times U_{12}]$

Atom	U_{11}	U_{22}	U_{33}	U_{23}	U_{13}	U_{12}
O(001)	30.4(5)	29.1(6)	34.0(5)	-6.8(4)	17.4(4)	-1.0(4)
N(002)	32.3(6)	21.0(6)	28.4(6)	1.2(5)	16.5(5)	-1.7(5)
C(003)	27.0(7)	20.8(7)	31.7(7)	5.6(5)	13.2(6)	8.0(5)
C(004)	27.9(7)	20.1(7)	27.2(7)	-1.0(5)	11.9(5)	-0.8(5)
C(005)	26.0(7)	20.6(7)	26.0(7)	-0.4(5)	9.9(5)	-1.5(5)
C(006)	27.4(7)	22.1(7)	23.4(6)	-7.0(5)	9.5(5)	-5.2(5)
C(007)	27.2(7)	22.0(7)	26.1(7)	0.0(5)	11.0(6)	0.3(5)
C(008)	29.1(7)	24.7(7)	30.0(7)	4.2(6)	12.8(6)	3.1(6)
C(009)	27.7(7)	22.0(7)	27.4(7)	2.3(5)	11.8(6)	1.3(6)
C(00A)	33.7(8)	19.5(7)	39.5(8)	1.0(6)	16.1(6)	3.6(6)

Atom	U_{11}	U_{22}	U_{33}	U_{23}	U_{13}	U_{12}
C(00B)	25.5(7)	30.3(8)	35.9(8)	3.9(6)	11.9(6)	4.7(6)
C(00C)	30.4(8)	41.4(9)	43.7(9)	11.4(7)	20.6(7)	8.6(7)
C(00D)	43.6(9)	27.0(8)	36.4(8)	-3.5(6)	15.7(7)	7.3(7)
C(00E)	44.0(9)	41.1(9)	36.8(8)	4.0(7)	23.1(7)	15.2(7)

Table 4: Bond Lengths in Å for **(±)-215**.

Atom	Atom	Length/Å
O(001)	C(006)	1.2397(16)
N(002)	C(006)	1.3353(18)
N(002)	C(007)	1.4547(16)
C(003)	C(008)	1.5079(19)
C(003)	C(00A)	1.398(2)
C(003)	C(00B)	1.3921(19)
C(004)	C(005)	1.5344(18)
C(004)	C(006)	1.5124(18)
C(005)	C(007)	1.5462(18)
C(005)	C(009)	1.5182(18)
C(008)	C(009)	1.5320(18)
C(00A)	C(00D)	1.387(2)
C(00B)	C(00C)	1.387(2)
C(00C)	C(00E)	1.386(2)
C(00D)	C(00E)	1.385(2)

Table 5: Bond Angles in ° for **(±)-215**.

Atom	Atom	Atom	Angle/°
C(006)	N(002)	C(007)	114.86(11)
C(00A)	C(003)	C(008)	120.61(13)
C(00B)	C(003)	C(008)	121.10(13)
C(00B)	C(003)	C(00A)	118.18(13)
C(006)	C(004)	C(005)	105.21(11)
C(004)	C(005)	C(007)	103.89(10)
C(009)	C(005)	C(004)	114.40(11)
C(009)	C(005)	C(007)	112.90(11)
O(001)	C(006)	N(002)	125.61(13)
O(001)	C(006)	C(004)	126.04(12)
N(002)	C(006)	C(004)	108.34(11)
N(002)	C(007)	C(005)	103.73(10)
C(003)	C(008)	C(009)	112.04(11)
C(005)	C(009)	C(008)	113.38(11)
C(00D)	C(00A)	C(003)	120.90(14)
C(00C)	C(00B)	C(003)	121.03(14)
C(00E)	C(00C)	C(00B)	120.03(14)
C(00E)	C(00D)	C(00A)	120.05(15)
C(00D)	C(00E)	C(00C)	119.79(14)

Table 6: Hydrogen Fractional Atomic Coordinates ($\times 10^4$) and Equivalent Isotropic Displacement Parameters ($Å^2 \times 10^3$) for **(±)-215**. U_{eq} is defined as 1/3 of the trace of the orthogonalized U_{ij}.

Atom	x	y	z	U_{eq}
H(002)	4371.01	5245.74	2417.98	31
H(00A)	4647.2	2462.87	5408.3	29
H(00B)	4042.58	1245.55	4182.11	29
H(005)	2566.56	2751.19	3513.97	29
H(00C)	2692.81	5305.54	2766.04	29
H(00D)	3525.83	5855.68	4222.89	29
H(00E)	1920.97	5671.77	4922.92	33
H(00F)	1249.5	4046.43	4576.67	33
H(00G)	3442.77	4161.85	6229.49	30
H(00H)	2774.49	2534.76	5916.32	30
H(00I)	2777.65	6307.55	7636.8	36
H(00J)	249.06	3340.16	6062.83	36
H(00K)	-115.51	3532.87	8156.72	44
H(00L)	2441.59	6433.93	9753.45	42
H(00M)	991.6	5054.11	10016.93	46

(*S*)-3-(Aminomethyl)-5-phenylpentanoic acid hydrochloride ((*S*)-257)

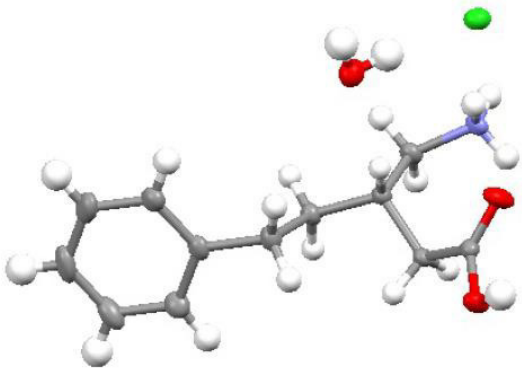

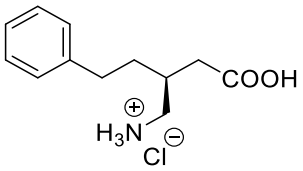

Table 1: Crystal data and structure refinement for **(*S*)-257**.

Chemical formula	$Cl \cdot C_{12}H_{18}NO_2 \cdot H_2O$
M_r	261.74
Crystal system, space group	Monoclinic, *P*21
Temperature (K)	123
a, *b*, *c* (Å)	6.3309 (2), 8.1505 (2), 13.7227 (4)
β (°)	101.228 (3)
V (Å^3)	694.54 (4)
Z	2
Radiation type	Cu *Kα*
μ (mm^{-1})	2.42
Crystal size (mm)	0.22 × 0.19 × 0.11
F(000)	280
Diffractometer	SuperNova, Single source at offset, Atlas
Absorption correction	Gaussian *CrysAlis PRO* 1.171.38.43 (Rigaku Oxford Diffraction, 2015) Numerical absorption correction based on gaussian integration over a multifaceted crystal model Empirical absorption correction using spherical harmonics, implemented in SCALE3 ABSPACK scaling algorithm.

T_{min}, T_{max}	0.808, 0.907
No. of measured, independent and observed [$I > 2\sigma(I)$] reflections	8612, 2879, 2826
R_{int}	0.029
$(\sin \theta/\lambda)_{max}$ (Å^{-1})	0.630
$R[F^2 > 2\sigma(F^2)]$, $wR(F^2)$, S	0.024, 0.063, 1.07
No. of reflections	2879
No. of parameters	163
No. of restraints	1
H-atom treatment	0.17, −0.15
Absolute structure	Flack x determined using 1276 quotients [(I+)-(I-)]/[(I+)+(I-)] (Parsons, Flack and Wagner, Acta Cryst. B69
$\Delta\rho_{max}$, $\Delta\rho_{min}$ (e Å^{-3})	H-atom treatment H atoms treated by a mixture of independent and constrained refinement(2013) 249-259).
Absolute structure parameter	−0.009 (7)

Table 2: Fractional Atomic Coordinates (×10^4) and Equivalent Isotropic Displacement Parameters (Å^2×10^3) for **(*S*)-257**. U_{eq} is defined as 1/3 of the trace of the orthogonalized U_{ij}.

Atom	x	y	z	U_{eq}
Cl1	1657.1(6)	5660.2(5)	-593.7(3)	27.58(12)
O1	9678.1(19)	5621(2)	2263.4(9)	28.4(3)
O2	6996(2)	5197.3(19)	972.4(10)	34.1(4)
O3	1517(2)	7742.7(19)	1293.5(11)	32.5(3)
N1	3917(3)	2494.5(19)	586.8(11)	23.8(3)
C9	4556(3)	3635(2)	2325.1(12)	18.6(3)
C12	7879(3)	4914(2)	1821.5(12)	19.4(3)
C10	3549(3)	2268(2)	1622.0(12)	23.3(4)
C8	3825(3)	3404(2)	3322.4(12)	20.1(3)
C7	4176(3)	4957(2)	3964.3(13)	23.9(3)
C11	7039(3)	3693(2)	2479.1(12)	19.6(3)
C2	3185(3)	4836(2)	4880.2(12)	22.1(3)
C1	1182(3)	5531(3)	4886.4(13)	28.1(4)
C3	4239(3)	4012(2)	5725.1(14)	28.2(4)
C5	1301(4)	4571(3)	6557.7(16)	37.9(5)

Atom	x	y	z	U_{eq}
C6	248(3)	5403(3)	5724.8(16)	36.2(5)
C4	3309(4)	3878(3)	6561.6(15)	35.7(5)

Table 3: Anisotropic Displacement Parameters ($\times 10^4$) **(*S*)-257**. The anisotropic displacement factor exponent takes the form: $-2p^2[h^2a^{*2} \times U_{11} + ... + 2hka^* \times b^* \times U_{12}]$

Atom	U_{11}	U_{22}	U_{33}	U_{23}	U_{13}	U_{12}
Cl1	23.50(19)	29.1(2)	28.35(19)	4.85(16)	0.68(13)	-0.38(17)
O1	24.1(6)	37.0(7)	22.3(5)	5.9(6)	0.3(4)	-8.9(7)
O2	32.4(7)	43.7(9)	21.9(6)	13.4(5)	-5.0(5)	-11.1(6)
O3	32.6(7)	31.9(7)	34.9(7)	5.9(6)	11.1(6)	0.9(6)
N1	26.3(7)	25.7(7)	17.4(6)	-4.4(5)	-0.3(5)	3.0(6)
C9	18.9(8)	19.4(8)	16.8(7)	0.7(5)	2.2(6)	0.0(6)
C12	18.3(8)	22.6(7)	17.0(7)	1.5(6)	2.9(6)	3.9(6)
C10	24.8(8)	25.1(9)	18.8(8)	-2.7(6)	1.7(6)	-3.3(6)
C8	22.9(8)	19.6(7)	18.0(7)	0.1(6)	4.7(6)	-2.1(6)
C7	29.0(9)	21.4(8)	22.2(8)	-2.3(6)	7.5(7)	-3.7(7)
C11	19.5(8)	23.3(8)	15.2(7)	2.9(6)	1.4(6)	0.5(6)
C2	28.5(9)	18.0(8)	20.4(8)	-5.1(6)	6.4(6)	-4.9(6)
C1	30.1(8)	29.3(9)	24.1(7)	-6.7(7)	3.5(6)	-0.3(8)
C3	36.2(10)	20.3(8)	28.2(9)	0.7(7)	6.4(7)	1.8(7)
C5	58.2(14)	33.4(10)	28.0(9)	-12.2(8)	23.0(9)	-12.6(10)
C6	35.2(10)	39.6(13)	37(1)	-17.6(9)	14.8(8)	-2.1(9)
C4	60.2(14)	24.8(9)	22.6(9)	1.7(7)	9.2(9)	-3.9(9)

Table 4: Bond Lengths in Å for **(*S*)-257**.

Atom	Atom	Length/Å
O1	C12	1.314(2)
O2	C12	1.212(2)
N1	C10	1.495(2)
C9	C10	1.529(2)
C9	C8	1.539(2)
C9	C11	1.546(2)
C12	C11	1.509(2)
C8	C7	1.533(2)

Atom	Atom	Length/Å
C7	C2	1.513(2)
C2	C1	1.391(3)
C2	C3	1.392(3)
C1	C6	1.396(3)
C3	C4	1.392(3)
C5	C6	1.383(4)
C5	C4	1.390(4)

Table 5: Bond Angles in ° for **(*S*)-257**.

Atom	Atom	Atom	Angle/°
C10	C9	C8	108.12(13)
C10	C9	C11	113.35(14)
C8	C9	C11	110.85(13)
O1	C12	C11	112.83(14)
O2	C12	O1	123.79(16)
O2	C12	C11	123.37(16)
N1	C10	C9	112.75(15)
C7	C8	C9	111.98(14)
C2	C7	C8	112.73(15)

Atom	Atom	Atom	Angle/°
C12	C11	C9	113.96(14)
C1	C2	C7	120.31(17)
C1	C2	C3	118.75(17)
C3	C2	C7	120.93(17)
C2	C1	C6	120.51(18)
C2	C3	C4	120.90(19)
C6	C5	C4	119.70(18)
C5	C6	C1	120.28(19)
C5	C4	C3	119.9(2)

Table 6: Hydrogen Fractional Atomic Coordinates ($\times 10^4$) and Equivalent Isotropic Displacement Parameters ($Å^2 \times 10^3$) for **(*S*)-257**. U_{eq} is defined as 1/3 of the trace of the orthogonalized U_{ij}.

Atom	x	y	z	U_{eq}
H1	10048.84	6298.37	1887.87	43
H3A	1500.95	7309.5	729.03	49
H1A	3142.83	1761.97	187.56	29
H1B	5307.33	2353.81	578.87	29
H1C	3519.02	3502.13	377.76	29
H9	3989.94	4686.88	2041.18	22
H10A	4152.17	1223.56	1876	28
H10B	2011.54	2235	1608.18	28
H8A	2309.16	3116.72	3196.33	24
H8B	4622.84	2503	3682.63	24
H7A	5709.94	5153.6	4166.98	29
H7B	3553.94	5886.83	3568.99	29
H11A	7618.12	3964.33	3167.5	24
H11B	7562.3	2609.96	2353.4	24
H1D	458.67	6085.67	4327.71	34
H3	5581.5	3545.66	5730.83	34
H5	668.17	4475.53	7112.59	45
H6	-1088.32	5878.52	5723.32	43
H4	4030.55	3326	7121.62	43
H3B	690(50)	8510(50)	1090(30)	51(9)

(*R*)-3-(Aminomethyl)-5-phenylpentanoic acid hydrochloride ((*R*)-257)

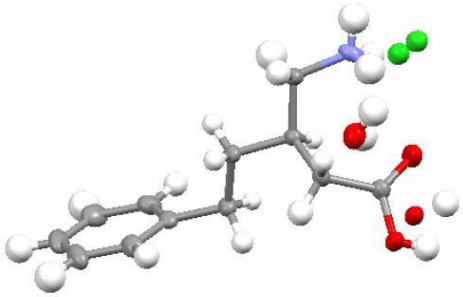

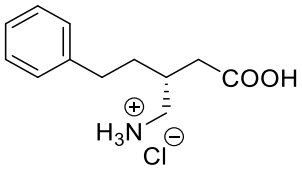

Table 1: Crystal data and structure refinement for**(*R*)-257**.

Chemical formula	$Cl \cdot C_{12}H_{18}NO_2 \cdot H_2O$
M_r	261.74
Crystal system, space group	Monoclinic, *P*21
Temperature (K)	123
a, *b*, *c* (Å)	6.3143 (3), 8.1582 (3), 13.6974 (5)
β (°)	101.031 (4)
V (Å^3)	692.56 (5)
Z	2
Radiation type	Cu *Kα*
μ (mm^{-1})	2.43
Crystal size (mm)	0.16 × 0.12 × 0.05
F(000)	280
Diffractometer	SuperNova, Single source at offset, Atlas
Absorption correction	Gaussian *CrysAlis PRO* 1.171.38.43 (Rigaku Oxford Diffraction, 2015) Numerical absorption correction based on gaussian integration over a multifaceted crystal model Empirical absorption correction using spherical harmonics, implemented in SCALE3 ABSPACK scaling algorithm.

T_{min}, T_{max}	0.878, 0.943
No. of measured, independent and observed [$I > 2\sigma(I)$] reflections	9612, 2866, 2713
R_{int}	0.052
$(\sin \theta/\lambda)_{max}$ (Å^{-1})	0.630
$R[F^2 > 2\sigma(F^2)]$, $wR(F^2)$, S	0.057, 0.159, 1.14
No. of reflections	2866
No. of parameters	240
No. of restraints	14
H-atom treatment	H atoms treated by a mixture of independent and constrained refinement
Absolute structure	Classical Flack method preferred over Parsons because s.u. lower.
$\Delta\rho_{max}$, $\Delta\rho_{min}$ (e Å^{-3})	0.31, −0.42
Absolute structure parameter	0.03 (3)

Table 2: Fractional Atomic Coordinates (×10^4) and Equivalent Isotropic Displacement Parameters (Å^2×10^3) for **(*R*)-257**. U_{eq} is defined as 1/3 of the trace of the orthogonalized U_{ij}.

Atom	***x***	***y***	***z***	U_{iso}*/U_{eq}	**Occ. (<1)**
Cl2	0.16519 (19)	0.43599 (13)	−0.05938 (18)	0.0300 (5)	0.942 (8)
O1	0.6991 (6)	0.4821 (4)	0.0968 (2)	0.0386 (9)	
O3	0.9683 (5)	0.4383 (5)	0.2264 (2)	0.0301 (8)	0.942 (8)
H3	1.001553	0.366720	0.190082	0.045*	0.942 (8)
O4	0.1519 (6)	0.2265 (5)	0.1288 (3)	0.0377 (8)	
H4C	0.075657	0.141168	0.113216	0.056*	
H4D	0.160702	0.279758	0.076238	0.056*	
N1	0.3918 (7)	0.7523 (5)	0.0585 (3)	0.0278 (8)	
C2	0.4570 (7)	0.6388 (4)	0.2325 (3)	0.0210 (8)	
C1	0.3562 (7)	0.7751 (5)	0.1626 (3)	0.0260 (9)	
C12	0.7891 (6)	0.5107 (5)	0.1817 (3)	0.0233 (8)	
C3	0.3833 (7)	0.6620 (5)	0.3325 (3)	0.0229 (8)	
H3A	0.463166	0.751899	0.368622	0.028*	
H3B	0.231377	0.690704	0.320065	0.028*	
C4	0.4182 (7)	0.5069 (5)	0.3964 (3)	0.0264 (8)	

Atom	*x*	*y*	*z*	U_{iso}*/U_{eq}	Occ. (<1)
C11	0.7044 (6)	0.6322 (5)	0.2475 (3)	0.0223 (8)	
C5	0.3182 (7)	0.5186 (5)	0.4883 (3)	0.0243 (8)	
C6	0.4241 (8)	0.6007 (5)	0.5729 (3)	0.0312 (9)	
C8	0.1293 (10)	0.5450 (7)	0.6563 (4)	0.0418 (13)	
C10	0.1181 (7)	0.4485 (6)	0.4890 (3)	0.0313 (9)	
C9	0.0231 (9)	0.4619 (6)	0.5730 (4)	0.0389 (12)	
C7	0.3304 (10)	0.6146 (6)	0.6563 (3)	0.0386 (11)	
H2	0.402 (9)	0.530 (7)	0.204 (4)	0.022 (12)*	
H4A	0.583 (10)	0.479 (7)	0.422 (4)	0.031 (14)*	
H4B	0.349 (8)	0.408 (7)	0.352 (4)	0.021 (12)*	
H6	0.575 (11)	0.659 (10)	0.571 (5)	0.041 (17)*	
H1D	0.417 (11)	0.879 (9)	0.183 (5)	0.041 (17)*	
H11A	0.763 (10)	0.739 (8)	0.233 (4)	0.031 (14)*	
H10	0.038 (10)	0.392 (8)	0.426 (5)	0.036 (16)*	
H8	0.057 (12)	0.554 (10)	0.716 (6)	0.05 (2)*	
H11B	0.769 (11)	0.606 (9)	0.319 (5)	0.040 (16)*	
H1E	0.211 (14)	0.783 (12)	0.163 (6)	0.06 (2)*	
H9	−0.110 (14)	0.410 (12)	0.571 (6)	0.06 (2)*	
H7	0.404 (14)	0.671 (12)	0.721 (7)	0.06 (2)*	
O2	0.993 (3)	0.507 (8)	0.173 (4)	0.0301 (12)	0.058 (8)
H2A	1.001225	0.481723	0.115939	0.045*	0.058 (8)
Cl1	0.147 (3)	0.419 (3)	−0.021 (3)	0.0298 (10)	0.058 (8)
H1A	0.347 (11)	0.653 (10)	0.029 (5)	0.042 (17)*	
H1B	0.330 (13)	0.820 (11)	0.014 (7)	0.06 (2)*	
H1C	0.537 (14)	0.771 (12)	0.056 (6)	0.06 (2)*	

Table 3: Anisotropic Displacement Parameters (×10^4) **(*R*)-257**. The anisotropic displacement factor exponent takes the form: $-2p^2[h^2a^{*2} \times U_{11} + ... + 2hka^* \times b^* \times U_{12}]$

Atom	U^{11}	U^{22}	U^{33}	U^{12}	U^{13}	U^{23}
Cl2	0.0290 (5)	0.0284 (5)	0.0304 (11)	0.0006 (4)	0.0004 (5)	−0.0051 (5)
O1	0.0408 (18)	0.044 (2)	0.0272 (14)	0.0114 (15)	−0.0022 (13)	−0.0149 (14)
O3	0.0281 (15)	0.0352 (17)	0.0251 (14)	0.0103 (16)	0.0003 (11)	−0.0063 (14)
O4	0.0389 (18)	0.0348 (18)	0.0408 (17)	−0.0004 (15)	0.0115 (14)	−0.0049 (14)
N1	0.0330 (19)	0.0258 (18)	0.0214 (15)	−0.0036 (15)	−0.0027 (12)	0.0055 (13)
C2	0.0244 (19)	0.0184 (17)	0.0192 (15)	0.0017 (13)	0.0019 (13)	−0.0005 (12)
C1	0.027 (2)	0.025 (2)	0.0237 (18)	0.0039 (15)	0.0005 (14)	0.0024 (14)
C12	0.0235 (18)	0.0229 (17)	0.0227 (17)	−0.0034 (15)	0.0023 (13)	−0.0039 (14)
C3	0.0276 (19)	0.0183 (15)	0.0229 (17)	0.0032 (14)	0.0049 (13)	−0.0010 (13)
C4	0.034 (2)	0.0220 (18)	0.0248 (17)	0.0052 (16)	0.0086 (15)	0.0020 (15)
C11	0.0243 (19)	0.0228 (19)	0.0189 (16)	−0.0014 (14)	0.0019 (13)	−0.0024 (13)
C5	0.033 (2)	0.0170 (17)	0.0237 (18)	0.0034 (14)	0.0067 (15)	0.0049 (13)

Atom	U^{11}	U^{22}	U^{33}	U^{12}	U^{13}	U^{23}
C6	0.042 (3)	0.0207 (17)	0.031 (2)	−0.0011 (17)	0.0058 (17)	−0.0018 (16)
C8	0.066 (4)	0.033 (2)	0.033 (2)	0.014 (2)	0.025 (2)	0.0133 (19)
C10	0.034 (2)	0.029 (2)	0.0293 (18)	0.0004 (19)	0.0035 (16)	0.0086 (17)
C9	0.039 (2)	0.039 (3)	0.041 (2)	0.001 (2)	0.0138 (19)	0.017 (2)
C7	0.065 (3)	0.025 (2)	0.027 (2)	0.002 (2)	0.011 (2)	−0.0012 (16)
O2	0.028 (2)	0.035 (2)	0.025 (2)	0.010 (2)	0.0003 (18)	−0.006 (2)
Cl1	0.0287 (15)	0.0283 (15)	0.0304 (18)	0.0005 (15)	0.0006 (16)	−0.0052 (16)

Table 4: Bond Lenghts in Å for **(*R*)-257.**

Atoms	Length/ Å	Atoms	Length/ Å
O1—C12	1.214 (5)	C3—C4	1.530 (5)
O3—H3	0.8200	C4—C5	1.515 (5)
O3—C12	1.319 (5)	C4—H4A	1.06 (6)
O4—H4C	0.8501	C4—H4B	1.05 (6)
O4—H4D	0.8512	C11—H11A	0.98 (7)
N1—C1	1.497 (5)	C11—H11B	1.00 (7)
N1—H1A	0.93 (8)	C5—C6	1.393 (6)
N1—H1B	0.86 (10)	C5—C10	1.389 (6)
N1—H1C	0.94 (9)	C6—C7	1.389 (7)
C2—C1	1.525 (5)	C6—H6	1.07 (7)
C2—C3	1.541 (5)	C8—C9	1.386 (9)
C2—C11	1.537 (6)	C8—C7	1.391 (9)
C2—H2	1.00 (6)	C8—H8	1.01 (8)
C1—H1D	0.95 (8)	C10—C9	1.399 (6)
C1—H1E	0.92 (9)	C10—H10	1.02 (6)
C12—C11	1.506 (6)	C9—H9	0.94 (9)
C12—O2	1.316 (15)	C7—H7	1.03 (9)
C3—H3A	0.9700	O2—H2A	0.8200
C3—H3B	0.9700	Cl1—H4D	1.7373

Table 5: Bond Angles in ° for **(*R*)-257**.

Atoms	Angle/°	Atoms	Angle/°
C12—O3—H3	109.5	C3—C4—H4A	113 (3)
H4C—O4—H4D	109.4	C3—C4—H4B	108 (3)
C1—N1—H1A	116 (5)	C5—C4—C3	112.7 (3)
C1—N1—H1B	117 (6)	C5—C4—H4A	106 (3)
C1—N1—H1C	110 (5)	C5—C4—H4B	109 (3)
H1A—N1—H1B	101 (7)	H4A—C4—H4B	108 (4)
H1A—N1—H1C	110 (7)	C2—C11—H11A	111 (4)
H1B—N1—H1C	101 (8)	C2—C11—H11B	110 (4)
C1—C2—C3	107.9 (3)	C12—C11—C2	114.3 (3)
C1—C2—C11	113.7 (3)	C12—C11—H11A	106 (3)
C1—C2—H2	109 (3)	C12—C11—H11B	109 (4)

Atoms	Angle/°
C3—C2—H2	108 (3)
C11—C2—C3	110.9 (3)
C11—C2—H2	107 (3)
N1—C1—C2	112.7 (3)
N1—C1—H1D	106 (4)
N1—C1—H1E	110 (5)
C2—C1—H1D	112 (4)
C2—C1—H1E	110 (6)
H1D—C1—H1E	106 (7)
O1—C12—O3	124.2 (4)
O1—C12—C11	123.0 (4)
O1—C12—O2	101 (2)
O3—C12—C11	112.8 (3)
O2—C12—C11	122 (2)
C2—C3—H3A	109.3
C2—C3—H3B	109.3
H3A—C3—H3B	107.9
C4—C3—C2	111.8 (3)
C4—C3—H3A	109.3
C4—C3—H3B	109.3

Atoms	Angle/°
H11A—C11—H11B	107 (5)
C6—C5—C4	120.7 (4)
C10—C5—C4	120.3 (4)
C10—C5—C6	119.0 (4)
C5—C6—H6	119 (4)
C7—C6—C5	120.8 (5)
C7—C6—H6	120 (4)
C9—C8—C7	119.8 (4)
C9—C8—H8	119 (5)
C7—C8—H8	122 (5)
C5—C10—C9	120.4 (4)
C5—C10—H10	119 (4)
C9—C10—H10	121 (4)
C8—C9—C10	120.0 (5)
C8—C9—H9	122 (5)
C10—C9—H9	118 (5)
C6—C7—C8	120.0 (5)
C6—C7—H7	124 (5)
C8—C7—H7	116 (5)
C12—O2—H2A	109.5

4 Curriculum Vitae

Personal data	
Name	Sabine Martha Kerres
Date of birth	February 1, 1990 in Burglengenfeld
Nationality	German
Email	Sabine.Kerres@chemie.uni-regensburg.de
Education	
Since 11/2014	PhD thesis in the group of Prof. Dr. O. Reiser at the University of Regensburg, Germany
09/2014	Master of Science in chemistry
1/2014-09/2014	Master thesis in the group of Prof. Dr. O. Reiser at the University of Regensburg, Germany
04/2014-07/2014	Research stay in the group of Prof. Dr. J. D. Aitken at Université Paris-Sud XI, Orsay, France
10/2012-09/2014	Advanced studies in chemistry, University of Regensburg, Germany
09/2012	Bachelor of Science in chemistry
10/2009-09/2012	Studies in chemistry, University of Regensburg, Germany
09/2000-06/2009	Allgemeine Hochschulreife (A-levels), Johann-Michael-Fischer-Gymnasium (secondary school), Burglengenfeld, Germany

Professional References

Prof. Dr. Oliver Reiser

Institut für Organische Chemie

Universität Regensburg, Universitätsstr. 31, 93053 Regensburg, Germany

Phone: 0049 941 943 4631

Prof. Dr. D. J. Aitken

Institut de Chimie Moléculaire et des Matériaux d'Orsay (ICMMO)

Université Paris-Sud XI

15 rue Georges Clemenceau, 91405 Orsay Cedex, France

Phone: 0033 1 69 15 32 38

List of publications

Visible Light Mediated Synthesis of γ-Cyclobutane Amino Acids
S. Kerres, S. Malcherek, J. Rehbein, O. Reiser, manuscript in preparation.

Photosensitised regioselective [2+2]-cycloaddition of cinnamates and related alkenes
S. K. Pagire, A. Hossain, L. Traub, S. Kerres, O. Reiser, *Chem. Comm.* **2017**, *53 (89)*, 12072-12075.

Asymmetric Synthesis of Both Enantiomers of Arteludovicinolide
A Kreuzer, S. Kerres, T. Ertl, H. Rücker, S. Amslinger, O. Reiser, *Org. Lett.* **2013**, *15*, 3420-3423.

Conferences

GdCh-Wissenschaftsforum 2017 (10.-14-09.2017), Berlin, Germany
"Photocatalytic Synthesis of γ-Cyclobutane Amino Acids and their Application in NPY Analogues" (Poster)

26th ISHC-Congress (03.-08.09.2017), Regensburg, Germany
"Synthesis of γ-Cyclobutane Amino Acids via Visible Light" (Poster)

6th EuCheMS Chemistry Congress (11.-15.09.2016), Sevilla, Spain
"Photocatalytic Synthesis of γ-Cyclobutane Amino Acids" (Poster)

GdCh-Wissenschaftsforum 2015 (30.08.-02.09.2015), Dresden, Germany
"Synthesis of γ-Cyclobutane Amino Acids and their Application in NPY Analogues" (Poster)

Annual GRK 1626 Report Meetings (oral presentation, 15 min)

Regularly Group Seminar Research Report (oral presentation, 15 min)

G Acknowledgment

Ich bedanke mich bei Prof. Oliver Reiser für die Überlassung des äußerst interessanten Themas und seine beständige Unterstützung während der gesamten Arbeit.

Für die ideelle als auch finanzielle Unterstützung während meiner Promotion bedanke ich mich bei der DFG Research Training Group GRK 1626 und der Friedrich-Ebert-Stiftung.

Vielen Dank an Simon Malcherek (AK Rehbein) für die Berechnungen zum Reaktionsmechanismus der [2+2] Photocycloaddition.

Vielen Dank auch an die Arbeitsgruppen von Prof. C. Cabrele für die Synthese der Peptidsequenzen und von Prof. A. Buschauer für die Durchführung der biologischen Tests.

Bei allen Mitarbeitern der zentralen Analytik bedanke ich mich insbesondere für die Aufnahme der Röntgenstrukturanalysen, der Durchführung der Massenspektroskopien und der NMR-Messungen. Vielen Dank auch an Regina Hoheisel für die CV-Messungen.

Ein herzliches Dankeschön an unsere Sekretärinnen, Antje Weigert und Michaela Schüle, für alle Hilfe organisatorischer Art. Insbesondere Antje Weigert, die immer ein offenes Ohr für jegliche Belange hatte.

Herzlichen Dank an Dr. Peter Kreitmeier für seine Hilfe bei technischen und chemischen Problemen sowie für die unzähligen fachlichen, aber besonders für die nicht fachlichen Diskussionen. Außerdem bedanke ich mich bei Klaus Döring, Roxane Harteis, Helena Konkel und Brigitte Eichenseher für die Unterstützung im Laboralltag.

Vielen lieben Dank an meine Laborkollegen, Corina Neumeister, Thomas Ertl, Michael Leitner, Robert Eckl und Eva Plut für die super Atmosphäre und Zusammenarbeit im Labor 33.1.19, die wissenschaftlichen Diskussionen und vor allem für die nicht chemischen Gespräche. Arbeiten mit Euch hat richtig Spaß gemacht.

Mein besonderer Dank gilt hierbei Corina und Tom. Wir waren ein wahres Powerlabor und ein super Team. Wir haben das alles gut hinbekommen ☺ Ich habe die Zeit mit Euch richtig genossen. Danke für die wunderbare Zeit mit Euch und Eure Freundschaft!

Lieber Michi, eine Laborseite mit dir zu teilen war einfach mega. Geordnetes Chaos lebe hoch! Danke für deine Geduld und deine Unterstützung vor allem in der Endphase dieser Promotion. Ohne dich wäre es nie im Leben noch so lustig geworden und ohne dich wäre auch einiges schwerer gefallen. Danke für unsere Freundschaft.

Lieben Dank an Thomas Ertl und Martin Hofmann für all die Hilfe rund um das Thema Aminosäuren und Peptide. Vor allem Thomas Ertl für die Unterstützung bei der HPLC und dem NPY-Thema und Martin Hofmann für die Hilfe mit jeglichem „Computerkram“. Besonderen Dank natürlich für den Spaß, den man immer mit Euch hatte. Durch Euch hat man sich von Anfang an am Arbeitskreis wohl gefühlt.

Liebe Verena, es war Freundschaft auf den zweiten Blick ;-) Danke für die gemeinsame Zeit vor allem in der Regensburger Innenstadt und für den Schlafplatz ab und an.

An meine Leidensgenossen Matthias Gnahn, Benjamin Kastl und Saerom Park ein herzliches Dankeschön. Mit Euch wurde sogar die Schreibphase ertragbarer Spaß ☺. Lieber Matze, es war immer wieder lustig mit dir und danke für deine Hilfsbereitschaft jeglicher Art. Liebe Saerom, danke für deine fröhliche und offene Art. Danke Euch dreien für die super entspannte und fröhliche Atmosphäre und gemeinsame Zeit im Office bzw. in der Handbib.

Vielen Dank für die unvergessliche Zeit mit Euch allen: Andi, Benjamin, Berni, Christian, Corina, Daniel, Easy, Felix, Jimmy, Lisa, Lu, Matze, Michi, Petermeister, Roxy, Saerom, Tom, Vreni!

Herzlichen Dank an alle aktuellen und ehemaligen Mitarbeiter des AK Reisers. Für die gute Zusammenarbeit, die schönen Aktivitäten am und außerhalb des Arbeitskreises. Insbesondere danke ich Andreas Bergmann, Francesca Besostri, Simon Budde, Daniel Dobler, Robert Eckl, Peter Ehrnsberger, Christian Eichinger, Thomas Ertl, Christian Faderl, Thomas Föll, Matthias Gnahn, Andreas Hartl, Martin Hofmann, Benjamin Kastl, Paul Kohls, Andreas Kreuzer, Christian Lankes, Verena Lehner, Michael Leitner, Roland Lindhardt, Sabine Möhle, Natalja Moor, Corina Neumeister, Andreas Okun, Saerom Park, Ludwig Pilsl, Eva Plut, Daniel Rackl, Thomas Rawner, Carina Sonnleitner, Lisa Stadler und Kathrin Ulbrich.

Für das gewissenhafte Korrekturlesen bedanke ich mich herzlichst bei Robert Eckl, Thomas Ertl, Kristina Hebauer, Verena Lehner, Michael Leitner, Corina Neumeister und Carina Sonnleitner.

Außerdem danke ich meinen ehemaligen Bachelorstudenten und Forschungspraktikant(inn)en Lukas Wein, Fabian Späth, Josefine Weiß, Alexander Röther, Robert Eckl, Bernhard Leitner.

Liebe Sabine, herzlichen Dank für die gemeinsame Studienzeit. Mit dir hat das Chemiestudium einfach Spaß gemacht. Vor allem bedanke ich mich für die wunderbare Zeit außerhalb der Uni und unserer Freundschaft trotz jeglicher räumlicher Distanz.

Natürlich bedanke ich mich über alles bei meinen Freunden von „*Dahoam*“. Ein unendliches Dankeschön Karina, Kristina, Carina, Dominique, Juli, Anna Z., Anna S., Max, Michael, Florian R, Martin, Christina, Bernhard, Markus, dass ihr immer für die notwendige Ablenkung gesorgt habt. Ohne Euch hätte es nicht funktioniert.

Lieber Benjamin, es ist unmöglich mein Dankeschön an dich in Worte zu fassen. Danke, dass du mich immer in allem unterstützt hast, für mich da warst, für unsere langjährige Freundschaft. Du bist für mich nicht mehr weg zu denken ☺

Lieber Florian, danke für deine unermüdliche Geduld, deine liebevolle Unterstützung, dein unendliches Vertrauen und deinen Rückhalt. Ohne dich hätte ich das nicht alles erreichen können.

Zu guter Letzt bedanke ich mich bei meiner ganzen Familie für die Liebe, Geborgenheit und Unterstützung. Ich bin so unendlich froh Euch alle zu haben. Danke, Schwesterlein, dass es dich gibt ☺ Danke Mama und Papa, dass ihr mich in all meinen Vorstellungen und Entscheidungen stets unterstützt und ermutigt habt. Ohne Euch wäre ich nie so weit gekommen.

H Declaration

Herewith I declare that this present thesis is a presentation of my original work prepared single-handed. Wherever contributions from others are involved all of them are marked clearly, with reference to the literature, license, and acknowledgement of collaborative research.

Regensburg, July 09, 2018

_____

Sabine Kerres